APPENDIX 17:

THIN SECTION REPORT
(ROGER MITCHELL – ALMAZ PETROLOGY)

PETROGRAPHIC REPORTS

ELDOR CARBONATITES

42829
68101
68119
68128
68138
68146
68151
68162
68171
68182
68184
68191
68193
68194
70059

ALMAZ PETROLOGY
ROGER H MITCHELL

NOVEMBER 2009

SUMMARY

This document summarises petrological observations on 15 samples of carbonatite derived from the Eldor complex, Northern Quebec. For each sample there is a brief petrographic description based on optical and back-scattered electron petrography coupled with X-ray spectrometric identification of the minerals present. In some instances semiquantitative compositional data are given for pyrochlore, ferrocolumbite, fersmite and other rare element-bearing minerals. Although these data are considered as semiquantitative they are considered as being "close" to the actual compositions. Quantitative data requires more extensive standardization than used in this overview of the mineralogy of the samples. This hard copy report of the petrographic description is accompanied by a CD which contains PowerPoint files of transmitted light and false-colour back scattered electron images for each sample. Note that standard optical methods are totally inadequate for the characterization of the mineralogy of these rocks. An Excel file on the CD provides a summary of the mineralogy of each sample.

The rocks investigated are mineralogically complex and differ substantially from sample to sample. The common mineralogical trait is that all contain ferroan dolomite; although this ranges in modal amounts from trace to major quantities. Some of the rocks contain the uncommon carbonate mineral breunnerite (magnesite-siderite solid solution), and those richest in siderite can be considered as ferrocarbonatites. Samples rich in calcite are minor components of this suite. The breunnerite and ferroan dolomite exhibit wide ranges in composition with respect to their Mg, Ca, Fe and Mn contents. Variations in these components might be used to assess the relative degree of evolution of members of this carbonatite suite, as it is evident that breunnerite forms prior to ferroan dolomite and the latter in turn before calcite.

The rocks appear to represent members of a suite of ferroan dolomite carbonatites and ferrocarbonatites that range from disrupted cumulates (apatite-magnetite carbonatites) to late stage hydrothermal-like rocks (fluorite-carbonatites). One important aspect of the mineralogy is the presence in many of the samples of quartz, potassium feldspar, magnesium arfvedsonite and aegirine. One sample contains the rare silicate bafertisite. The silicate assemblage is essentially syenitic, and coupled with the enrichment of some of the carbonatites in fluorite and REE-fluorocarbonates suggests derivation from an anorogenic (A-type) peralkaline syenitic/granitoid source. The high U and Ta content of the pyrochlores might be in accord with such a source. The common resorption and complex alteration of most of the rare element-bearing minerals indicates that they have formed from magmas which are not represented by their current host rocks, i.e. they are a rheologically transported assemblage. The samples do not contain nepheline or diopsidic pyroxenes typical of the ijolite-carbonatite suite and any genesis or affinity related to "typical" Nb-rich carbonatite complexes such as Oka or Araxa is unlikely.

In the absence of any geological data regarding the occurrence and field disposition of these samples further commentary on their genesis is not warranted in this petrographic report.

	bruennerite	fe-dolomite	calcite	apatite	magnetite	pyrochlore	ferrocolumbite	REE-F-carbs	fluorite	monazite	aeschynite	other minerals of interest
68101		x		x				x		x	x	Mg-arfvedsonite, phlogopite, Y-thorogummite
68119			x	x	x						x	minor pyrochlore; phlogopite; trace REE-carbs
68128		x						x		x		Quartz, K-feldspar; Y-phases; CeF3; trace phlogopite
68138		x						x	x			trace fersmite, zircon; phlogopite
68146	x	x			x		x			x		major Mg-arfvedsonite; pyrite; zircon
68151		x		x	x	x					x	fersmite; chlorite;
68162		x		x		x 2 types		x	x		x	K-feldspar, phlogopite
68171		x		x	x	x					x	common diopside; fersmite; zircon
68182		x	x	x	x	x						common chlorite; trace baddeleyite; zircon
68184			x	x	x	x						pyrite
68191	x	x		x	x	x	x					quartz, aegirine, pyrite; zircon
68193		x		x						x		K-feldspar, chlorite (after phlogopite); albite
68194	x	x		x	x	x	x			x		quartz; Mg-arfvedsonite;aegirine; zircon
70059	x	x						x		x		K-feldspar, albite, pyrite;Fe oxides/hydroxides;molybdenite; niobian rutile
42829	x	x						x	x	x		quartz;Mg-arfvedsonite; bafertisite, trace xenotime

ELDOR 42829

This fine grained sample is cut by numerous random thin veins of colourless-to-deep purple fluorite (Fig.1). Similar fluorite occurs disseminated throughout the carbonatite intergrown with carbonates (Fig. 2, 6, 12). The fluorite veins consist of anhedral interlocking crystals of fluorite and lack breunnerite and dolomite. They typically lack rare earth fluorocarbonates but do contain very thin (15 um) veins of unidentifiable Sr-Ba-Ce-carbonates (Fig. 4).

The carbonatite matrix to the fluorite veins consists principally of a very complex, fine grained intimate intergrowth of anhedral fluorite, breunnerite, diverse ferroan dolomites and quartz (Figs 3-11). Quartz is the latest mineral to form and occurs as rounded "pools" in the carbonate matrix (Figs. 7-9). Fluorite forms irregular aggregates of anhedral crystals which in some instances are connected to fluorite veins (Fig. 6). Breunnerite (as magnesian siderite) is the earliest carbonate to form, and occurs as aggregates of anhedral crystals that can be rimmed by ferroan dolomite (Fig. 7). Dolomites with diverse Fe contents form a matrix in which most of the other components of the sample are set (Figs. 5-8). Trace amounts of silicates present in the rock include subhedral prisms of blue-green magnesioarfvedsonite and elongated laths (<200um) of orange bafertisite [$Ba(Fe,Mn)_2TiSi_2O_7(O,OH)_2$] (Figs 3,5,9). Also present in the groundmass are rare small (<50 um) subhedral crystals of niobian rutile (10-15 wt.% Nb_2O_5) and niobian ilmenite. Pyrite is present as large (<0.4mm) euhedral-to-rounded crystals (Figs.14-15). These typically contain small (< 10um) inclusions of galena. Sphalerite occurs in groundmass fluorite as anhedral (< 200 um) crystals (Fig.12).

ELDOR 42829

This sample is not rich in rare element-bearing minerals, as these are present in trace amounts (c. <<5 vol%). Pyrochlore, fersmite, ferrocolumbite, and apatite are absent. The principal rare earth element-bearing phases are bastnaesite-(Ce) and monazite-(Ce). These occur principally as anhedral-to-rounded aggregates of small crystals (<100 um) disseminated in fluorite aggregates (Fig.6,12) or throughout the dolomite matrix (Figs 8-9. 14-15). The fluorite veins do not appear to contains these minerals. Late stage quartz can contain small crystals of thorian monazite (Fig. 8). Very rarely, small (<20 um) crystals of xenotime and Y-Th-Nb-oxide can be found within dolomite (Fig. 10). Monazite rarely occurs as veins cross-cutting the carbonate-fluorite matrix (Fig. 13).

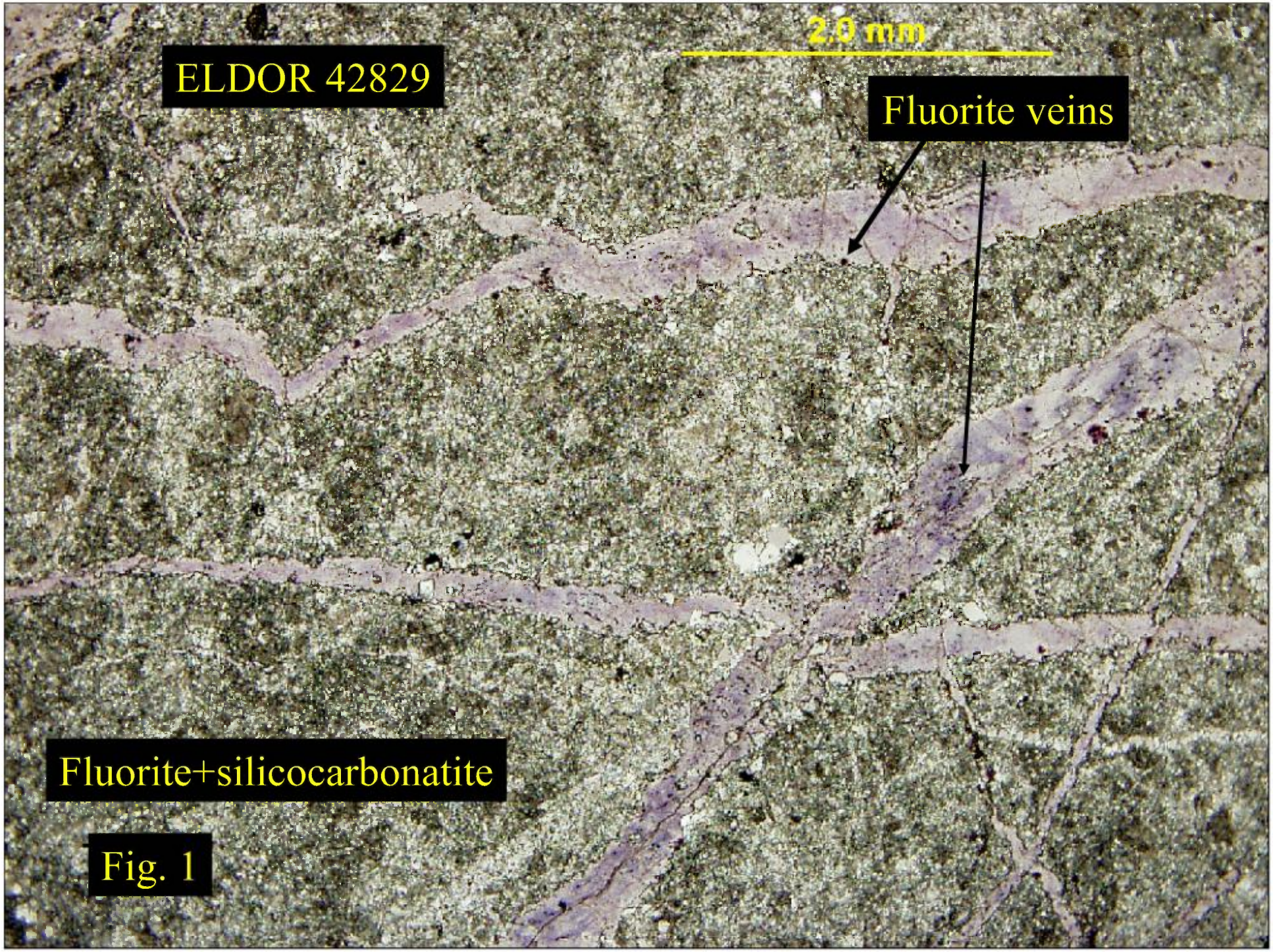
2.0 mm
ELDOR 42829
Fluorite veins
Fluorite+silicocarbonatite

Fig. 1

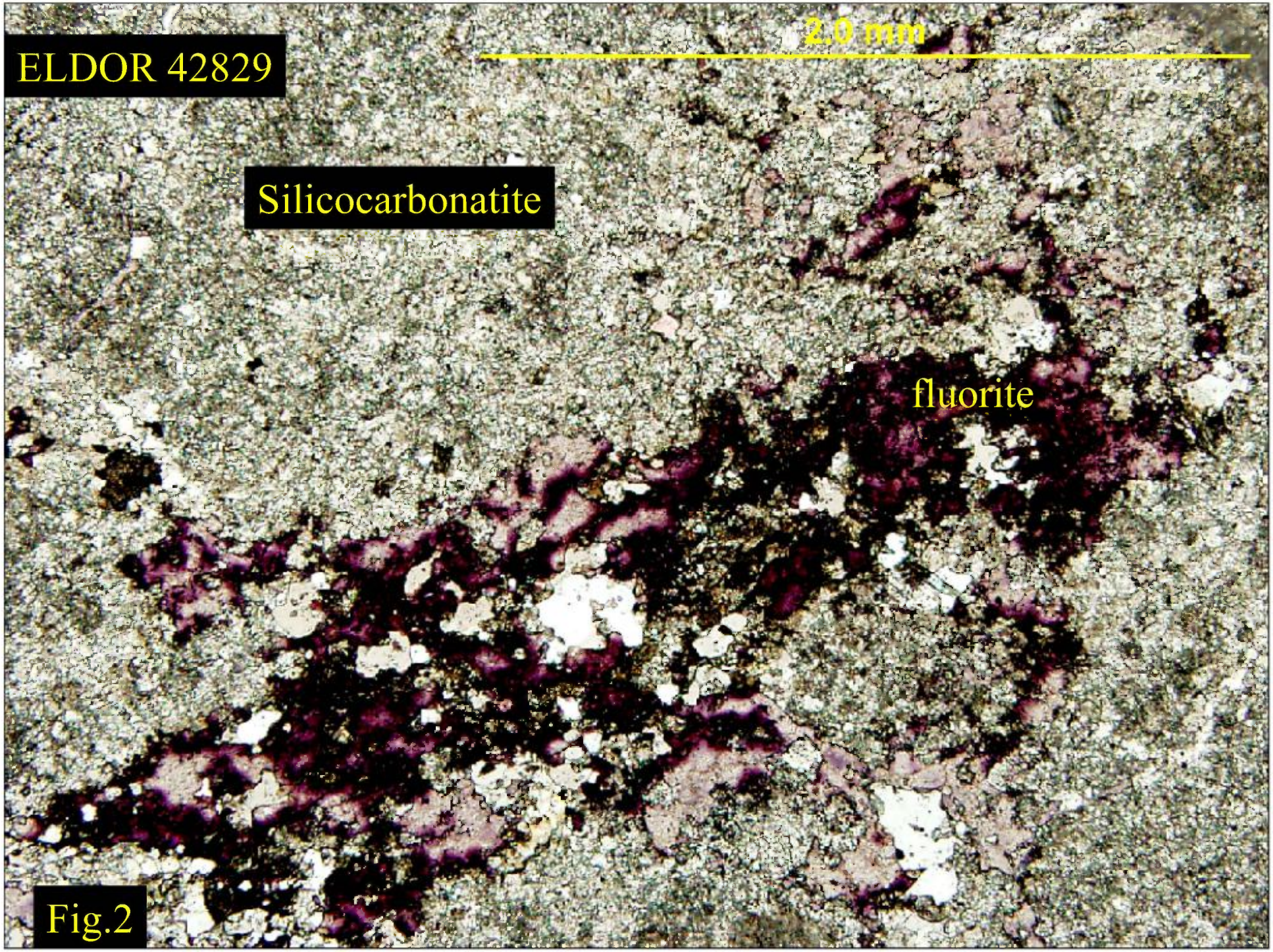

Fig.2

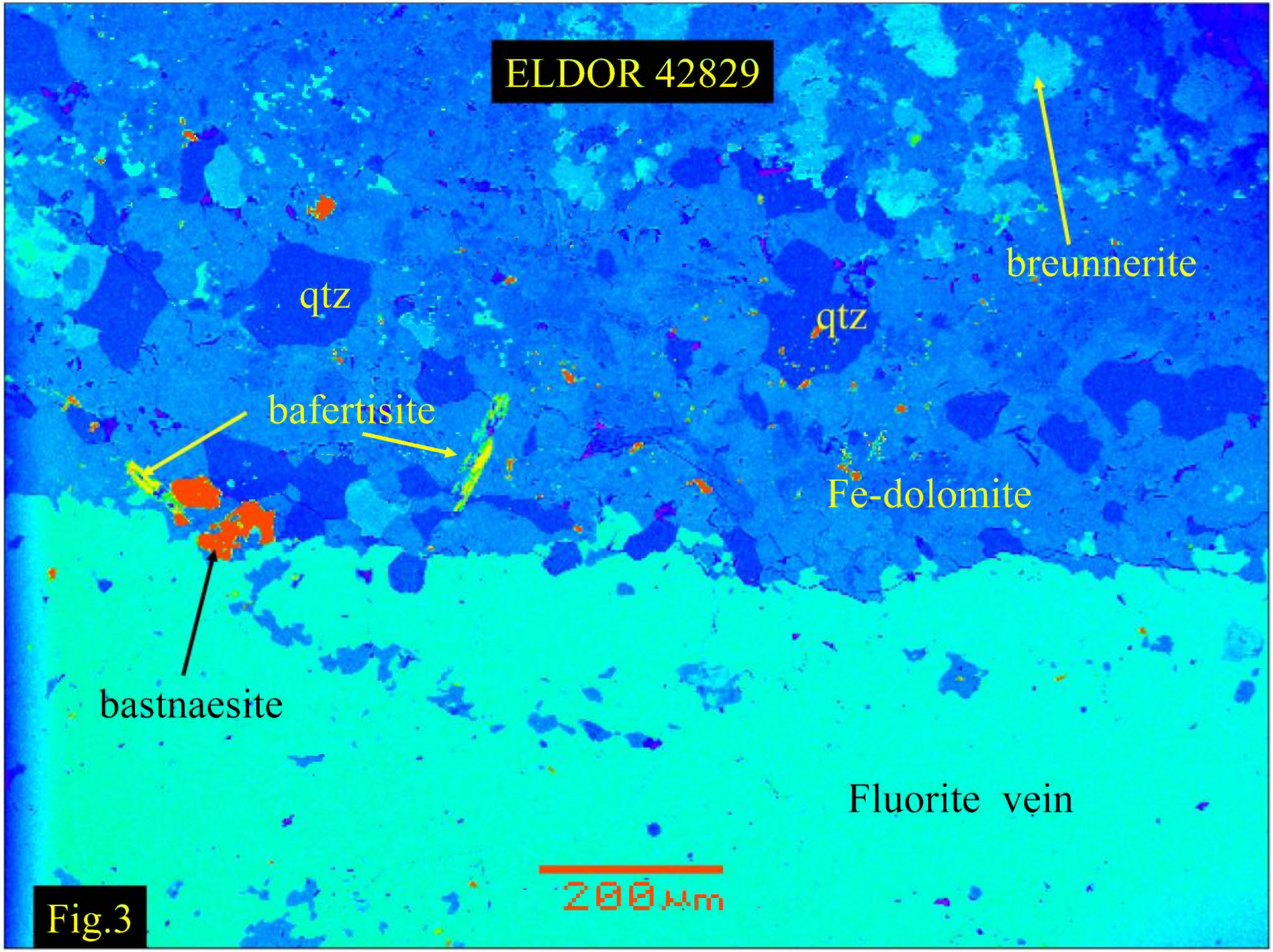
ELDOR 42829
qtz
qtz
breunnerite
bafertisite
Fe-dolomite
bastnaesite
Fluorite vein
200 µm

Fig.3

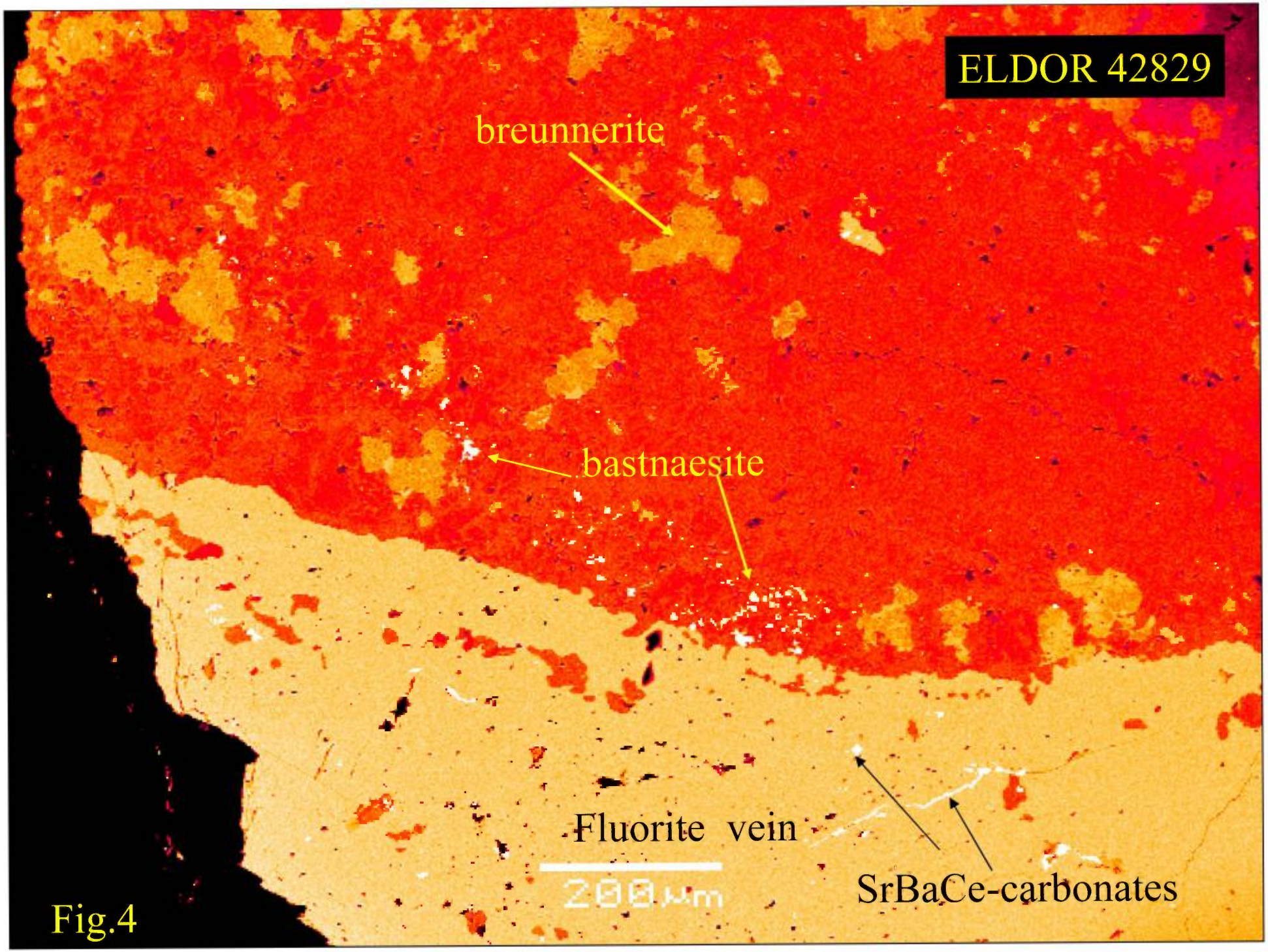
ELDOR 42829
breunnerite
bastnaesite
Fluorite vein
200µm
SrBaCe-carbonates

Fig.4

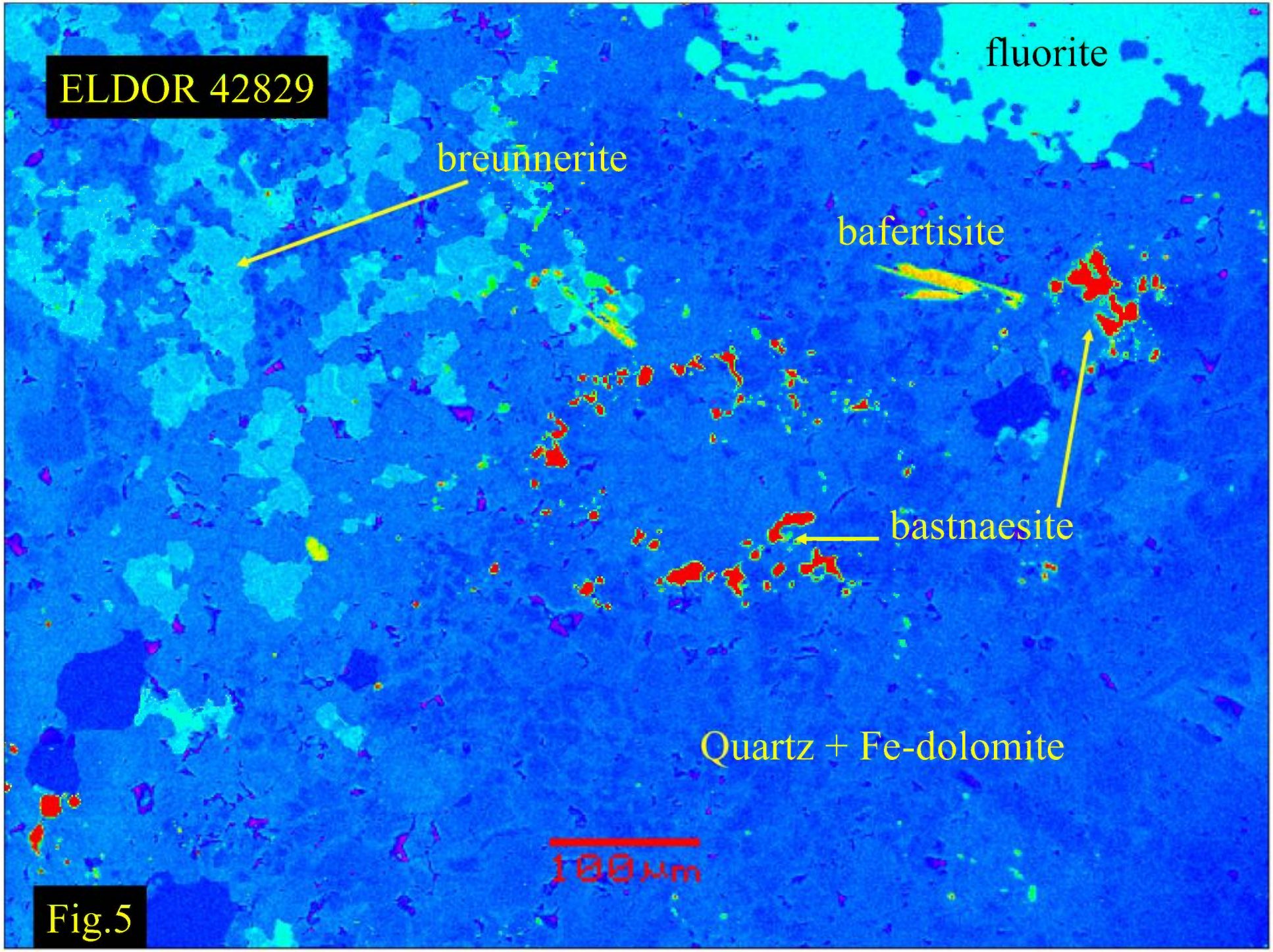
ELDOR 42829
fluorite
breunnerite
bafertisite
bastnaesite
Quartz + Fe-dolomite
100 µm

Fig.5

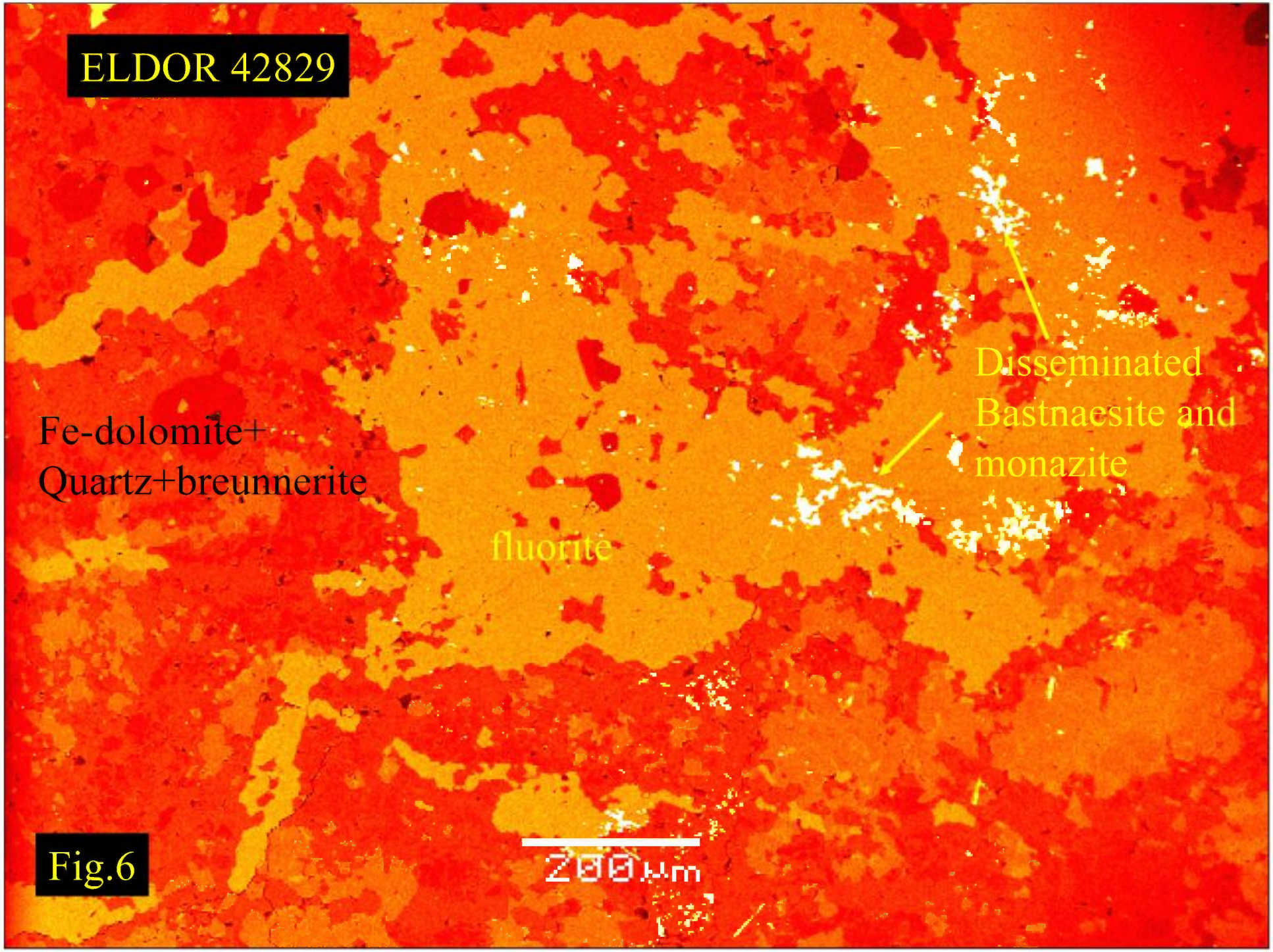
ELDOR 42829
Fe-dolomite+
Quartz+breunnerite
fluorite
Disseminated
Bastnaesite and
monazite
200µm

Fig.6

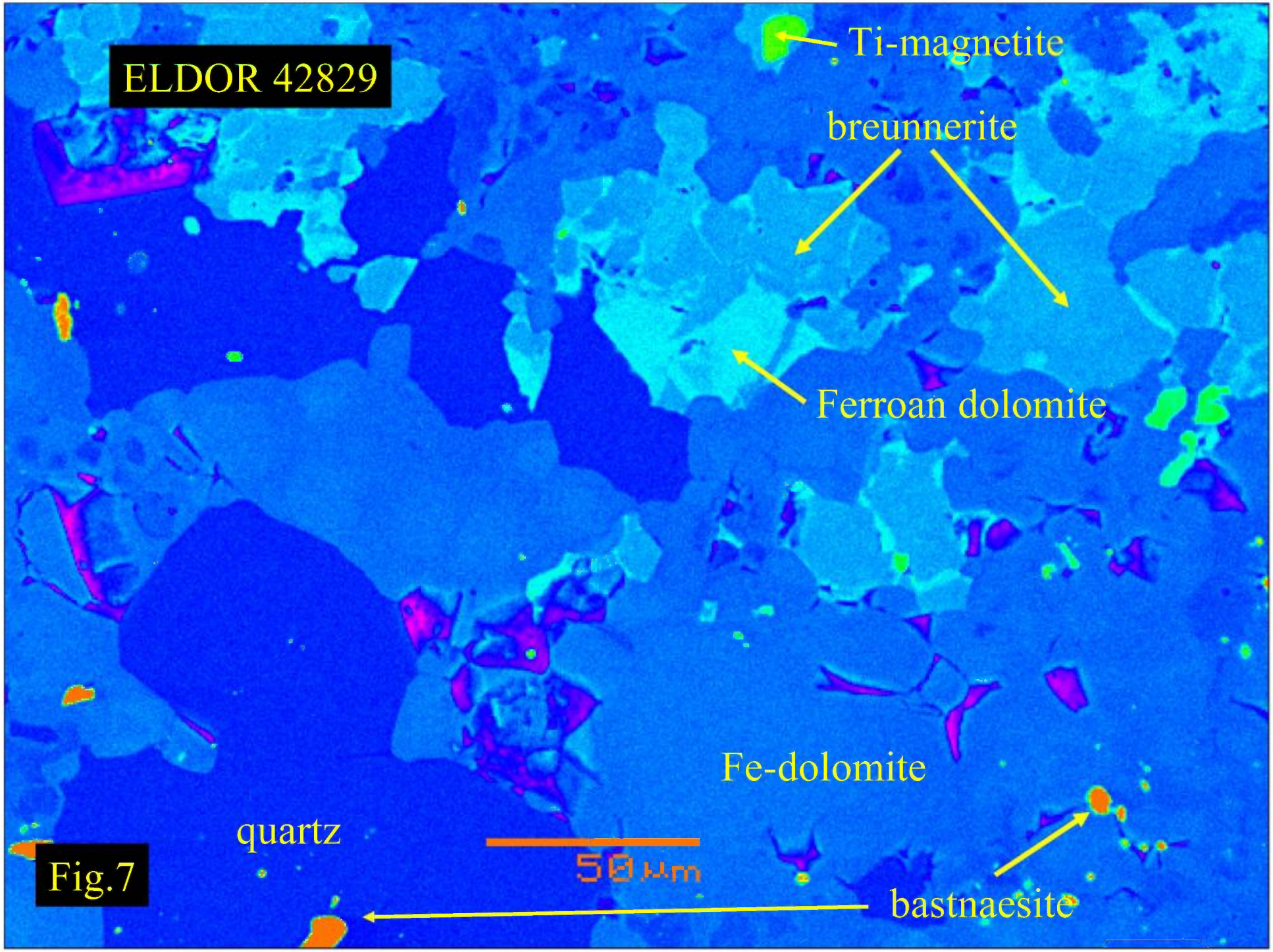
ELDOR 42829
Ti-magnetite
breunnerite
Ferroan dolomite
Fe-dolomite
quartz
50 µm
bastnaesite

Fig.7

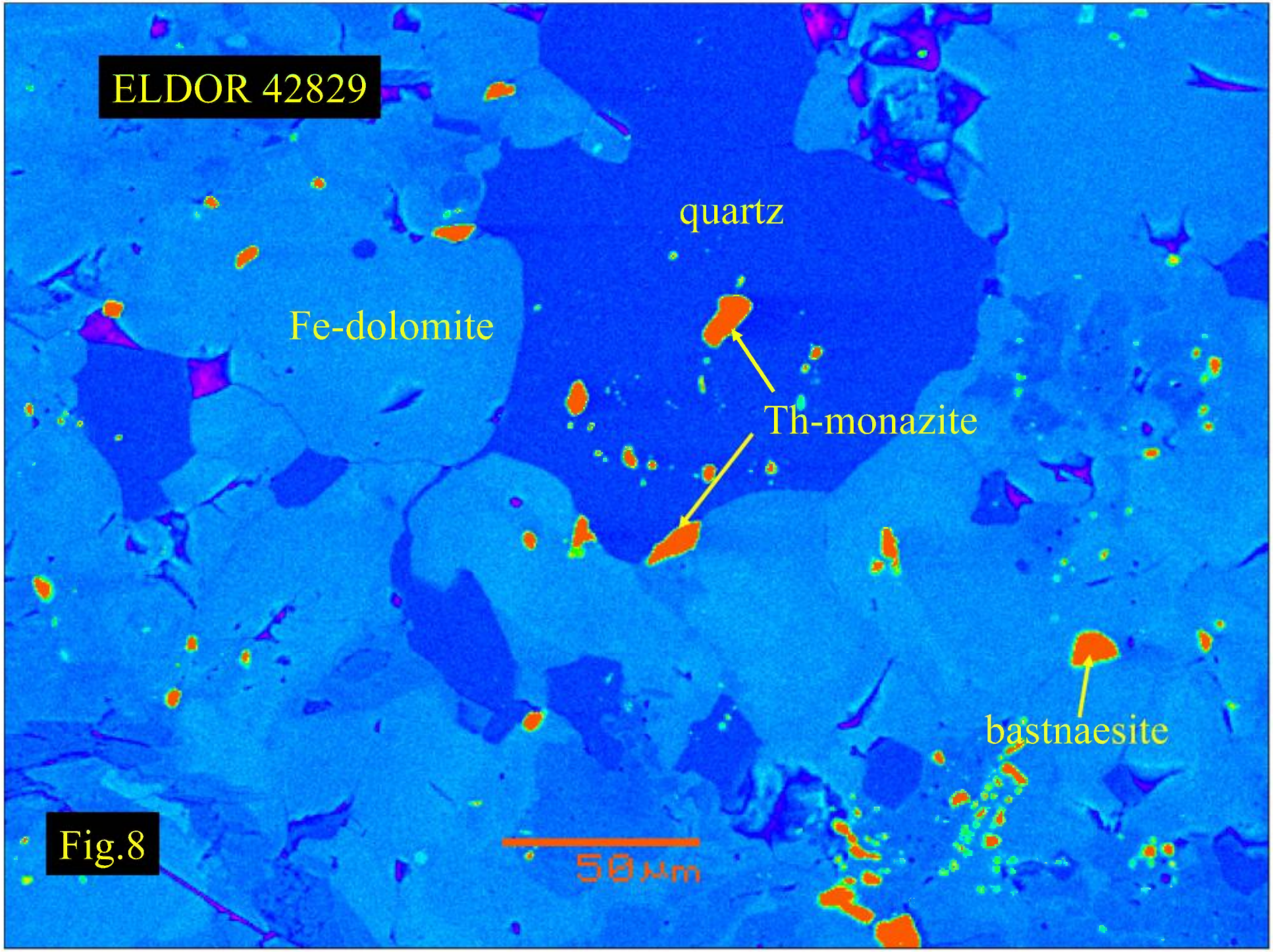
ELDOR 42829
quartz
Fe-dolomite
Th-monazite
bastnaesite
50 µm

Fig.8

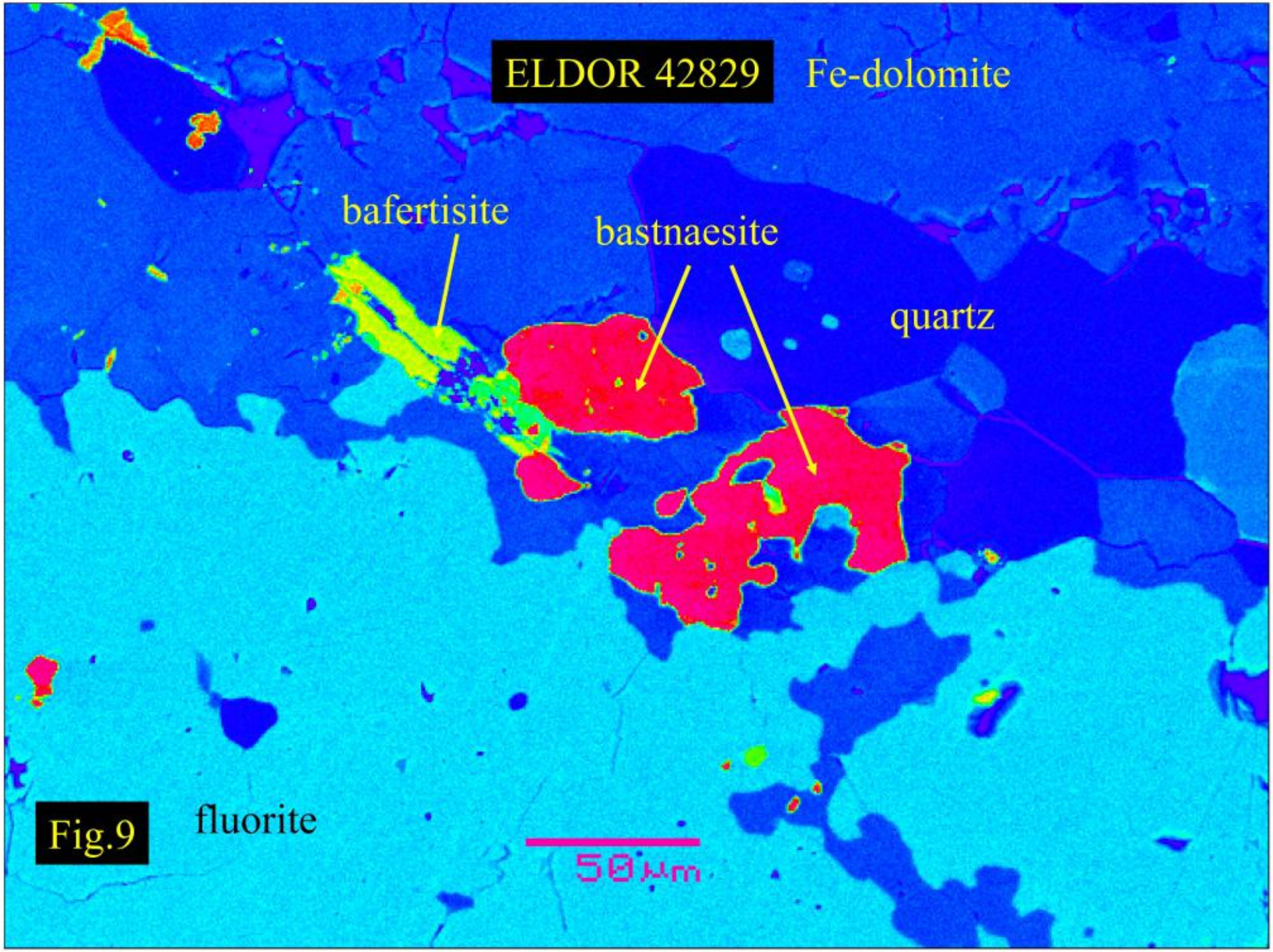
ELDOR 42829
Fe-dolomite
bafertisite
bastnaesite
quartz
fluorite
50 µm

Fig.9

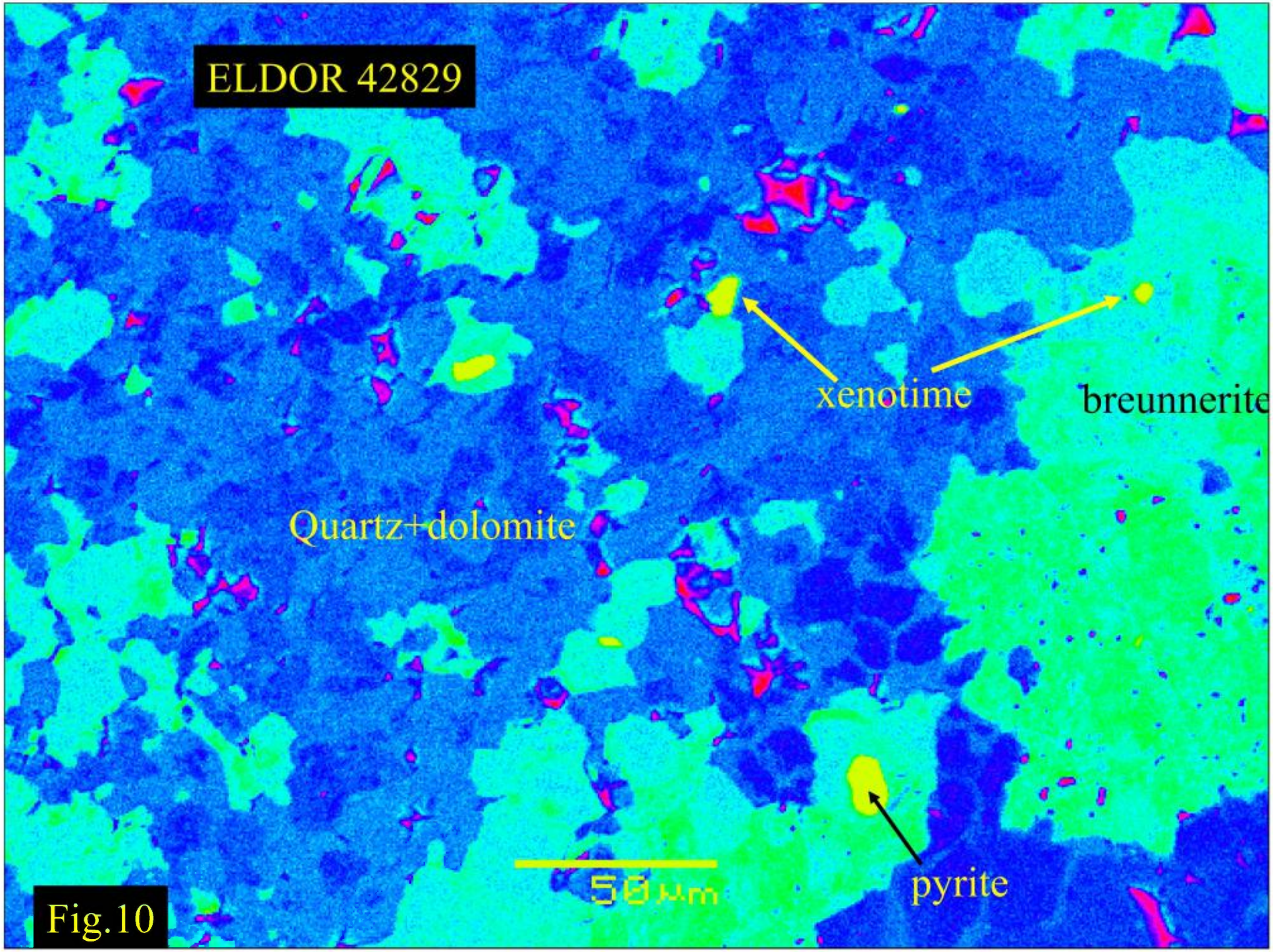
ELDOR 42829
xenotime
breunnerite
Quartz+dolomite
50 µm
pyrite

Fig.10

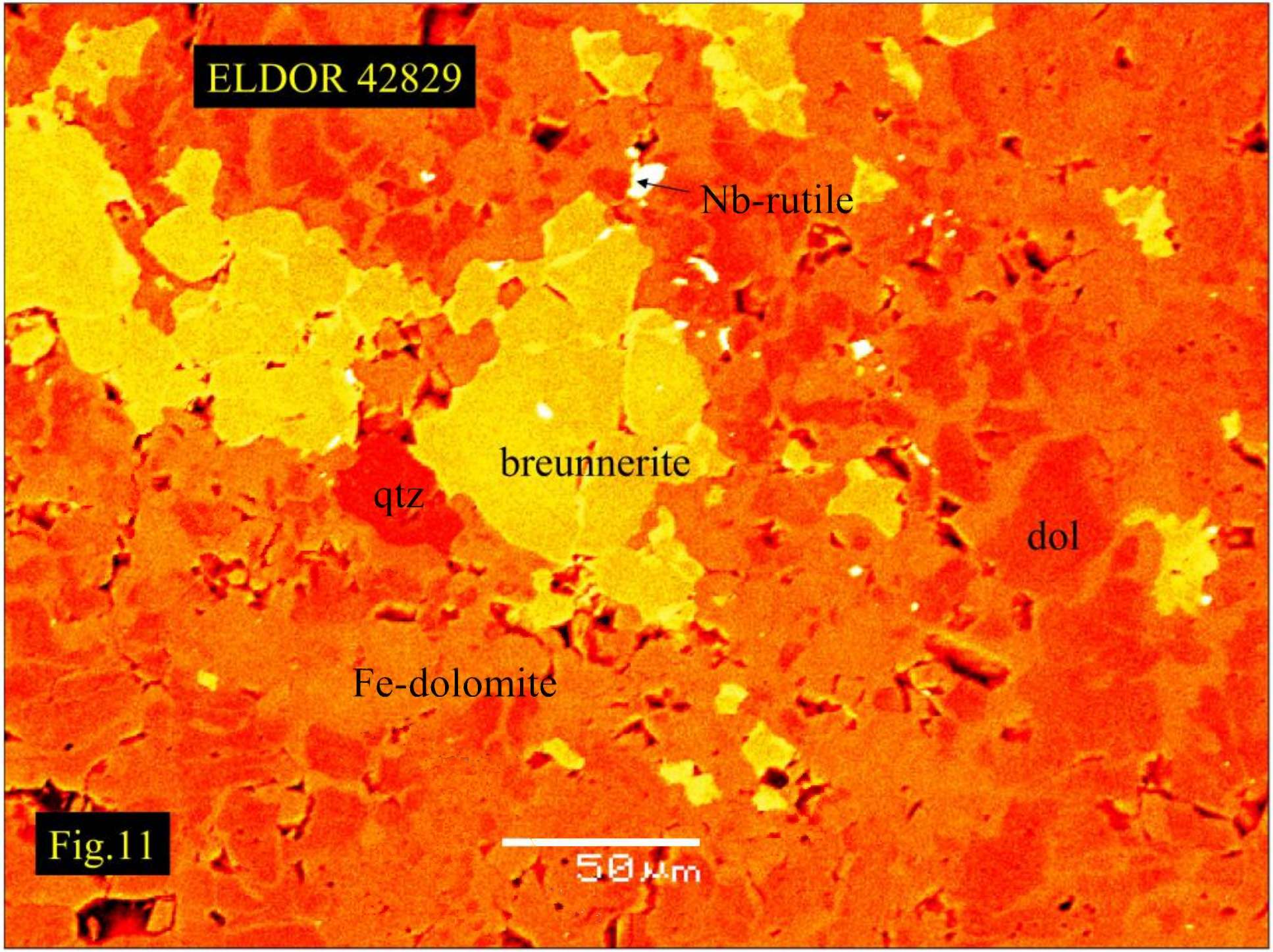

Fig.11

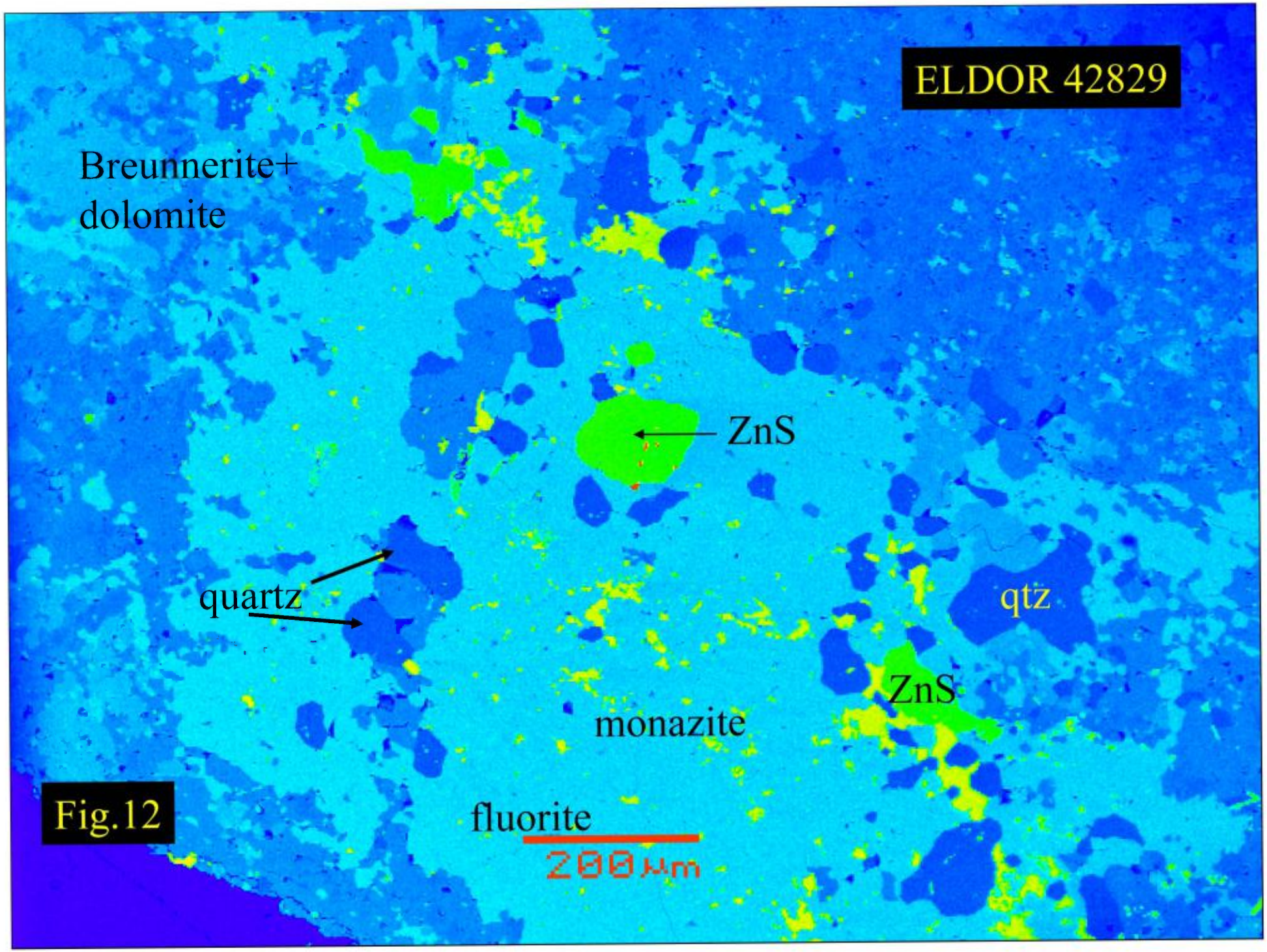
ELDOR 42829
Breunnerite+
dolomite
ZnS
quartz
qtz
ZnS
monazite
fluorite
200 µm

Fig.12

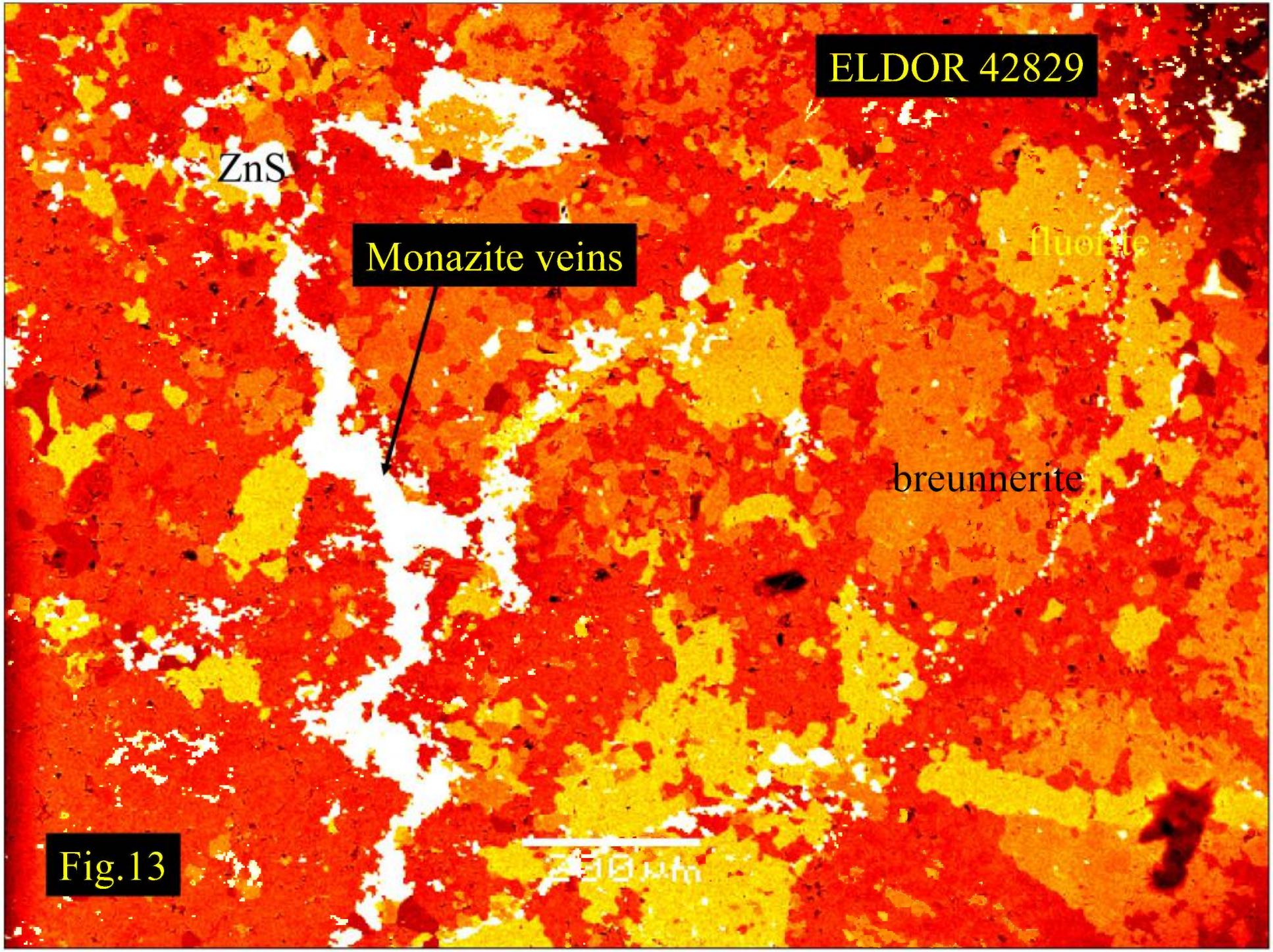
ELDOR 42829
ZnS
Monazite veins
fluorite
breunnerite
Fig.13

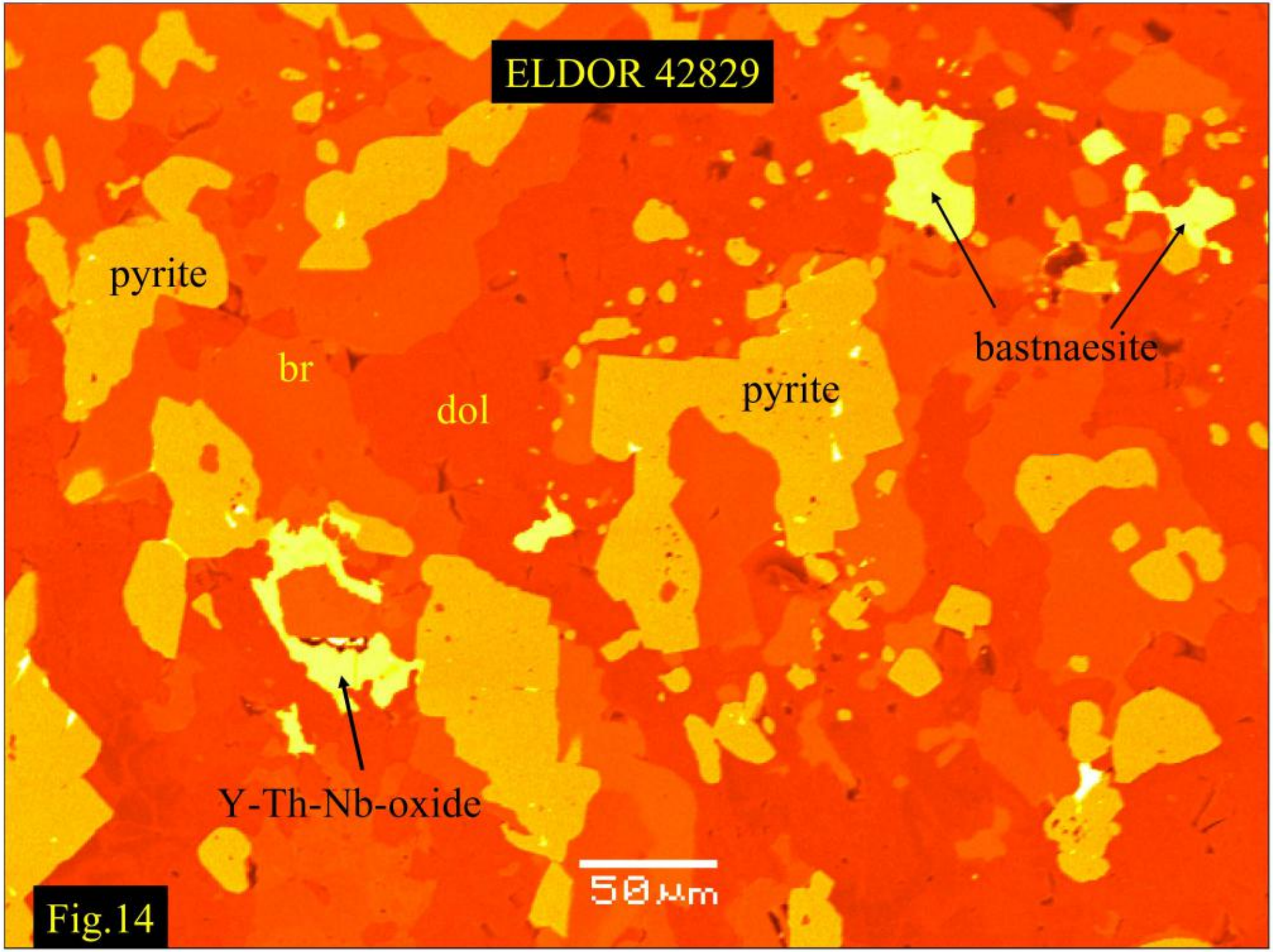
ELDOR 42829
pyrite
br
dol
pyrite
bastnaesite
Y-Th-Nb-oxide
50 µm

Fig.14

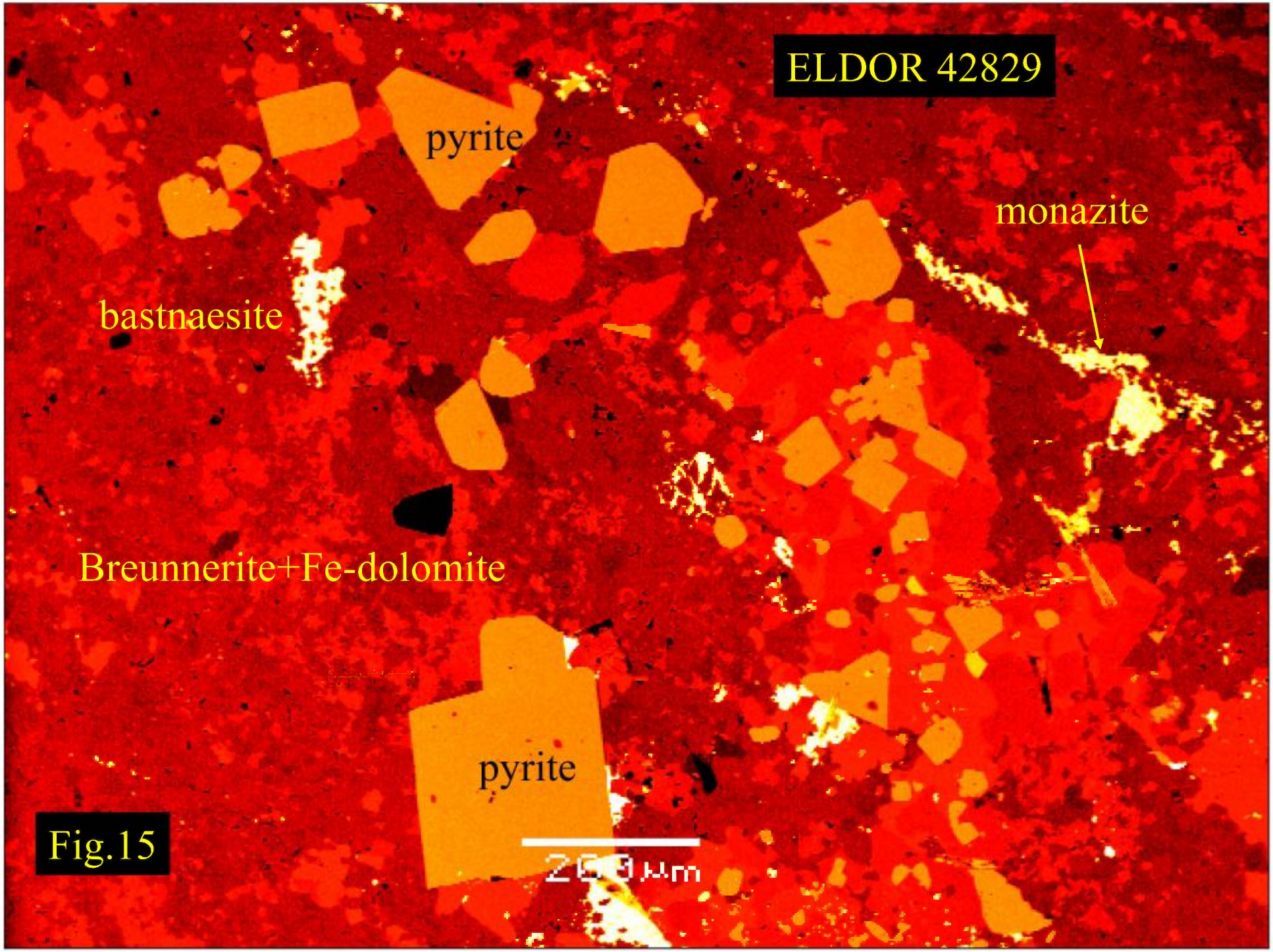
ELDOR 42829
pyrite
monazite
bastnaesite
Breunnerite+Fe-dolomite
pyrite
Fig.15

ELDOR 68101

ELDOR 68101 *REE-fluorocarbonatite-bearing ferroan dolomite carbonatite*

This a very fine grained banded ferroan dolomitic carbonatite (Fig 1) characterized by anhedral interlocking dolomite crystals with thin bands consisting of aggregates of blue pleochroic prisms of magnesioarfvedsonite and plates of brown phlogopite (Figs. 2 &3). These silicate minerals define the foliation evident in the rock. Accompanying these silicates are small euhedral opaque plates of pyrite. Although most of the dolomite is fine grained, coarser "boudin-like" patches of dolomite occur (Fig.1). These are poorer in Fe (5 wt.% FeO) than the fine grained dolomite (FeO 8- 10 wt.%; MnO 0.5- 2 wt.%). Rare anhedral crystals of quartz are scattered throughout the fine grained dolomite. Interstitial to the dolomite crystals is very dark coloured high relief material. In some areas this forms thin bands aligned parallel to the silicate bands (Fig.1). Commonly, this material is too fine grained to identify by optical methods. In some areas interstitial patches are coarser and are seen to consist of high relief, high birefringent fluorocarbonates and monazite. Abundances of all fluorocarbonates are low (< 5 vol.%). Rare rounded near-opaque crystals of optically un-identifiable trace accessory phases are scattered throughout the rock. BSE imagery and X-ray EDS show these to include: pyrite, sphalerite, galena, aeschynite and thorogummite.

ELDOR 68101

Three rare earth fluorocarbonates are common in this rock (Figs. 4-9). These are bastnaesite, synchysite and parisite. Typically bastnaesite-(Ce) forms anhedral crystals and has crystallized before the other REE-fluorocarbonates (Fig.4). Synchysite-(Ce) and parisite-(Ce) commonly coexist as syntaxial intergrowths developed on bastnaesite crystals (Figs 5-9). All REE-fluorocarbonates are Ce-rich and light REE enriched varieties.

Typical semi-quantitative compositions are:

	bastnaesite	parisite	synchysite
CaO	0.3	10.35	13.8
SrO	0.4	0.6	0.54
La_2O3	18.2	14.5	10.8
Ce_2O_3	38.4	30.6	24.7
Pr_2O_3	4.6	3.6	1.9
Nd_2O_3	14.8	11.9	9.9
Sm_2O_3	1.5	1.6	0.6
ThO_2	0.5	0.4	0.4
F	7.3	6.5	5.5

ELDOR 68101

Trace accessory phases in this rock are monazite-(Ce); yttrian thorogummite; and aeschynite-(Nd).

*Monazite-(Ce)*occurs as anhedral round crystals scattered throughout ferroan dolomite matrix and subhedral crystals in interstitial areas where it is overgrown by bastnaesite-(Ce) (Figs. 4 & 6). A typical semi-quantitative composition (wt.%) is: 28.8 P_2O_5 : 13.2 La_2O_3 ; 35.1 Ce_2O_3 4.0 Pr_2O_3 12.1 Nd_2O_3; 1.3 Sm_2O_3; 0.9 ThO_2

Yttrian thorogummite [$(Th,Y)SiO_4(OH)_4$] occurs rarely as anhedral rounded crystals within REE-fluorocarbonates (Fig 10) and as thin mantles on corroded aeschynite-(Nd) (Fig. 11). A typical semi-quantitative composition (wt.%) is: 18.6 wt.% SiO_2; 12.1 Y_2O_3; 56.8 ThO_2; 1.3 UO_2. .

Aeschynite-(Nd) [$(Nd,Ce,Y,Ca)(Ti,Nb)_2(O,OH)_6$], occurs as irregular resorbed crystals (Fig. 11) These are strongly zoned with respect to their REE, Y and Th contents with the margins of the crystals being enriched in Th relative to the core. The ultimate expression of the Th enrichment is the formation of yttrian thorogummite rims on corroded aeschynite cores. A typical semi-quantitative composition (wt.%) of aeschynite-(Nd) is: 2.3 CaO; 27.1 TiO_2 ; 25.6 Nb_2O_5; <0.4 La_2O_3 ; 3.9 Ce_2O_3; 1.3 Pr_2O_3 ; 9.9 Nd_2O_3; 5.5 Sm_2O_3; 2.4 Eu_2O_3; 3.7 Gd_2O_3; 8.2 ThO_2 ; 4.9 Y_2O_3

Nomenclature: REE-fluorocarbonatite-bearing ferroan dolomite carbonatite

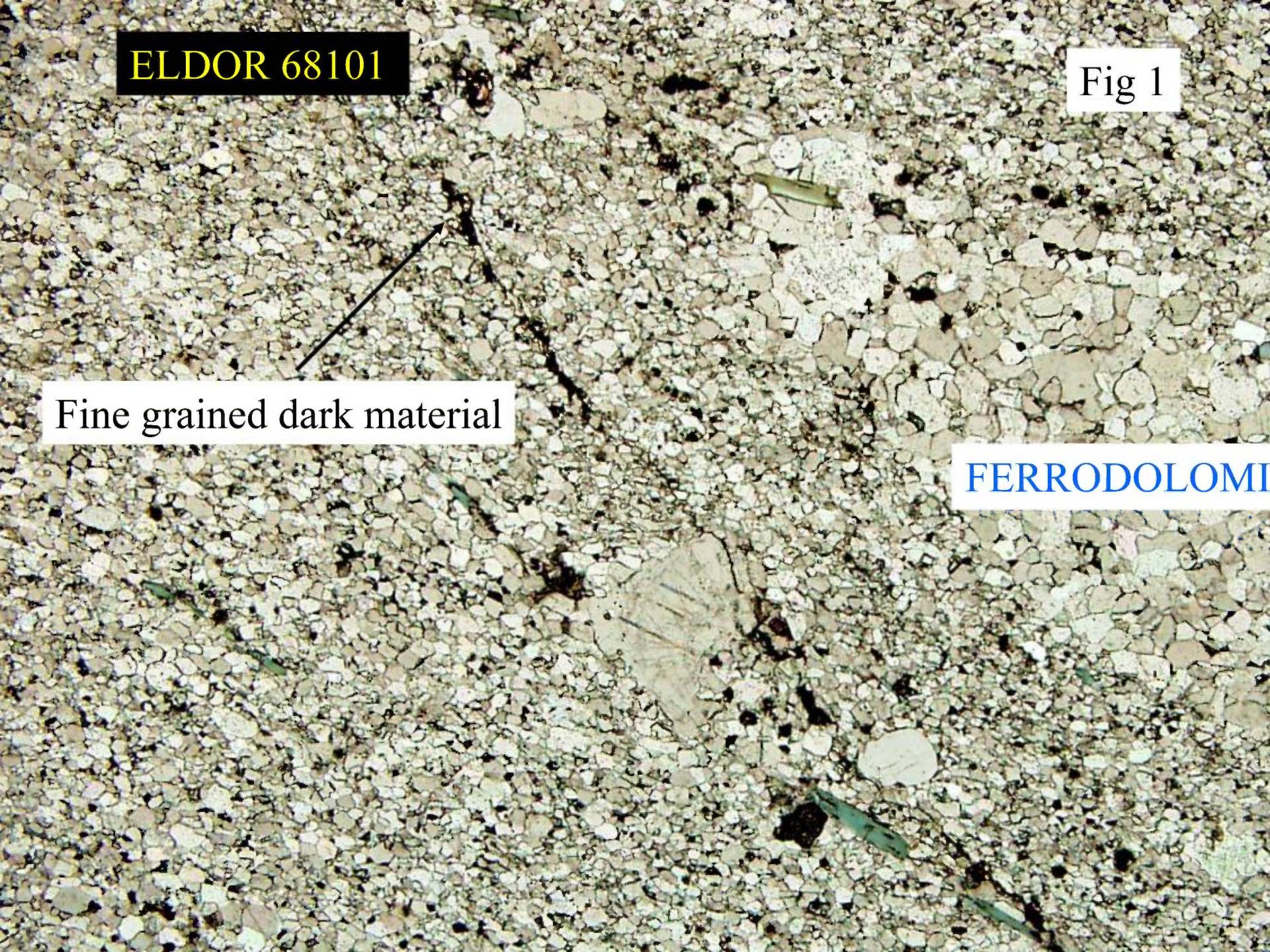
ELDOR 68101
Fig 1
Fine grained dark material
FERRODOLOMI

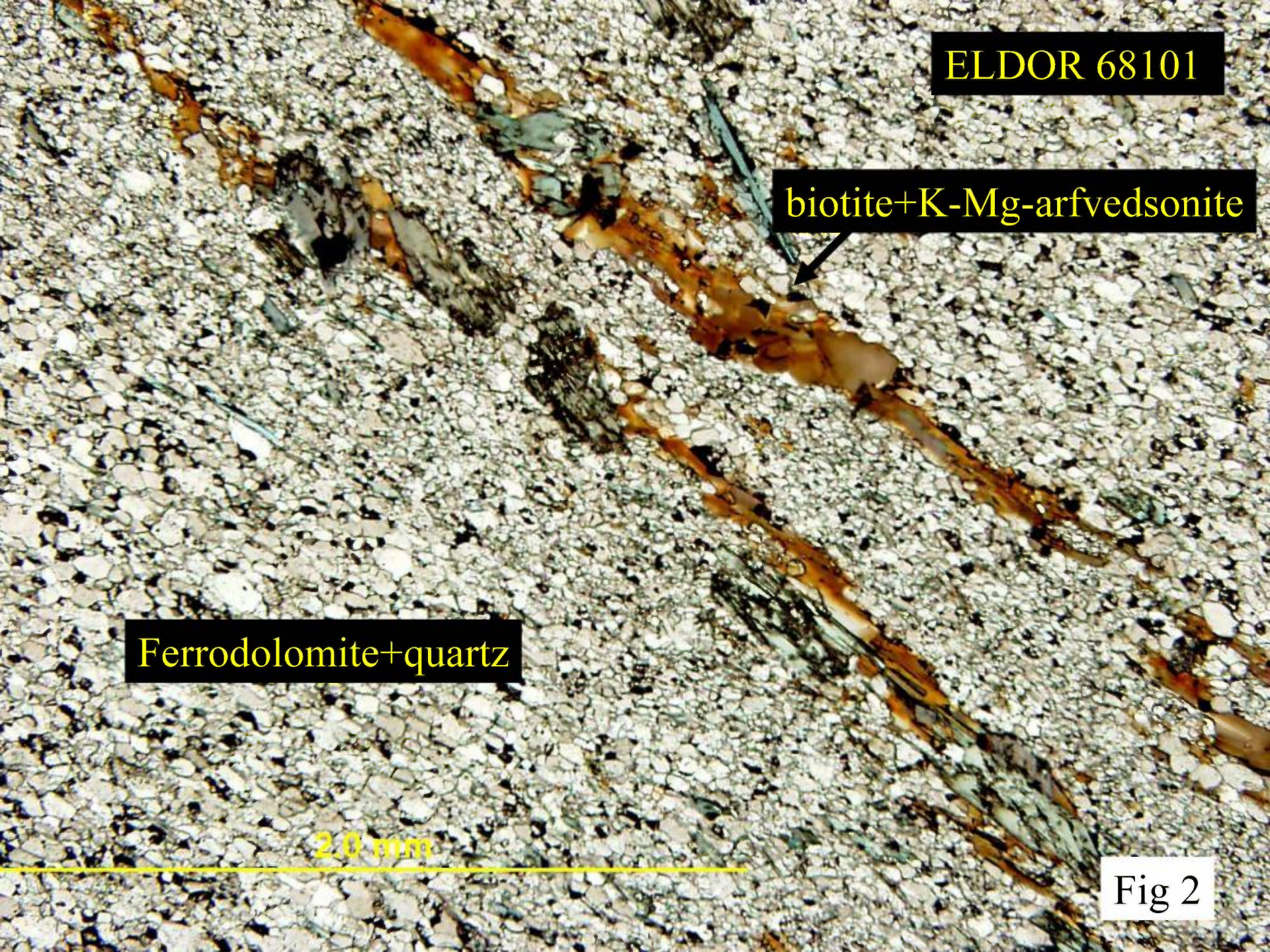
ELDOR 68101
biotite+K-Mg-arfvedsonite
Ferrodolomite+quartz
2.0 mm

Fig 2

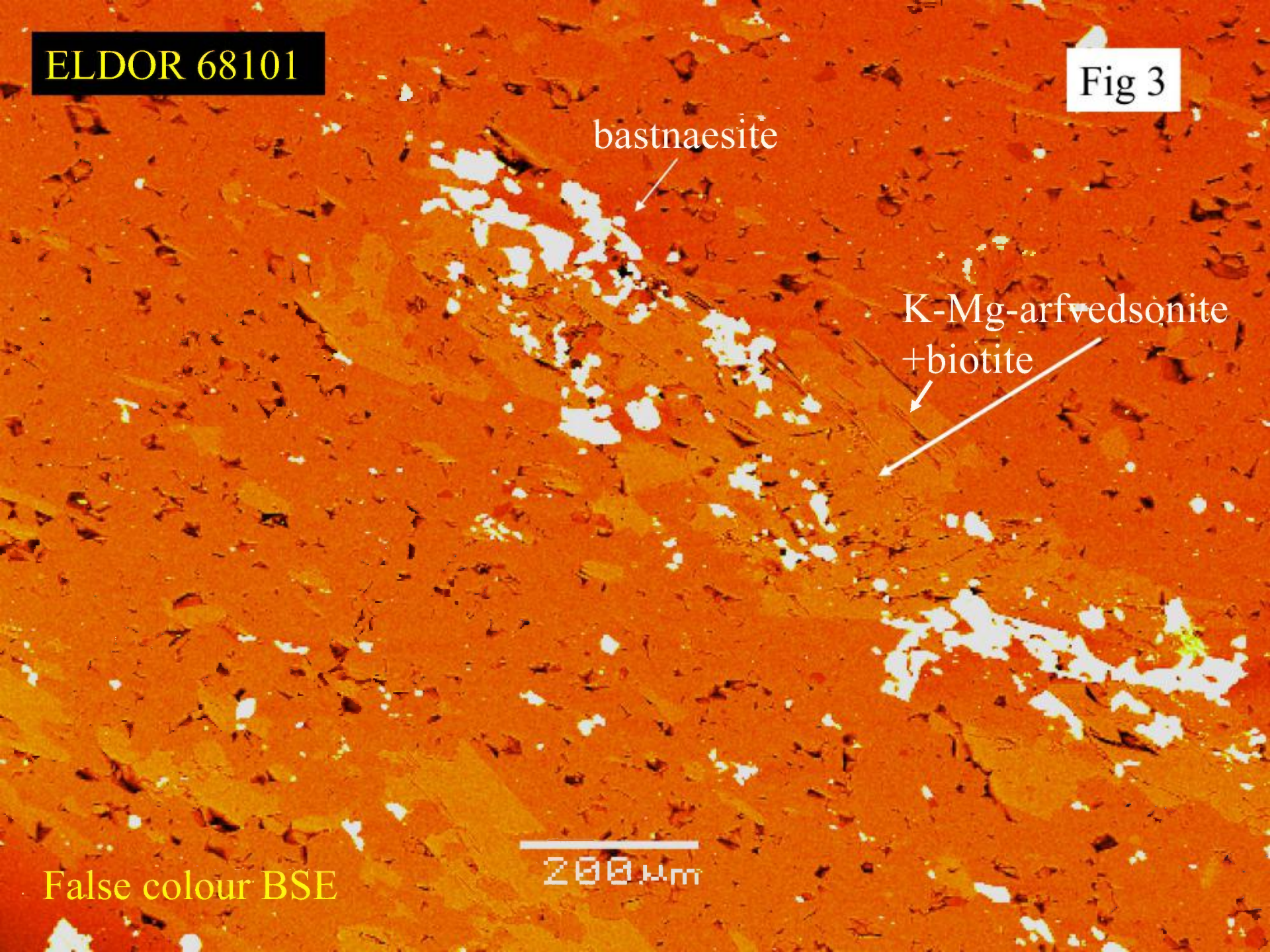
ELDOR 68101
Fig 3
bastnaesite
K-Mg-arfvedsonite
+biotite
200µm
False colour BSE

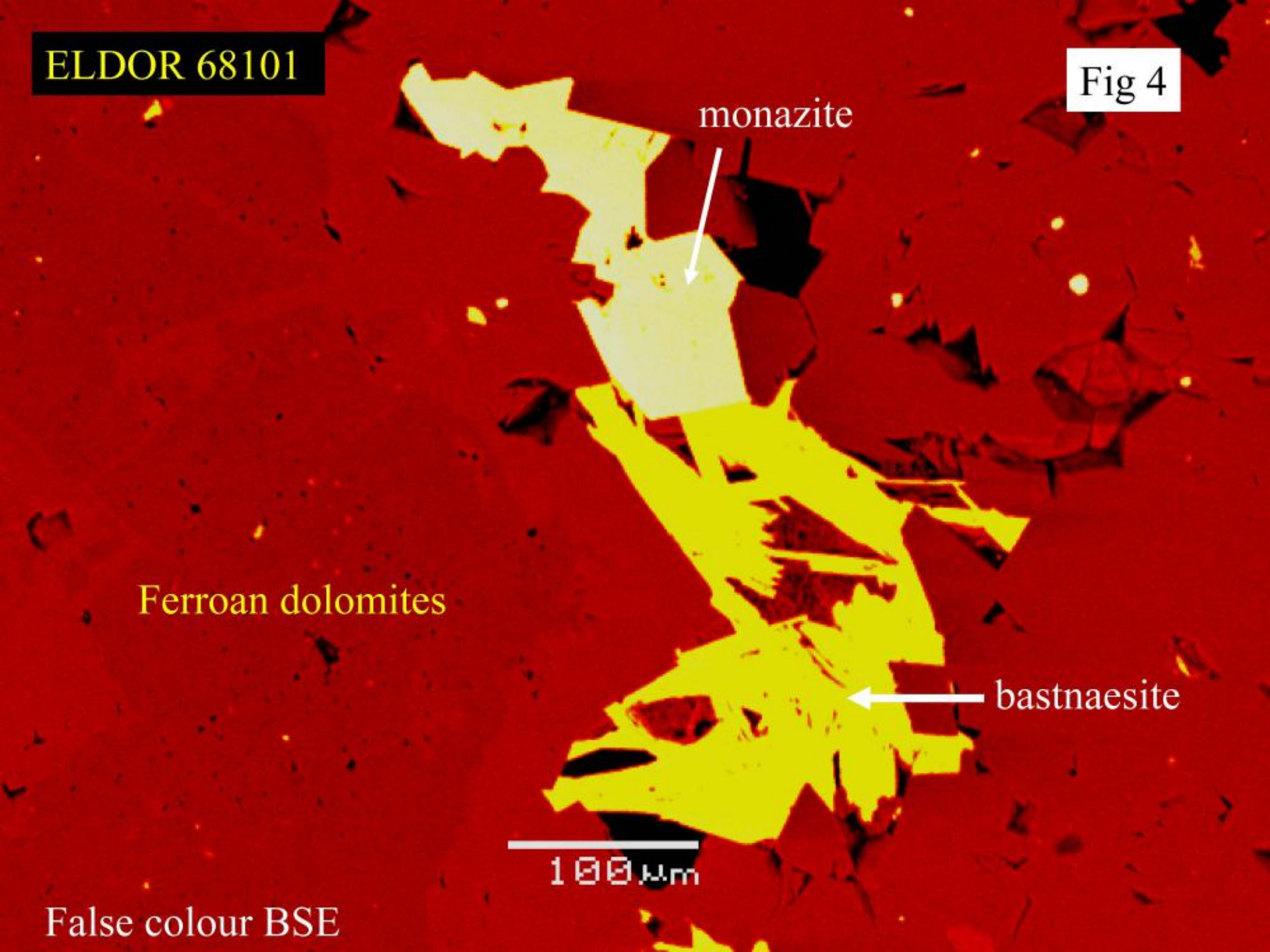
ELDOR 68101
Fig 4
monazite
Ferroan dolomites
bastnaesite
100 µm
False colour BSE

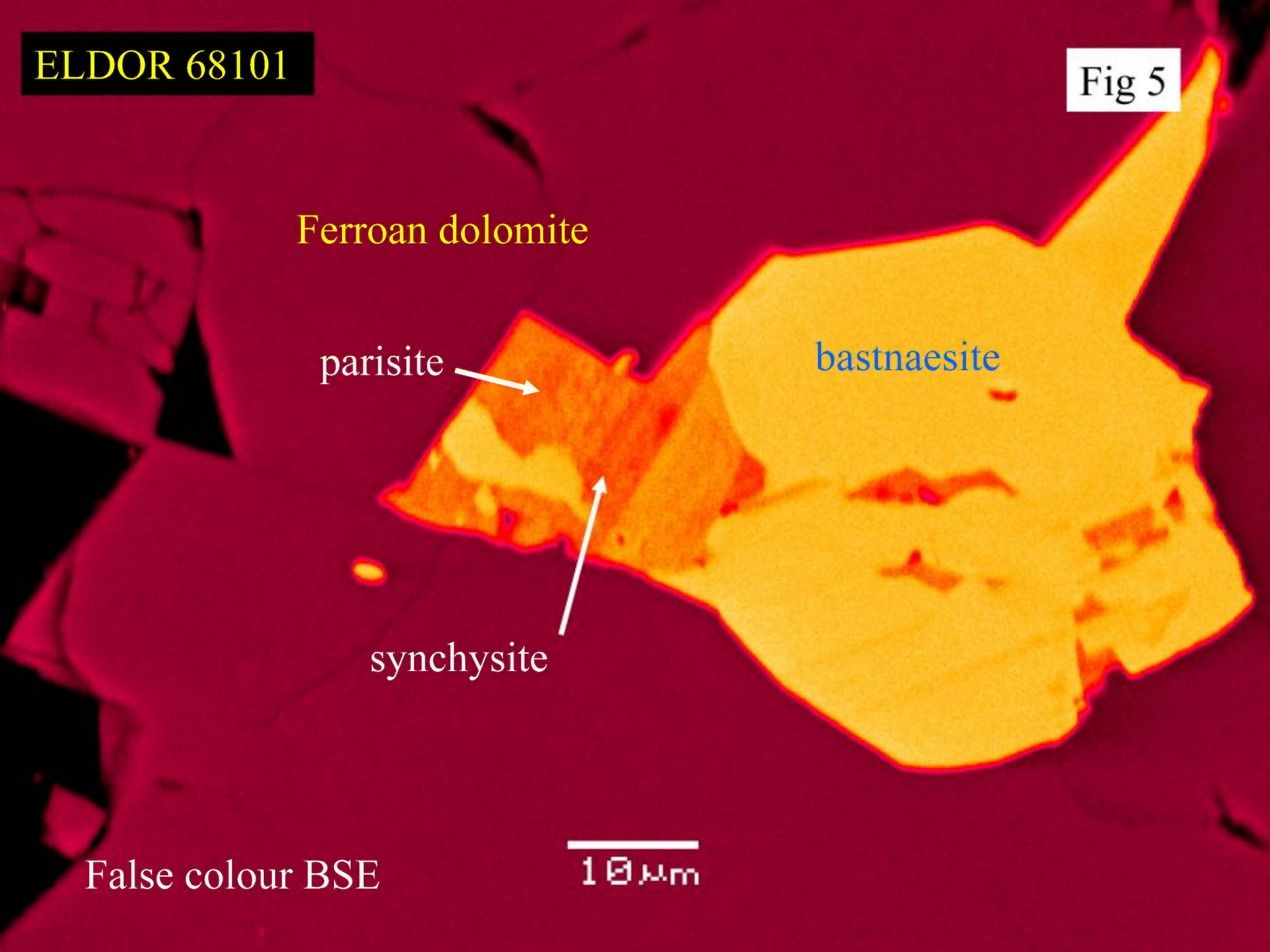
ELDOR 68101
Fig 5
Ferroan dolomite
parisite
bastnaesite
synchysite
False colour BSE
10 µm

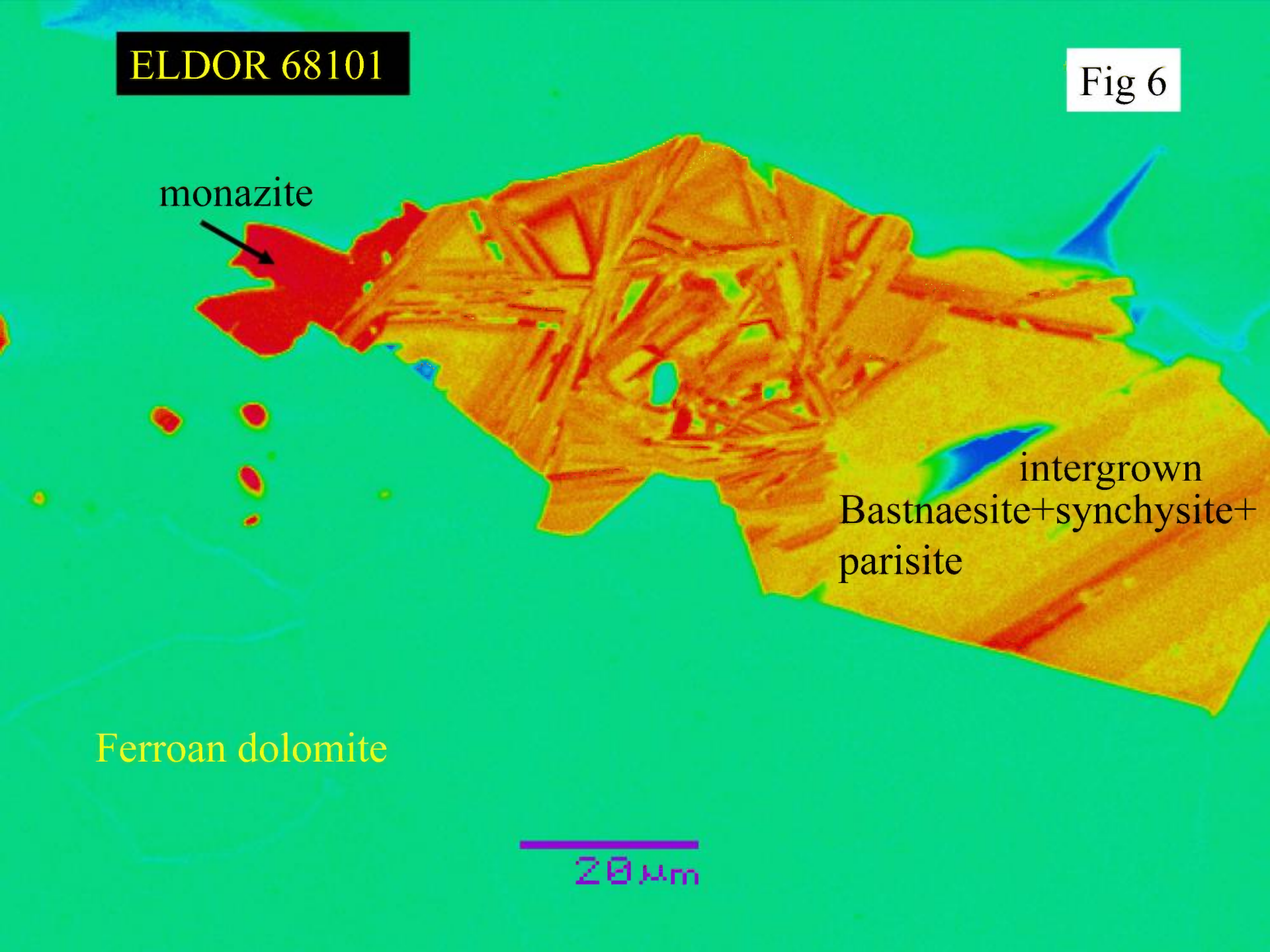
ELDOR 68101
Fig 6
monazite
intergrown
Bastnaesite+synchysite+
parisite
Ferroan dolomite
20 µm

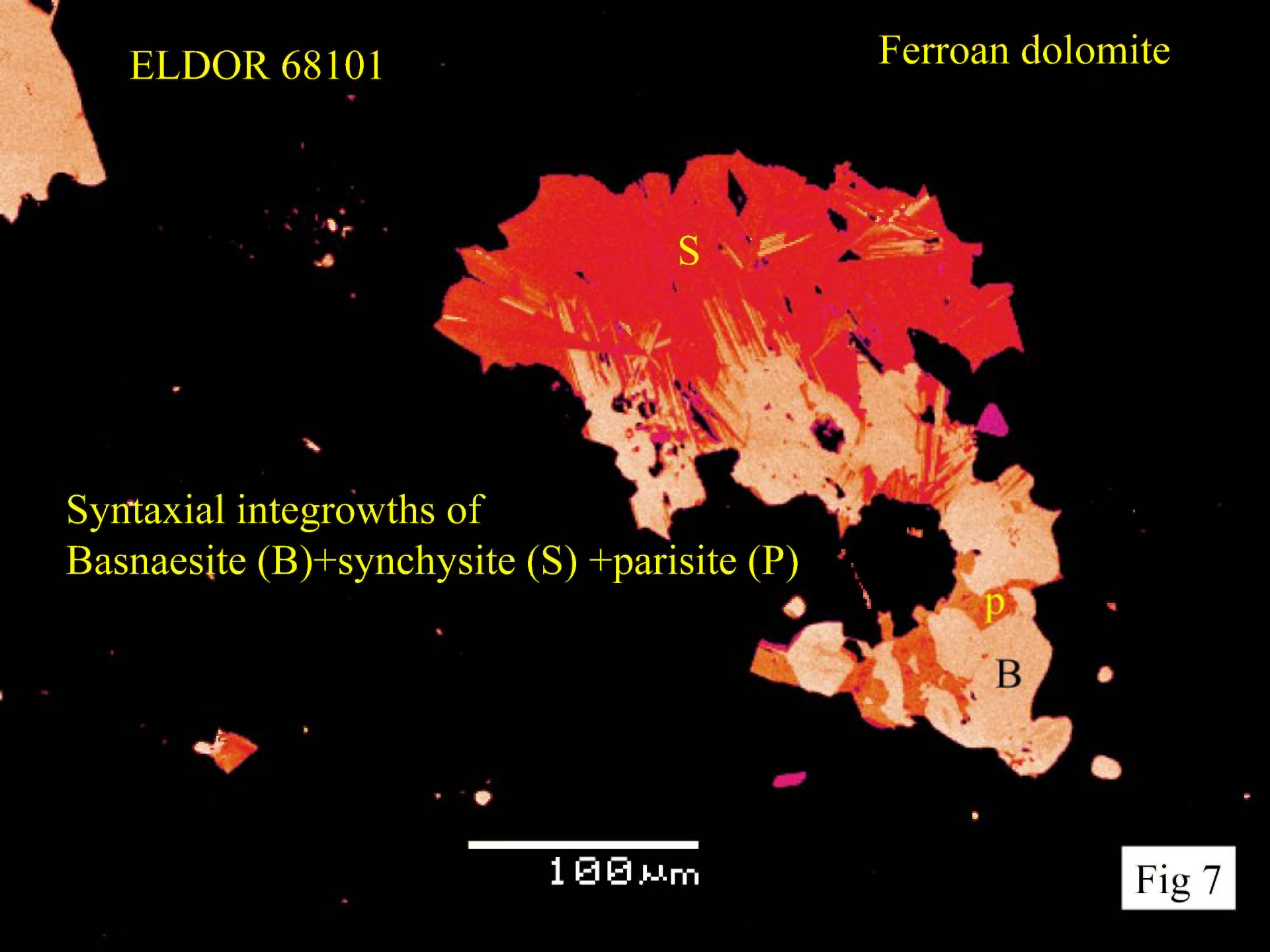
ELDOR 68101
Ferroan dolomite
S
Syntaxial integrowths of
Basnaesite (B)+synchysite (S) +parisite (P)
p
B
100µm

Fig 7

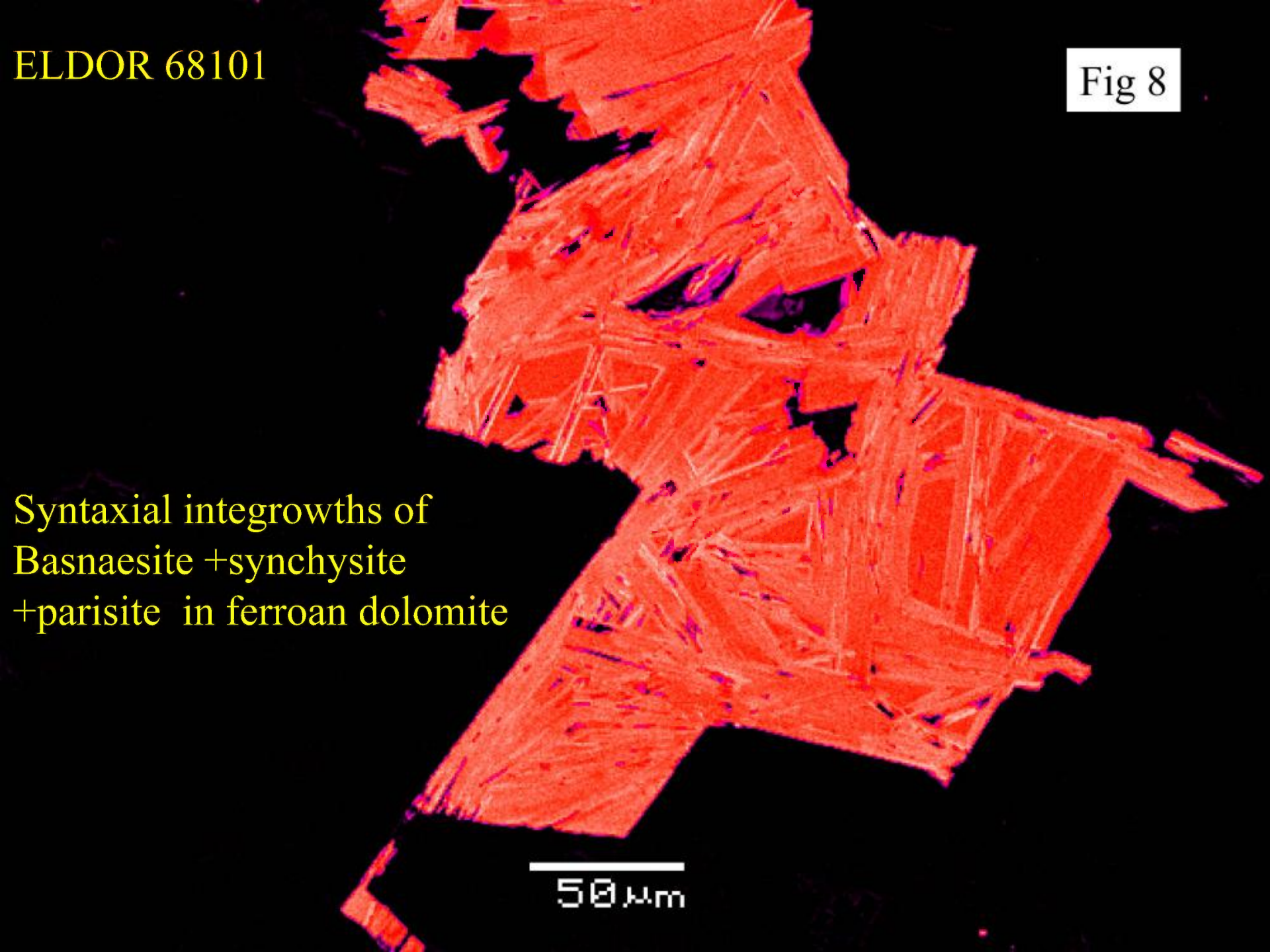
ELDOR 68101
Fig 8
Syntaxial integrowths of
Basnaesite +synchysite
+parisite in ferroan dolomite
50 µm

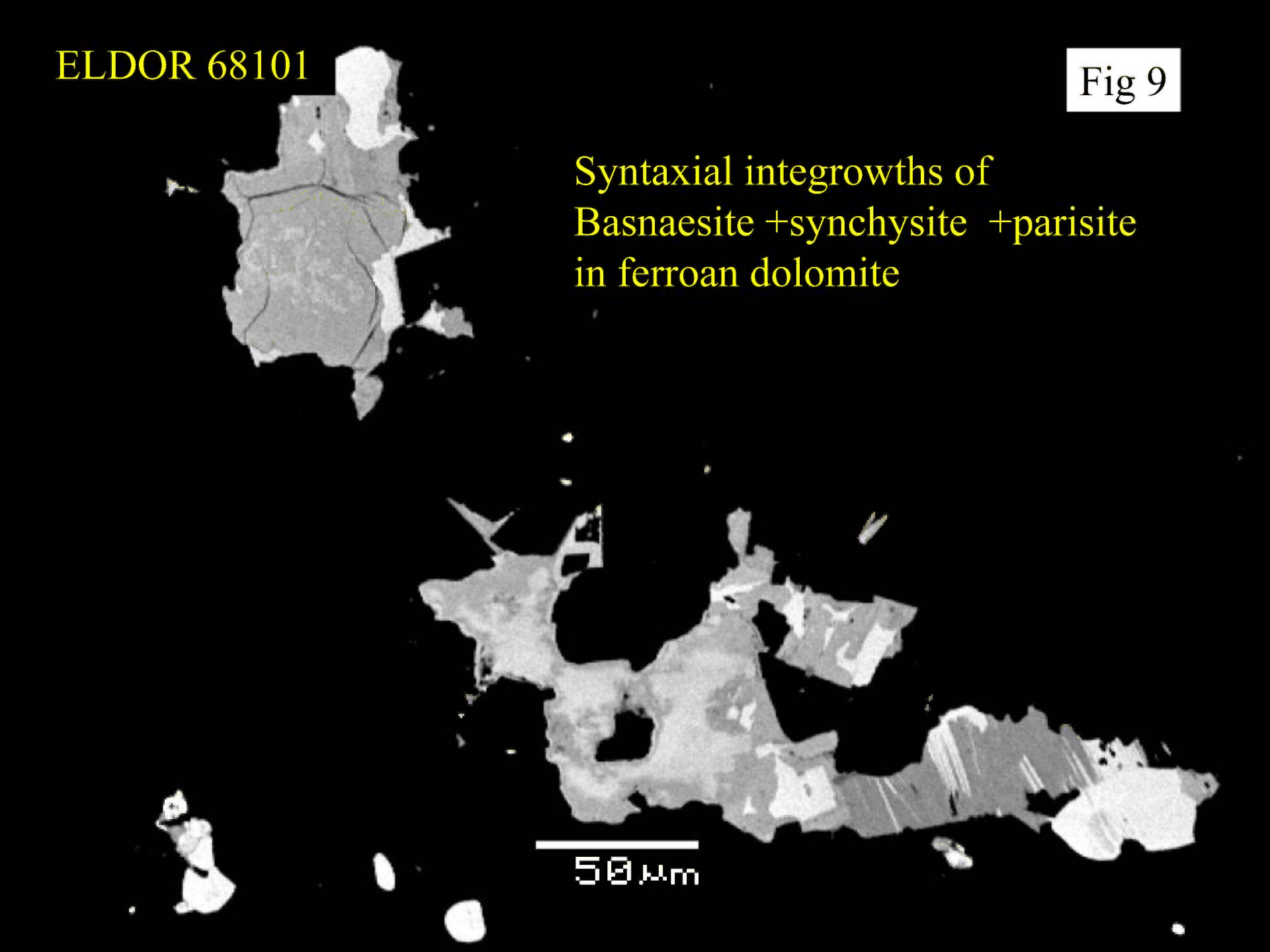
ELDOR 68101
Fig 9
Syntaxial integrowths of
Basnaesite +synchysite +parisite
in ferroan dolomite
50 µm

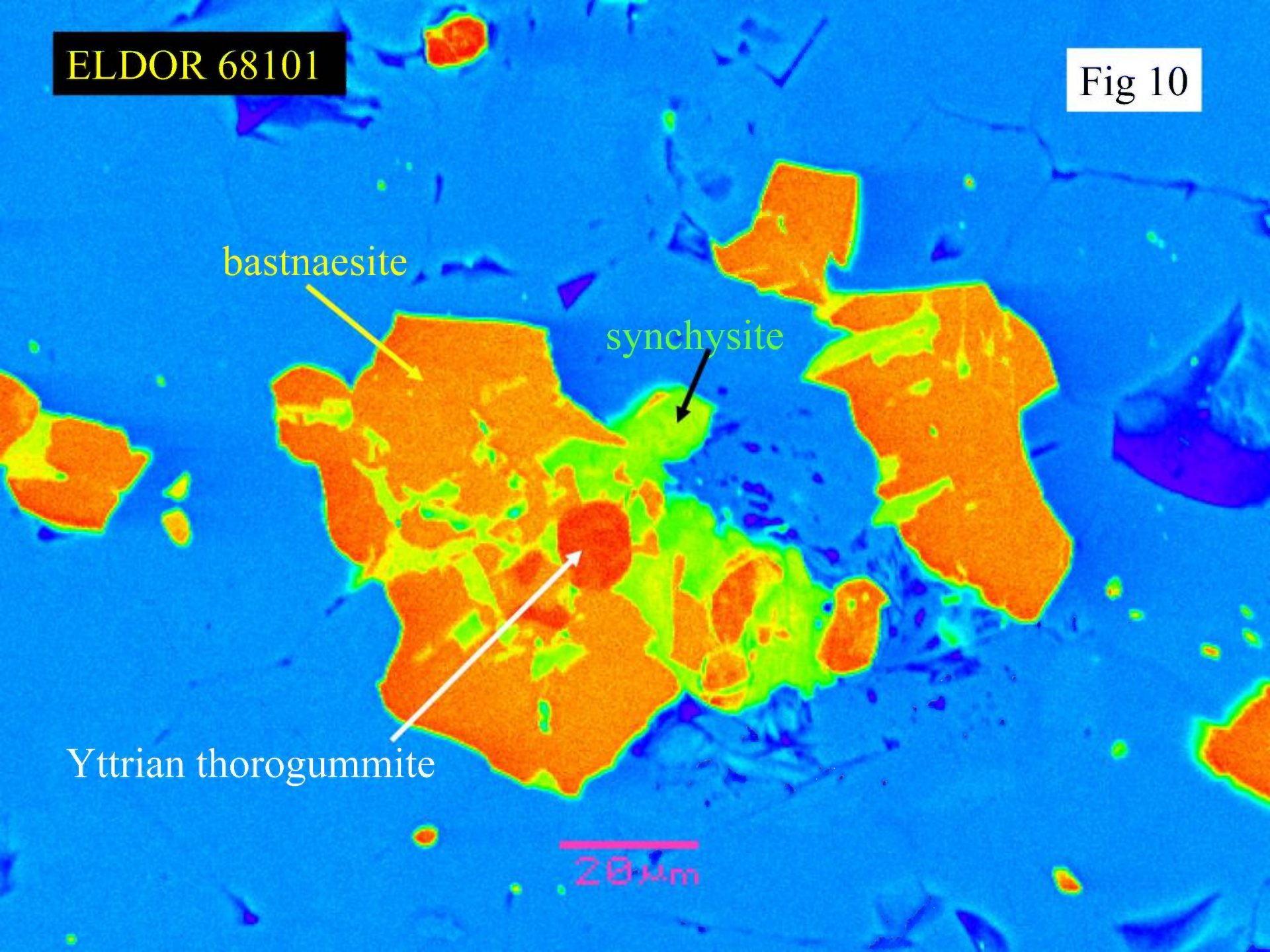
ELDOR 68101
Fig 10
bastnaesite
synchysite
Yttrian thorogummite
20 µm

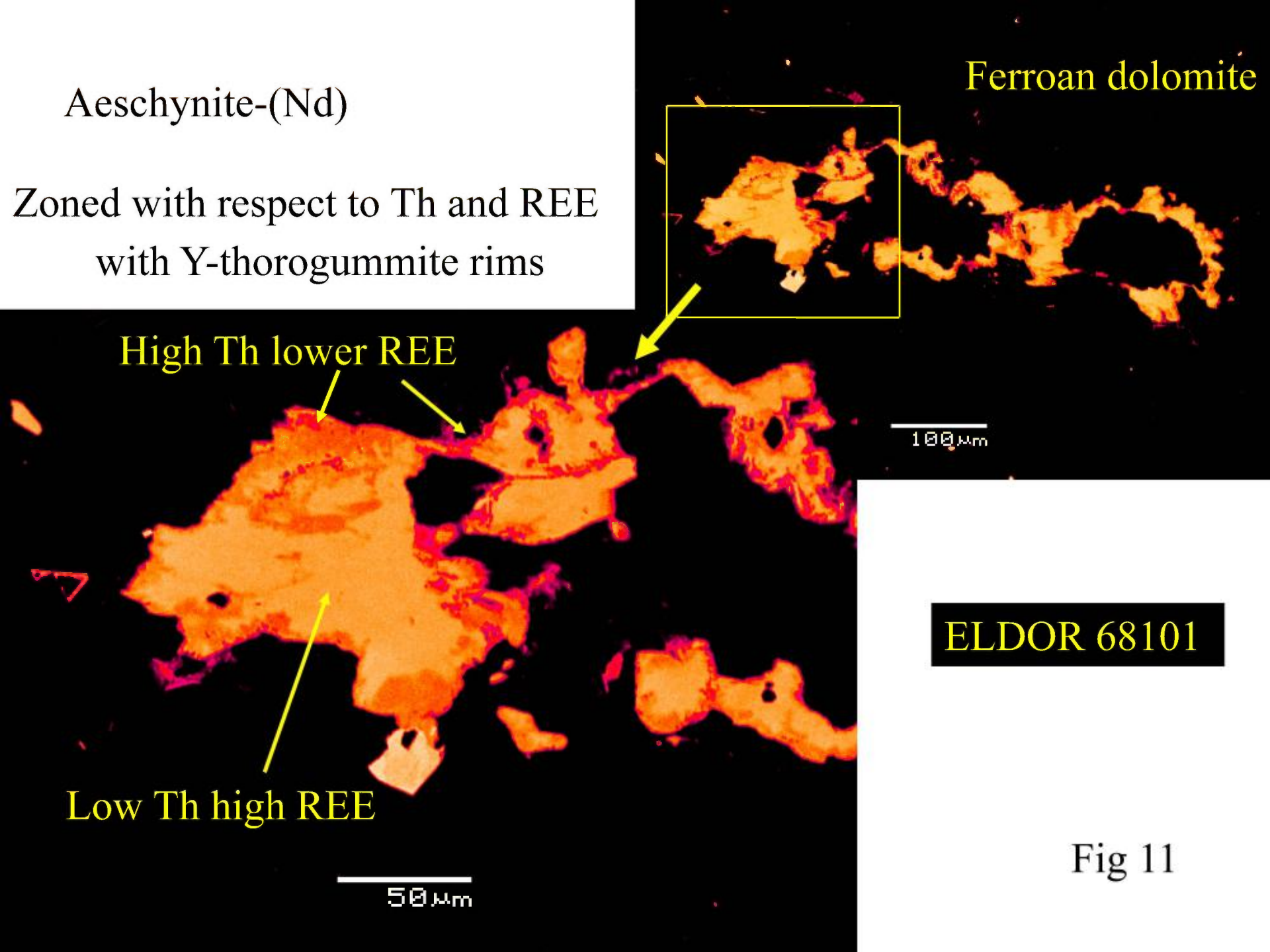
Aeschynite-(Nd)
Zoned with respect to Th and REE
with Y-thorogummite rims
Ferroan dolomite
High Th lower REE
Low Th high REE
100µm
50µm
ELDOR 68101

Fig 11

ELDOR 68119

ELDOR 68119 *Magnetite apatite calcite carbonatite*

This sample is heterogeneous with respect to the distribution of the principal constituents, i.e. magnetite, apatite and calcite (Figs 1 & 2). Apatite was the first mineral to form and occurs as aggregates or discrete rounded crystals (Figs 1-5). These can be found included in both magnetite and calcite. Euhedral prisms of apatite are rare. The apatite is of uniform composition and poor in Sr and rare earth elements (< 0.5 wt.% oxides). Magnetite occurs as large (up to 8 mm) irregular, anhedral crystals which are typically strongly fractured (Figs 1-4, 6-9). Small subhedral inclusions of Mn-bearing ilmenite (5-8 wt.% MnO) are common (Fig. 11); some of these are rarely found as orientated exsolution lamellae. Fractures are commonly partially-filled with irregular small (< 50 um) crystals of aeschynite (fig. 11). The magnetite is homogeneous with respect to its composition and poor in Ti, Mg and Mn (<0.5 wt.% oxides). Ragged laths of pale brown phlogopite are common in this sample and are typically altered to pale green chlorite (Figs. 1 & 3)2; opaque sphalerite has been introduced along the cleavages in some examples. Calcite forms the bulk of the groundmass in which all of the earlier-formed constituents are set . This occurs as large interlocking crystals that exhibit well-developed polysynthetic twinning (Figs 1-2). Fe-poor dolomite (2-3 wt.% FeO) is also present in minor amounts (Figs. 6 & 7) and is typically found in association with magnetite, where it occurs as anhedral crystals developed at the margins of the magnetite crystals (Fig. 8). Other late forming minerals include trace quantities of synchysite, pyrite, galena and sphalerite. Very small (<20 um) subhedral crystals of monazite-(Ce) can be very rarely found growing marginal to apatite crystals.

ELDOR 68119

The sample is relatively poor in Nb-U-minerals (c. < 5 vol.%). Fersmite and ferrocolumbite are not present. The principal Nb-bearing phase is aeschynite-(Ce). This occurs as a late stage mineral in the calcite groundmass and along fractures in magnetite crystals (Figs 10 & 11). Most examples are small (< 50 um) irregular zoned crystals. Larger aggregates of this material (c. 0.2mm), with inclusions of zircon and sphalerite, can rarely be found (Fig. 10). The aeschynite is of variable composition and ranges from Th-poor to Th-rich varieties. Representative semiquantitative compositions are given below.

Pyrochlore is very rare in this sample (< 1 vol.%) and occurs only as small (<30 um) irregular resorbed grains that can be mantled by aeschynite and synchysite (Figs. 12 & 13). The pyrochlores show a wide range of composition with Th-rich varieties being mantled by Th-poor types. Representative semiquantitative compositions are given below.

ELDOR 68119

Representative semiquantitative compositions of pyrochlore

Wt.%	aeschynite	Th-aeschynite	pyrochlore	Th-pyrochlore
F	n.d.	n.d.	n.d.	n.d.
Na_2O	n.d.	n.d.	n.d.	n.d..
SiO_2	0.7	0.8	1.4	0.7.
BaO	n.d.	n.d.	n.d.	n.d.
CaO	2.5	4.4	11.3	4.9
TiO_2	24.9	21.2	4.9	0.9
FeO	1.7	6.2	4.3	5.2
Nb_2O_5	33.8	28.6	59.3	53.6
Ta_2O_5	0.4	1.7	3.9	1.2
La_2O_3	4.6	1.7.	0.7	0.8.
Ce_2O_3	17.4	8.2	3.3	7.7
Pr_2O_3	1.4	1.4	0.6.	1.8
Nd_2O_3	7.4	6.7	1.6	7.3.
ThO_2	3.6	13.3	1.8	10.7
UO_2	n.d.	1.0	2.6	0.5

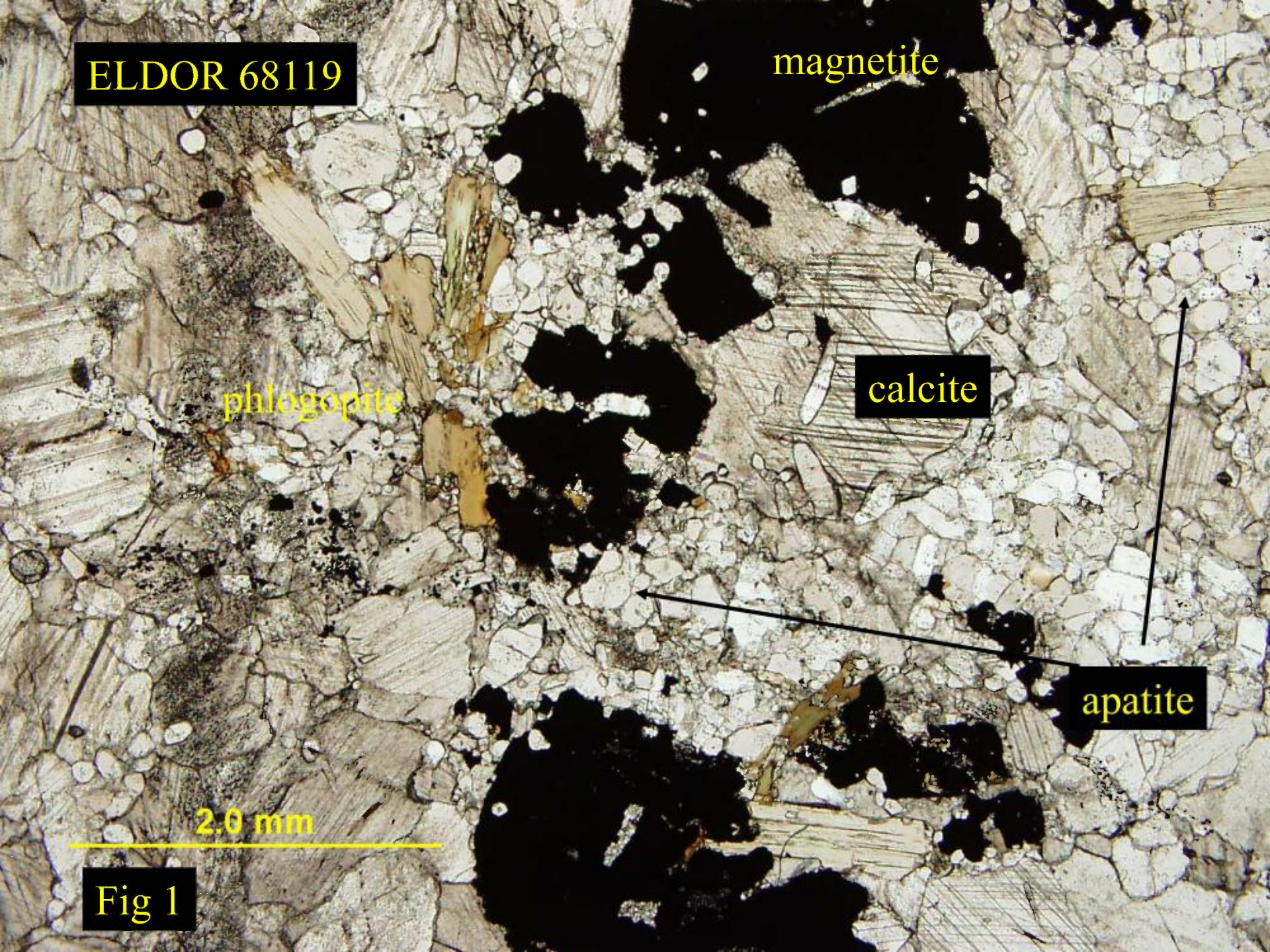

Fig 1

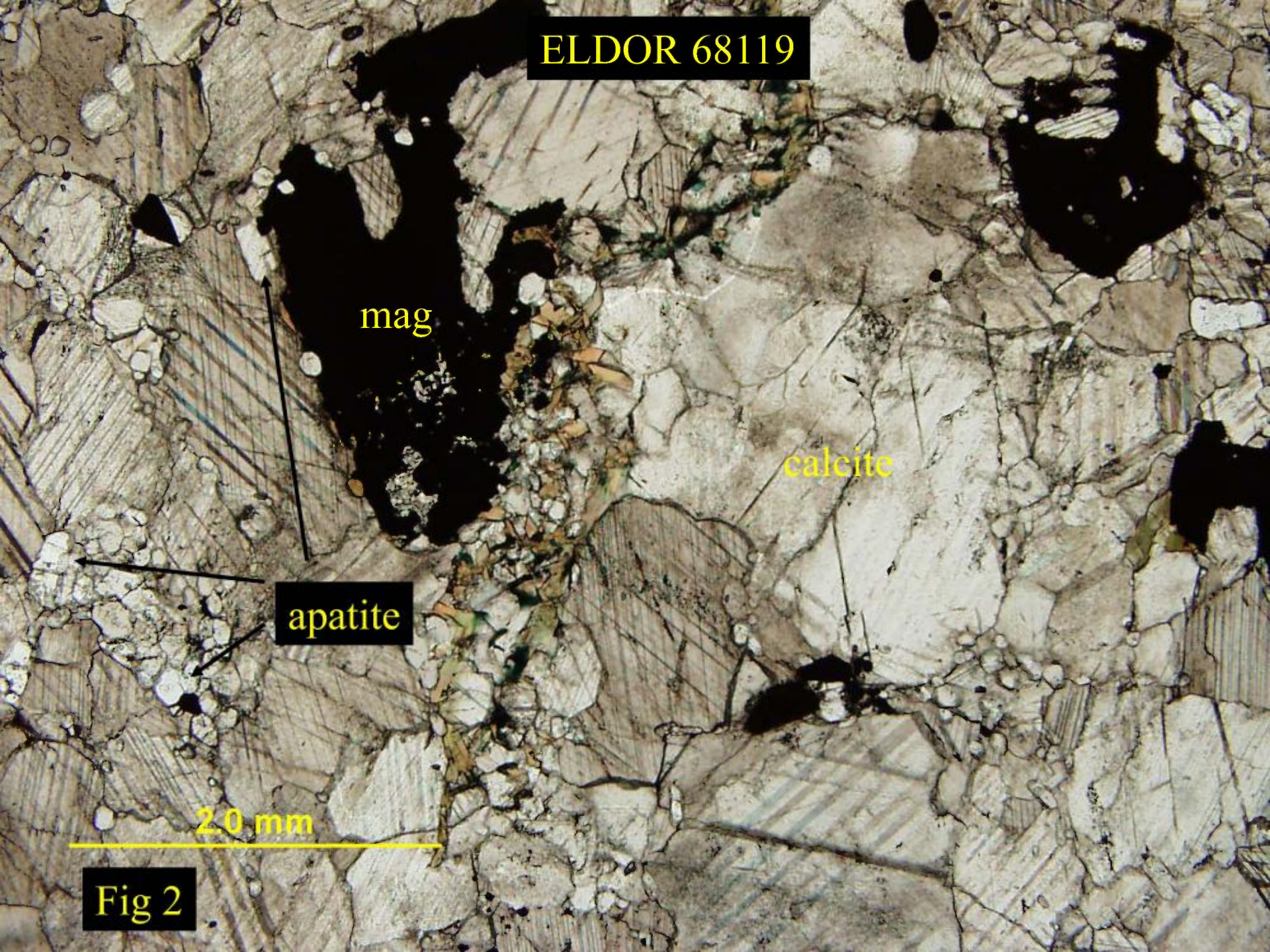

Fig 2

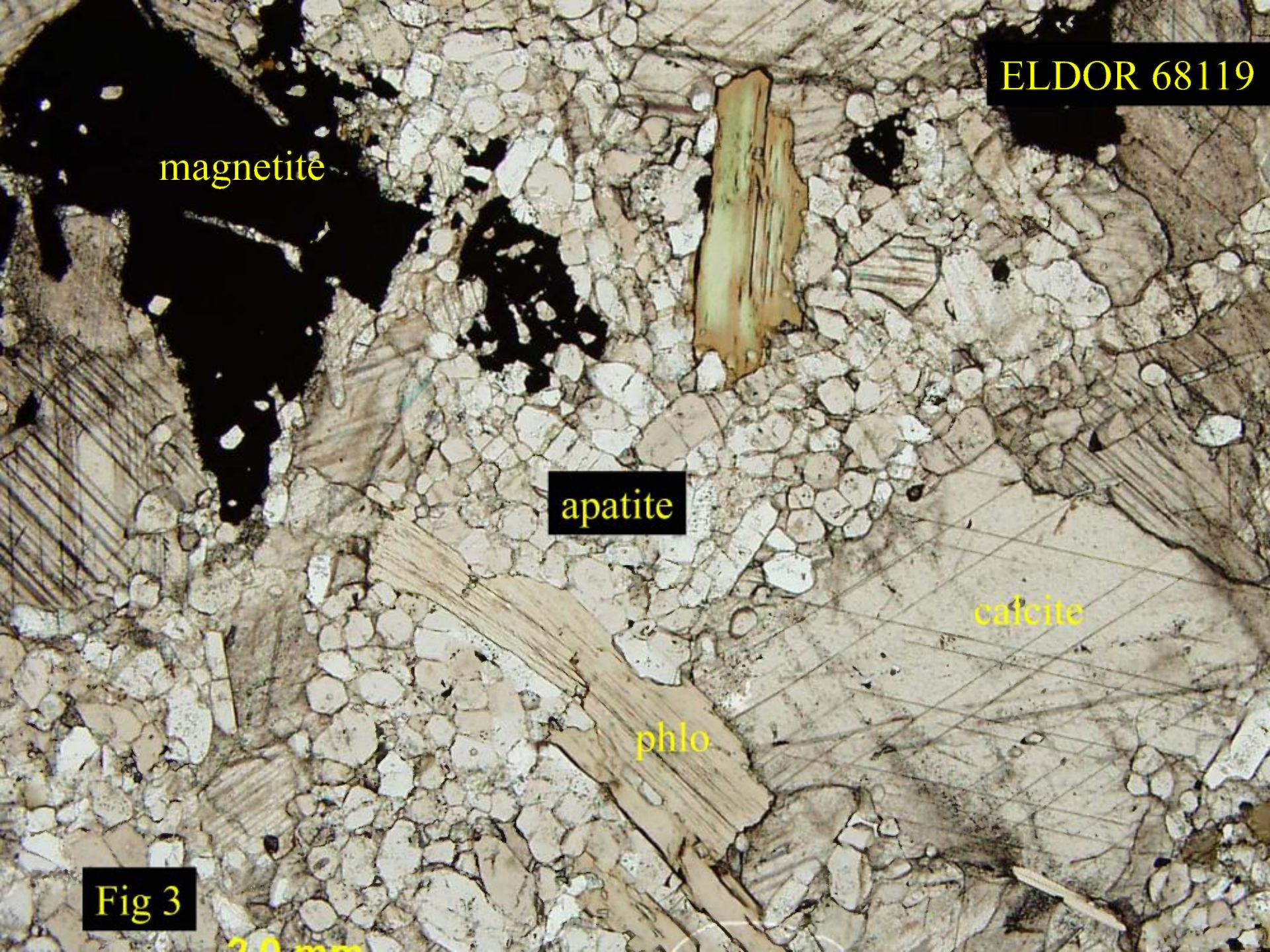
ELDOR 68119
magnetite
apatite
calcite
phlo
Fig 3

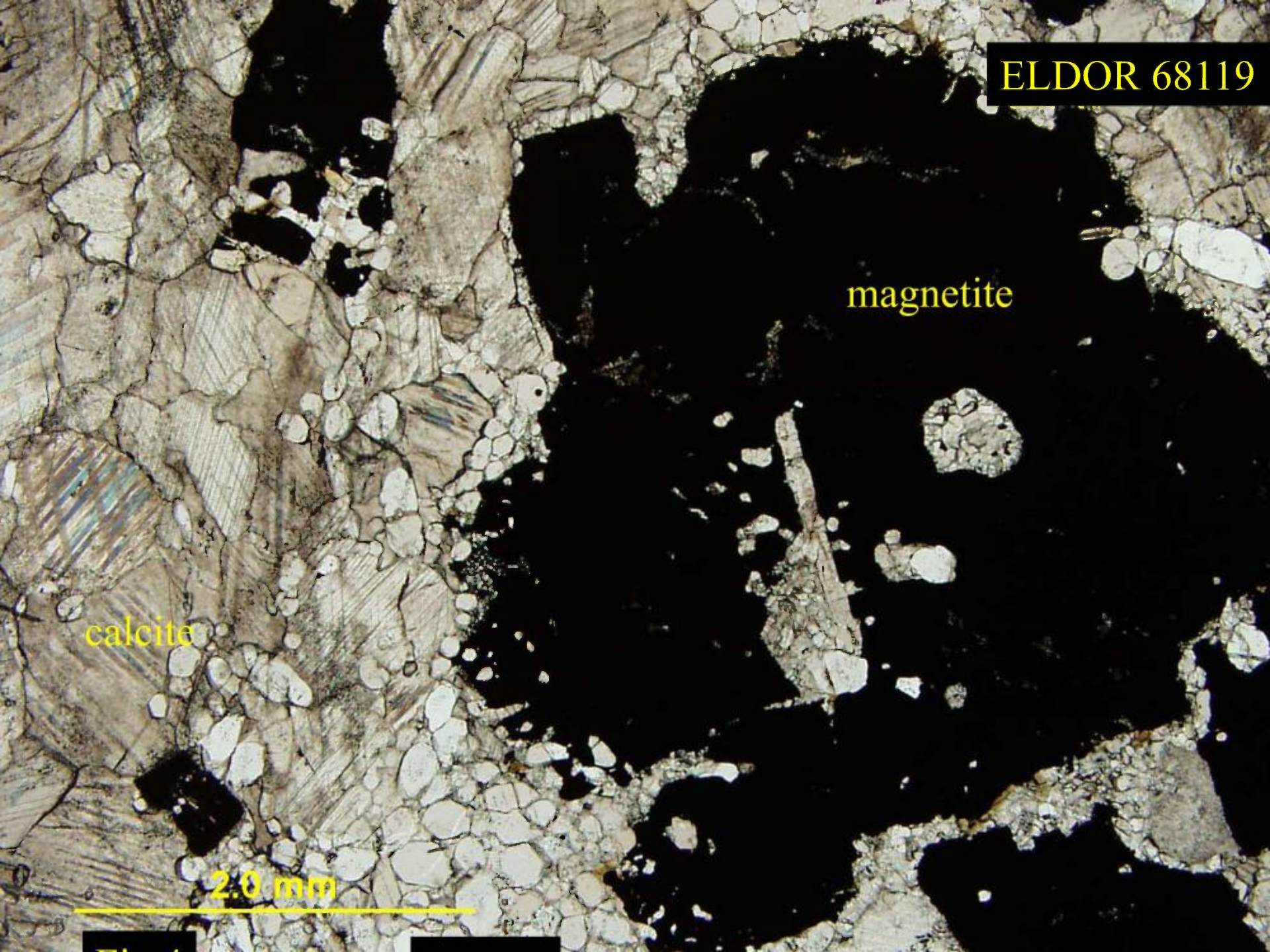
ELDOR 68119
magnetite
calcite
2.0 mm

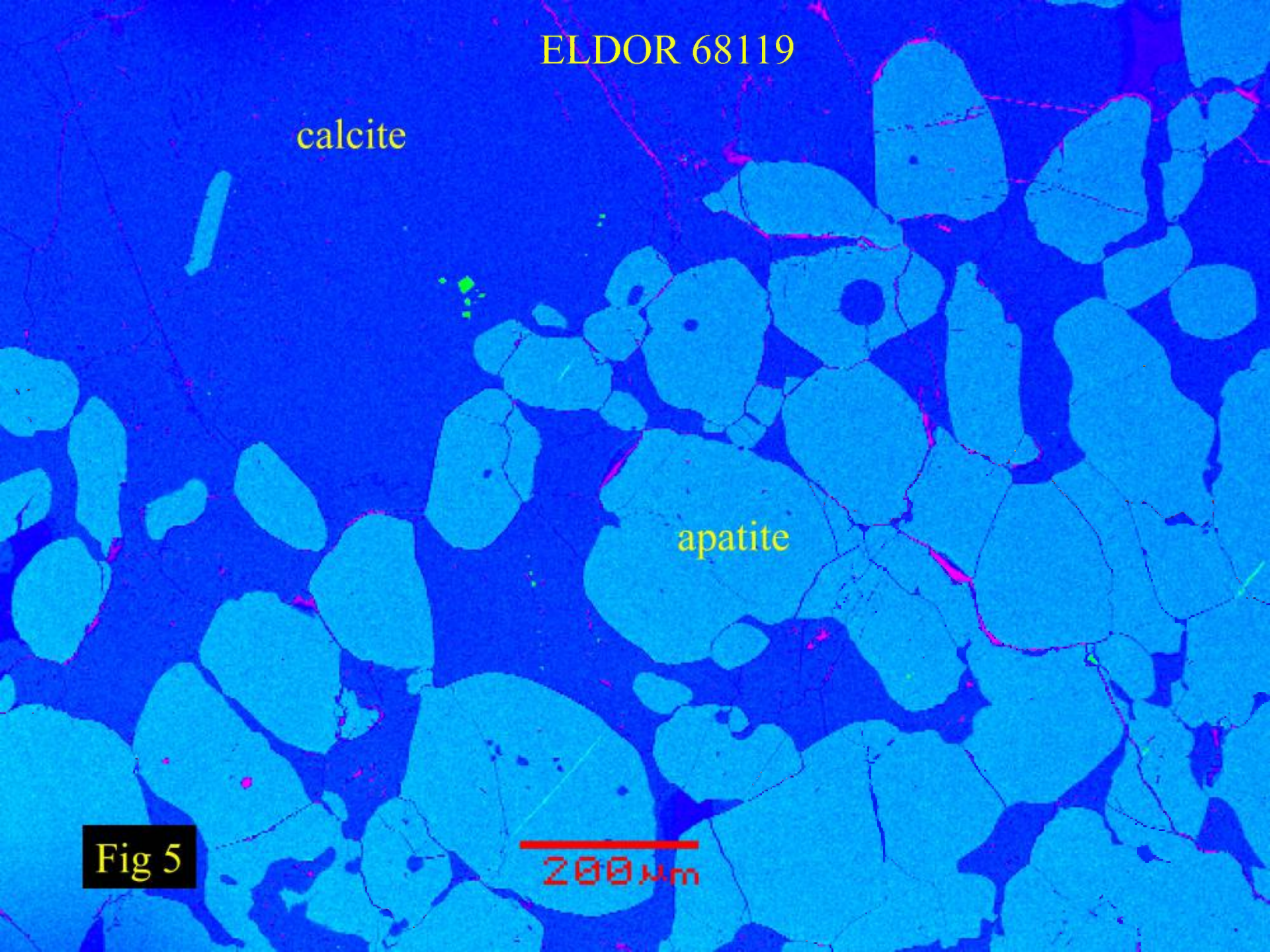

Fig 5

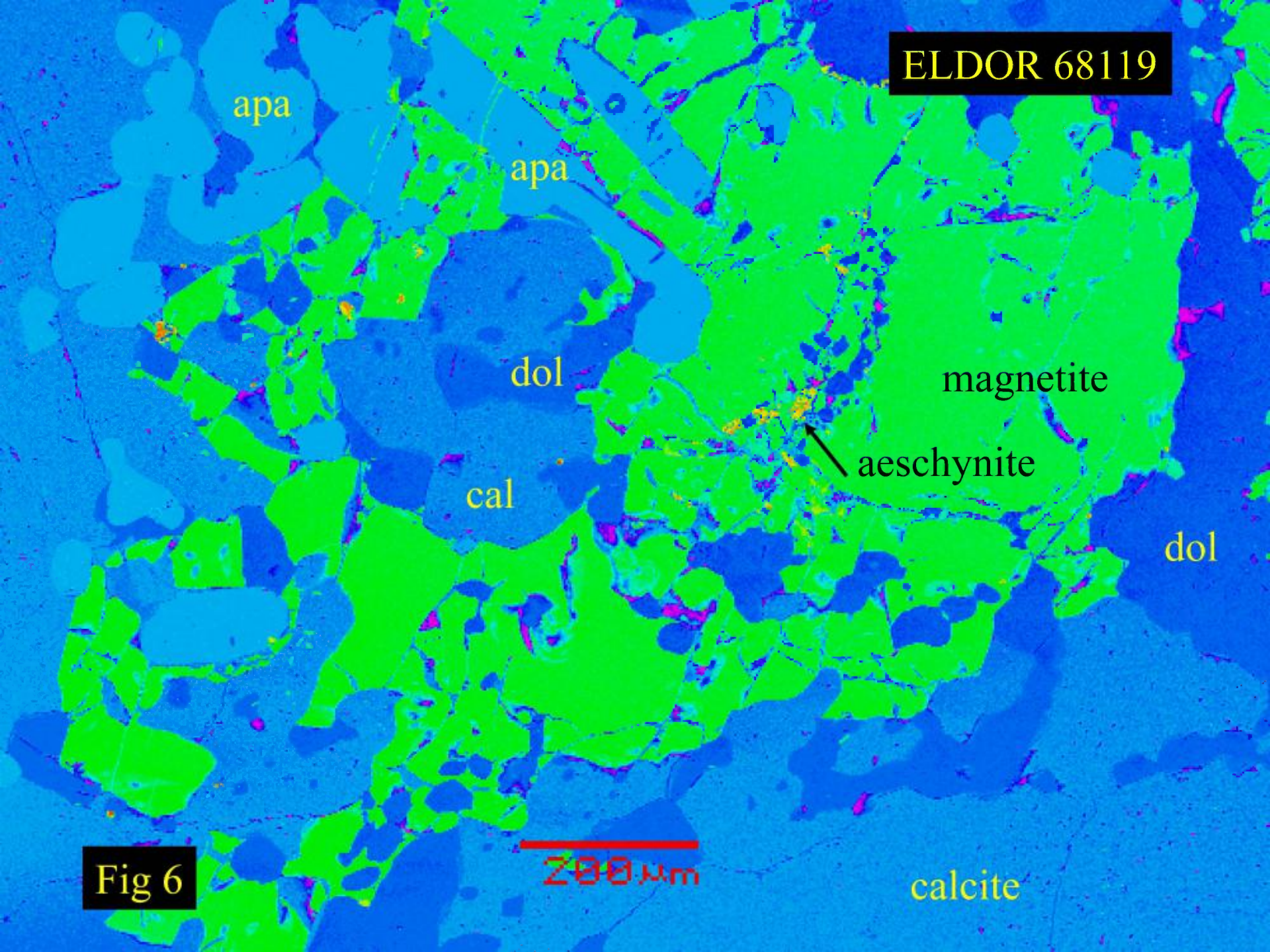
ELDOR 68119
apa
apa
dol
magnetite
aeschynite
cal
dol
200 µm
calcite

Fig 6

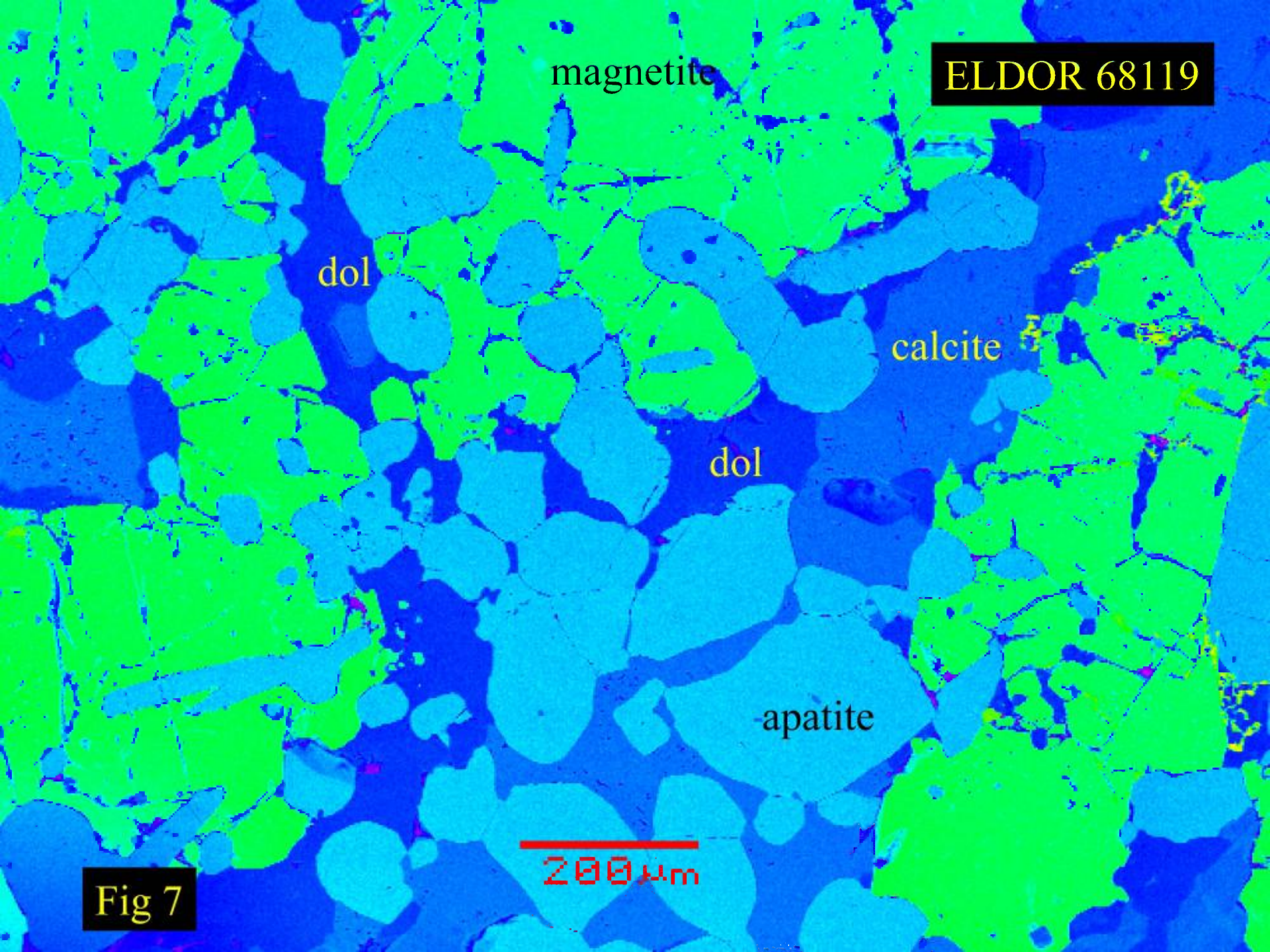

Fig 7

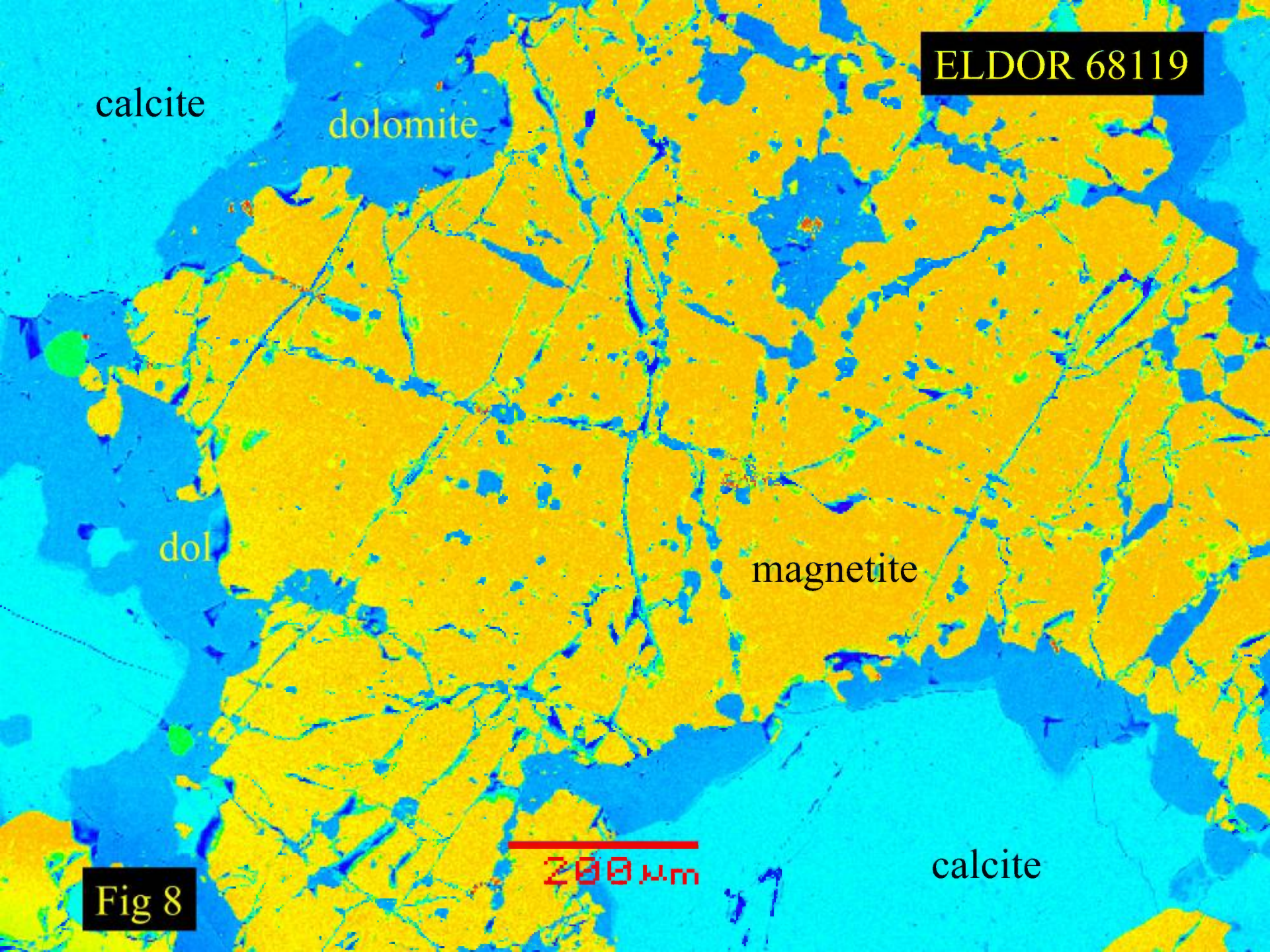

Fig 8

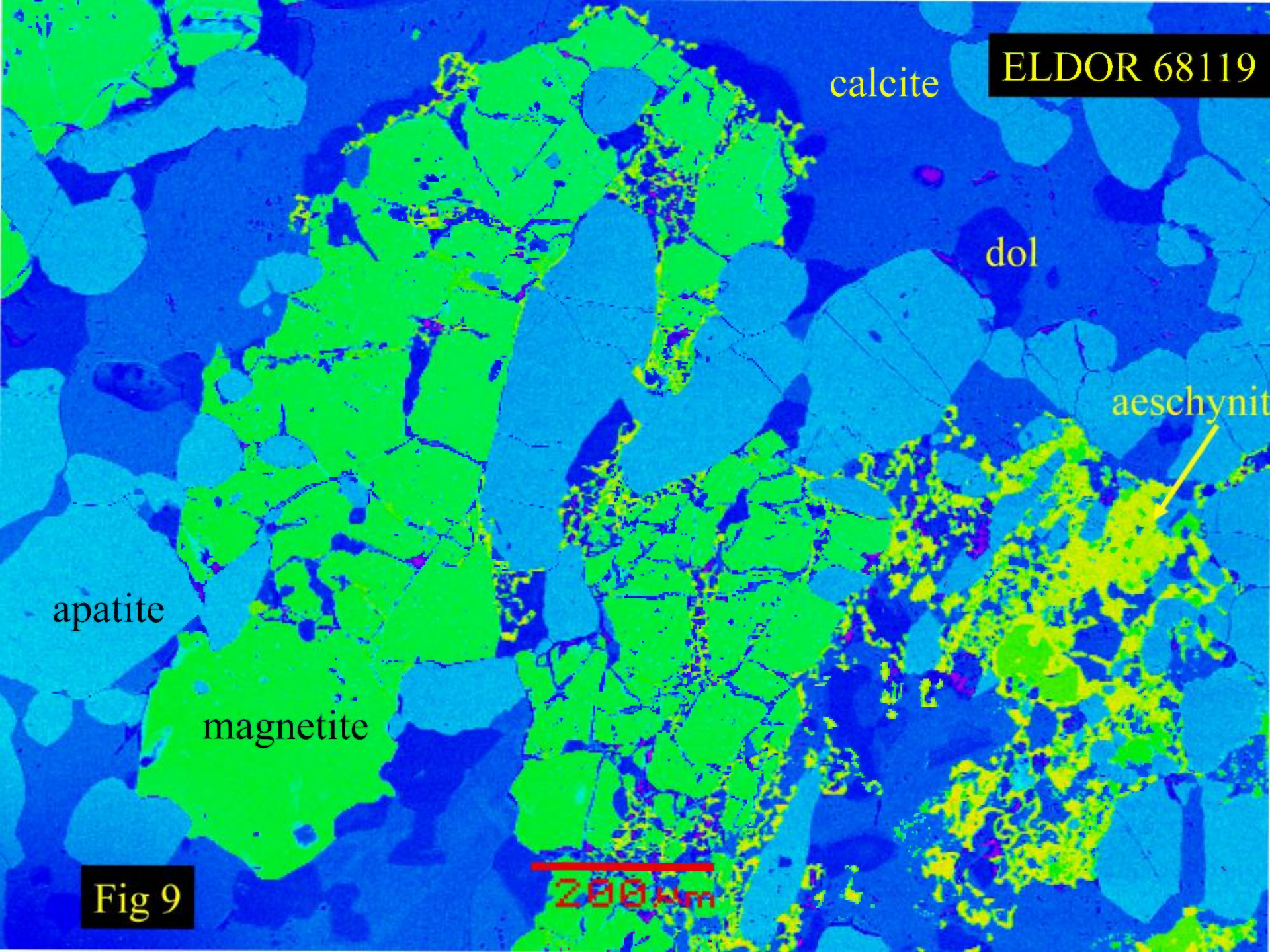
ELDOR 68119
calcite
dol
aeschynit
apatite
magnetite
200µm
Fig 9

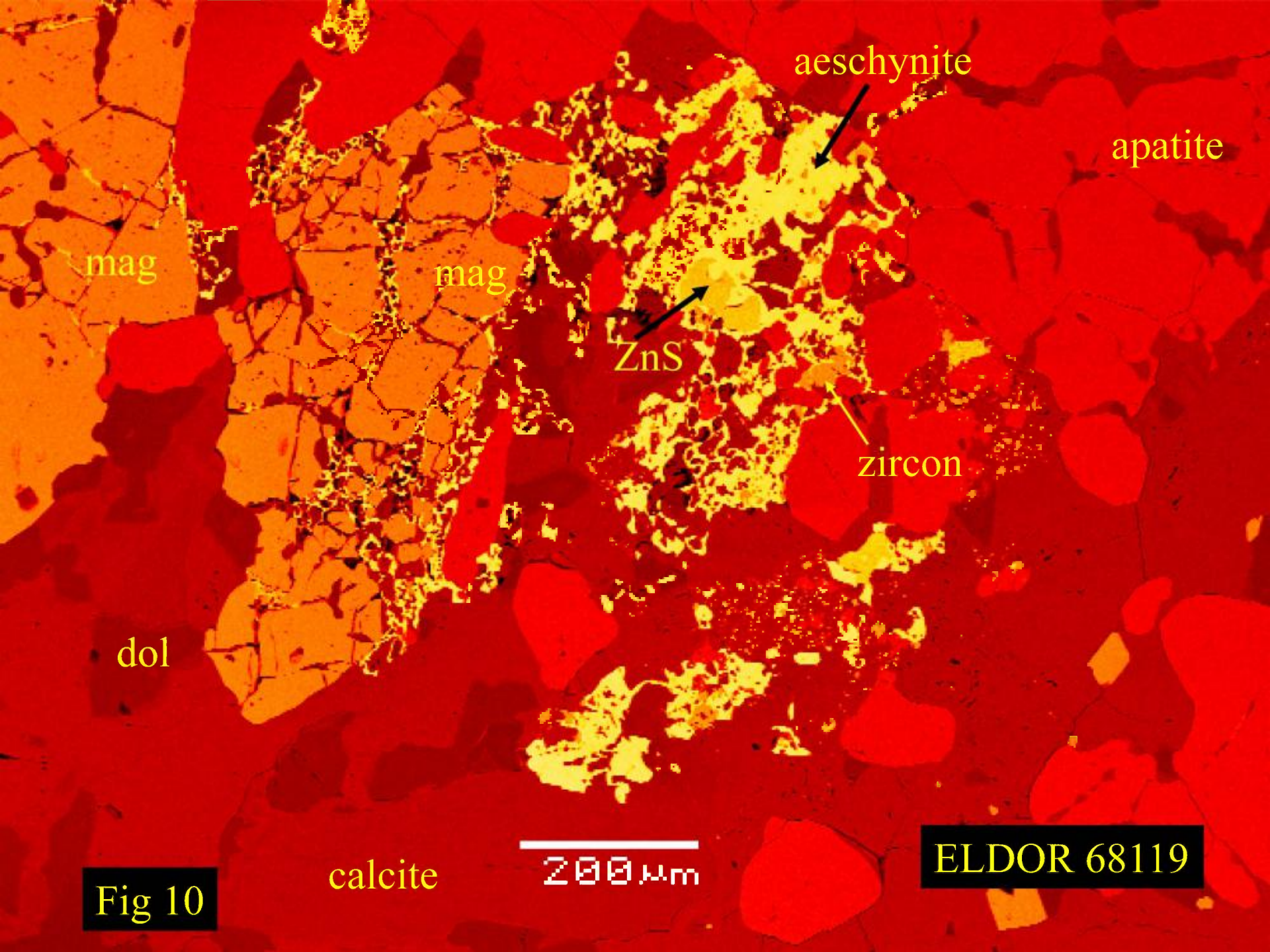
aeschynite
apatite
mag
mag
ZnS
zircon
dol
calcite
200µm
ELDOR 68119

Fig 10

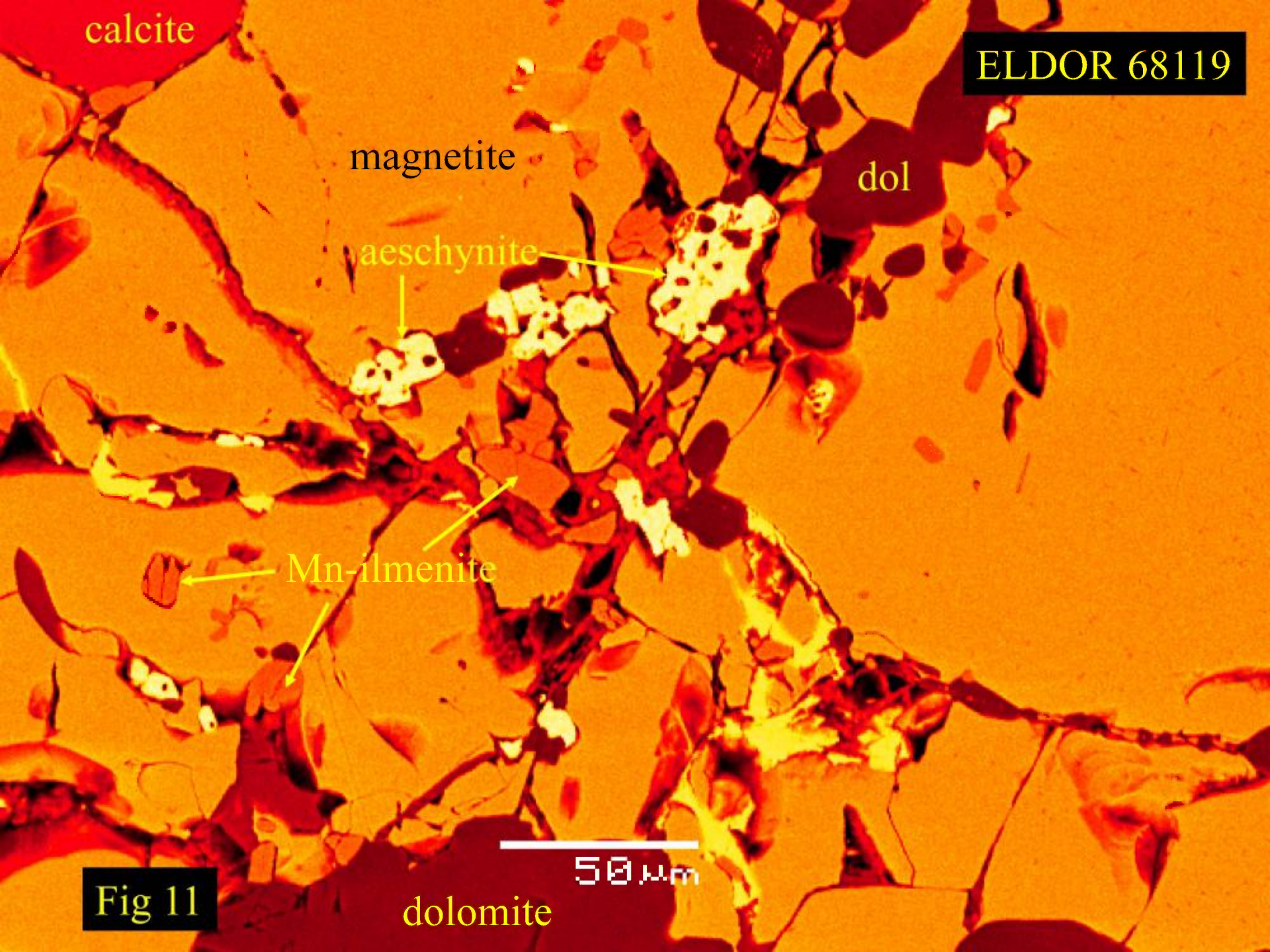
calcite
ELDOR 68119
magnetite
dol
aeschynite
Mn-ilmenite
50 µm
dolomite

Fig 11

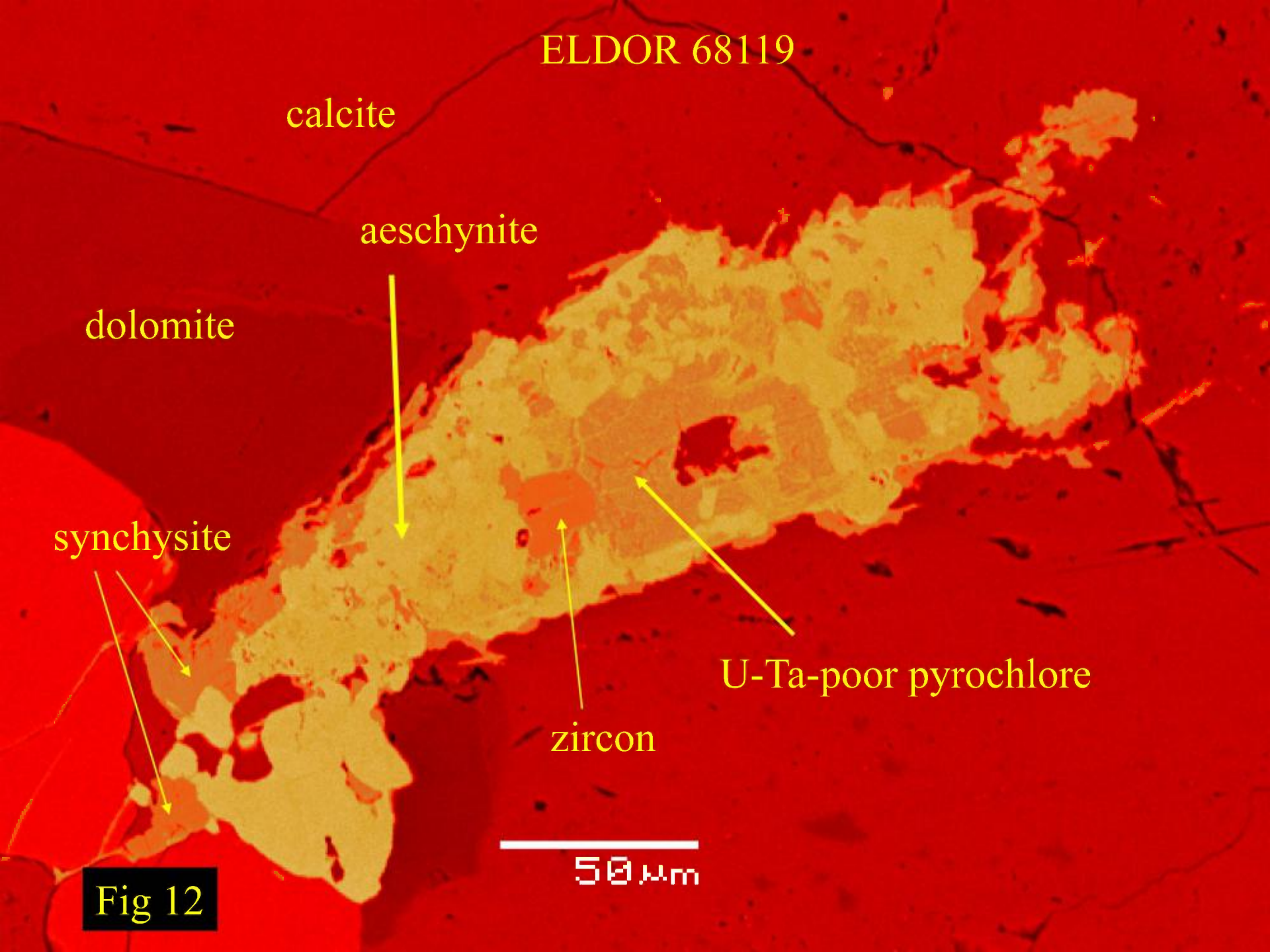
ELDOR 68119
calcite
aeschynite
dolomite
synchysite
U-Ta-poor pyrochlore
zircon
50 µm

Fig 12

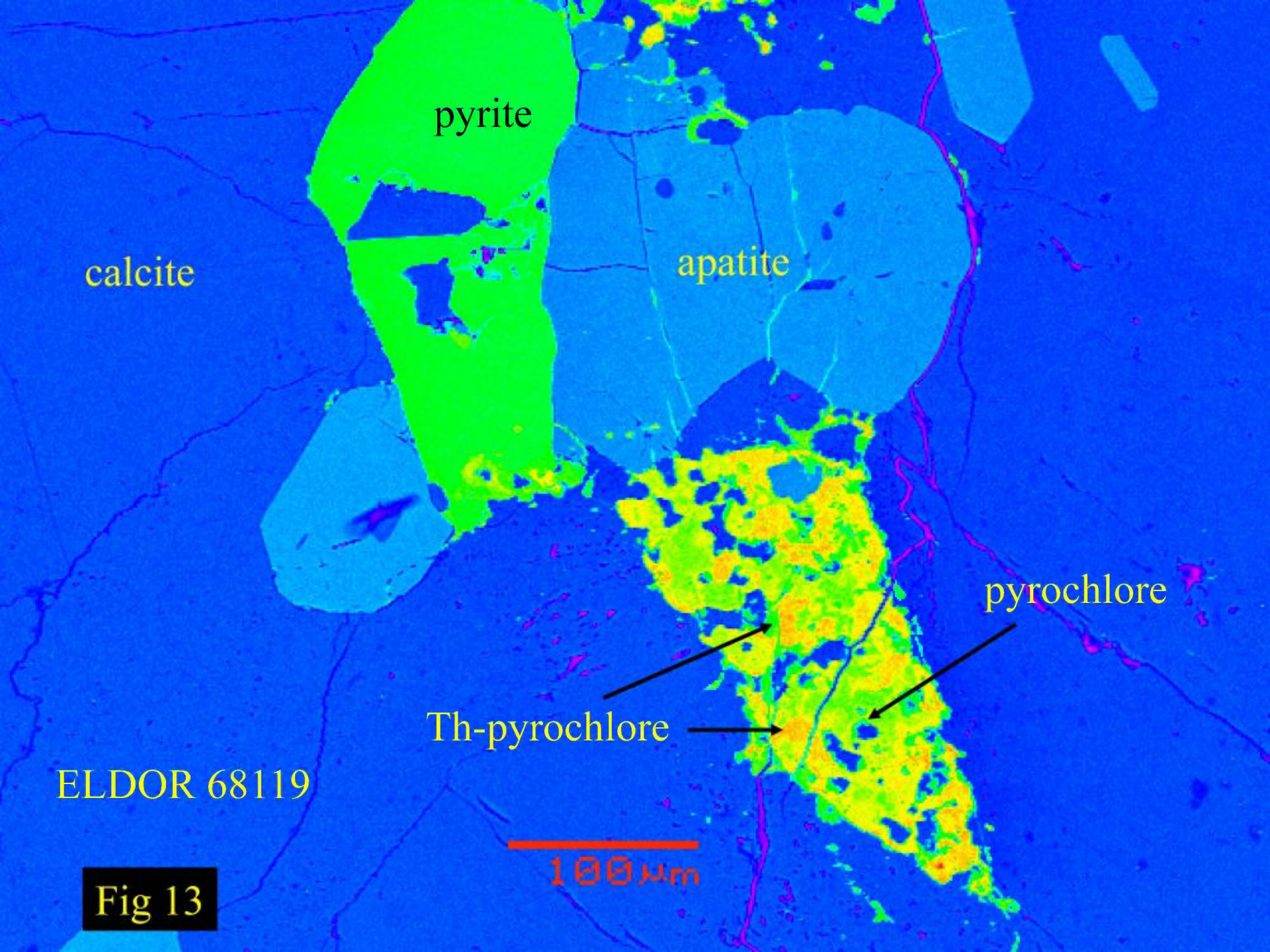
pyrite
calcite
apatite
pyrochlore
Th-pyrochlore
ELDOR 68119
100µm

Fig 13

ELDOR 68128

ELDOR 68128 *Monazite dolomite carbonatite*

Overall this is an extremely fine grained porous dolomite carbonatite that is cut by veins consisting of relatively coarser dolomite (Fig.1). Apart from these thin veins, some areas of the fine grained material appear to have been brecciated consequent upon introduction of the coarse material (Fig.2). Thin bands consisting of opaque-rich fine grained material transect the fine grained dolomite (Fig. 1). Ragged phlogopite grains with pleochroic haloes about inclusions occur rarely. Apatite, magnetite and pyrochlore are absent.

The rock consists primarily of early-forming fine grained ferroan dolomite (9-10 wt.% FeO) with trace amounts of anhedral intergrown pure potassium feldspar (Figs.4 & 5) and quartz (Fig. 5). The latter appears to represent one of the last phases to crystallize. BSE-imagery and X-ray spectrometry demonstrate that much of the very fine grained, brownish-to-opaque optically unidentifiable material seen in figures 1 and 2 consists of disseminated monazite-(Ce), basnaesite-(Ce) and minor fluocerite-(Ce) [$(Ce,La)F_3$].

Monazite fills interstices and pores between dolomite crystals and ranges in size to up 250 um in maximum dimension. Fluocerite occurs similarly but seldom exceeds 100 um in size. Rare earth fluorocarbonates can be found as small crystals (<50um) intergrown with monazite and as larger plates (up to 300 um) in the coarser dolomite veins. Pyrite occurs principally as small euhedral grains in the opaque-rich thin bands (Fig.1) in association with monazite and synchysite (Fig. 7).

ELDOR 68128

Areas in which residual fluids have concentrated contain Y-bearing minerals and some unidentified V-bearing titanates. All of these minerals are very small (< 20 um) present only in trace quantities.

Fig. 11 illustrates an occurrence of xenotime-(Dy) [wt.%: 4.7 Dy_2O_3 ; 2.1 Gd_2O_3 ; 3.0 Er_2O_3) which has formed in a paragenesis with monazite-(Ce), synchysite-(Ce), pyrite, sphalerite, and an unnamed Y-bearing Th-Nb-silicate (wt.%: 3.0 Y_2O_3; 7.1 SiO_2; 3.2 CaO; 21.9 TiO_2; 21.7 Nb_2O_5 ; 24.3 ThO_2.

Fig. 12 illustrates a highly corroded isolated unidentified Y-silicate-(Nd) that contains high levels of heavy REE [wt.%: 4.6 Sm_2O_3; 5.7 Gd_2O_3; 4.3 Dy_2O_3 ; 1.5 Er_2O_3) set in ferrodolomite.

Fig. 13 illustrates a decomposing unidentified REE-poor, Y-Th-P-silicate [wt.% 9.8 SiO_2; 4.0 P_2O_5; 8.8 Y_2O_3; 53.4 ThO_2] in association with monazite-(Ce) and pyrite. This is probably an yttrian variety of the thorite-huttonite-thorogummite series.

Fig. 14 illustrates two unidentified titanates. On is a V-Nb-titanite [wt.% 45.6 TiO_2; 20.6 V_2O_3; 33.4 Nb_2O_5]; the other is a V-Fe-titanate [wt.%: 60.9 TiO_2; 16.0 V_2O_3; 16.4 FeO] that is similar to the unnamed mineral $(Fe, Mg, Mn)_2(Ti,Cr.V)_5O_{12}$. Note that V, Nb and Ti can be highly mobile in some hydrothermal environments, hence the occurrence of these titanates in these rocks is not unexpected.

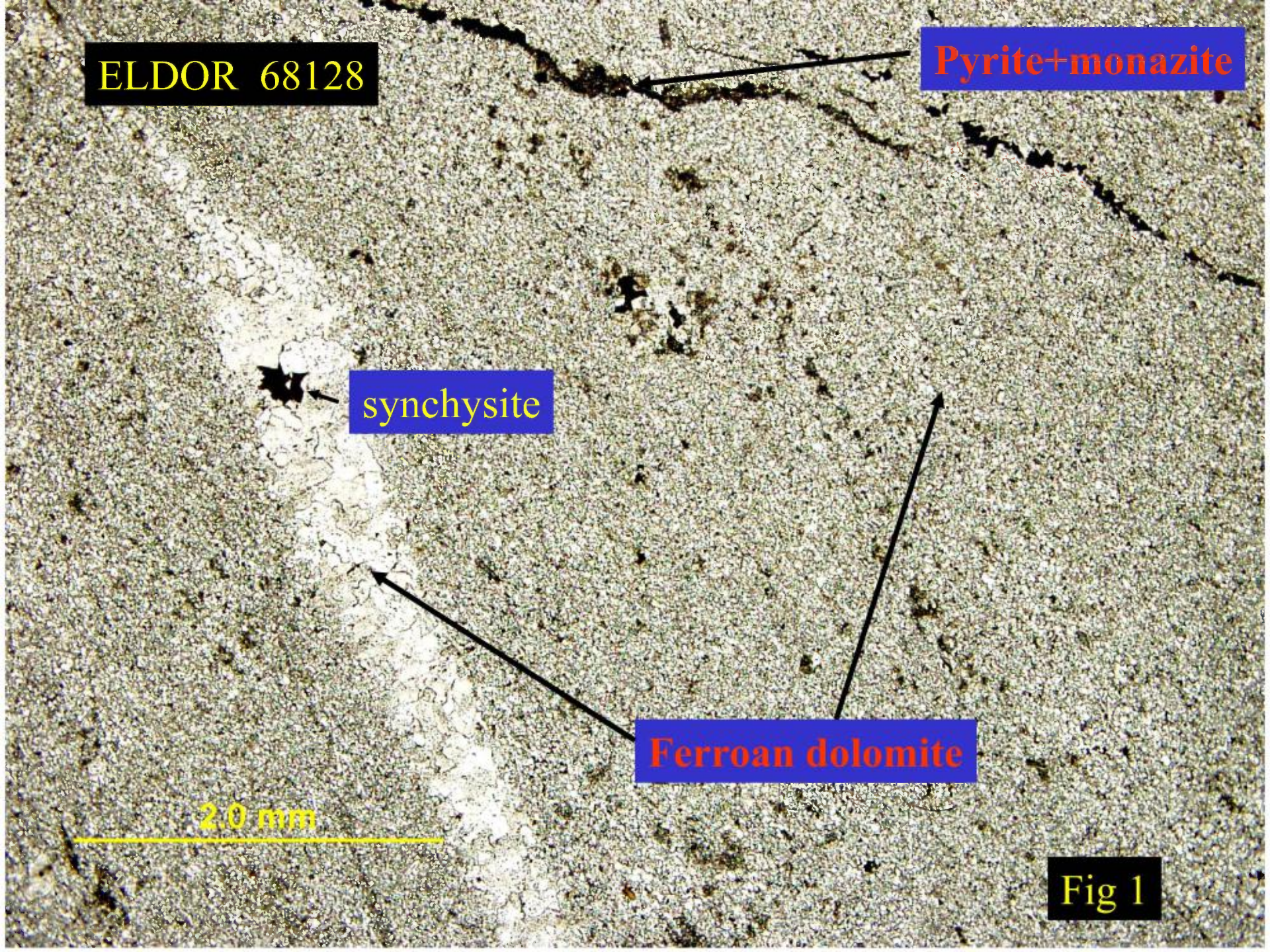
ELDOR 68128
Pyrite+monazite
synchysite
Ferroan dolomite
2.0 mm
Fig 1

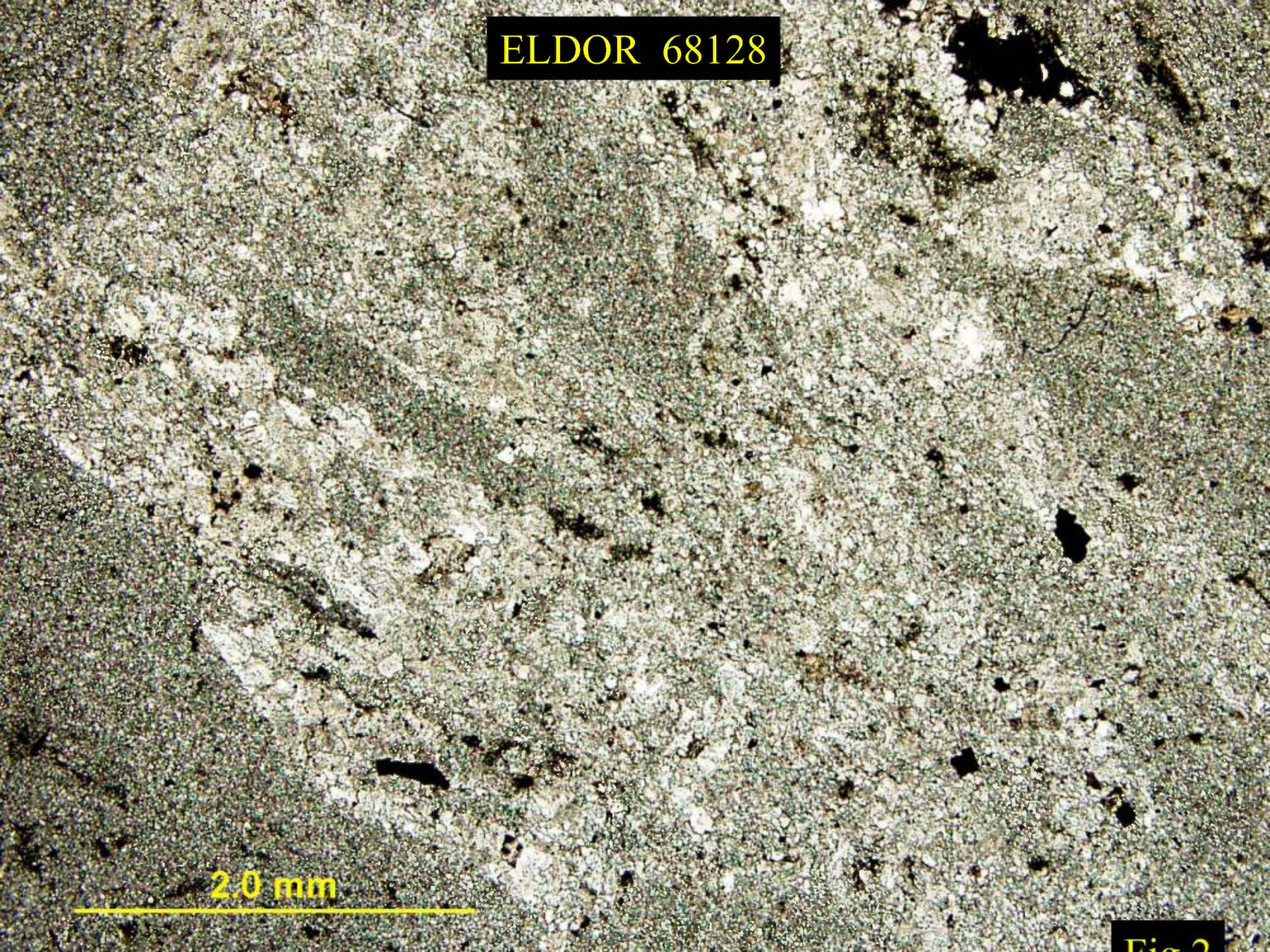

Fig 2

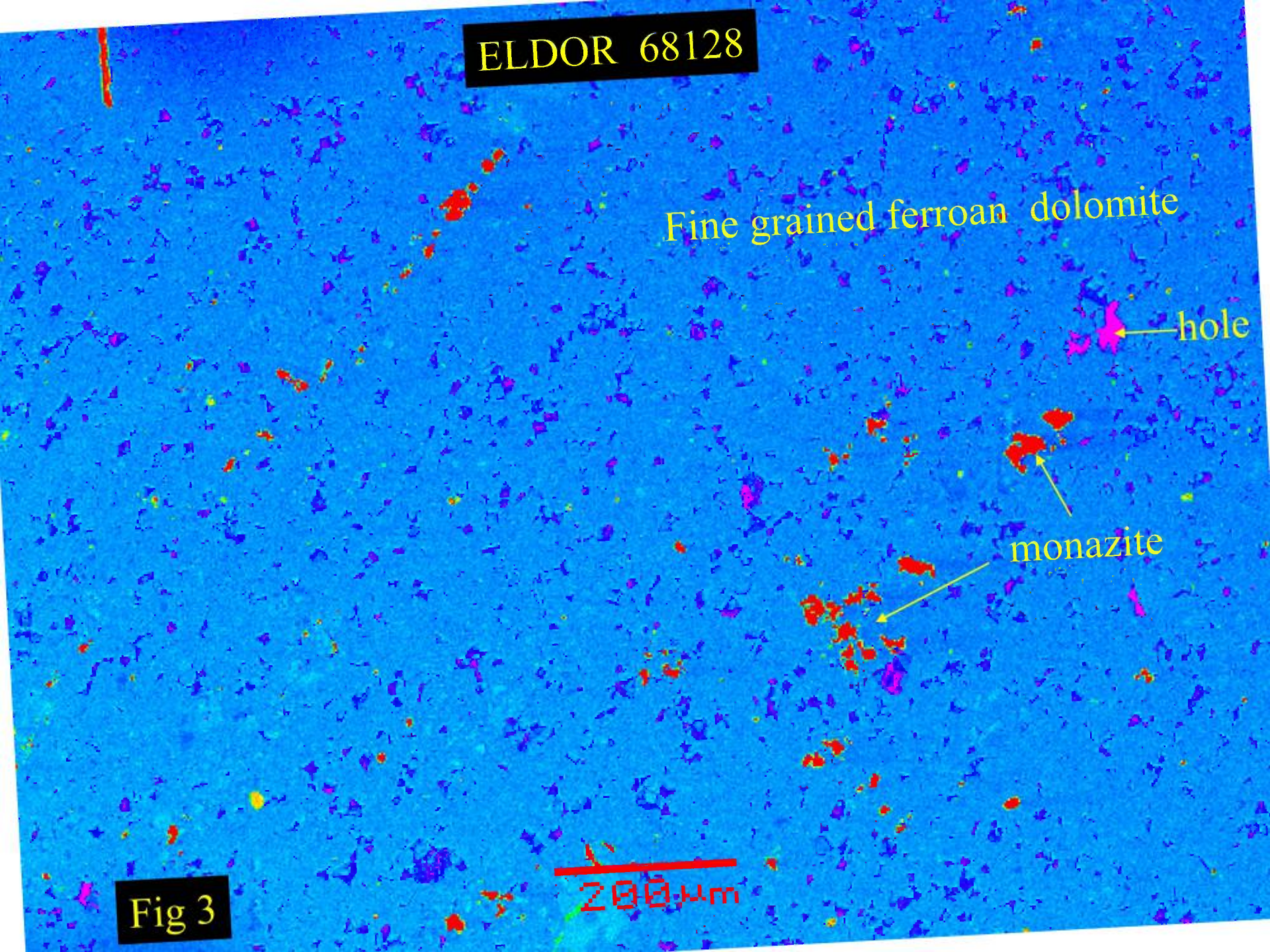
ELDOR 68128
Fine grained ferroan dolomite
hole
monazite
200µm

Fig 3

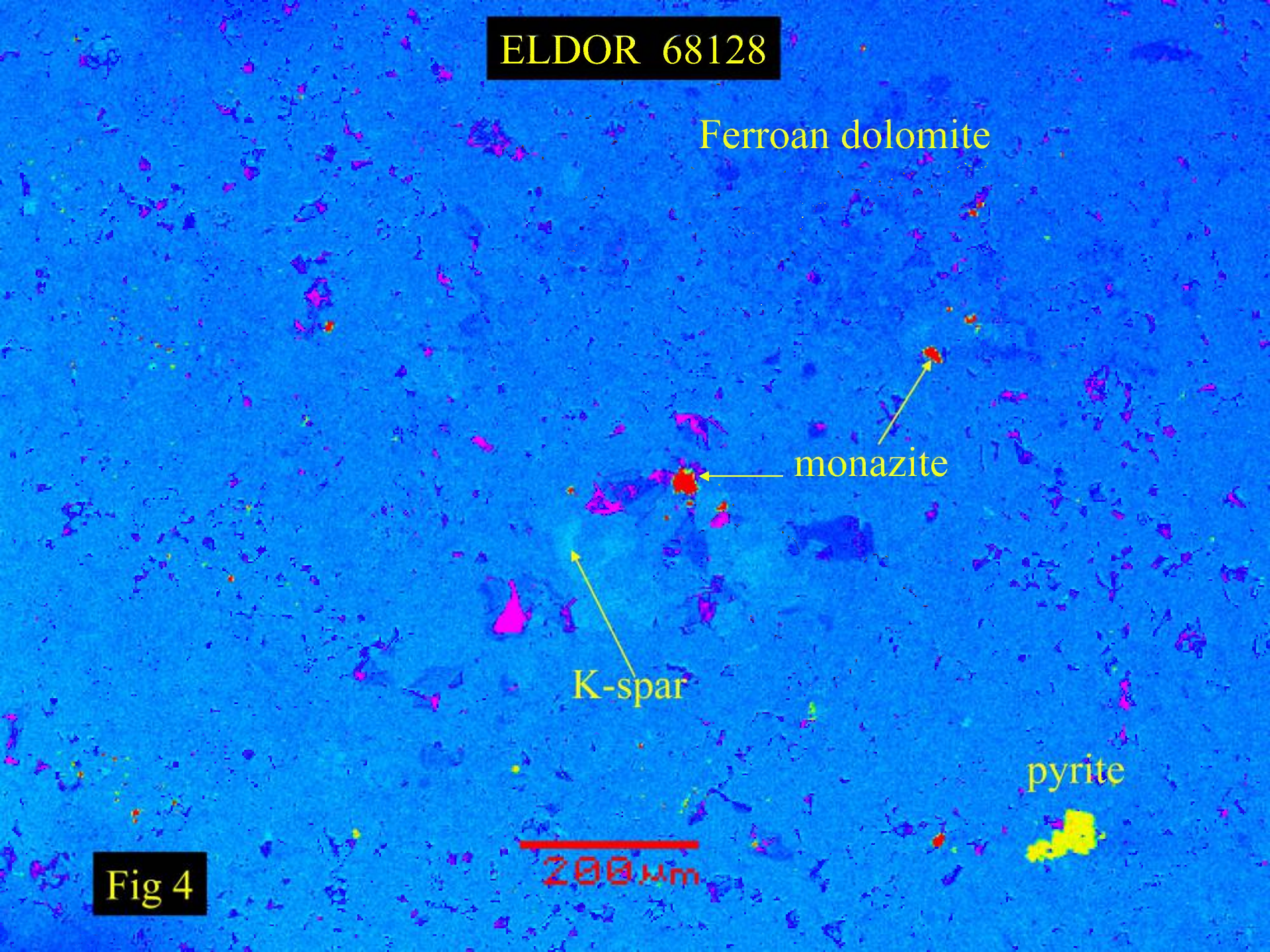

Fig 4

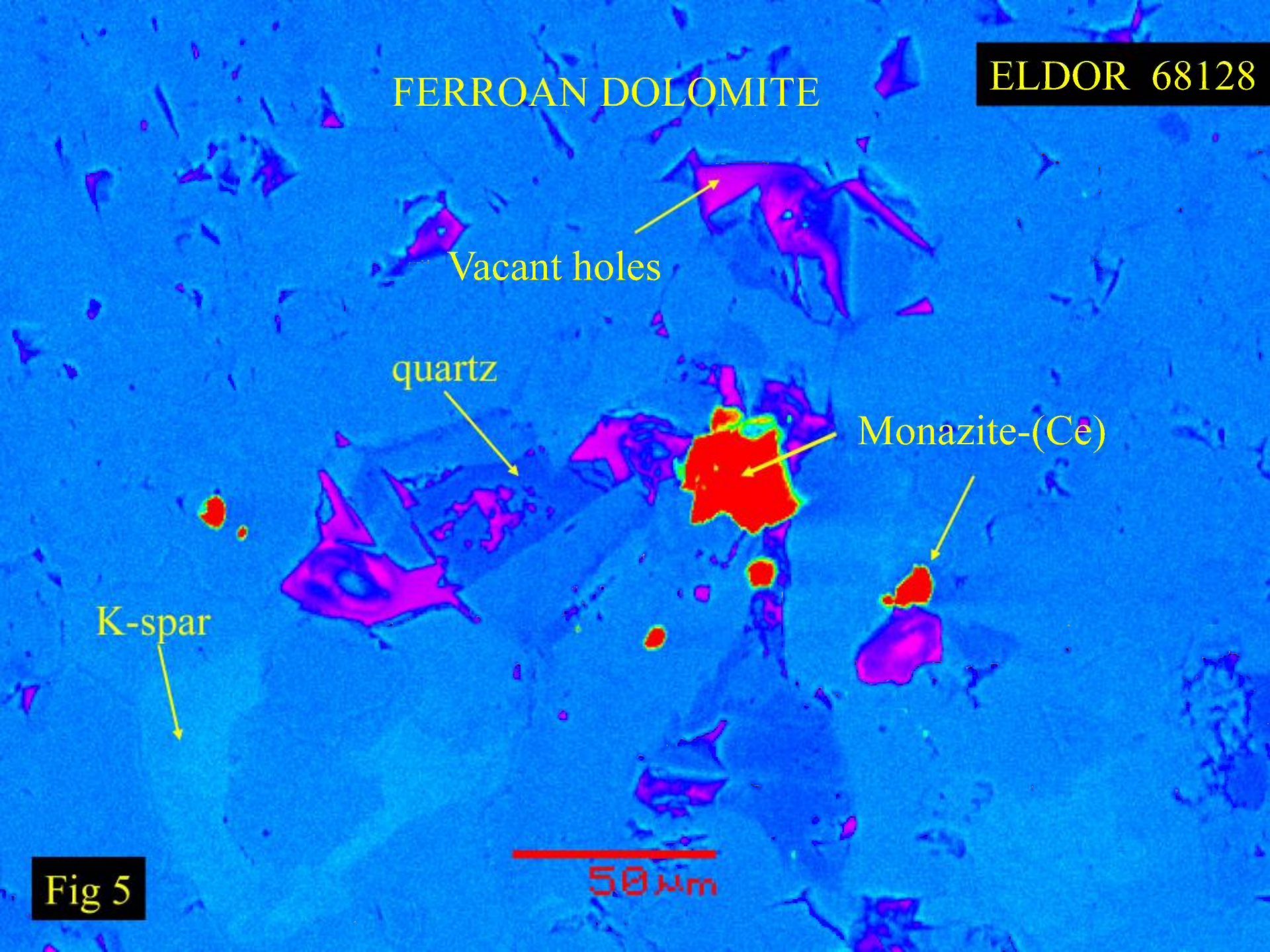
ELDOR 68128
FERROAN DOLOMITE
Vacant holes
quartz
Monazite-(Ce)
K-spar
50 µm

Fig 5

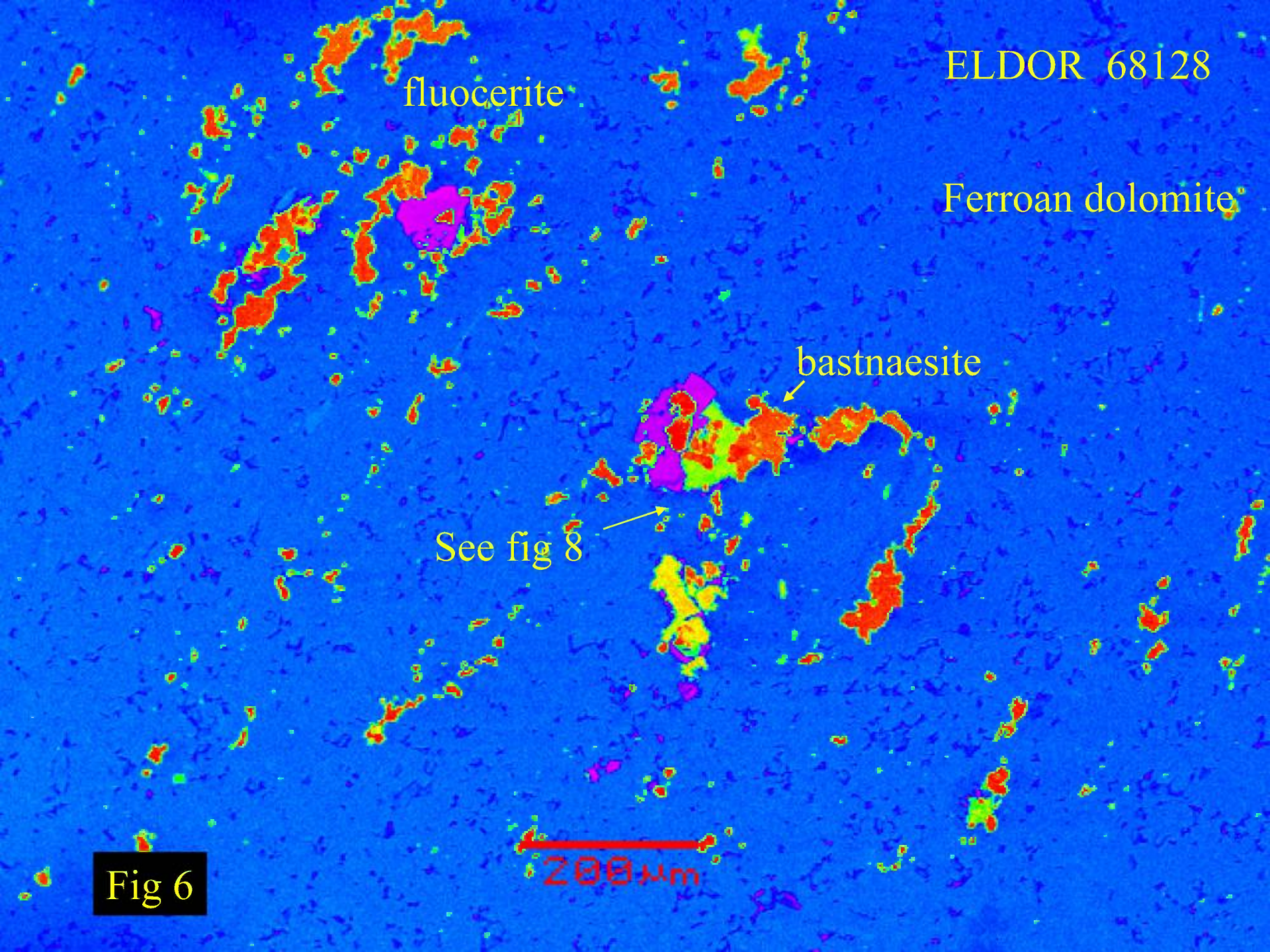
ELDOR 68128
fluocerite
Ferroan dolomite
bastnaesite
See fig 8
200µm

Fig 6

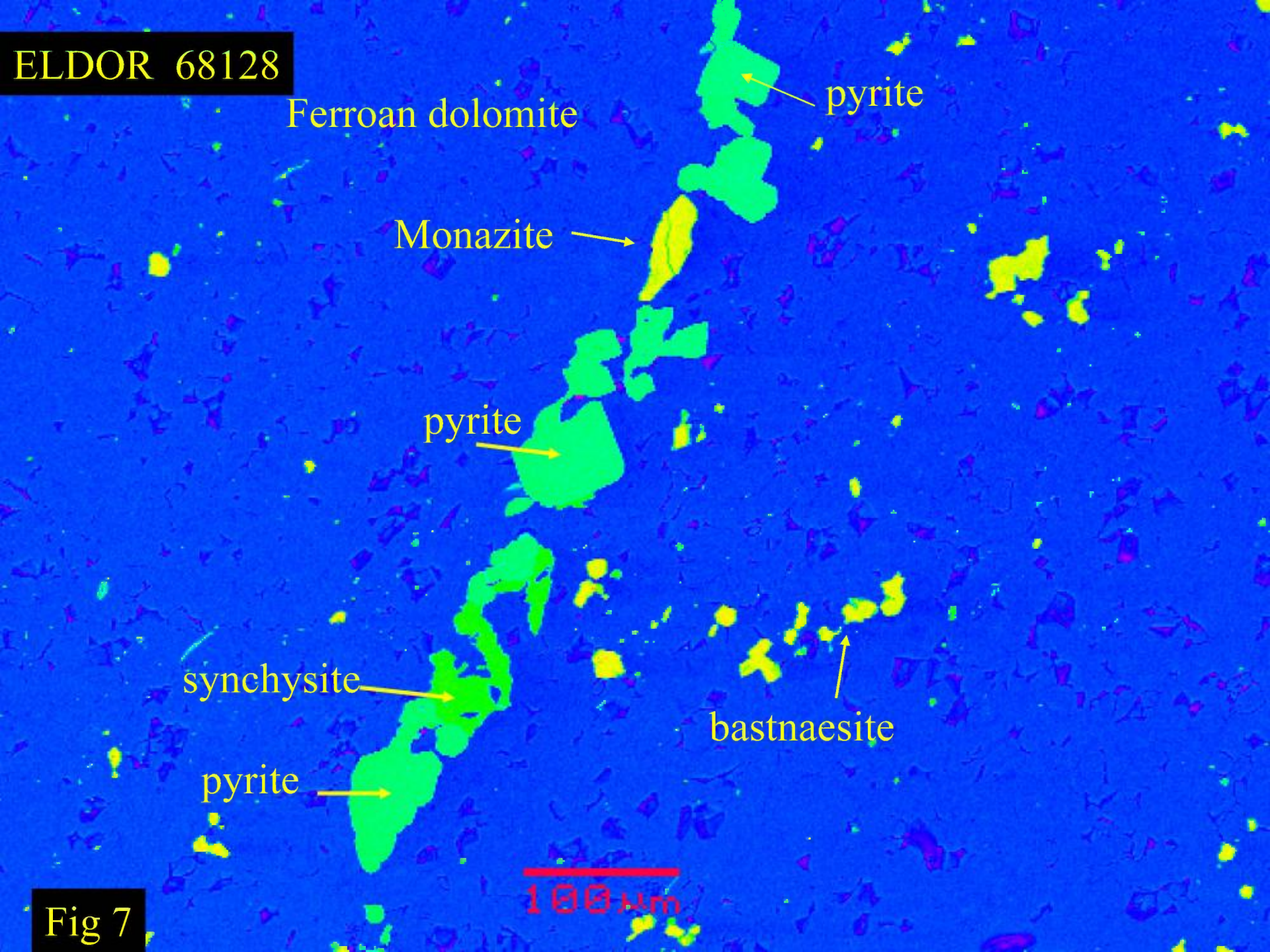
ELDOR 68128
Ferroan dolomite
pyrite
Monazite
pyrite
synchysite
bastnaesite
pyrite
100 µm

Fig 7

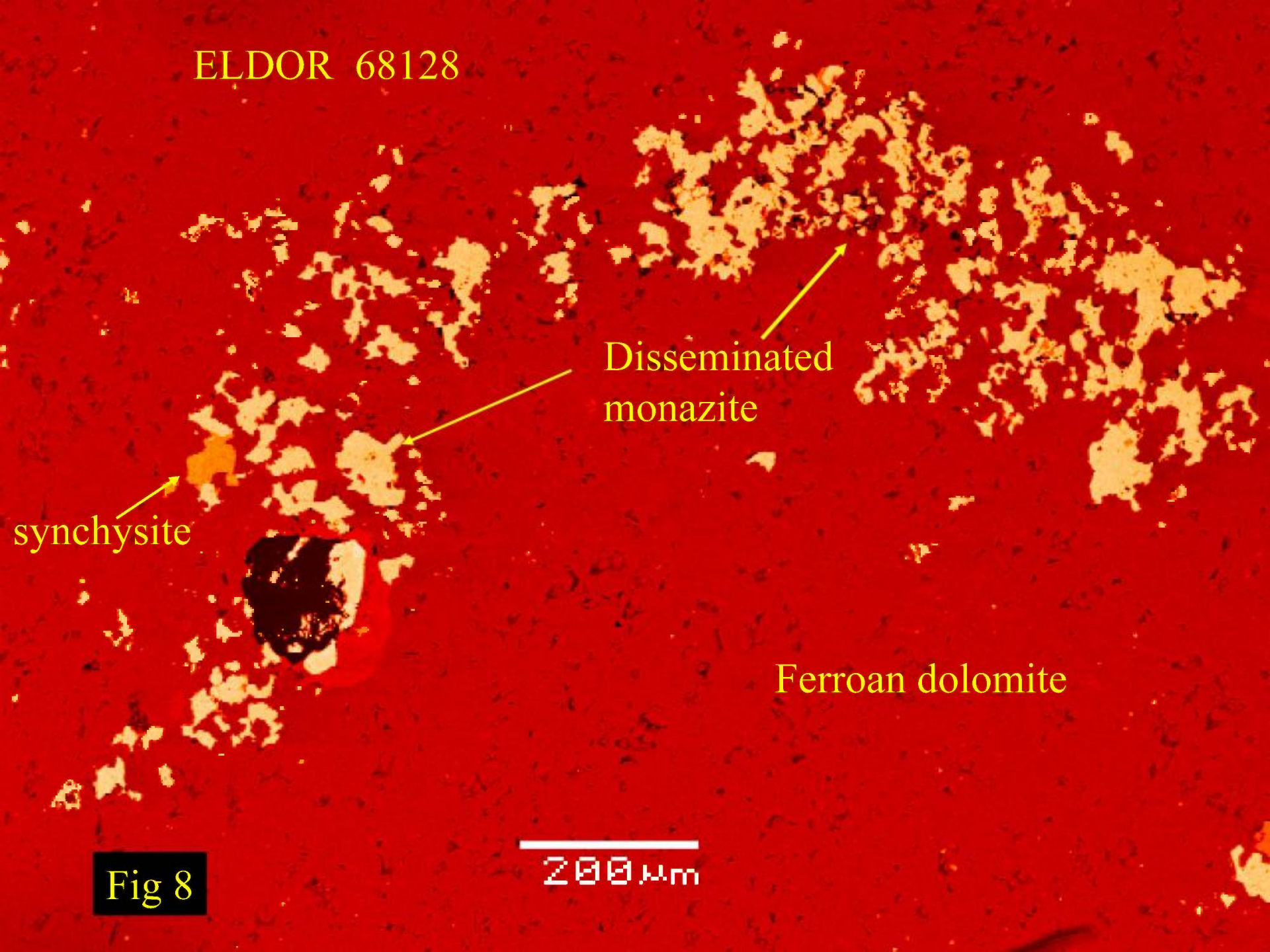
ELDOR 68128
Disseminated
monazite
synchysite
Ferroan dolomite
200 µm

Fig 8

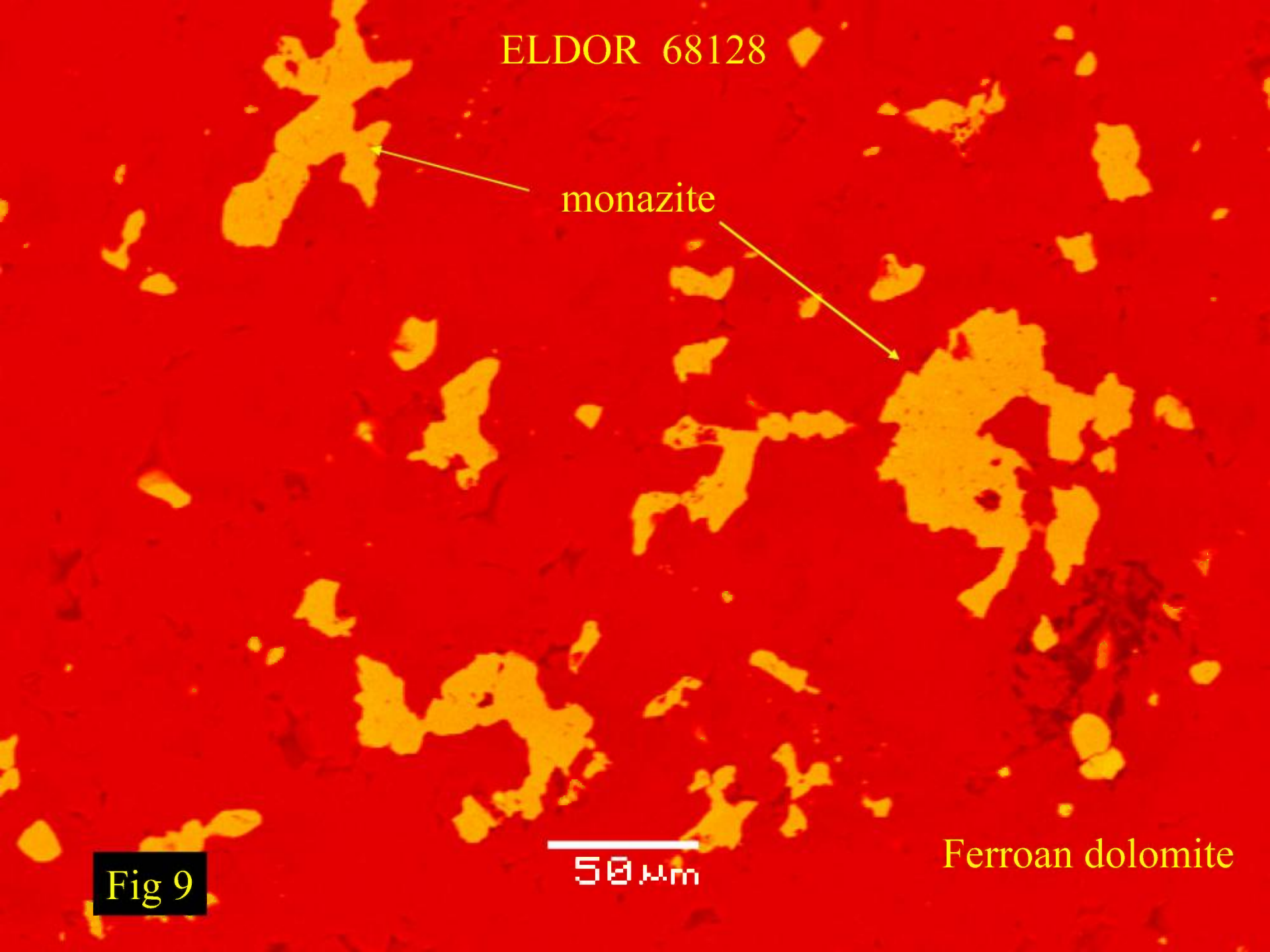

Fig 9

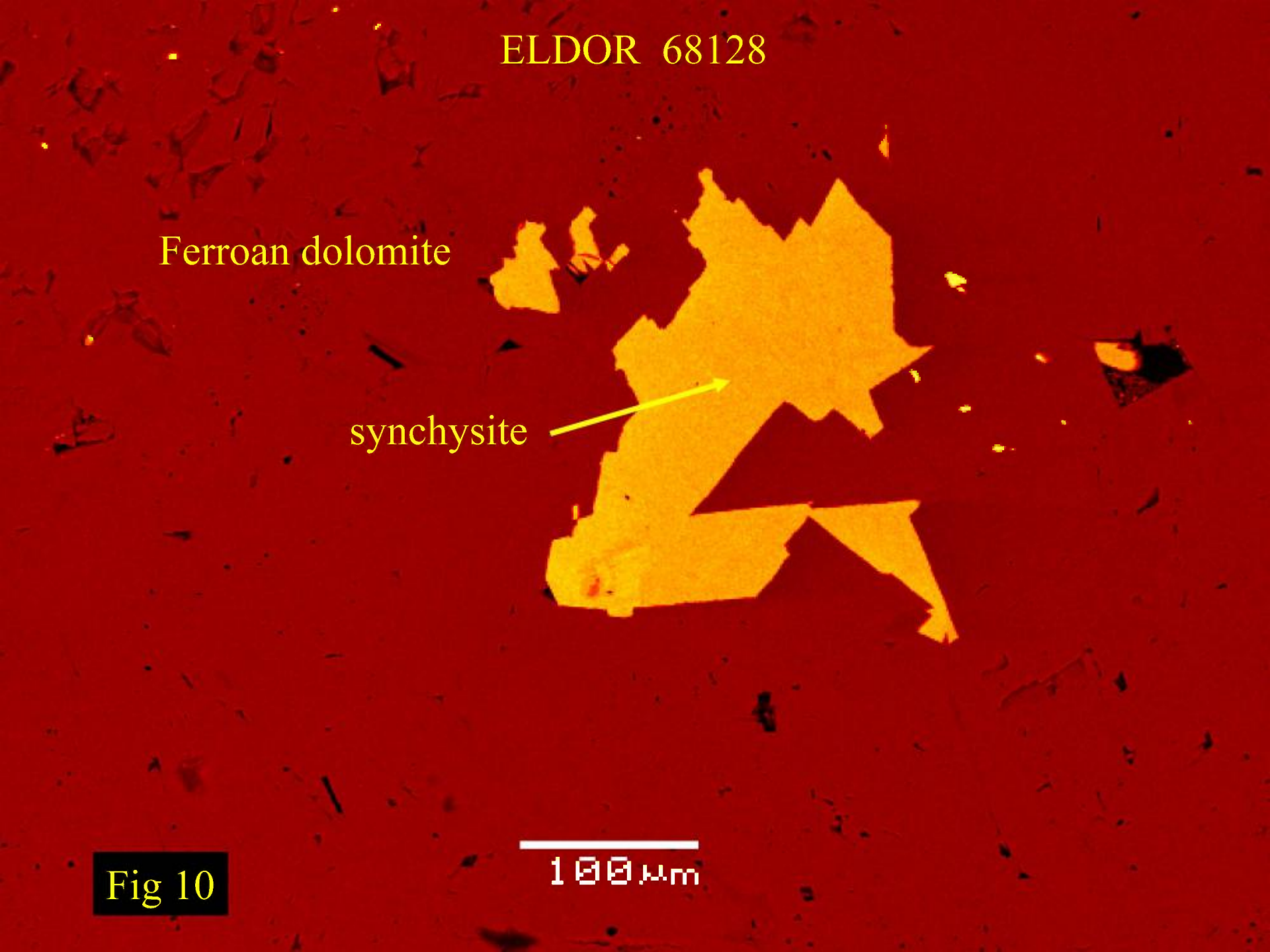

Fig 10

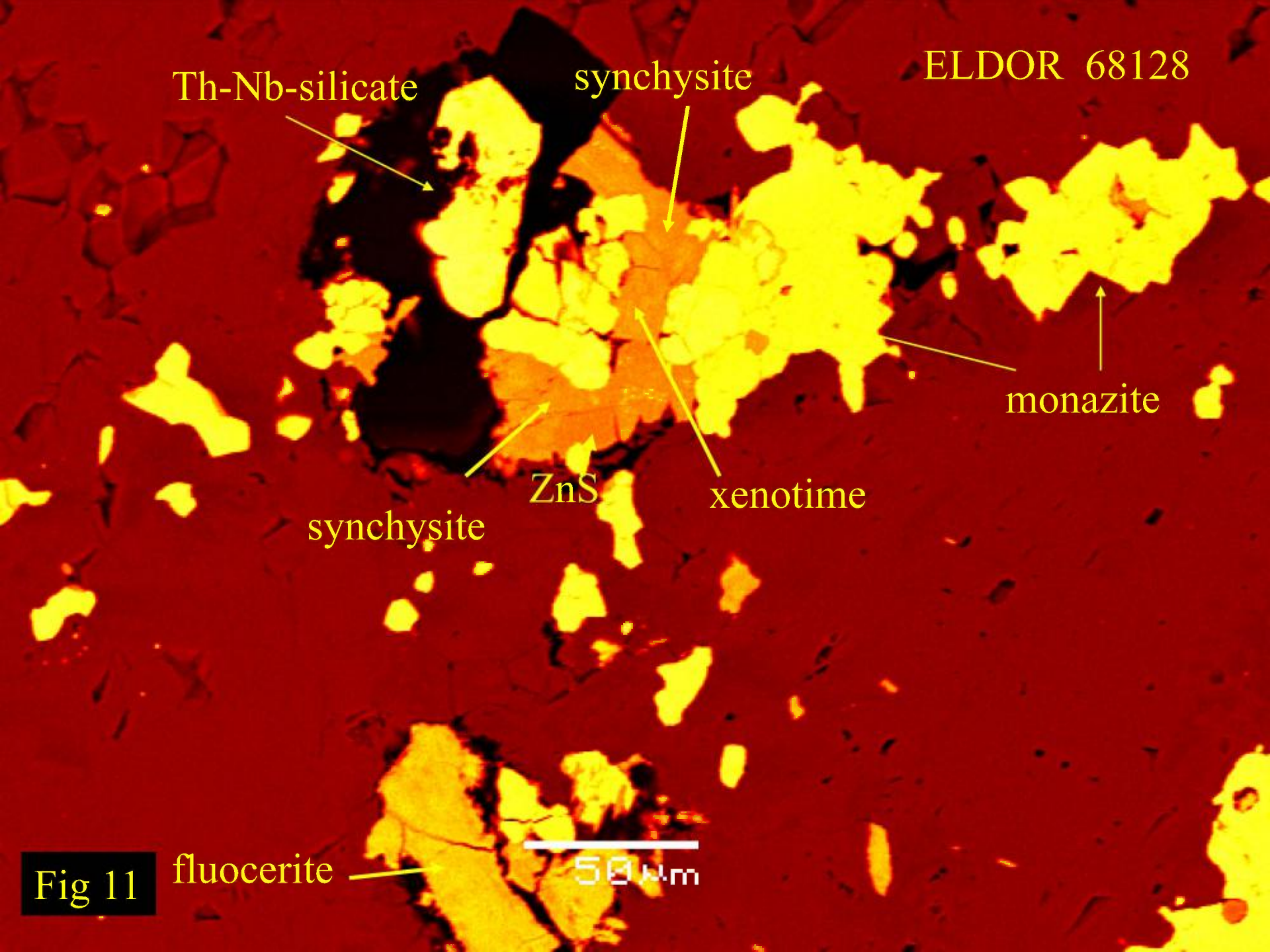
ELDOR 68128
Th-Nb-silicate
synchysite
monazite
synchysite
ZnS
xenotime
fluocerite
50µm

Fig 11

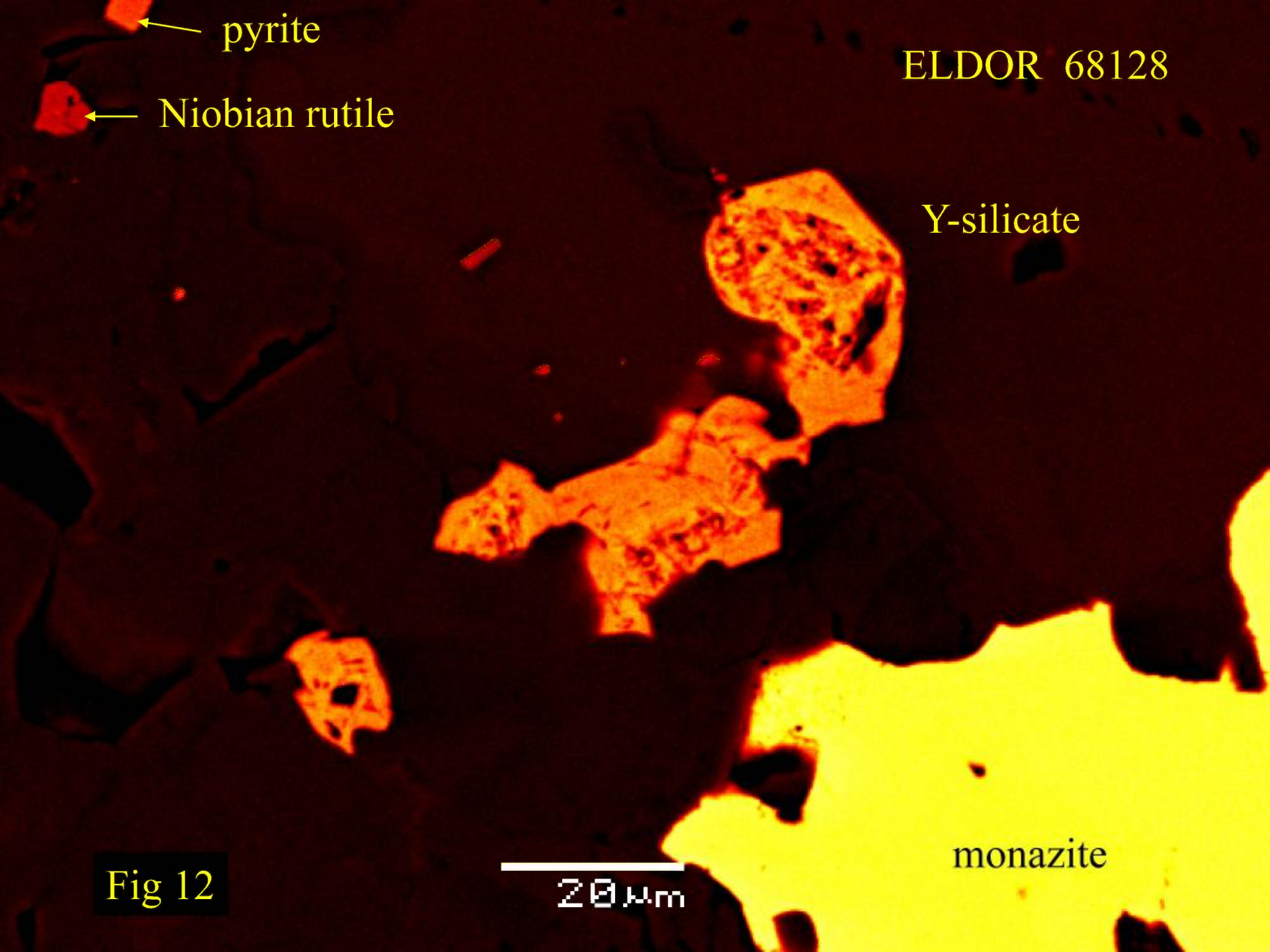
pyrite
Niobian rutile
ELDOR 68128
Y-silicate
monazite
20µm

Fig 12

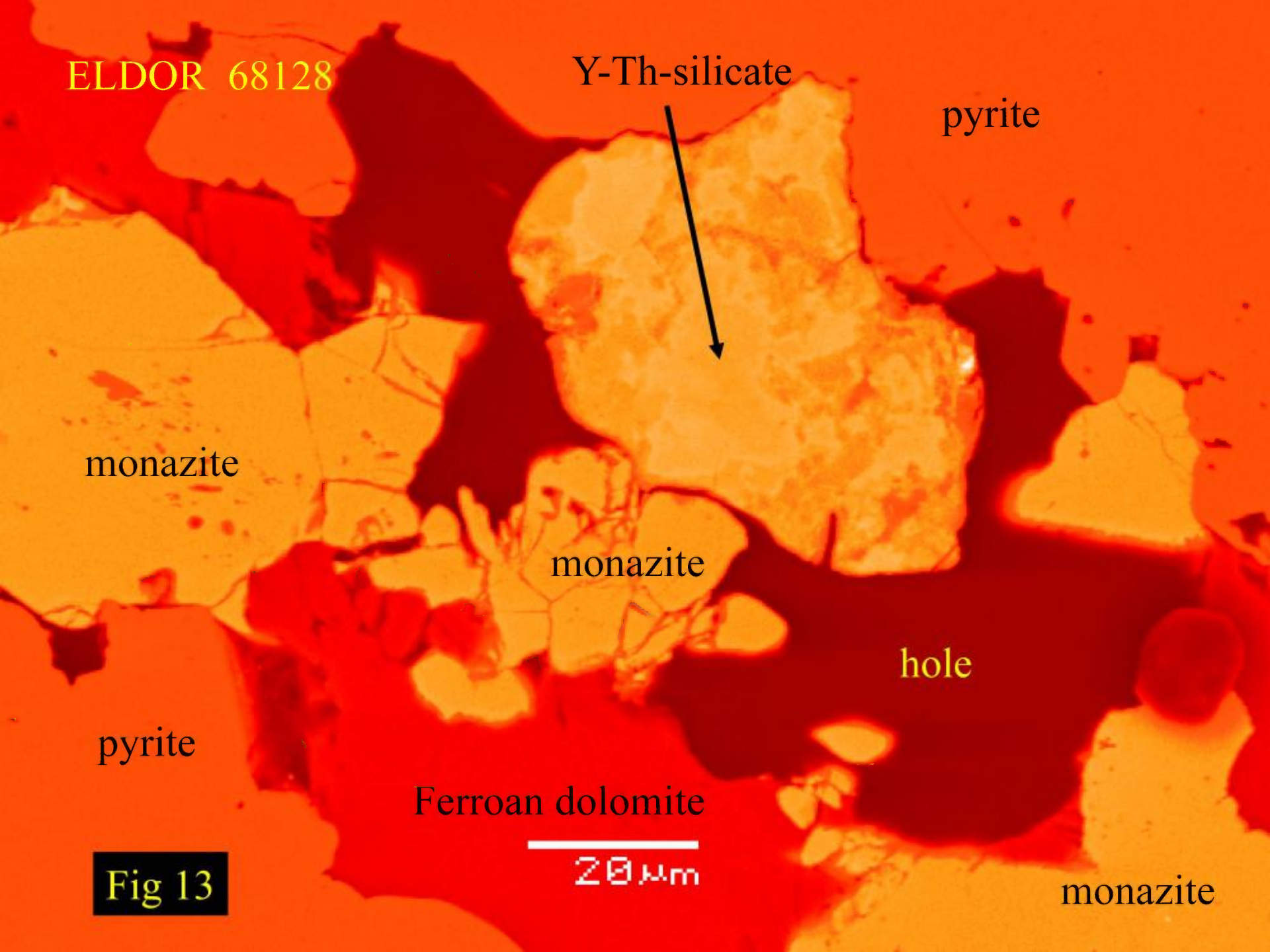
ELDOR 68128
Y-Th-silicate
pyrite
monazite
monazite
hole
pyrite
Ferroan dolomite
20 µm
monazite

Fig 13

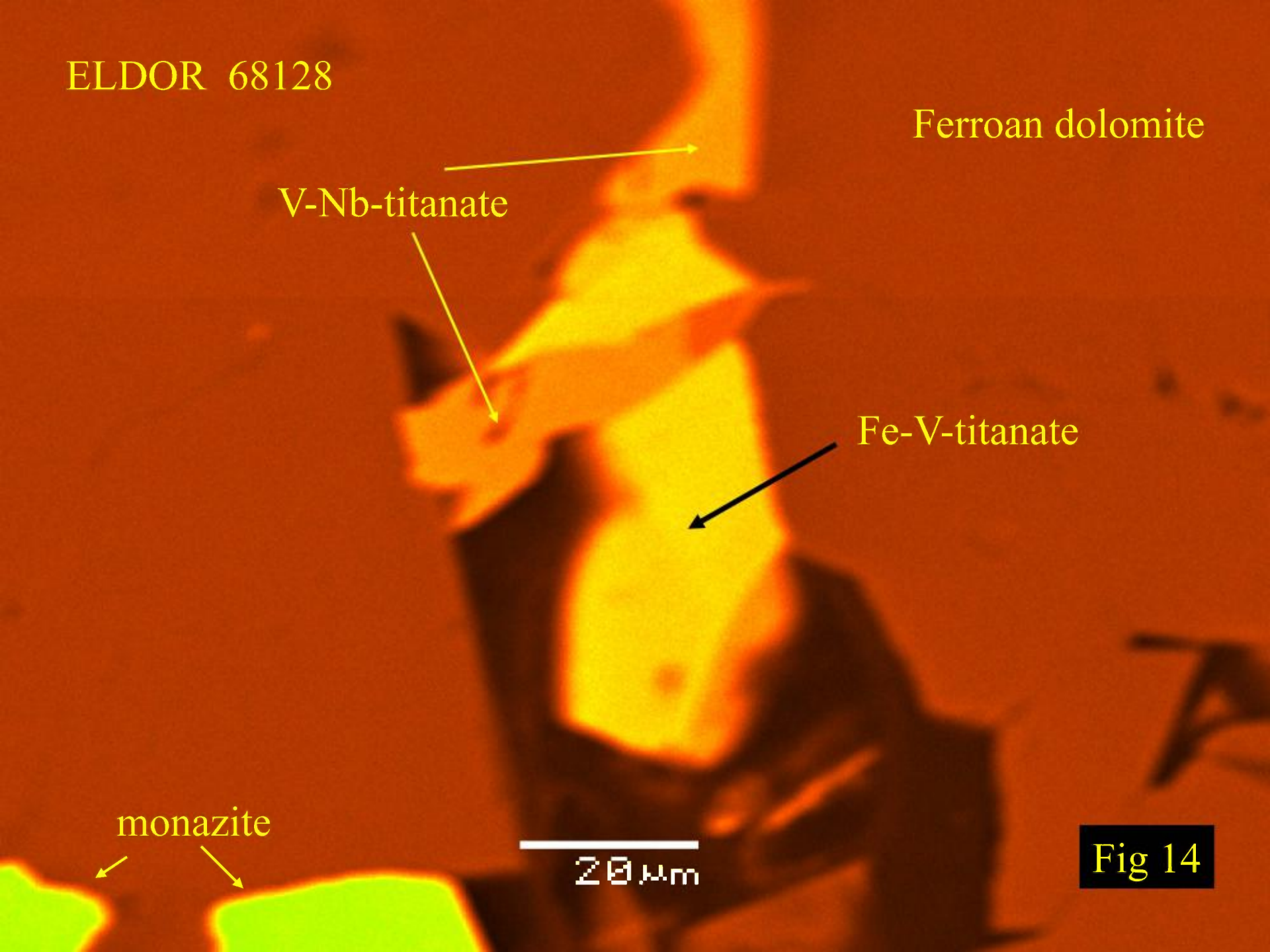
ELDOR 68128
Ferroan dolomite
V-Nb-titanate
Fe-V-titanate
monazite
20 µm

Fig 14

ELDOR 68138

ELDOR 68138 ***Fluorite dolomite carbonatite***

This sample is a banded rock consisting of alternate bands dominated by, or consisting entirely of, fluorite or dolomite (Figs 1-4). Bands can range up to 1 cm in thickness. Fluorite forms allotriomorphic granular aggregates that range in colour from colourless to deep purple (Figs 1-5) This no doubt reflects variations in trace element abundances. The fluorite has numerous very small (< 20um) single phase fluid inclusions and many very small (< 20um) optically unidentifiable inclusions of high birefringence. BSE-images and X-ray spectrometry show these to be either rounded zircon crystals or REE-fluorocarbonates (Figs. 6-7). Exact identification of the carbonates is not possible because of secondary fluorescence from Ca in the matrix fluorite; however they are considered to be either bastnaesite, parisite or synchysite. Rare fersmite was also identified. Dolomite is principally a low Fe-variety (c. 3-6 wt.% FeO). It forms allotriomorphic granular aggregates as monomineralic bands or intergrowths with fluorite. In common with the fluorite, very small inclusions of zircon and fluorocarbonates are present (Figs. 6-7). The only silicates present are laths of colourless-to-pale brown phlogopite which are aligned, at their contacts, parallel to the fluorite-dolomite bands. Some areas of the sample contain a yellow-brown phase (Figs 4-6). BSE-imagery and X-ray spectrometry show this to be ferroan dolomite of similar composition to other dolomite in this sample. The yellow-brown colour is considered to be an alteration feature. REE-bearing phases are not intergrown with this material. Pyrochlore, magnetite and apatite are not present in this sample which has the textural characteristics of a late-forming hydrothermal vein deposit; the economic potential is low.

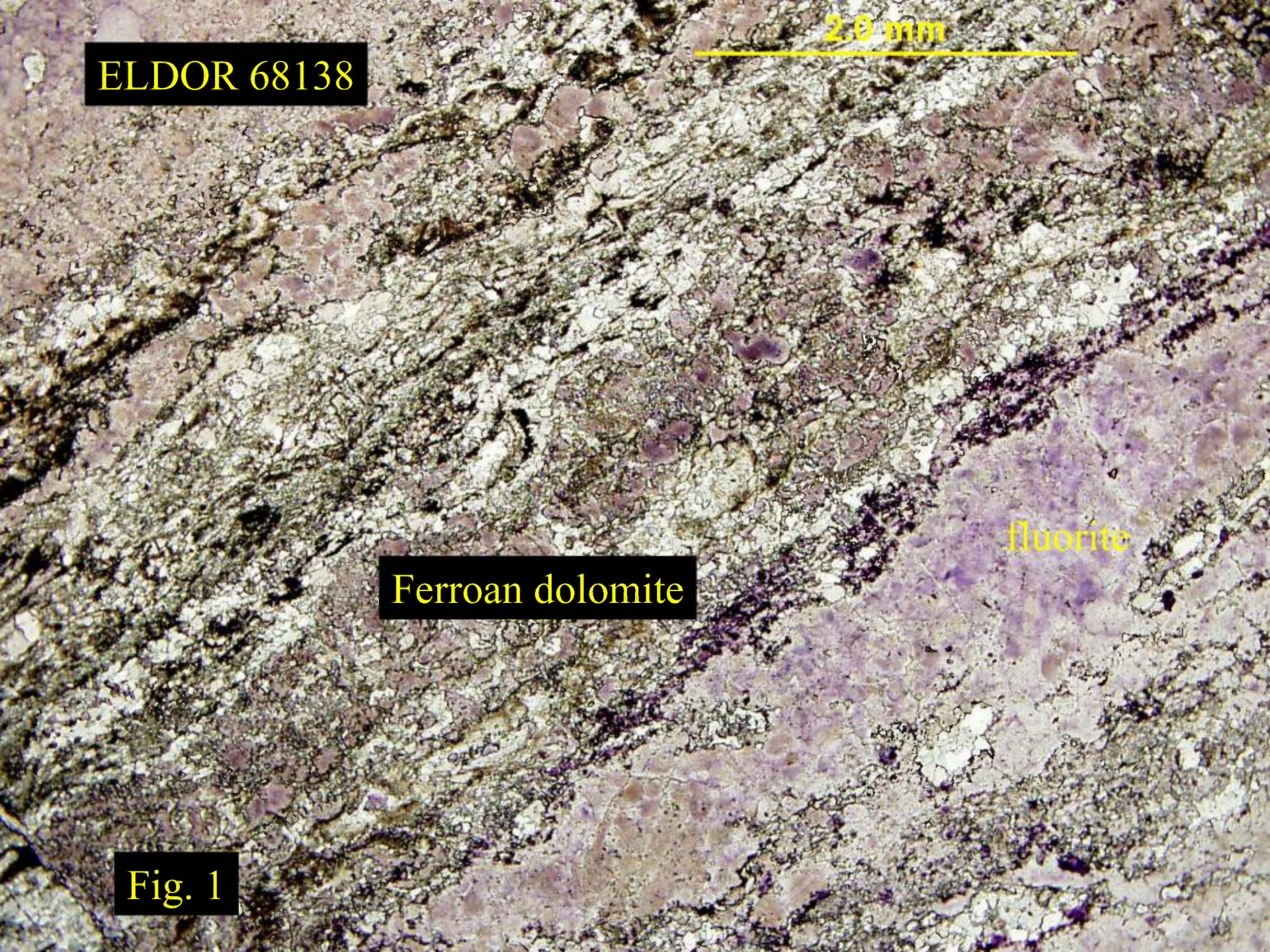

Fig. 1

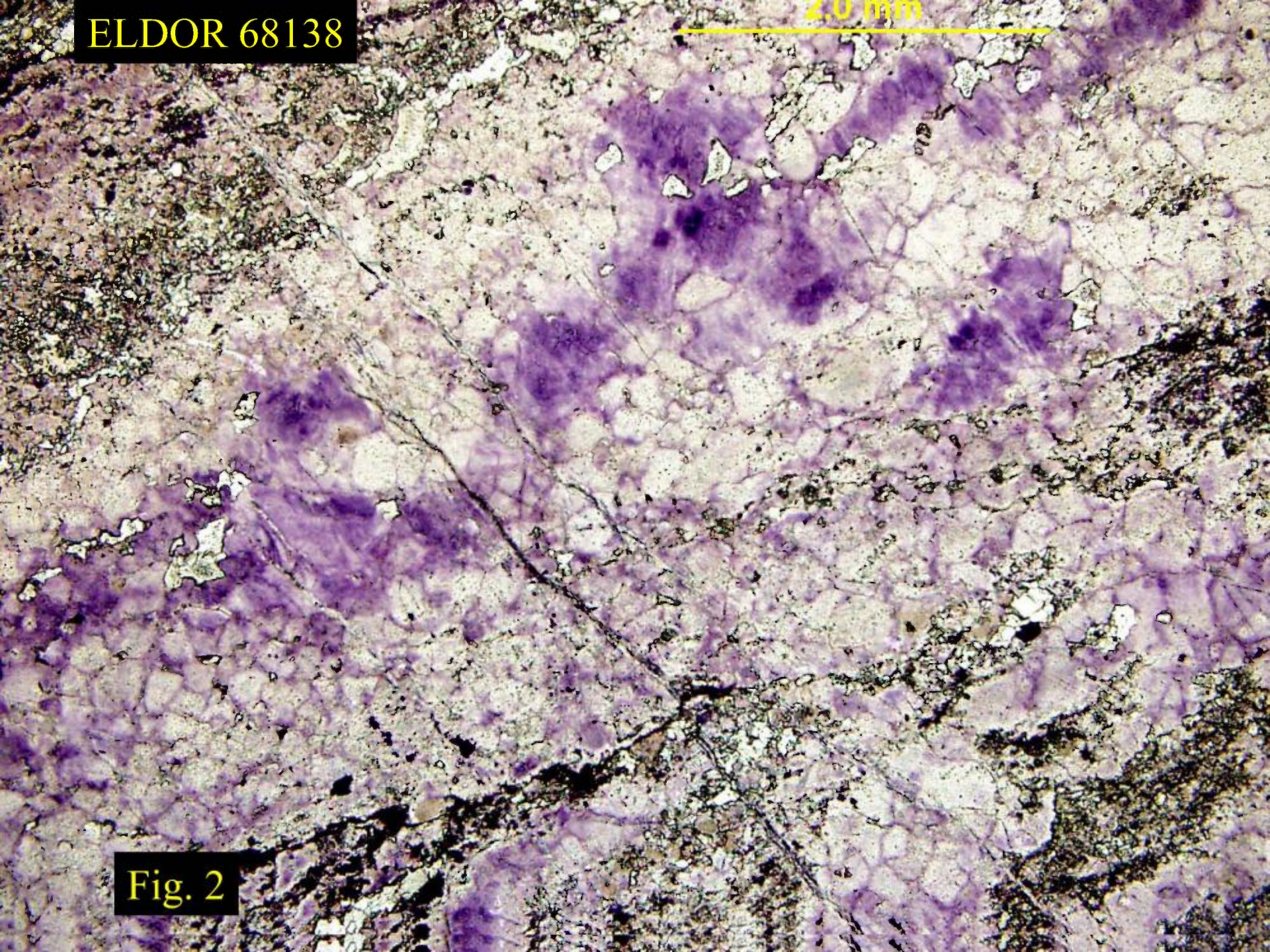

Fig. 2

Fig. 3

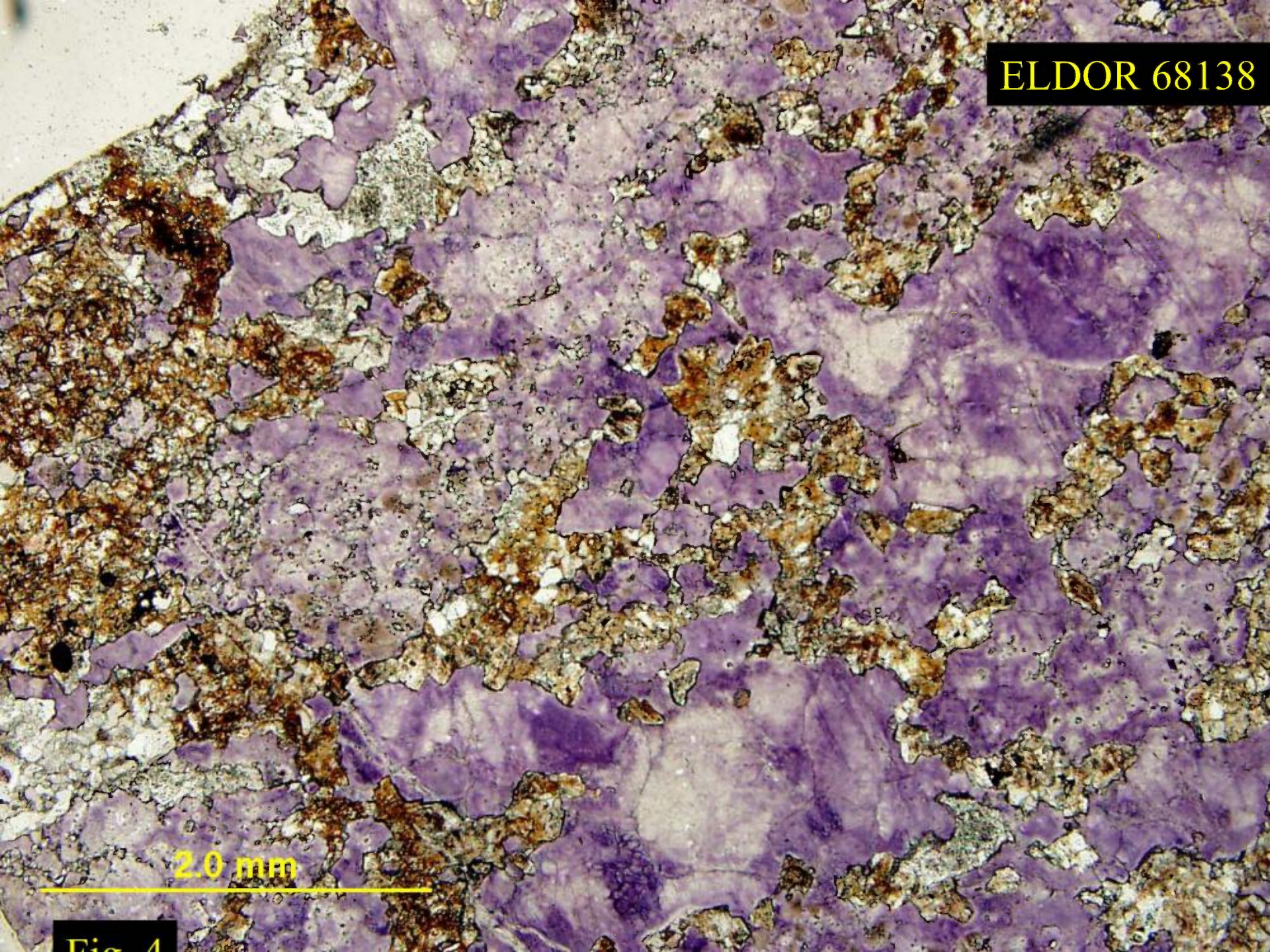

Fig. 4

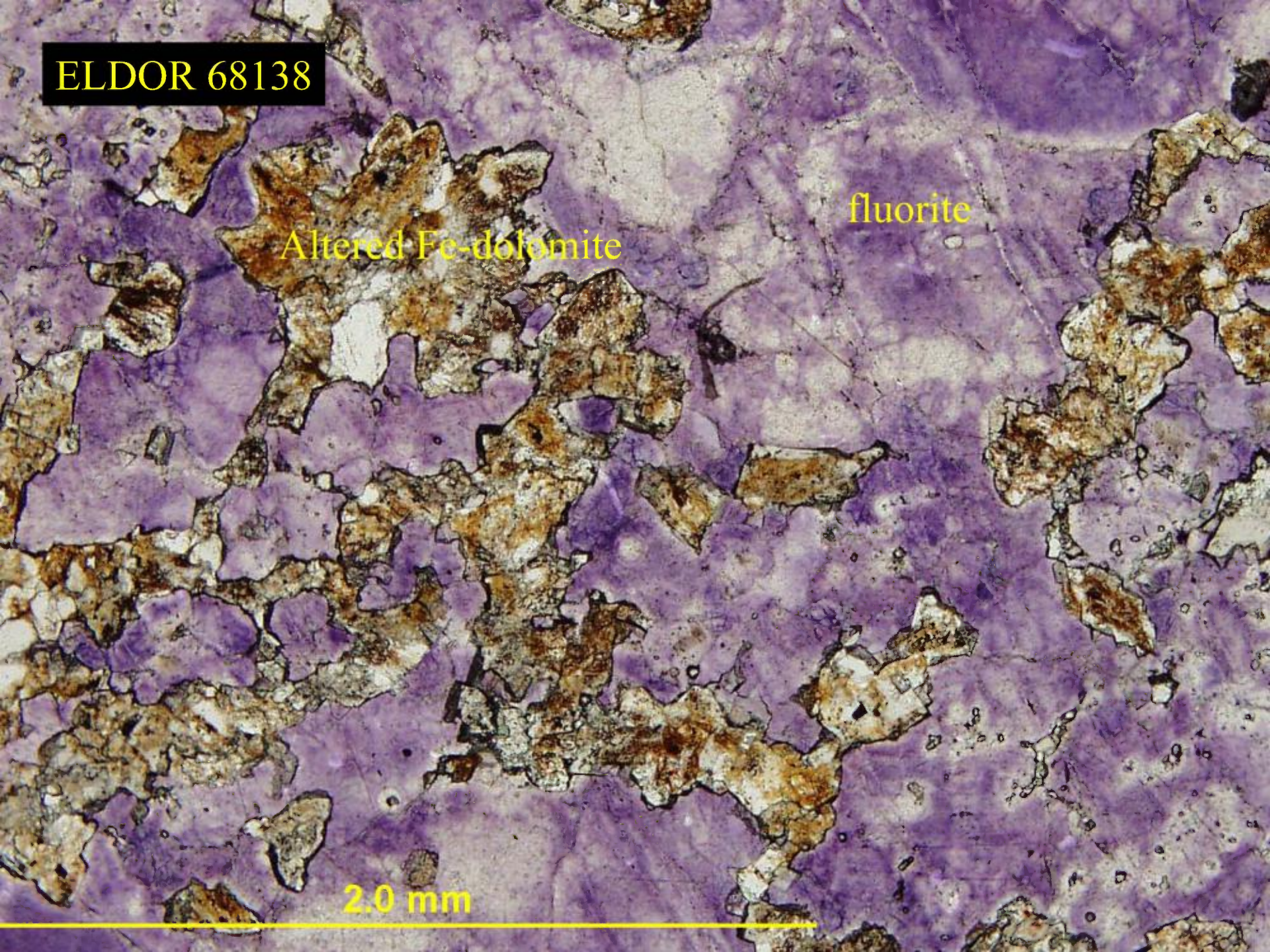
ELDOR 68138
Altered Fe-dolomite
fluorite
2.0 mm

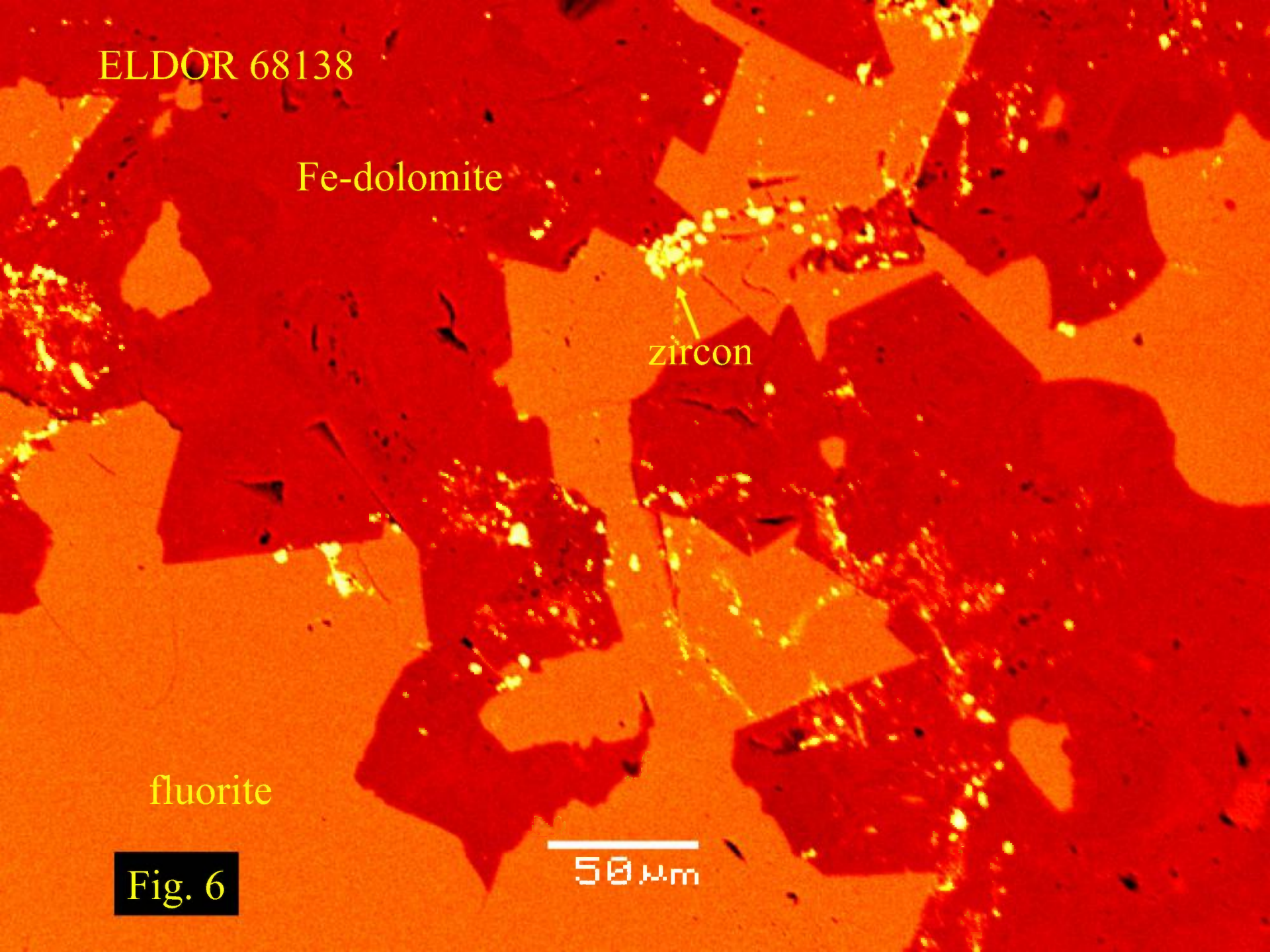

Fig. 6

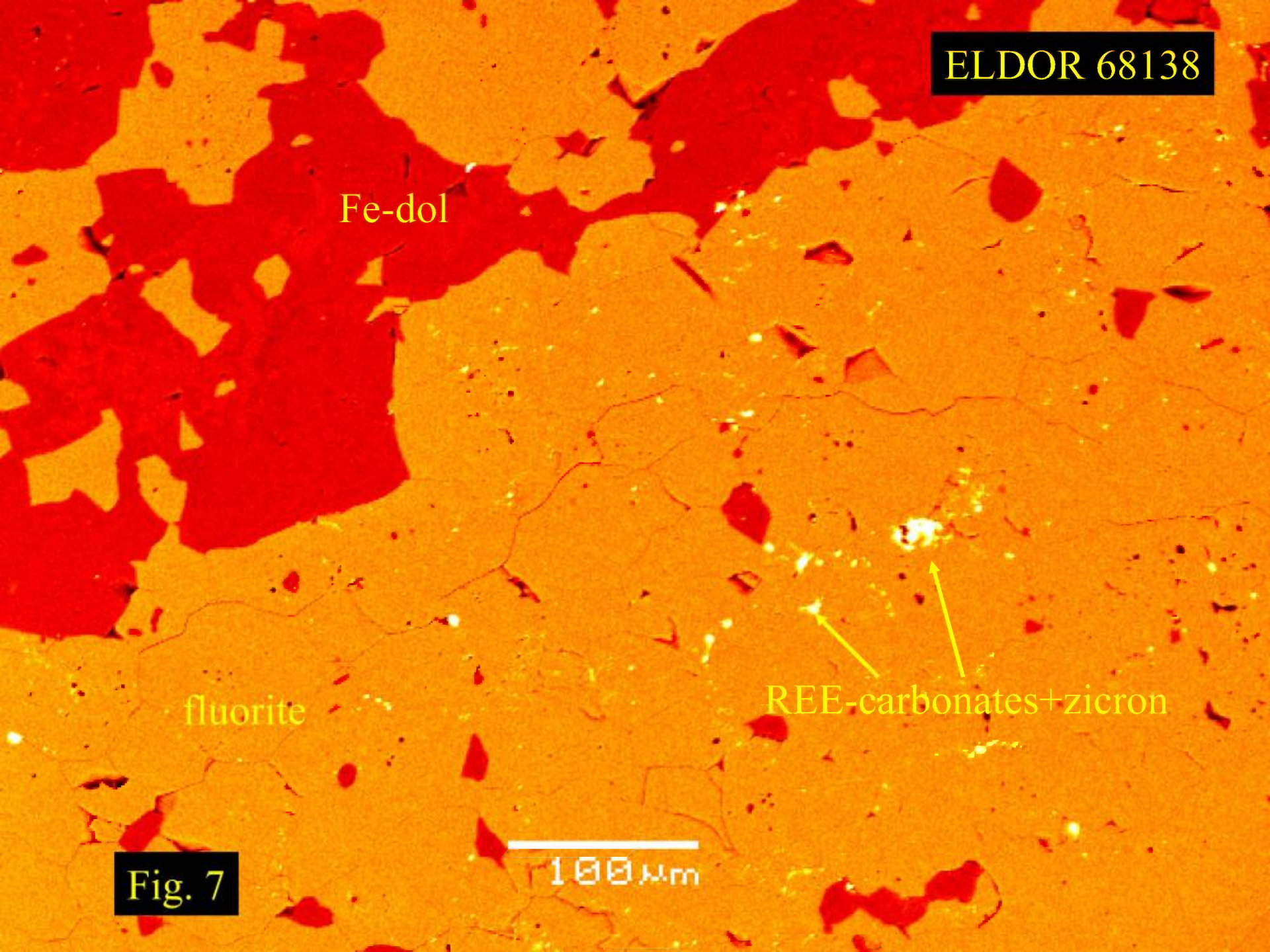

Fig. 7

ELDOR 68146

This sample (Figs 1-3) is characterized by the presence of abundant (c. 50 vol.%) irregular large (up to 0.5cm) crystals of magnetite and euhedral pyrite (up to 0.5cm) set in a matrix of blue green magnesioarfvedsonite, breunnerite and ferroan dolomite (Fig 4). The rock is heterogeneous with respect to the modal distribution of magnetite and pyrite, and magnetite-rich areas (Fig. 5) can be found. The amphibole prisms, together with minor amounts of pale yellow phlogopite, impart a distinct foliation (Fig.2).

The magnetite appears for the most part to represent a fragmented cumulate as few euhedral crystals are evident. Inclusions of ferrocolumbite are present in some, but not all, of the magnetite crystals (Figs. 5-6). The magnetite contains no detectable Mg, Ti or Mn and ilmenite exsolution lamellae are absent. However, subhedral to euhedral crystals of monazite-(Ce) and ilmenite decorate the margins of some magnetite crystals (Fig.7). Similar subhedral discrete ilmenite occurs throughout the groundmass. Pyrite forms large euhedral plates and typically lacks inclusions, although in some instances resorbed ferrocolumbite crystals are present (Fig.8).

The matrix consists of significant amountsof magnesioarfvedsonite (c. 15 vol%) intergrown with small crystals of siderite-rich breunnerite set in a mesostasis of late-forming ferroan dolomite (Fig. 4 and 10). Also present in the mesostasis are small (< 20 um) anhedral crystals of zircon and plates of colourless chlorite. Zircon is also found as reaction mantles formed upon anhedral resorbed crystals of baddeleyite (Fig.9).

ELDOR 68146

Ferrocolumbite occurs as irregular, corroded crystals (up to 0.4 mm) scattered randomly throughout the sample (Figs 5, 7-9). The ferrocolumbite can occurs as inclusions in magnetite or pyrite and a discrete crystals in the carbonate matrix. All ferrocolumbites contain small (< 20 um) anhedral inclusions of uranium-bearing (14- 19 wt.% UO_2) thorite [$(Th,U)SiO_4$] and small (<20 um) anhedral inclusions of zircon (Figs 8,10-11). Euhedral crystals of late-forming ilmenite have nucleated in some instances at the margins of the ferrocolumbite crystals (Fig.11). Pyrochlore, fersmite and apatite are not present on this sample.

The ferrocolumbite is a Ta-poor variety (compared to those in for example sample 68194). Representative semiquantitative compositions are:

wt.%	FC-1	FC-2
TiO_2	4.8	4.1
FeO	17.9	17.7
Nb_2O_5	73.8	73.1
Ta_2O_5	1.1	3.1

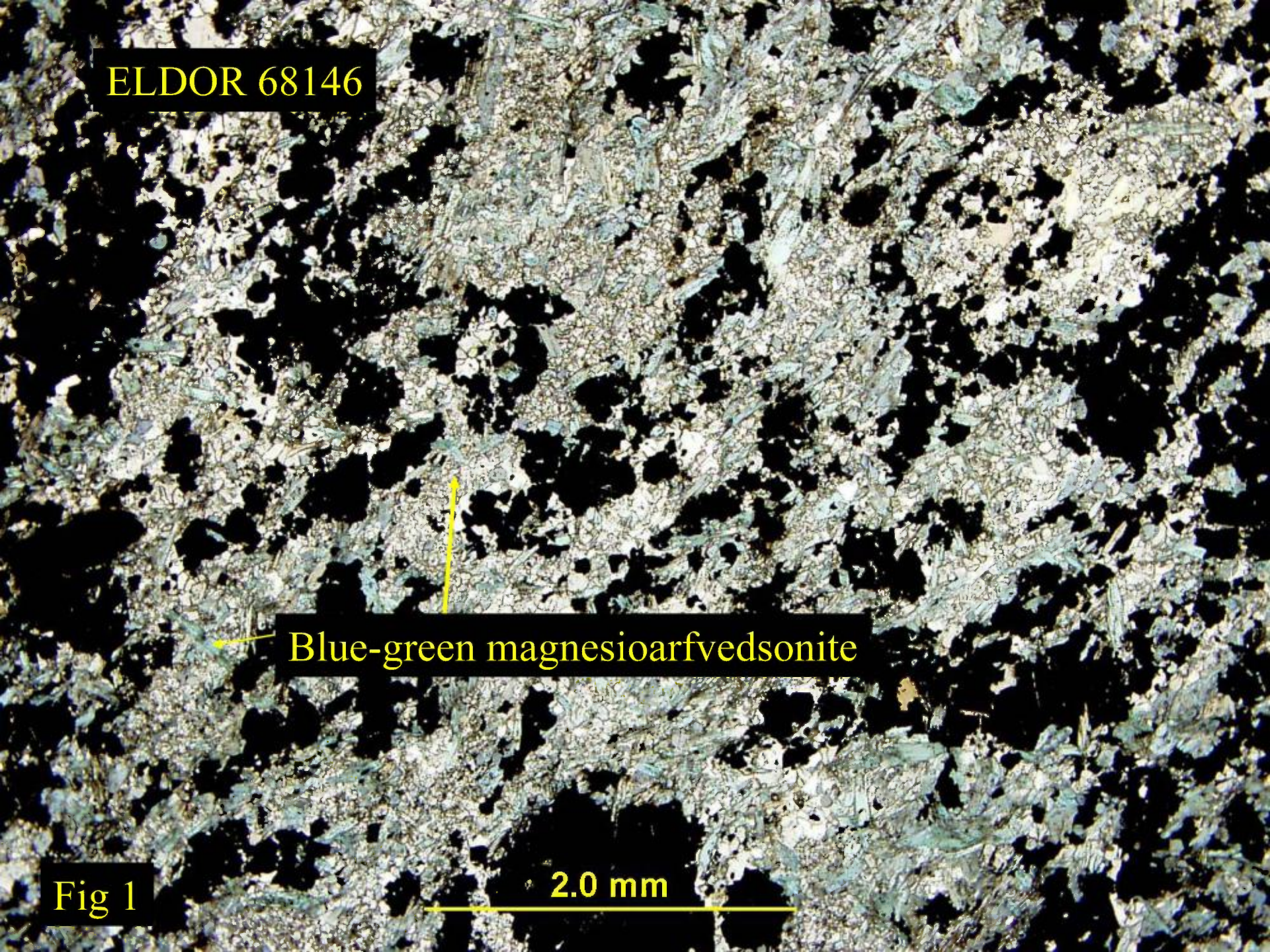

Fig 1

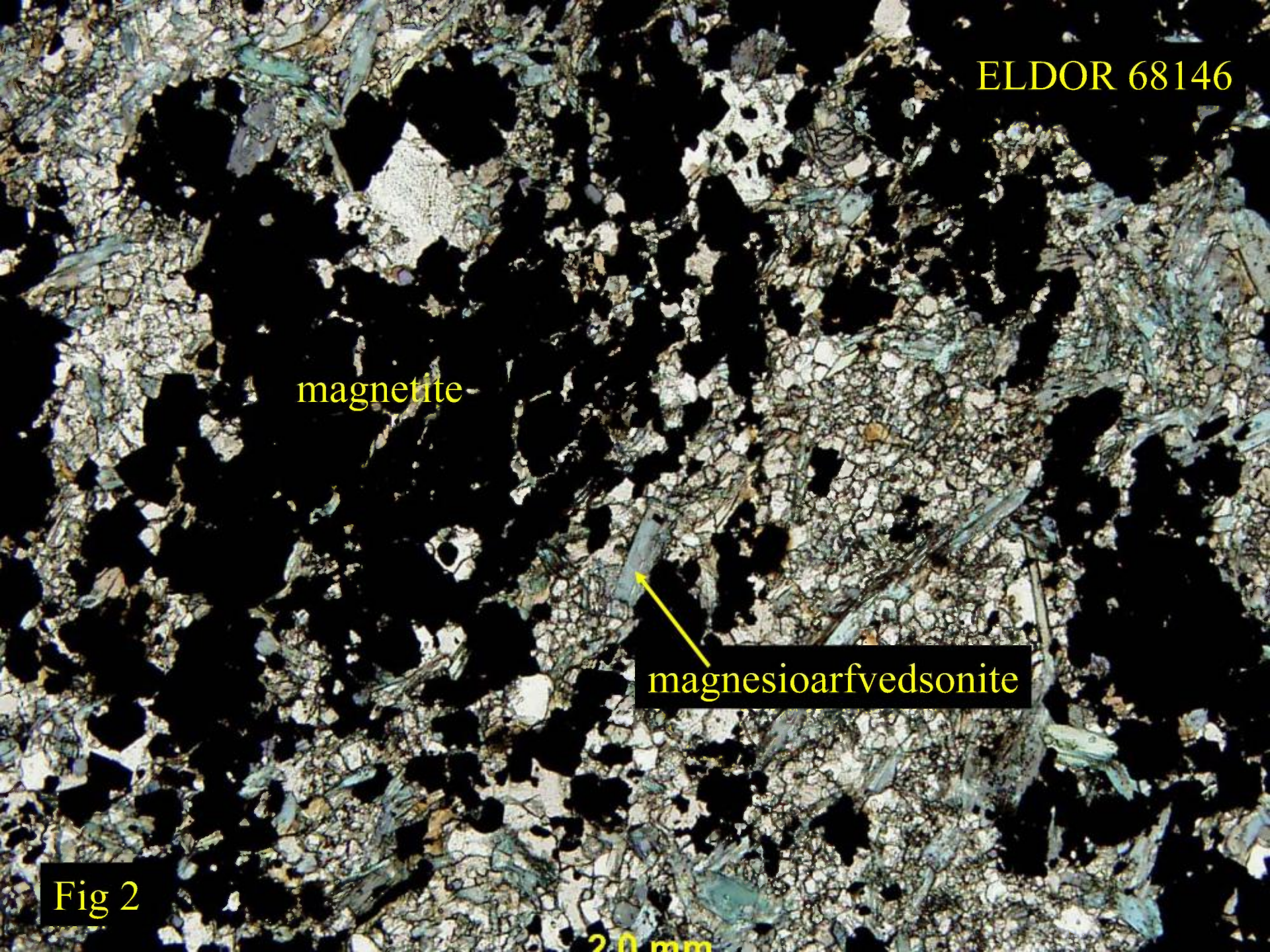

Fig 2

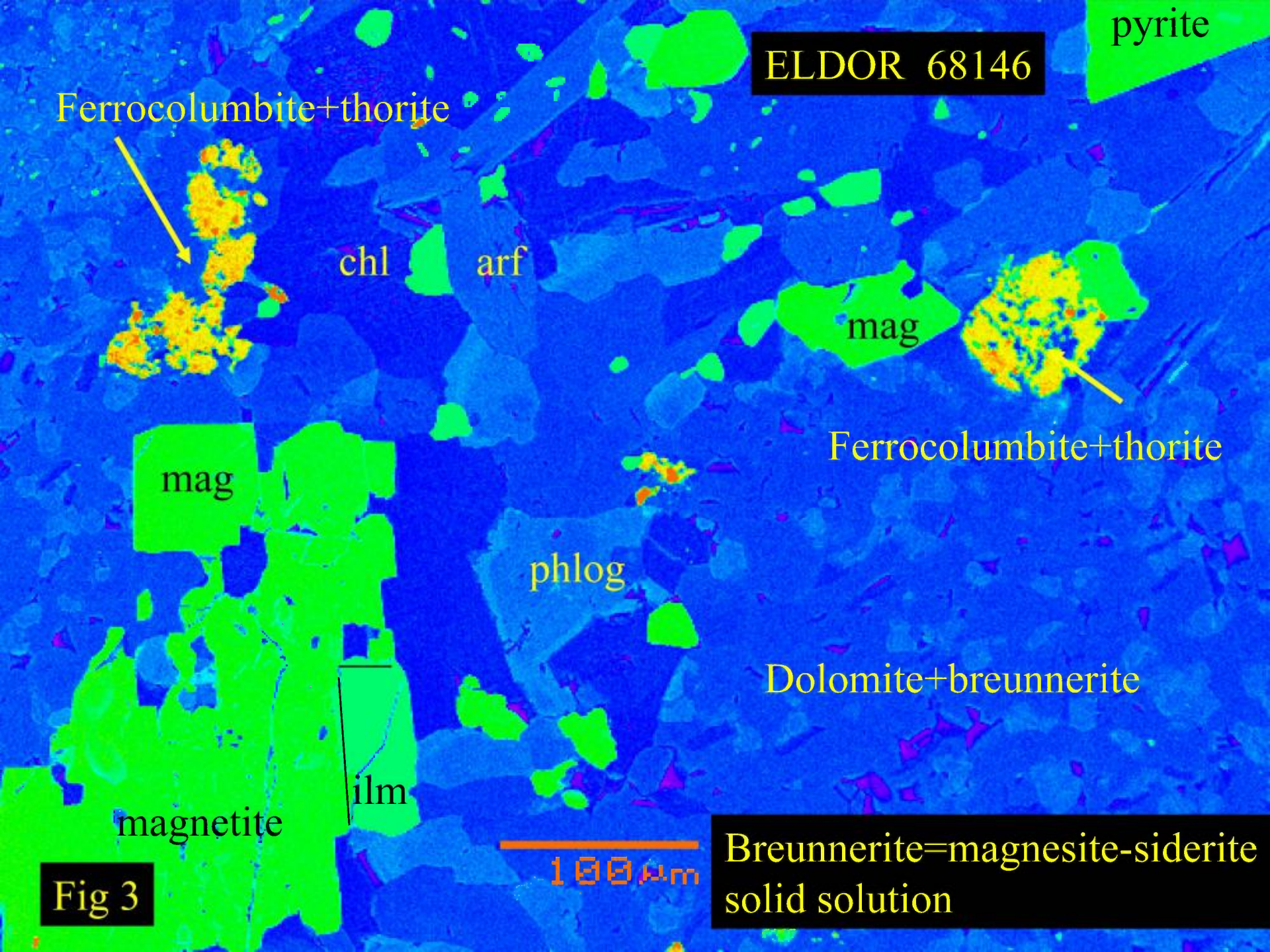
ELDOR 68146
pyrite
Ferrocolumbite+thorite
chl
arf
mag
Ferrocolumbite+thorite
mag
phlog
Dolomite+breunnerite
ilm
magnetite
100 µm
Fig 3
Breunnerite=magnesite-siderite solid solution

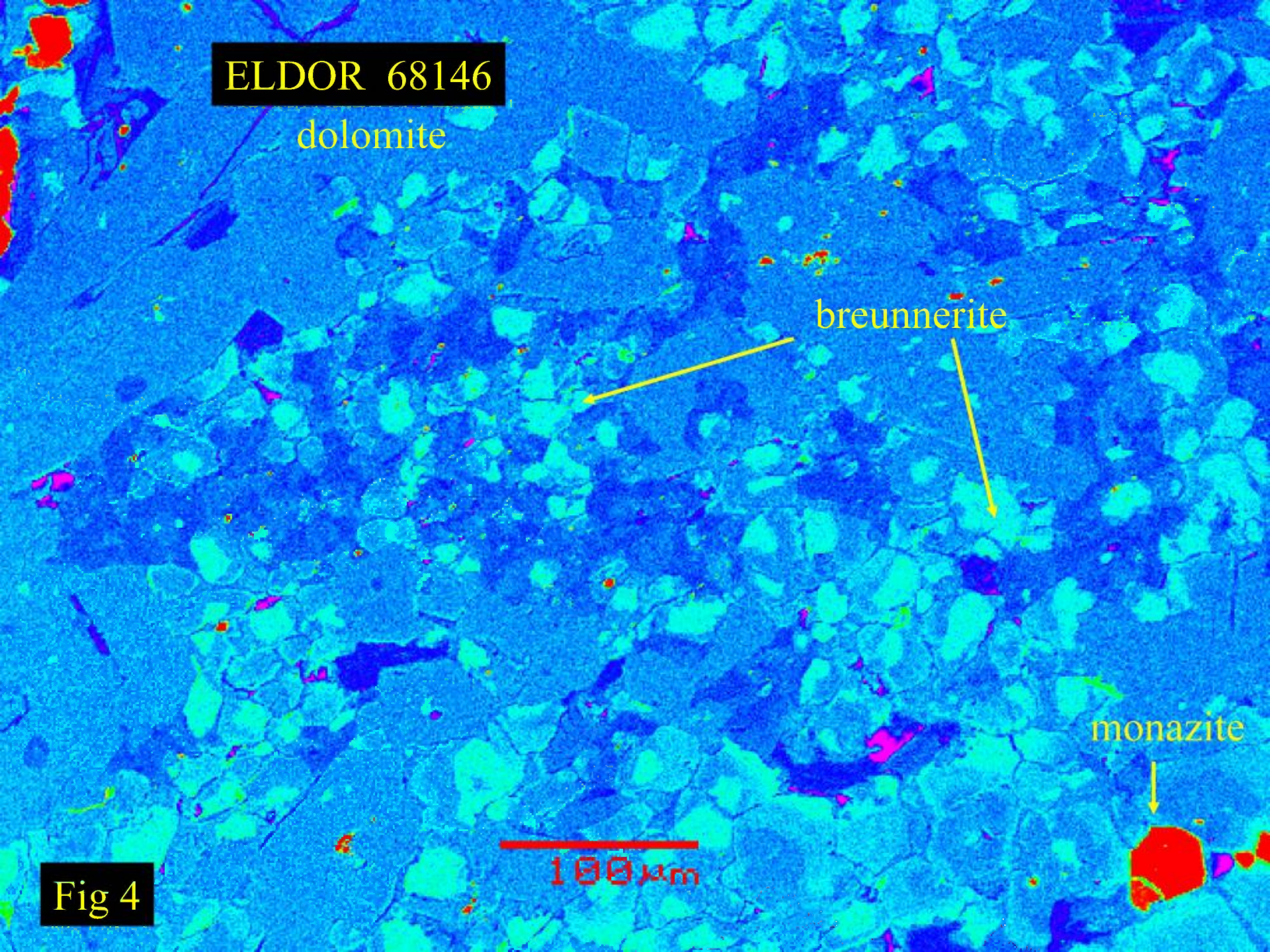

Fig 4

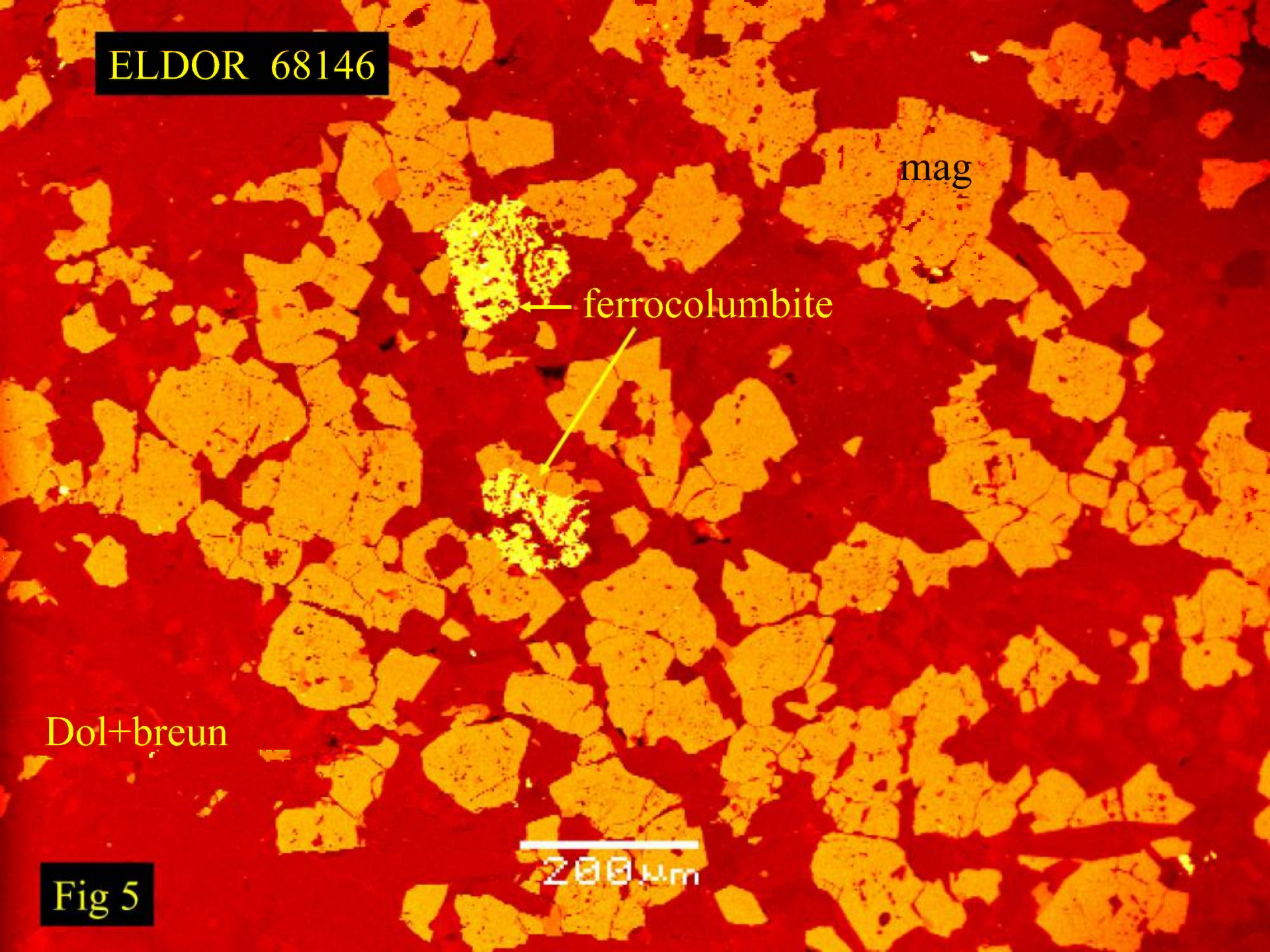

Fig 5

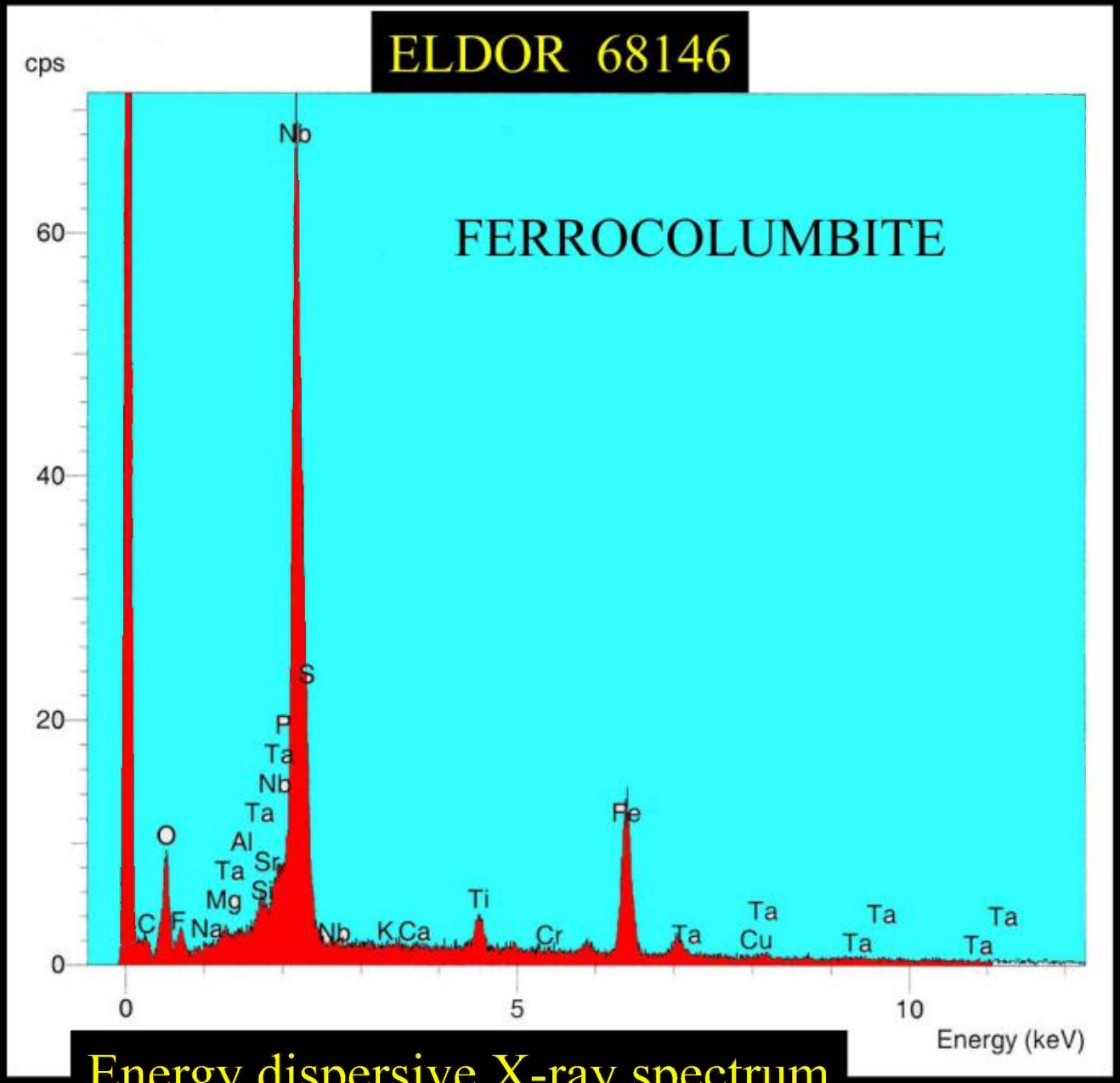

Energy dispersive X-ray spectrum

Fig 6

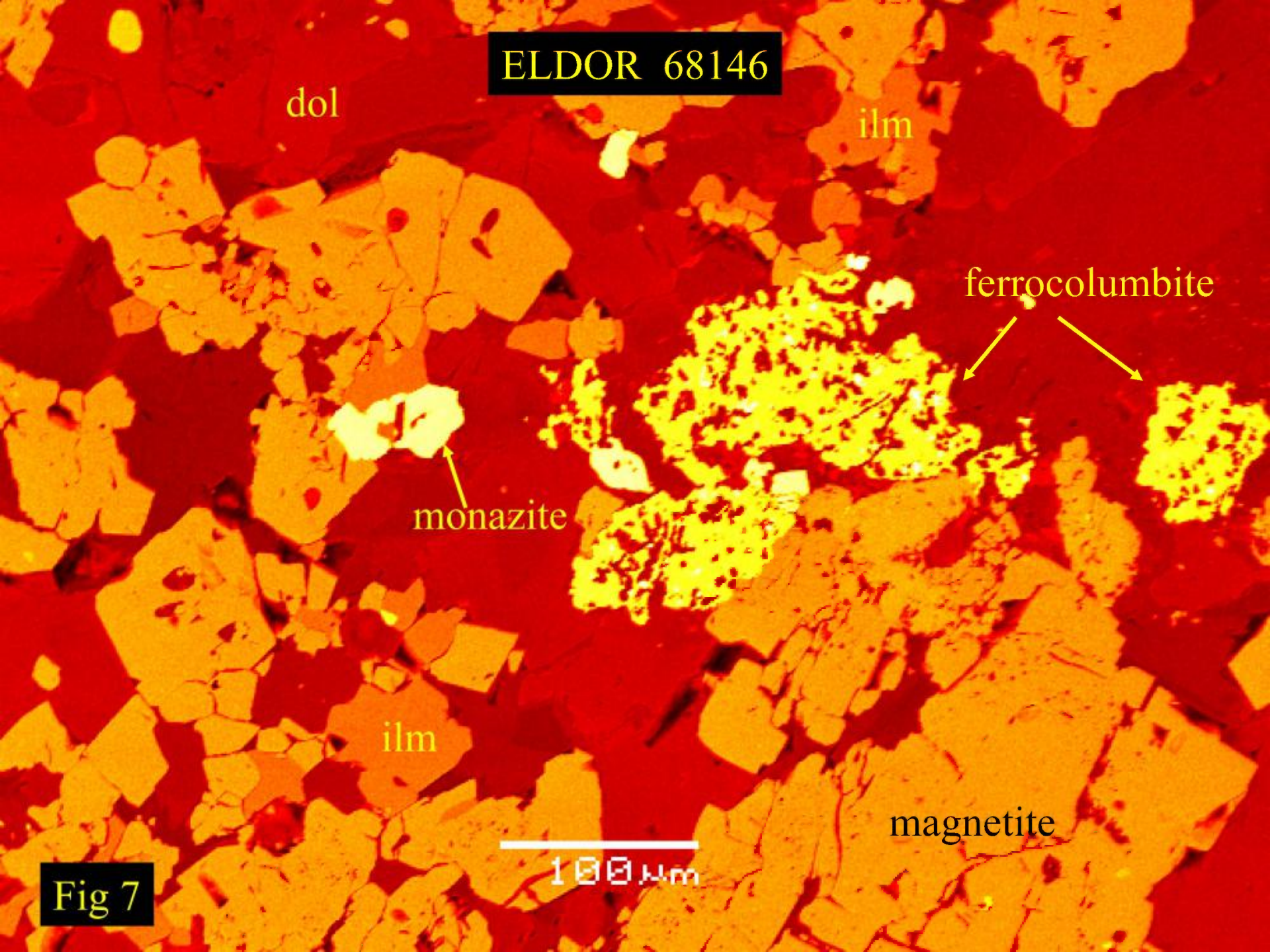
ELDOR 68146
dol
ilm
ferrocolumbite
monazite
ilm
magnetite
100µm

Fig 7

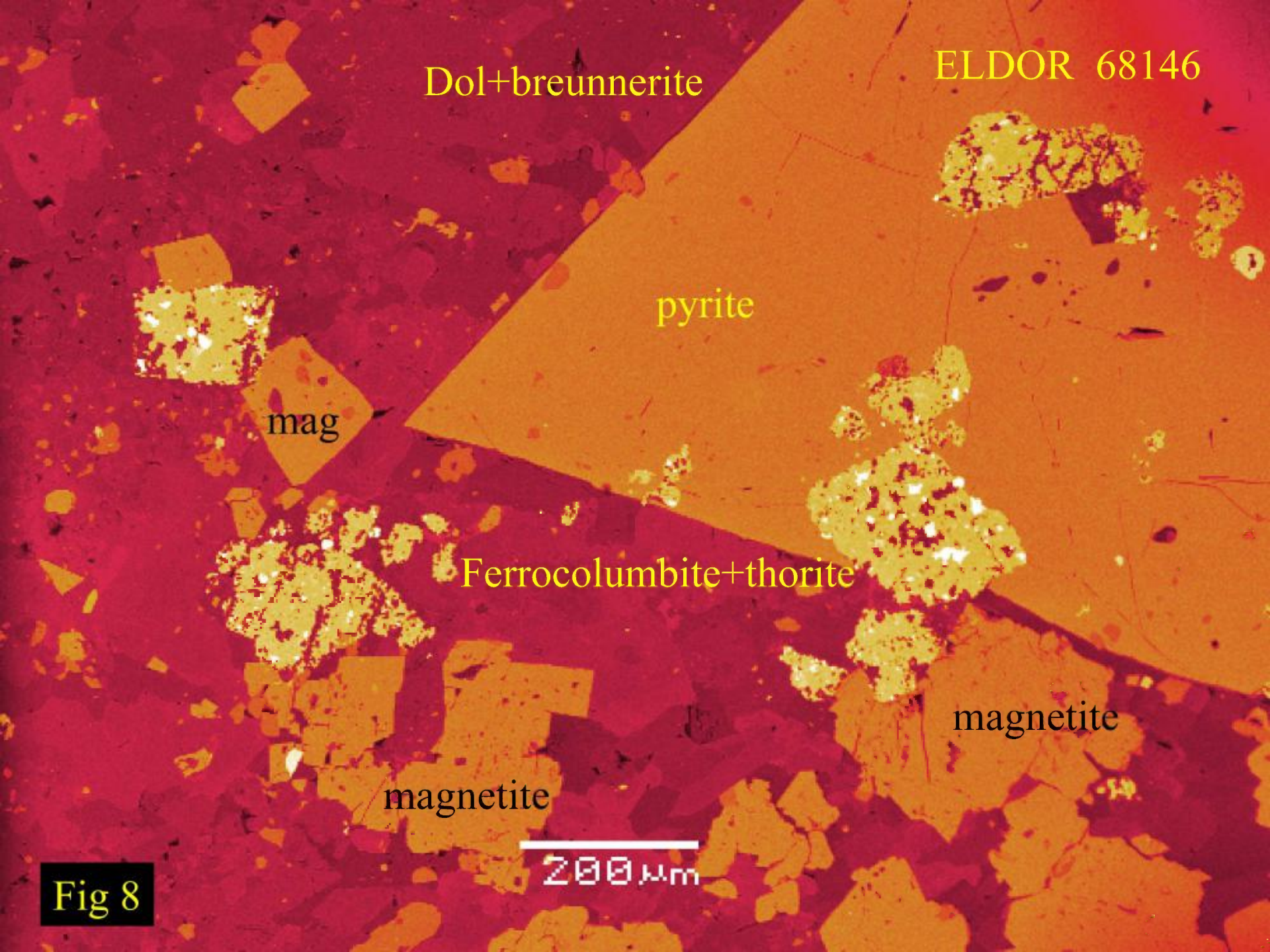
ELDOR 68146
Dol+breunnerite
pyrite
mag
Ferrocolumbite+thorite
magnetite
magnetite
200 µm

Fig 8

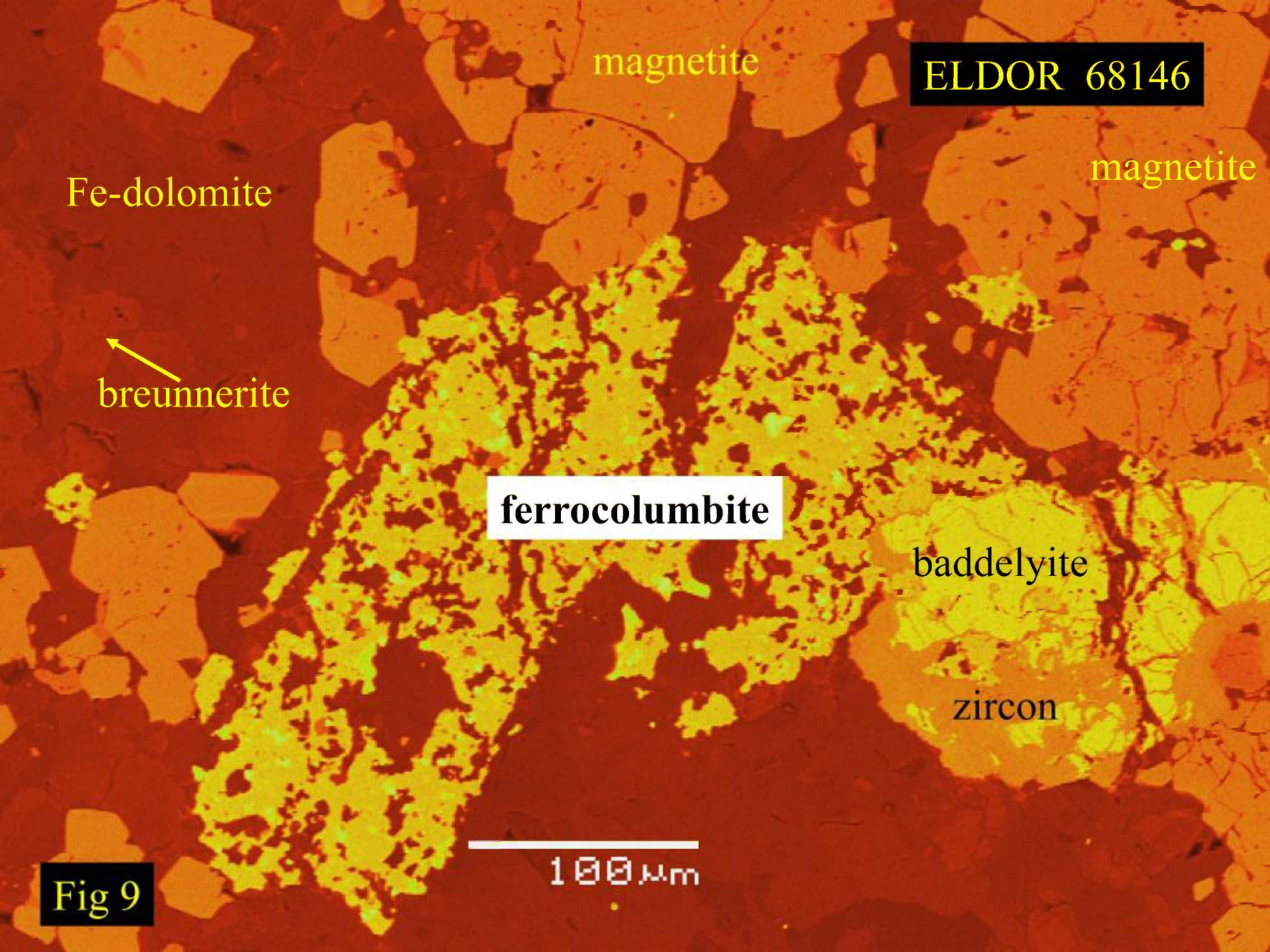
magnetite
ELDOR 68146
magnetite
Fe-dolomite
breunnerite
ferrocolumbite
baddelyite
zircon
100 µm

Fig 9

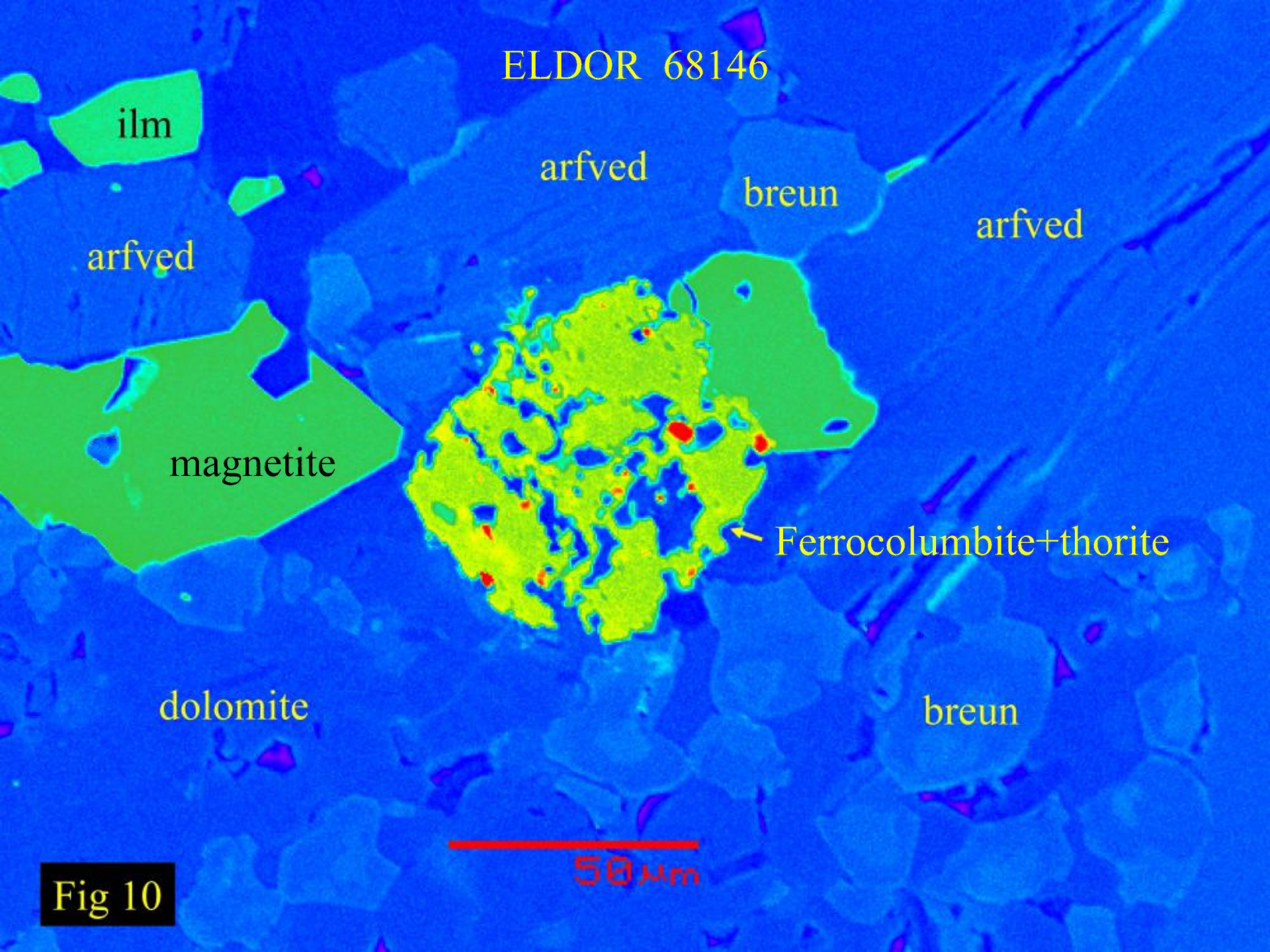
ELDOR 68146
ilm
arfved
breun
arfved
arfved
magnetite
Ferrocolumbite+thorite
dolomite
breun
50 µm

Fig 10

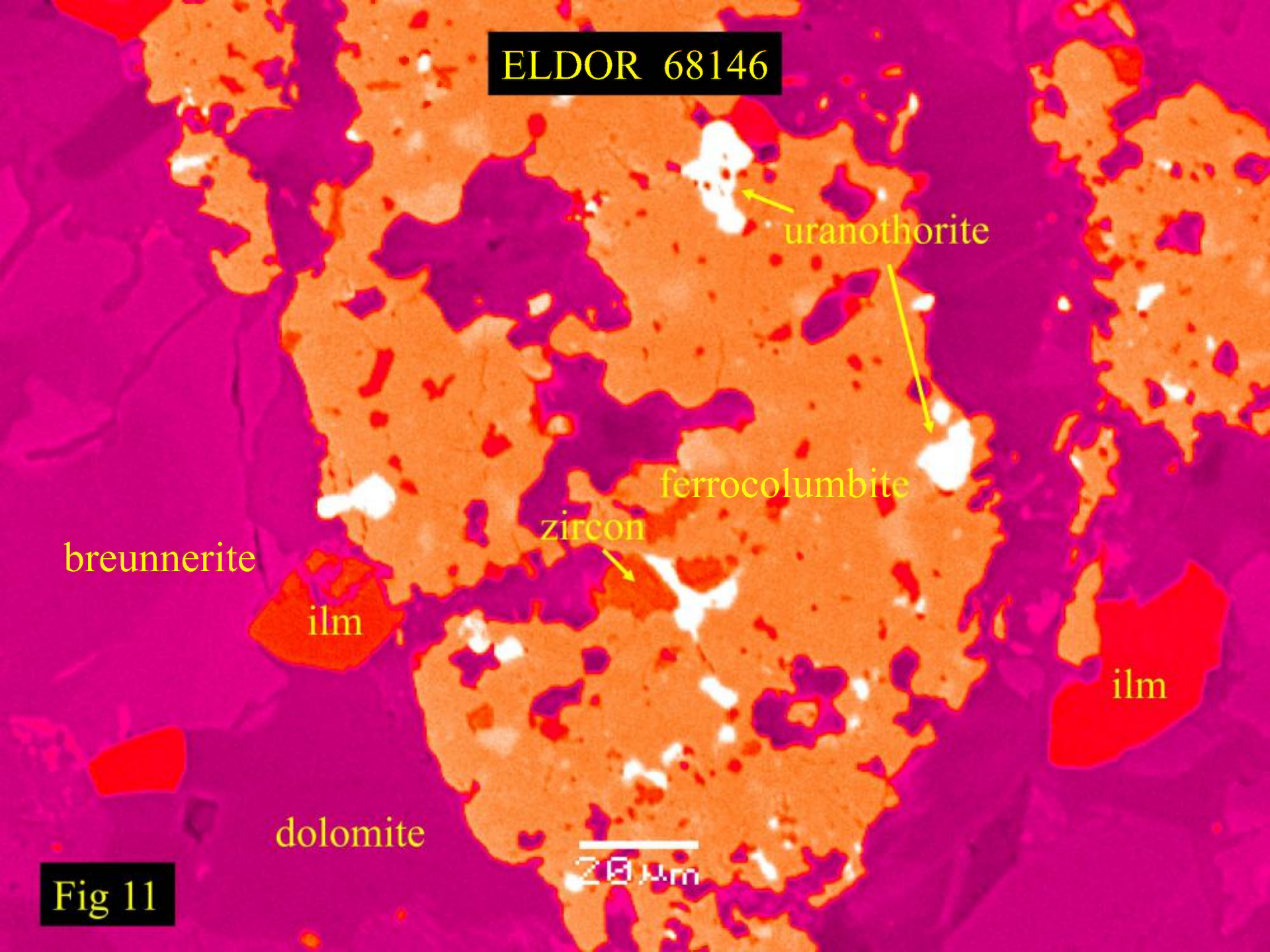
ELDOR 68146
uranothorite
ferrocolumbite
zircon
breunnerite
ilm
ilm
dolomite
20 µm

Fig 11

ELDOR 68151

ELDOR 68151 ***Apatite-"silicate"-magnetite dolomite carbonatite***

This sample is modally heterogeneous with some portions being enriched in magnetite whereas other portions are rich in carbonate and/or apatite (Figs. 1-3). The principal minerals present are magnetite, apatite, chlorite pseudomorphs after an unidentifiable silicate, "pyrochlore" and ferroan dolomite.

Magnetite forms subhedral to irregular angular crystals (Figs. 1-2, 4) and crystal fragments that range in size up to 0.5 cm in width. The magnetite lacks detectable Ti, Mg and Mn and ilmenite exsolution lamellae are not present. Inclusions occurring in the magnetite are ZnS, PbS, apatite, and rare $Ca(Zr,Nb)O_3$. Apatite forms anhedral crystals (Figs, 3-4, 6-9) which are typically inclusion-free. The apatite contains no detectable Sr or rare earth elements. Magnetite-rich (25-35 vol%) portions of the rock are also enriched in similar amounts of a subhedral-to-euhedral phase which has been completely pseudomorphed by laths of Mg-Fe chlorite, anhedral dolomite, anhedral calcite and thin small plates of magnetite (Figs 1-2). The habit is suggestive of former) pyroxene or olivine. The matrix in which the above and the "pyrochlore" are set consists of coarse grained ferroan dolomite (Figs.3, 4-7) and thin laths and plates of Mg-Al-Fe chlorite. The habit of the latter suggests they are pseudomorphs after former phlogopite. Hence, the original matrix was phlogopite set in a mesostasis of ferroan dolomite. Minor amounts of calcite are present (figs. 6 & 7). Common in the dolomite-chlorite matrix (Figs. 12 & 14) are clusters of small prisms of pyrophanite [$(Mn,Fe)TiO_3$].

ELDOR 68151

"Pyrochlore" is common throughout the samples as large (up to 500 um) euhedral through subhedral to resorbed irregular crystals (Figs. 11-18). Commonly these occur as discrete crystals in the dolomite matrix but can also be found intergrown with magnetite and/or apatite. BSE-imagery and X-ray spectrometry demonstrates that the "pyrochlore" is a very complex multi-phase mixture consisting of pyrochlores of diverse composition, fersmite, zircon and (Th, U,Pb)O_2 . Figures 12-13 and 15-18, demonstrate the complexity of the intergrowths. Pyrochlores are uranopyrochlores of various Ta-U-contents together with a discrete Th-rich pyrochlore. Representative compositions are given below. Fersmite occurs intergrown with the pyrochlores and in many instances forms prismatic crystals that appear to have formed prior to the pyrochlore (Fig. 13). However, apparently late-forming fersmite can also be observed (Fig.15). Ferrocolumbite and high Ta_2O_5 (> 15 wt.%) - high UO_2 (>20 wt.%) pyrochlores (as found in sample 68194) are absent from this sample.

Wt.%	Th-pyro	U-Ta-pyro	U-Ta-pyro	fersmite	aeschynite-(Ce)
Na_2O	0.5	n.d.	n.d.	0.4	n.d.
SiO_2	1.0	1.9	0.8	0.6	n.d.
CaO	6.5	14.6	10.1	13.9	3.5
TiO_2	0.5	9.2	10.9	3.5	25.0
FeO	5.9	3.3	3.0	1.3	3.3
Nb_2O_5	45.8	41.2	40.0	71.4	29.8
Ta_2O_5	n.d	7.7	6.7	1.1	1.8
La_2O_3	0.7	0.9	0.6	0.5	5.2
Ce_2O_3	4.0	1.9	2.3	2.3	15.7
Pr_2O_3	0.6	0.2	0.7	0.2	1.5
Nd_2O_3	3.1	0.4	1.6	1.2	5.1
ThO_2	21.9	9.3	11.8	2.3	7.9
UO_2	1.2	6.9	6.3	n.d.	n.d.

ELDOR 68151

Late-forming aeschynite is common in the groundmass of the sample as discrete prismatic crystals set in the dolomite mesostasis (Fig. 19) or more rarely as overgrowths on magnetite (Fig. 20) or pyrochlore (Fig 21). Note that pyrochlores juxtaposed to aeschynite-bearing parts of the sample are not typically overgrown by this mineral (Fig 20).

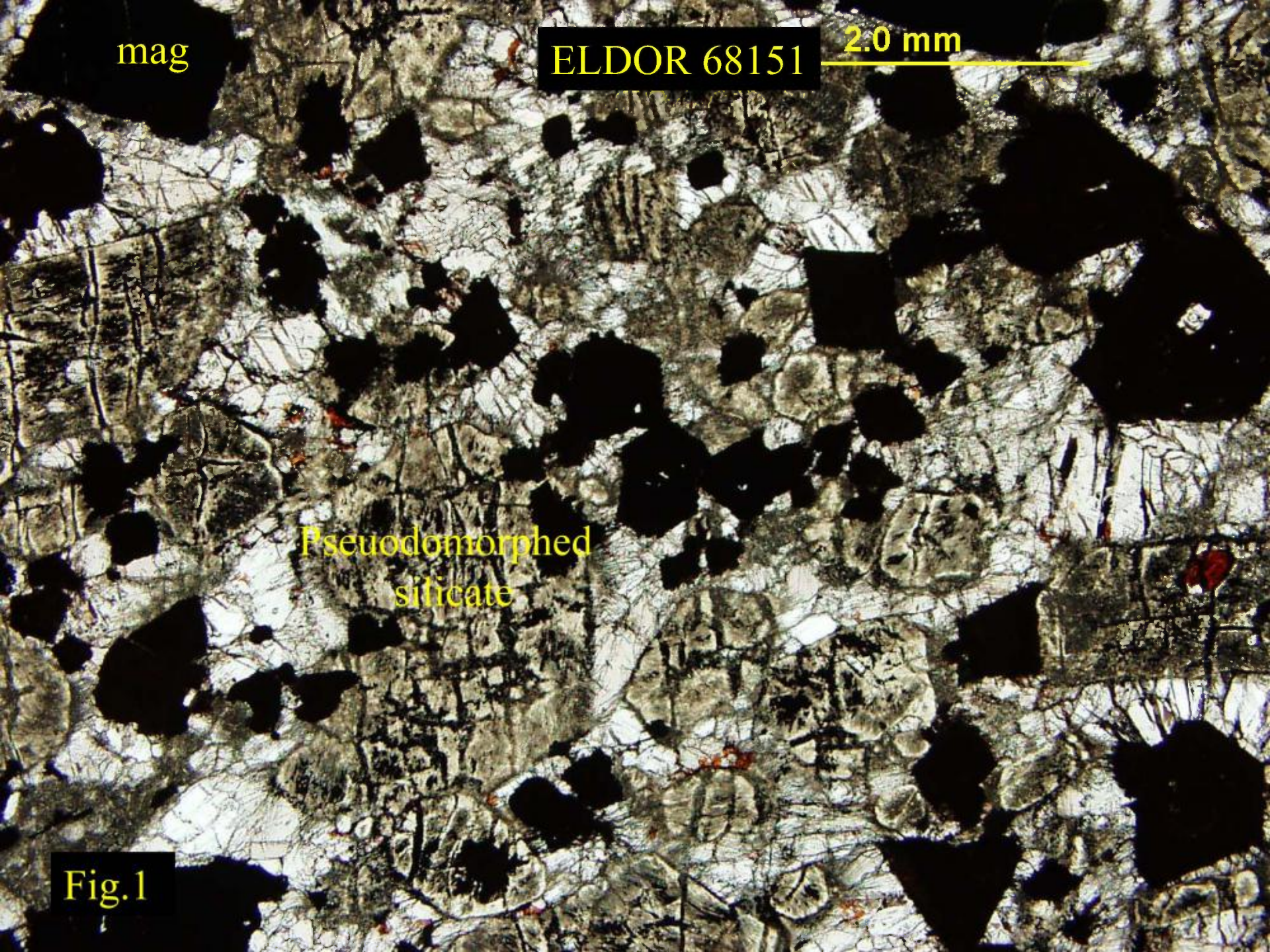

Fig.1

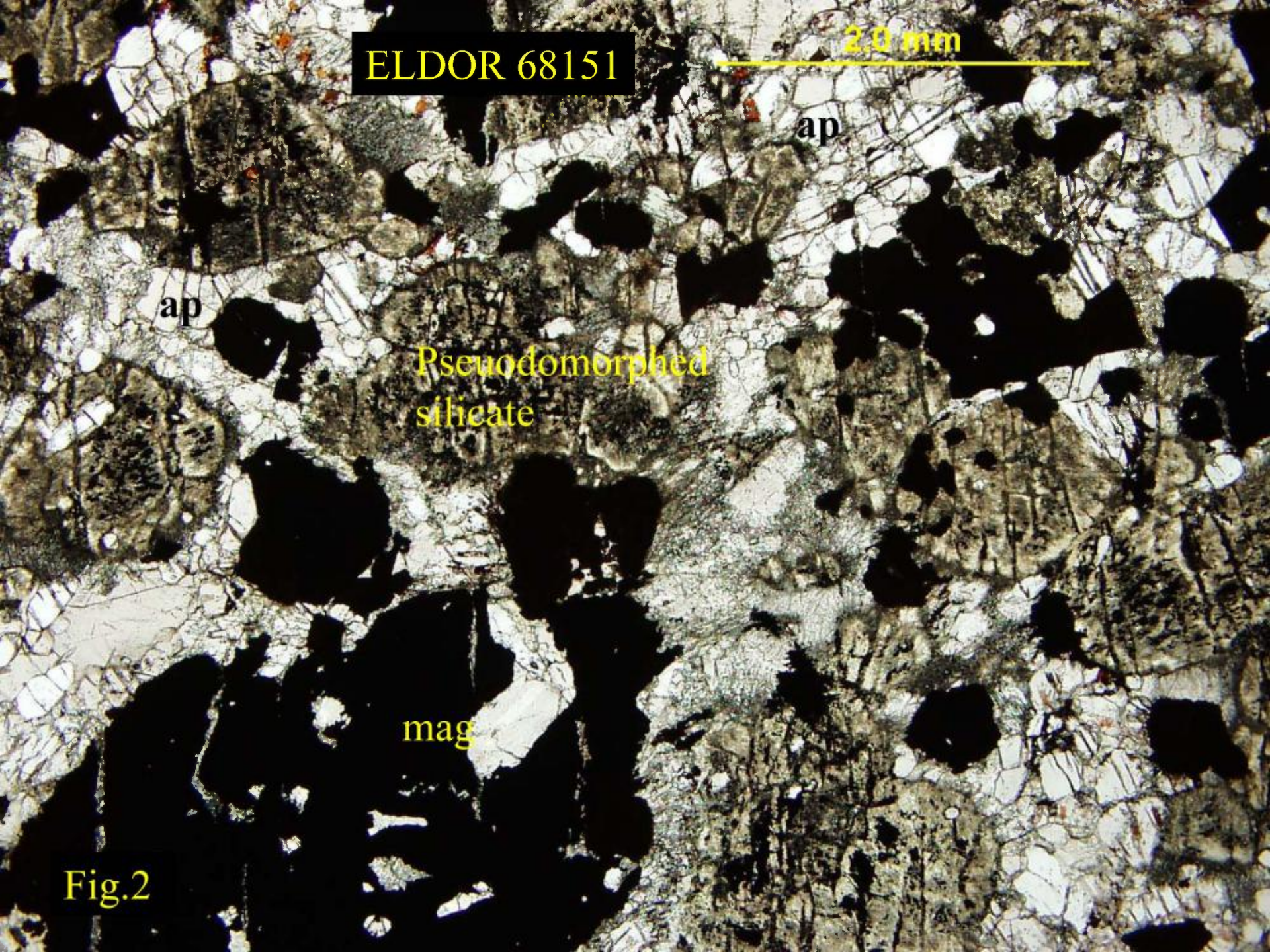

Fig.2

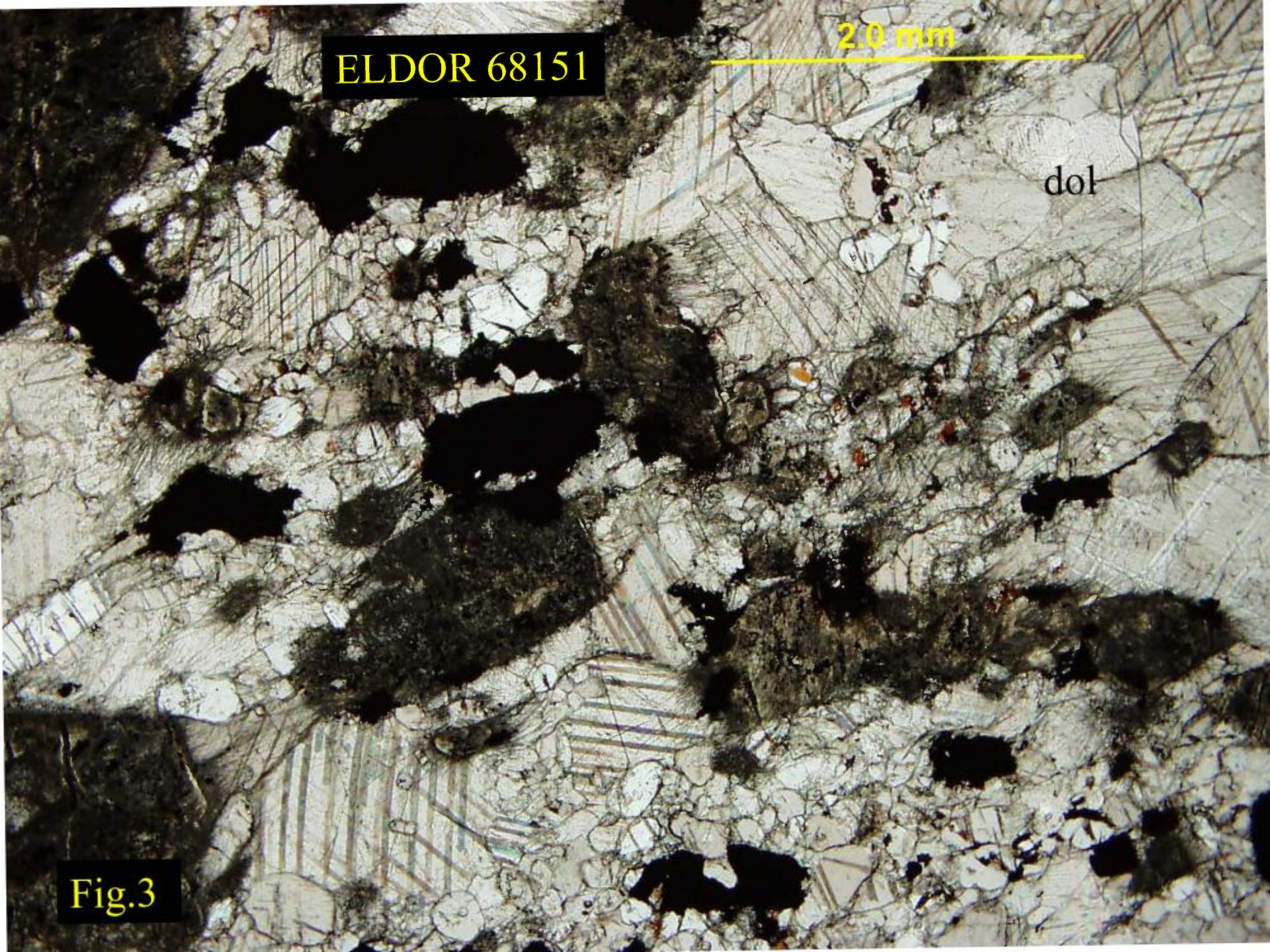

Fig.3

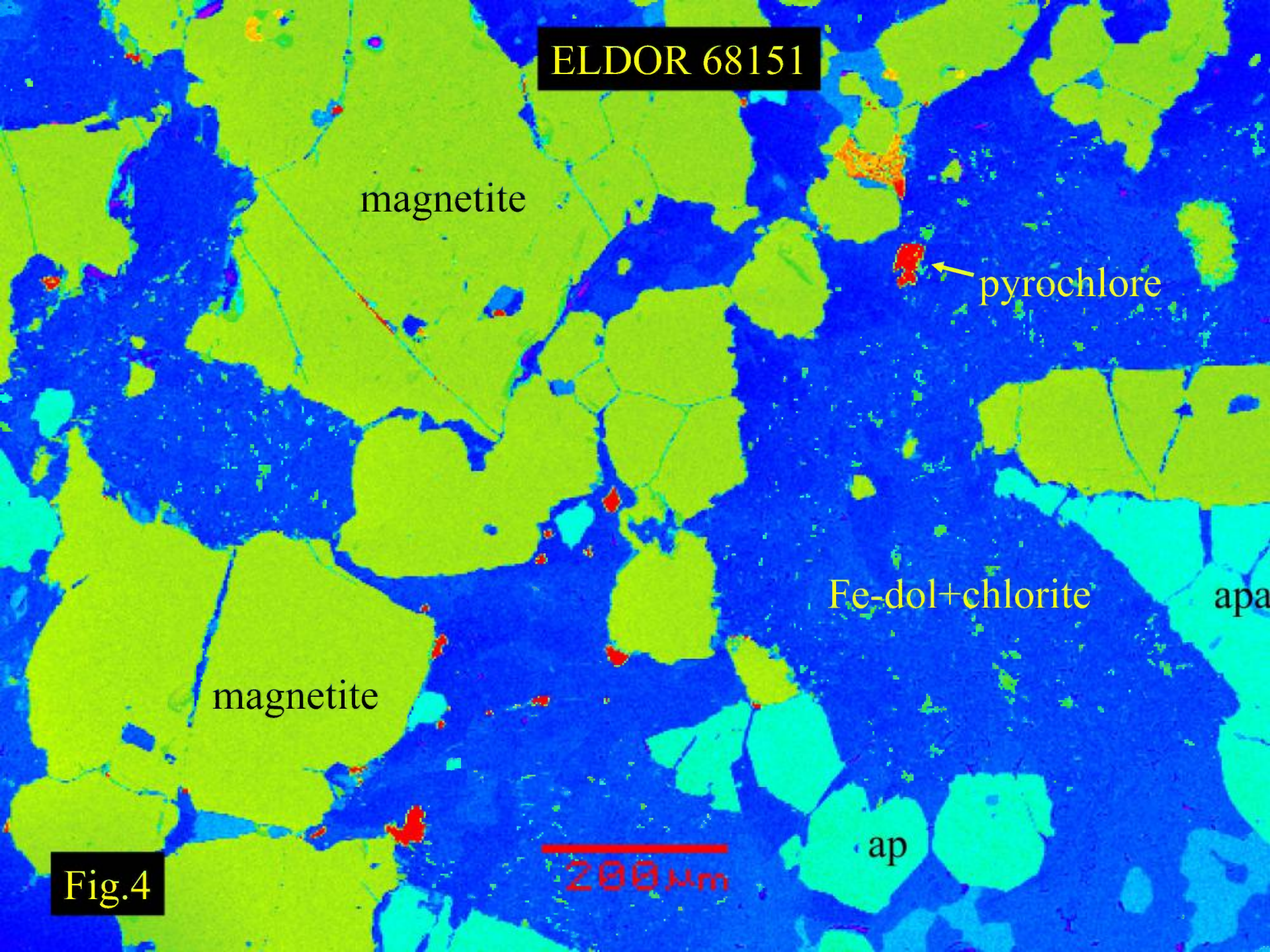
ELDOR 68151
magnetite
pyrochlore
Fe-dol+chlorite
apa
magnetite
ap
200µm

Fig.4

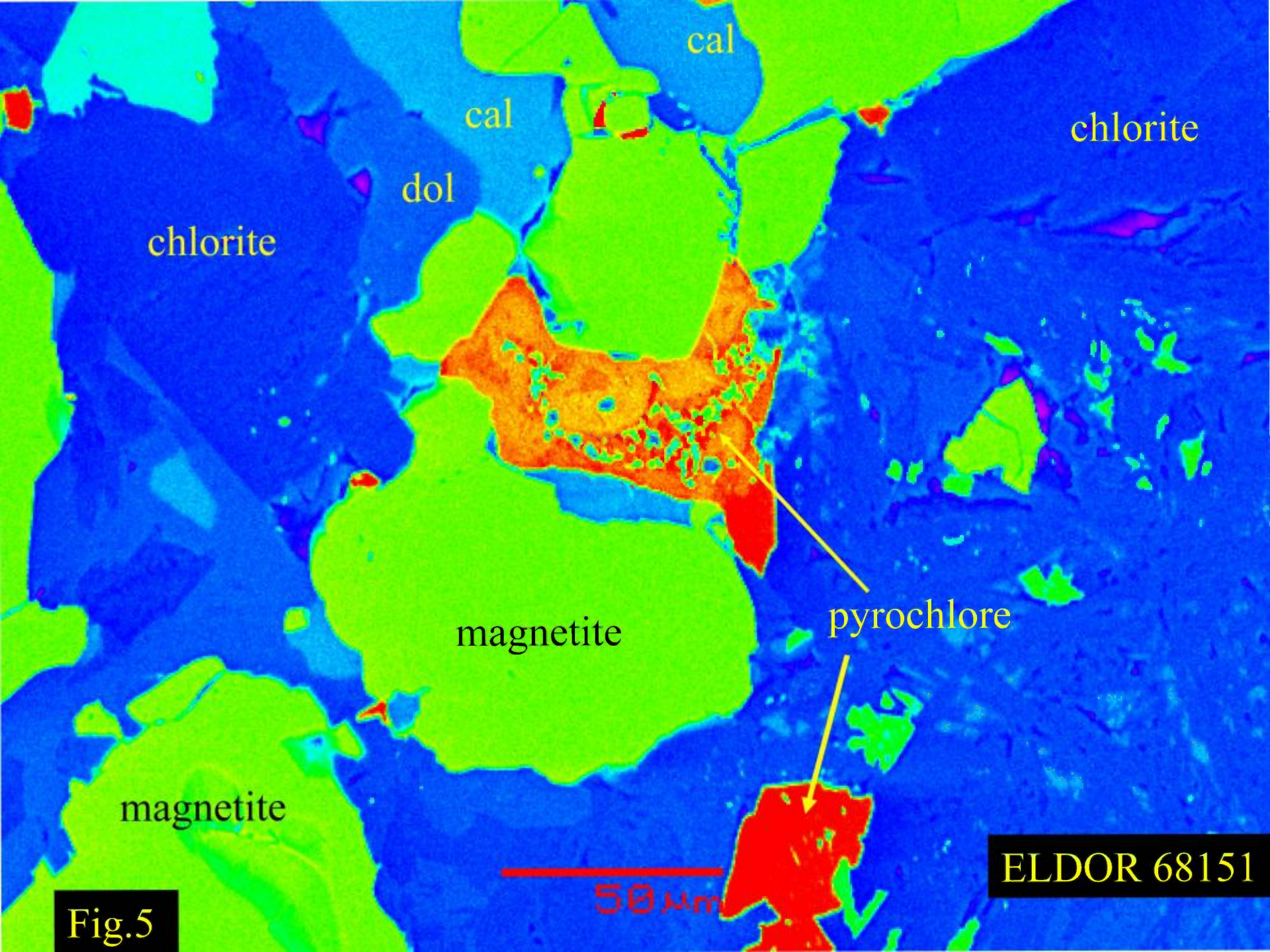
cal
cal
dol
chlorite
chlorite
magnetite
magnetite
pyrochlore
50 µm
ELDOR 68151

Fig.5

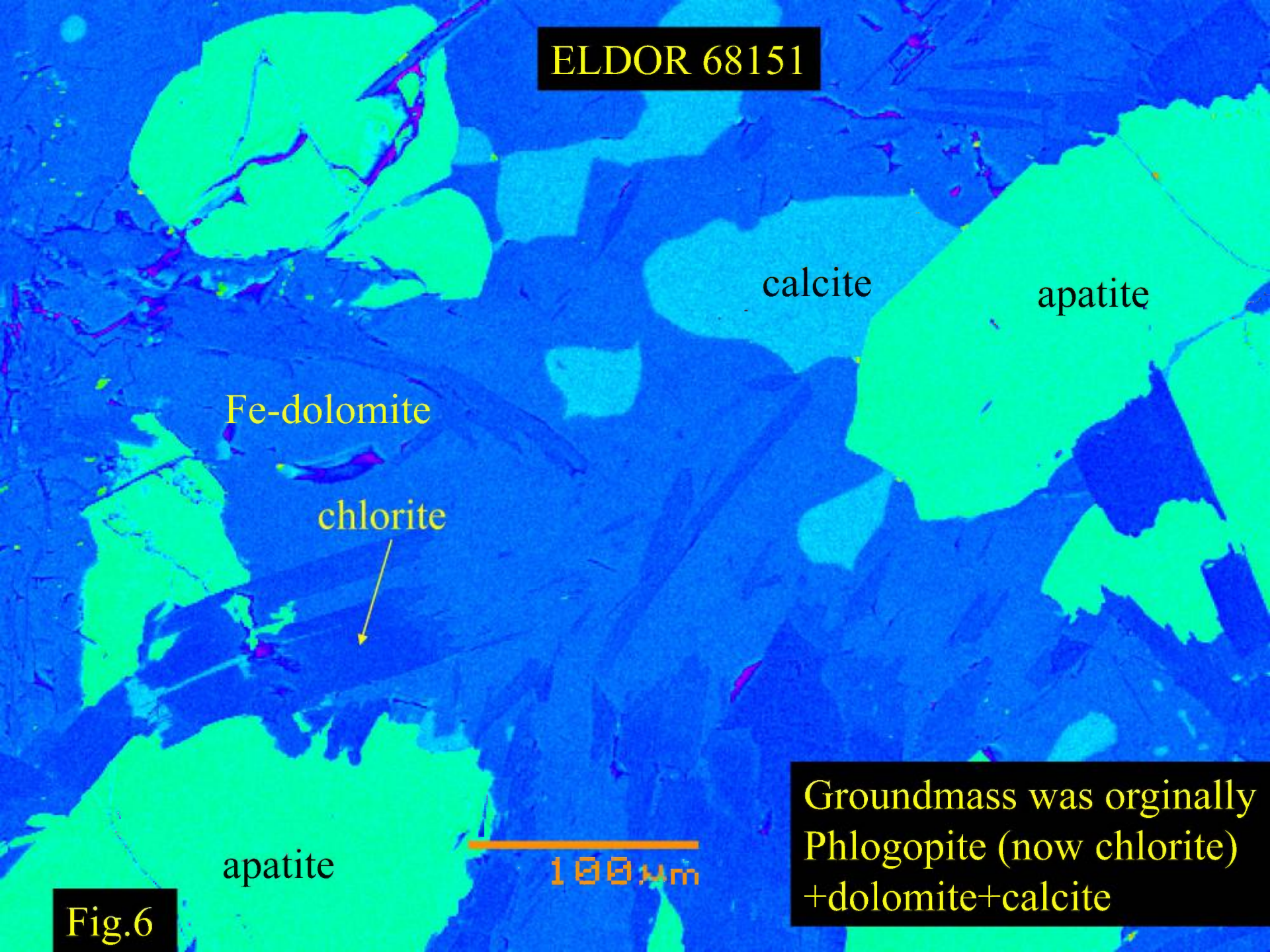
ELDOR 68151
calcite
apatite
Fe-dolomite
chlorite
apatite
100µm
Groundmass was orginally
Phlogopite (now chlorite)
+dolomite+calcite

Fig.6

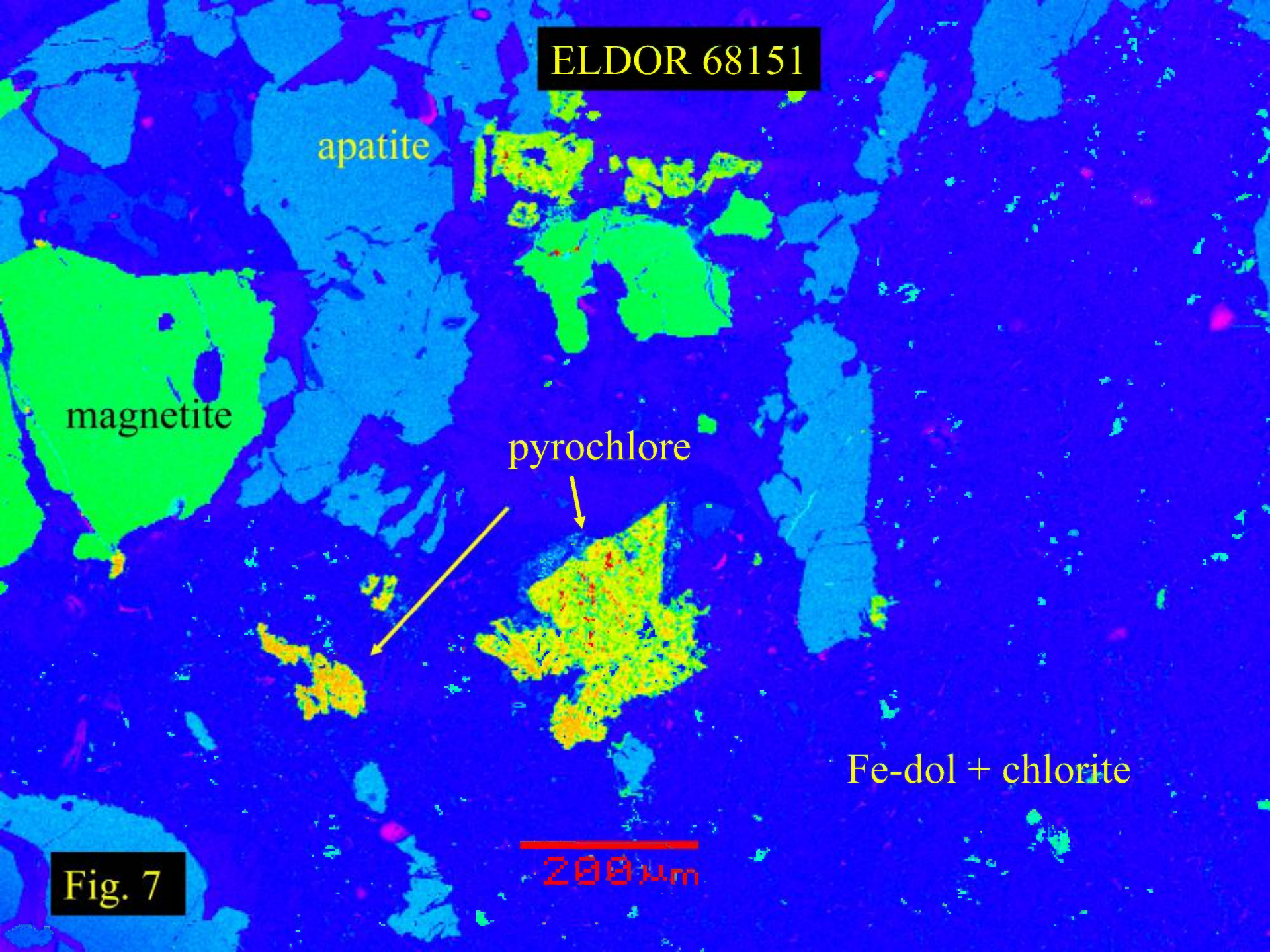
ELDOR 68151
apatite
magnetite
pyrochlore
Fe-dol + chlorite
200µm

Fig. 7

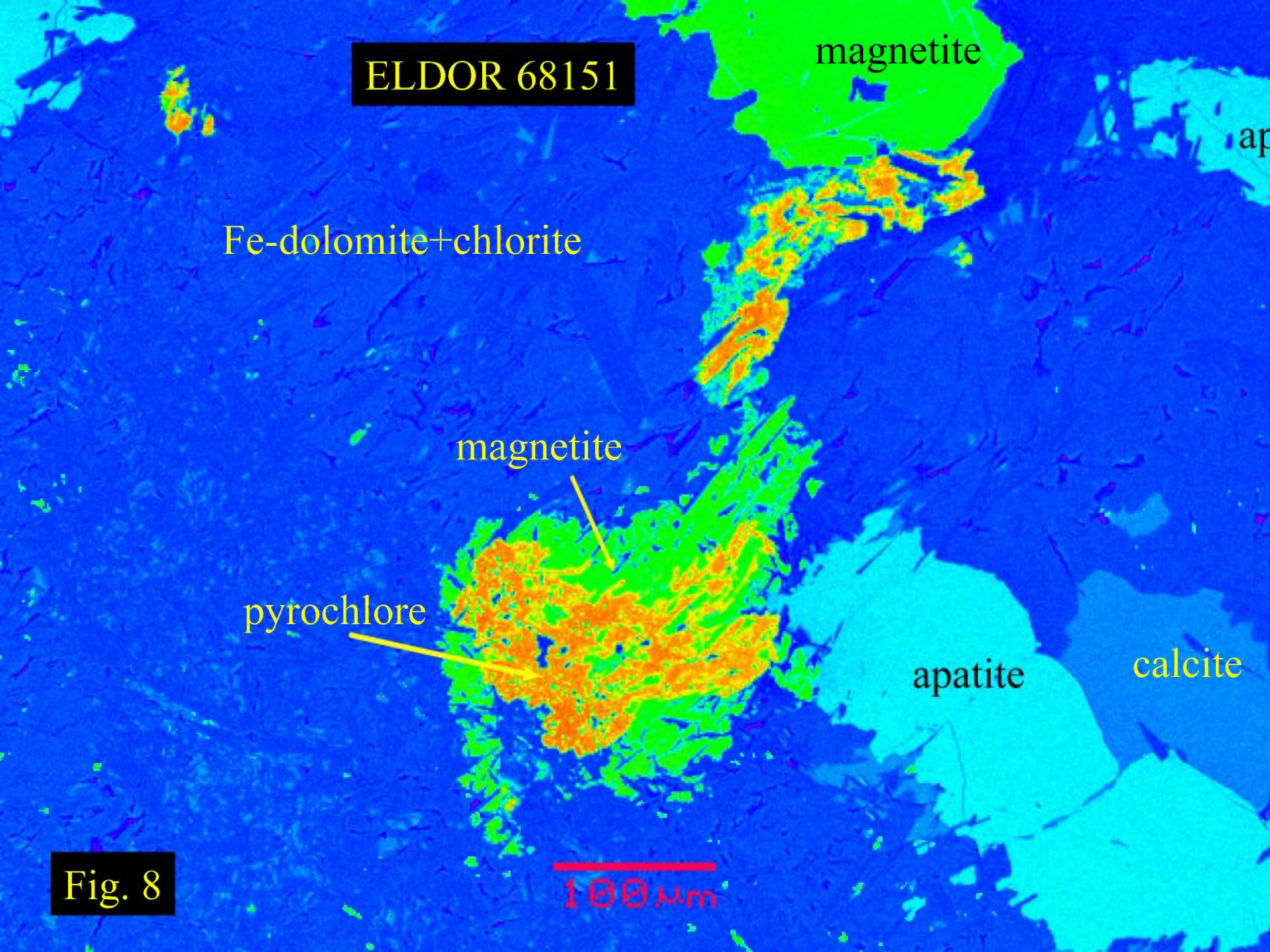
ELDOR 68151
magnetite
Fe-dolomite+chlorite
magnetite
pyrochlore
apatite
calcite
100 µm

Fig. 8

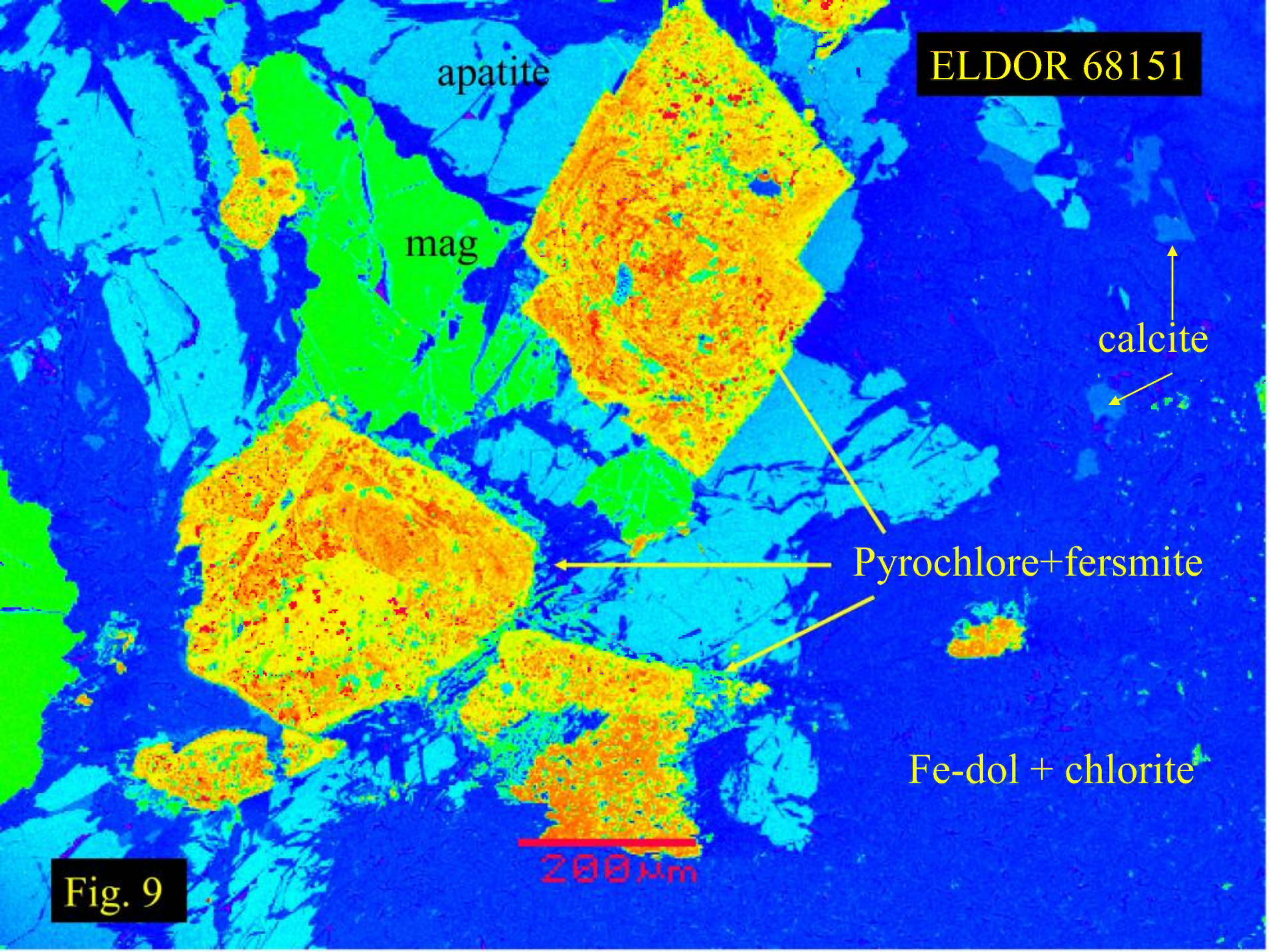
ELDOR 68151
apatite
mag
calcite
Pyrochlore+fersmite
Fe-dol + chlorite
200µm

Fig. 9

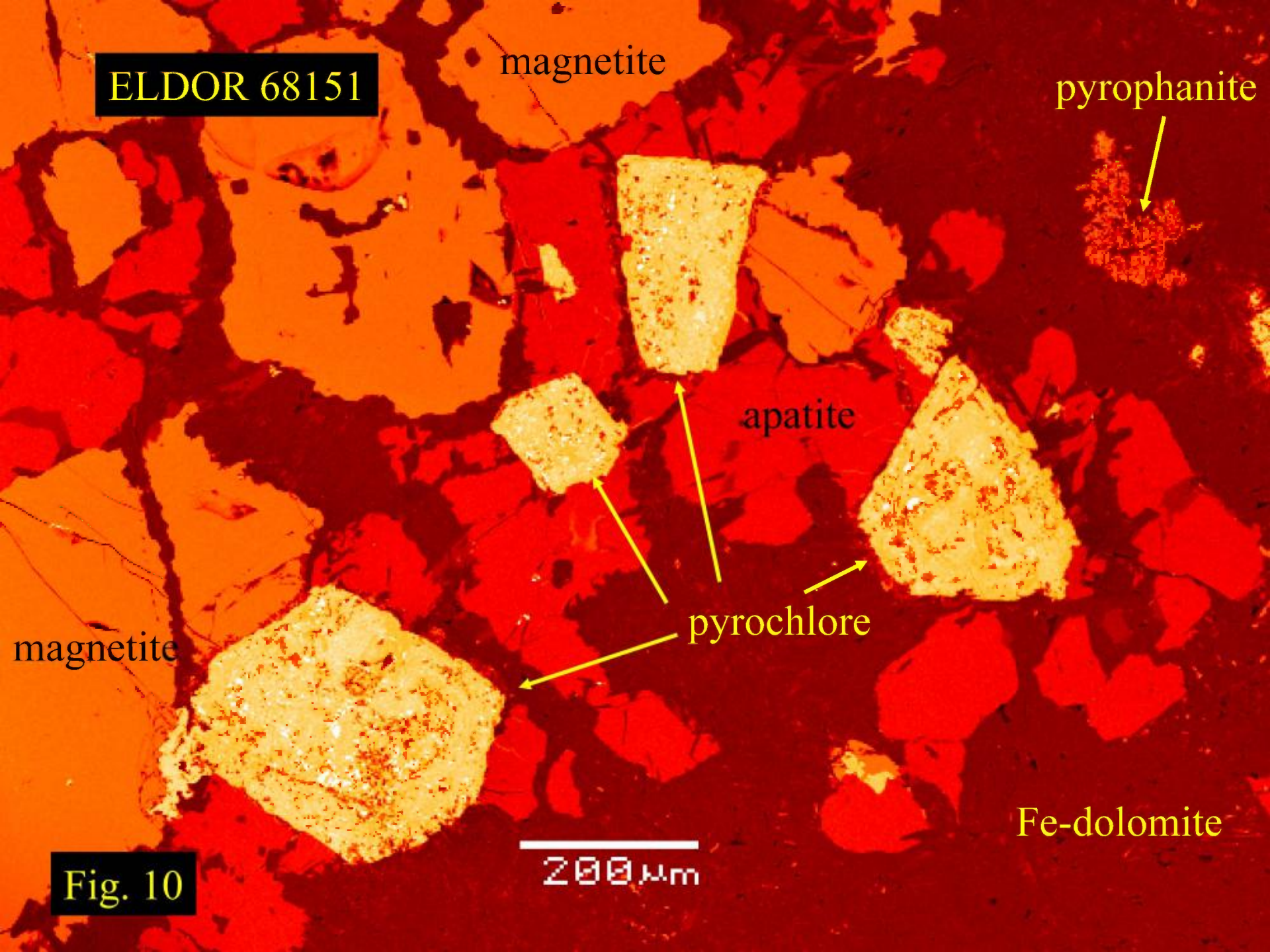
ELDOR 68151
magnetite
pyrophanite
apatite
pyrochlore
magnetite
Fe-dolomite
200µm

Fig. 10

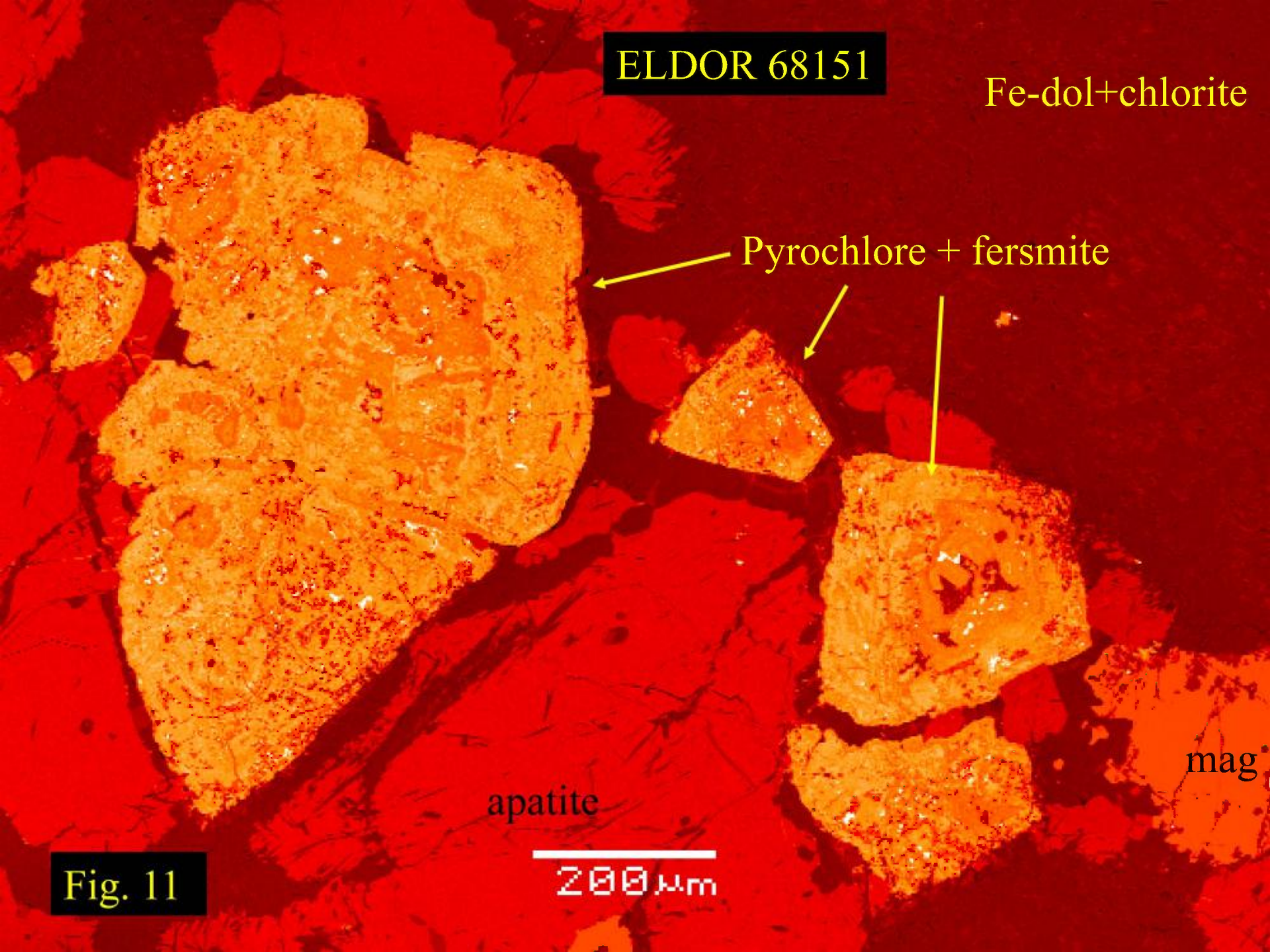
ELDOR 68151
Fe-dol+chlorite
Pyrochlore + fersmite
mag
apatite
200µm

Fig. 11

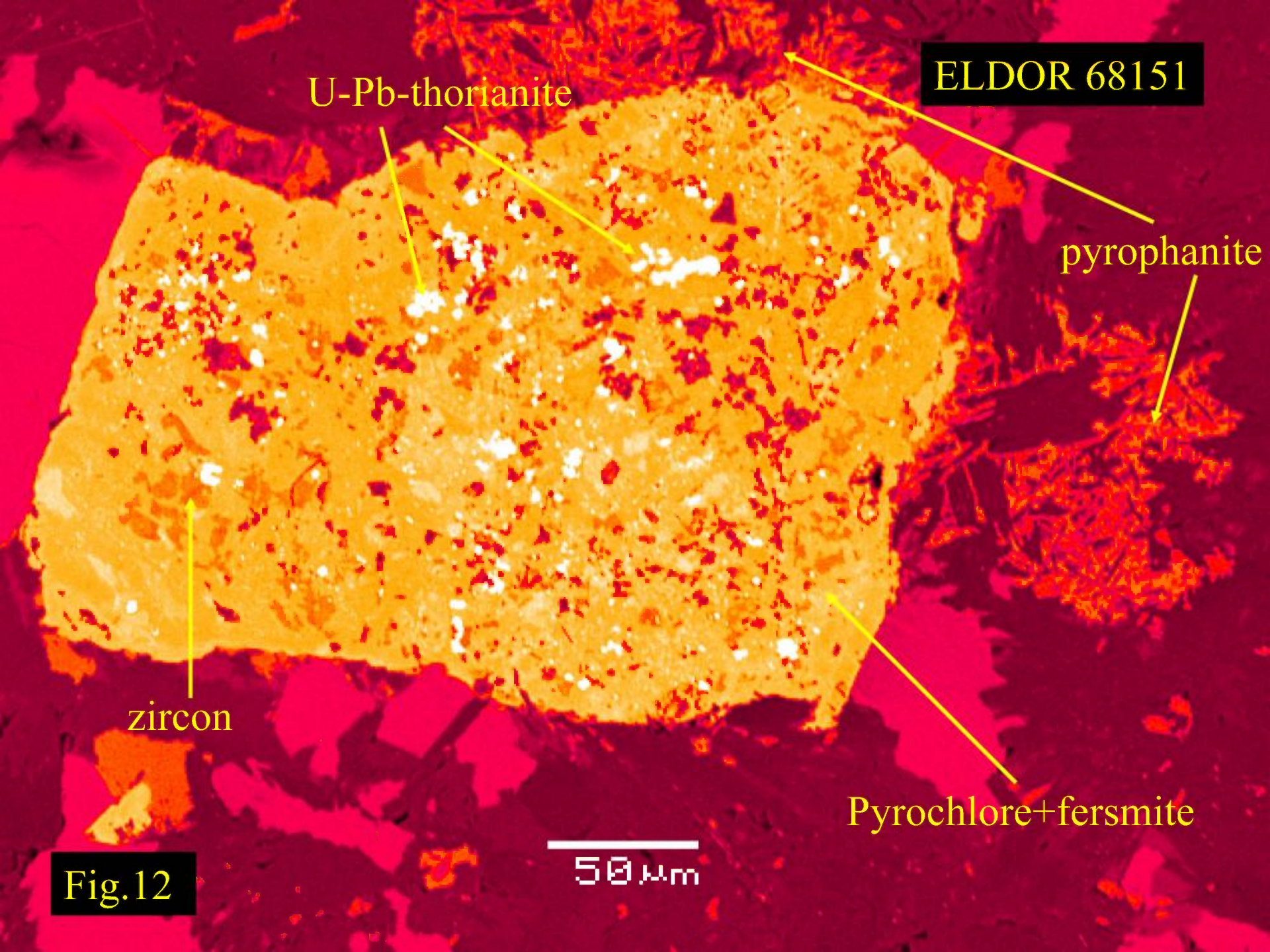
ELDOR 68151
U-Pb-thorianite
pyrophanite
zircon
Pyrochlore+fersmite
50 µm

Fig.12

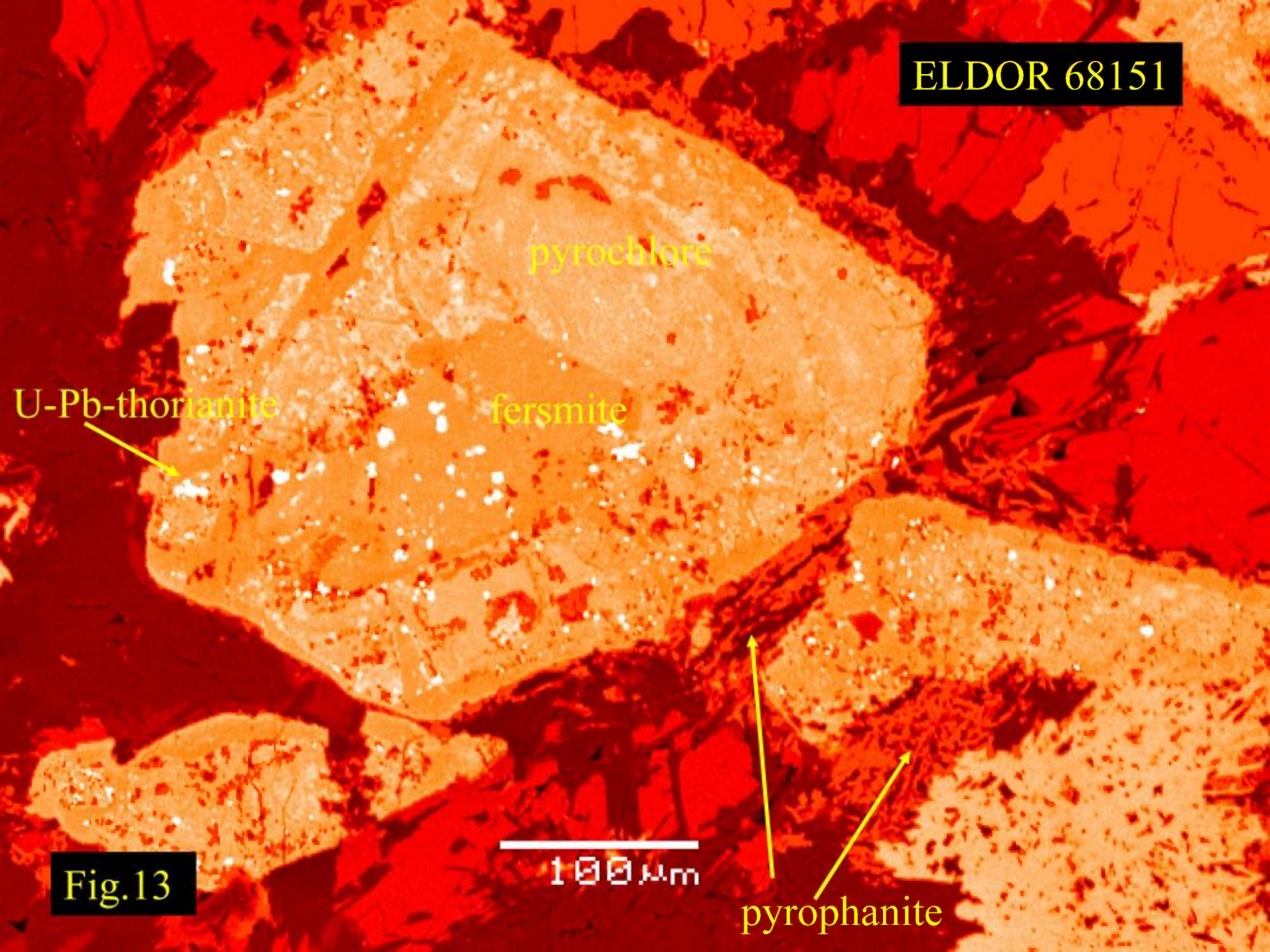
ELDOR 68151
pyrochlore
U-Pb-thorianite
fersmite
100 µm
pyrophanite

Fig.13

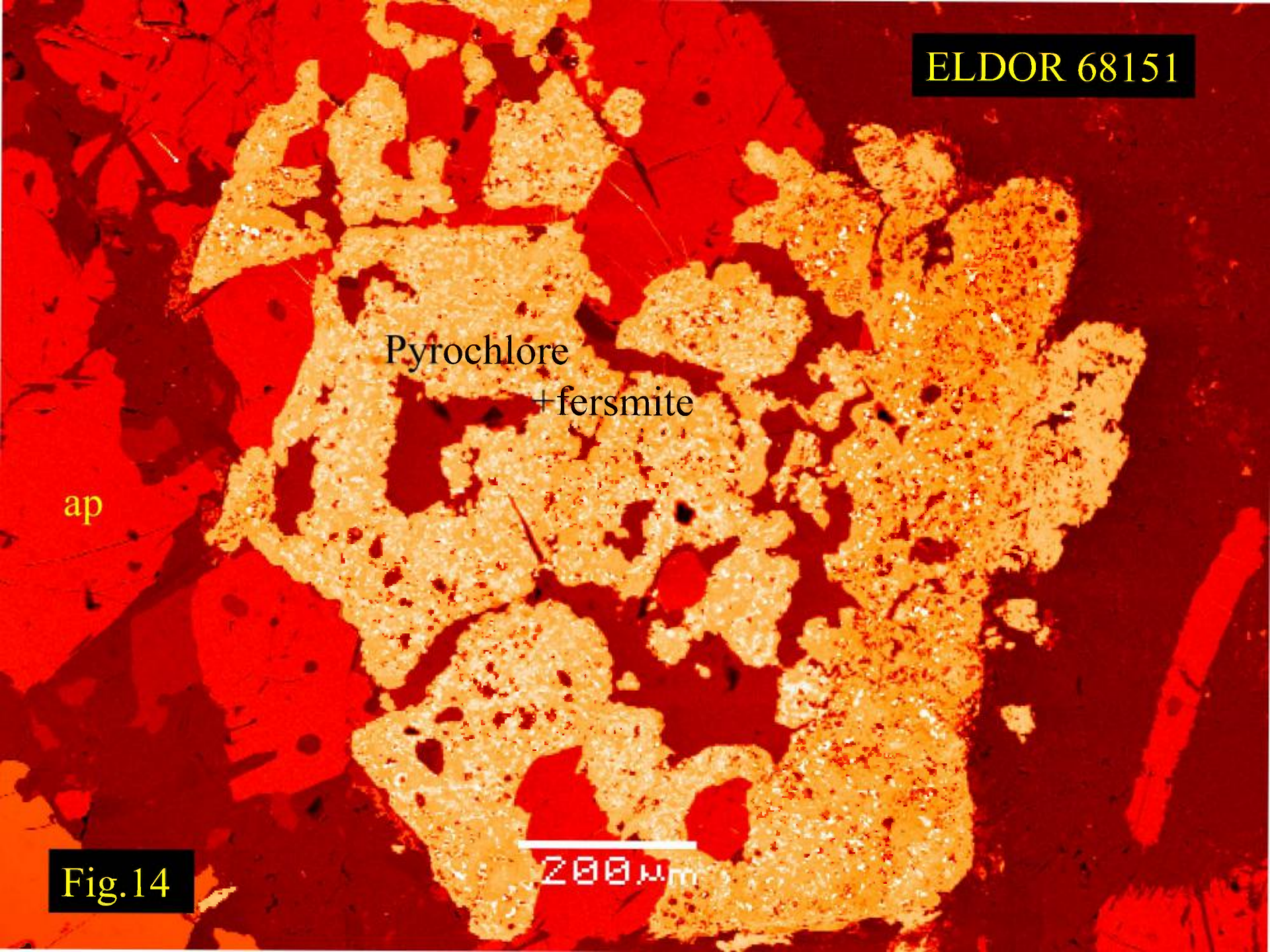

Fig.14

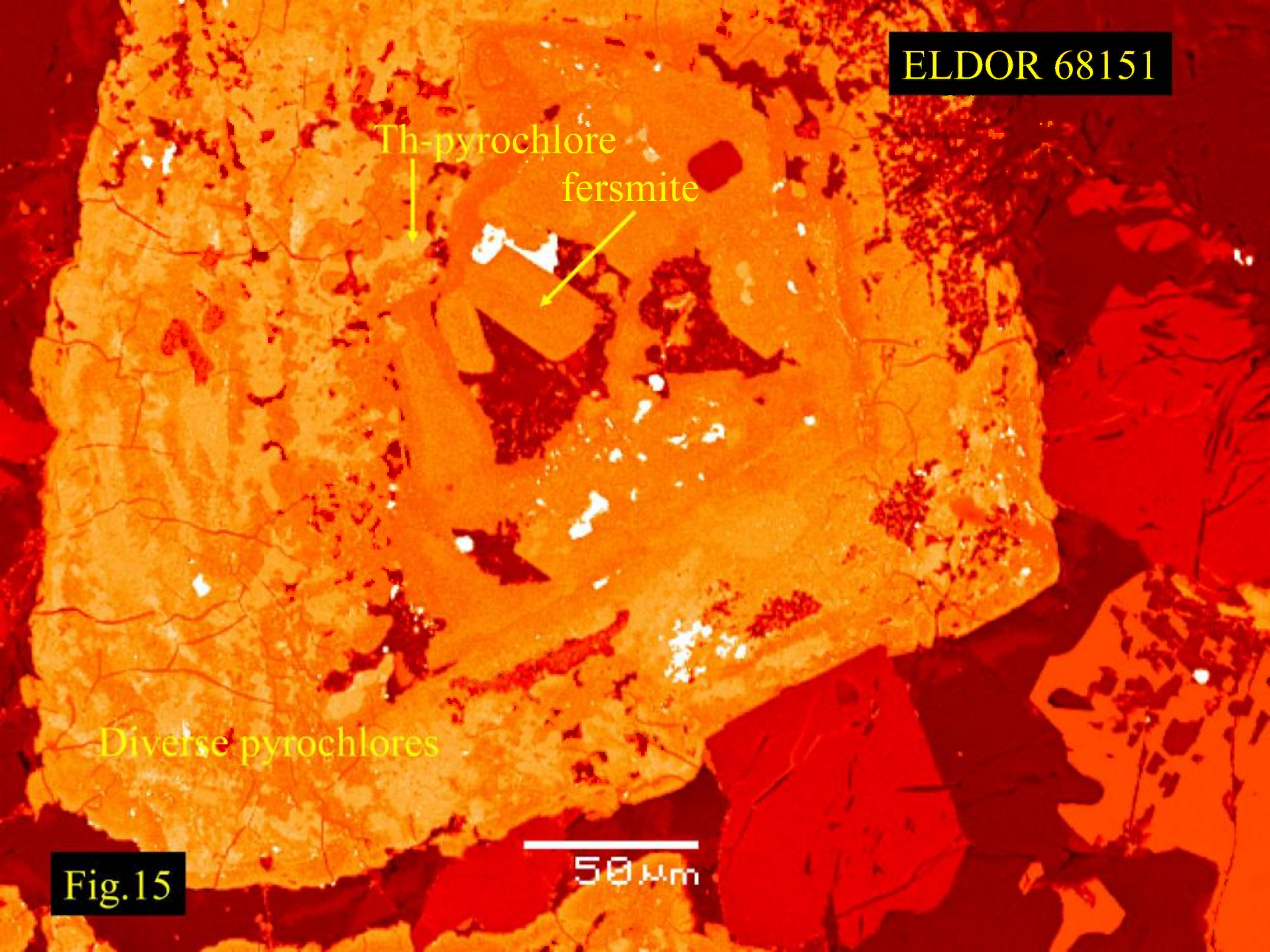
ELDOR 68151
Th-pyrochlore
fersmite
Diverse pyrochlores
50µm

Fig.15

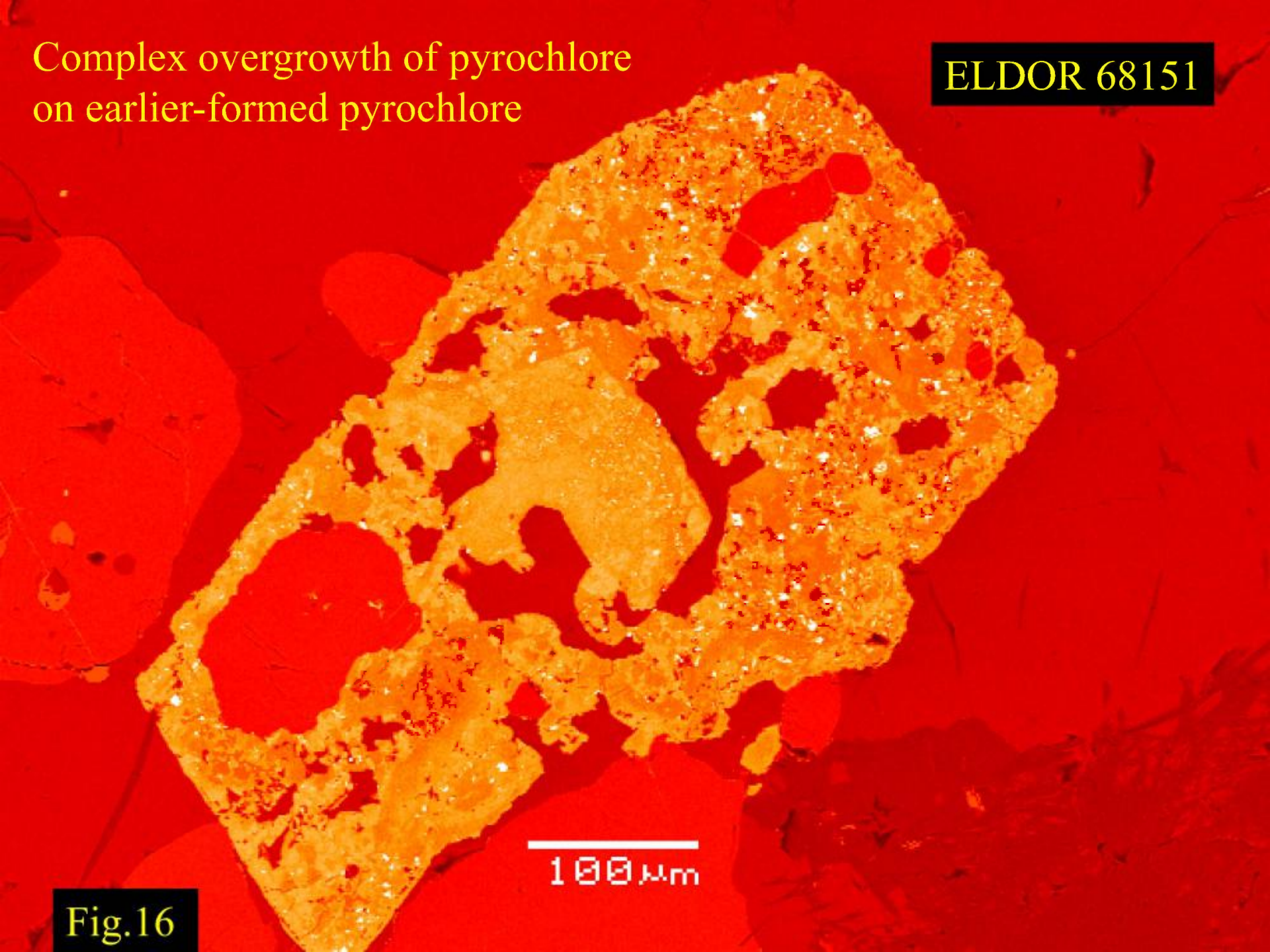
Complex overgrowth of pyrochlore
on earlier-formed pyrochlore
ELDOR 68151
100 µm
Fig.16

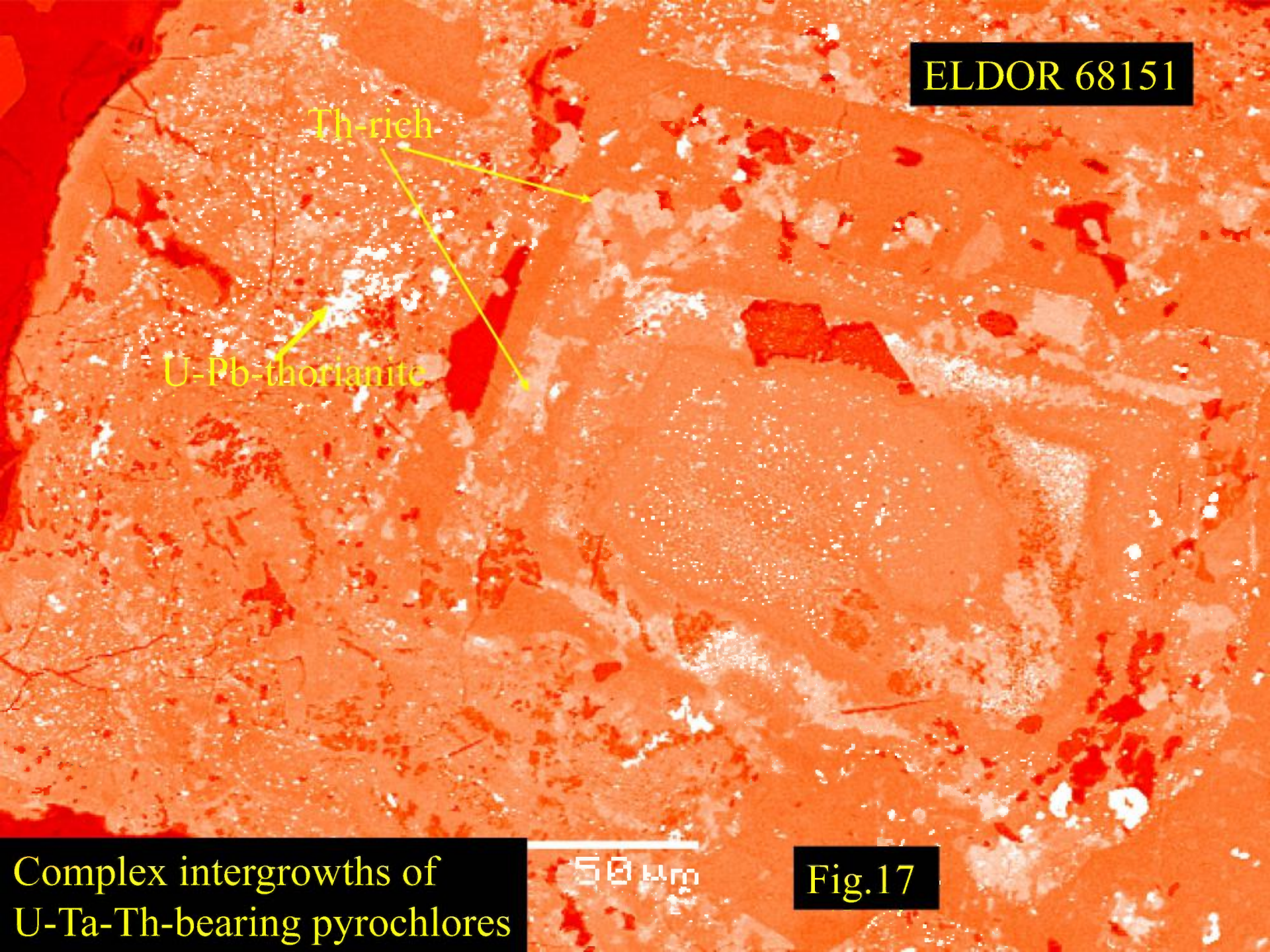

Complex intergrowths of U-Ta-Th-bearing pyrochlores

Fig.17

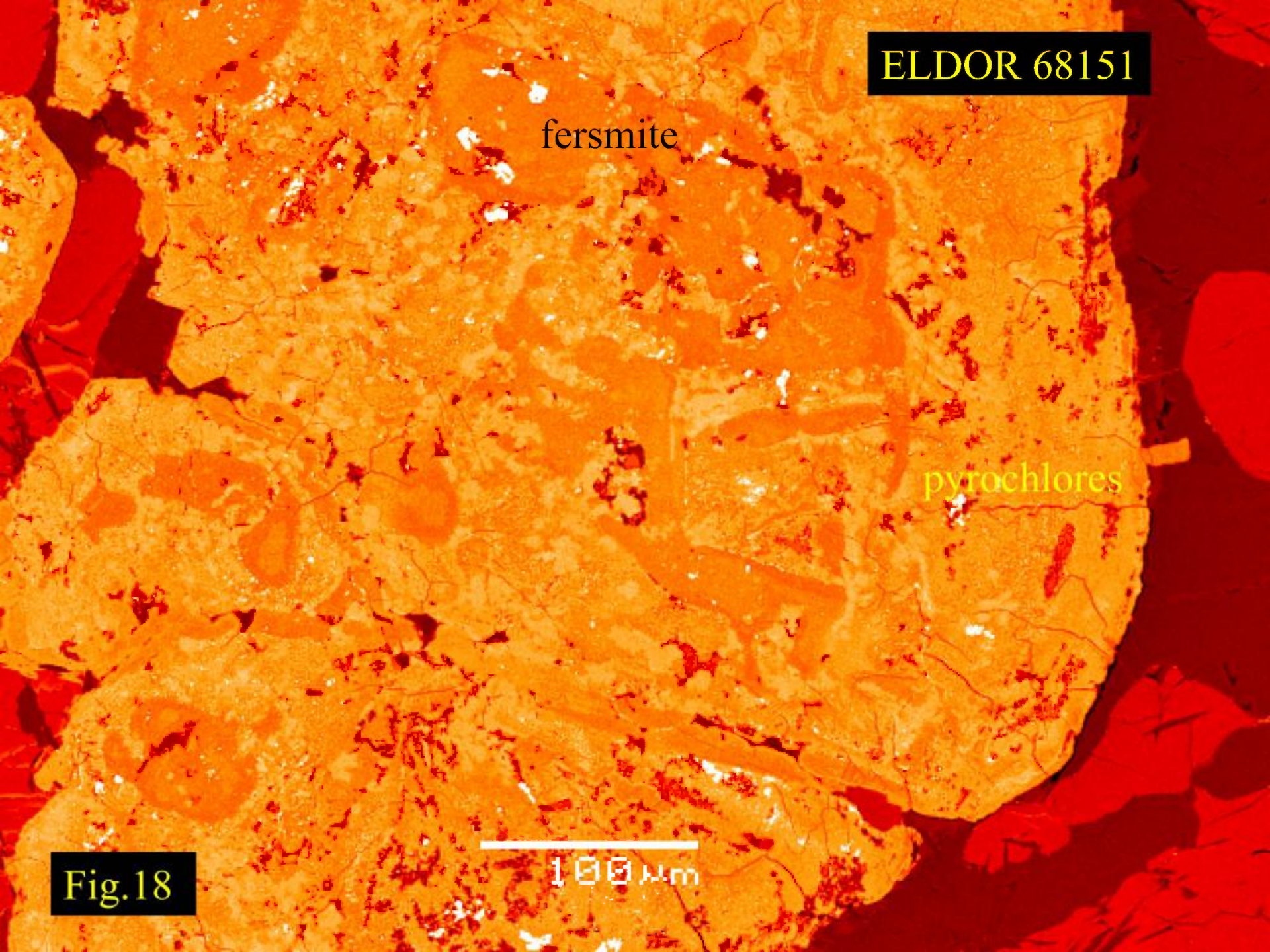

Fig.18

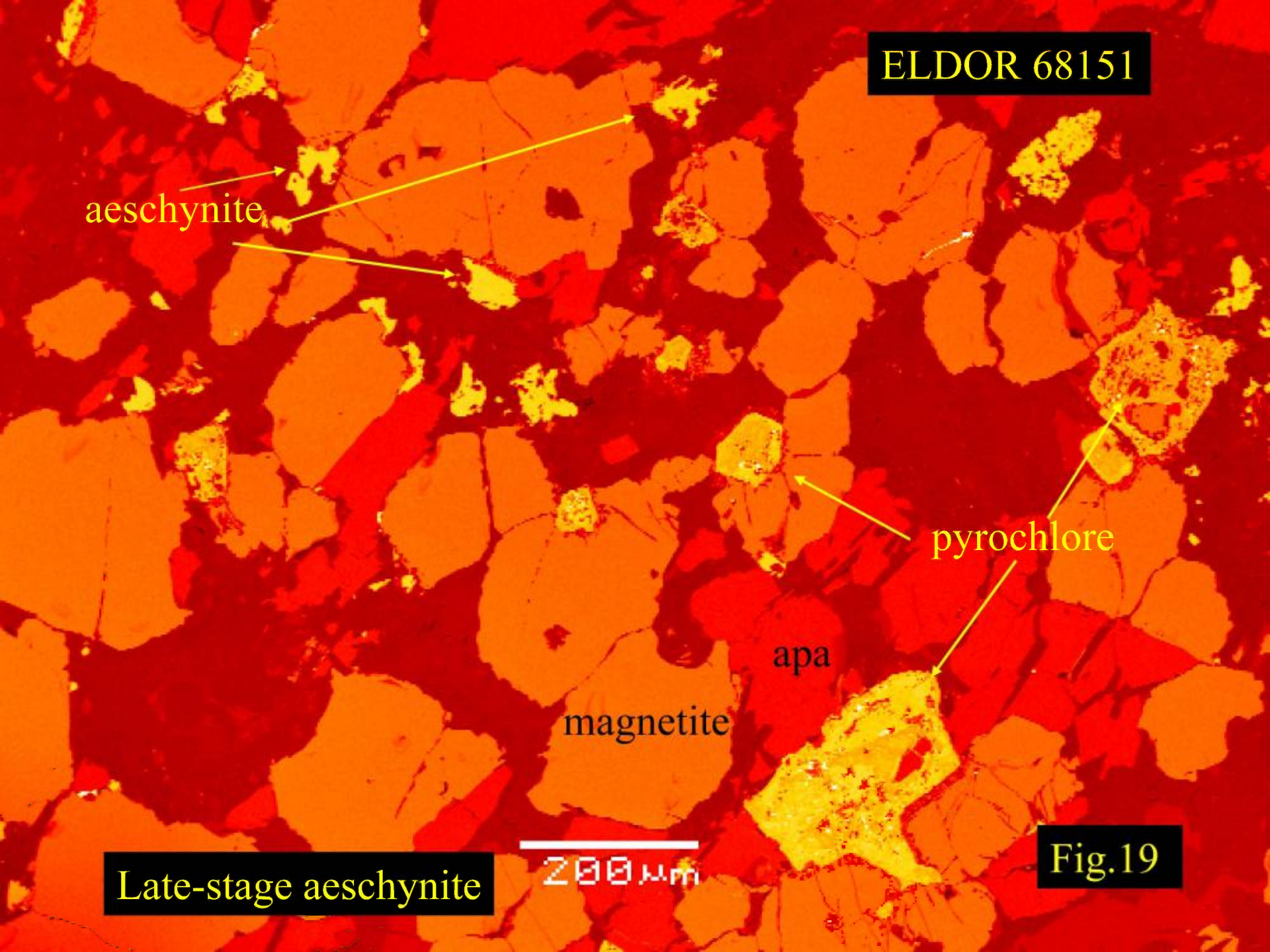

Late-stage aeschynite

Fig.19

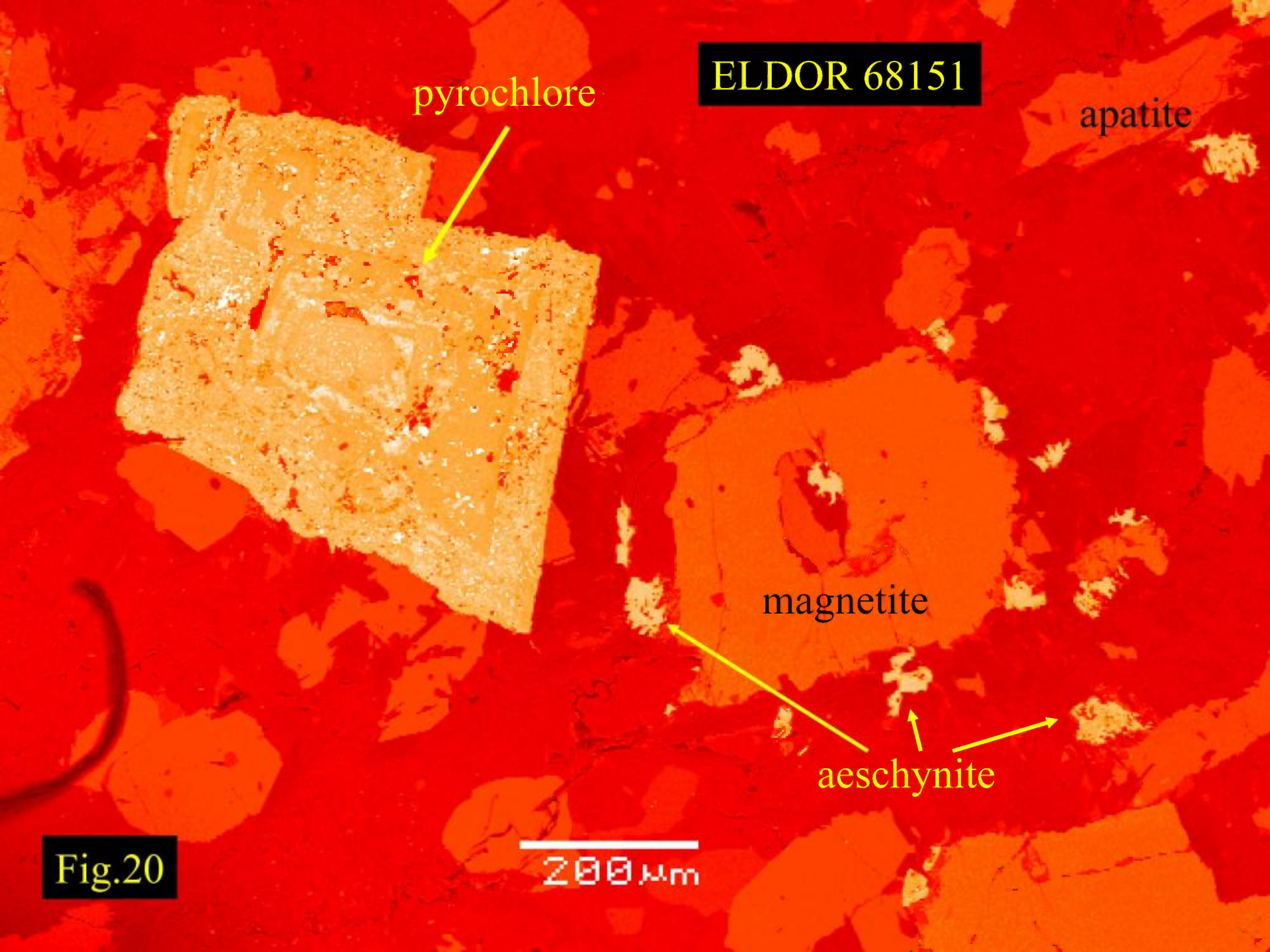
ELDOR 68151
pyrochlore
apatite
magnetite
aeschynite
200 µm

Fig.20

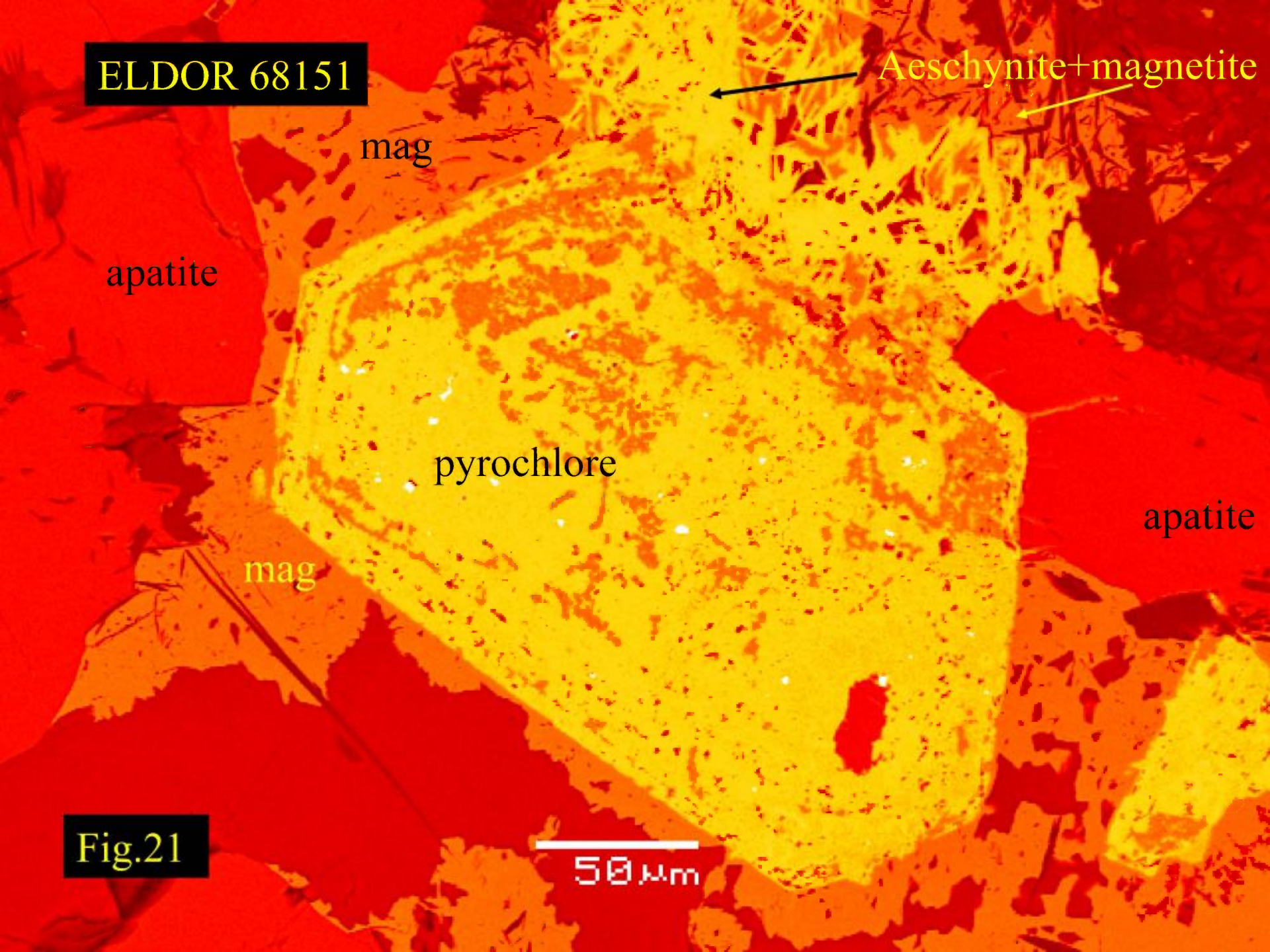
ELDOR 68151
Aeschynite+magnetite
mag
apatite
pyrochlore
apatite
mag
50 µm

Fig.21

ELDOR 68162

ELDOR 68162 *Phlogopite apatite dolomite carbonatite*

This sample is relatively poor in oxide minerals and consists principally of apatite and ferroan dolomite together with lesser phlogopite, fluorite and potassium feldspar. Phlogopite occurs as pale brown laths commonly intergrown with purple fluorite. Magnetite appears to be absent.

Figures 1-3 show the presence of rounded crystals of apatite set in a matrix of ferroan dolomite Opaque phases in Figure 1 &2 are pyrochlores and/or pyrite. Apatite is of uniform composition and has no detectable Sr, or rare earth elements (< 0.4 wt.%). Figs. 3-4 shows that subhedral crystals of potassium feldspar are intergrown with some, but not all apatite crystals. These have the appearance of clasts. The feldspar contains no detectable Na, Ba or Fe and does not exhibit any twinning in crossed polarized light. This feldspar is thus considered to be orthoclase and not microcline or sanidine. Pyrite occurs principally as subhedral-to-euhedral small (<50 um) crystals (Fig.5), although rare large anhedral (c. 0.5cm) aggregates can be found (Fig. 15). Only the latter contain inclusions of other phases, i.e. pyrochlore and REE-fluorocarbonates. Ferroan dolomite (c. 13 wt.% FeO) forms the matrix of the rock, and occurs as interlocking fine grained crystals. Interstices (200um) in the dolomite are commonly filled by fluorite and syntaxial intergrowths of REE-fluorocarbonates (Figs. 5-8). In these earlier formed irregular clast-like bastnaesite-(Ce) is overgrown by syntaxial parisite-(Ce) and synchysite-(Ce). Also present in this sample are irregularly-shaped masses (200 um) of bastnaesite-(Ce) lacking syntaxial overgrowths set the dolomite matrix (Fig.8). Small (<20um) rounded crystals of niobian rutile occur in the dolomite matrix, and as inclusions in pyrochlore (fig.12).

ELDOR 68162

Two principal varieties of early-forming “pyrochlore” are present in this sample. The earliest formed pyrochlore is termed here “pyrochlore-1"; the other is a later-forming Na-Ca-pyrochlore, termed “pyrochlore-2. Overgrowths of “pyrochlore-2" can be found on cores of “pyrochlore-1" (Fig.11), and inclusions of “pyrochlore-1" can be found in “pyrochlore-2 (Fig 12).
In addition, there is a late-stage interstitial variety, termed “pyrochlore-2a”, which also forms overgrowths on pyrochlore-2.

Pyrochlore-1 is rare relative to pyrochlore-2 (approx ratio1:20). All “pyrochlore-1" is a complex multi-phase pyrochlore that can be a mixture of U-Ba-pyrochlore plus Th-pyrochlore with overgrowths of Na-Ca pyrochlore and ferrocolumbite (Fig.9). All “pyrochlore-2" is of relatively uniform composition and consists of U-Th-poor sodian calcian pyrochlore. Small (<10 um) inclusions of baddeleyite are present in most crystals. Some crystals overgrowths (Fig. 14) of pyrochlore-2a that are relatively UO_2-rich compared to their cores and represent a late stage pyrochlore forming event. Both pyrochlore-1 and pyrochlore-2 can be juxtaposed in the dolomite matrix (Figs 10 & 13), and evidently represent a rheologically mixed assemblage. In addition to the above, pyrochlore-2a forms small subhedral-to-poikilitic crystals forming as very late stage a mineral in the interstices of the dolomite groundmass (Figs. 8 & 16) contemporaneously with the REE-fluorocarbonates. These pyrochlores are of relatively uniform composition (see data below) and of low Ta-contents.

ELDOR 68162

Representative semiquantitative compositions of pyrochlore are given below:

Wt.%	Th-pyro-1	U-pyro-1	U-pyro-1	Na-Ca-pyro-2	Na-Ca-pyro-2a	
F	n.d.	N.d.	N.d.	3.9	n.a	N.d
Na_2O	n.d.	n.d.	n.d.	5.3.	6.8	0.5
SiO_2	1.4	3.1	4.8	n.d.	n.d.	2.6
BaO	n.d.	1.9	n.d.	n.d.	n.d.	0.7
CaO	7.0	7.9	5.7	15.3	15.4	6.5
TiO_2	2.9	5.5	5.4	4.4	1.3	4.1
FeO	7.0	2.1	4.4	0.2	n.d	6.3
Nb_2O_5	72.6	59.9	58.9	68.0	75.3	59.5
Ta_2O_5	n.d.	3.7	6.0	0.7	n.d.	N.d.
La_2O_3	n.d.	N.d.	n.d.	n.d.	n.d.	N.d.
Ce_2O_3	0.7	2.6	n.d.	0.7	0.4	1.34
Pr_2O_3	n.d.	n.d.	n.d.	n.d	n.d.	n.d.
Nd_2O_3	n.d.	3.7	n.d.	n.d.	n.d.	n.d
ThO_2	3.5	2.7	0.5	1.2	n.d.	n.d.
UO_2	n.d.	4.1	7.1	n.d.	n.d.	14.7

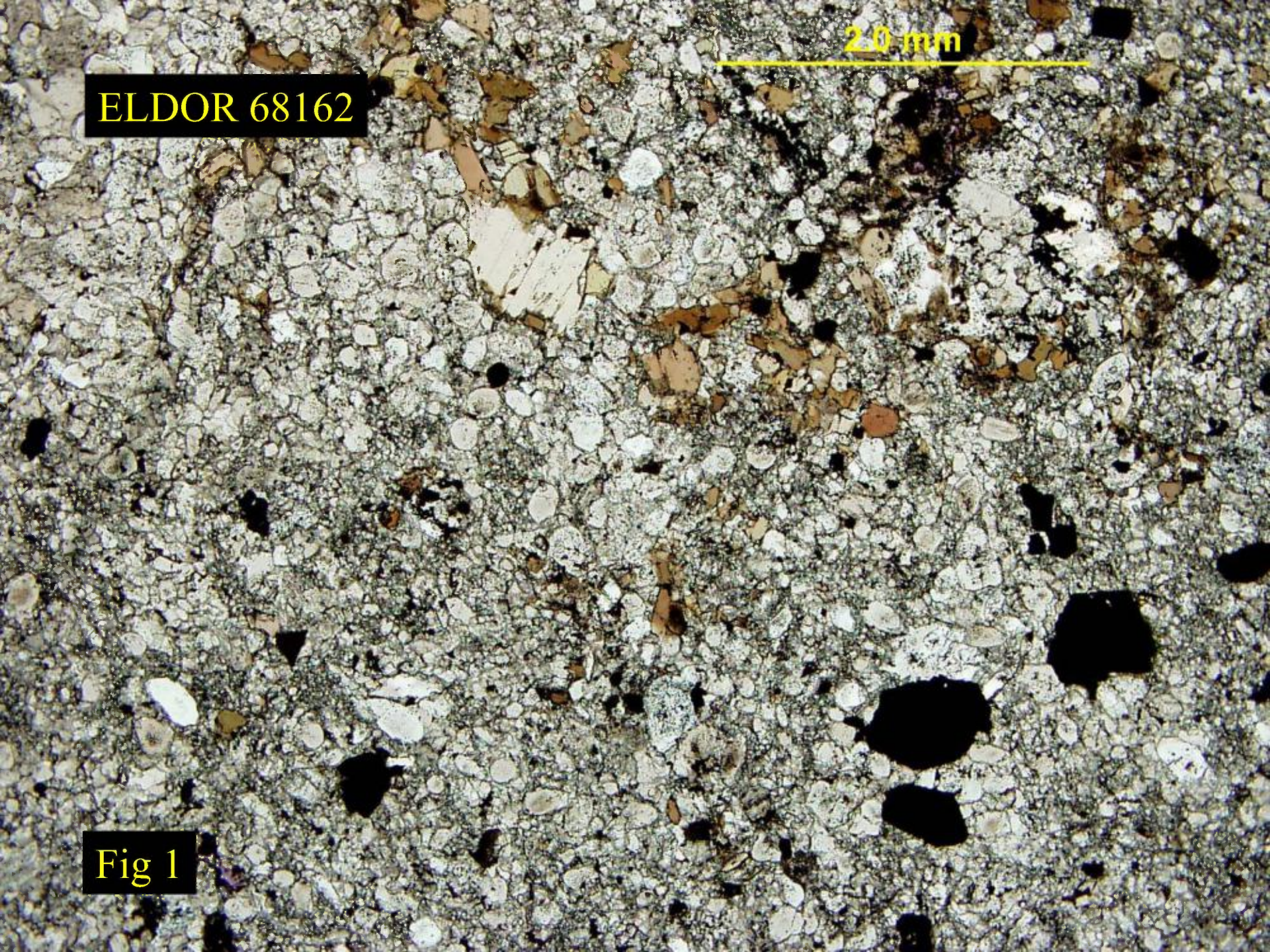

Fig 1

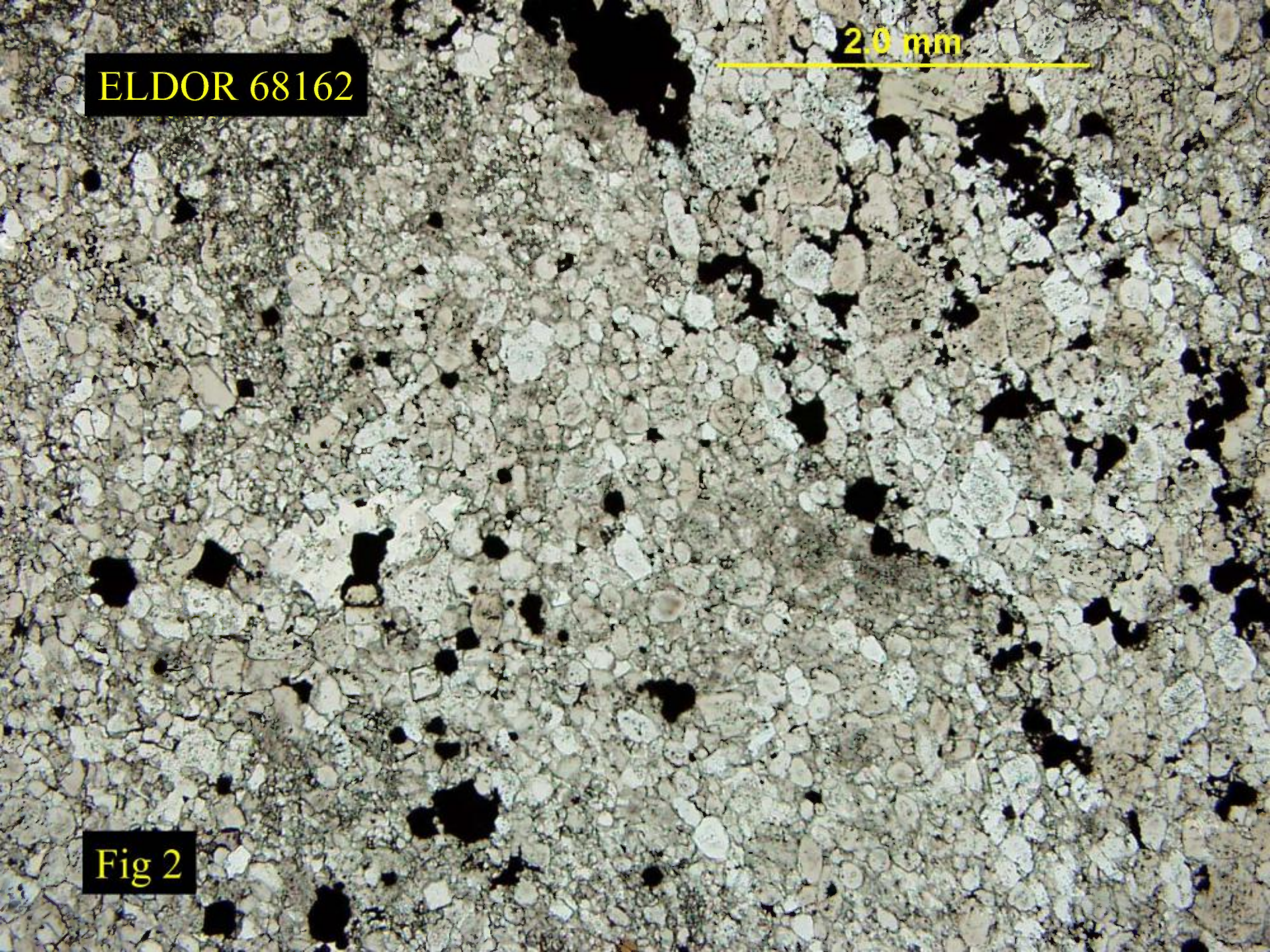

Fig 2

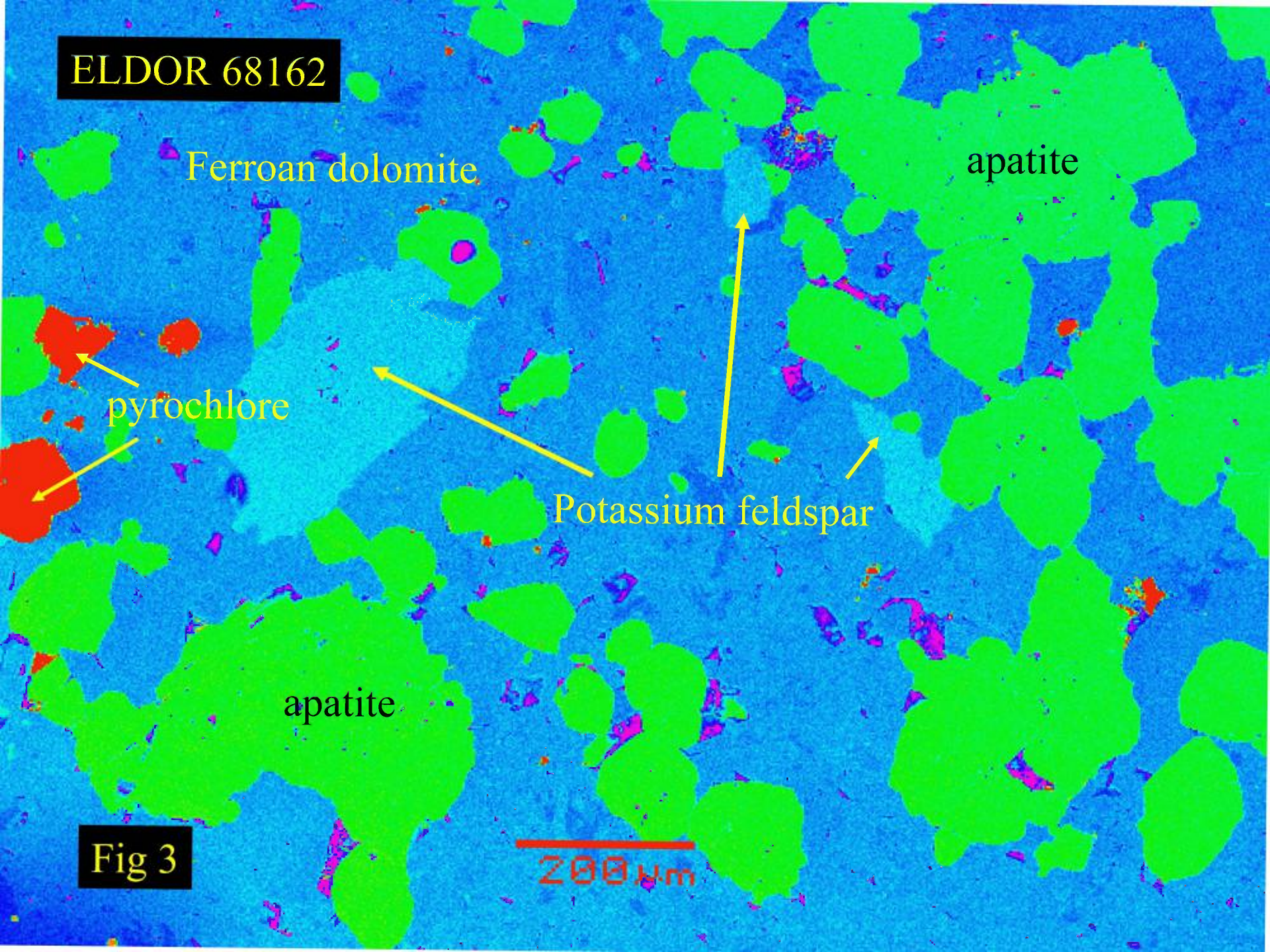
ELDOR 68162
Ferroan dolomite
apatite
pyrochlore
Potassium feldspar
apatite
200 µm
Fig 3

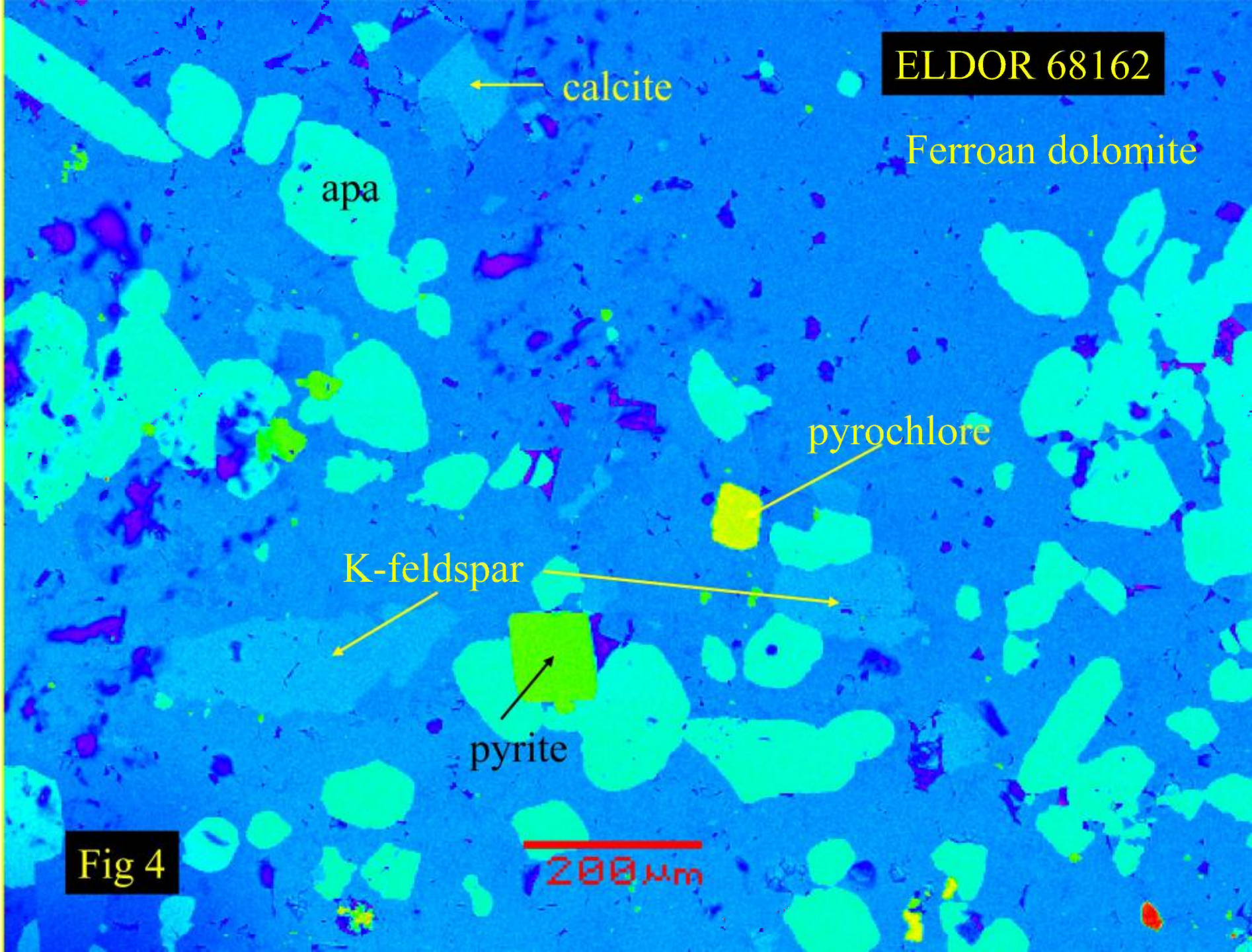
ELDOR 68162
calcite
Ferroan dolomite
apa
pyrochlore
K-feldspar
pyrite
200 µm

Fig 4

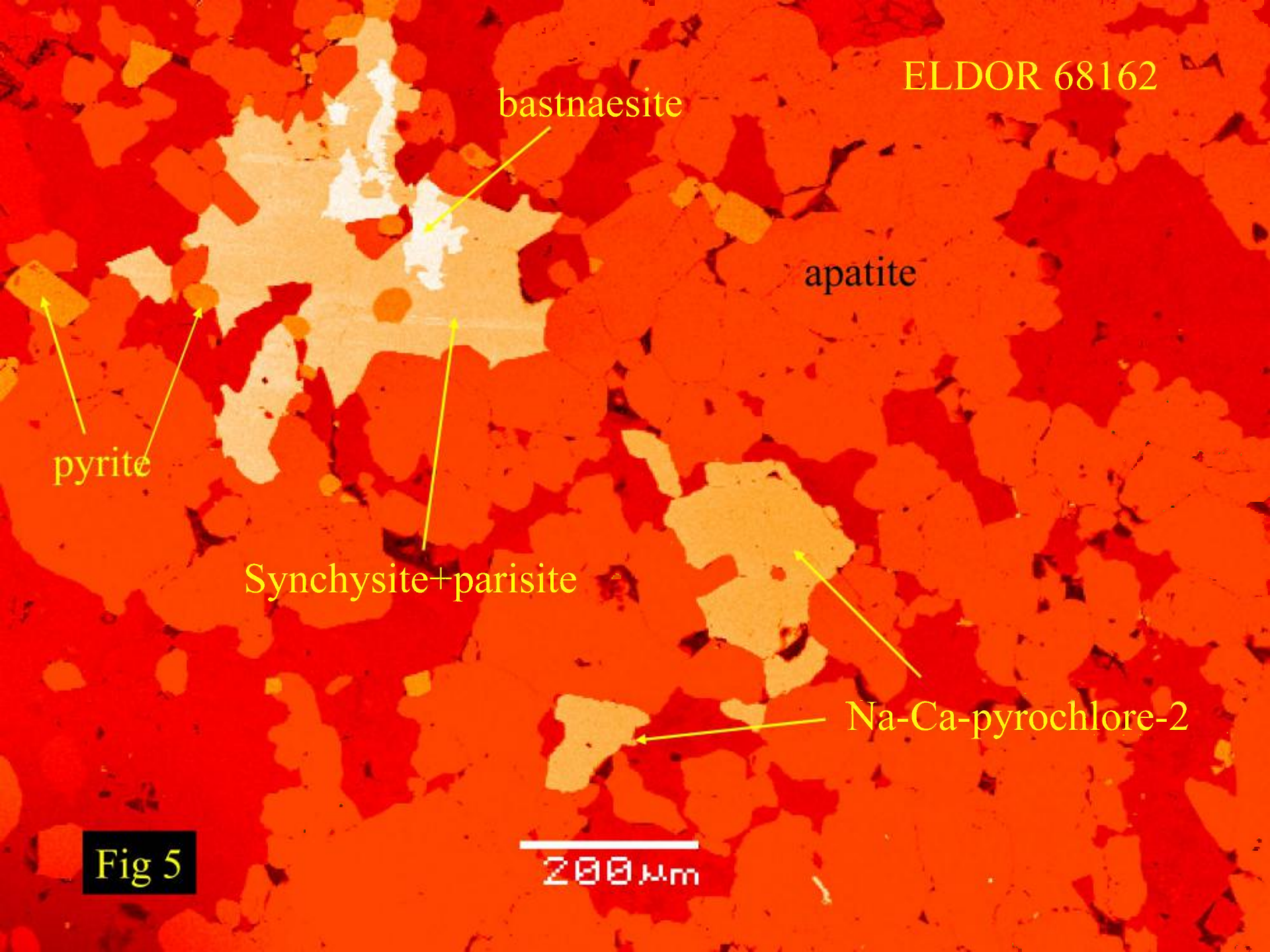
ELDOR 68162
bastnaesite
apatite
pyrite
Synchysite+parisite
Na-Ca-pyrochlore-2
200µm

Fig 5

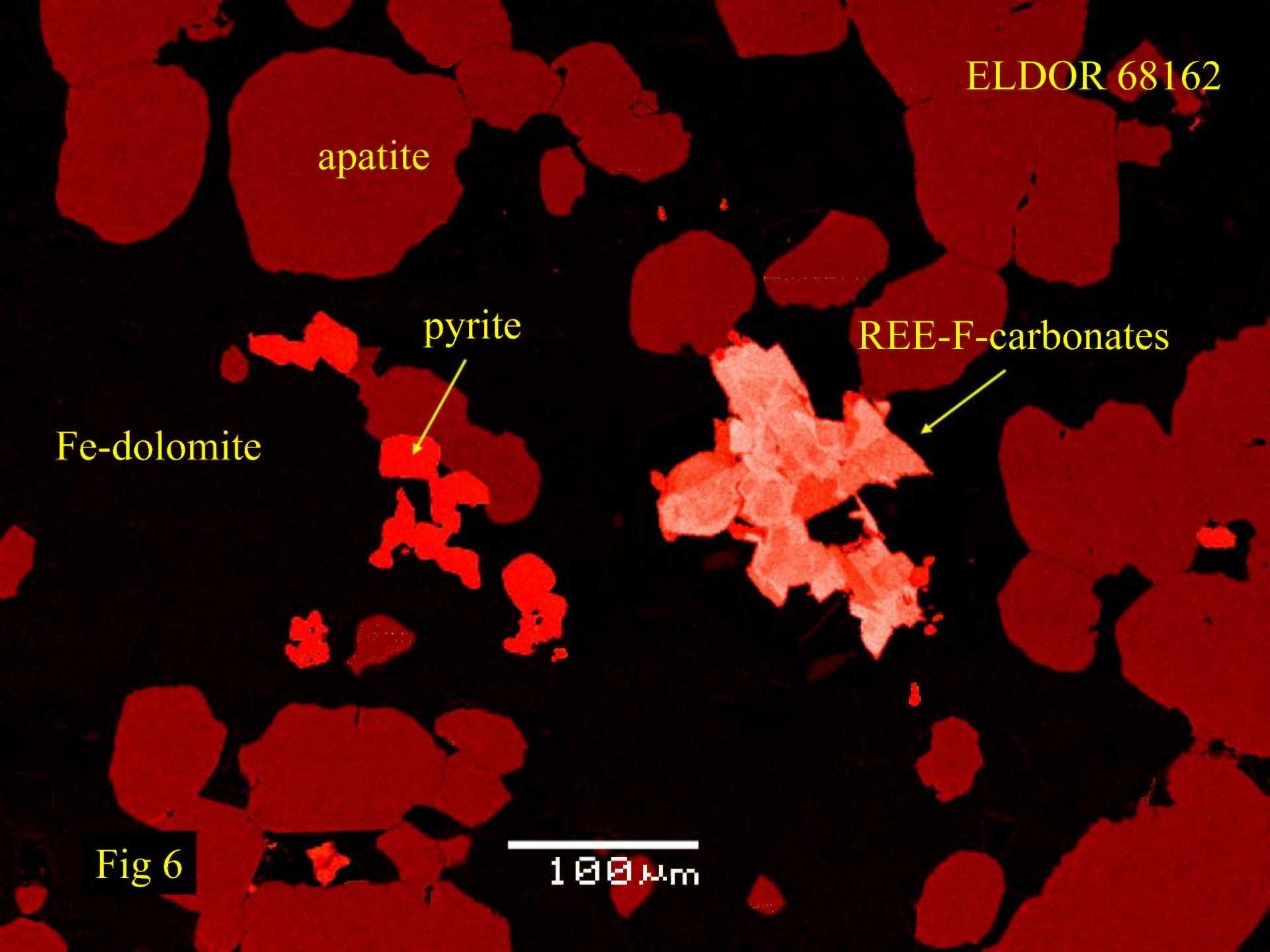
ELDOR 68162
apatite
pyrite
REE-F-carbonates
Fe-dolomite
100µm

Fig 6

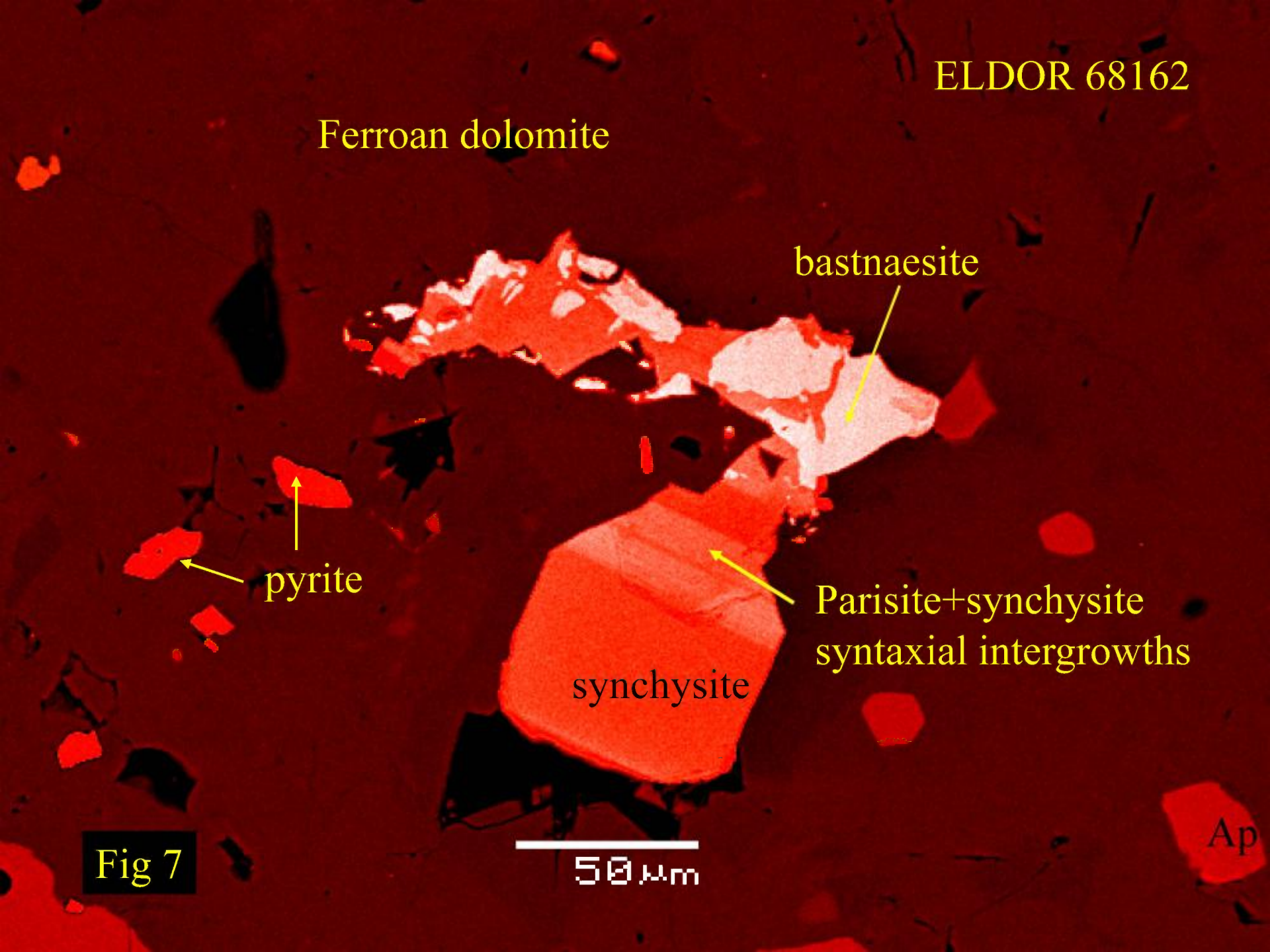
ELDOR 68162
Ferroan dolomite
bastnaesite
pyrite
Parisite+synchysite
syntaxial intergrowths
synchysite
50 µm
Ap

Fig 7

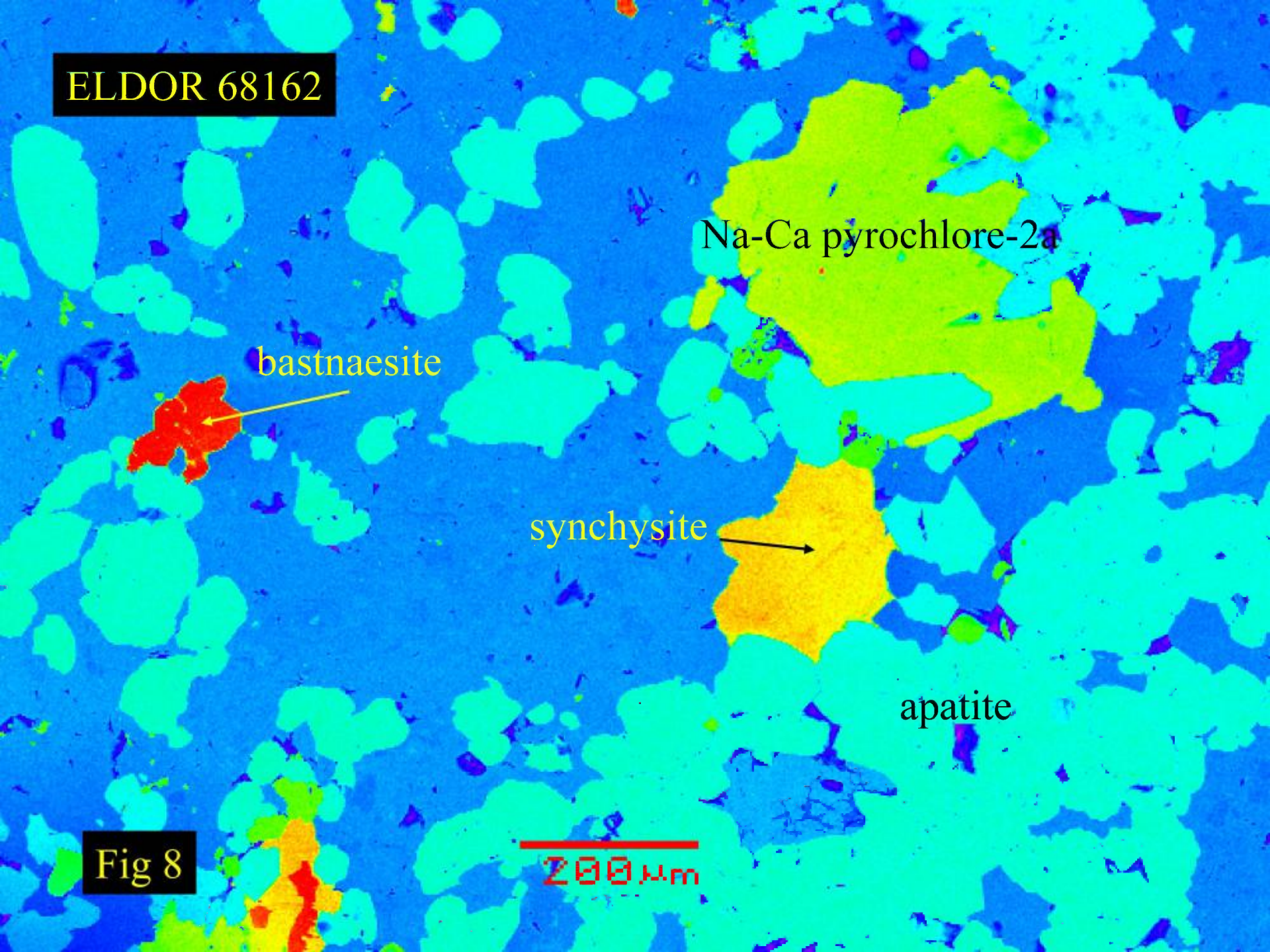
ELDOR 68162
Na-Ca pyrochlore-2a
bastnaesite
synchysite
apatite
200 µm

Fig 8

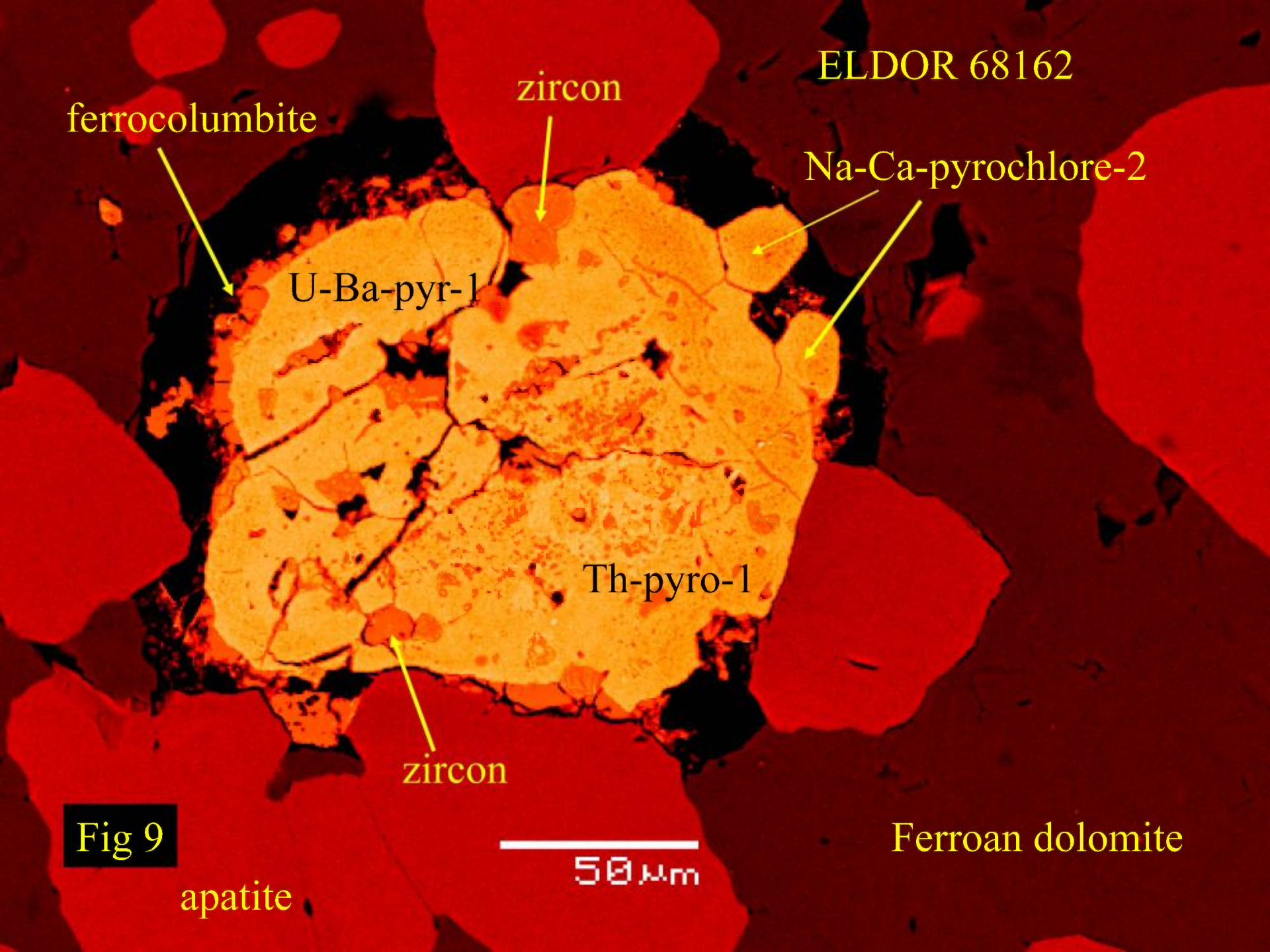
ELDOR 68162
zircon
ferrocolumbite
Na-Ca-pyrochlore-2
U-Ba-pyr-1
Th-pyro-1
zircon
Fig 9
50 µm
Ferroan dolomite
apatite

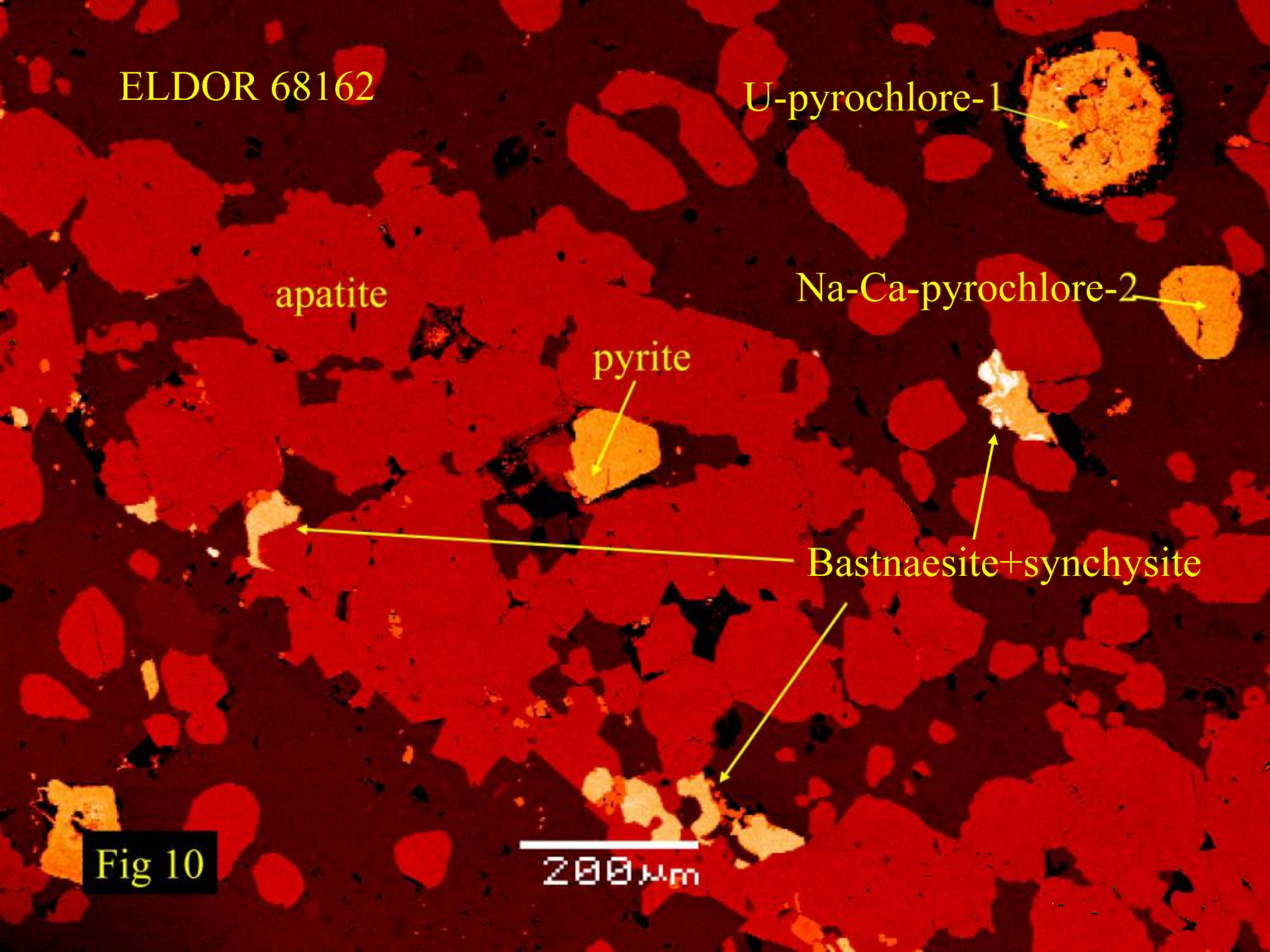
ELDOR 68162
U-pyrochlore-1
apatite
Na-Ca-pyrochlore-2
pyrite
Bastnaesite+synchysite
200µm

Fig 10

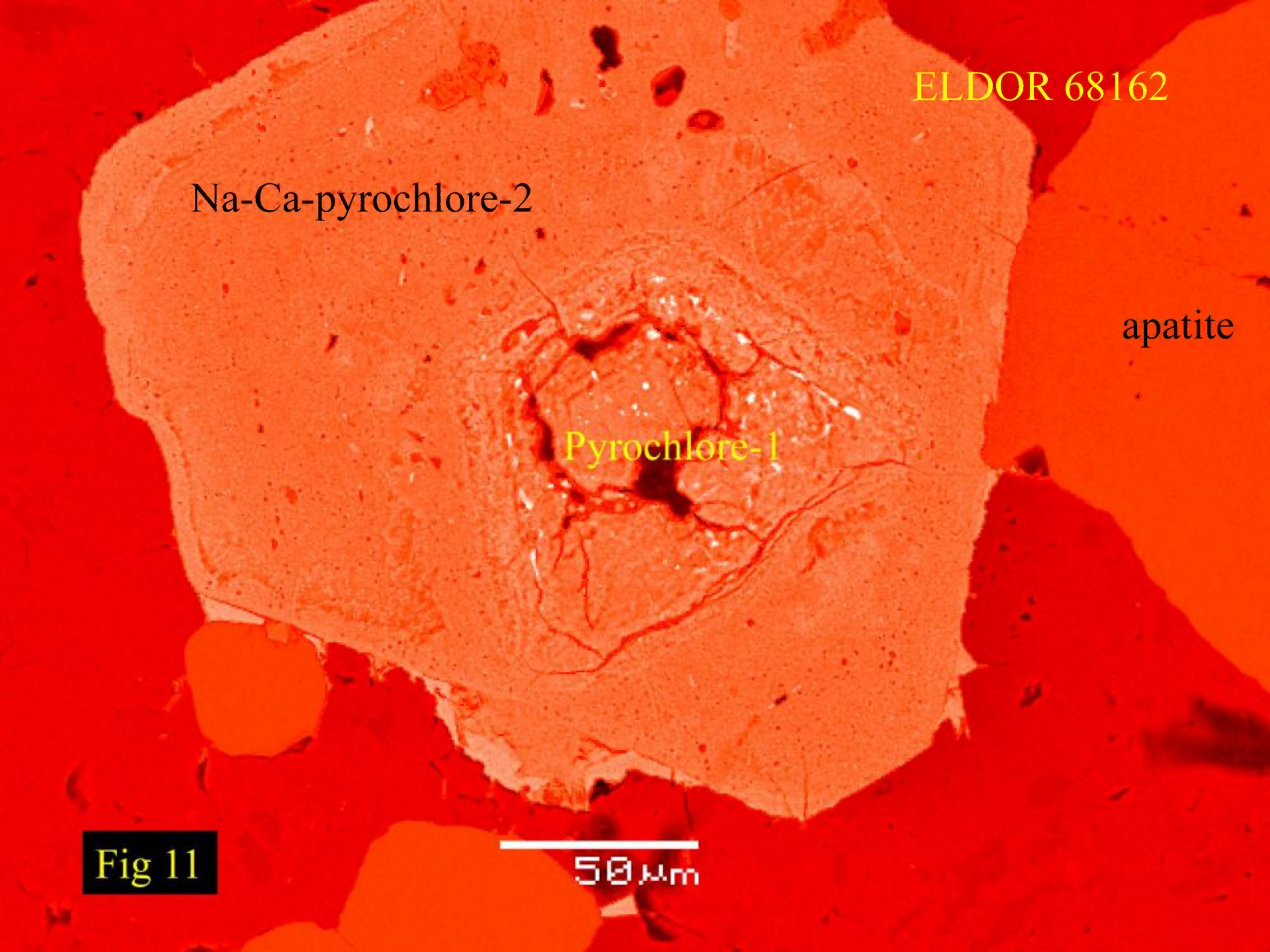

Fig 11

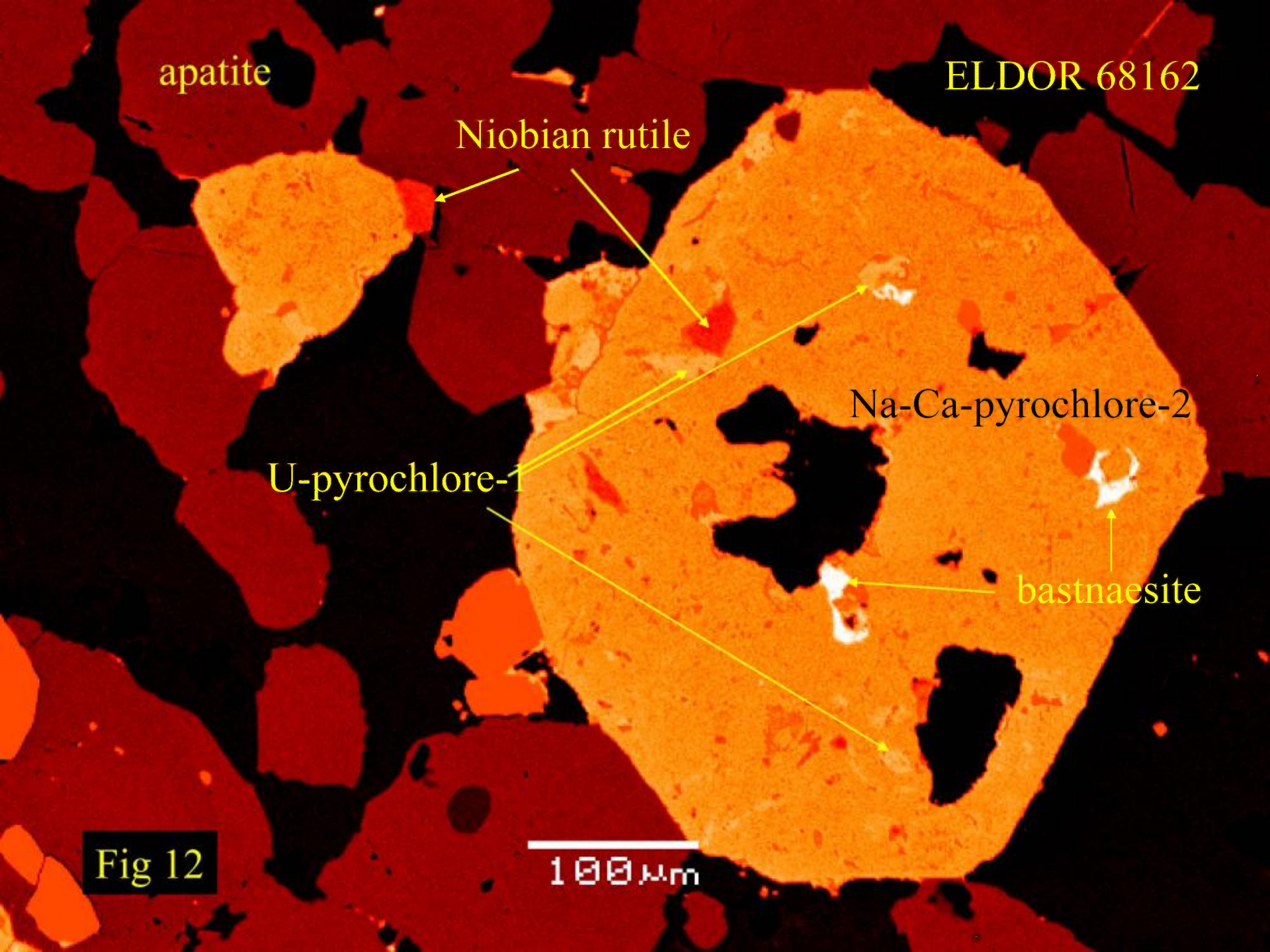
apatite
ELDOR 68162
Niobian rutile
Na-Ca-pyrochlore-2
U-pyrochlore-1
bastnaesite
100 µm

Fig 12

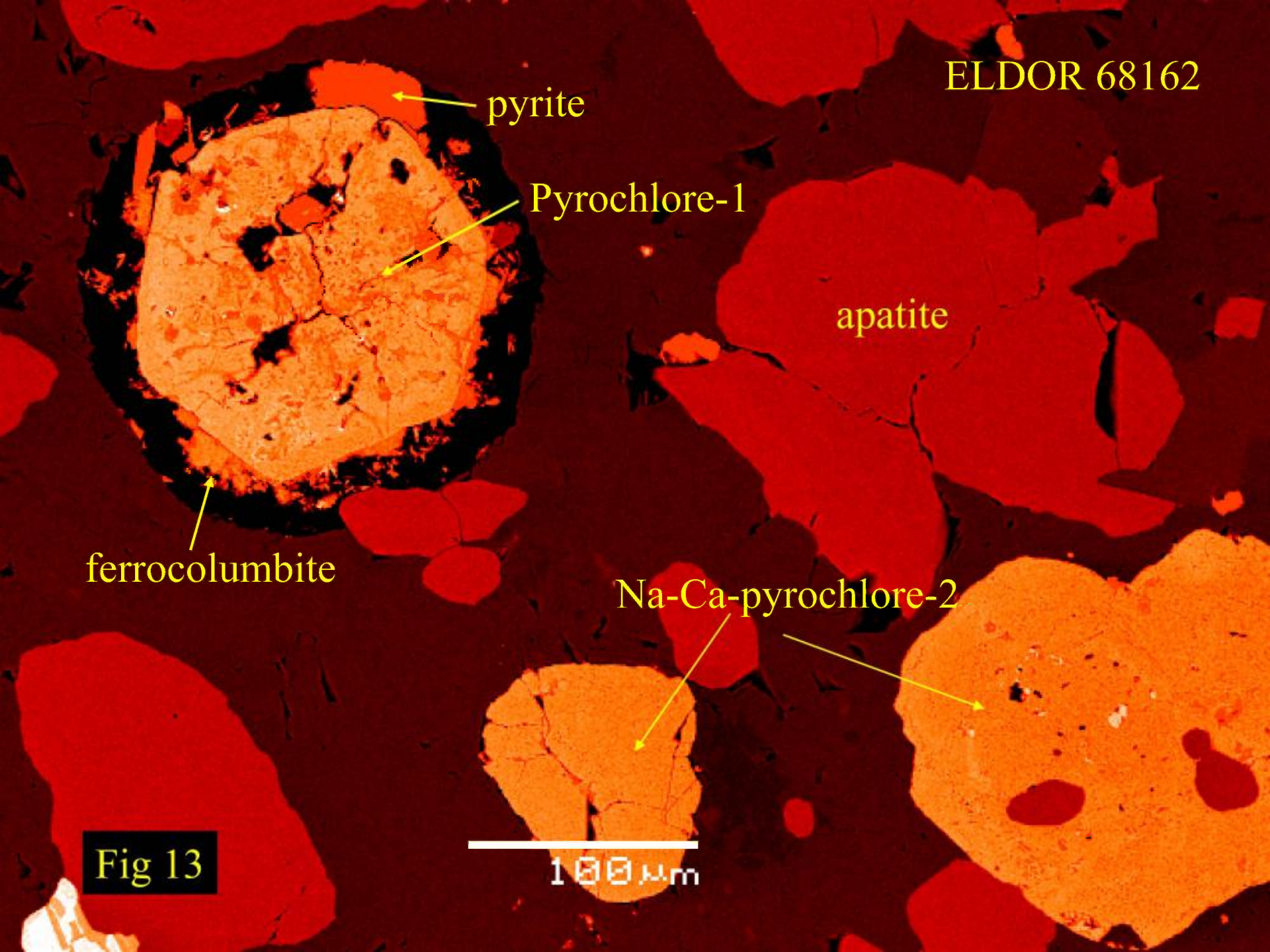
ELDOR 68162
pyrite
Pyrochlore-1
apatite
ferrocolumbite
Na-Ca-pyrochlore-2
100 µm

Fig 13

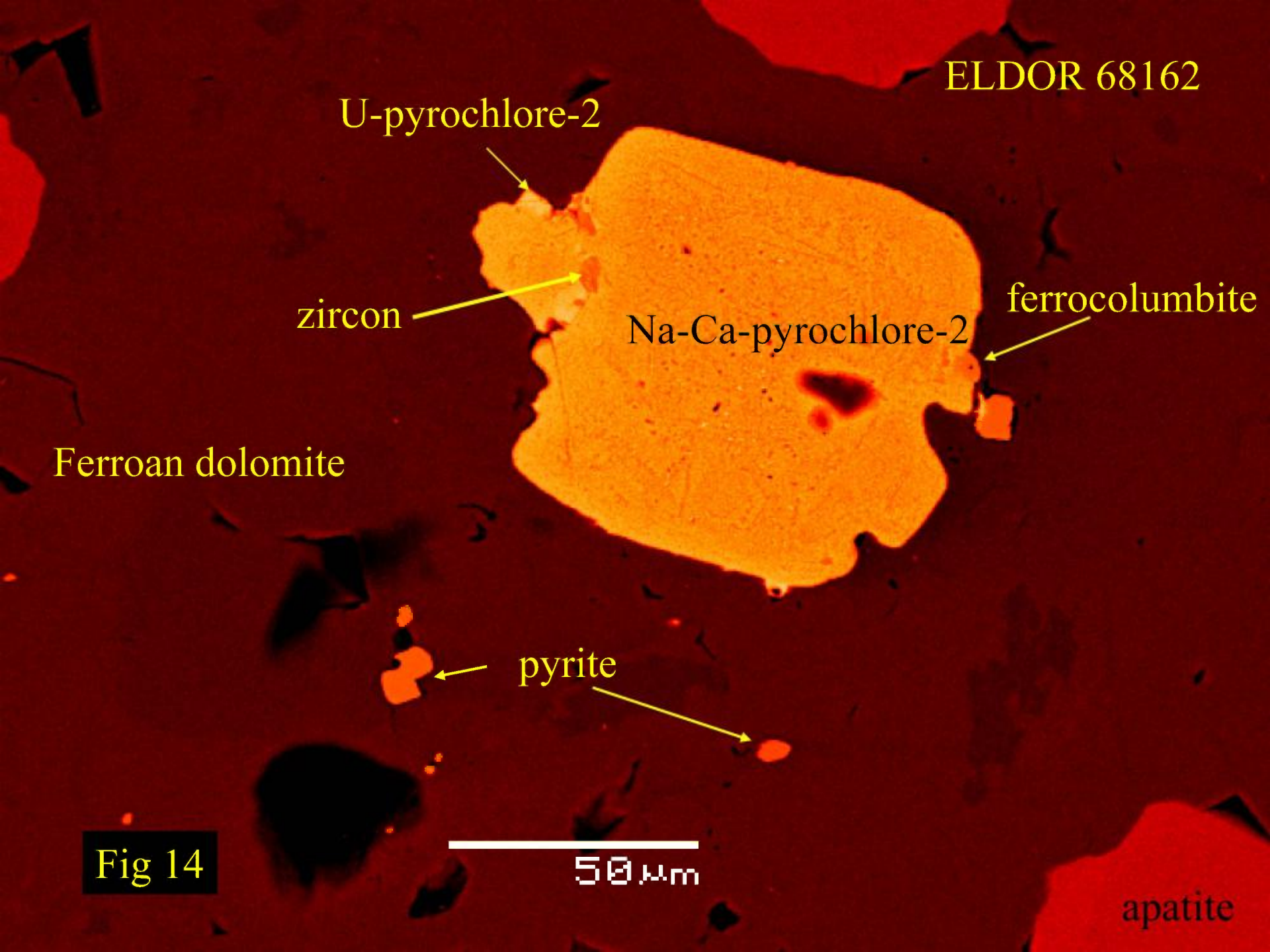
ELDOR 68162
U-pyrochlore-2
zircon
Na-Ca-pyrochlore-2
ferrocolumbite
Ferroan dolomite
pyrite
50 µm
apatite

Fig 14

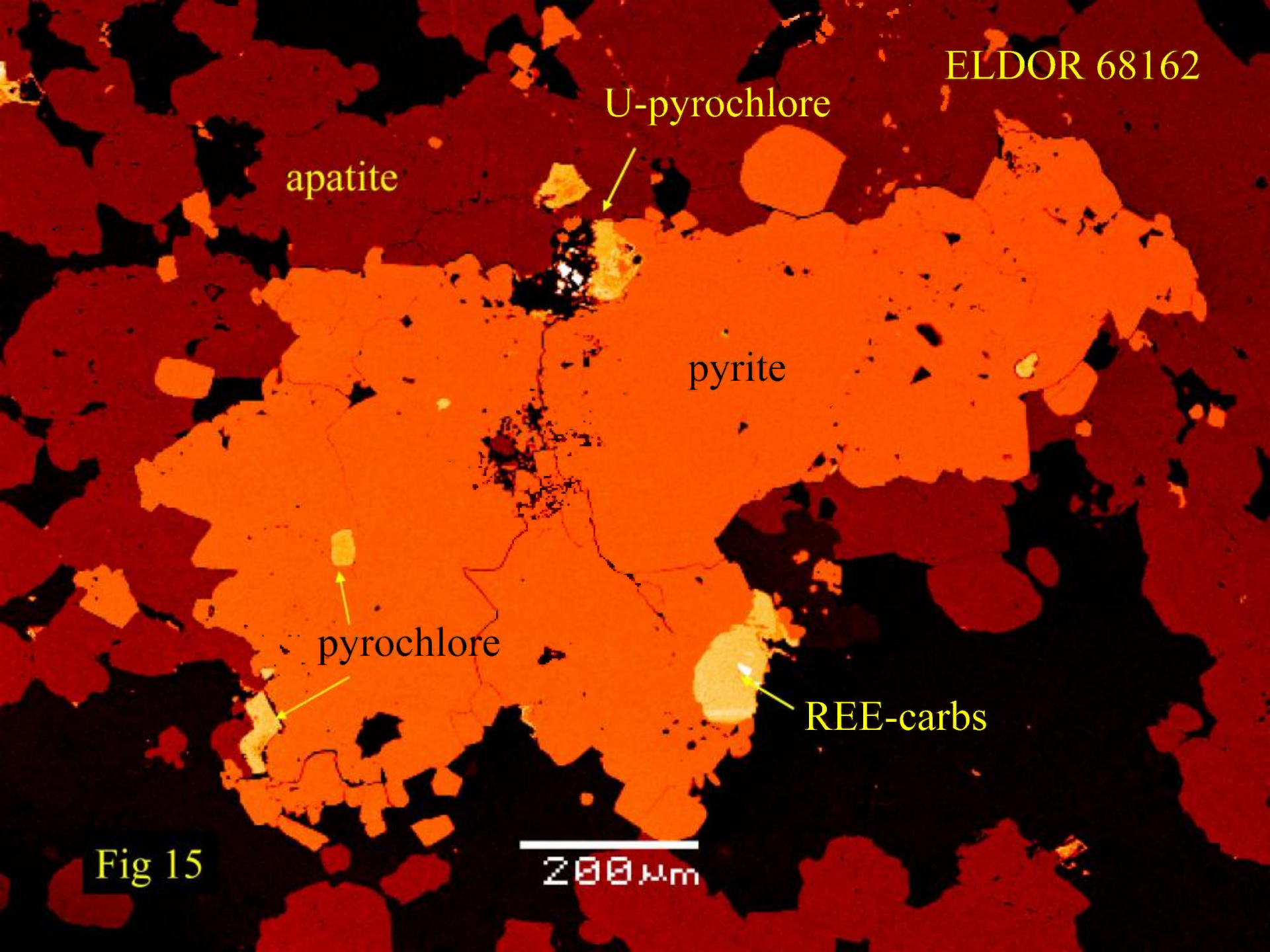
ELDOR 68162
U-pyrochlore
apatite
pyrite
pyrochlore
REE-carbs
200µm

Fig 15

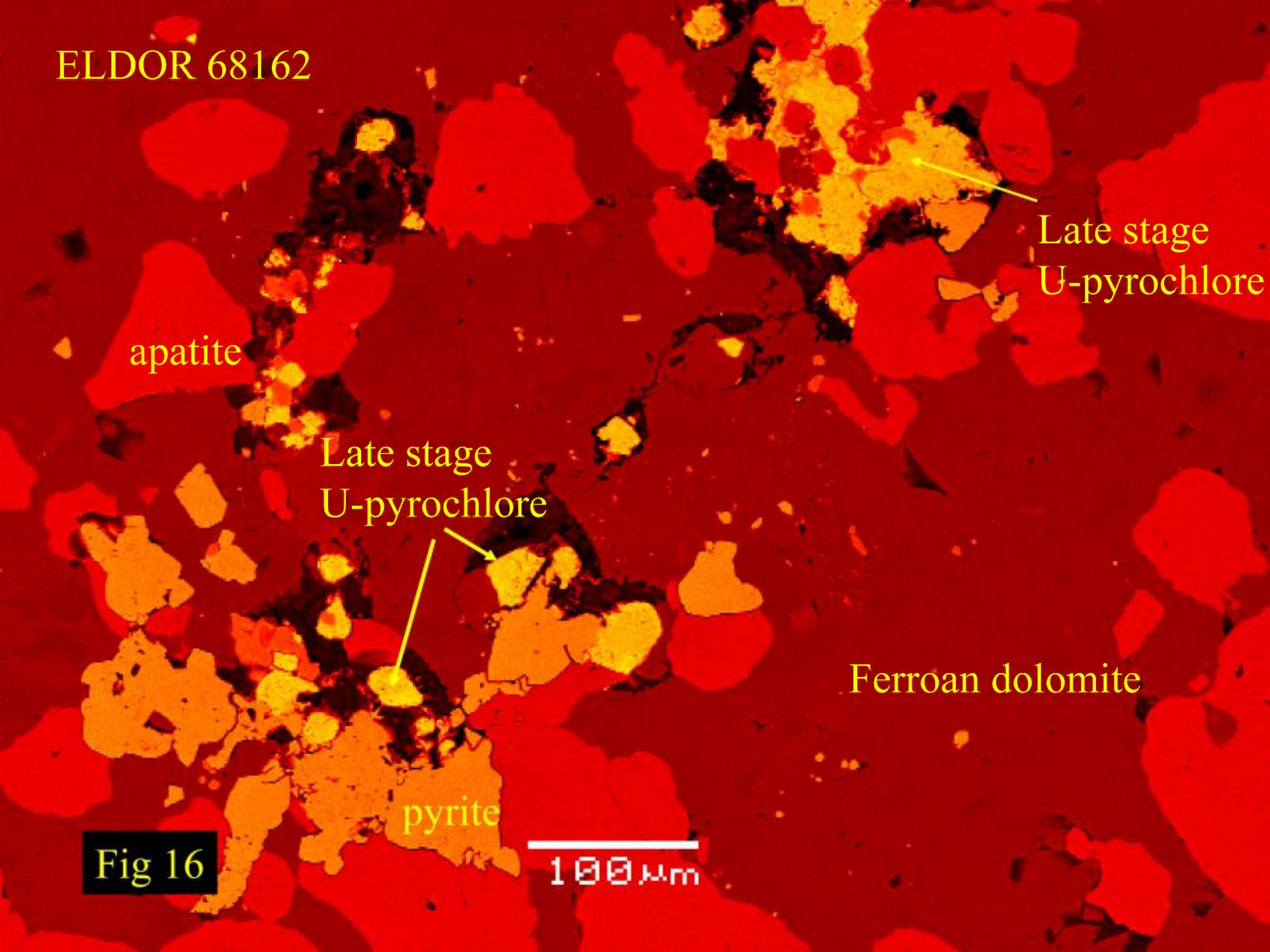
ELDOR 68162
Late stage
U-pyrochlore
apatite
Late stage
U-pyrochlore
Ferroan dolomite
pyrite
100 µm

Fig 16

ELDOR 68171

ELDOR 68171 *Magnetite diopside apatite dolomite carbonatite*

This relatively homogeneous sample consists principally of magnetite, apatite, diopside and Fe-bearing dolomite (Figs 1 & 2). Magnetite occurs as irregular anhedral crystals that are overgrown by, and intergrown with, apatite (Figs. 1-2, 6,8). The magnetite is extensively fractured (Figs. 6 & 8), and is homogeneous with respect to its composition. Inclusions of ilmenite are absent, and the magnetite is poor in Ti, Mg, and Mn (<0,5 wt.%). Irregular small (< 20 um) crystals of galena and aeschynite occur rarely along the fracture planes. Apatite forms irregular aggregates of anhedral and corroded crystals (Figs 1-4, 7). The apatite is of uniform composition and is poor in Sr and rare earth elements (<0.5 wt.% oxides). Pale green-to-colourless diopside is intergrown with apatite as subhedral prisms (figs 1-2). Typically these have resorbed margins (Fig.5), thus the diopside is evidently not stable in the current host. The groundmass consists of large (Figs 1-2) and small interlocking crystals of Fe-bearing (<5 wt.% FeO) dolomite. Within these plates anhedral resorbed crystals (<0.2mm) of calcite can be found (Fig. 5). These are typically surrounded by irregular mantles (Fig.5) of ferroan dolomite (>5 wt.% FeO).

ELDOR 68171

"Pyrochlores" occur as discrete ragged resorbed crystals (< 0.4 um) in association with magnetite and apatite (Figs. 4, 6-8). EDS-images and X-ray spectrometry shows that the "pyrochlores" are actually complex intimate intergrowths (Fig. 9) consisting principally of pyrochlore and fersmite with lesser zircon and $(Th,Pb)O_2$. Both Th and U -rich pyrochlores are present but the small size (<15 um) of these intergrown phases renders exact analysis impossible. The fersmite host to these pyrochlore is a low Th variety (< 1 wt. ThO_2). Pyrochlore-fersmite aggregates are also observed to have nucleated on irregular and/or prismatic baddeleyite crystals (Figs.10-11). The latter are commonly mantled by zircon. Ferrocolumbite is not present.

The groundmass contains trace amounts of aeschynite-(Ce) as irregular resorbed crystals (Fig. 12). These show a wide range in composition with respect to their rare earth (Ce_2O_3 8.4 - 14.9 wt.%) and ThO_2 contents (7.6 10.5 wt.%) and are U-poor (<0.5 wt.% UO_2).

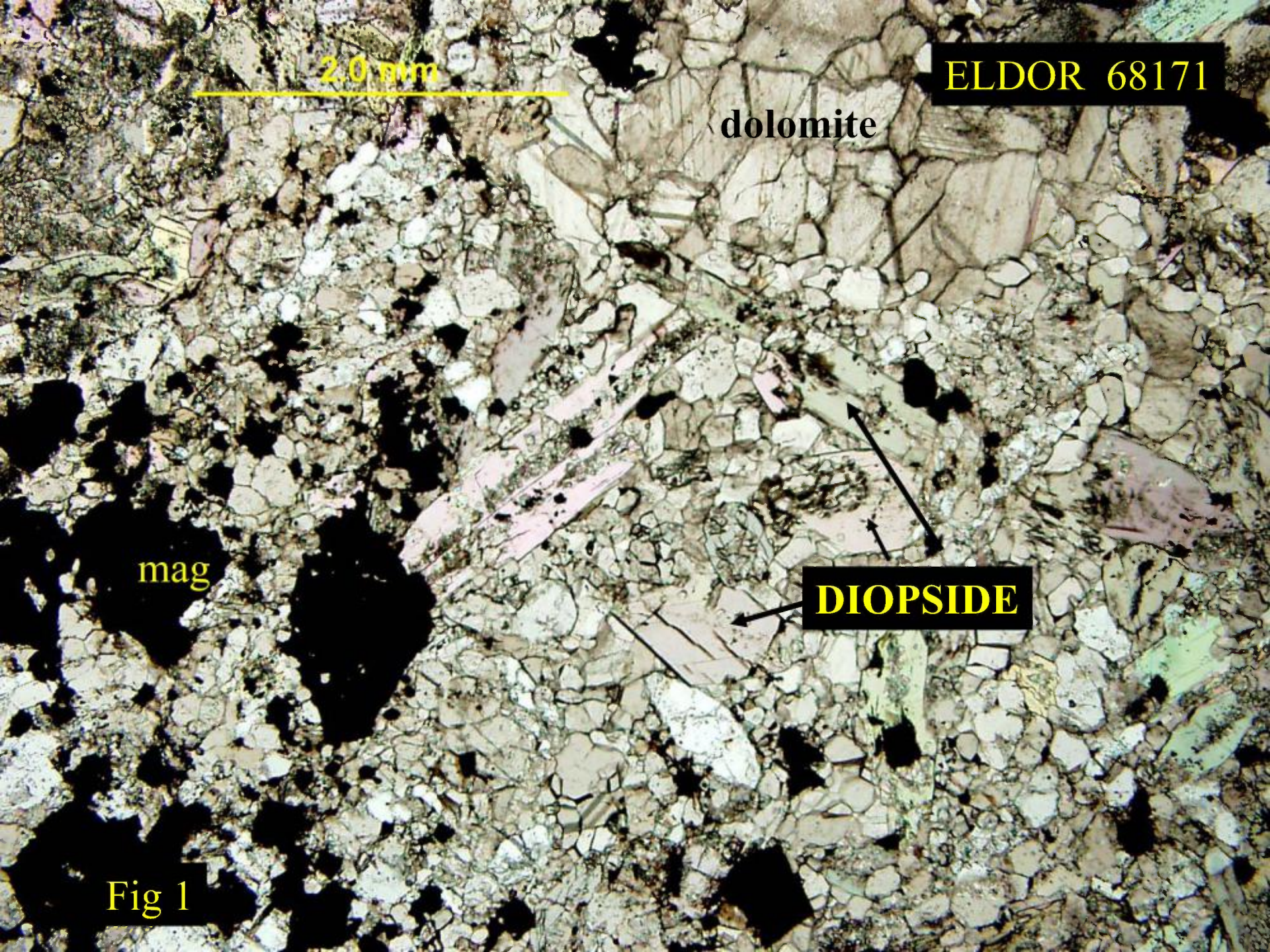

Fig 1

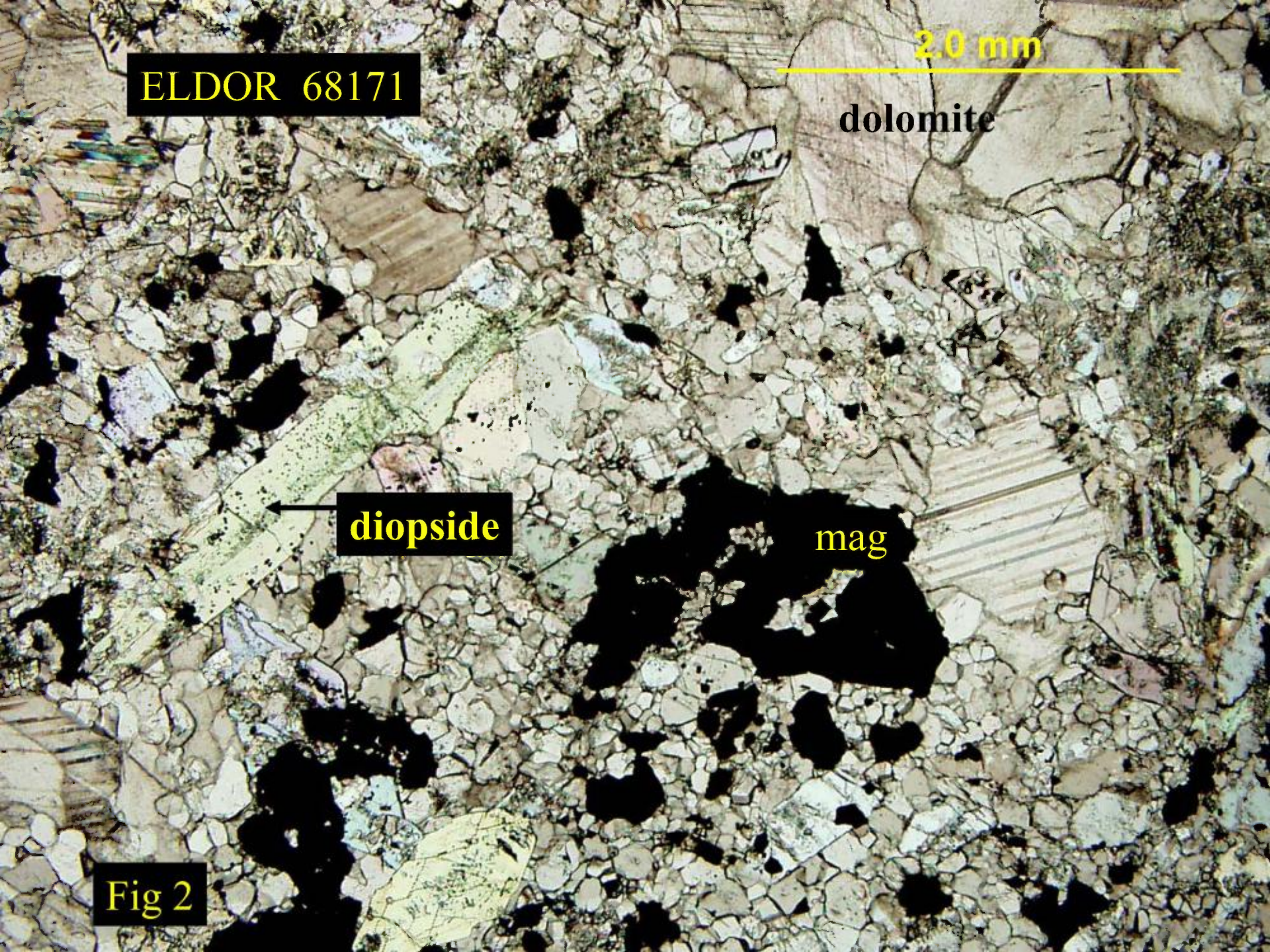
ELDOR 68171
2.0 mm
dolomite
diopside
mag
Fig 2

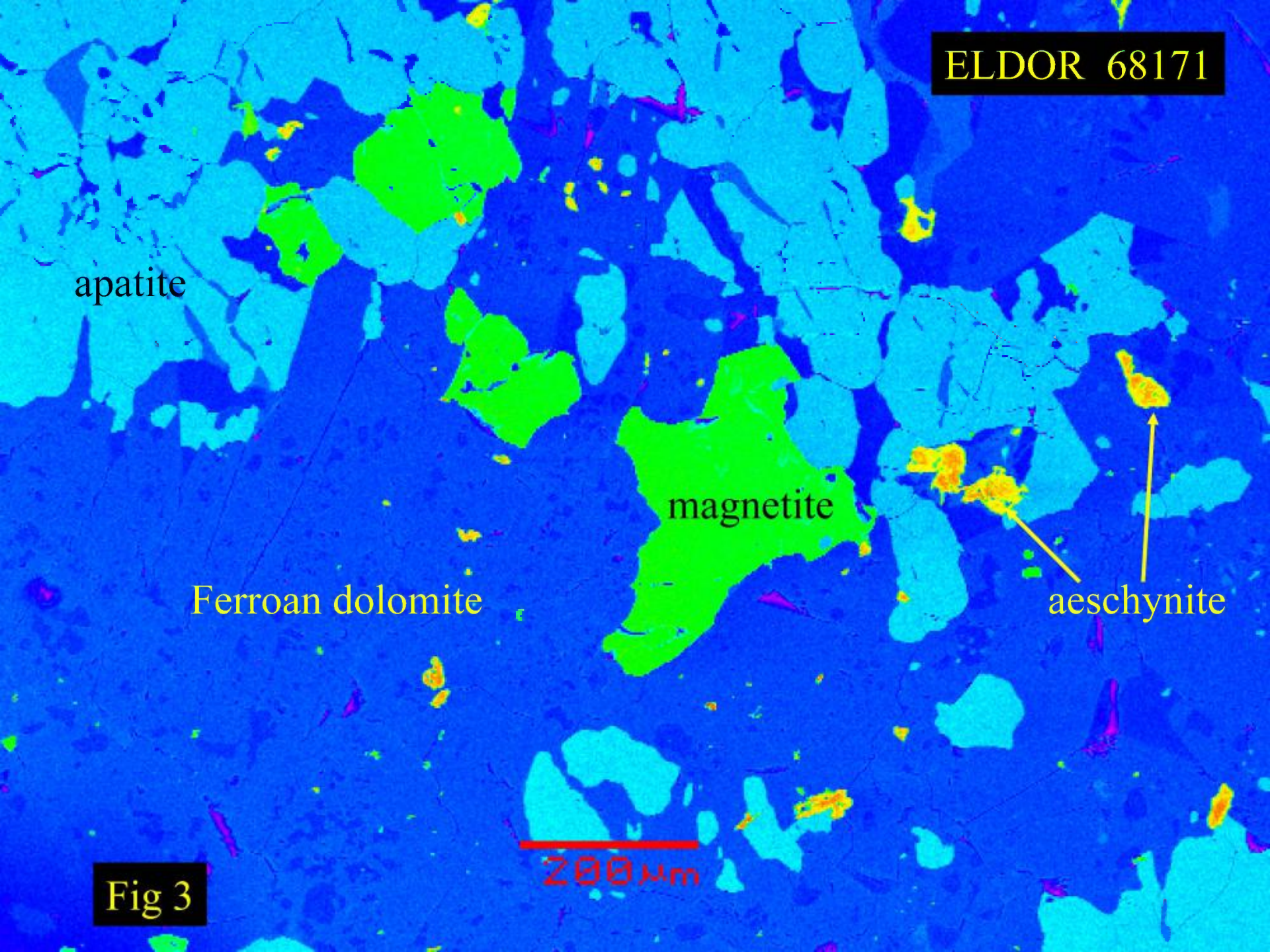
ELDOR 68171
apatite
magnetite
Ferroan dolomite
aeschynite
200µm

Fig 3

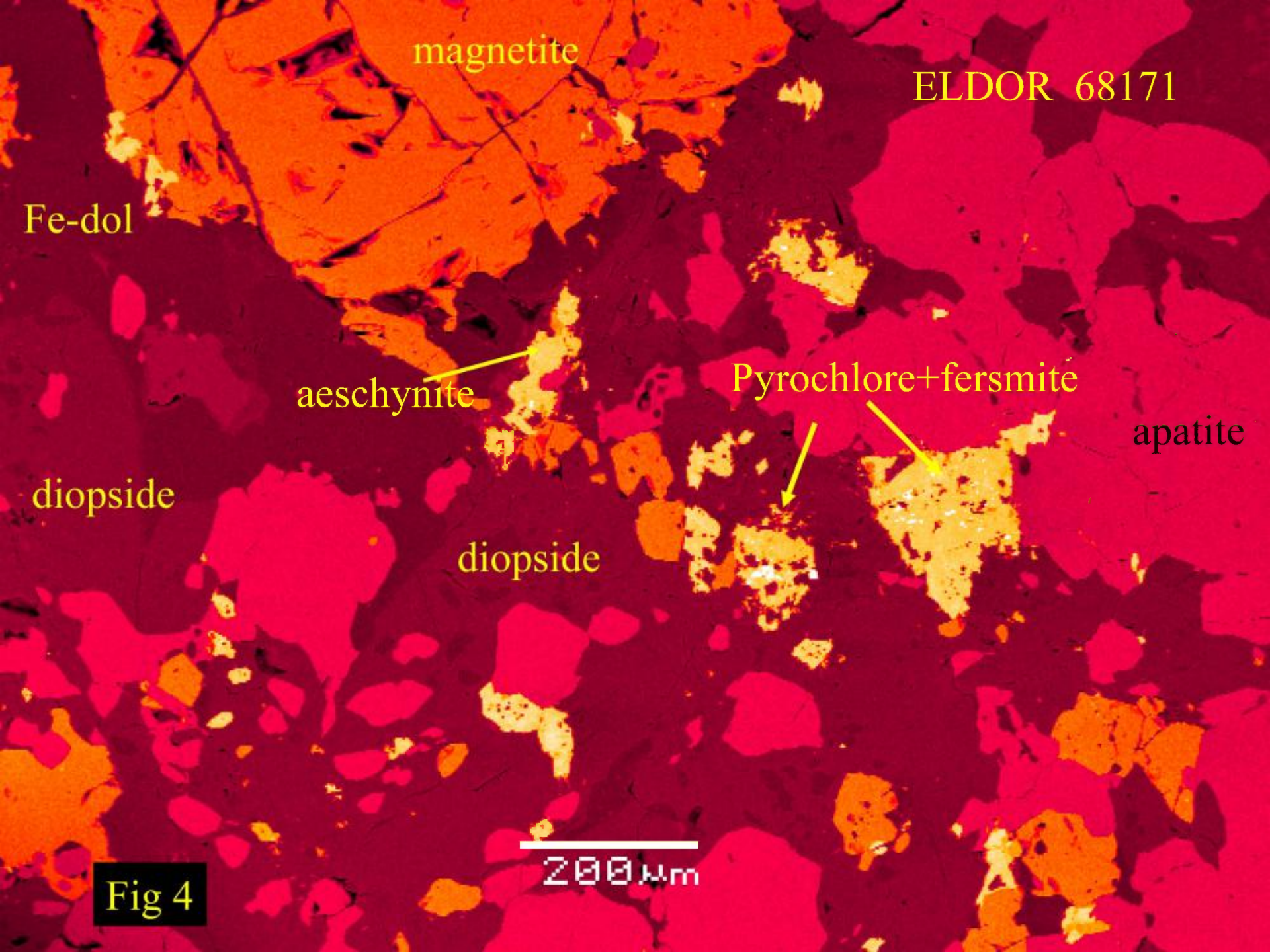
magnetite
ELDOR 68171
Fe-dol
aeschynite
Pyrochlore+fersmite
apatite
diopside
diopside
200µm

Fig 4

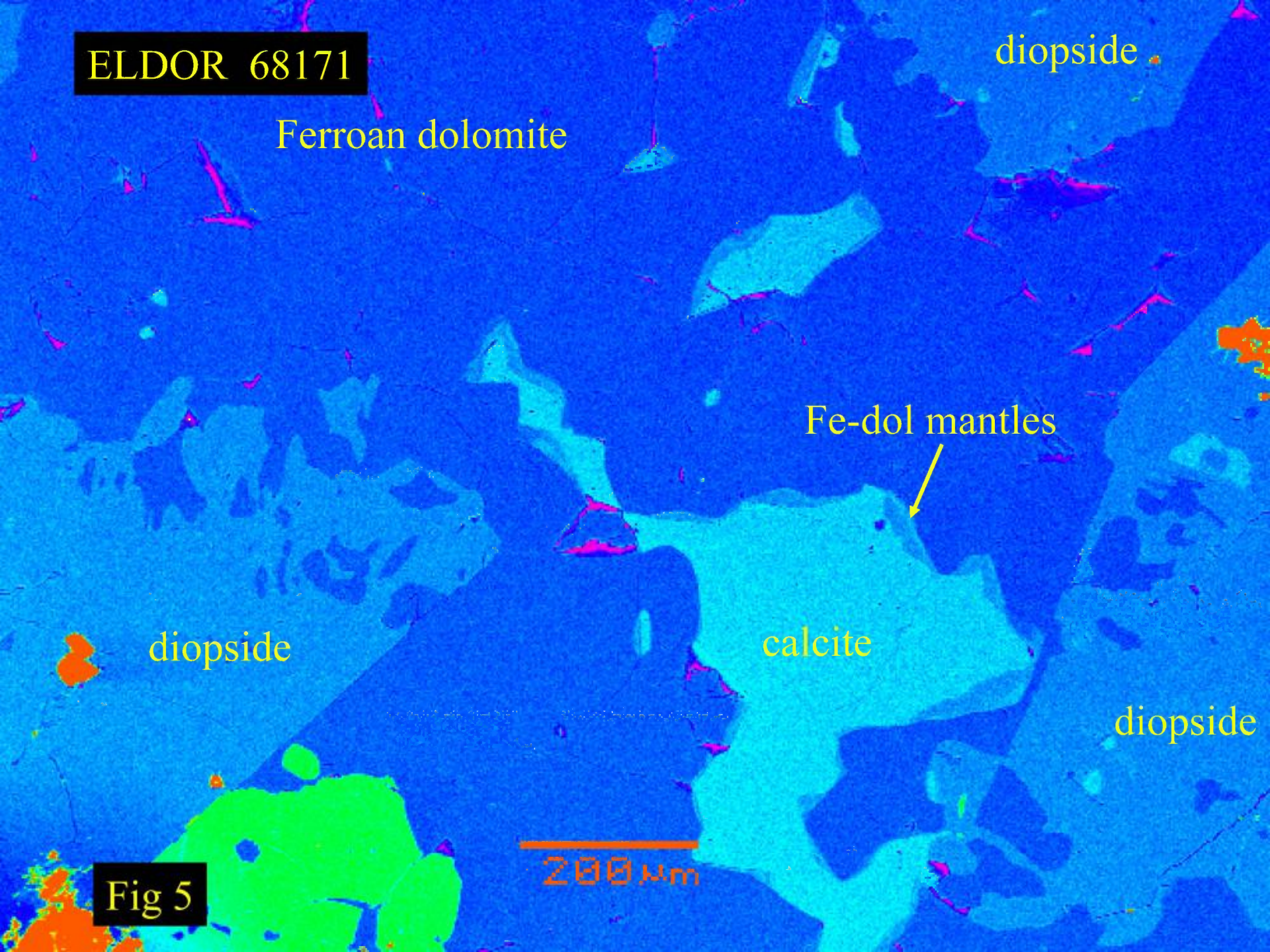
ELDOR 68171
Ferroan dolomite
diopside
Fe-dol mantles
diopside
calcite
diopside
200 µm
Fig 5

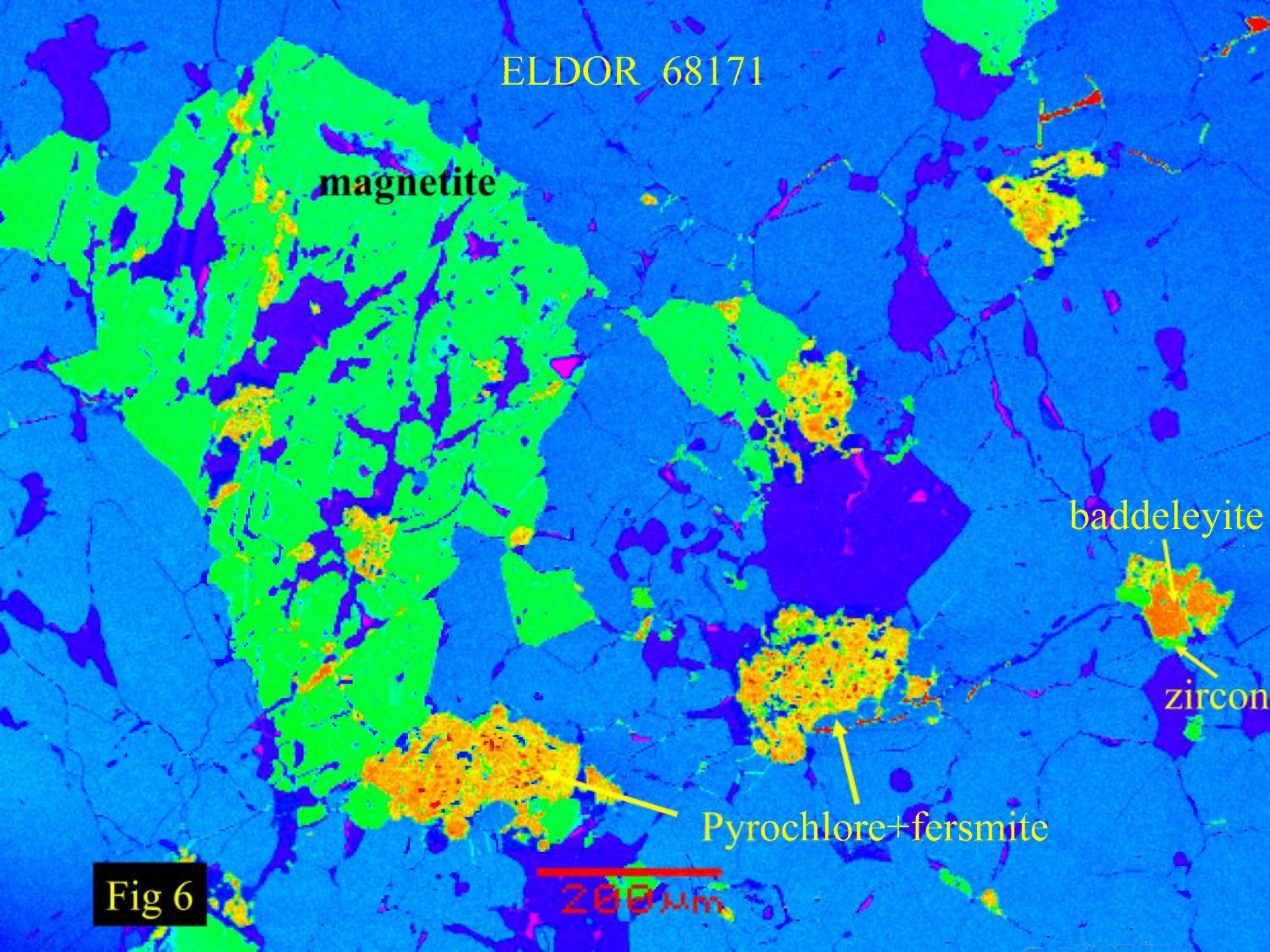
ELDOR 68171
magnetite
baddeleyite
zircon
Pyrochlore+fersmite
200µm

Fig 6

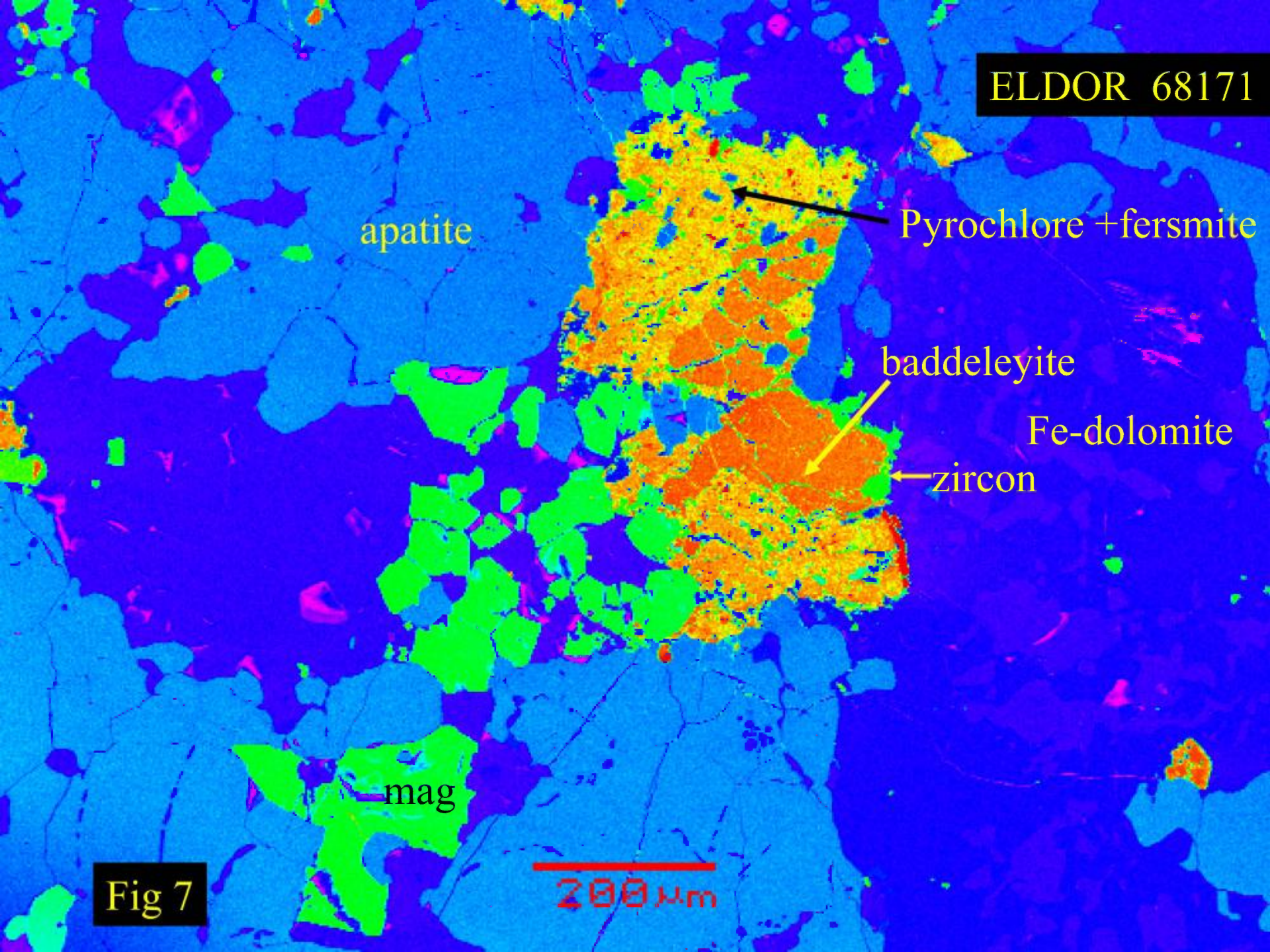
ELDOR 68171
apatite
Pyrochlore +fersmite
baddeleyite
Fe-dolomite
zircon
mag
200 µm

Fig 7

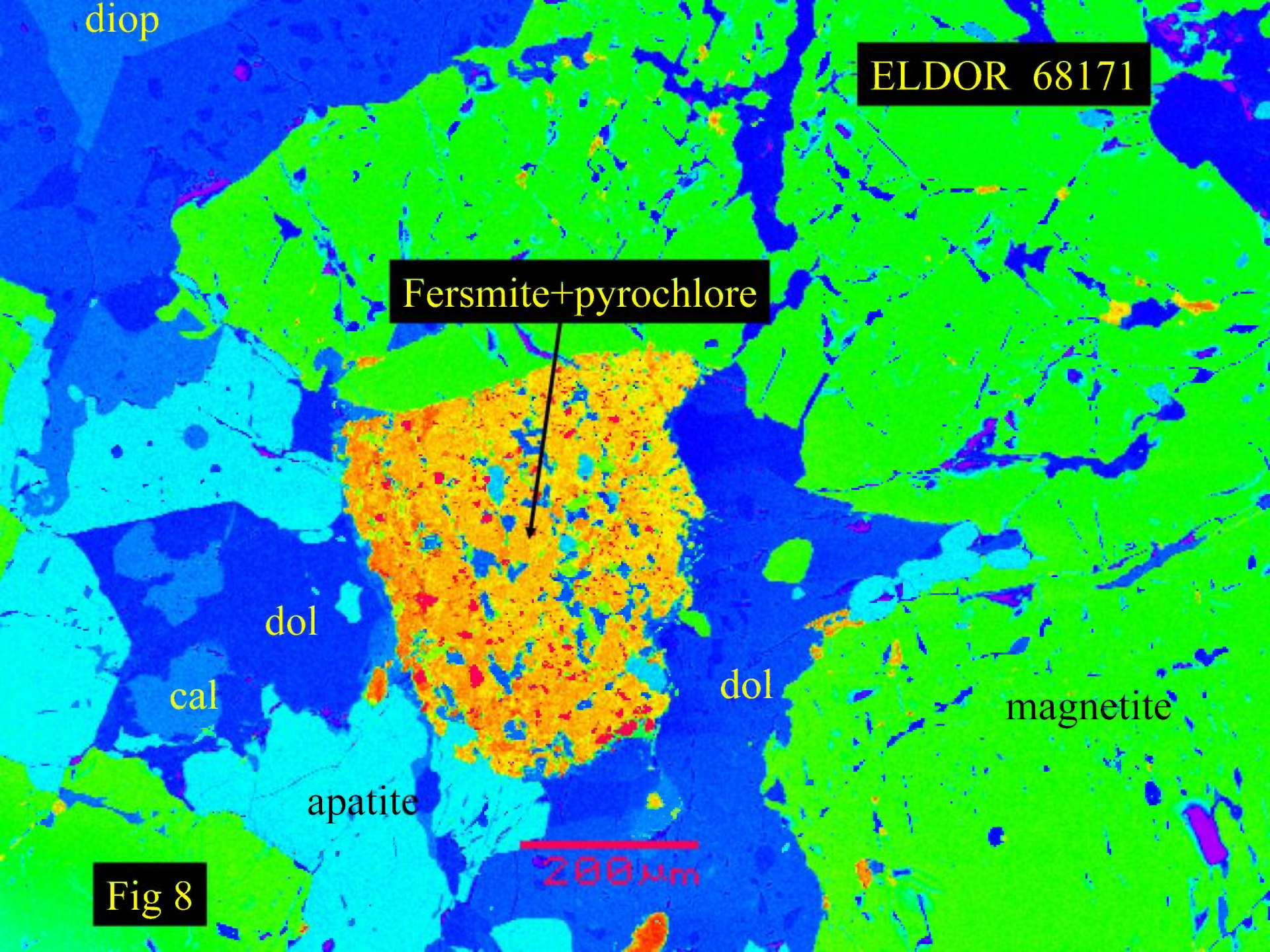
diop
ELDOR 68171
Fersmite+pyrochlore
dol
cal
dol
magnetite
apatite
200µm

Fig 8

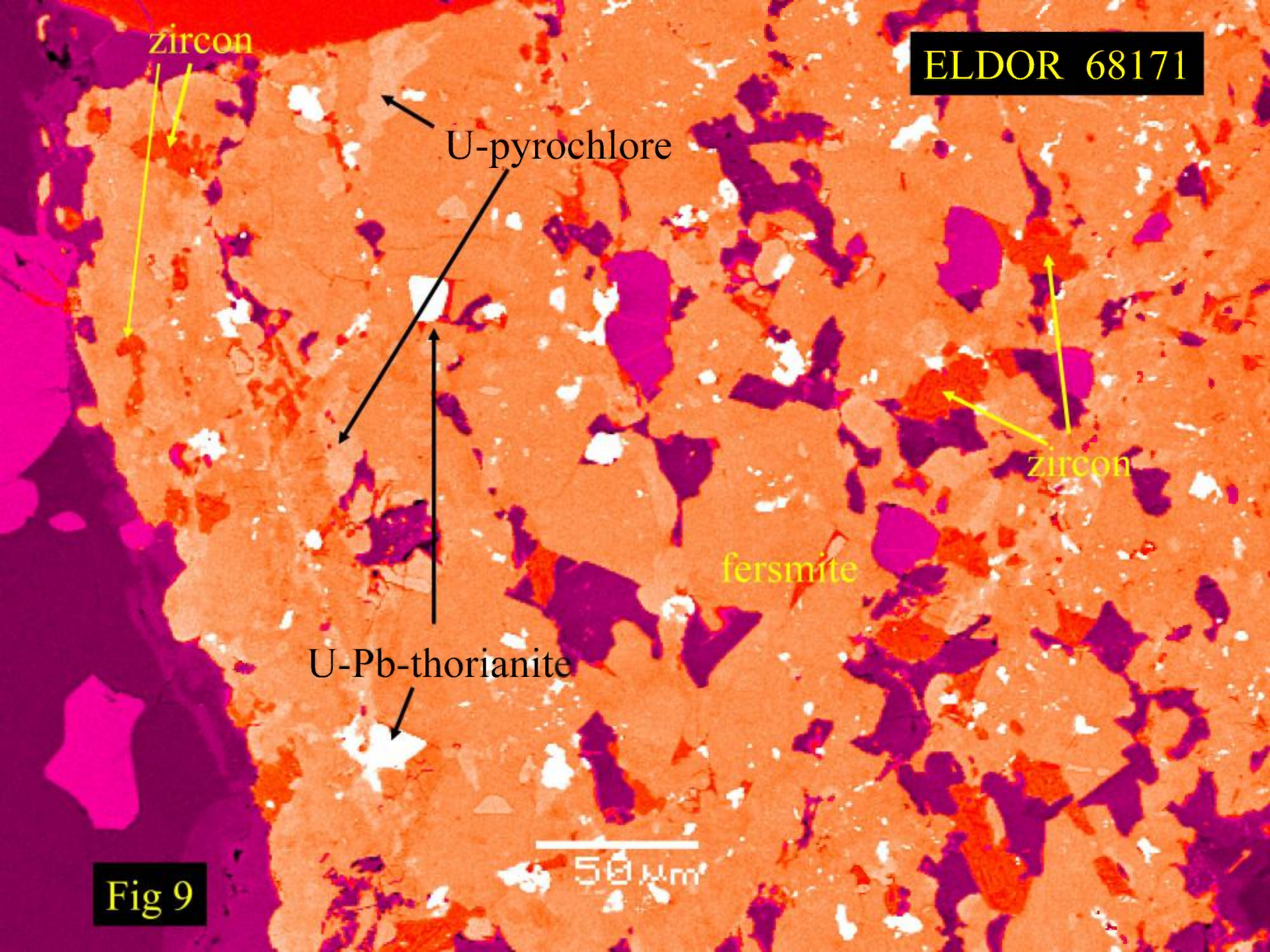
zircon
ELDOR 68171
U-pyrochlore
zircon
fersmite
U-Pb-thorianite
50 µm

Fig 9

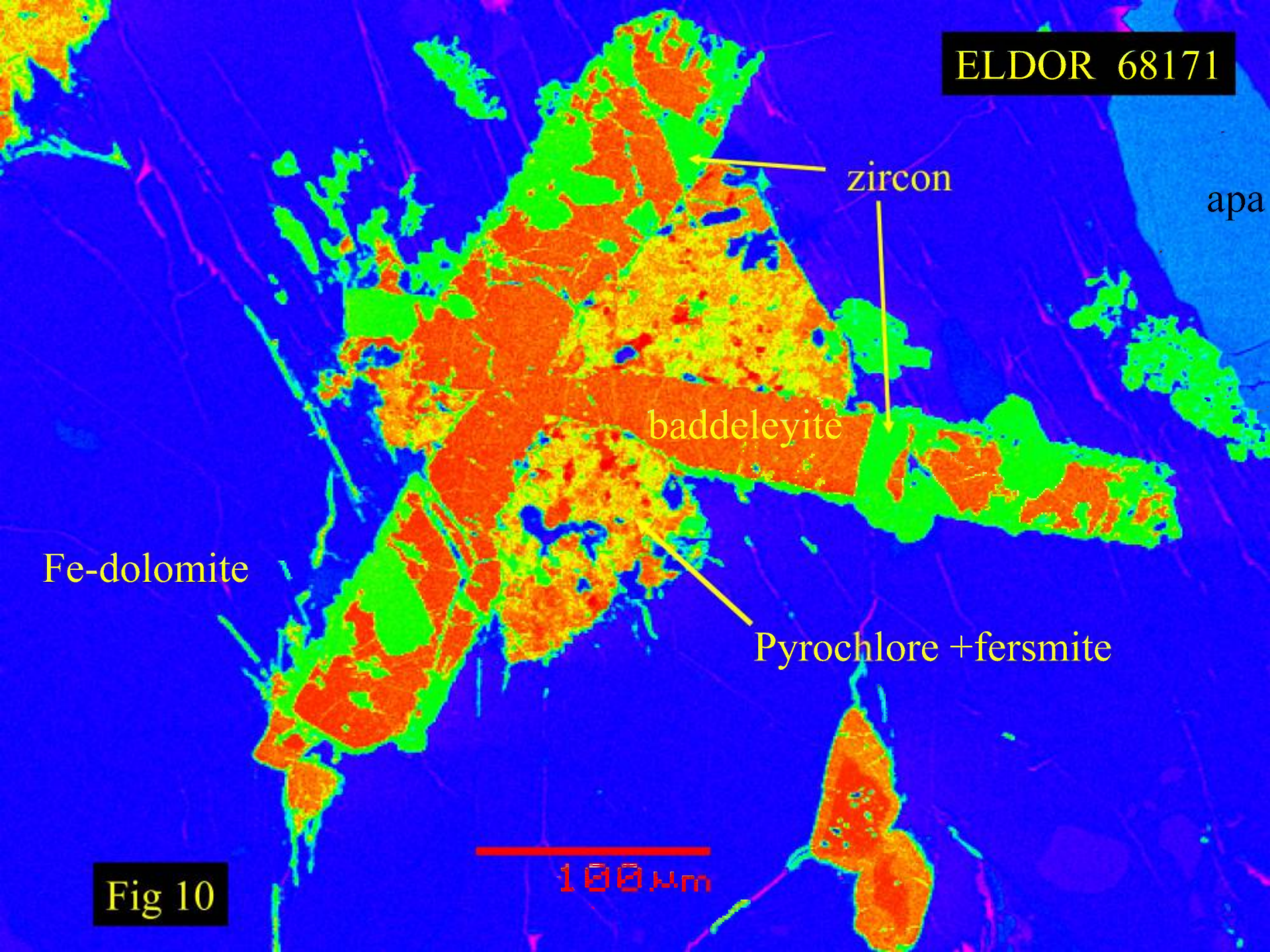
ELDOR 68171
zircon
apa
baddeleyite
Fe-dolomite
Pyrochlore +fersmite
100µm

Fig 10

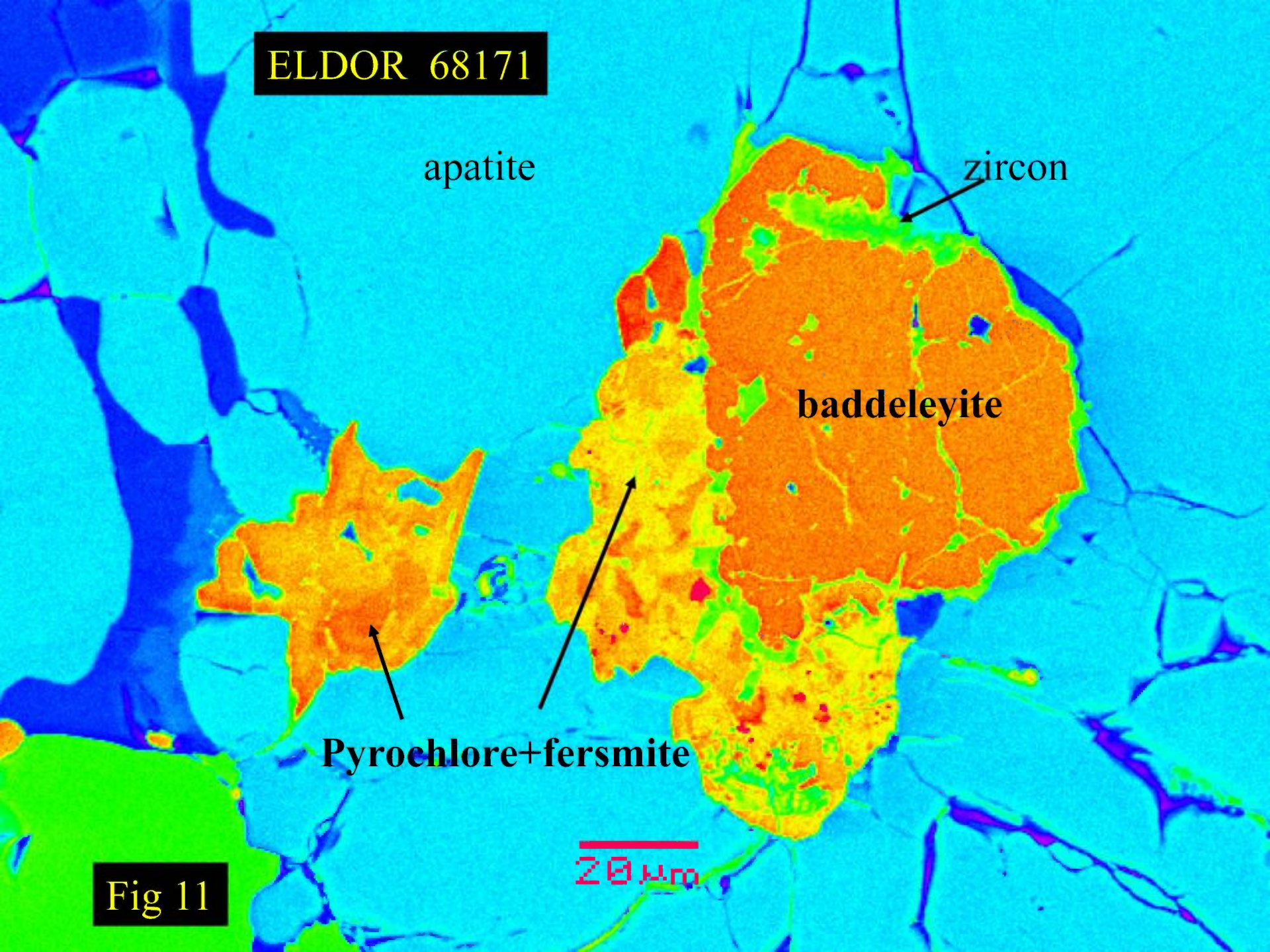
ELDOR 68171
apatite
zircon
baddeleyite
Pyrochlore+fersmite
20 µm

Fig 11

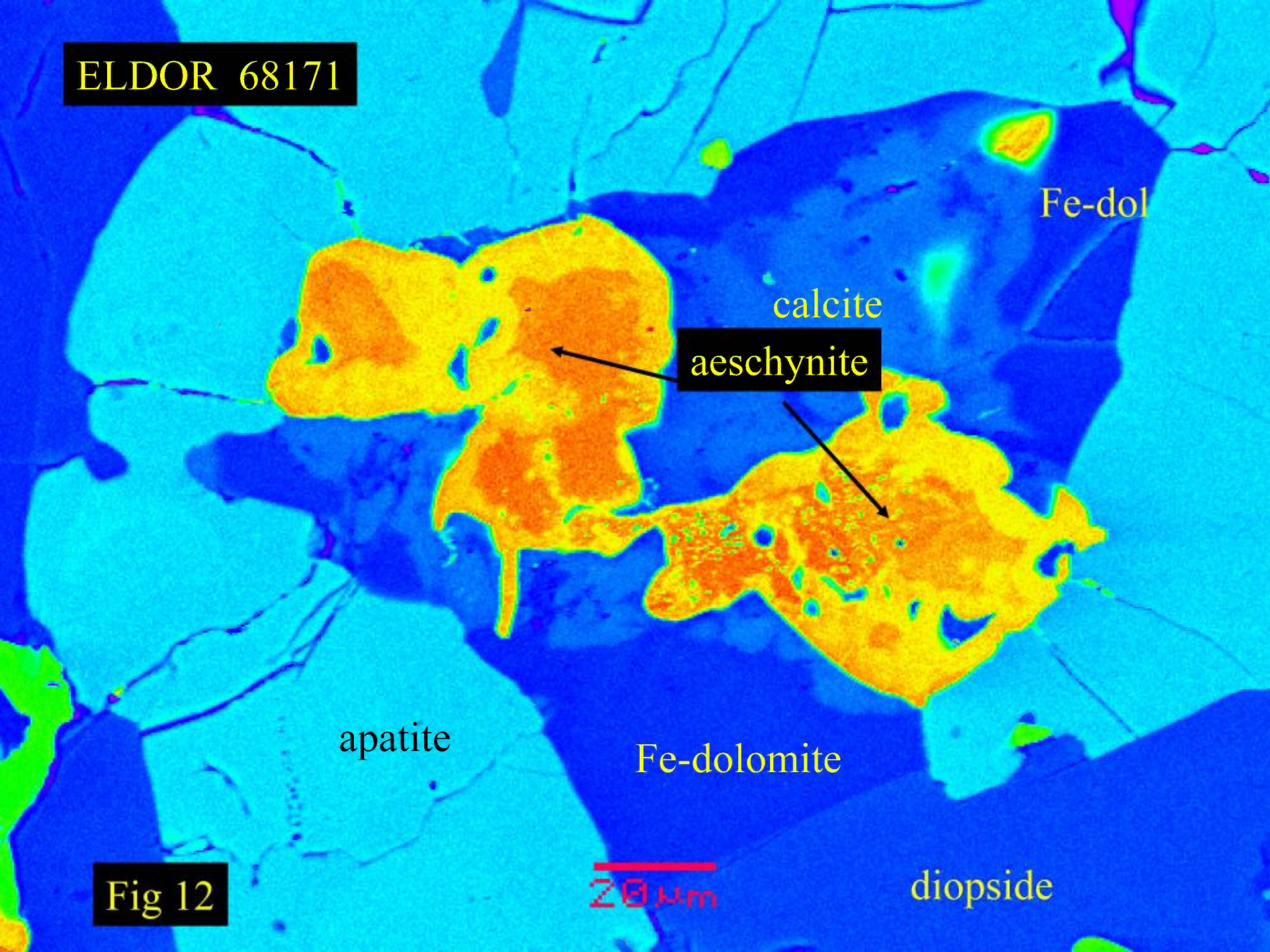
ELDOR 68171
Fe-dol
calcite
aeschynite
apatite
Fe-dolomite
diopside
20 µm

Fig 12

ELDOR 68182

ELDOR 68182 *Chlorite magnetite apatite calcite carbonatite.*

This heterogeneous sample consists principally of magnetite, apatite, chlorite pseudomorphs after an unidentified mineral, and calcite (Figs. 1-3). Some parts of the sample consist of apatite "cumulates" (fig.2), whereas others are enriched in apatite, magnetite and "pyrochlores"(Figs 1 & 7). Areas that are magnetite-poor and dominated by chlorite pseudomorphs are found (Figs 3 & 5).

Magnetite occurs as large (up to 0.7 mm) irregular crystals (Figs 5 & 7). The crystals are fractured, and galena can be found occupying portions of these fractures. Inclusions of ilmenite are not present. Magnetite appears to have formed subsequent to apatite. The magnetite is of uniform composition and poor in Ti, Mg, and Mn (<0.5 wt.% oxides). Magnetite is characterized by fibrous overgrowths of Mg-chlorite pseudomorphs after mica (Fig.1). Fe-bearing dolomite can be found cementing magnetite and apatite "cumulates". Apatite forms anhedral-to-irregular resorbed aggregates (Fig. 5 & 7) and cumulate-like masses of anhedral crystals (Figs. 2 & 6). The apatite is of uniform composition, and poor in Sr and rare earths (<0.5 wt.%). Large (<0.3mm) pale green euhedral crystals (Fig. 3) are Mg-chlorite (plus minor calcite) pseudomorphs after former phlogopite (Fig. 5). The groundmass of the sample is composed an intimate mixture of calcite and Mg-chlorite pseudomorphs after phlogopite (Fig. 4) or large anhedral plates of calcite (Fig. 2). Relicts of the mica can be observed in some instances in transmitted light. The original groundmass was thus phlogopite and calcite.

"Pyrochlores" are relatively abundant in the sample and form large (up to 0.4mm) irregular resorbed crystals intergrown with apatite and magnetite (Figs. 5 & 8-9). Euhedral crystals are rarely found (Fig.12). BSE-imagery and X-ray spectrometry show that all pyrochlores are complex intimate intergrowths of fersmite and diverse Th-U-Ta-bearing pyrochlores. Sphalerite, baddeleyite, zircon, galena and $(Th,Pb)O_2$ can be found as inclusions. Fersmites are typically poor in Ta and U. The pyrochlores range in composition from U-Ta pyrochlore to Th-pyrochlore. Representative semiquantitative compositions are given below. Ferrocolumbite is not present.

Baddeleyite lacking "pyrochlore-fersmite" overgrowths can also be found in the groundmass of the sample as subhedral small crystals (Fig. 9).

Representative semiquantitative compositions of pyrochlore and fersmite:

Wt.%	U-Ta-pyroch	Th-pyrochlore	fersmite
F	n.d.	n.d.	n.d.
Na_2O	n.d.	n.d.	n.d.
SiO_2	2.87	0.9	0.4
BaO	n.d.	n.d.	n.d.
CaO	5.5	3.7	13.9
TiO_2	3.6	2.3	0.5
FeO	4.5	3.2	3.7
Nb_2O_5	43.9	45.7	78.9
Ta_2O_5	11.3	4.3	1.8
La_2O_3	1.5	0.9	n.d.
Ce_2O_3	4.2	2.8	0.8
Pr_2O_3	n.d.	1.4	n.d..
Nd_2O_3	1.5	2.0	n.d.
ThO_2	n.d.	26.4	0.9
UO_2	15.0.	3.1	n.d.

ELDOR 68182

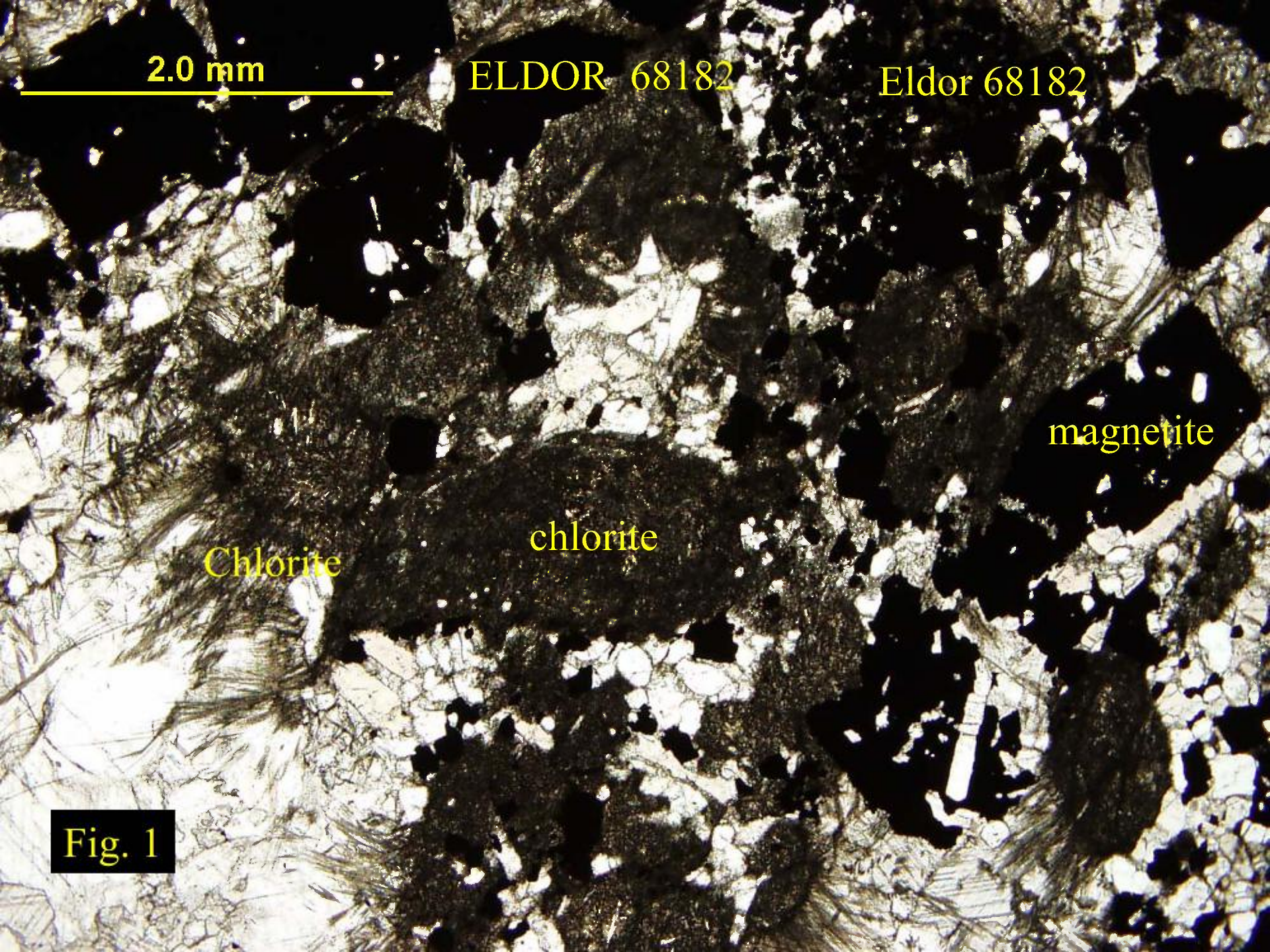

Fig. 1

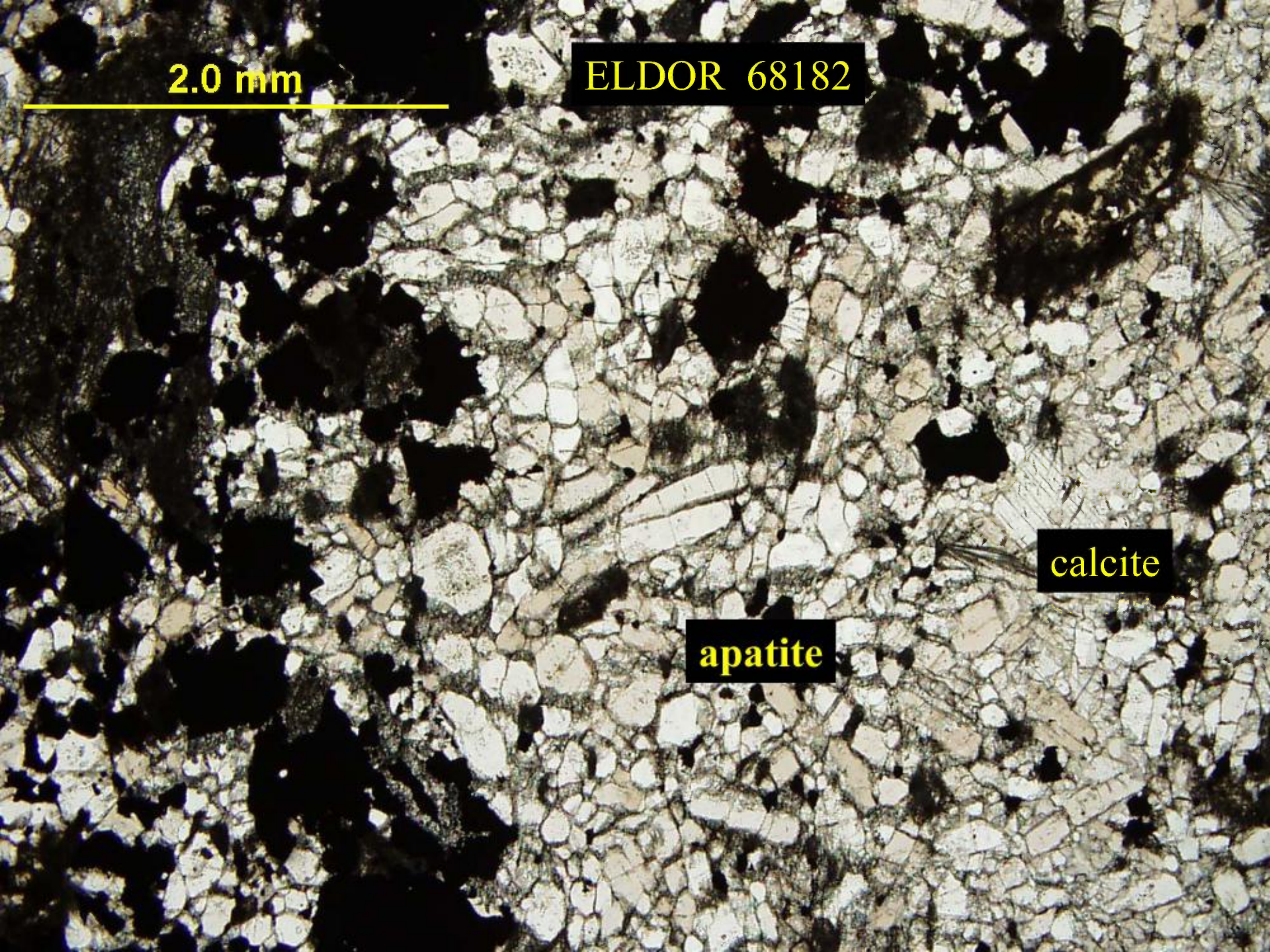
2.0 mm
ELDOR 68182
calcite
apatite

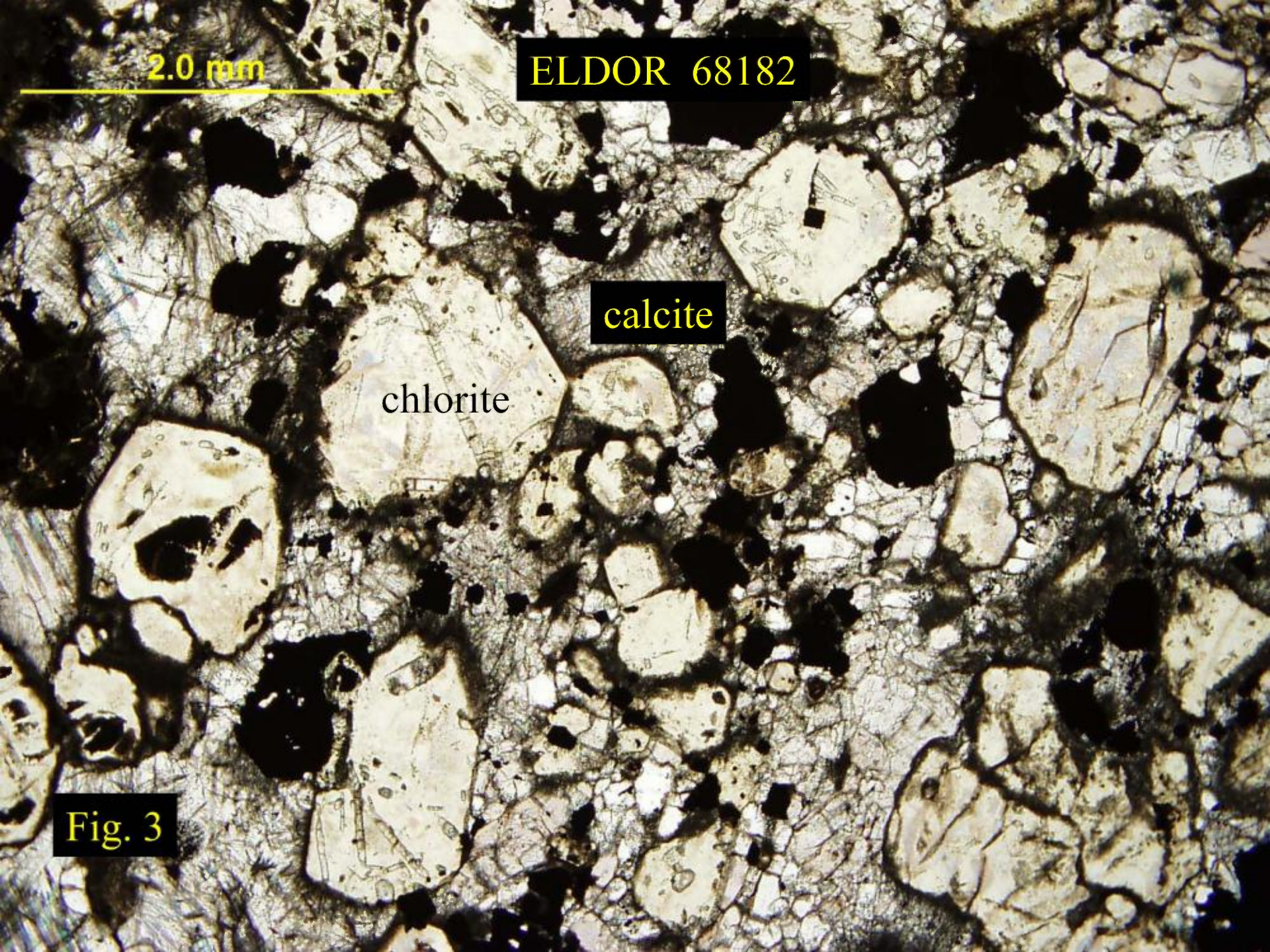

Fig. 3

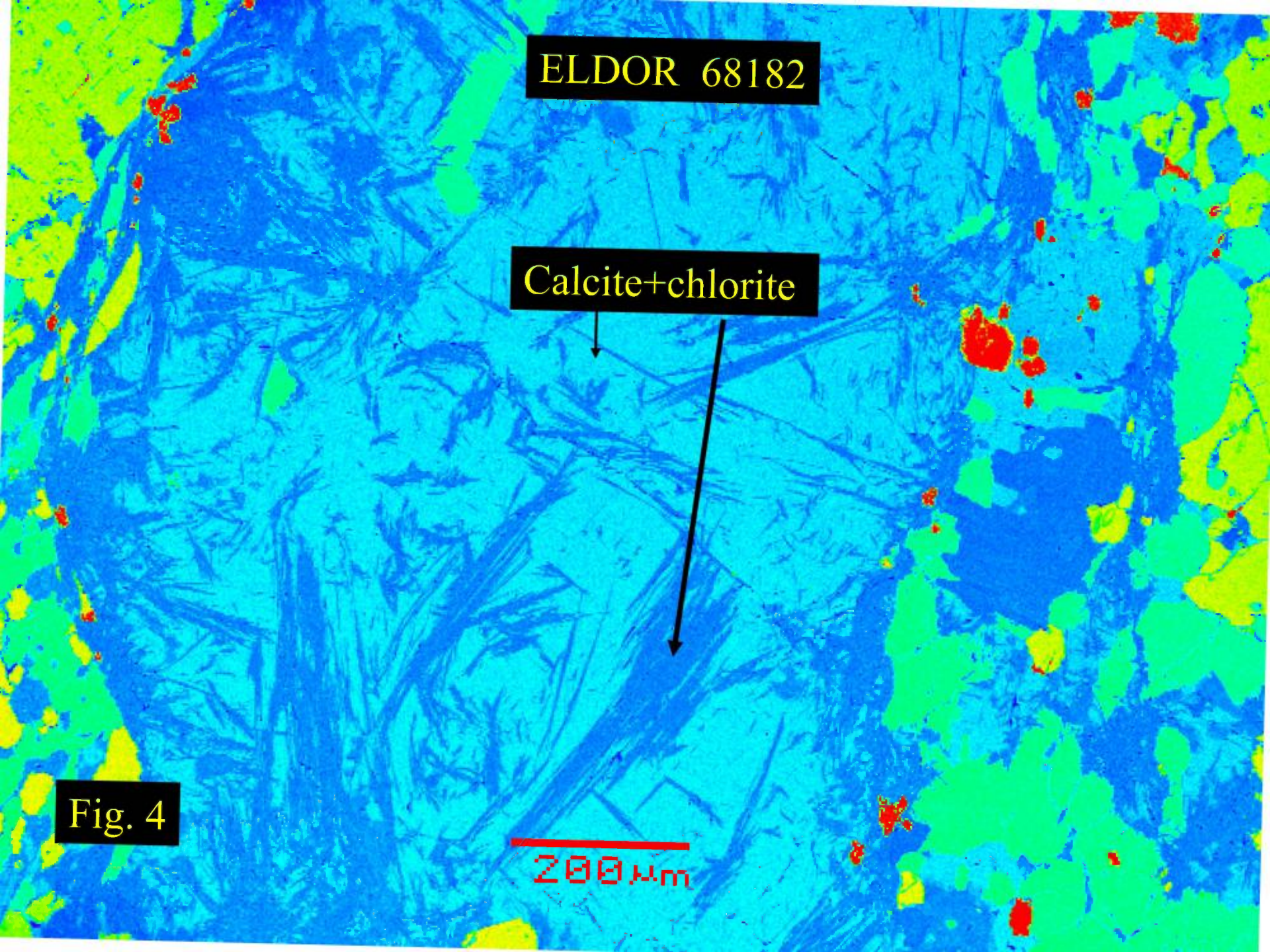

Fig. 4

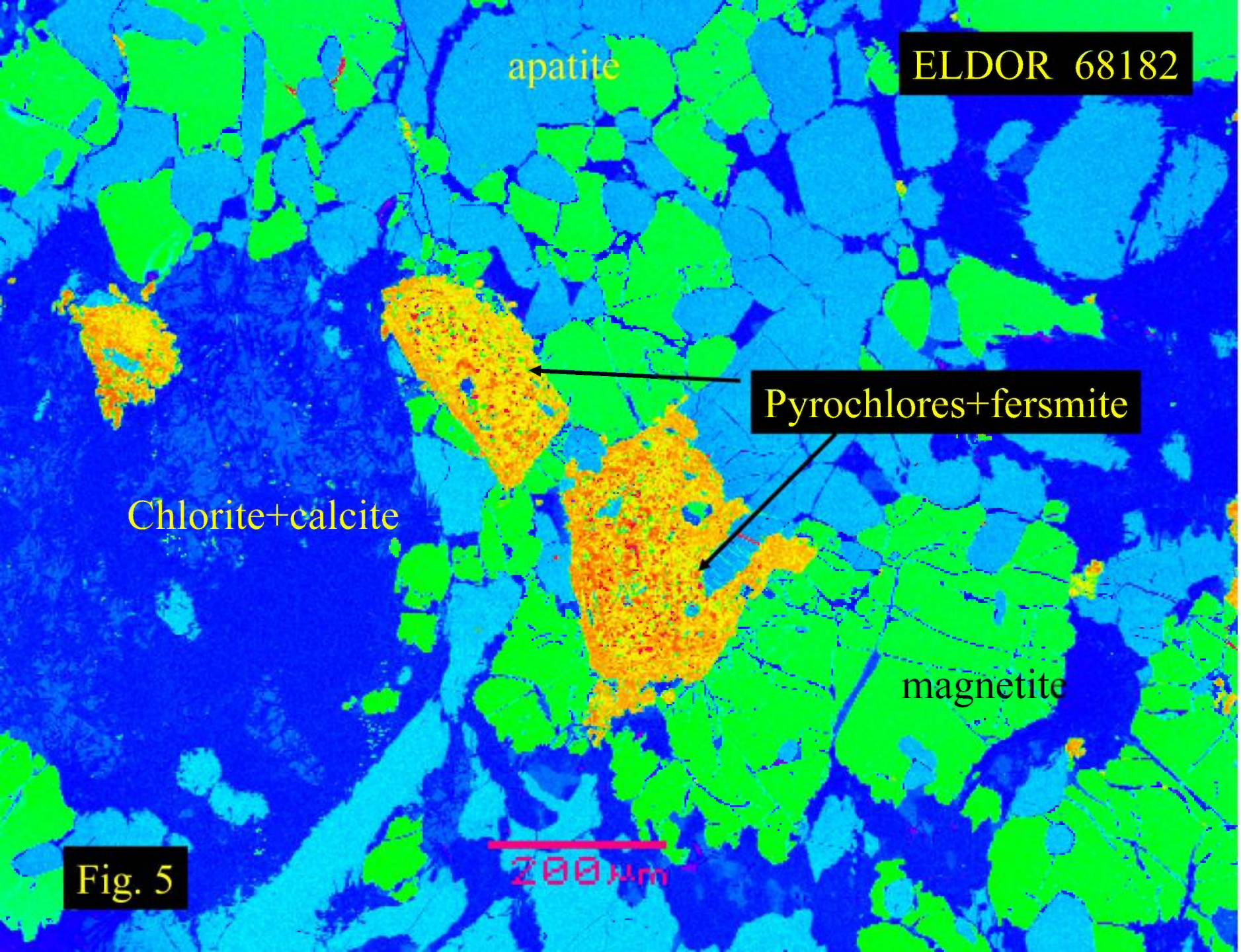
apatite
ELDOR 68182
Pyrochlores+fersmite
Chlorite+calcite
magnetite
200µm

Fig. 5

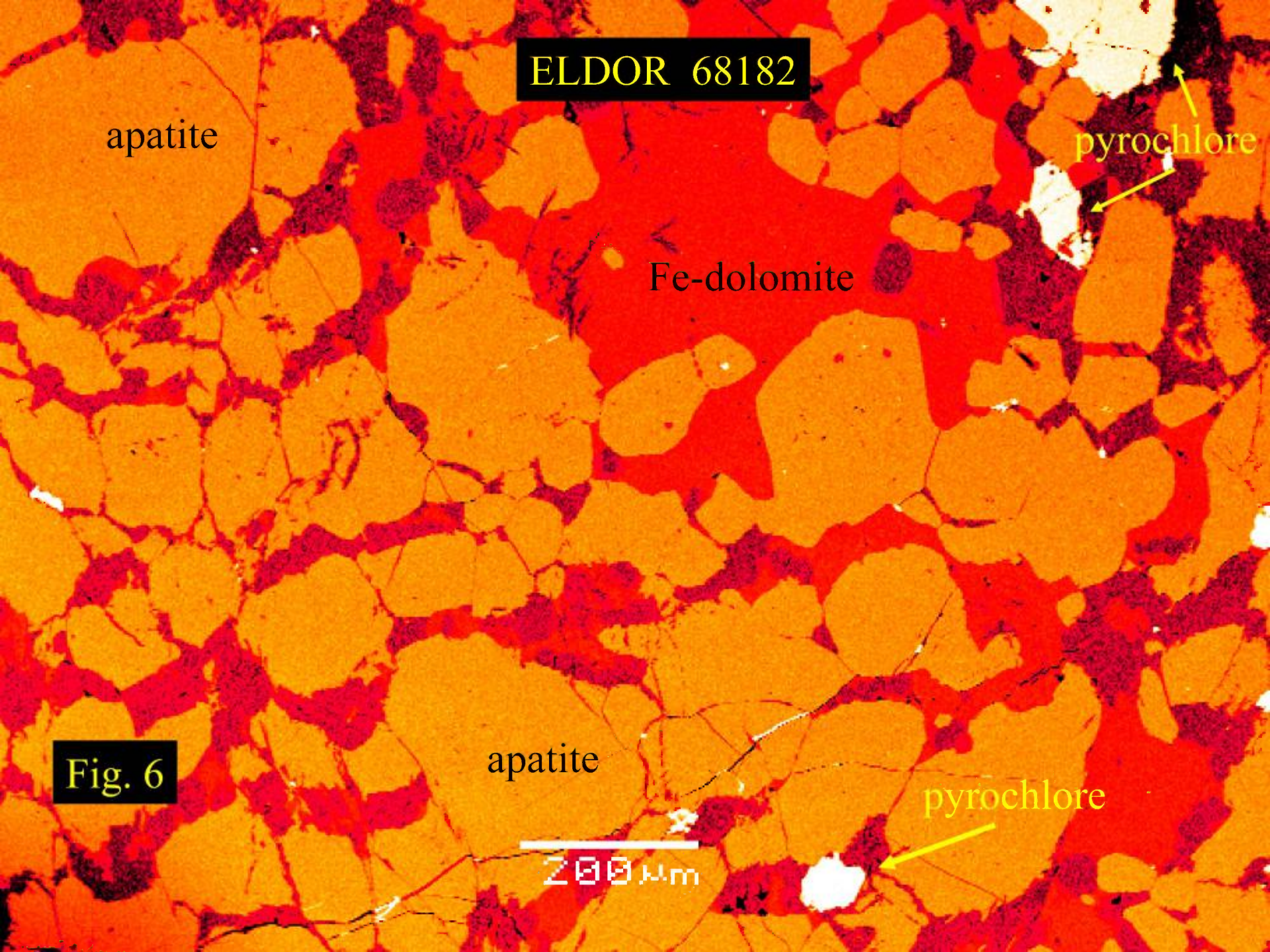
ELDOR 68182
apatite
pyrochlore
Fe-dolomite
apatite
pyrochlore
200µm

Fig. 6

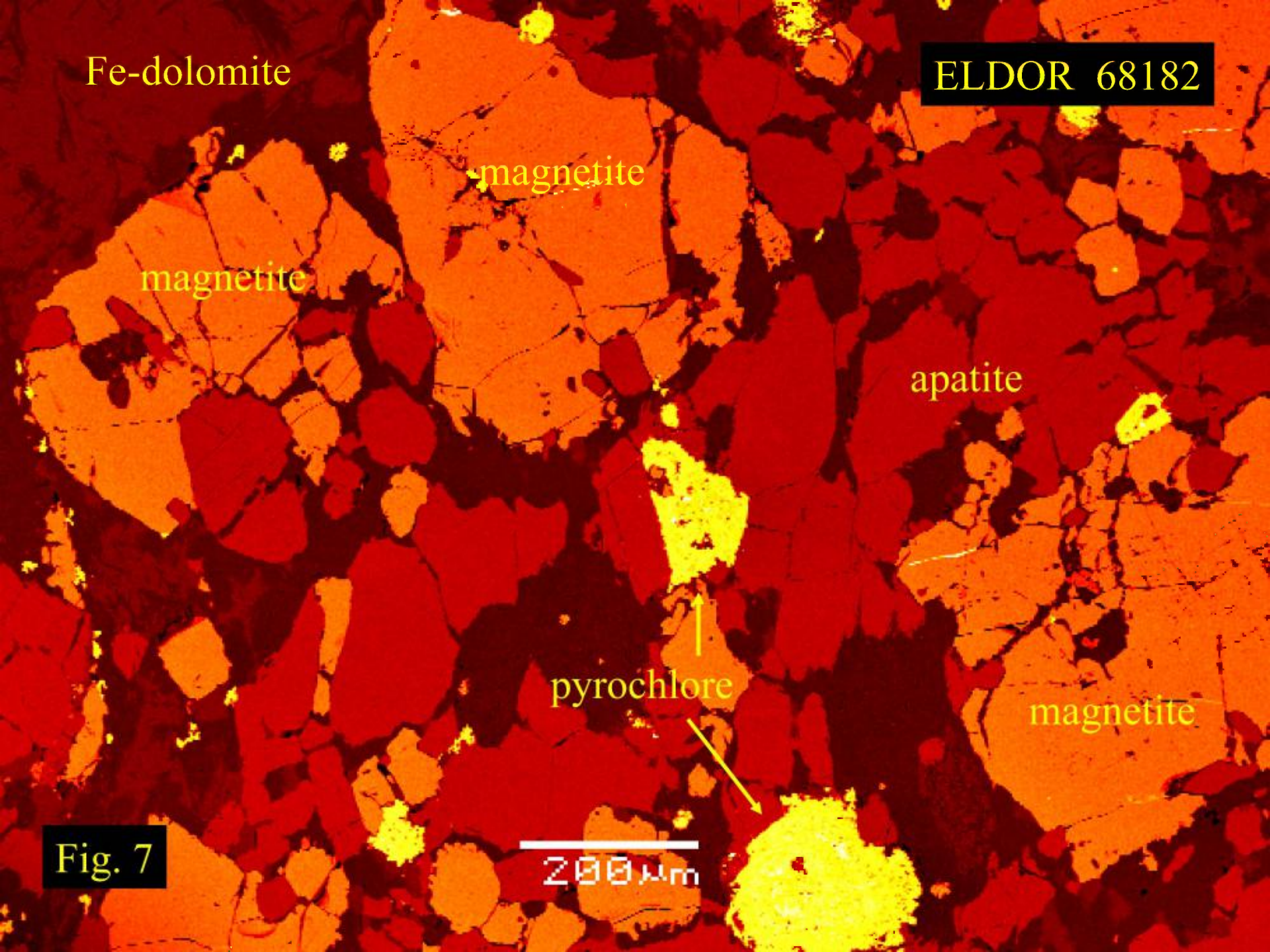
Fe-dolomite
ELDOR 68182
magnetite
magnetite
apatite
pyrochlore
magnetite
200µm

Fig. 7

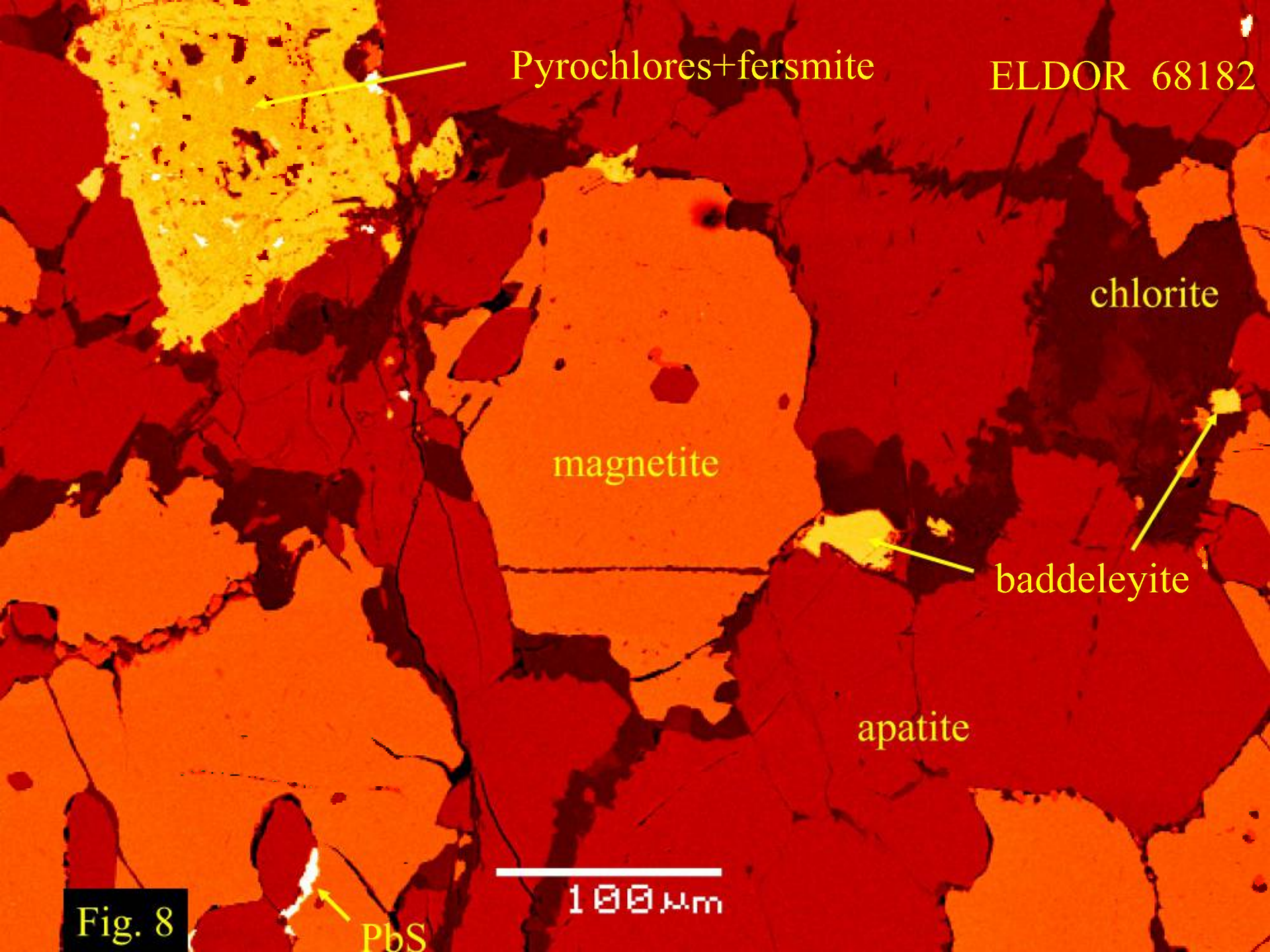
Pyrochlores+fersmite
ELDOR 68182
chlorite
magnetite
baddeleyite
apatite
100µm
PbS

Fig. 8

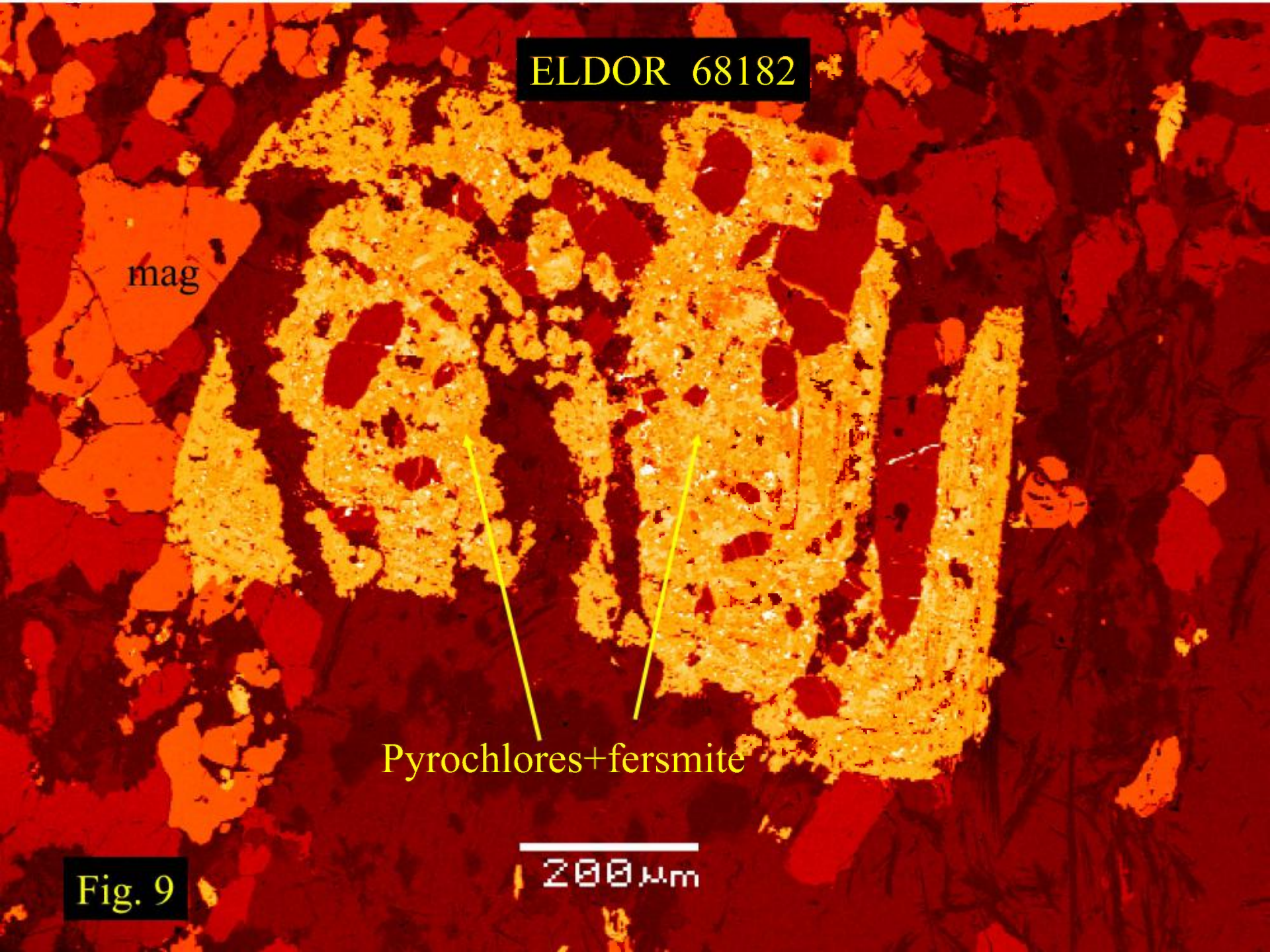

Fig. 9

BSE-image – grey scale

ELDOR 68182

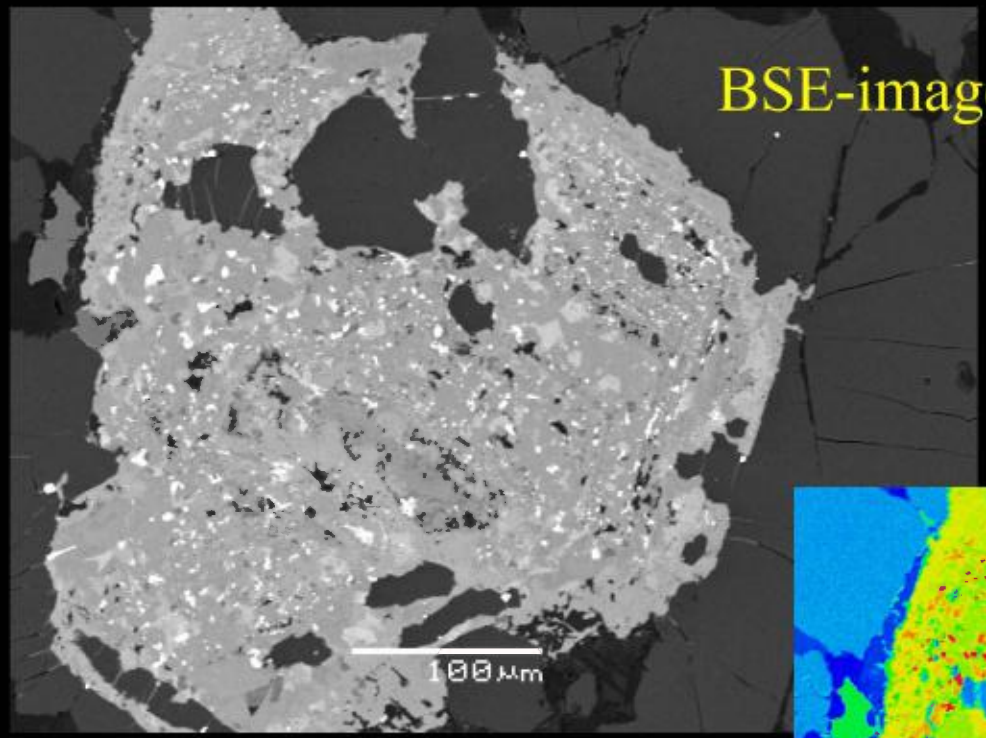

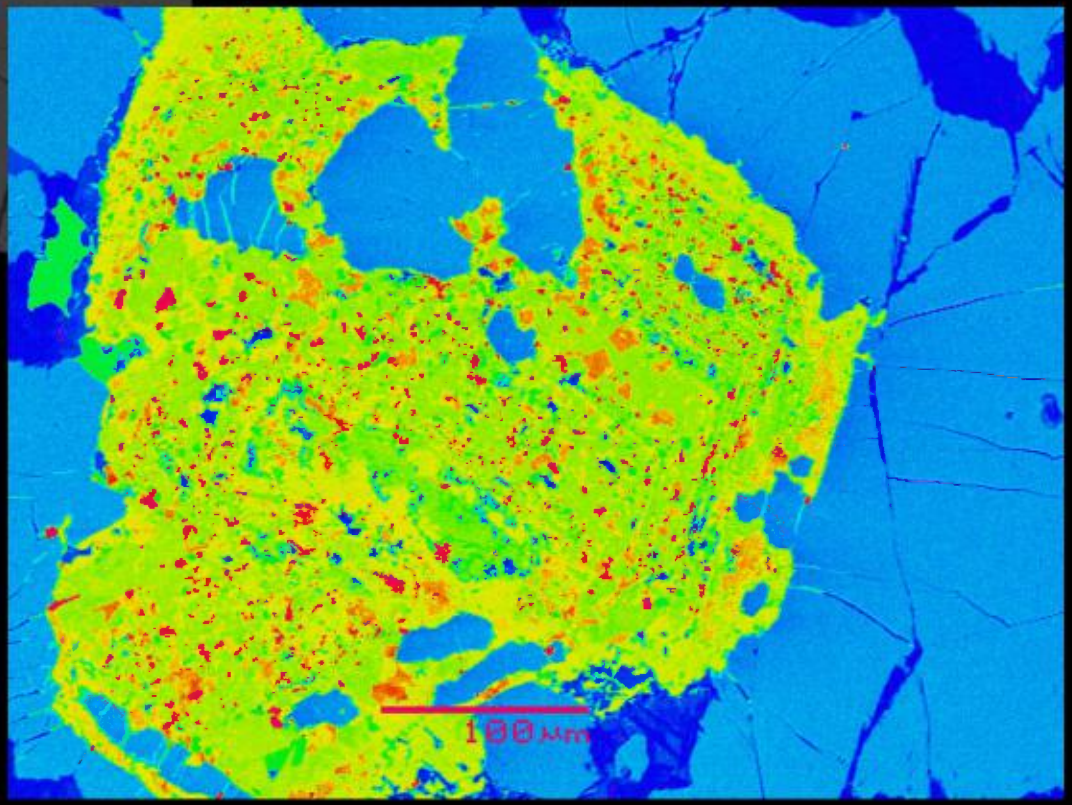

Complex “pyrochlore”

Fig. 10

BSE-image - false colour

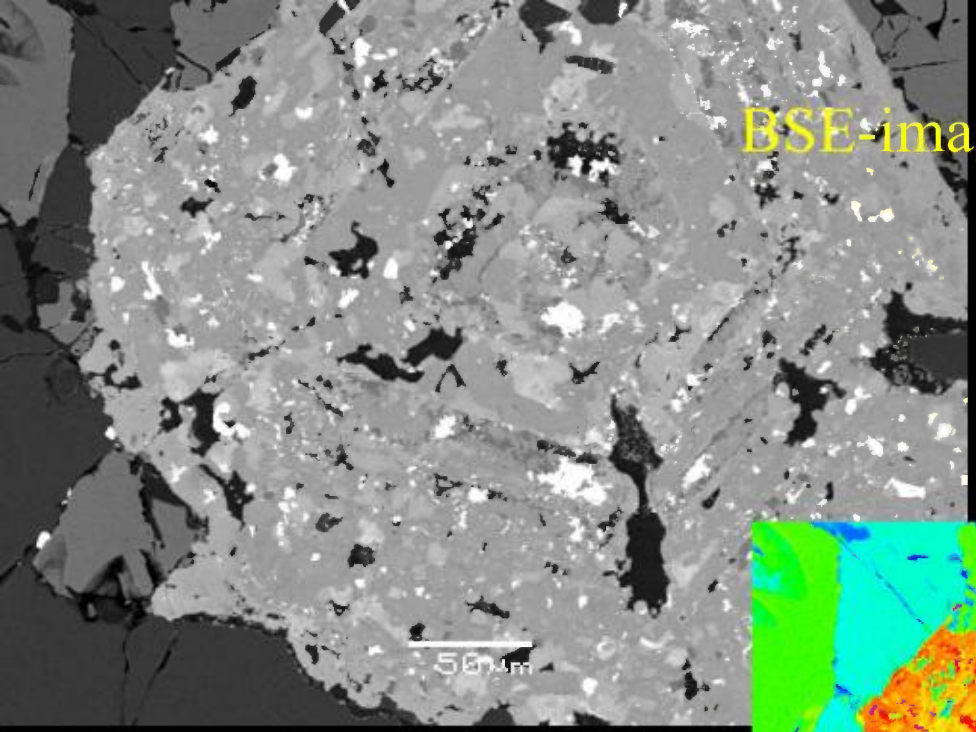

BSE-image – grey scale

ELDOR 68182

BSE-image - false colour

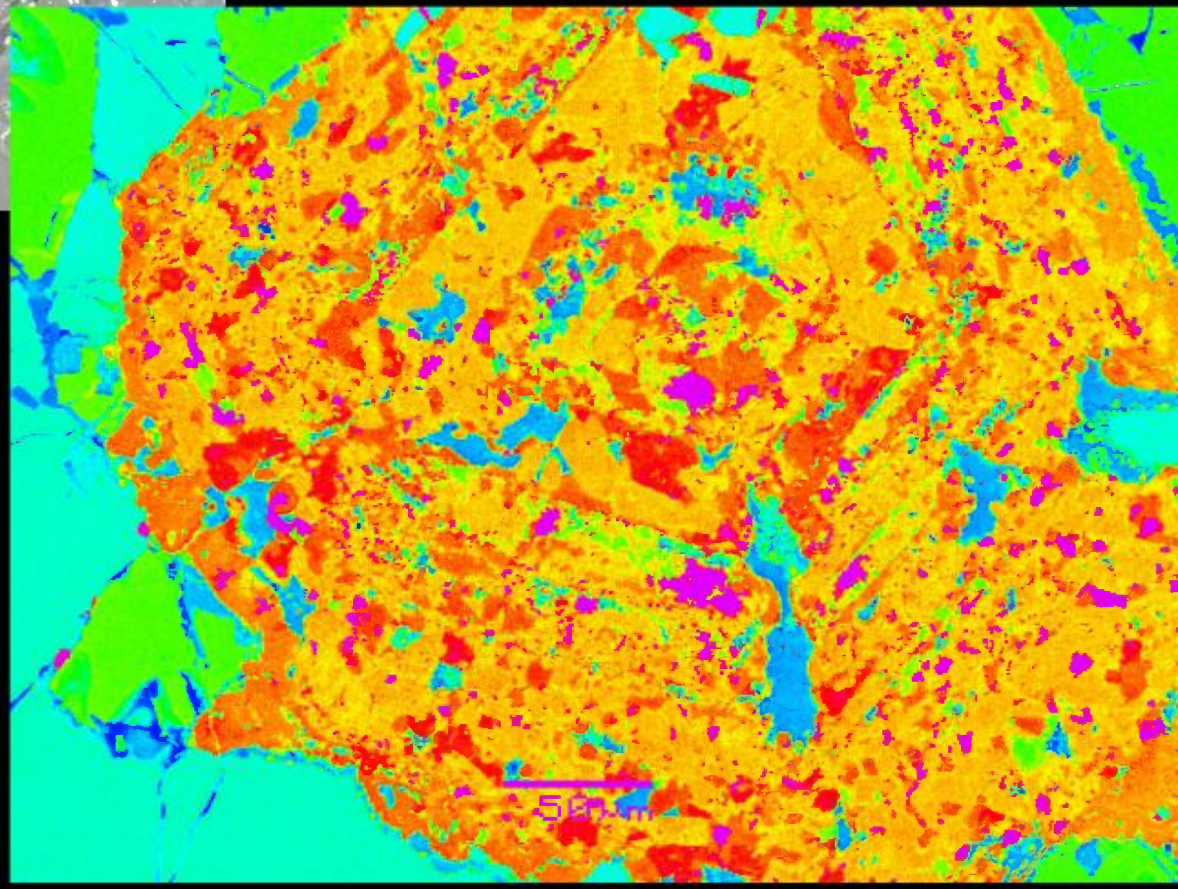

Complex “pyrochlore”

Fig.11

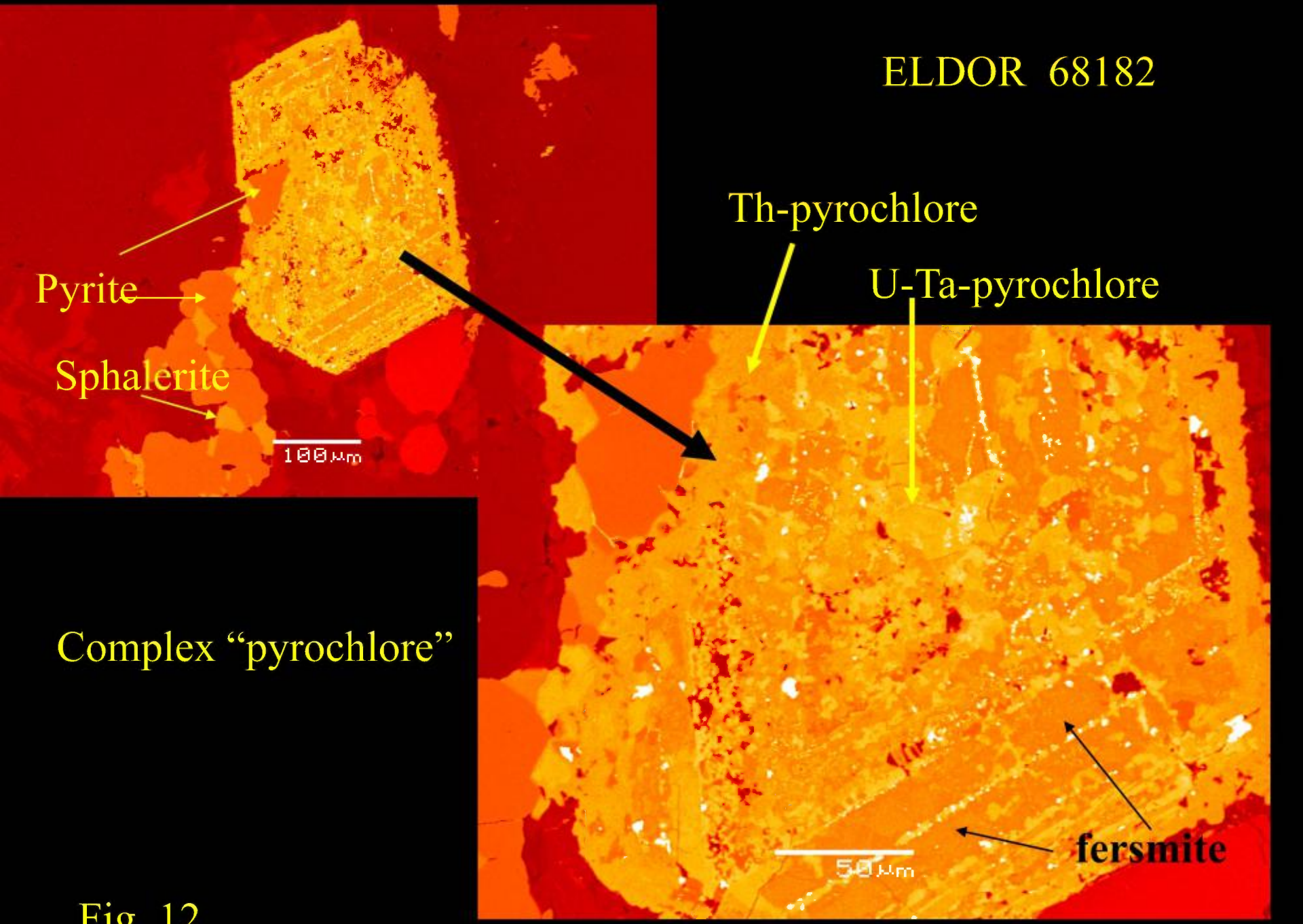

Complex “pyrochlore”

Fig. 12

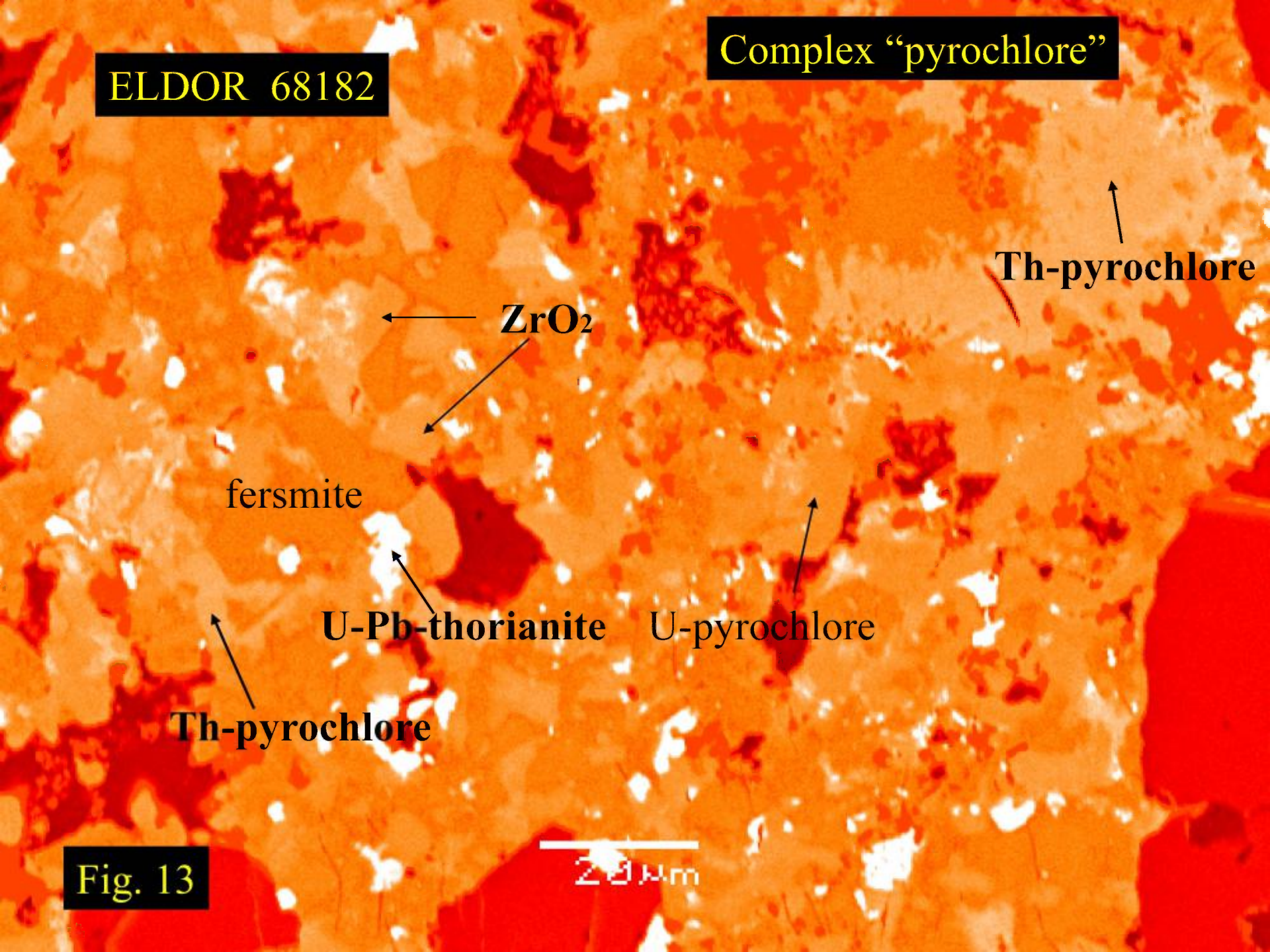
ELDOR 68182
Complex “pyrochlore”
Th-pyrochlore
ZrO2
fersmite
U-Pb-thorianite
U-pyrochlore
Th-pyrochlore
20 µm

Fig. 13

ELDOR 68184

68184 ***Pyrochlore magnetite apatite calcite carbonatite***

This sample is a coarse grained apatite calcite carbonatite with accessory magnetite, pyrite and pyrochlore (Figs 1-2). The sample exhibits well-defined banding resulting principally from variations in the abundance of apatite relative to that of calcite. Calcite crystals range in size from 2 mm down to several hundred microns and form allotriomorphic granular aggregates. The calcite exhibits well-defined polysynthetic twinning. Intergrown with the calcite are laths of pale green to light brown pleochroic phlogopite (Fig. 2) and minor amounts of Fe-poor dolomite (Fig 5). The pale green colour results from alteration of phlogopite to chlorite. Apatite forms rounded subhedral prisms, many of which are aligned parallel to the modal banding (Figs 4-6). Apatites are of uniform composition in BSE-images and poor in Sr and rare earth elements (< 1 wt.%). Pyrochlore, magnetite and pyrite are distributed relatively uniformly throughout the rock. All of these phases appear to have formed subsequent to apatite crystallization. Inclusions of apatite can be found in the pyrochlores (Fig 6). The latter fill interstices between apatite crystals (Fig 8) or occur as subhedral crystals set in the calcite matrix (Figs. 7 & 10). Many pyrochlore crystals are pale brown in colour and surrounded by radial crack filled with chlorite (Fig.3). These cracks result from expansion of the crystal during alteration and metamictization. Subhedral pyrite is a late-forming phase crystallizing after apatite and pyrochlore but prior to calcite. Late stage anhedral zircon is found in association with altered phlogopite (Fig. 4). Magnetites have no detectable Ti , Mg, or Mn and do not contain ilmenite exsolution lamellae. Rarely they occur intergrown with REE-rich pyrochlore (Fig. 7).

Pyrochlores range in size from <100 um to 600 um, the majority occurring in the 200-400 um size range. Habits range from subhedral to irregular resorbed crystals. Only inclusions of apatite are found in the pyrochlores. BSE-imagery shows that all pyrochlores consists of two phases; a crystal of relatively uniform composition (pyrochlore-1) that has been replaced along fractures and cleavages and margins by a second pyrochlore (pyrochlore-2). Small (<50 um) rounded crystal of pyrochlore-2 occur throughout the calcite matrix.

Pyrochlore-1 is an A-site deficient Na-Ca-pyrochlore with low contents of REE (< 2 wt.% REE_2O_3) coupled with low Ta (< 2 wt.% Ta_2O_5), Th (< 3 wt.% $ThO_{2)}$ and U contents (n.d.). This pyrochlore also contains significant amounts of ZrO_2 (c. 3.wt.%).

Pyrochlore-2 is a Na- and U- free, low Ta variety that is enriched in REE ((< 35 wt.% REE_2O_3) and Y_2O_3 (2 - 3 wt.%) relative to pyrochlore-1

ELDOR 68184

Representative semiquantitative compositions are;

wt.%	PYR-1	PYR-2	wt.%	PYR-1	PYR-2
F	5.4	1.7	Ta_2O_5	1.3	1.0
Na_2O	5.8	n.d.	La_2O_3	n.d.	1.9
CaO	13.6	3.4	Ce_2O_3	1.2	17.6
FeO	1.4	3.7	Pr_2O_3	0.6	2.3
SrO	1.2	0.5	Nd_2O_3	0.5	11.4
Y_2O_3	n.d.	2.4	Ta_2O_5	1.3	1.1
ZrO_2	3.3	n.d.	ThO_2	2.4	2.8
Nb_2O_5	65.0	54.4	UO_2	n.d.	n.d.

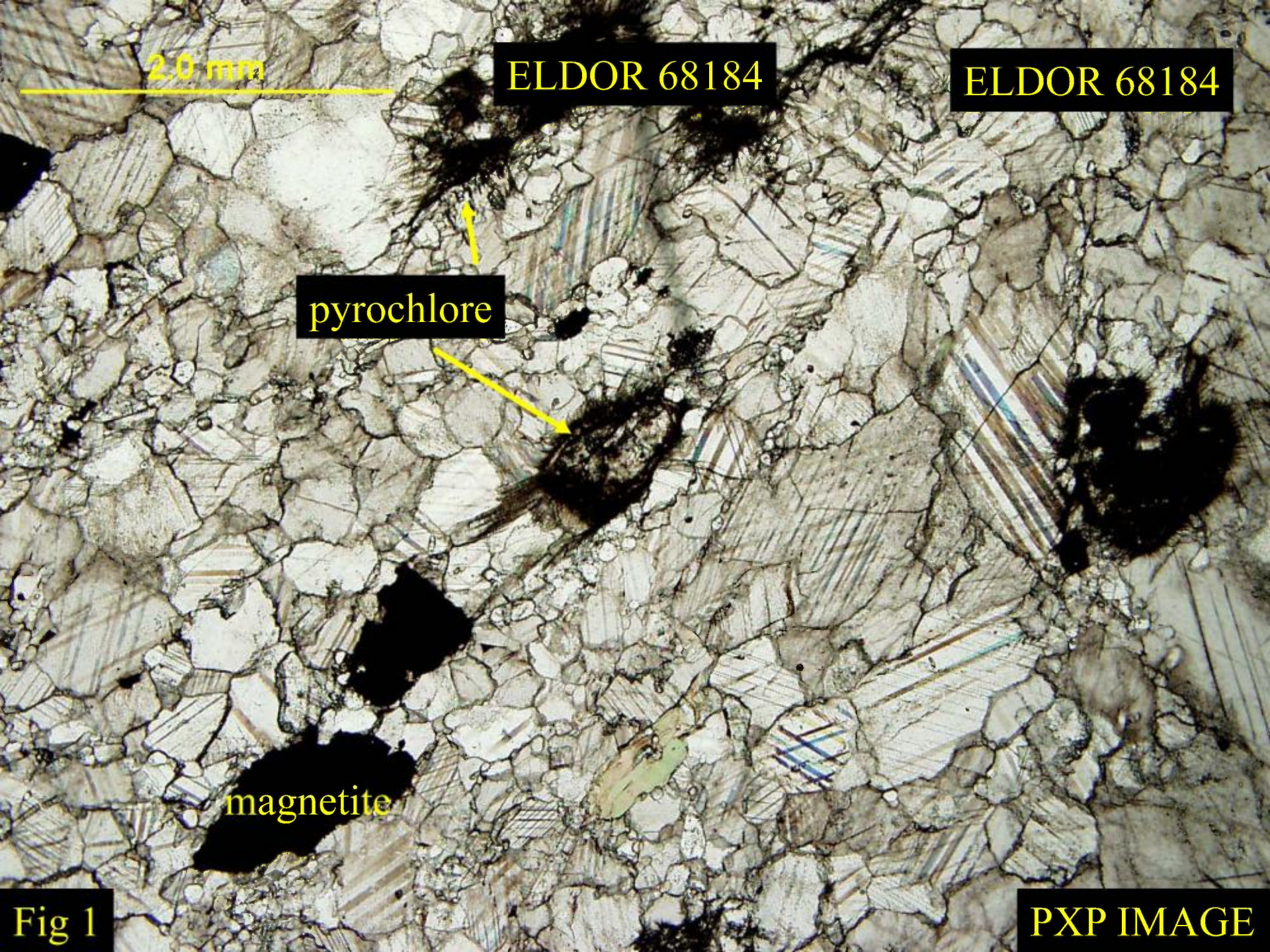
2.0 mm
ELDOR 68184
ELDOR 68184
pyrochlore
magnetite
Fig 1
PXP IMAGE

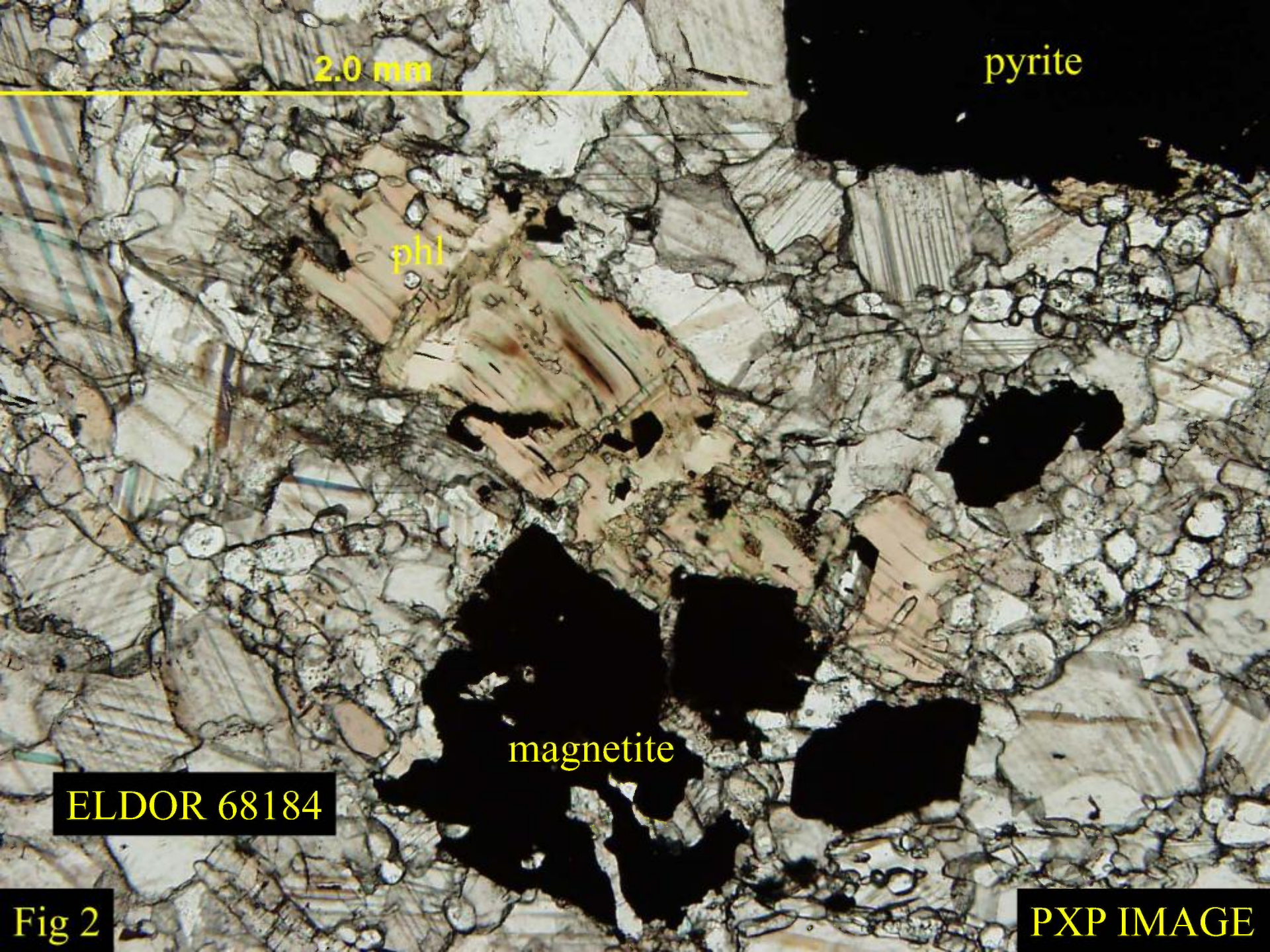
2.0 mm
pyrite
phl
magnetite
ELDOR 68184
Fig 2
PXP IMAGE

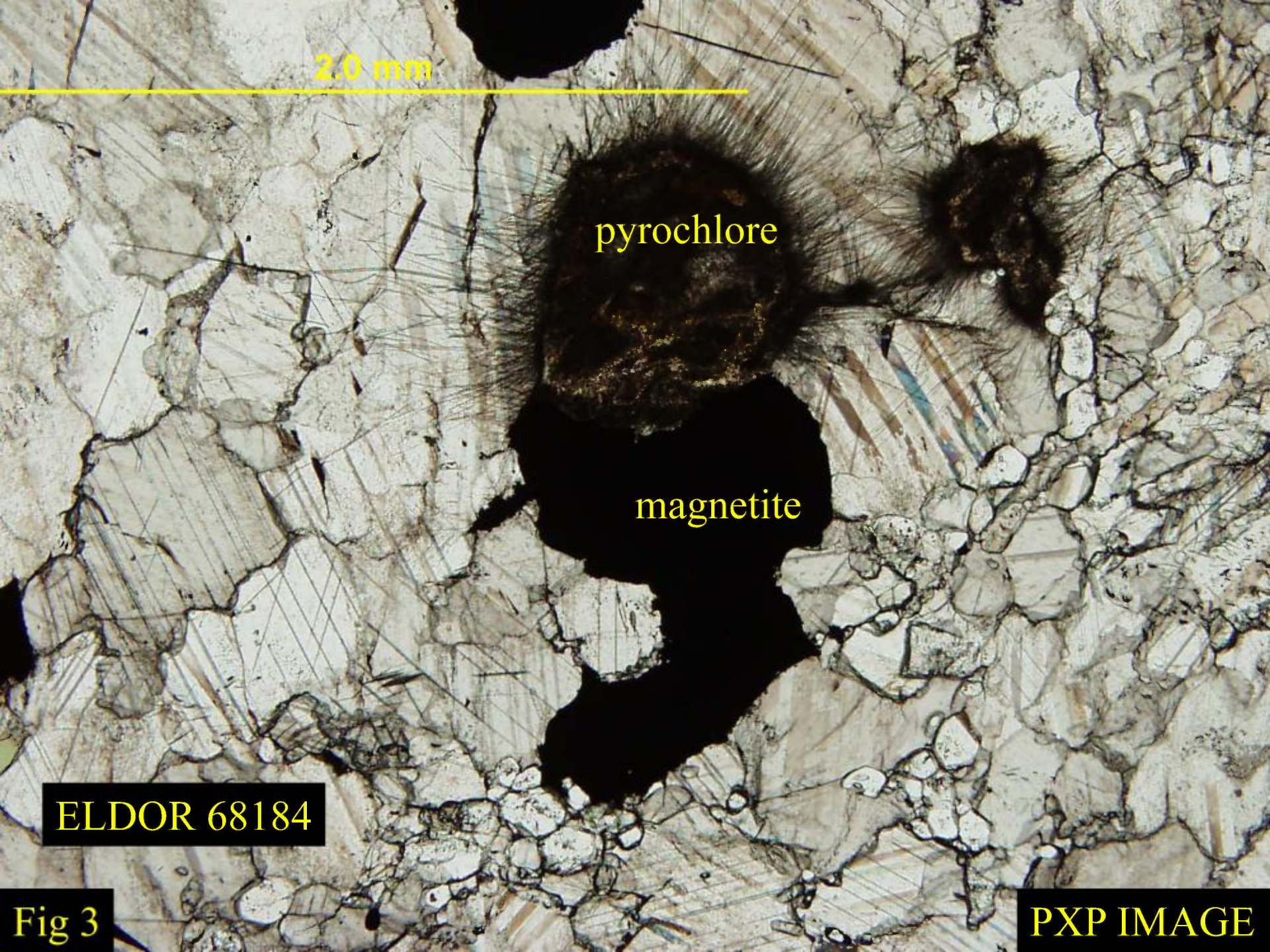
2.0 mm
pyrochlore
magnetite
ELDOR 68184
Fig 3
PXP IMAGE

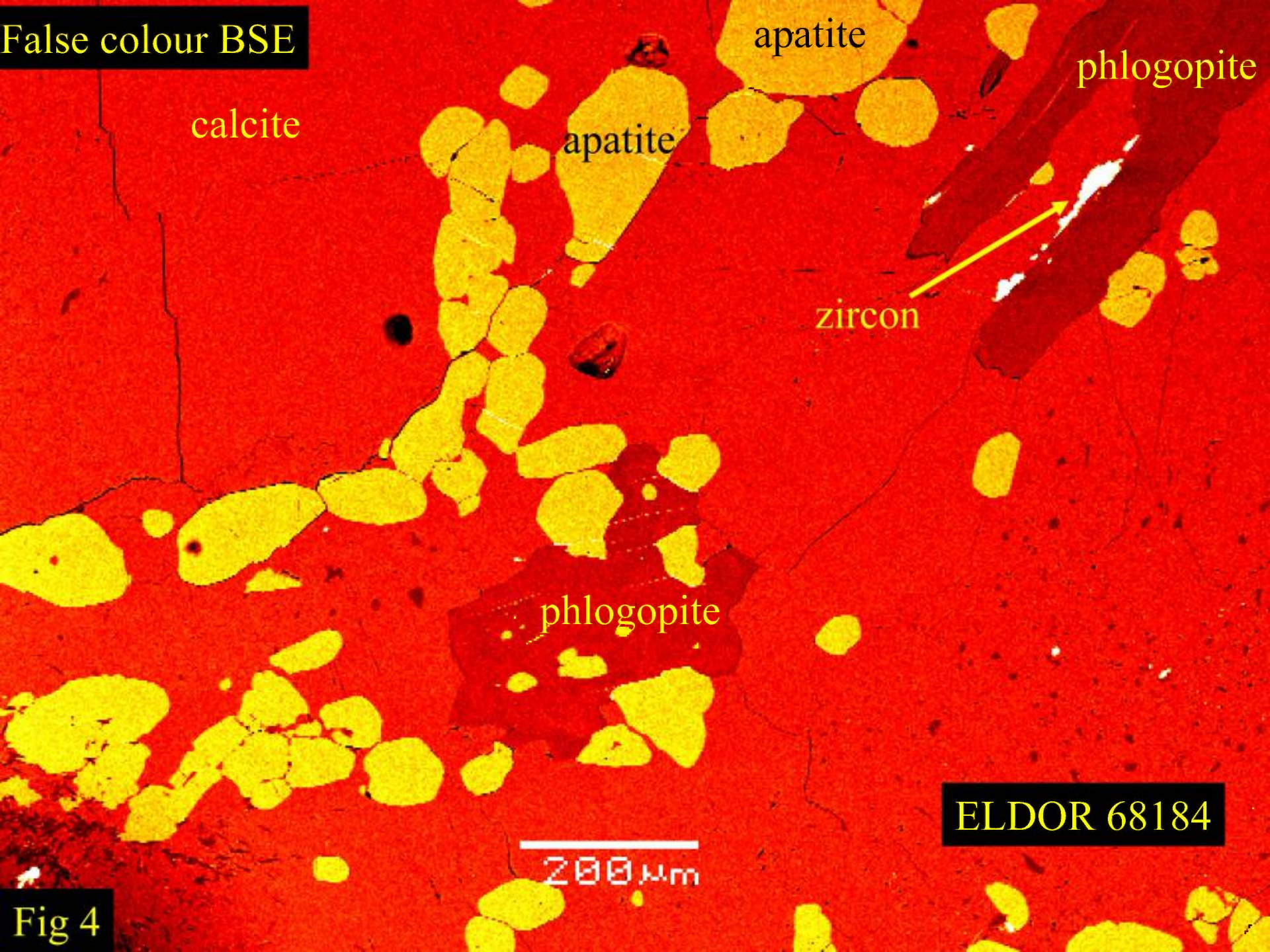
False colour BSE
apatite
phlogopite
calcite
apatite
zircon
phlogopite
ELDOR 68184
200µm

Fig 4

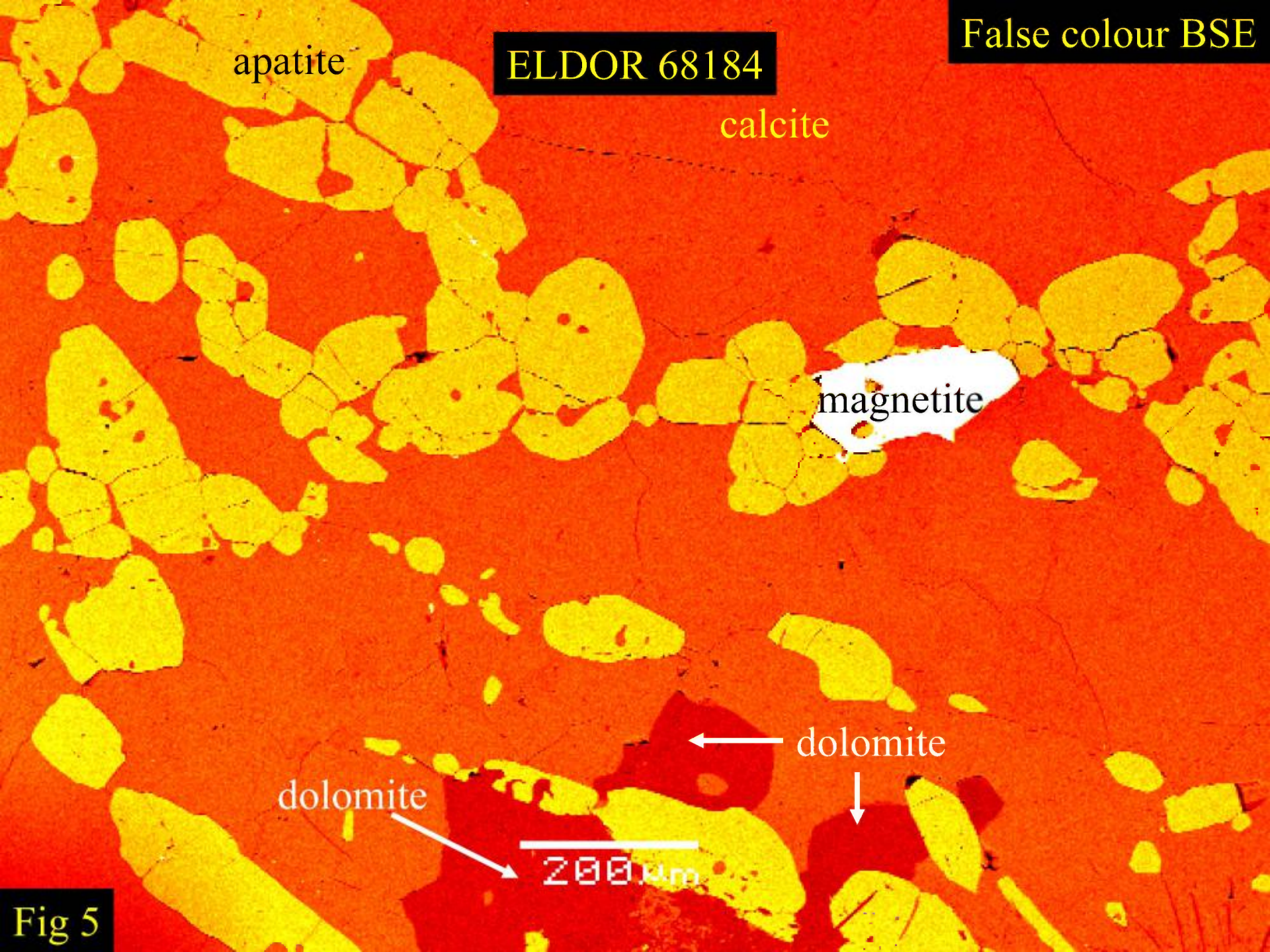
False colour BSE
ELDOR 68184
apatite
calcite
magnetite
dolomite
dolomite
200 µm

Fig 5

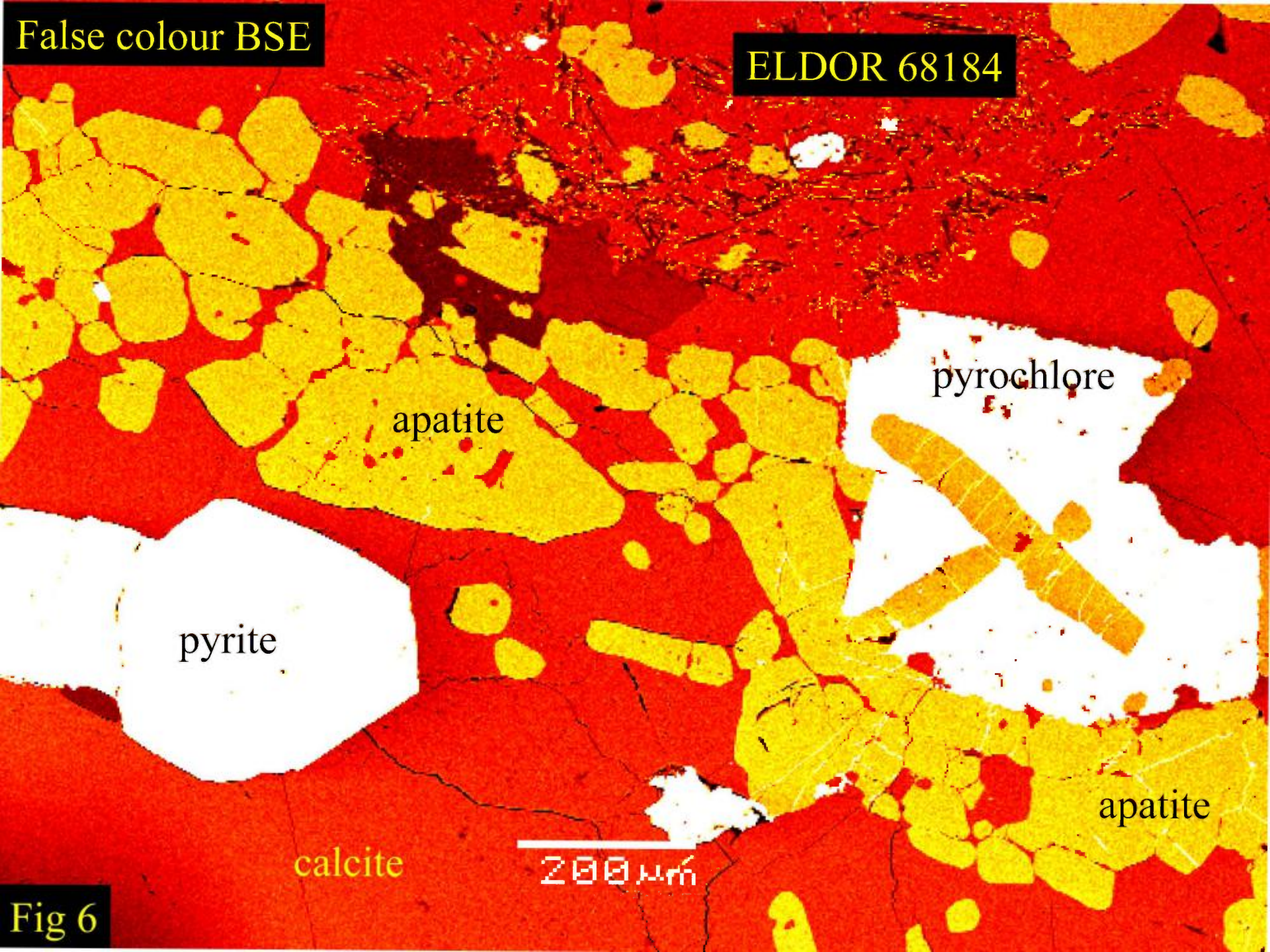
False colour BSE
ELDOR 68184
pyrochlore
apatite
pyrite
apatite
calcite
200 µm

Fig 6

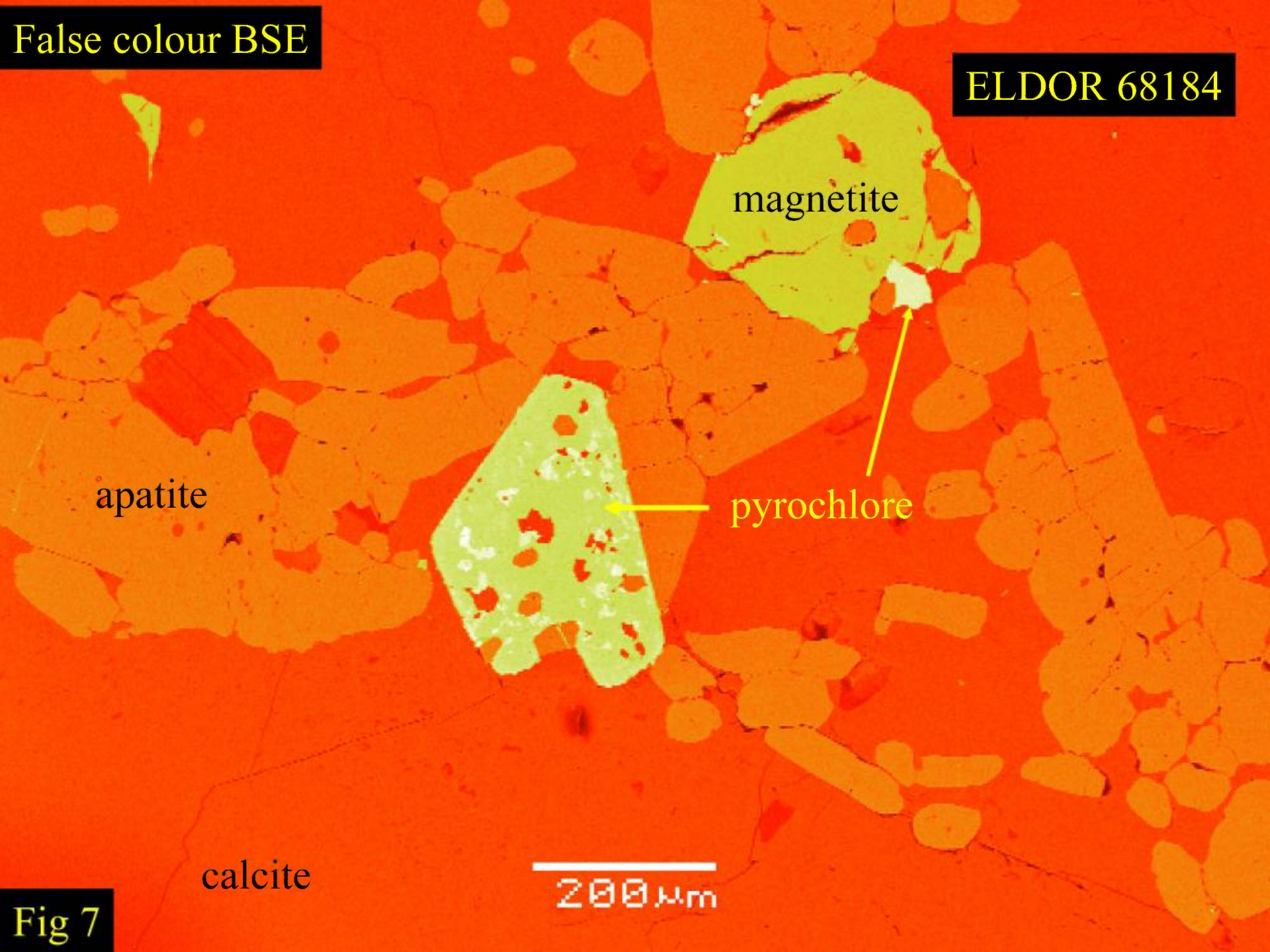
False colour BSE
ELDOR 68184
magnetite
apatite
pyrochlore
calcite
200µm

Fig 7

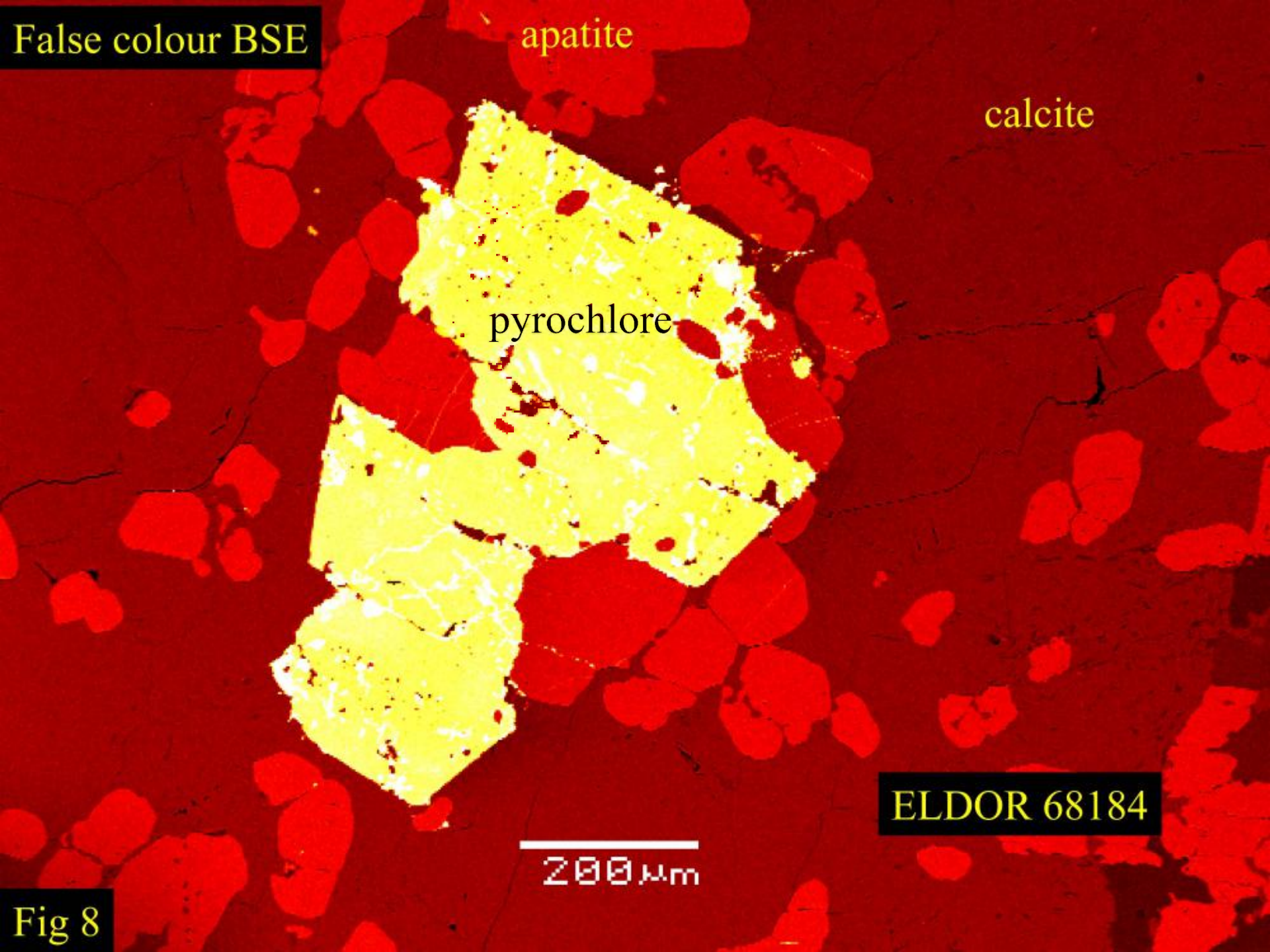
False colour BSE
apatite
calcite
pyrochlore
ELDOR 68184
200µm

Fig 8

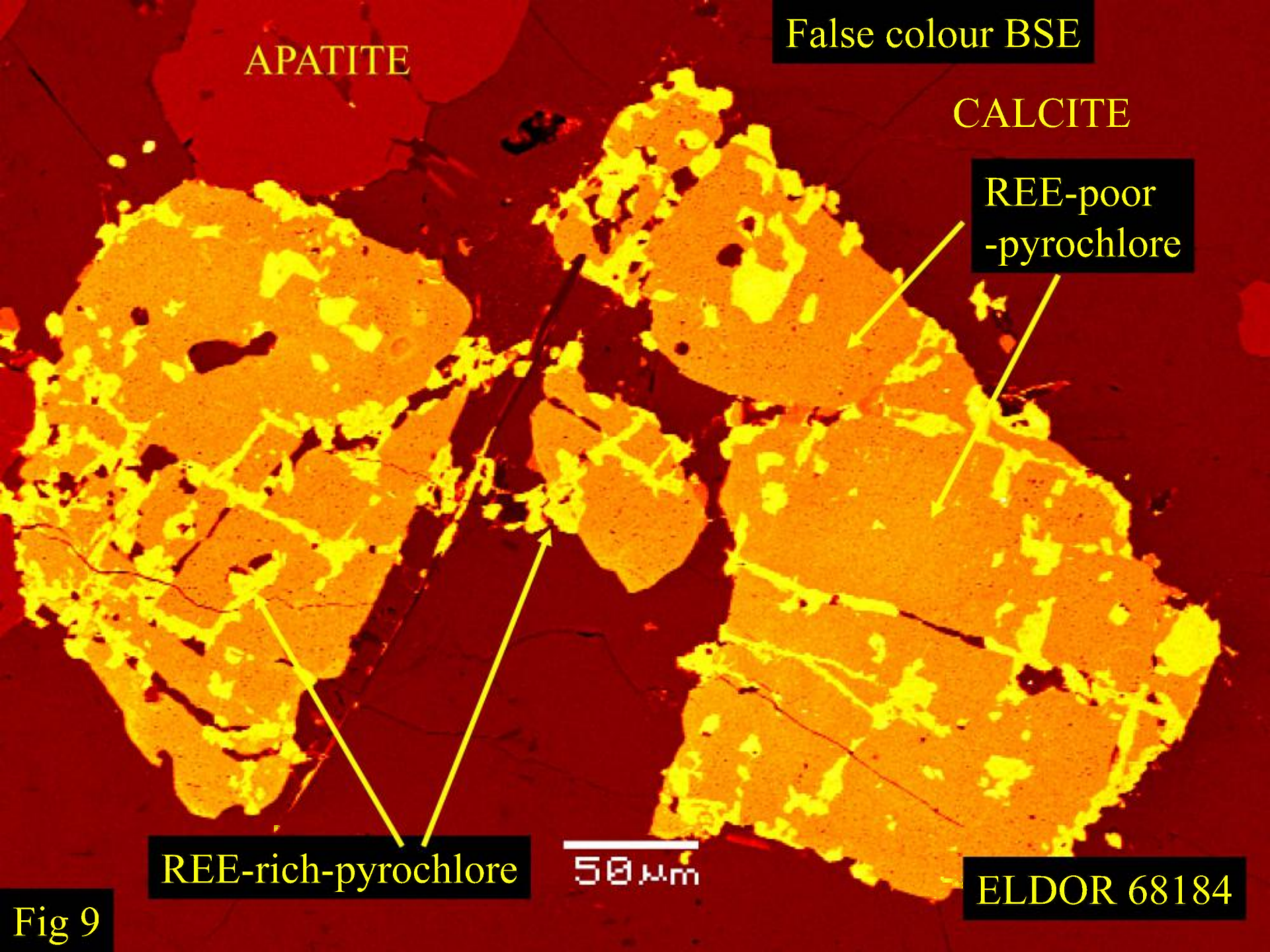
False colour BSE
APATITE
CALCITE
REE-poor
-pyrochlore
REE-rich-pyrochlore
50 µm
ELDOR 68184

Fig 9

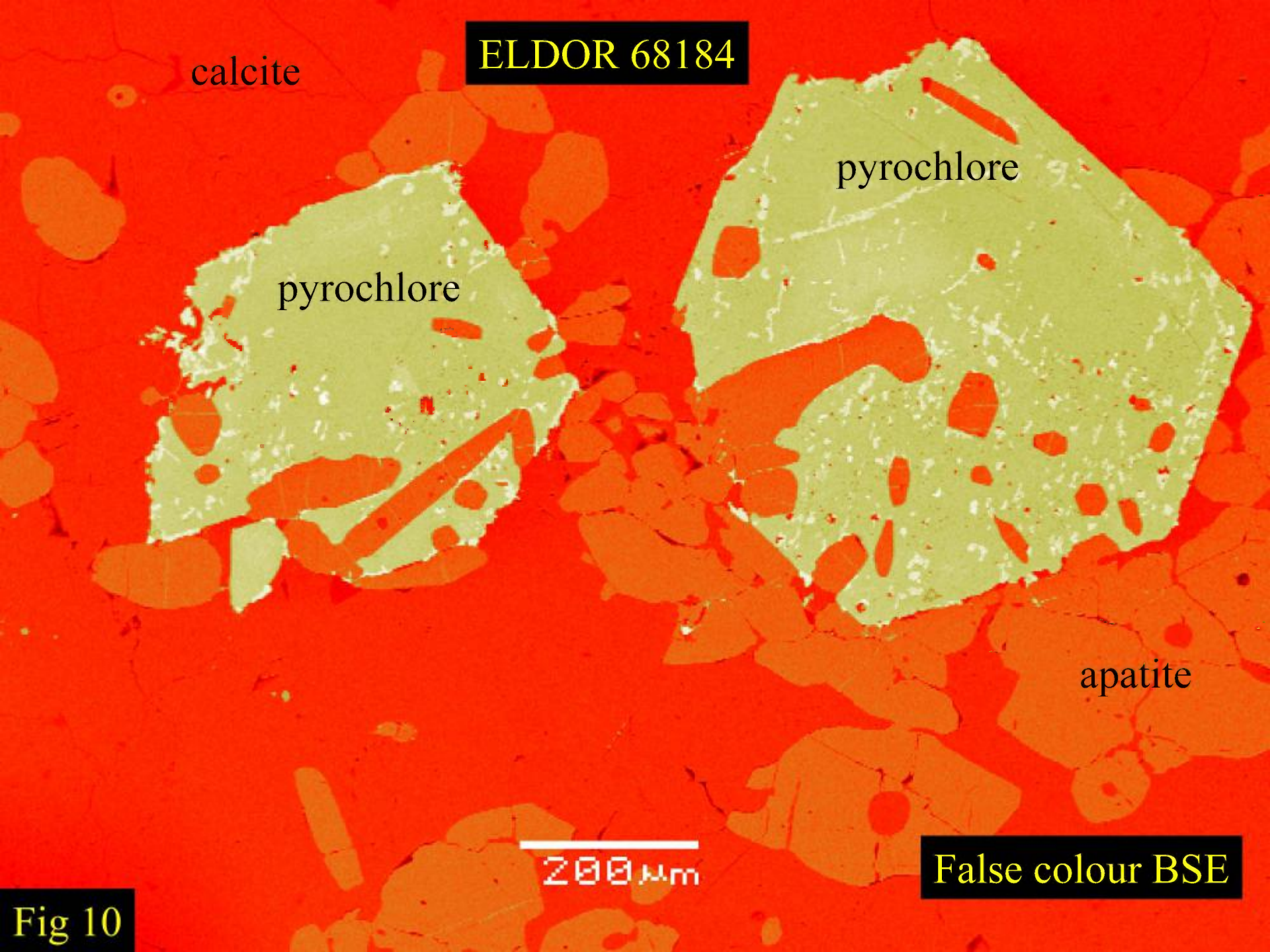
ELDOR 68184
calcite
pyrochlore
pyrochlore
apatite
200µm
False colour BSE

Fig 10

ELDOR 68191

A weakly-banded heterogeneous silicate-poor fine grained magnetite breunnerite ferroan dolomite-apatite rock consisting principally of irregular-to subhedral interlocking apatite crystals; many of the latter exhibit triple junction contacts (Figs 1-3). This rock can be termed an "apatitite". Magnetite forms irregular ragged large crystals which lack exsolution textures or inclusions of other minerals. The magnetite is Ti and Mn- poor (< 0.5 wt.% oxides). Ferroan dolomite (c 20 -22 wt.% FeO; c. 1-2 wt.% MnO) occurs as thin bands of small anhedral interlocking crystals (Fig.1) commonly in association with breunnerite and minor anhedral strained quartz crystals, subhedral-to-euhedral pale green aegirine-rich clinopyroxene and subhedral pyrite (Figs.2-4) The pyroxenes are intimately intergrown and/or overgrown with minor amounts of blue-green arfvedsonite (Fig.4). The principal accessory minerals are: pyrochlore, zircon and minor monazite

ELDOR 68191

In thin sections zircon forms subhedral grey-brown to opaque discrete crystals associated with apatite (Figs 3 & 5). These are overgrown by opaque pyrochlore (150-300 um). Many crystals are surrounded by radial fractures resulting from expansion of the pyrochlore during metamictization. The pyrochlore occurs as partial, irregular, resorbed overgrowths on anhedral resorbed zircon. Back-scattered electron imagery (BSE-imagery) demonstrates that none of the pyrochlores are monomineralic crystals and that they consist of core regions with complex amoeboid intergrowths of small (< 20 um) ferrocolumbite set in a matrix of U-Ta pyrochlore (Figs. 6 - 8). Common inclusions (< 1 um) in these complex pyrochlores are subhedral grains of $(Th,Pb)O_2$ and rare irregular anhedral zircons. The margins of the complex pyrochlore-ferrocolumbite intergrowths are mantled by discontinuous patches of BSE-uniform high U-Ta-pyrochlore (Figs 6 - 8). Other reaction mantles consist of ferrocolumbite and pyrite. Rare rounded grains (<1 um) of galena are also present.

The BSE-uniform pyrochlore mantles have the highest U and Ta content, although none have sufficiently high Ta contents that they can be termed microlite. A representative X-ray energy dispersive spectrum is shown in figure 9. A typical semi-quantitative composition is:

	wt.%		wt.%
Na_2O	n.d.	Nb_2O_5	36.04
SiO_2	n.d.	La_2O_3	n.d.
CaO	2.65	Ce_2O_3	n.d
TiO_2	7.03	Ta_2O_5	16.94
MnO	n.d.	PbO	1.45
FeO	3.88	ThO_2	0.64
SrO	2.58	UO_2	28.40
Y_2O_3	n.d.	F	n.d.

Note the absence of Na and F . These pyrochlores are thus A-site deficient varieties. Loss of Na is related to alteration associated with metamictization. The pyrochlores as found result from the decomposition of an earlier-formed pyrochlore that has reacted with magma/fluid. The pyrochlores represent a transported assemblage that have not crystallized from the magma which formed their current host rocks

Zircon occurs as anhedral irregular resorbed crystals commonly with pyrochlore overgrowths (Fig. 5) in association with apatite, and as subhedral crystals within late-forming ferro-dolomite (Fig. 10) and quartz. Some zircons contain anhedral inclusions of baddeleyite (ZrO_2).

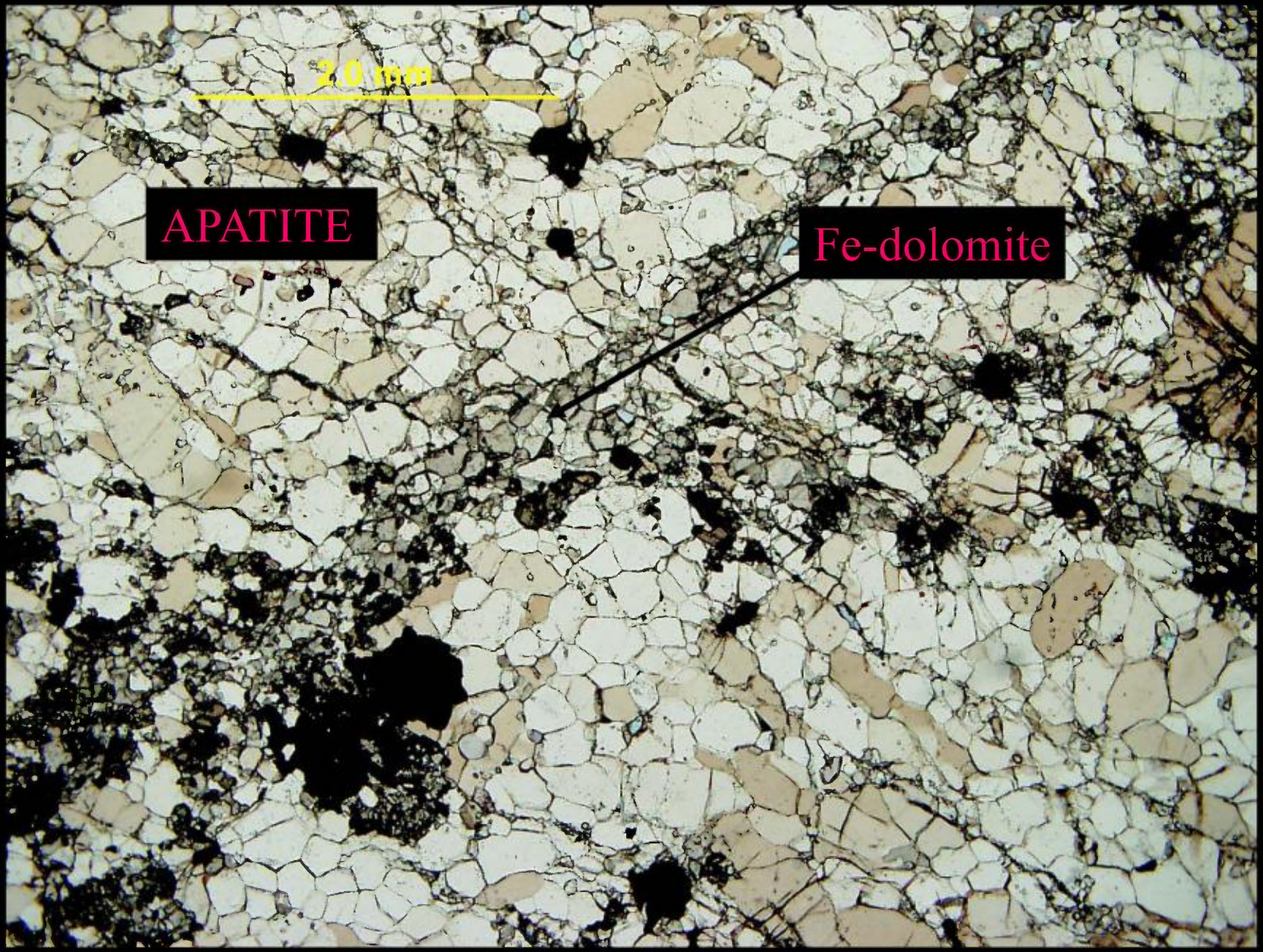

Fig 1 ELDOR 68191 PXP-IMAGE

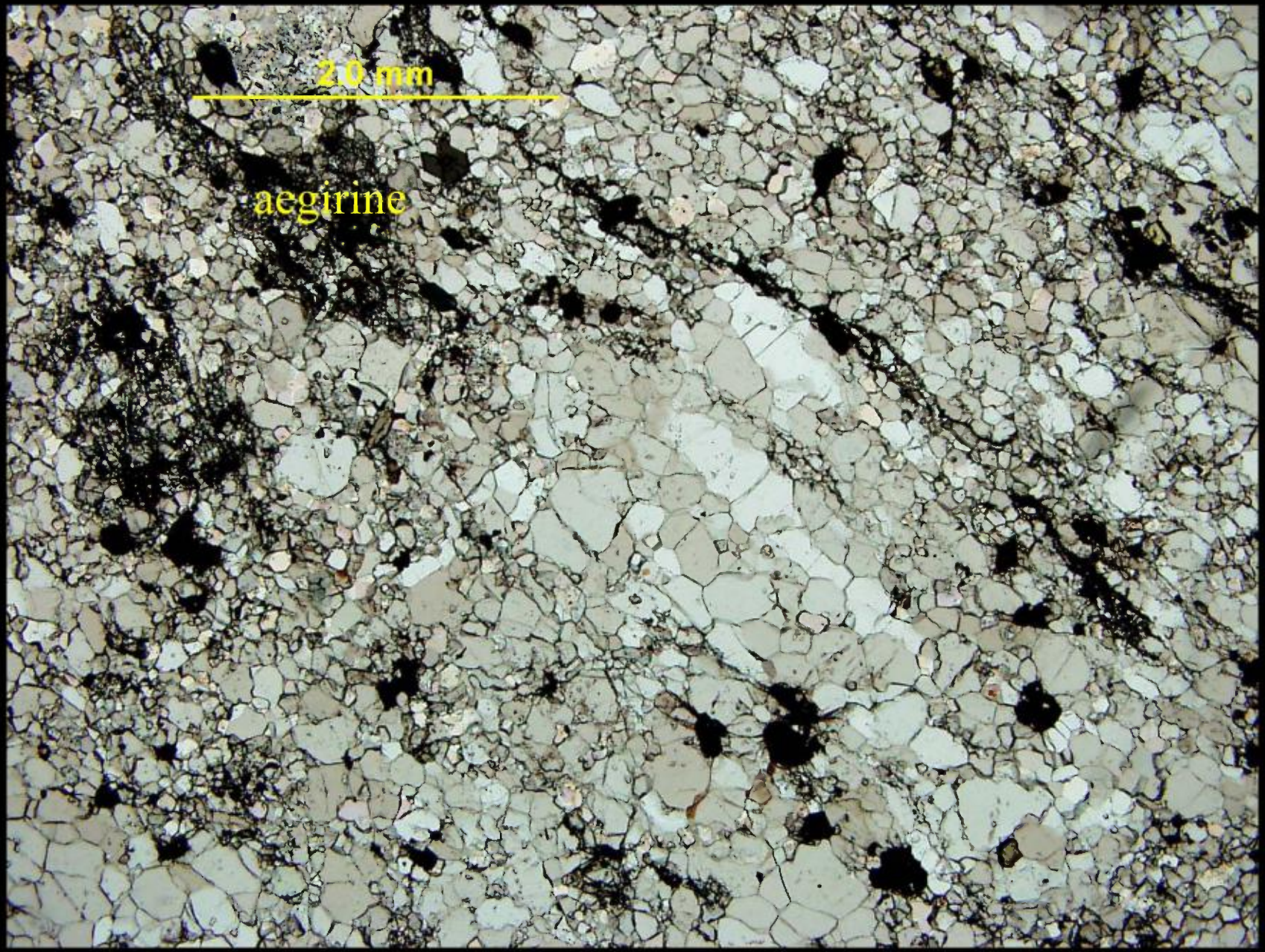

Fig 2 ELDOR 68191 PXP-IMAGE

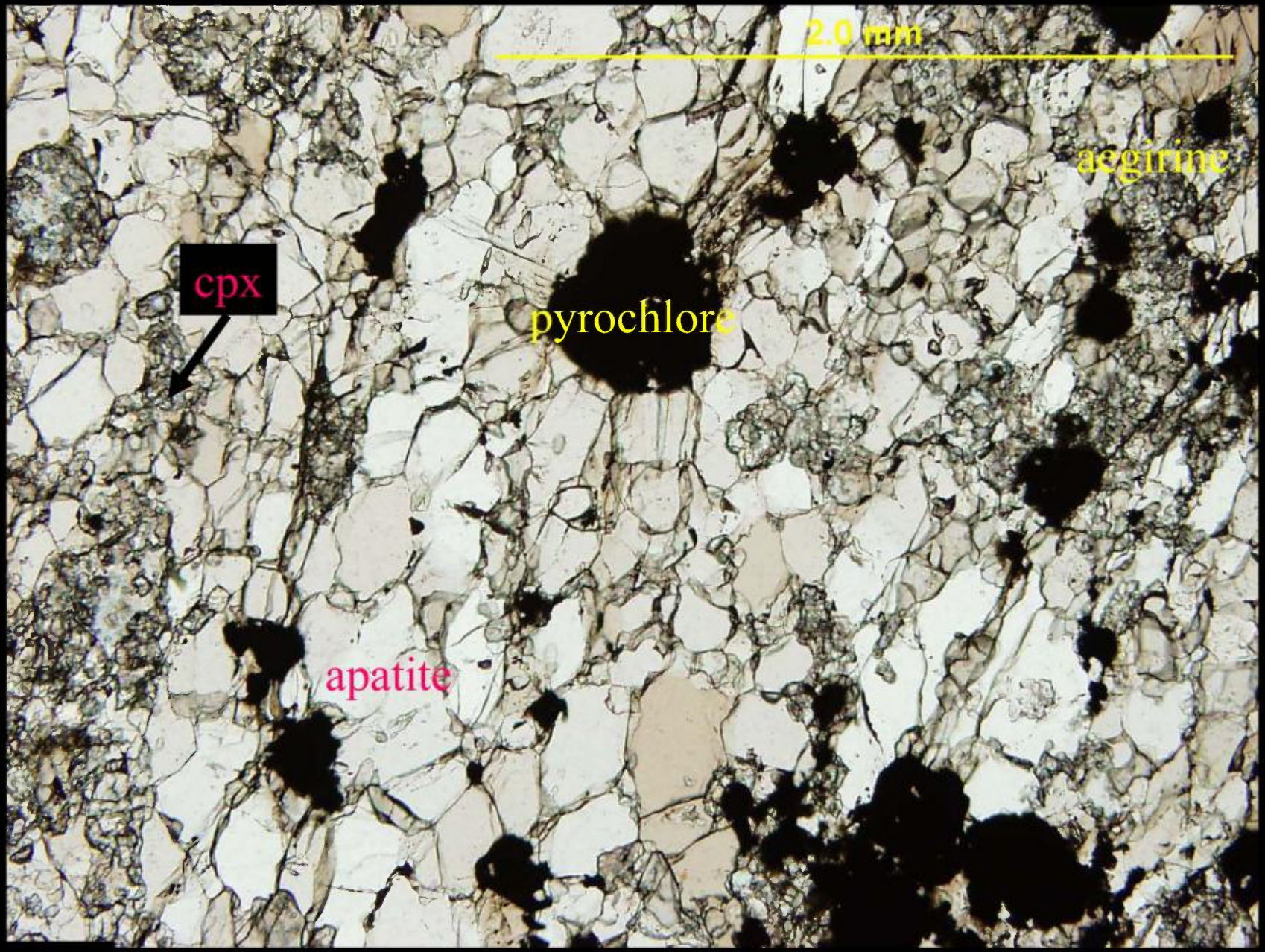

Fig 3

ELDOR 68191 PXP-IMAGE

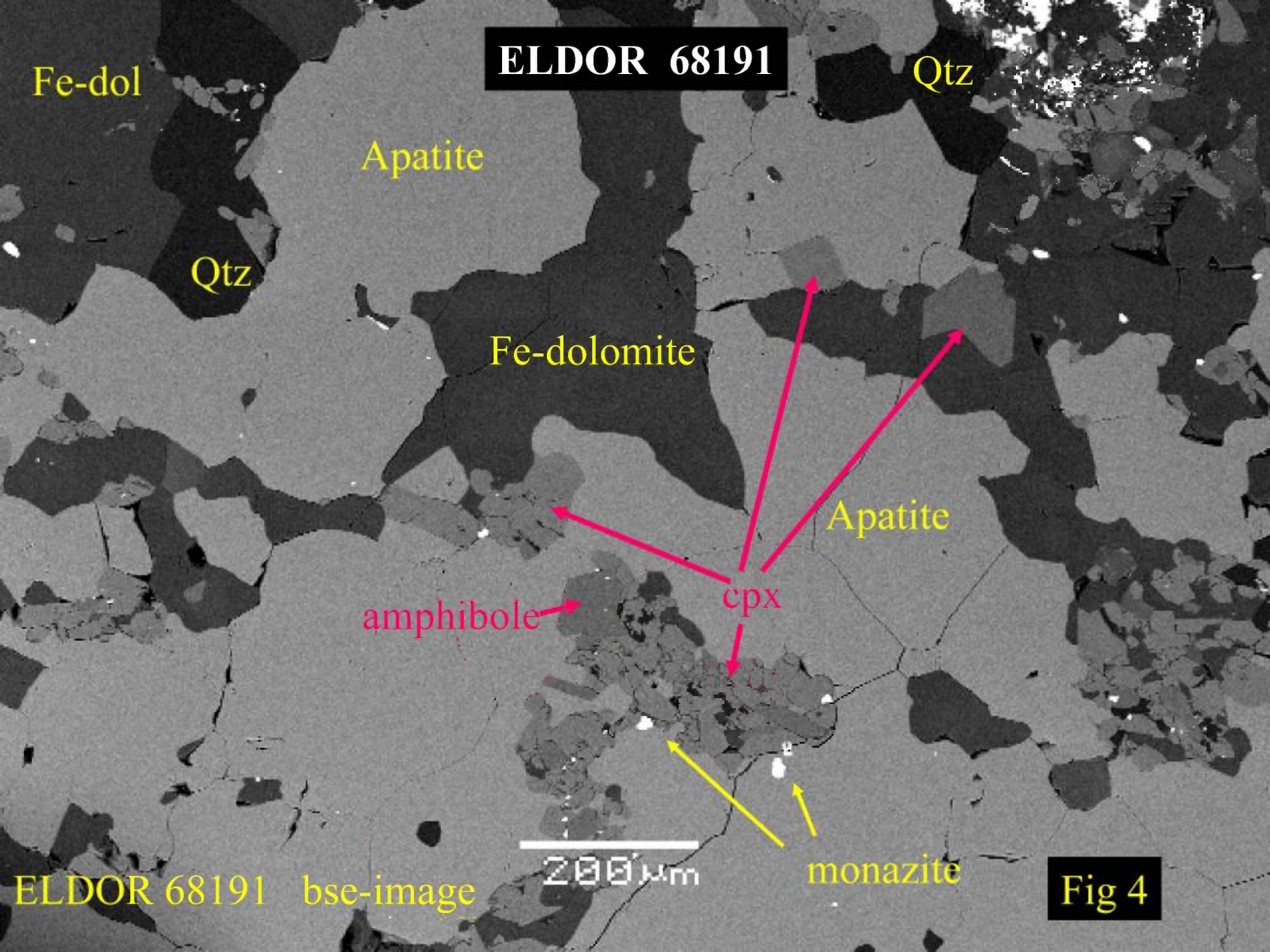
ELDOR 68191
Fe-dol
Qtz
Apatite
Qtz
Fe-dolomite
Apatite
cpx
amphibole
200 µm
monazite
ELDOR 68191 bse-image
Fig 4

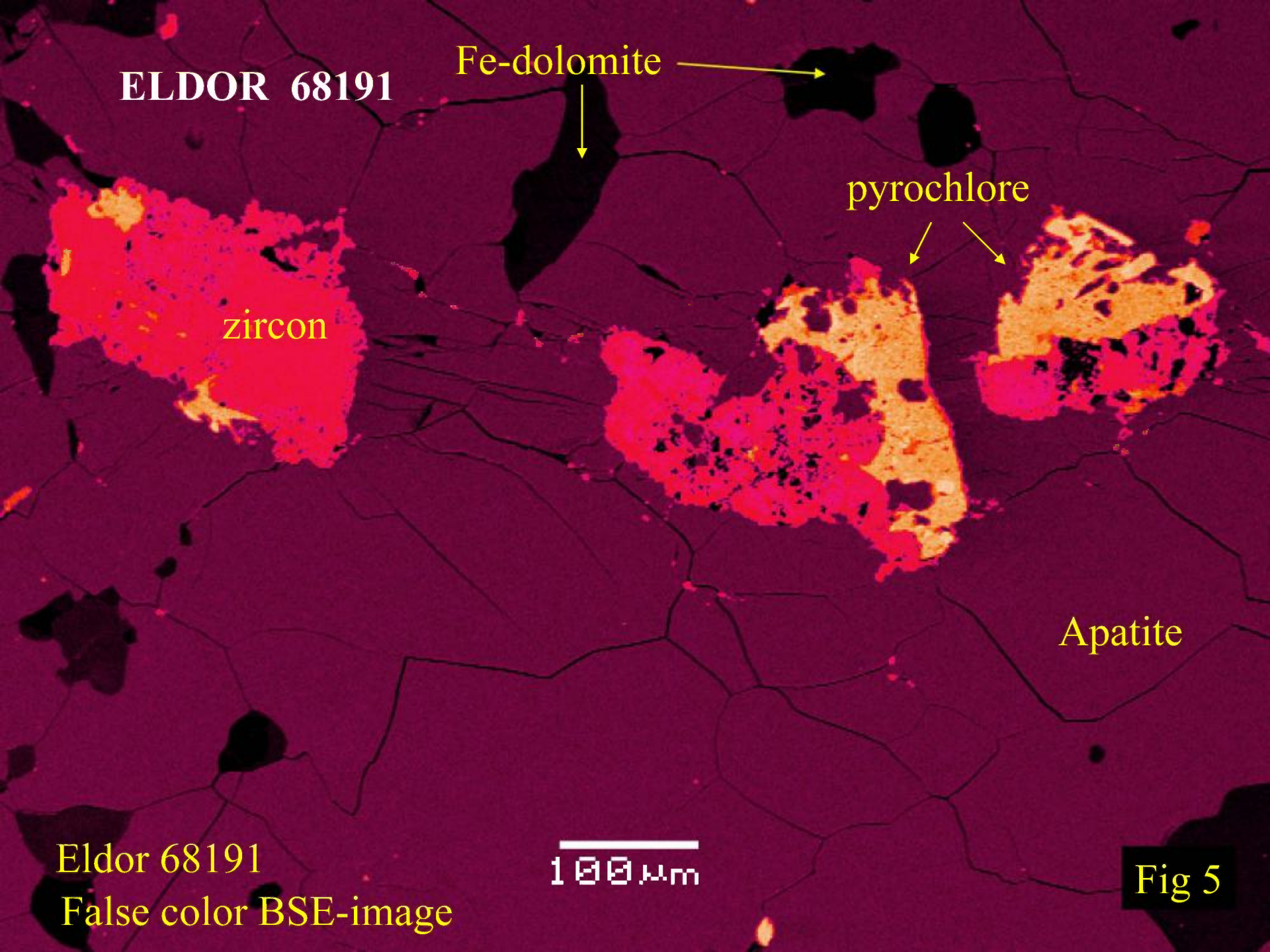

Eldor 68191
False color BSE-image

Fig 5

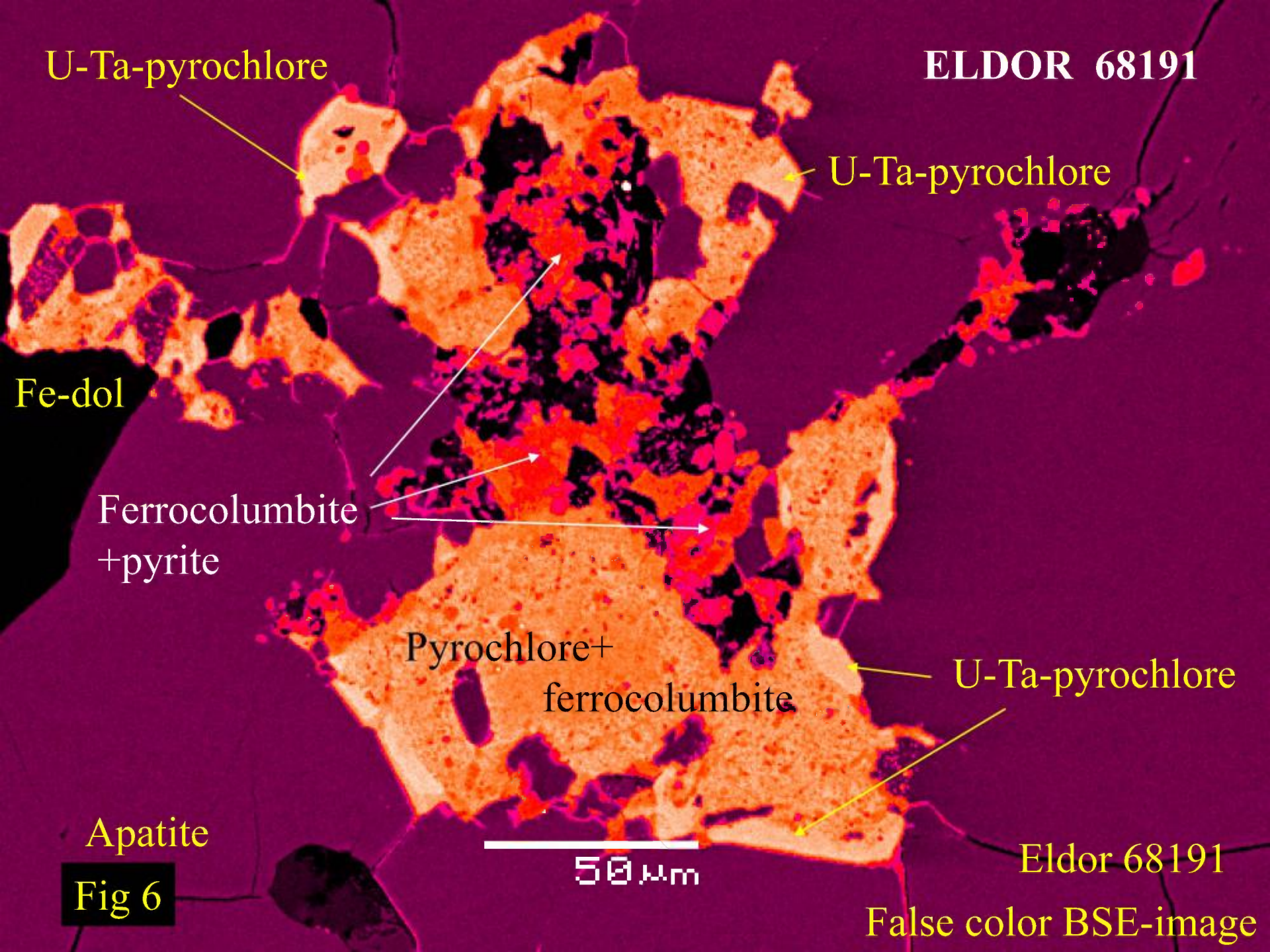
U-Ta-pyrochlore
ELDOR 68191
U-Ta-pyrochlore
Fe-dol
Ferrocolumbite
+pyrite
Pyrochlore+
ferrocolumbite
U-Ta-pyrochlore
Apatite
50 µm
Fig 6
Eldor 68191
False color BSE-image

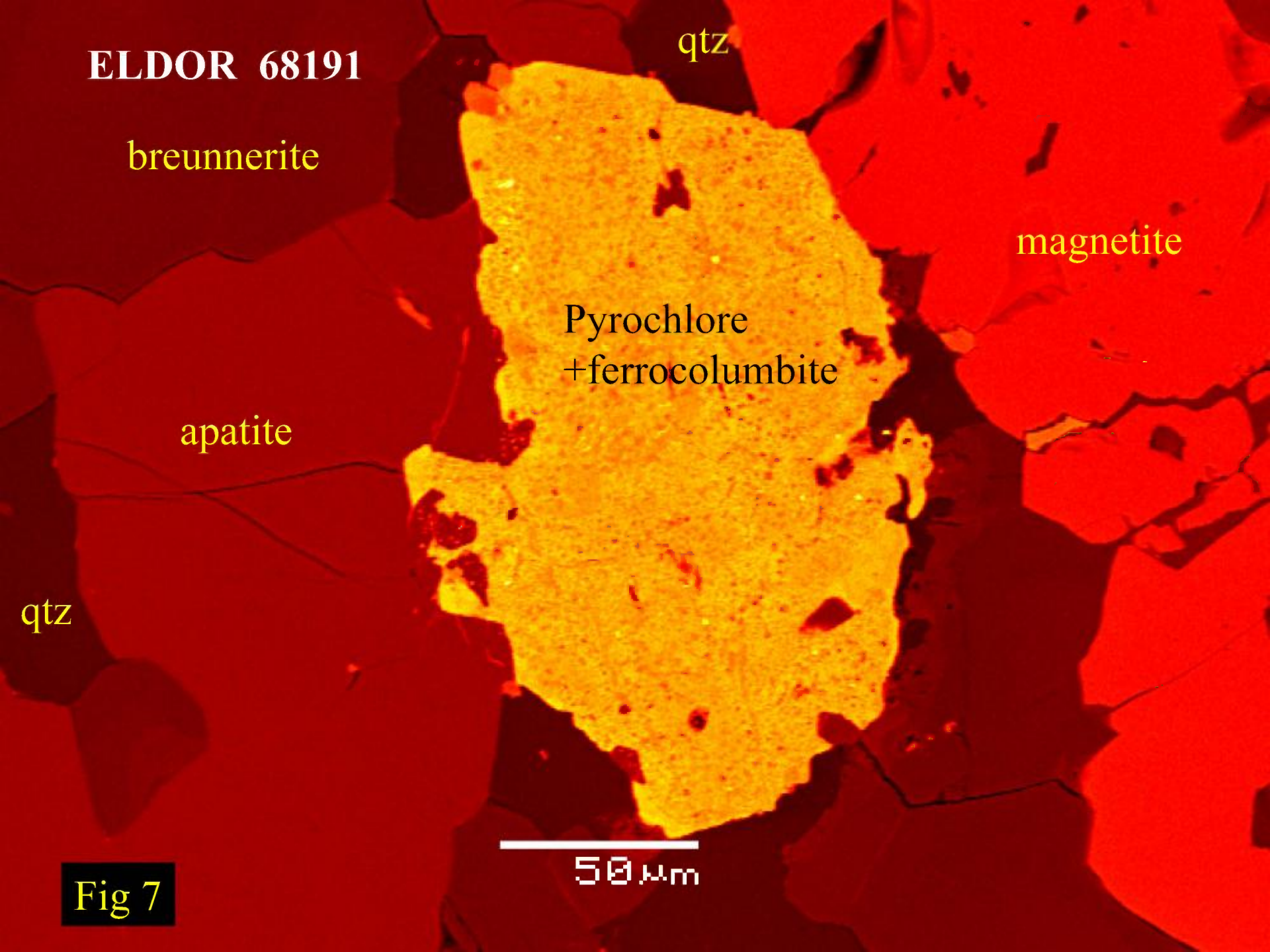
ELDOR 68191
qtz
breunnerite
magnetite
Pyrochlore
+ferrocolumbite
apatite
qtz
50 µm

Fig 7

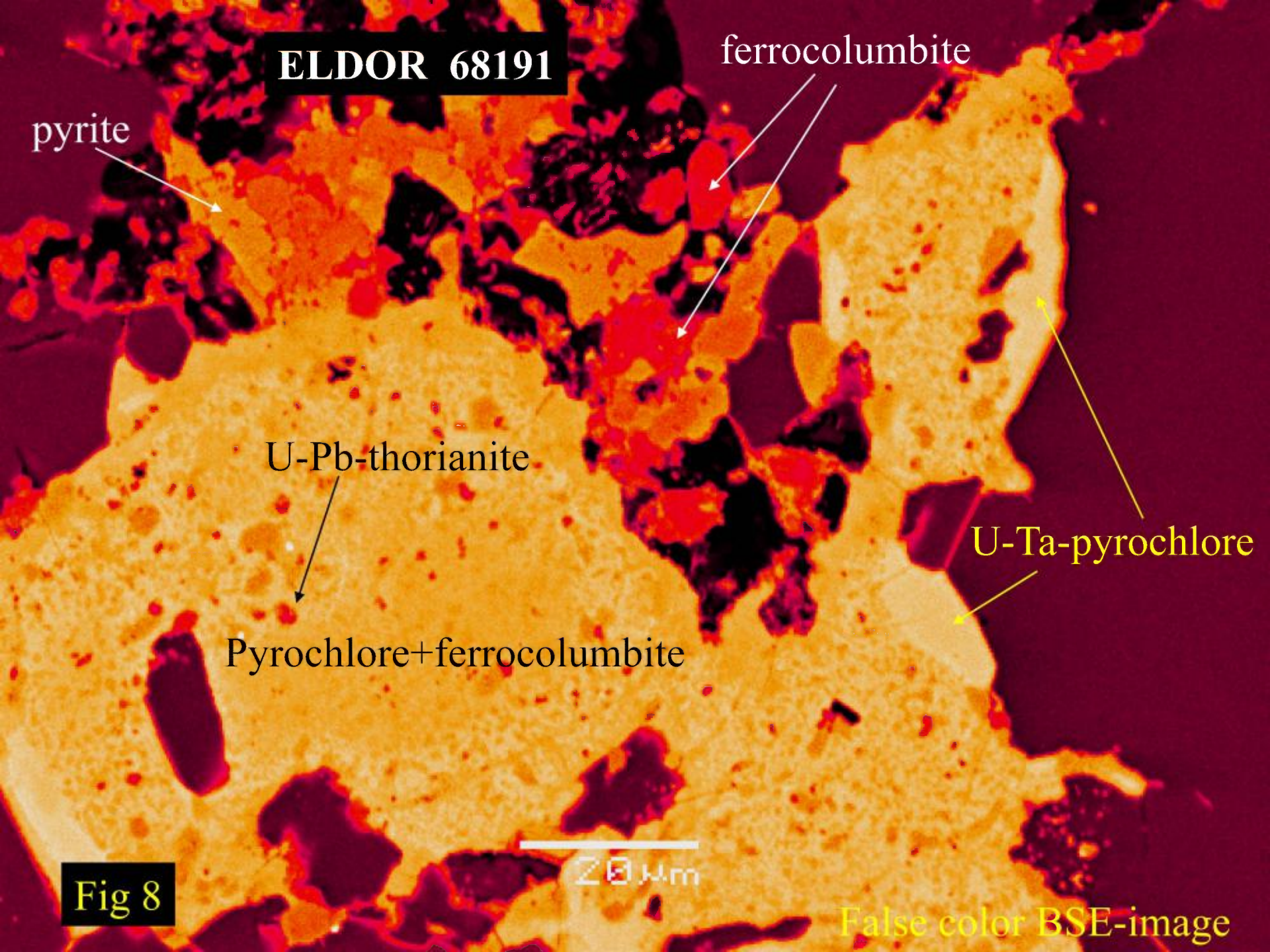
ELDOR 68191
ferrocolumbite
pyrite
U-Pb-thorianite
U-Ta-pyrochlore
Pyrochlore+ferrocolumbite
20 µm
Fig 8
False color BSE-image

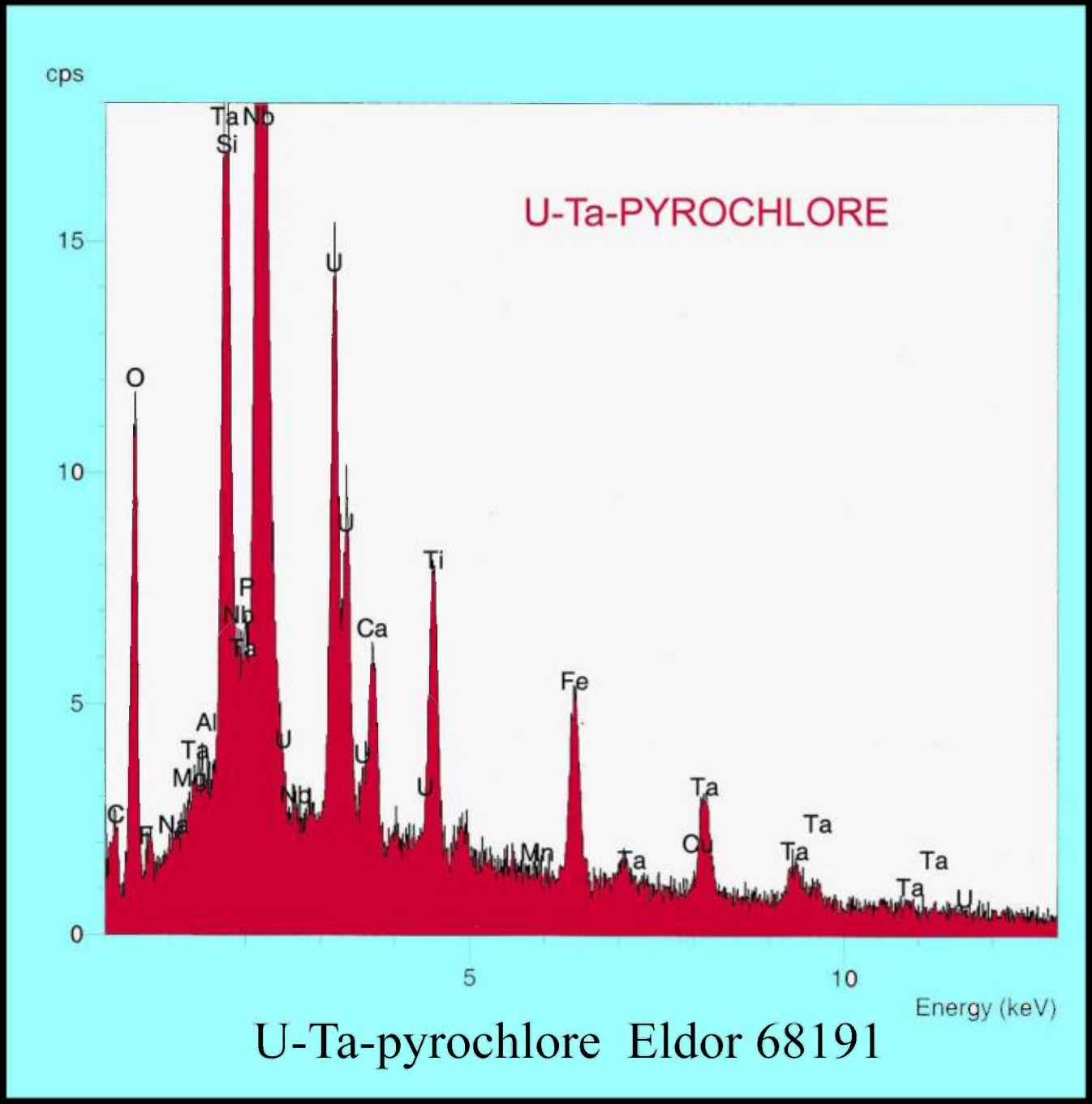

U-Ta-pyrochlore Eldor 68191

X-ray EDS

Eldor 68191

Fig 9

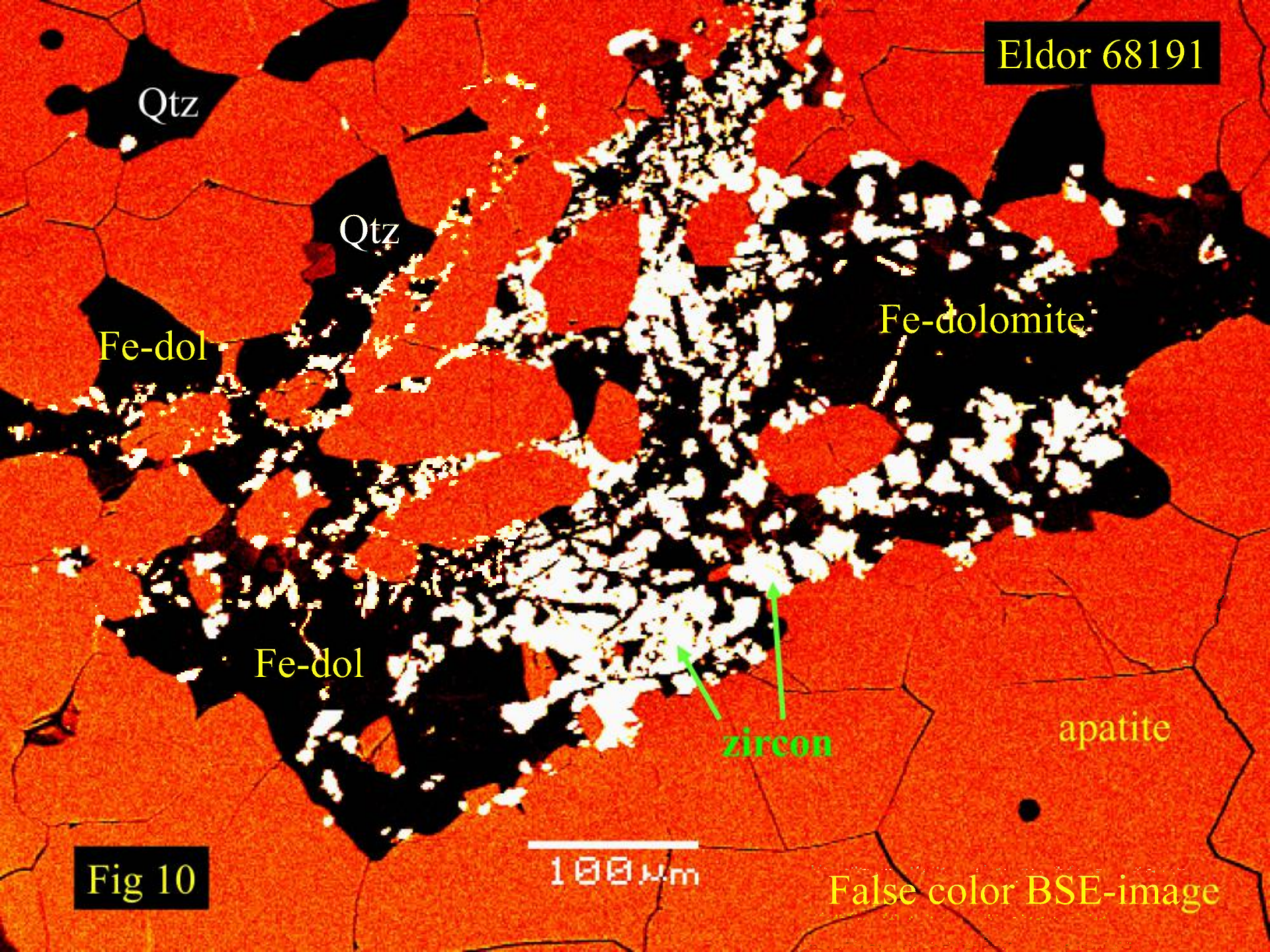
Eldor 68191
Qtz
Qtz
Fe-dol
Fe-dolomite
Fe-dol
zircon
apatite
100µm
Fig 10
False color BSE-image

ELDOR 68193

ELDOR 68193 *Orthoclase apatite ferroan dolomite carbonatite*

This heterogeneous and weakly banded sample consists principally of apatite, potassium feldspar and ferroan dolomite (Figs 1-3). Magnetite, fersmite, breunnerite and rare earth fluorocarbonates are not present. The rock is characterized by large (1 cm) patches of interlocking prismatic weakly-aligned apatite crystals (Figs 2 & 9). Opaque pyrochlore is commonly surrounded by radial fractures resulting from expansion of the crystal during metamictization (Figs 3 & 10).

Apatite is one of the earliest phases to form and occurs primarily as ragged monomineralic aggregates of interlocking anhedral crystals (Figs 2 & 9). The apatite is of uniform composition and lacks detectable Sr and rare earth elements. Inclusions of resorbed pyrochlore are characteristic (see below) of this apatite (Figs 4-7), and essentially bi-mineralic bands relatively enriched in pyrochlore and apatite are present. Twin-free potassium feldspar (orthoclase) and ferroan dolomite (5 -6 wt.% FeO) form the groundmass in which apatite crystals are set. These form complex intergrowths (Figs. 4-7). From their textural relationships it is apparent that the feldspar formed before the carbonate. The feldspars lacks detectable Na, Ba, and Fe. Rare anhedral crystals of pure albite and laths of Mg-Al-Fe-chlorite pseudomorphs after phlogopite are also observed in this groundmass. Late-forming very small (<20 um) anhedral zircon and galena occur in the dolomite-feldspar matrix (Fig. 8). Very small (<20 um) subhedral crystals of Th-rich (4-8 wt.% ThO_2) monazite-(Ce) can be observed to have nucleated rarely at the margins of the apatite crystals (Fig 8).

ELDOR 68193

Pyrochlore is characteristically found intergrown with apatite (Figs 4-7). The pyrochlores form ragged resorbed grains up to 0.5cm in width/diameter (Fig. 11). Resorption has taken place prior to their inclusion in apatite. Radial fractures surrounding pyrochlores can be filled with an unidentified U-silicate (Fig.10). All pyrochlores are heterogeneous and consist of complex intergrowths of Ta-bearing ferrocolumbite and minor PbS set in U-Ta-pyrochlore (Figs 12-15). The scale of the intergrowths is on the order of <10 um and hence determination of the composition of each phase is very difficult. Analysis of the coarser regions shows that Ta-content of ferrocolumbite in juxtaposed different crystals is different and ranges from 3 - 6 wt.% Ta_2O_5. The coexisting pyrochlores are Th-poor and apparently of very variable composition with respect to their Ta and U contents (up to 10 wt.% Ta_2O_5, and 24 wt.% UO_2).

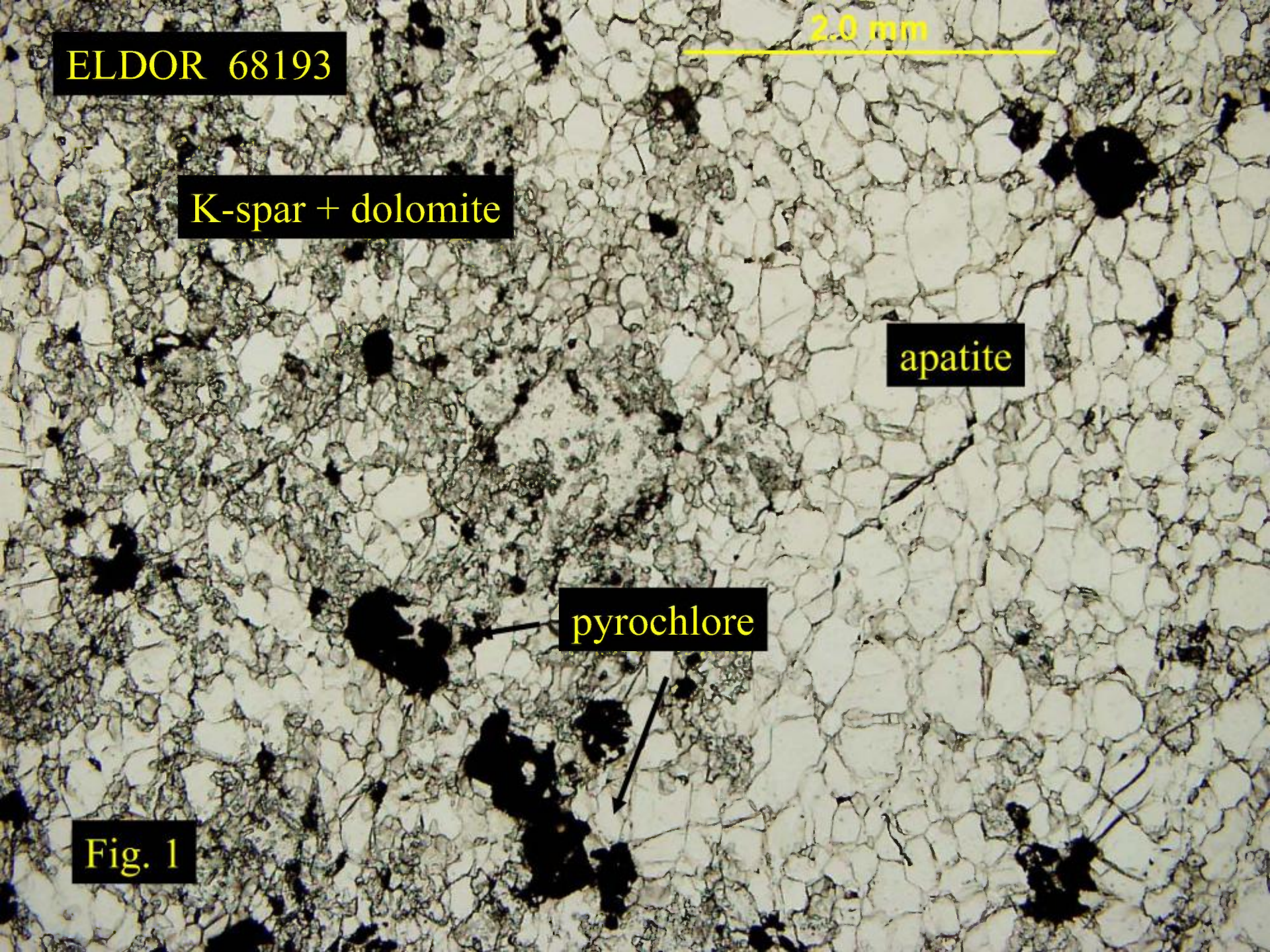

Fig. 1

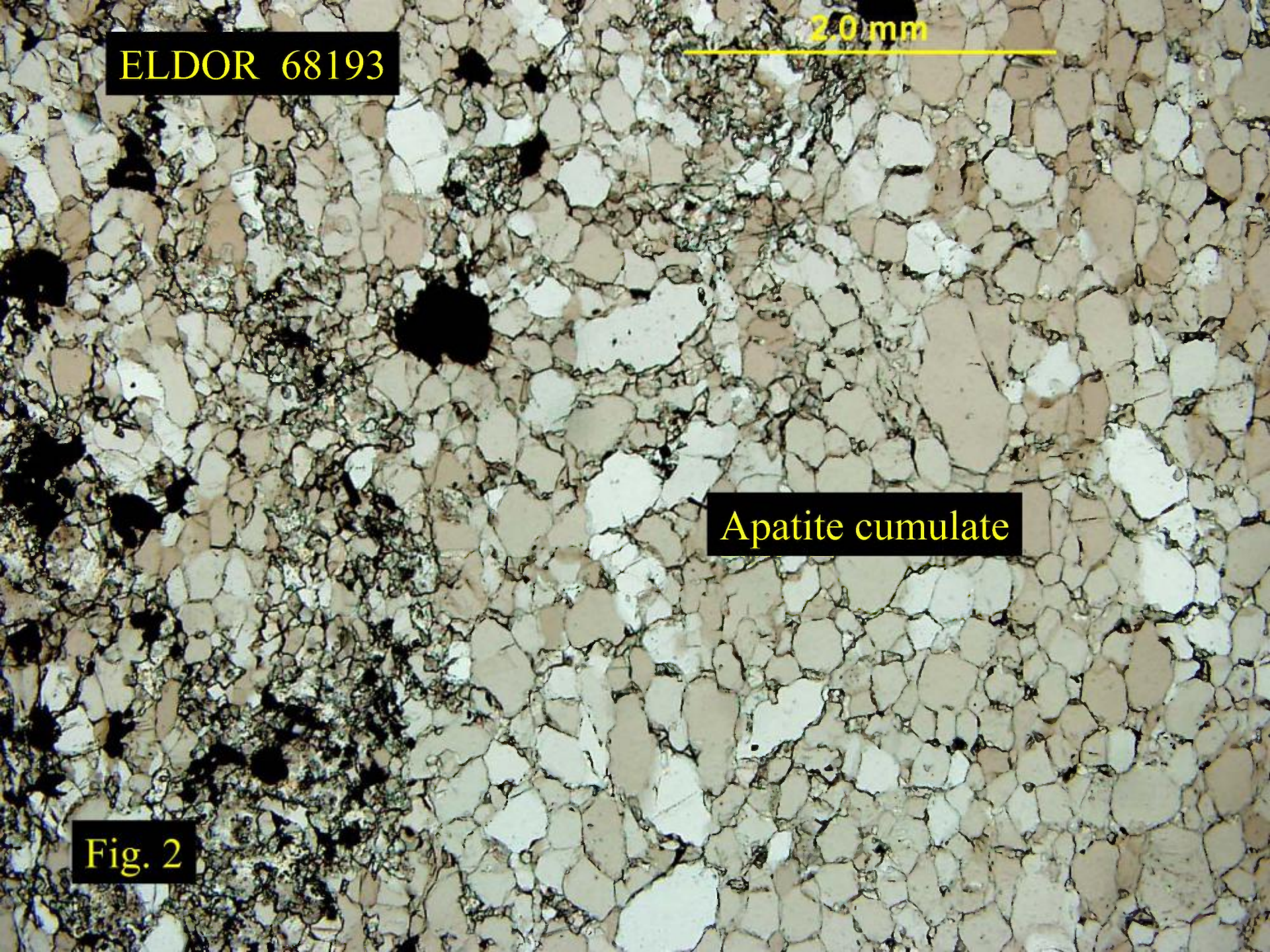

Fig. 2

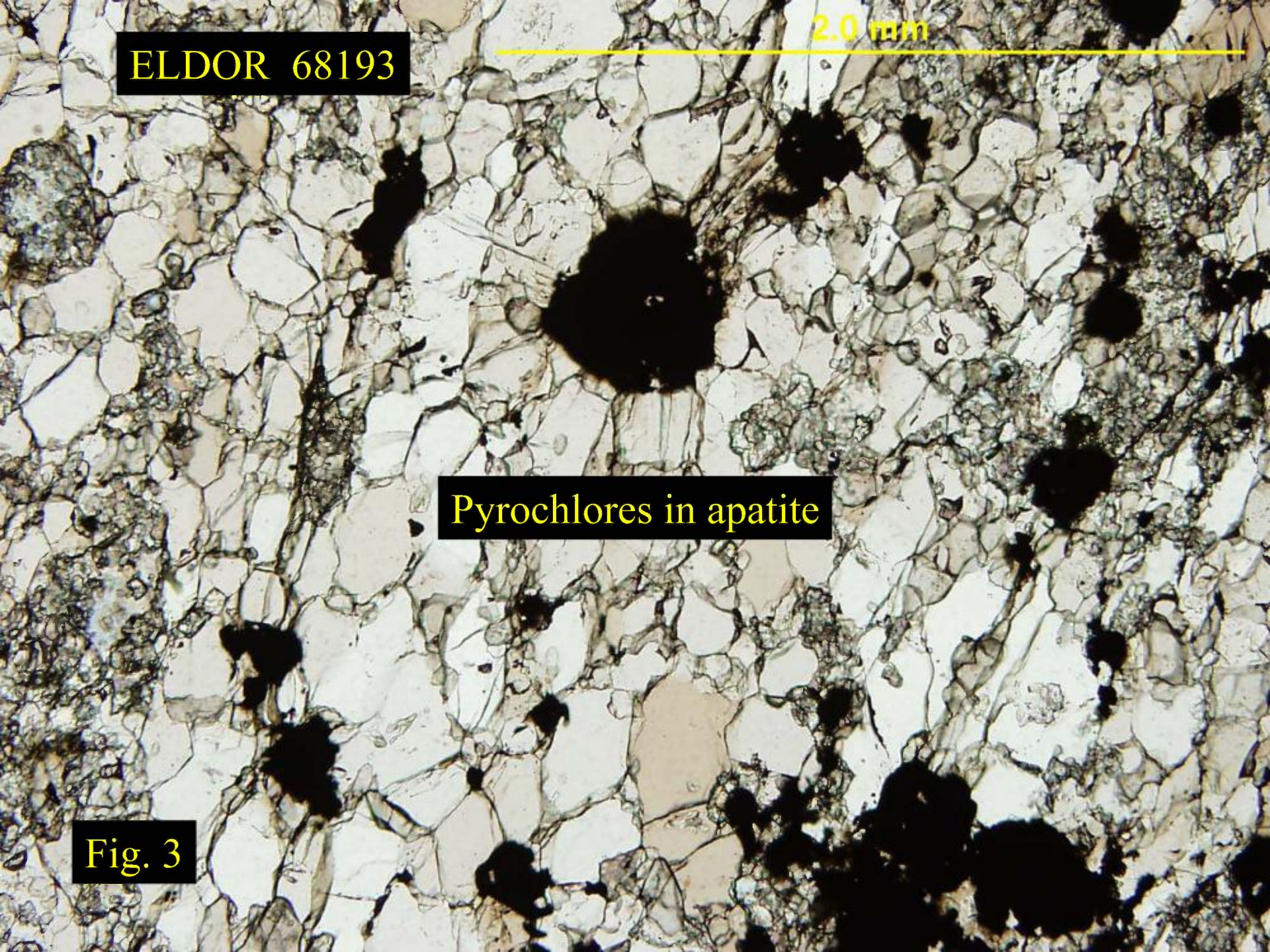

Fig. 3

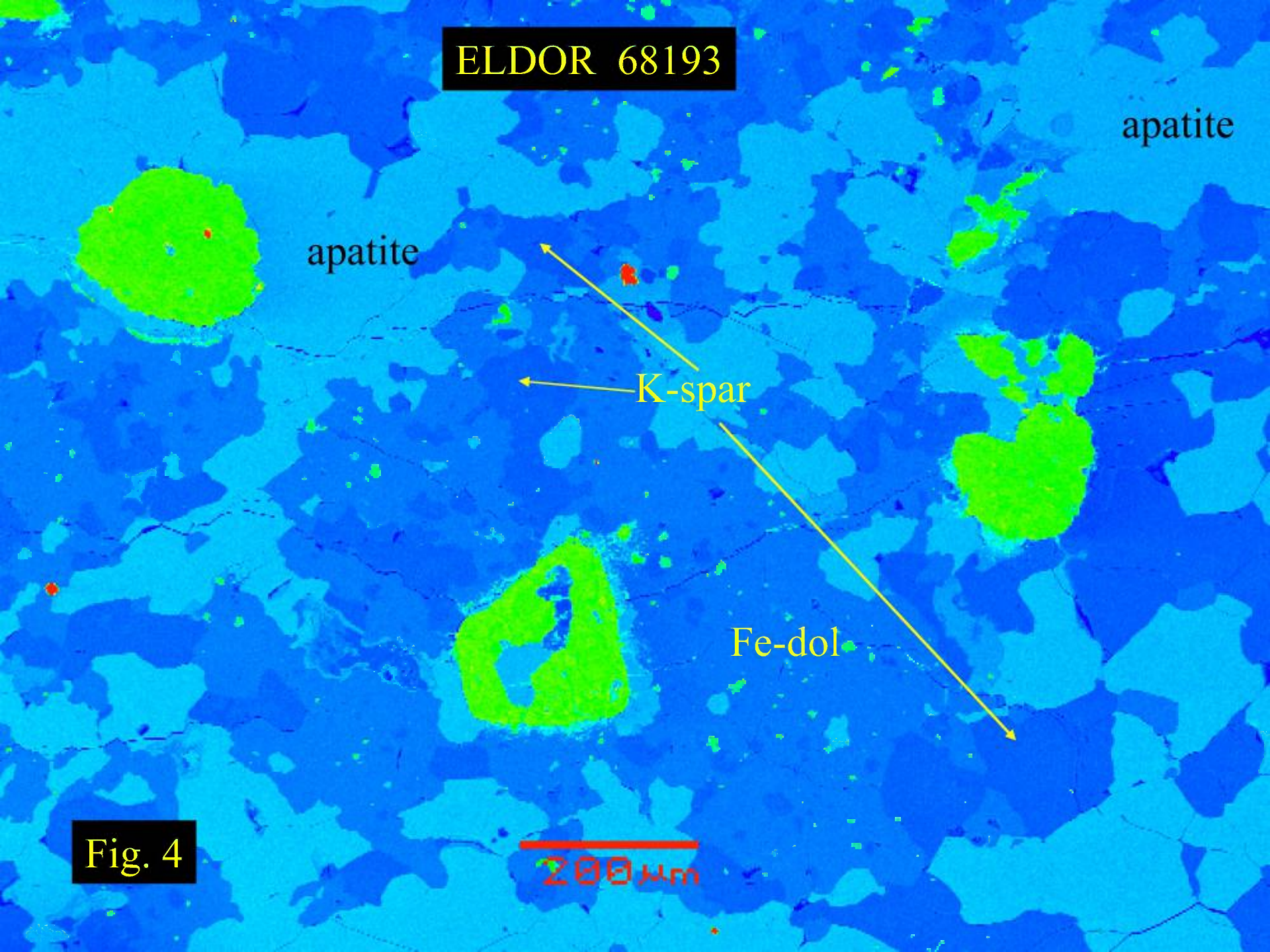

Fig. 4

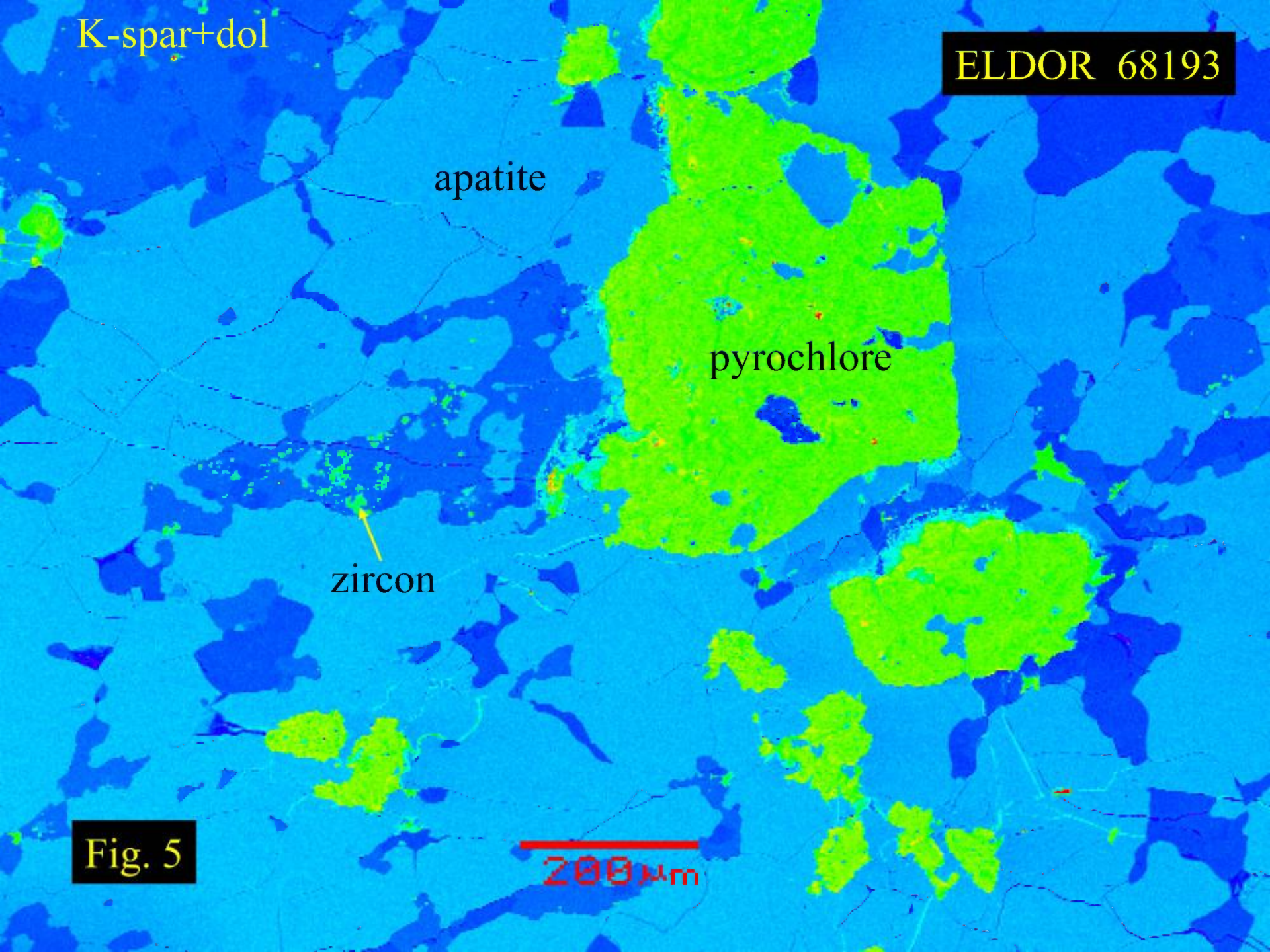

Fig. 5

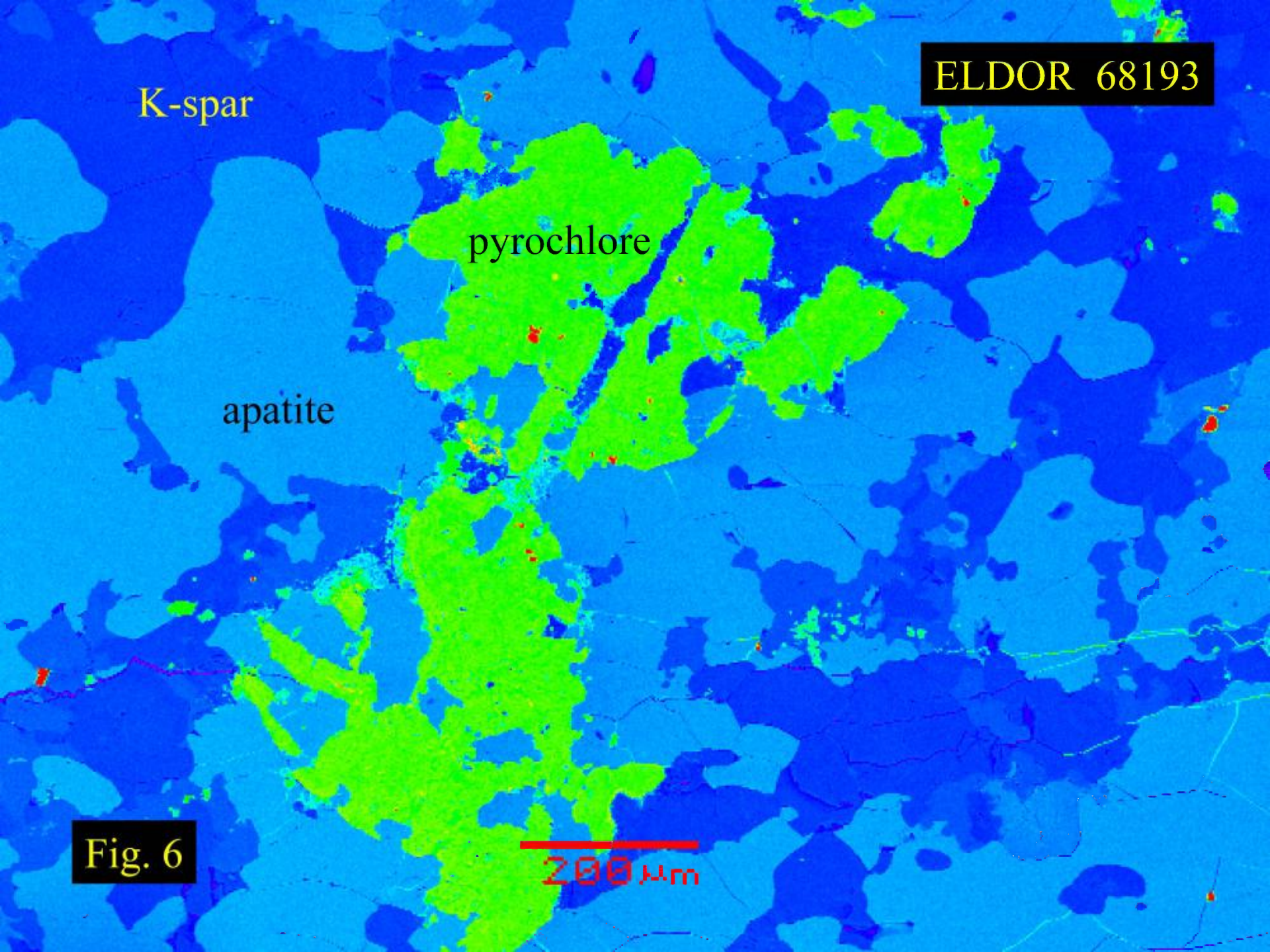

Fig. 6

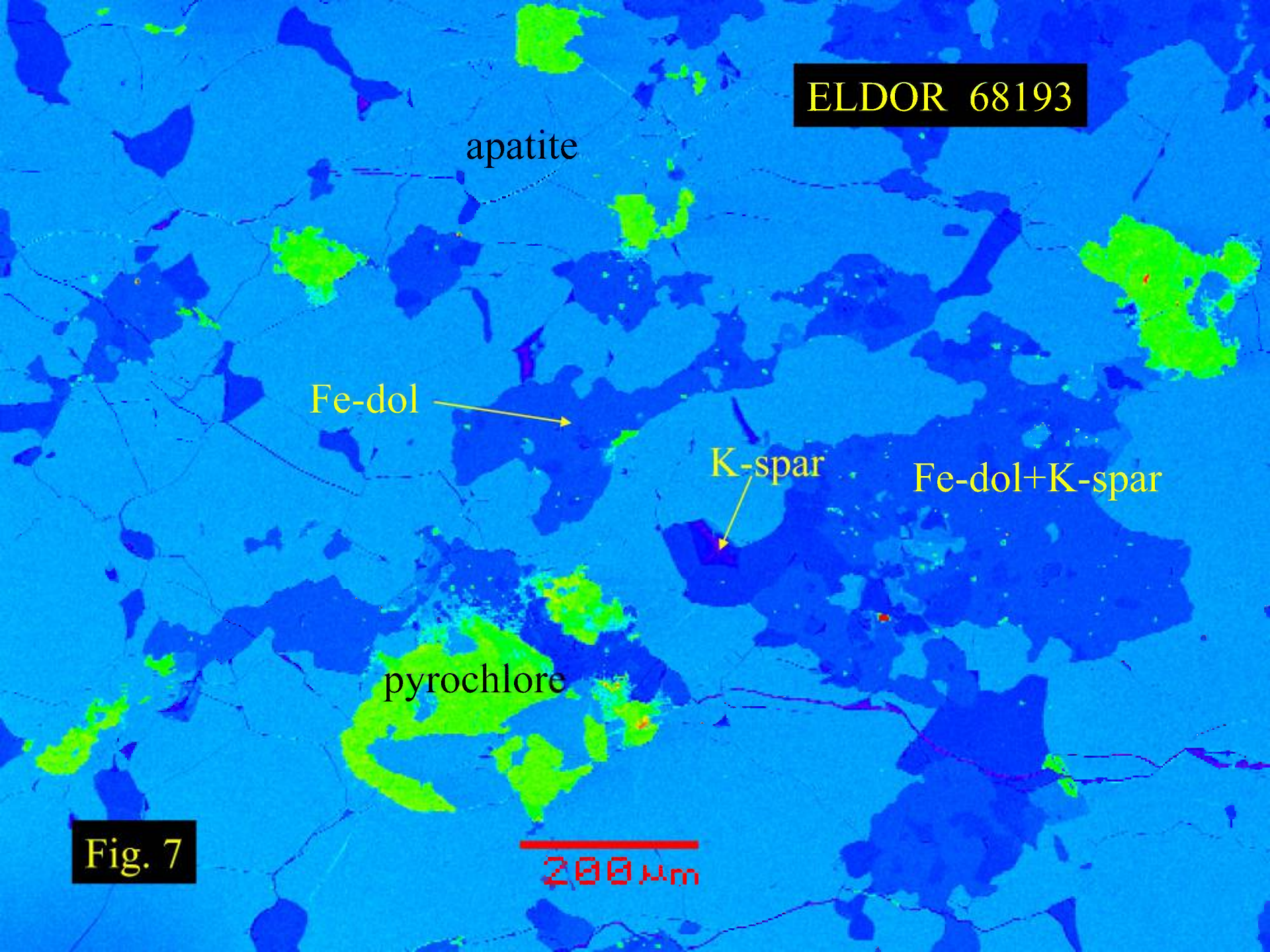
ELDOR 68193
apatite
Fe-dol
K-spar
Fe-dol+K-spar
pyrochlore
200 µm

Fig. 7

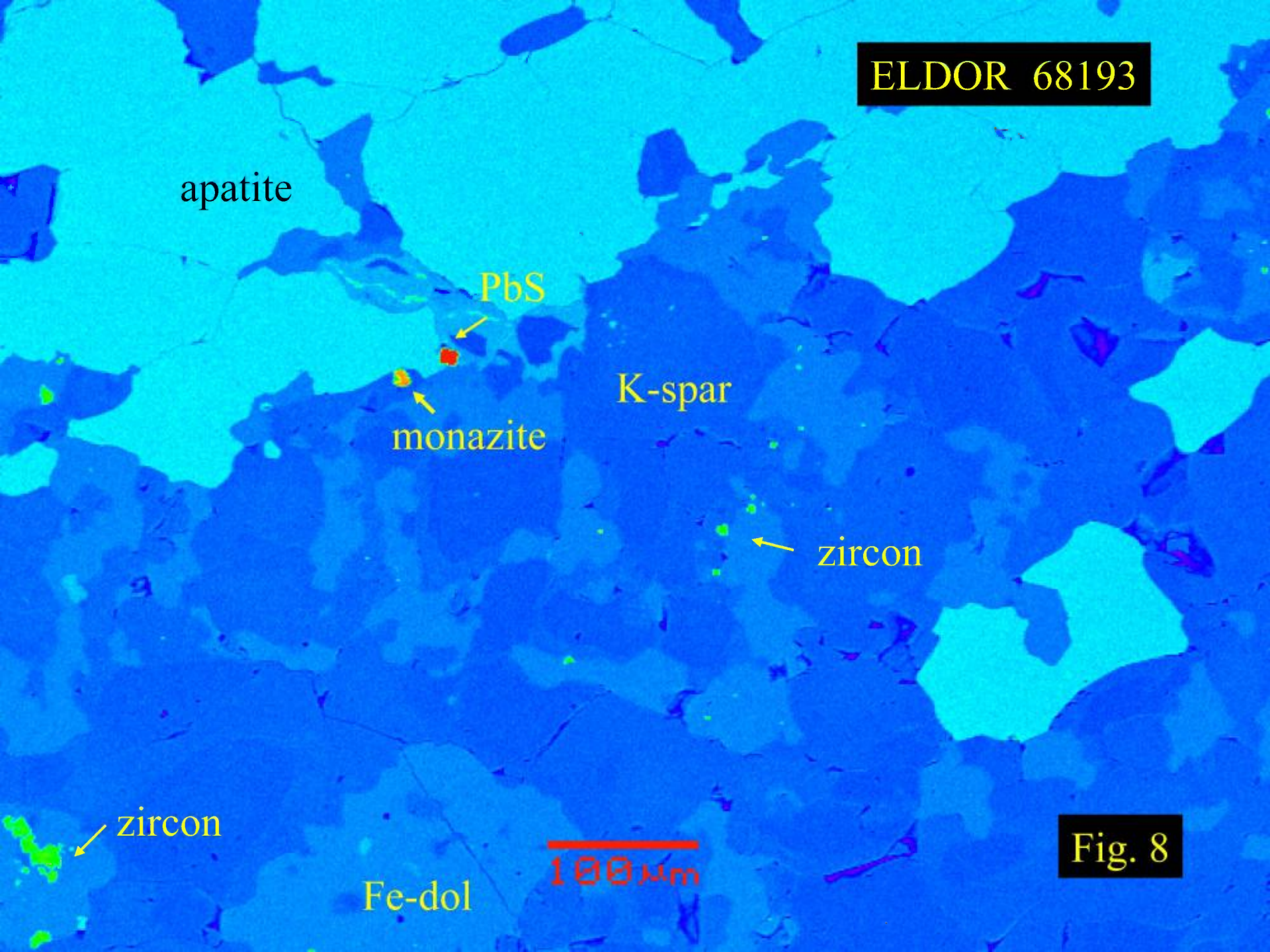
ELDOR 68193
apatite
PbS
monazite
K-spar
zircon
zircon
100 µm
Fe-dol
Fig. 8

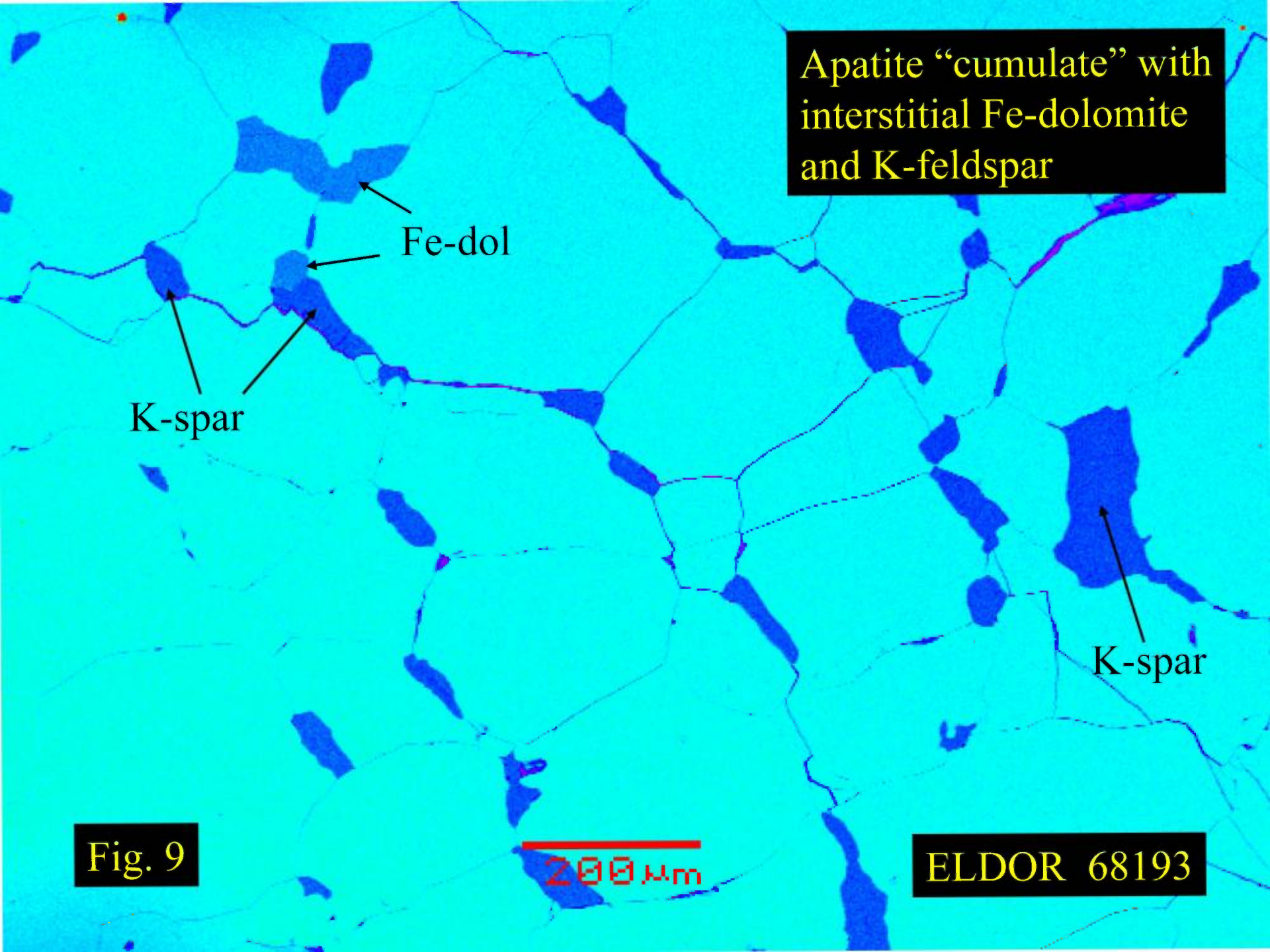
Apatite “cumulate” with interstitial Fe-dolomite and K-feldspar
Fe-dol
K-spar
K-spar
200 µm
ELDOR 68193

Fig. 9

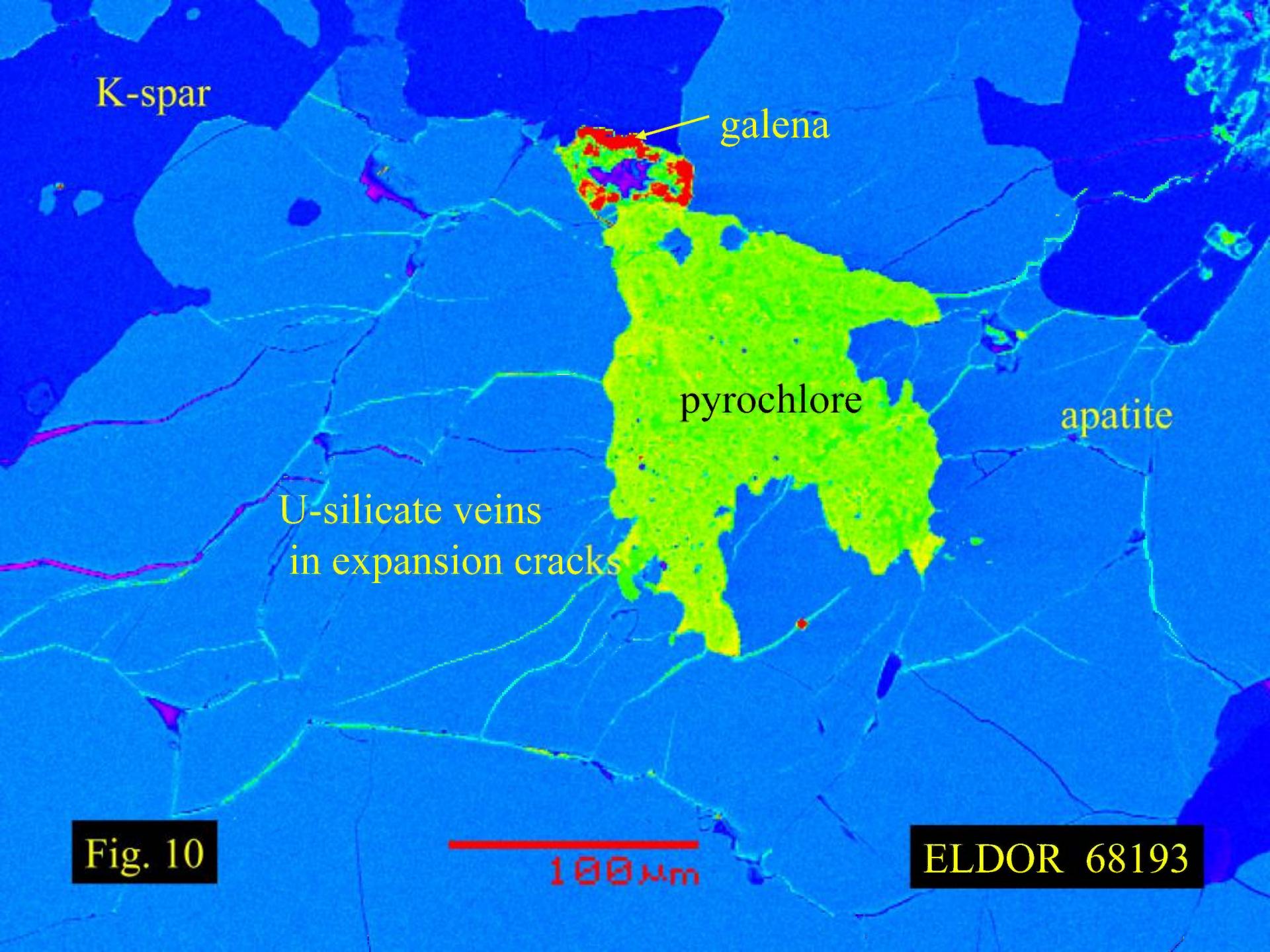
K-spar
galena
pyrochlore
apatite
U-silicate veins
in expansion cracks
100 µm
Fig. 10
ELDOR 68193

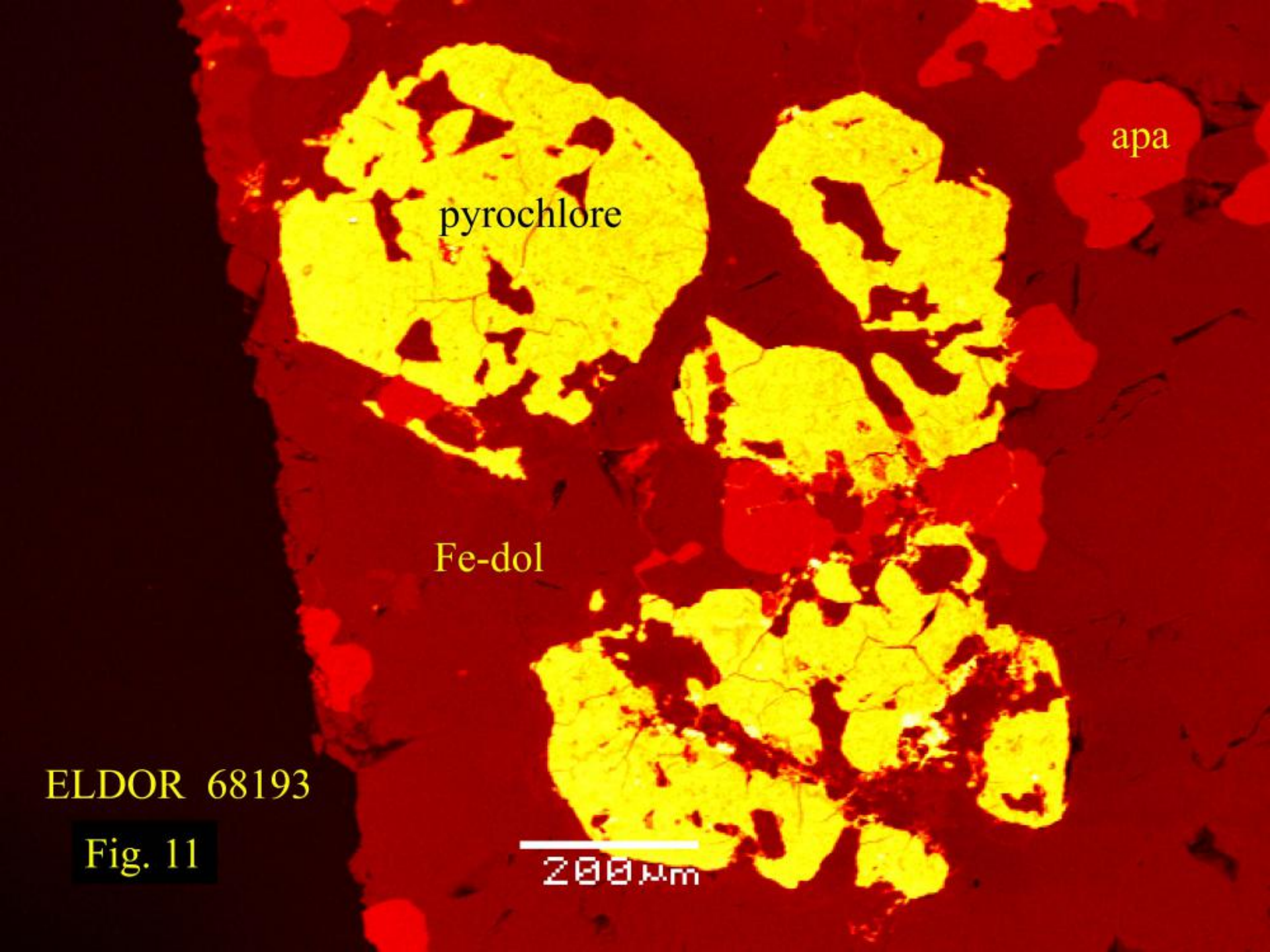

ELDOR 68193

Fig. 11

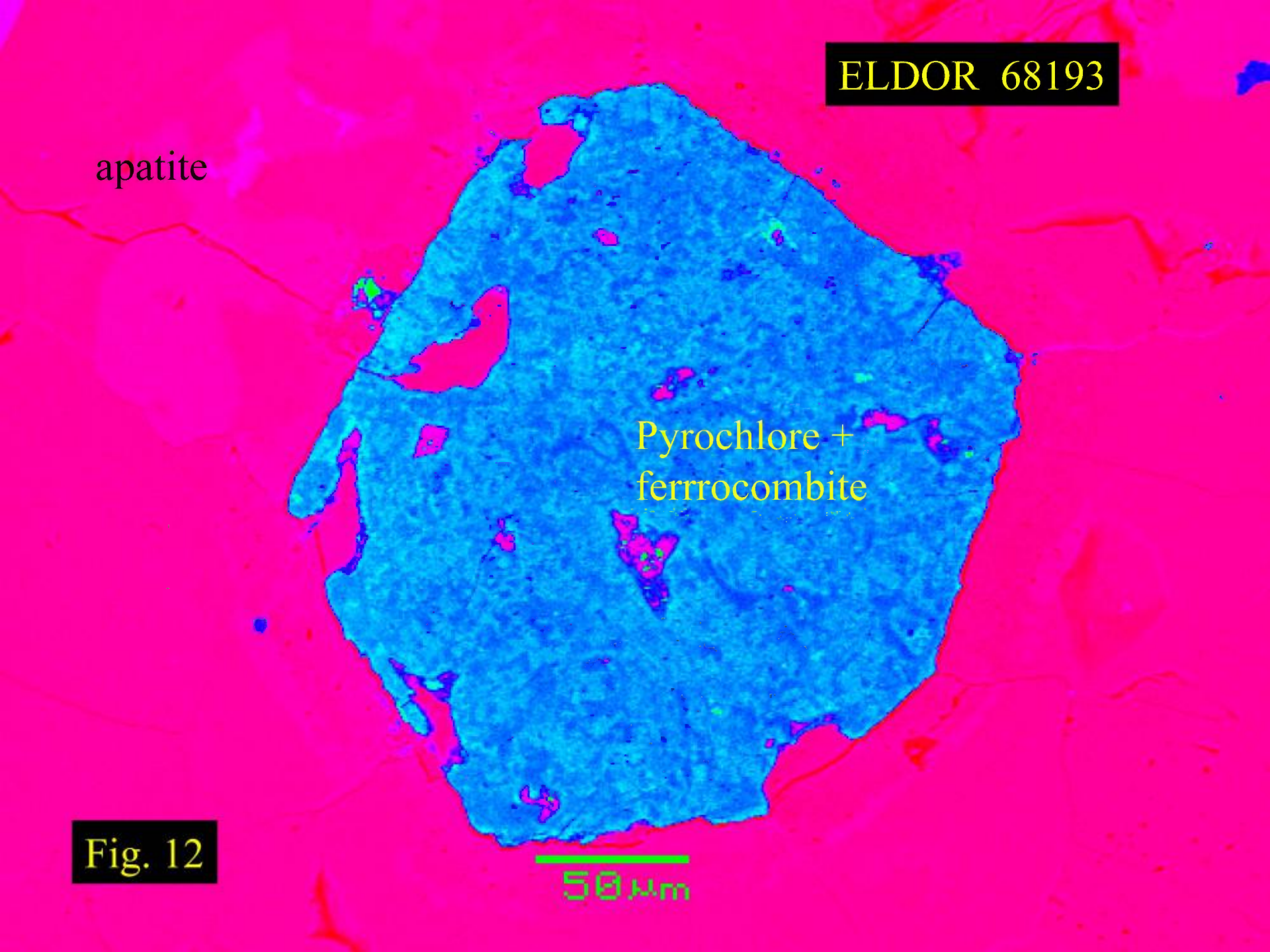

Fig. 12

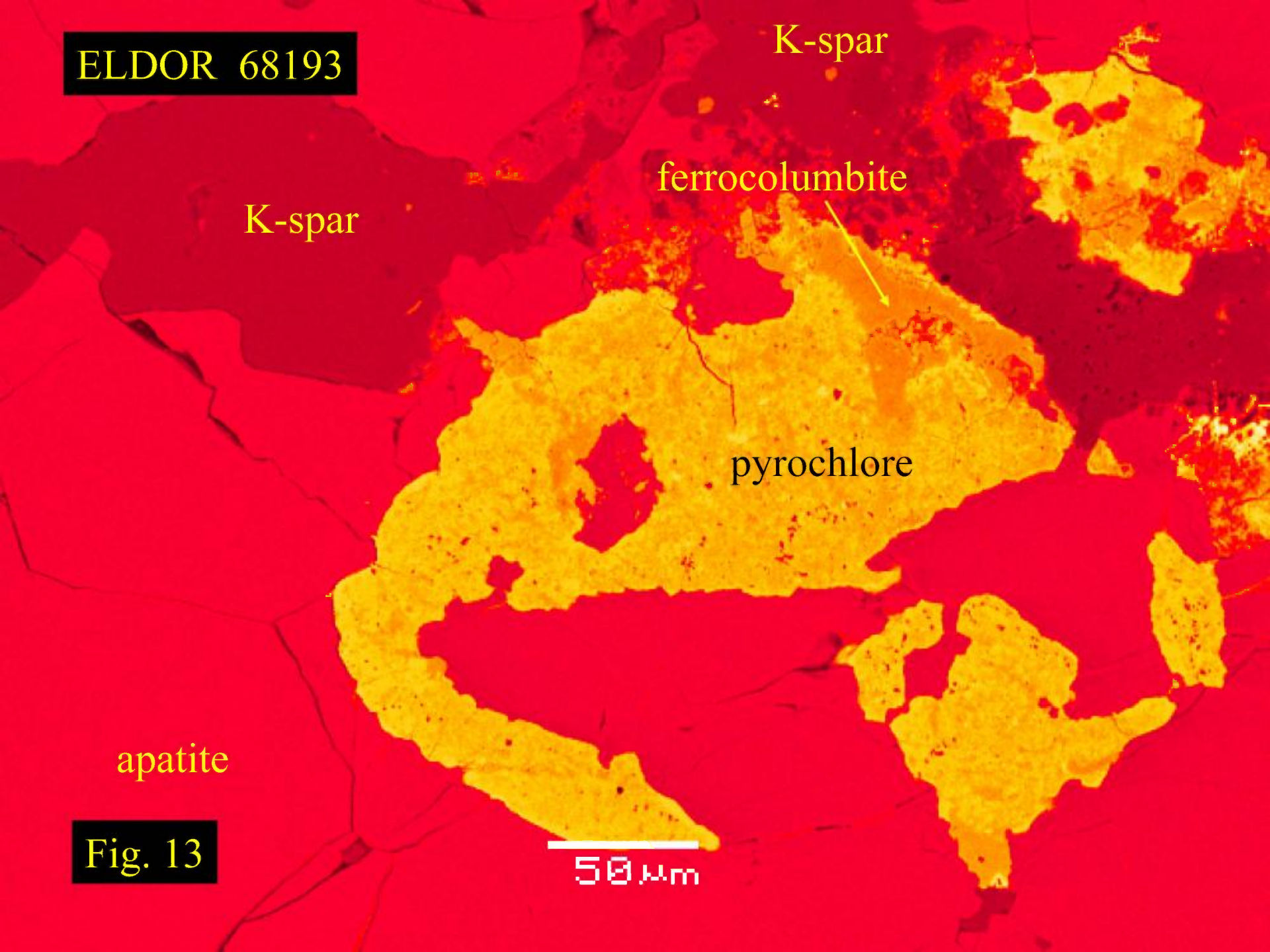
ELDOR 68193
K-spar
ferrocolumbite
K-spar
pyrochlore
apatite
50 µm

Fig. 13

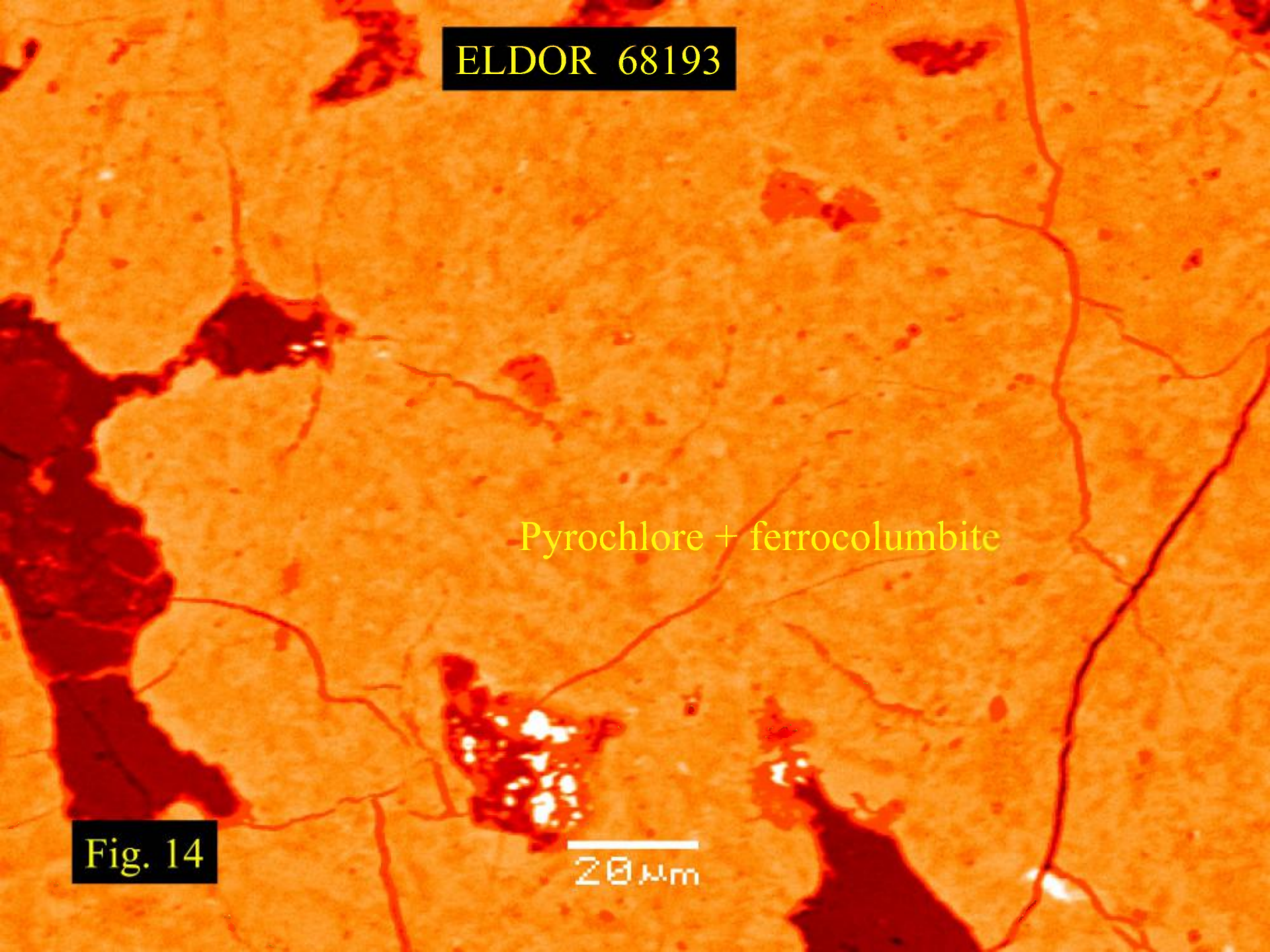

Fig. 14

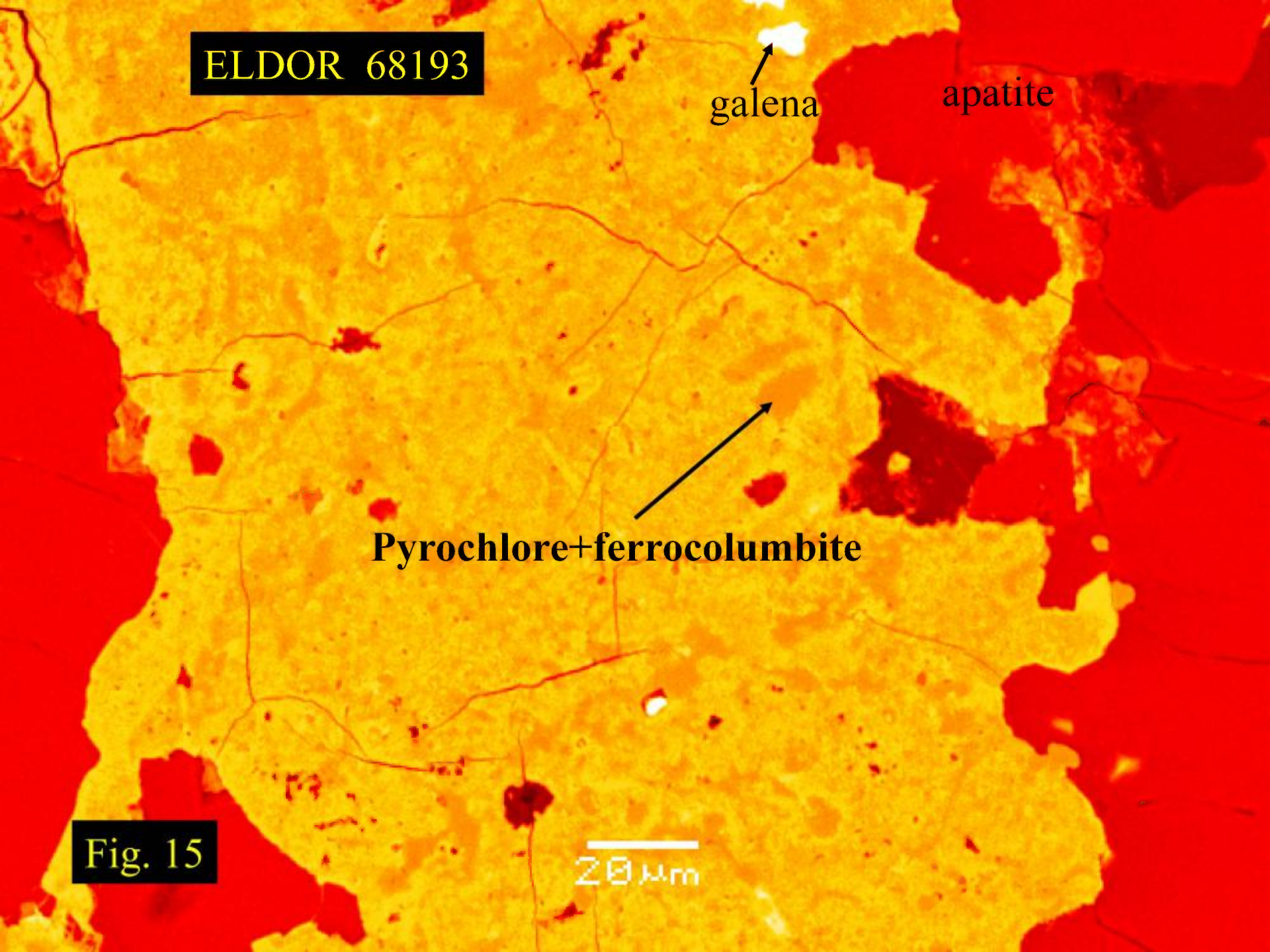
ELDOR 68193
galena
apatite
Pyrochlore+ferrocolumbite
20 µm

Fig. 15

ELDOR 68194

ELDOR 68194 ***Magnetite-apatite breunnerite carbonatite***

This sample is essentially a magnetite-apatite cumulate (Figs 1-5) that has been brecciated and cemented by a later forming breunnerite carbonatite. Magnetite forms irregular broken crystals up to 1 cm in size. Some crystals are brecciated and veined by breunnerite (Fig.7) together with lesser amounts of aegirine, Fe-rich chlorite and minor galena. The magnetite contains no detectable Ti, Mg or Mn, and contains rare small (< 20 um) anhedral inclusions of Ta-bearing Nb-Fe-titanate (niobo-ilmenorutile?). Exsolution ilmenite is not present. Apatite forms large (up to 1 cm) masses of interlocking subhedral prisms and anhedral crystals.(Figs. 4-5, 14) The texture is that of a cumulate (Fig. 14). The small amounts of interstitial material consist of breunnerite and/or ferroan dolomite. The apatite is of uniform composition and poor in Sr and REE (< 0.5 wt.). Small (<20 um) anhedral crystal of monazite-(Ce) are present in some apatite crystals. The breunnerite forms aggregates of anhedral interlocking complexly zoned crystals and cements or surrounds masses of apatite. The breunnerite is intergrown in many instances with later-forming ferroan dolomite and rounded late-stage quartz (Figs 8-10, 13). Late stage quartz-rich "pools" commonly contain small prisms of blue-green to violet arfvedsonite (Figs 8-9) and minor small (<20um) anhedral crystals of monazite-(Ce). A characteristic feature of the rock is the presence of significant amounts of aegirine. This occurs as clast-like angular intergrowths of apatite and aegirine or, more commonly, as rounded crystals of apatite which are poikilitically enclosed by large plates of aegirine (Figs 1, 5, and 11).

ELDOR 68194

The sample contains rounded-to-subhedral crystals (up to 400 um) of a pale brown phase of high relief. These are commonly, but not always, surrounded by irregular aggregates of opaque material (Figs. 1-3, 6). Radial expansion fractures filled with chlorite commonly surround this material (Figs. 1-3, 6 and 13). BSE-imagery and X-ray spectrometry shows that the pale brown phase is zircon and the opaque material is a "pyrochlore".

The margins of the zircon crystals are typically resorbed (Figs. 11, 15-16), and all crystals are homogeneous in their composition. Inclusions are not present. The "pyrochlores" are irregular, rounded resorbed crystals (up to 400 um in diameter; most 200-300). They consist of amoeboid irregular small inclusions of Ta-bearing ferrocolumbite enclosed within a matrix U-Ta-pyrochlore of relatively uniform composition (Figs. 17-18). Small (< 10 um) inclusions of galena are present. Th-pyrochlores and fersmite are not present.

Representative semiquantitative compositions of pyrochlore (PYR) and ferrocolumbite(FERROCOL) are:

wt.%	PYR	FERROCOL	wt.%	PYR	FERROCOL
SiO_2	2.2	1.2	TiO_2	6.6	3.4
Na_2O	n.a.	n.a	La_2O_3	n.d.	n.d.
CaO	1.9	n.d	Ce_2O_3	0.5	n.d.
FeO	6.6	19.2	Pr_2O_3	n.d.	n.d.
SrO	1.4	n.d.	Nd_2O_3	n.d.5	n.d
Y_2O_3	n.d.	n.d.	Ta_2O_5	17.8	5.6
ZrO_2	n.d.	n.d.	ThO_2	n.d.	N.d
Nb_2O_5	37.6	71.1	UO_2	28.6.	n.d.

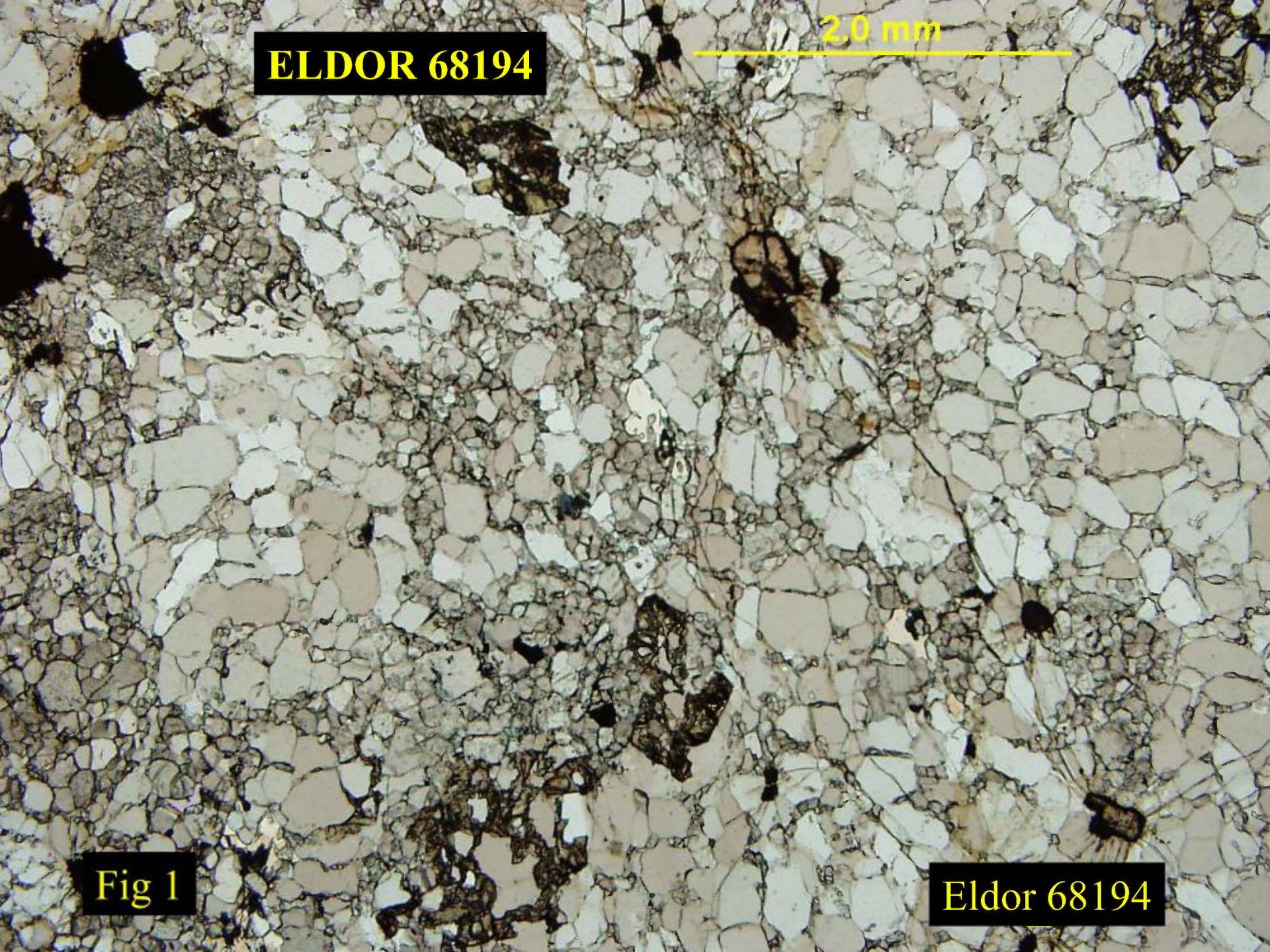
ELDOR 68194
2,0 mm
Fig 1
Eldor 68194

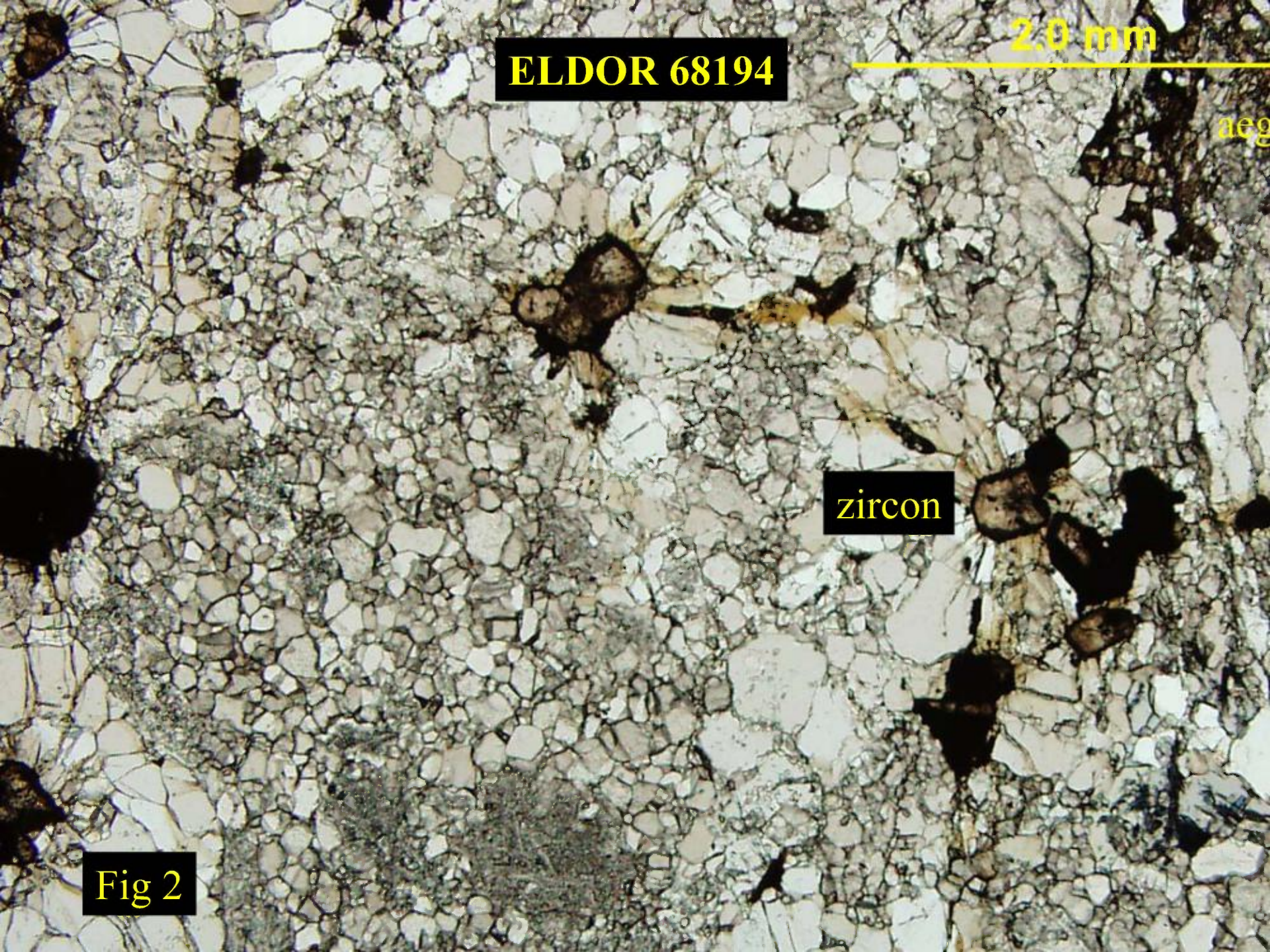

Fig 2

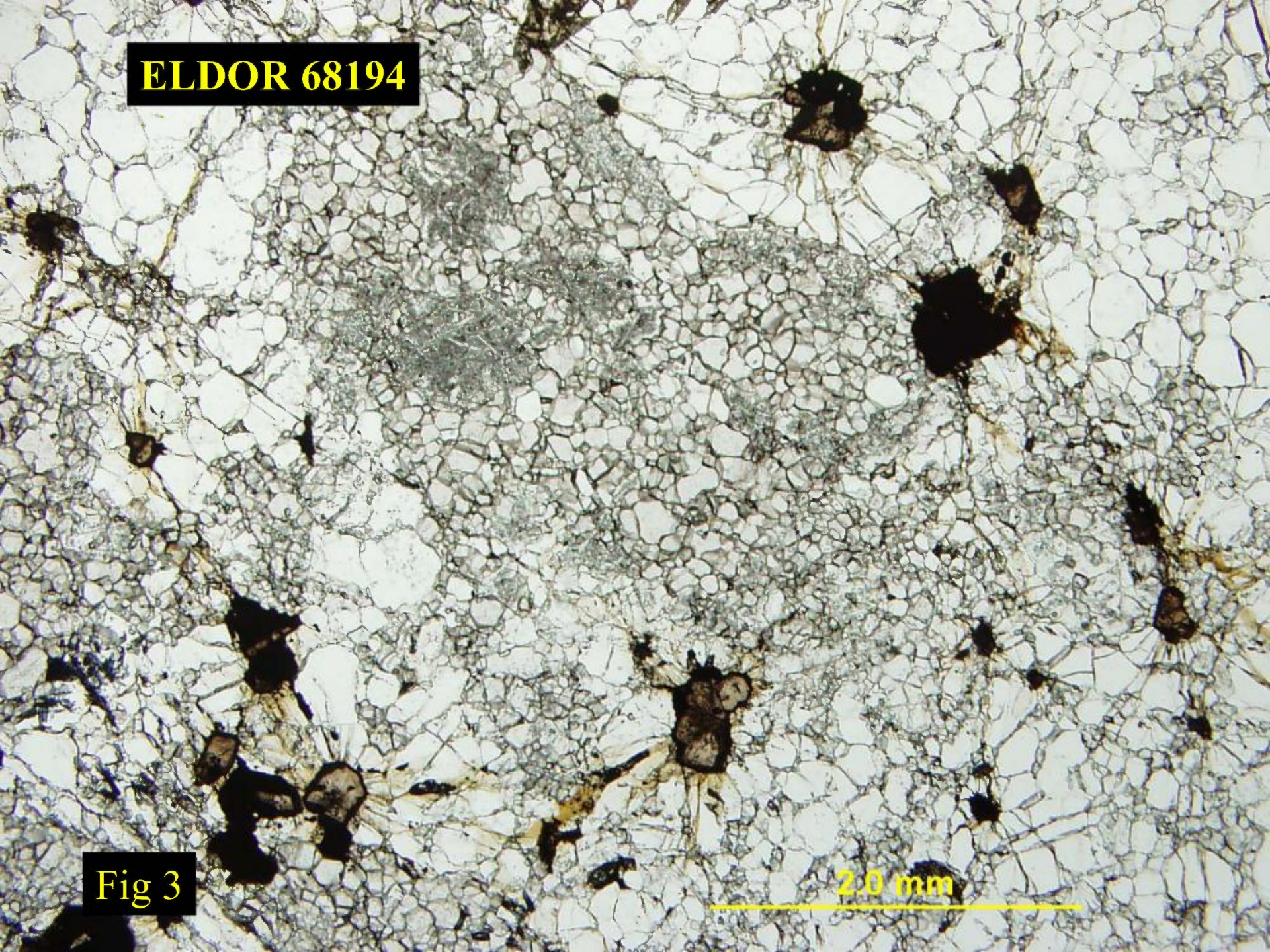

Fig 3

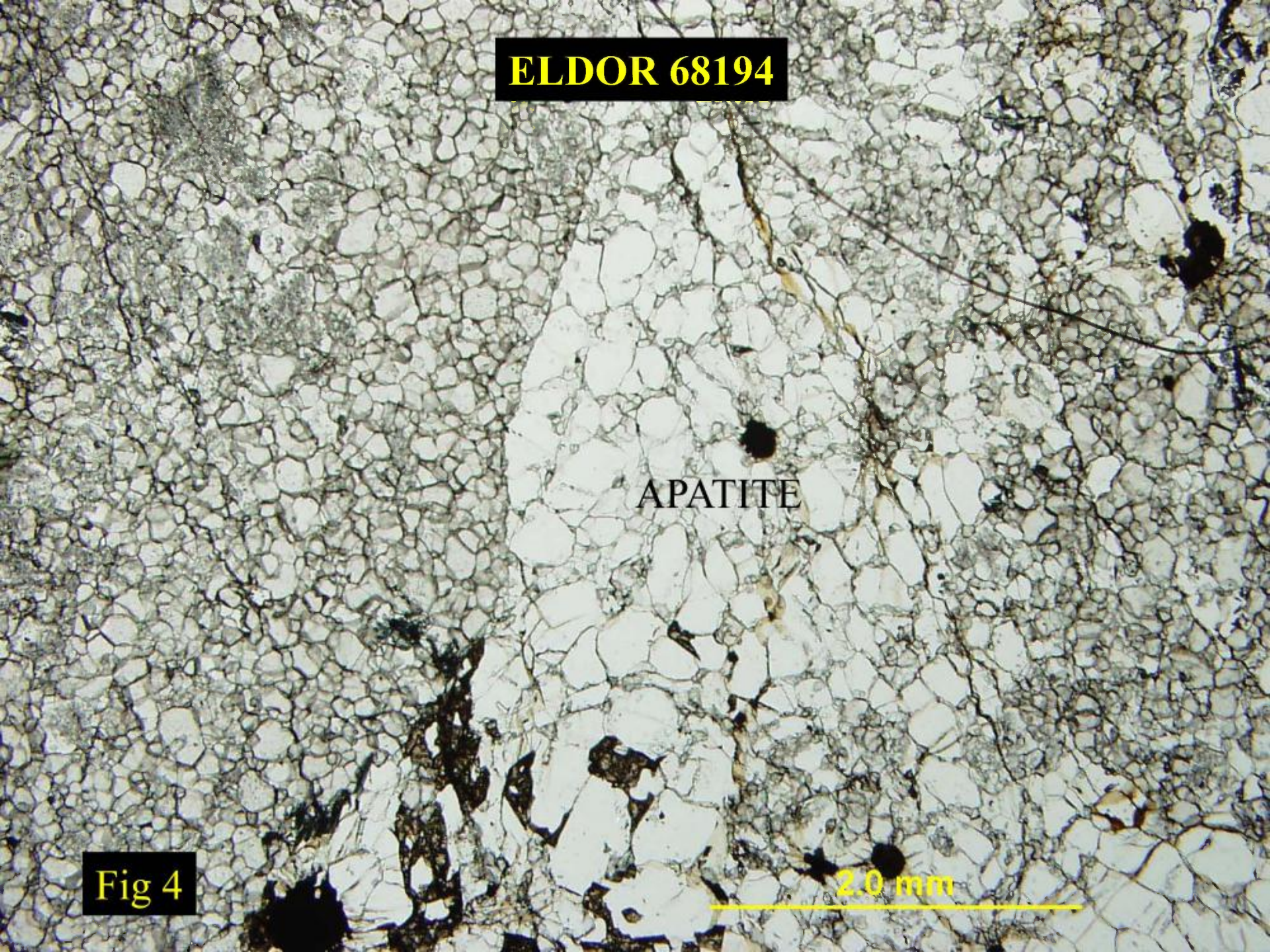

Fig 4

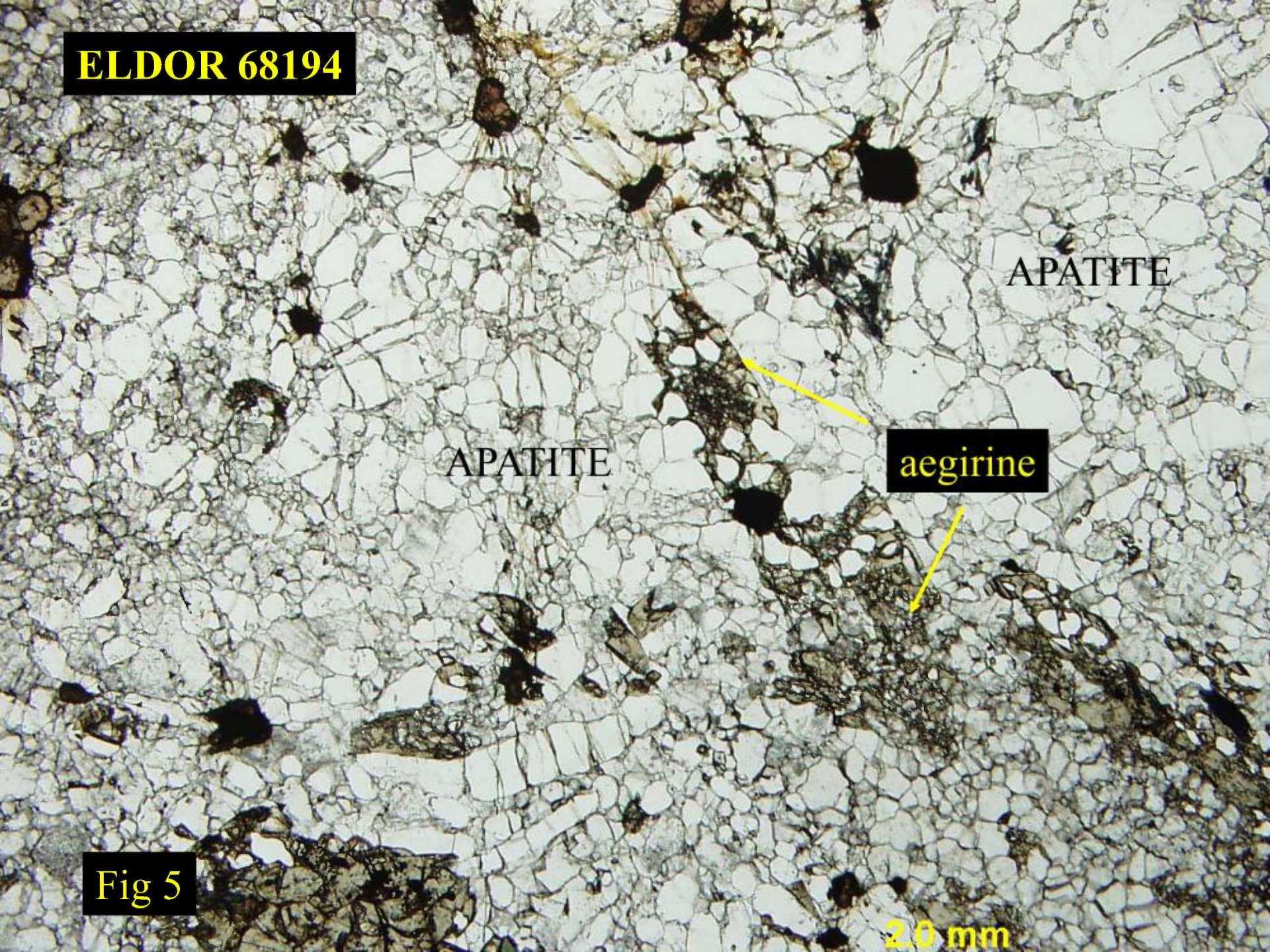
ELDOR 68194
APATITE
APATITE
aegirine
Fig 5
2.0 mm

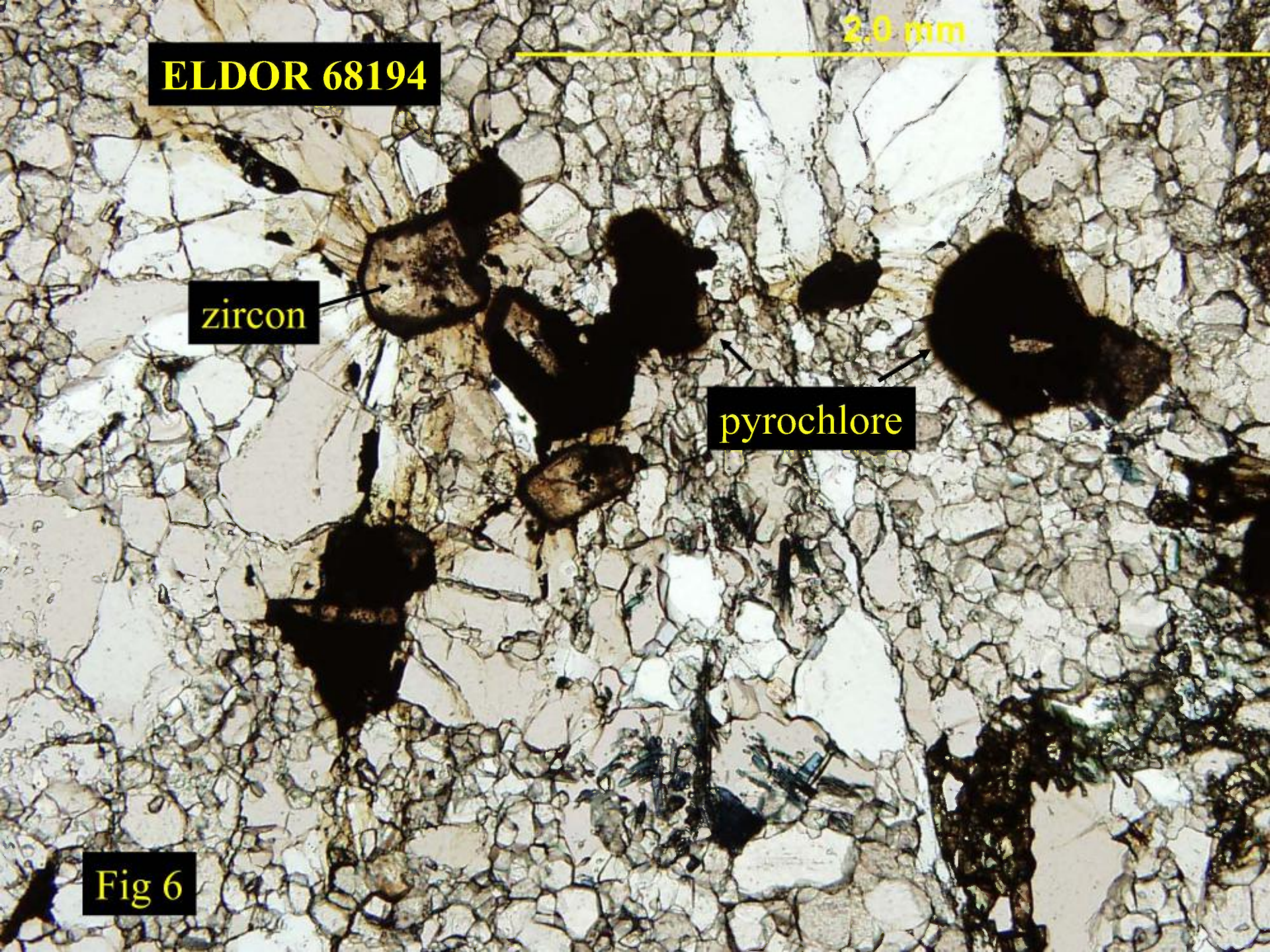

Fig 6

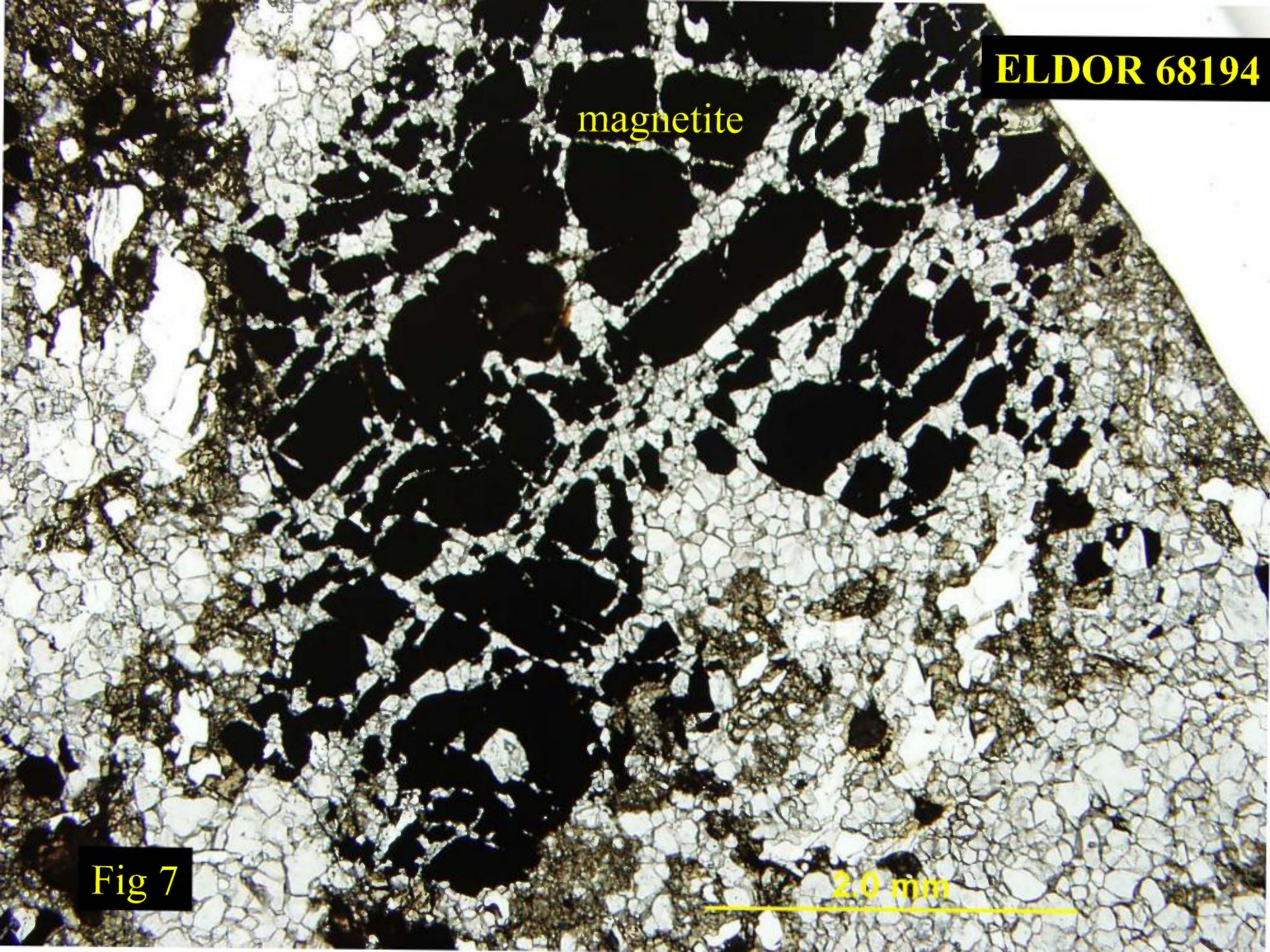
ELDOR 68194
magnetite
Fig 7
2.0 mm

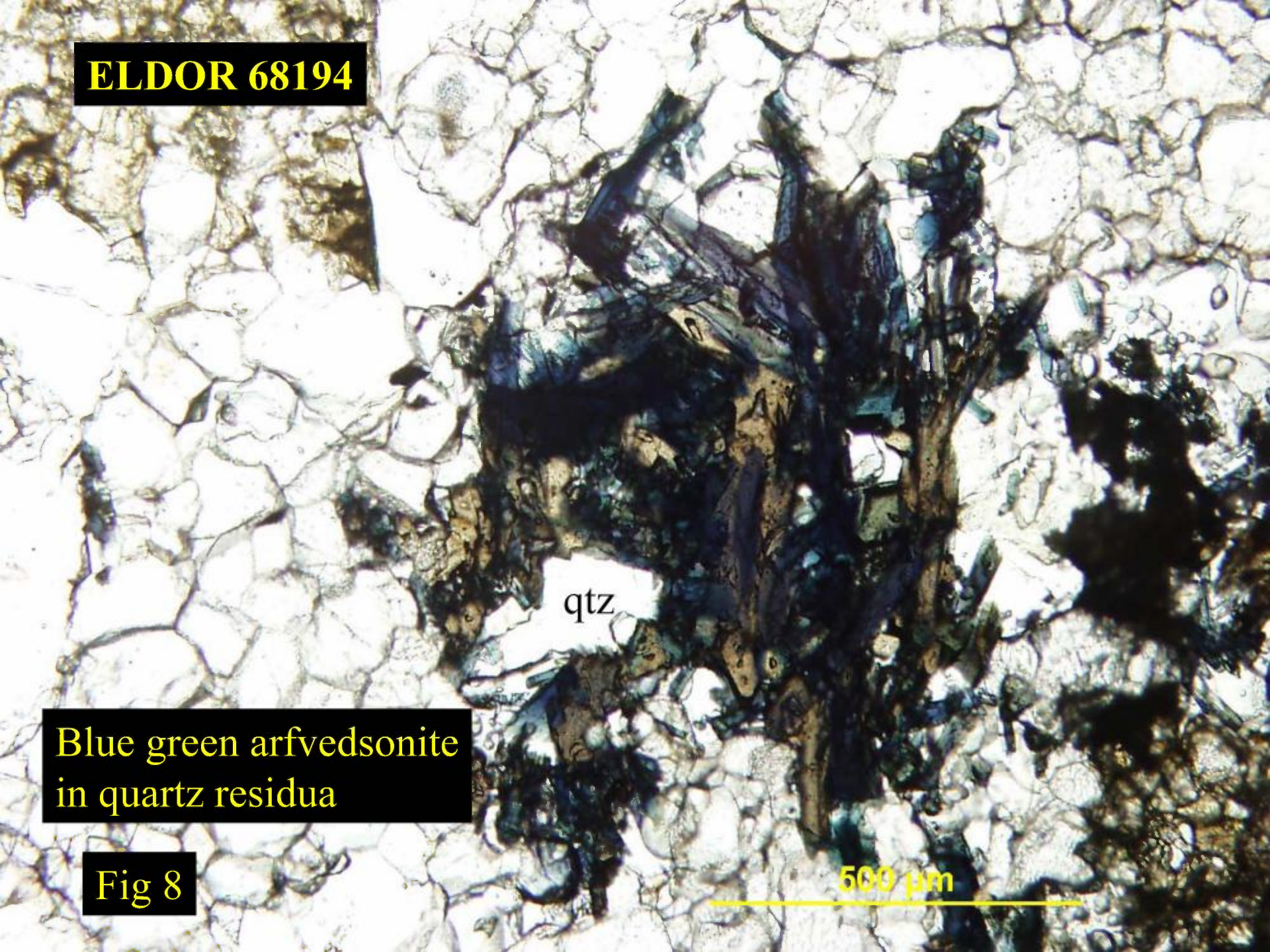

Blue green arfvedsonite in quartz residua

Fig 8

ELDOR 68194

ARFVEDSONITE PRISMS
IN QUARTZ MATRIX

Fig 9

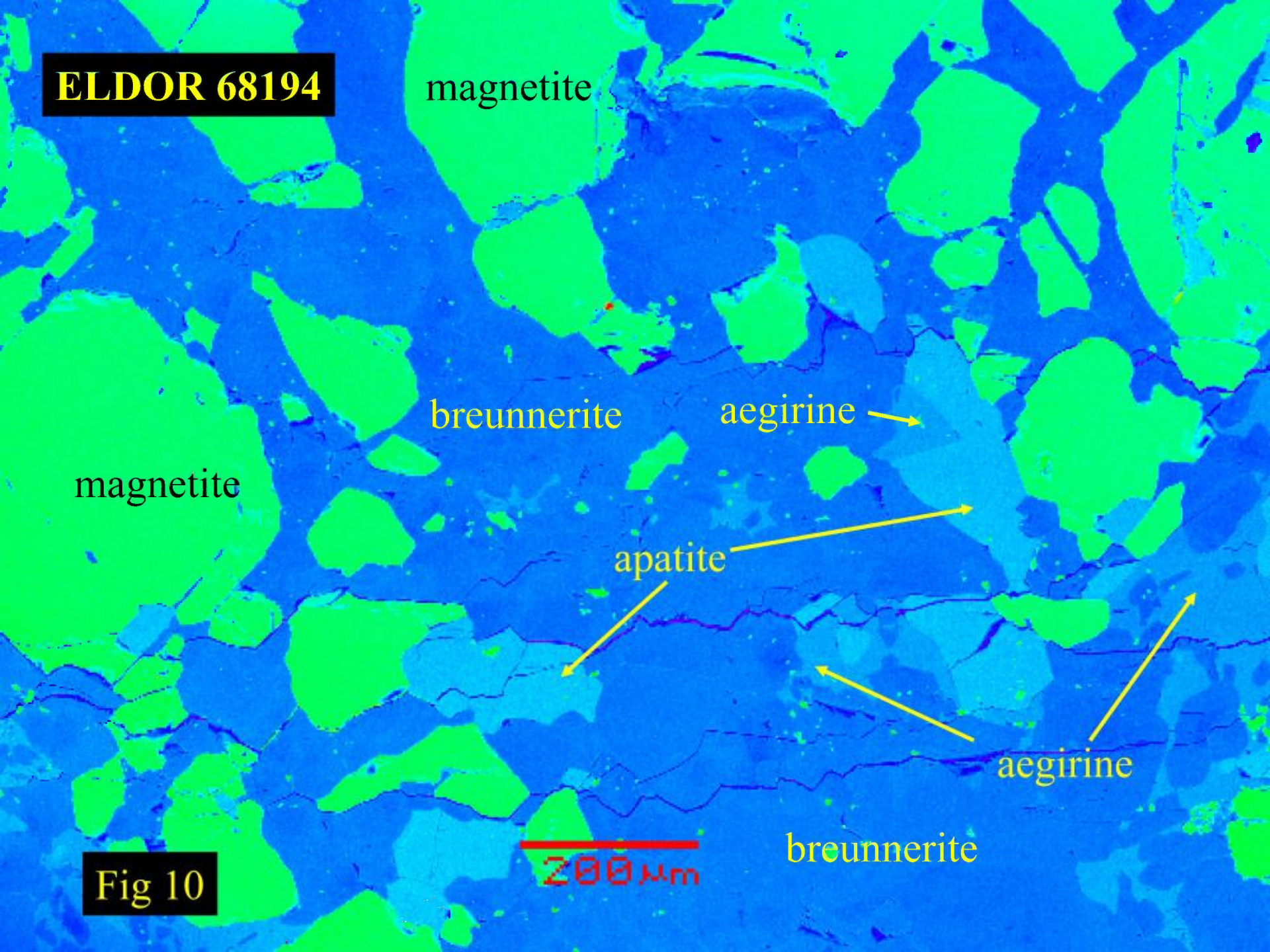
ELDOR 68194
magnetite
breunnerite
aegirine
magnetite
apatite
aegirine
breunnerite
200 µm
Fig 10

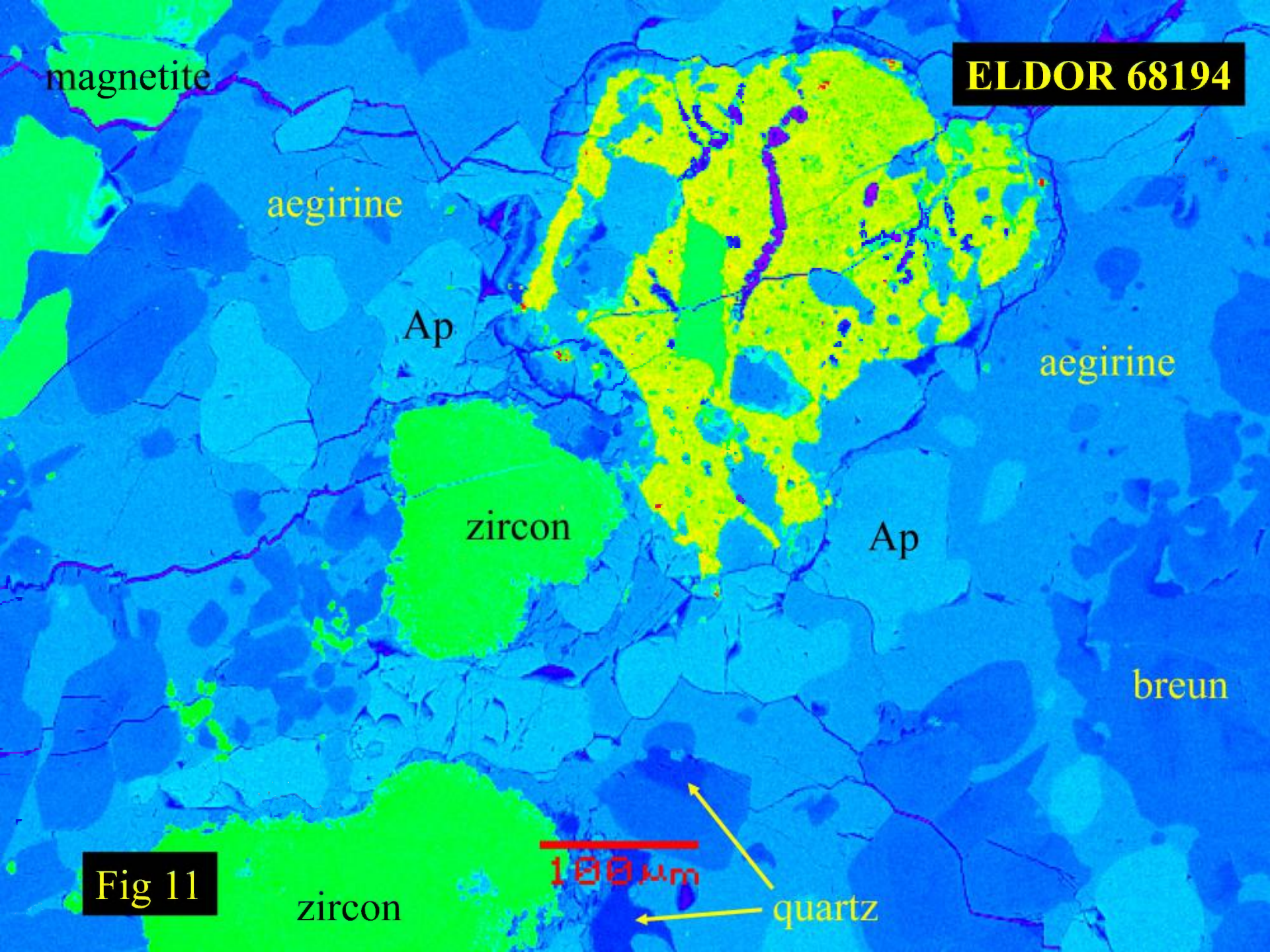
magnetite
ELDOR 68194
aegirine
Ap
aegirine
zircon
Ap
breun
100µm
zircon
quartz

Fig 11

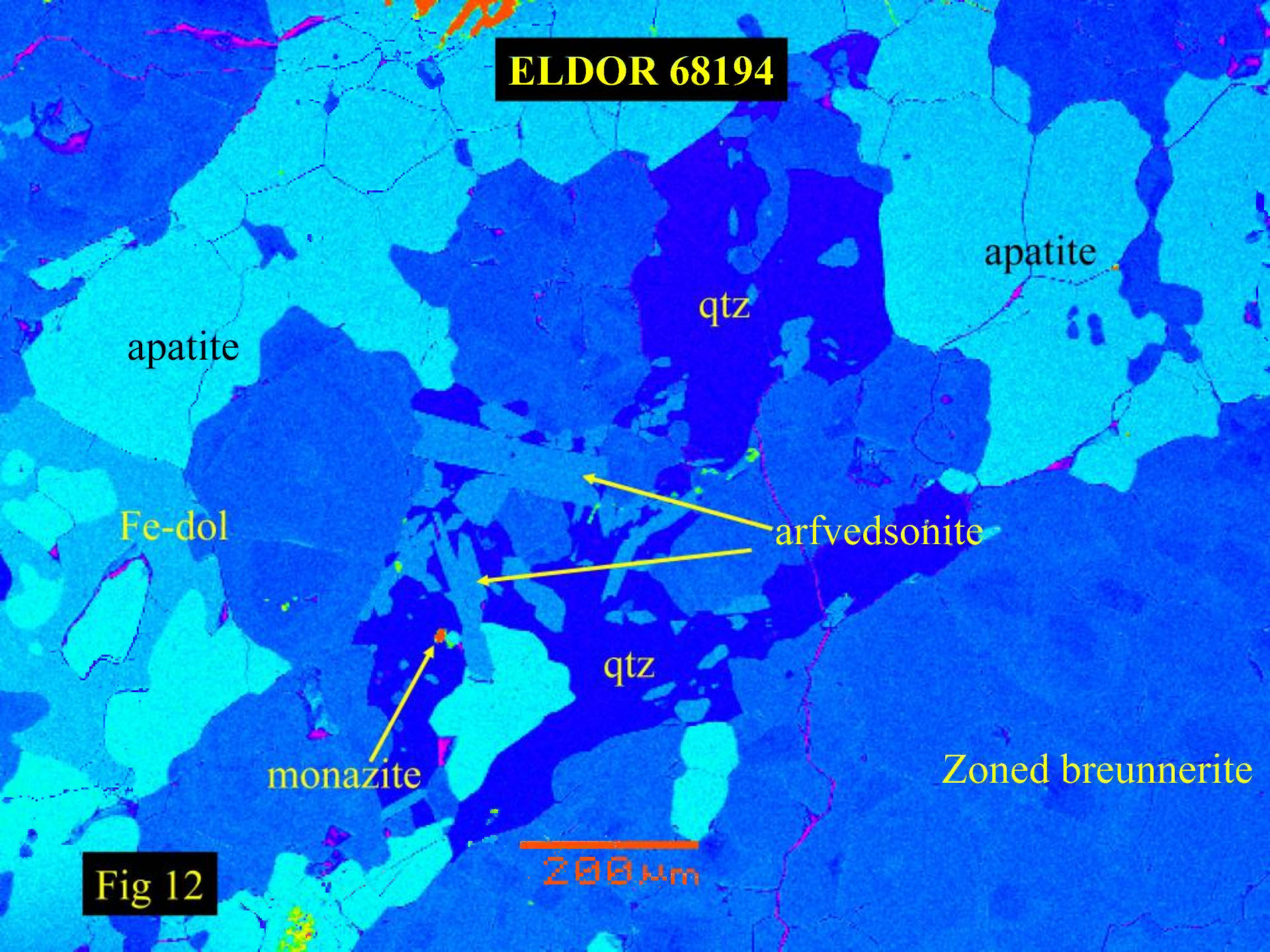
ELDOR 68194
apatite
qtz
apatite
Fe-dol
arfvedsonite
qtz
monazite
Zoned breunnerite
200 µm

Fig 12

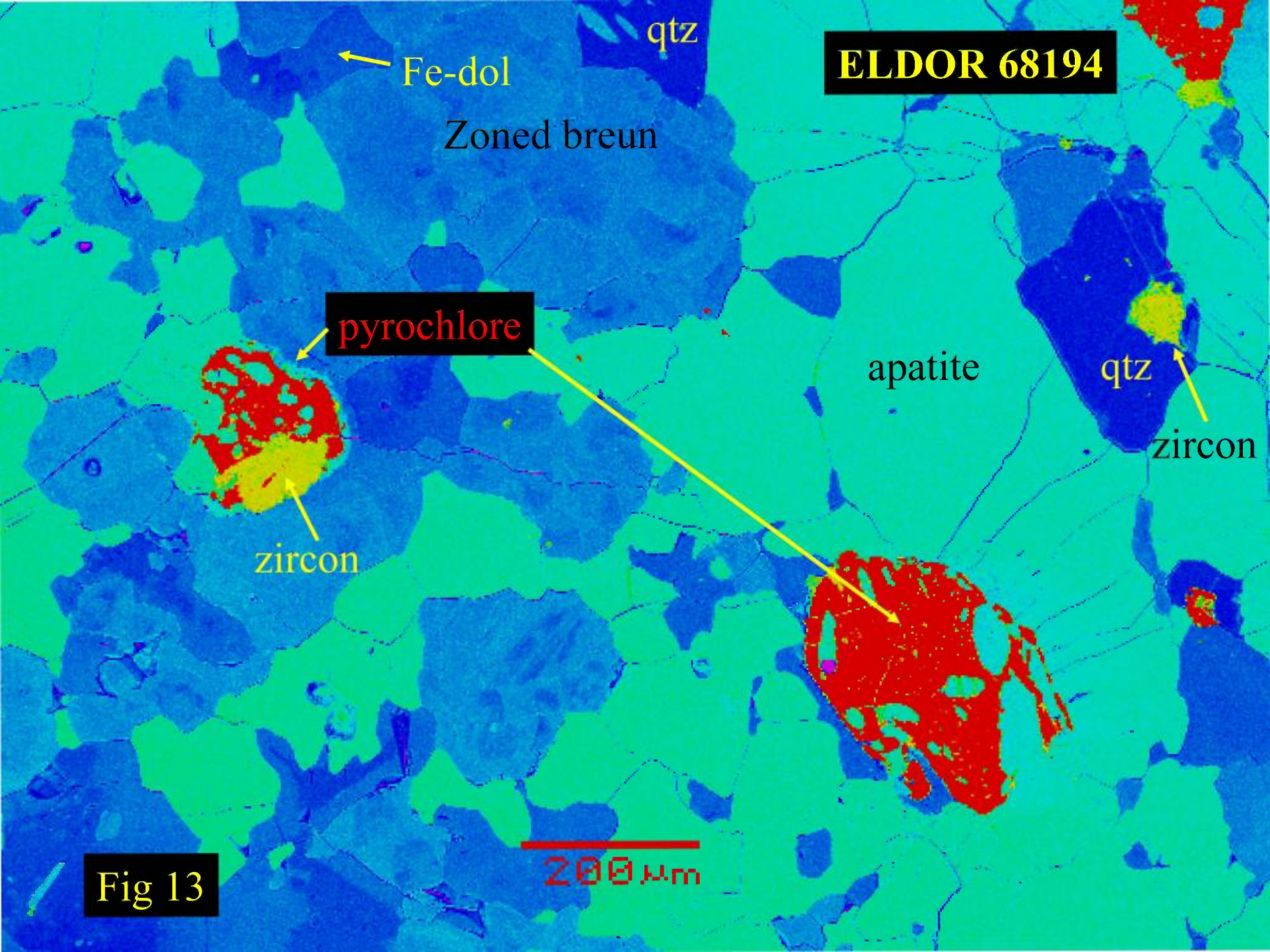
qtz
Fe-dol
ELDOR 68194
Zoned breun
pyrochlore
apatite
qtz
zircon
zircon
200 µm

Fig 13

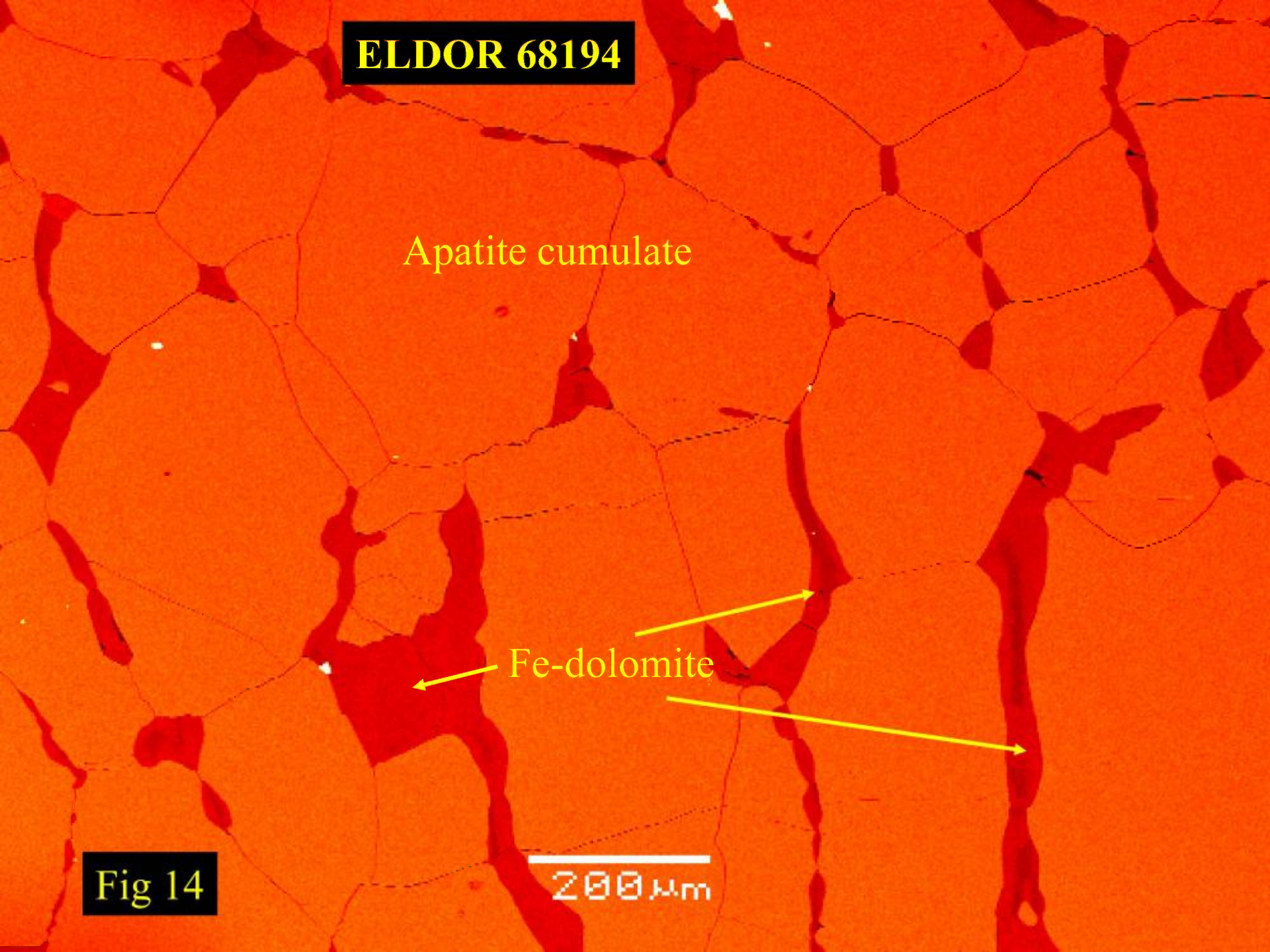

Fig 14

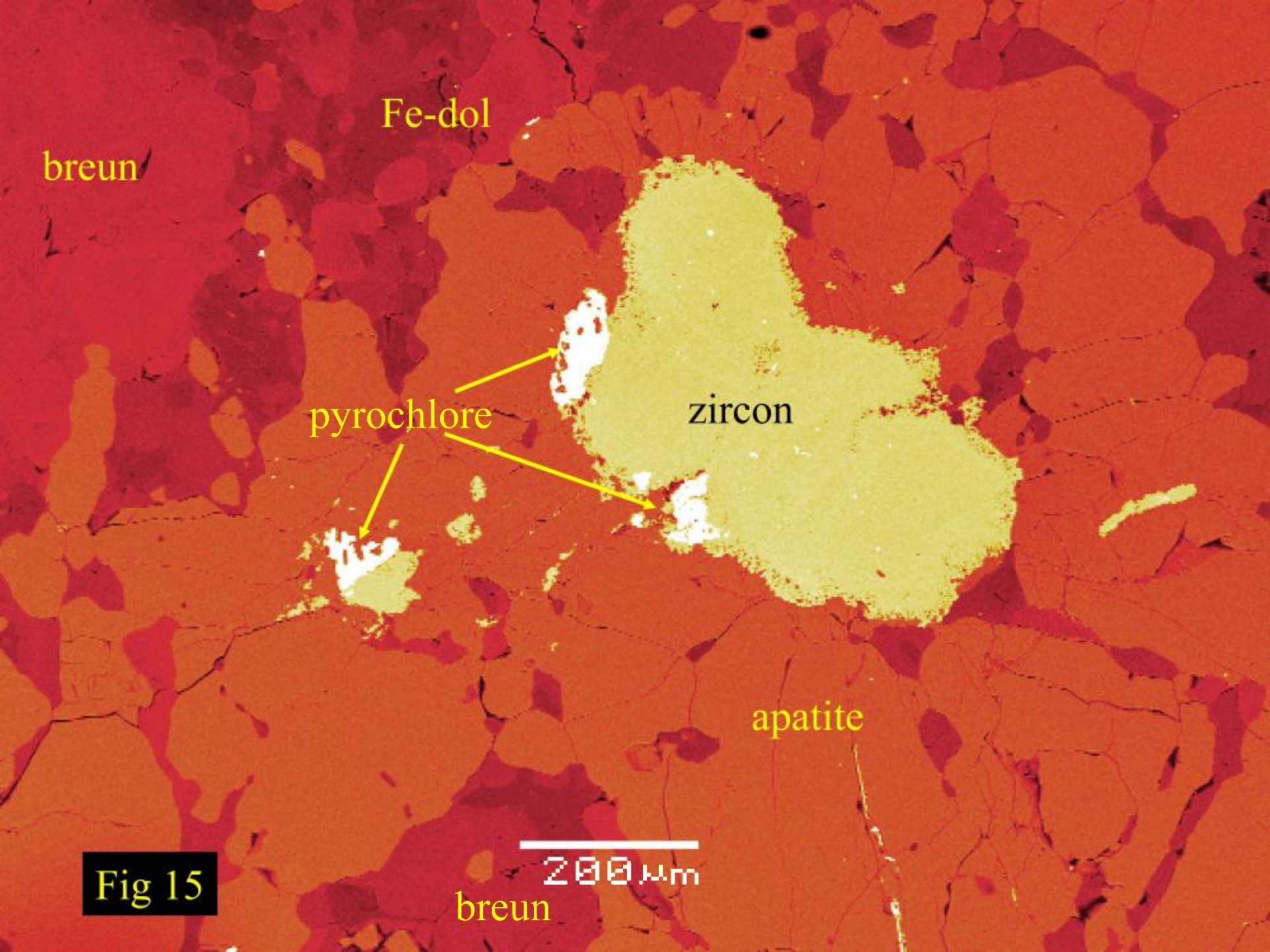

Fig 15

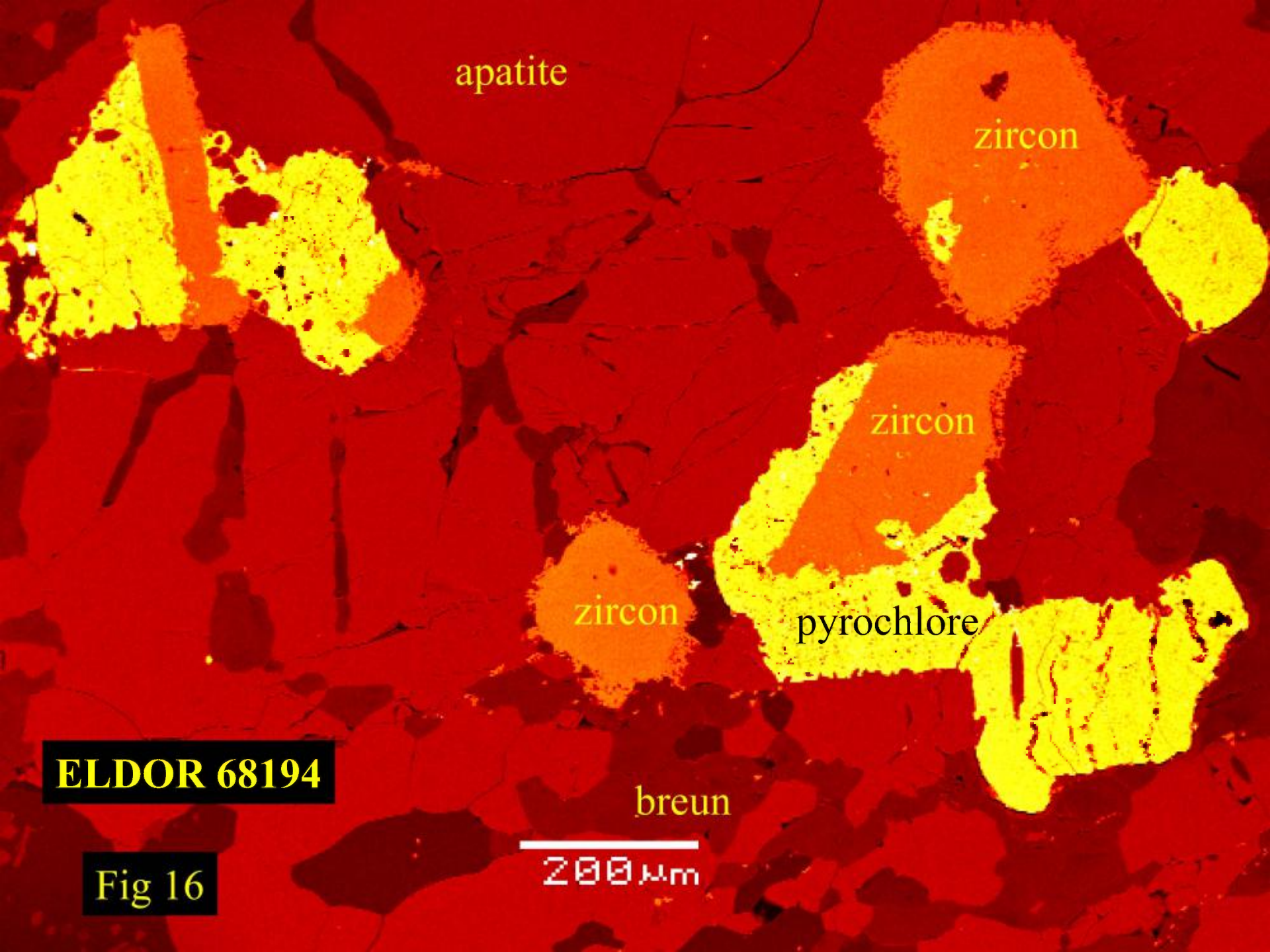

ELDOR 68194

Fig 16

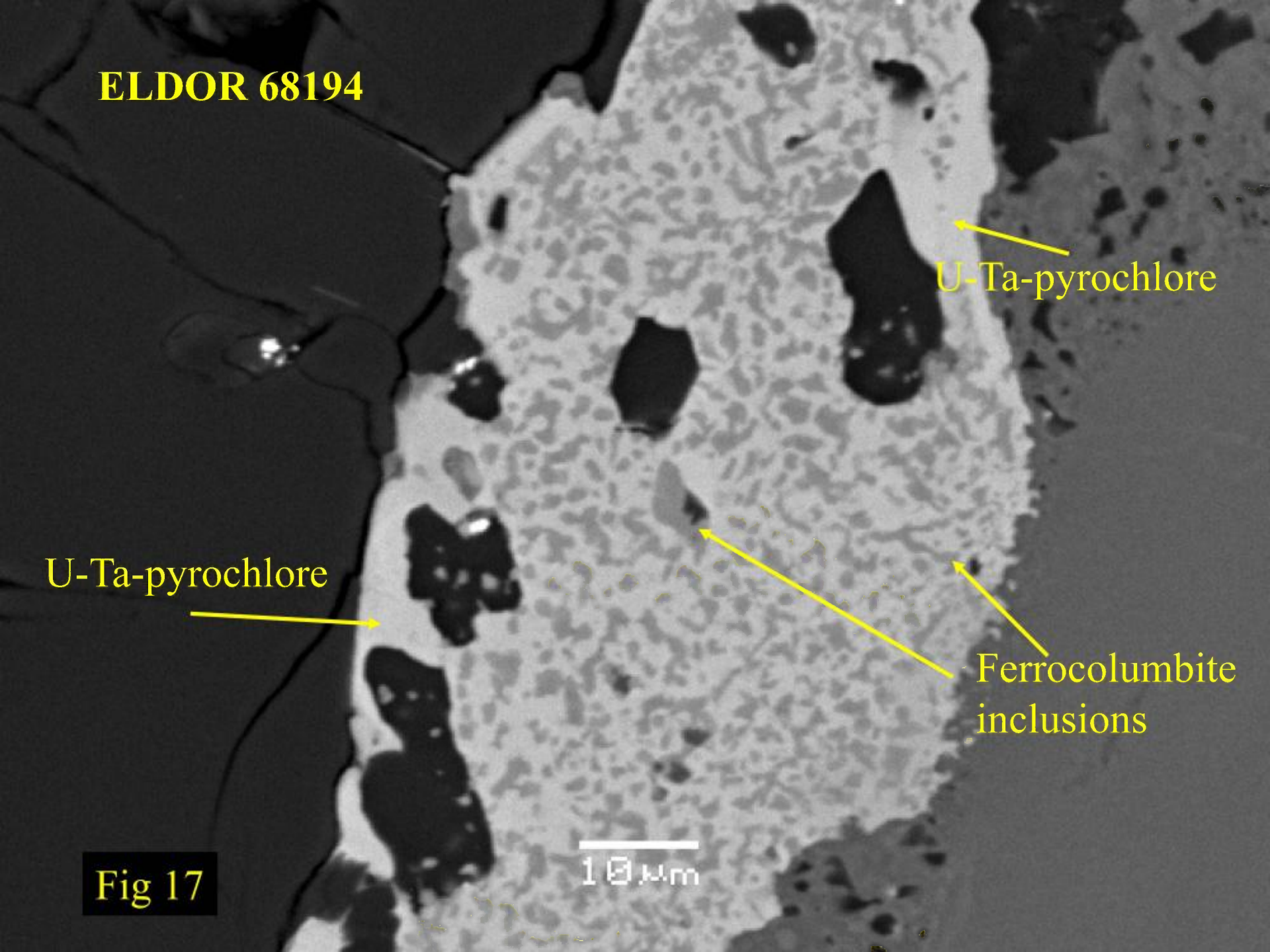
ELDOR 68194
U-Ta-pyrochlore
U-Ta-pyrochlore
Ferrocolumbite inclusions
10 µm

Fig 17

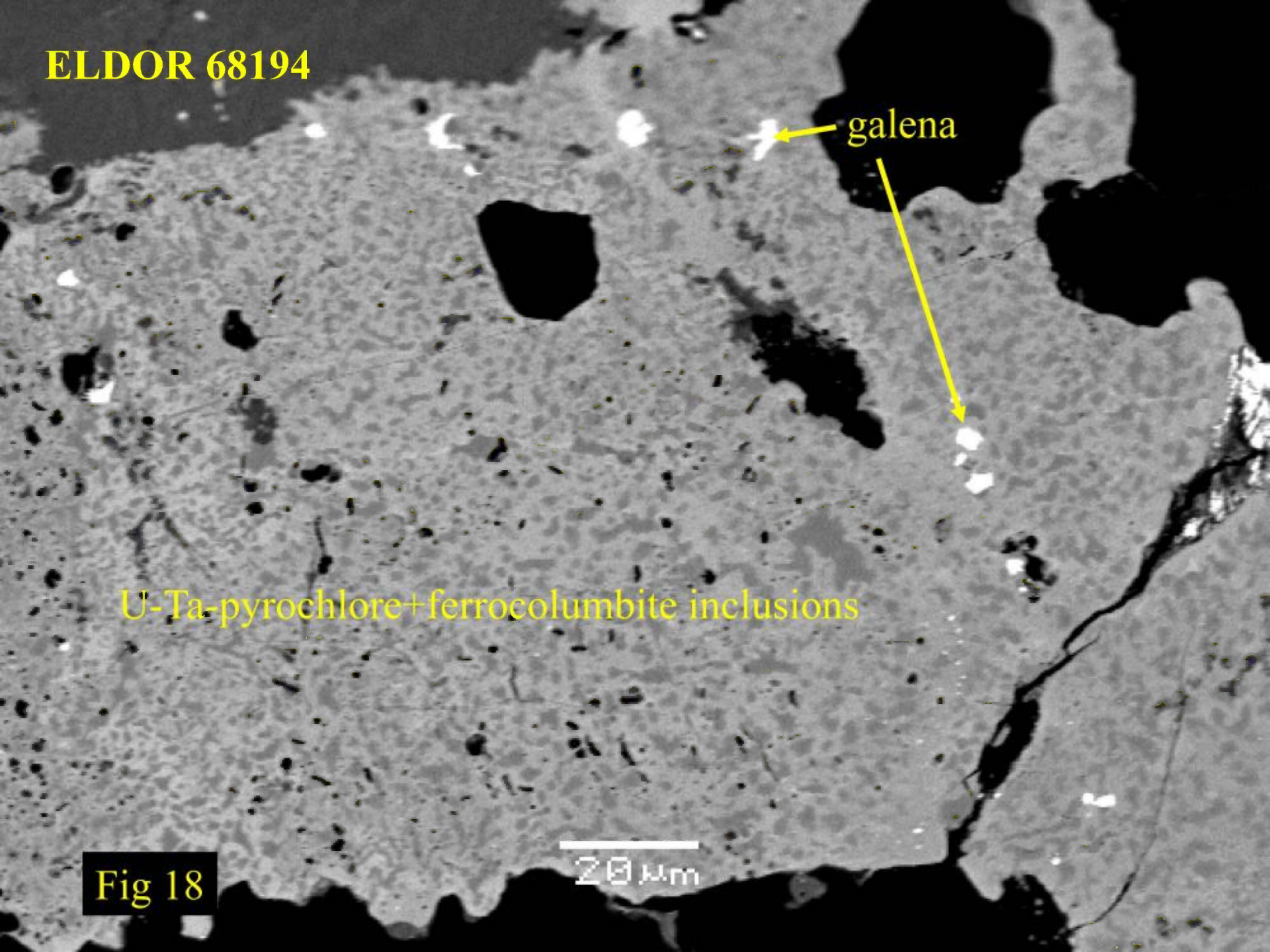
ELDOR 68194
galena
U-Ta-pyrochlore+ferrocolumbite inclusions
20 µm

Fig 18

ELDOR 70059

ELDOR 70059 *Bastnaesite feldspathic breunnerite Fe-dolomite carbonatite*

This complex heterogeneous rock is composed principally of breunnerite and ferroan dolomite with lesser K-feldspar, albite, pyrite and disseminated bastnaesite. Optically the sample is fine grained and leucocratic with bands and clasts of near-opaque material scattered throughout a matrix of interlocking anhedral carbonate crystals (Figs. 1-3). The near-opaque bands poikilitically enclose discrete anhedral carbonate crystals (Fig.3). Rare small (<100 um) laths of chloritized biotite are present. BSE-imagery and X-ray spectrometry show that the near-opaque material in the bands is composed of breunnerite and Fe-oxide/hydroxide pseudomorphs after breunnerite.

Typically, breunnerite is the earliest phase to crystallize and forms aggregates of anhedral crystals (Figs. 8-10). These range in composition from ferroan magnesite to magnesian siderite. Crystals can be relatively unaltered and surrounded by a thin mantle of Fe-rich material (Figs. 8 & 11); considered to be a mixture of Fe-oxides/hydroxides, or completely replaced by the latter material as complex interleaved platelets (Figs. 9 & 10). Breunnerite crystals can be enclosed in a variety of matrices; ranging from pure K-feldspar (Fig. 8-10), through pure albite and/or ferroan dolomite (Figs. 11 & 15) to pyrite (Figs. 16 & 17). Clast-like aggregates of breunnerite and/or breunnerite plus pyrite can be found in the ferroan dolomite matrix (Fig. 11).

ELDOR 70059

The dominant matrix of the rock is ferroan dolomite (6- 12 wt.% FeO) occurring as anhedral interlocking crystals (Figs 1-5). Interstices can be filled with potassium feldspar (Fig.5) and/or albite plus bastnaesite (Fig 12 & 13). The potassium feldspar contains no detectable Ba, Na, or Fe; and the albite lacks K and Ca. Albite commonly encloses residua composed of anhedral small crystals of bastnaesite and monazite (Fig.13). Pyrite is essentially paragenetically associated with breunnerite, and forms poikilitic plates about breunnerite crystals (Fig 16). The pyrite typically has small (<20um) inclusions of galena. Small laths of molybdenite (< 60um) are commonly found along the breunnerite-pyrite grain boundaries (Fig. 17). Rare anhedral plates of (< 100 um) of niobian rutile (5 - 8 wt.% Nb_2O_5) with very small inclusions (<15 um) of Ba-Mg-carbonate can be found interstially to breunnerite (Fig.10).

Rare earth element bearing minerals are represented only by monazite-(Ce) and bastnaesite-(Ce). Pyrochlore, fersmite, aeschynite and apatite are not present. Both monazite and bastnasite form anhedral-to-rounded masses of crystals (up to 250 um) disseminated throughout the ferroan dolomite matrix (Figs 4 & 5); and have evidently formed subsequent to breunnerite crystallization. Barite is commonly found as trace constituents in association with both minerals (Fig.7). Monazite commonly contains small (<50 um) anhedral inclusions of thorite (Figs 6 & 7)..

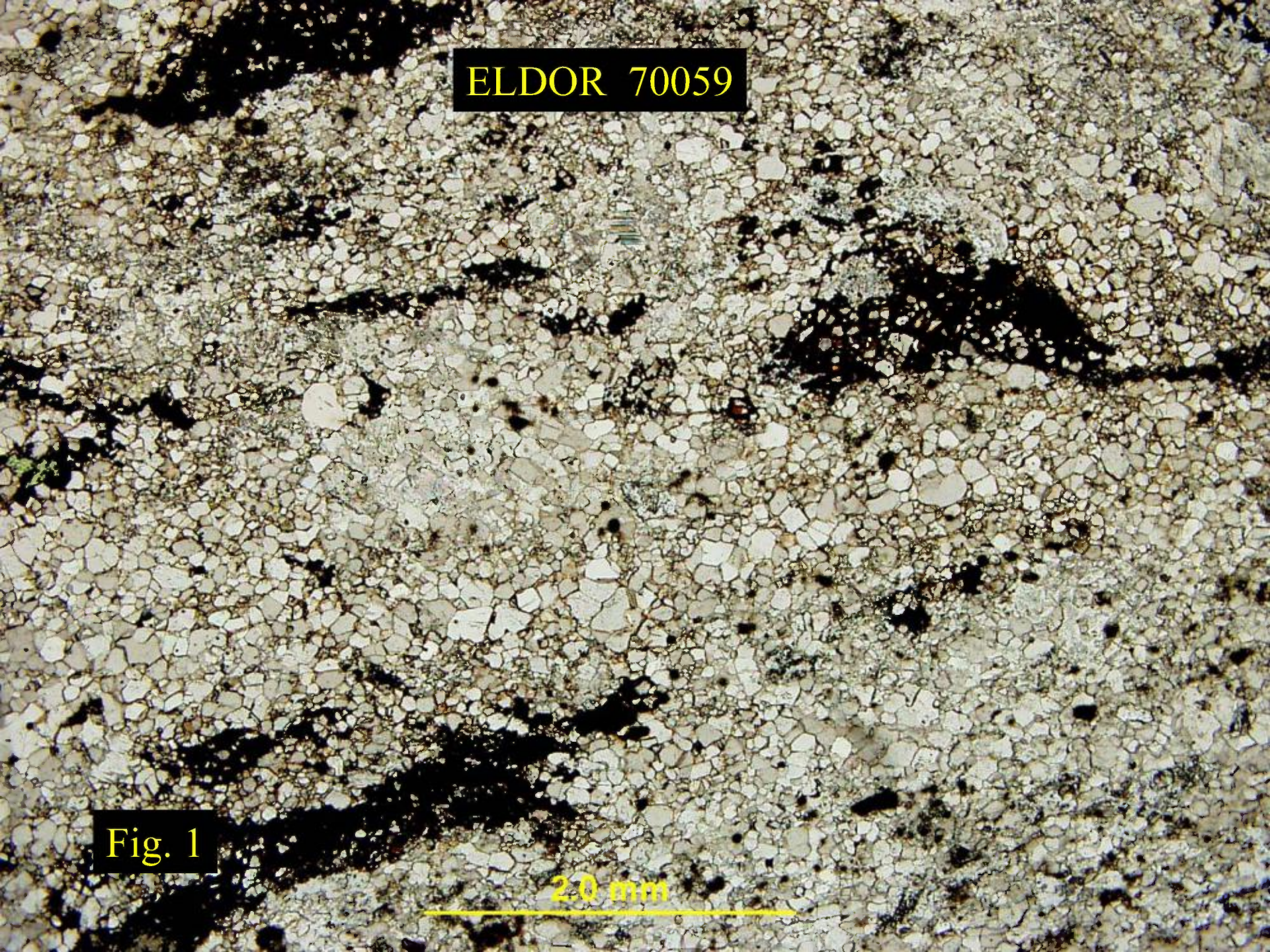

Fig. 1

Fig. 2

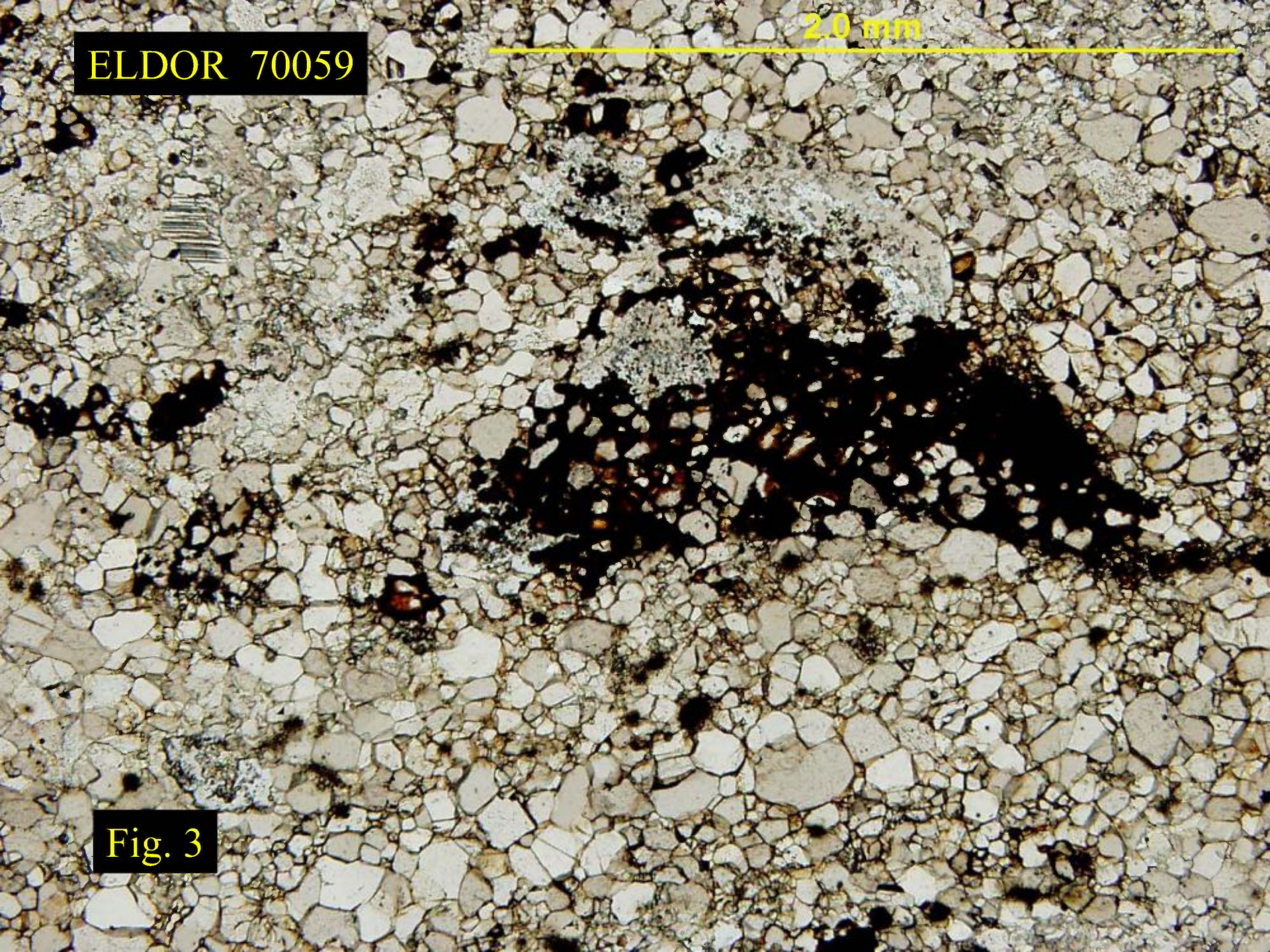

Fig. 3

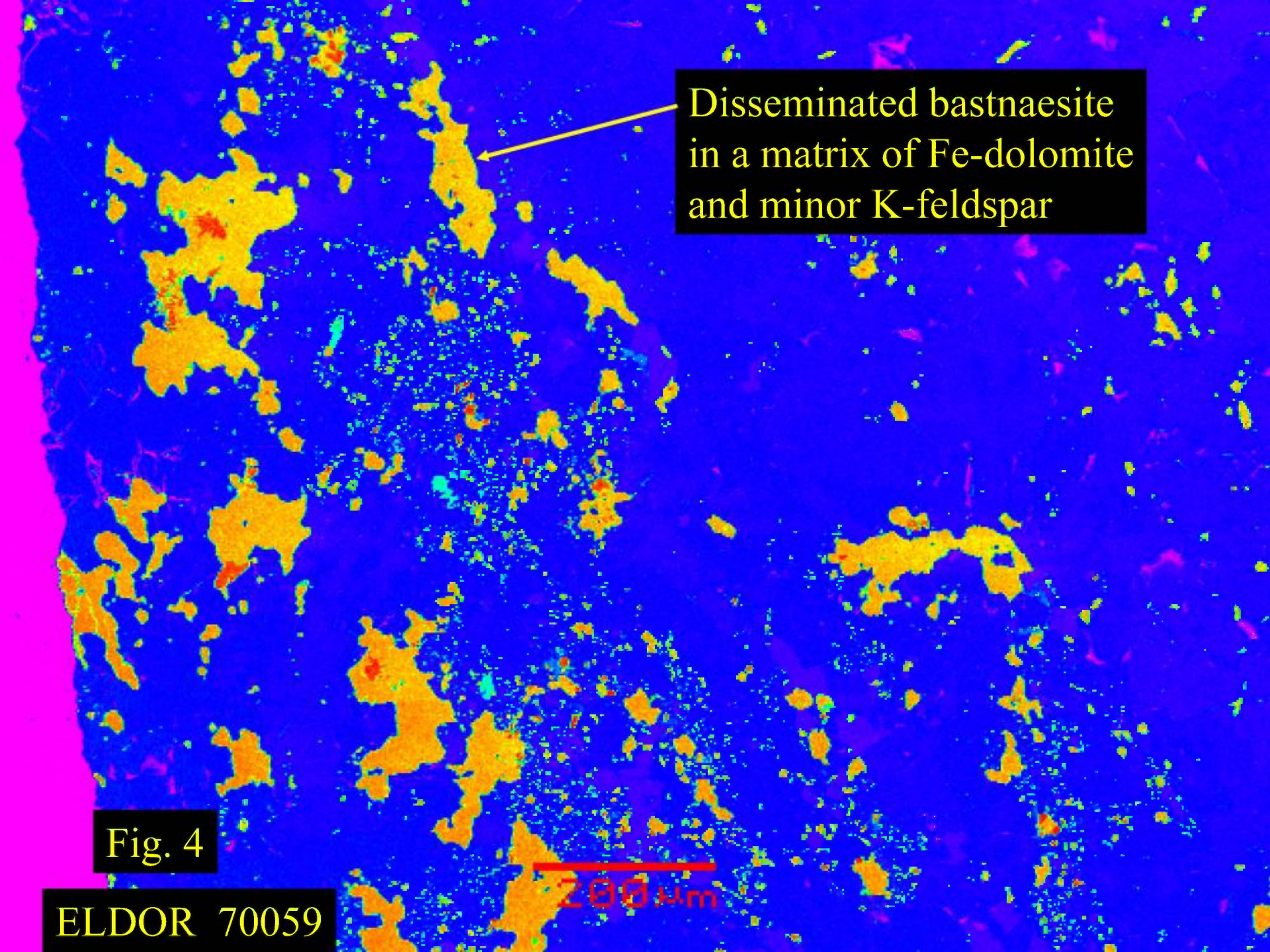

Fig. 4

ELDOR 70059

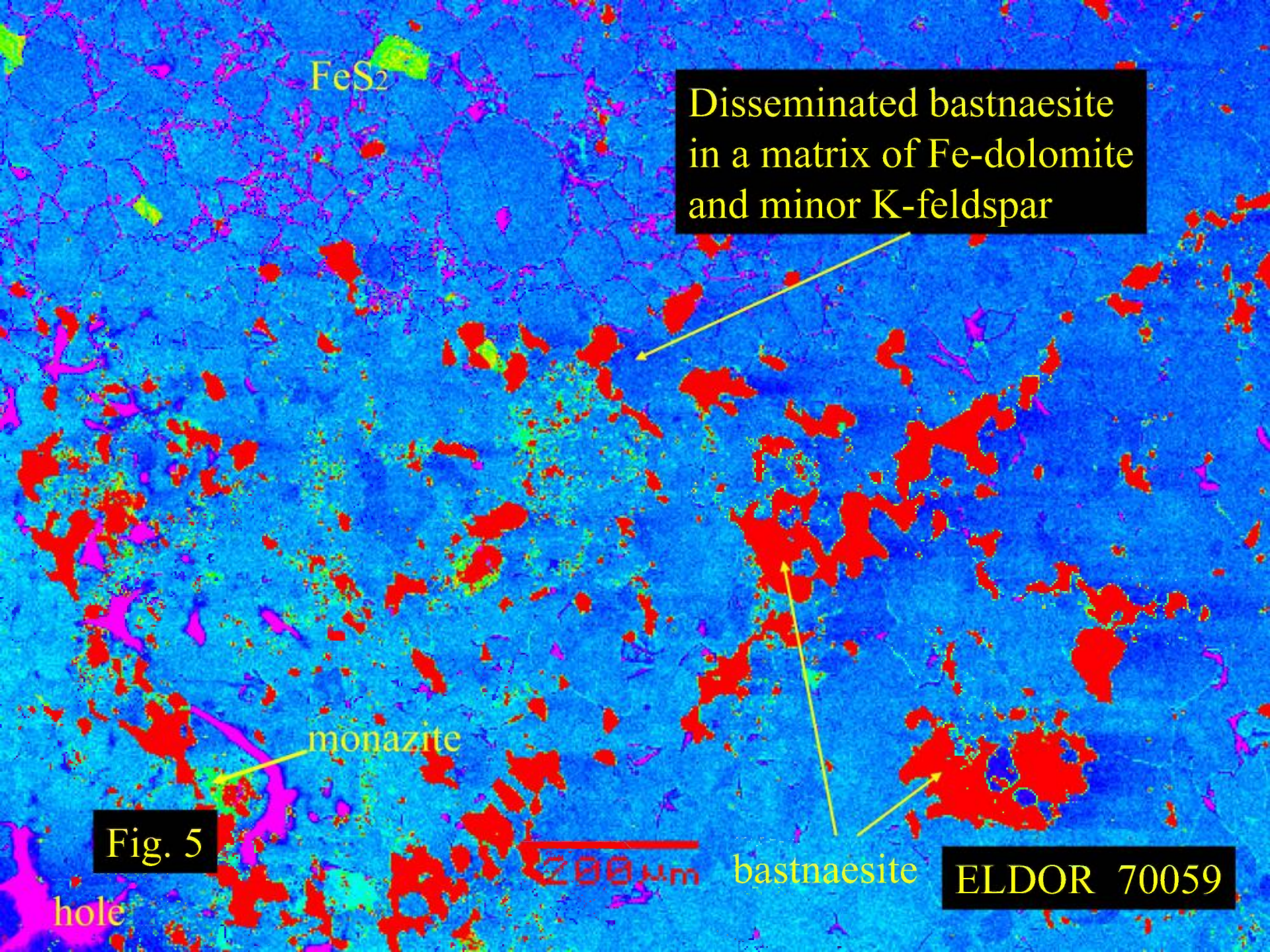
FeS2
Disseminated bastnaesite in a matrix of Fe-dolomite and minor K-feldspar
monazite
200µm
bastnaesite
ELDOR 70059
hole

Fig. 5

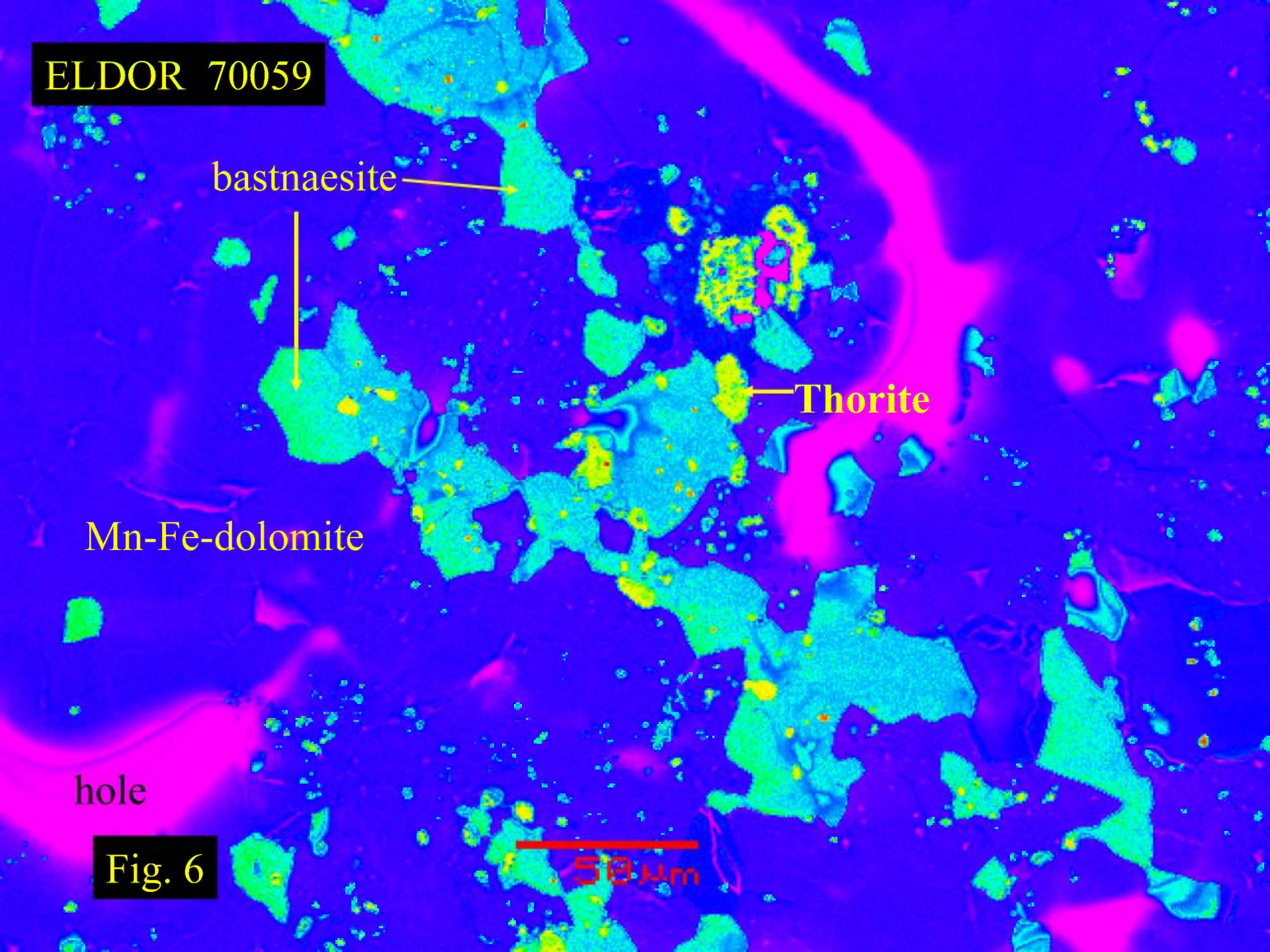

Fig. 6

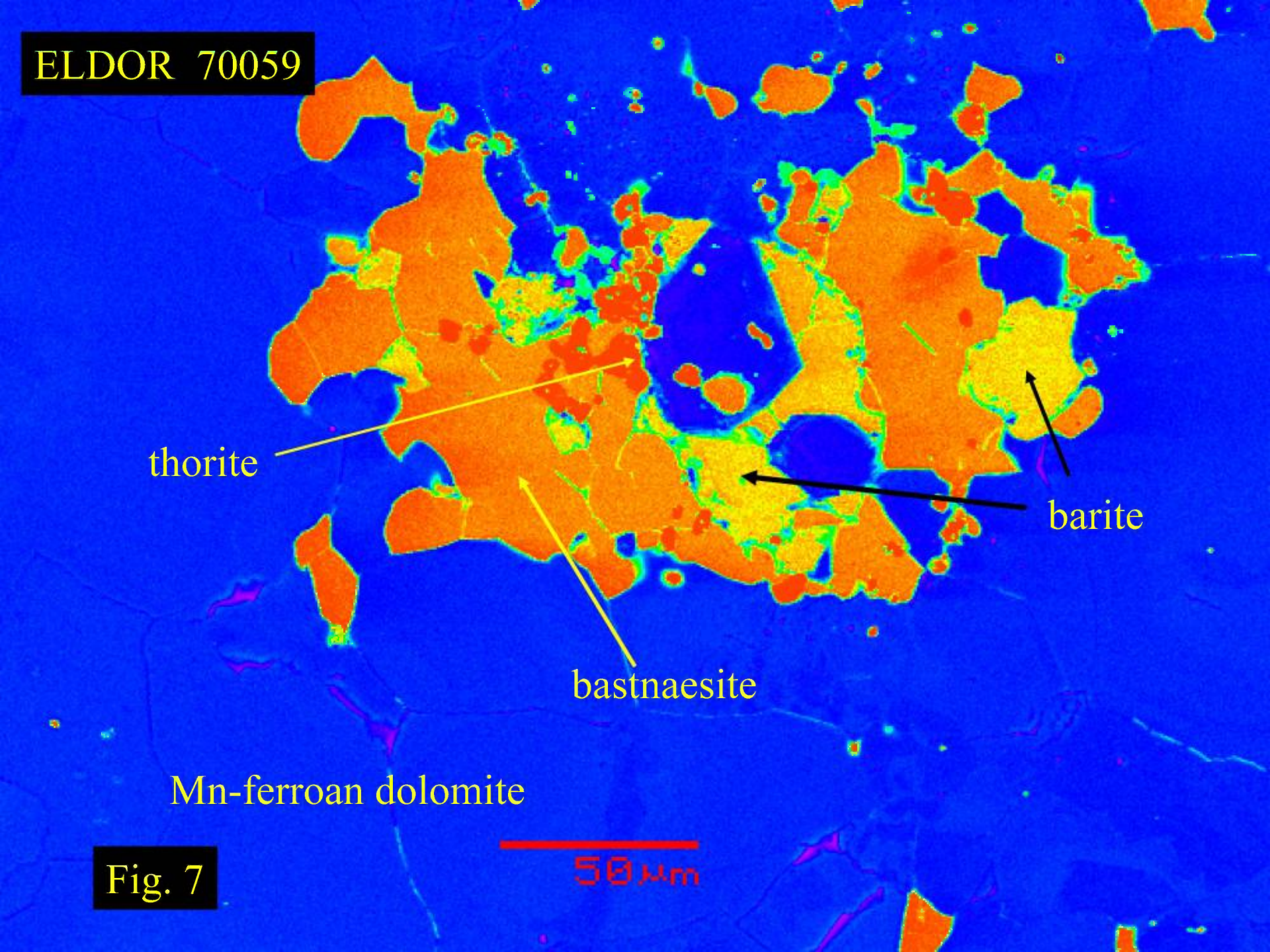
ELDOR 70059
thorite
barite
bastnaesite
Mn-ferroan dolomite
50 µm

Fig. 7

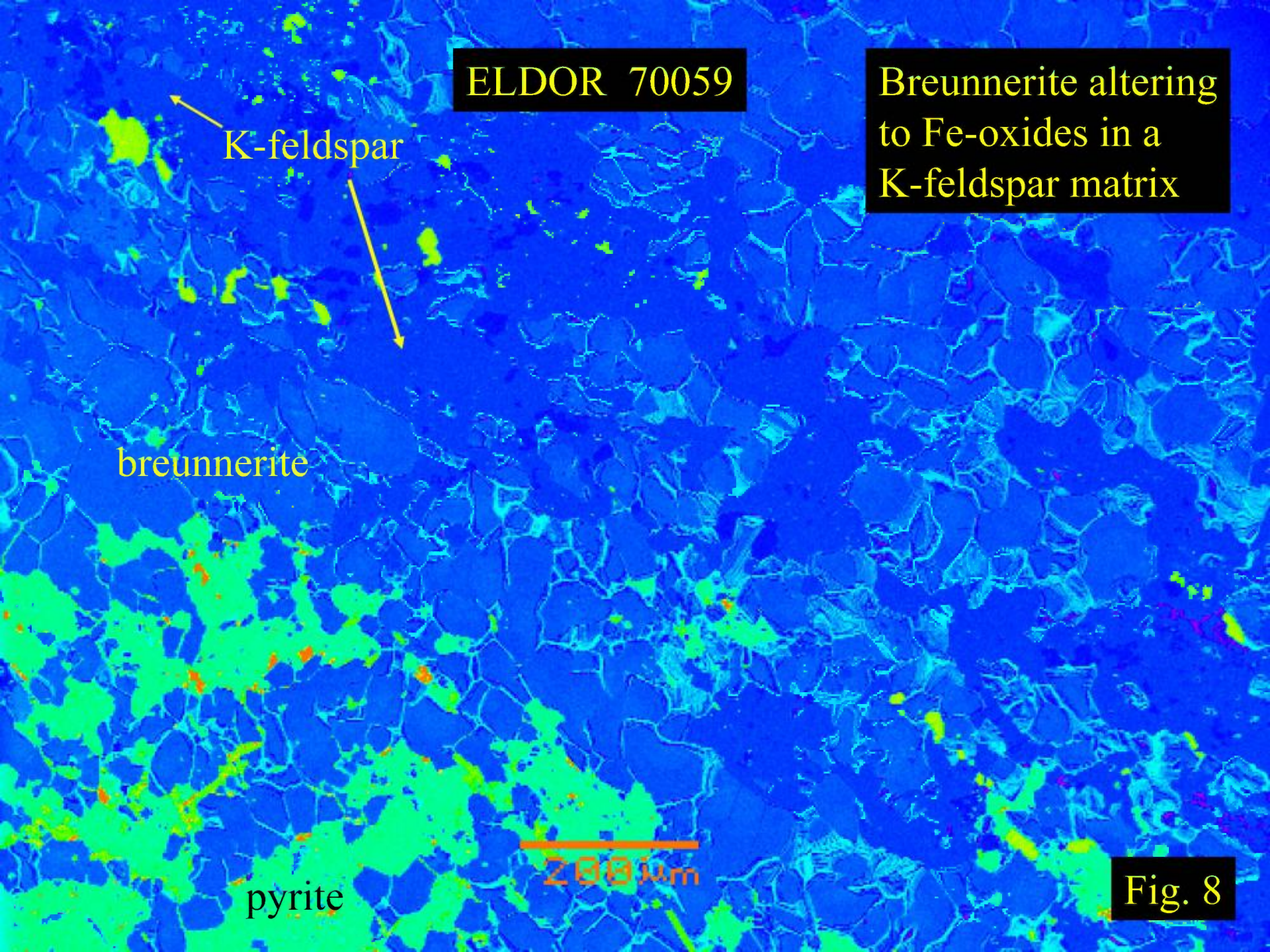
ELDOR 70059
Breunnerite altering to Fe-oxides in a K-feldspar matrix
K-feldspar
breunnerite
pyrite
200µm
Fig. 8

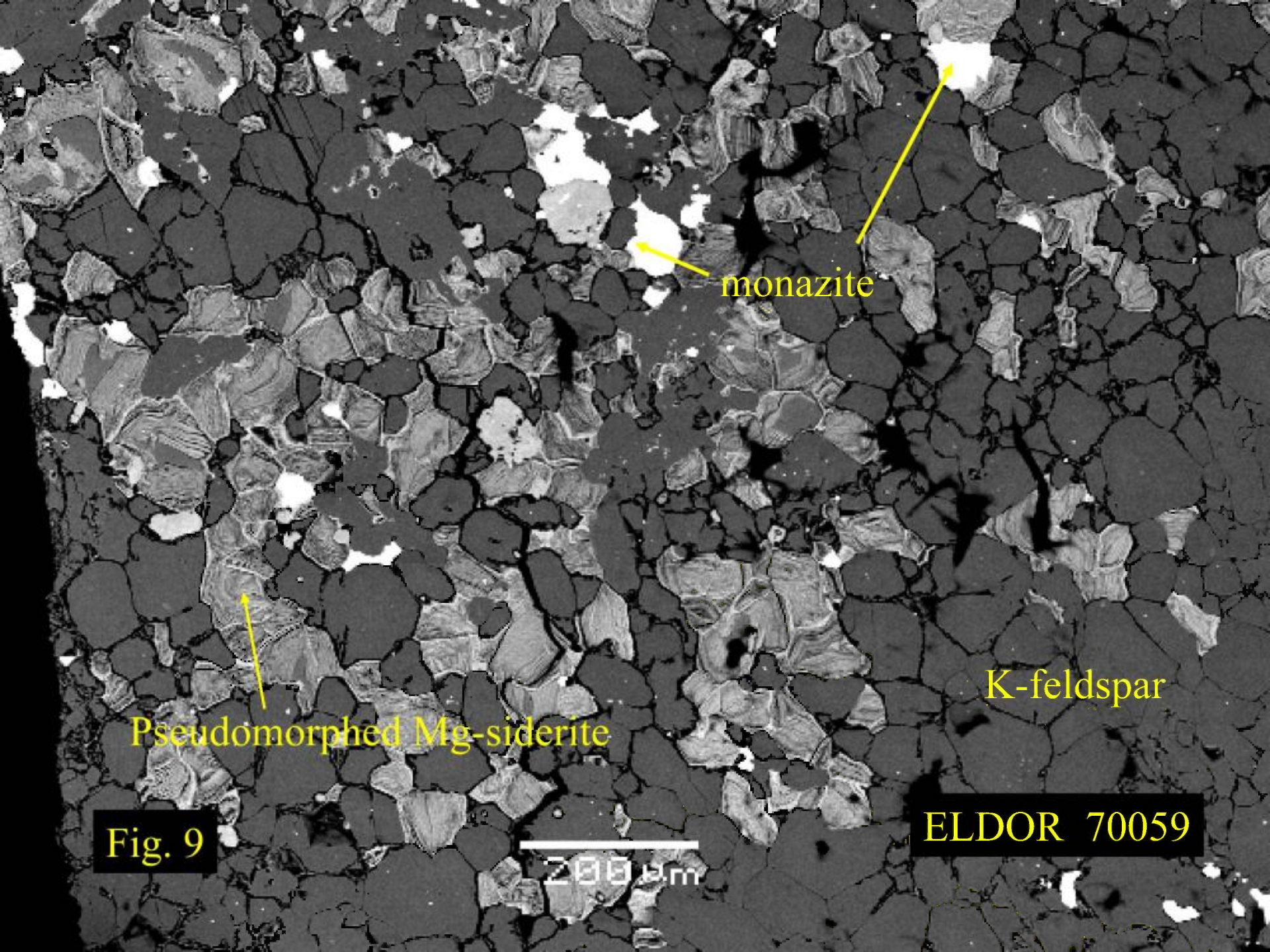
monazite
Pseudomorphed Mg-siderite
K-feldspar
ELDOR 70059
200 µm

Fig. 9

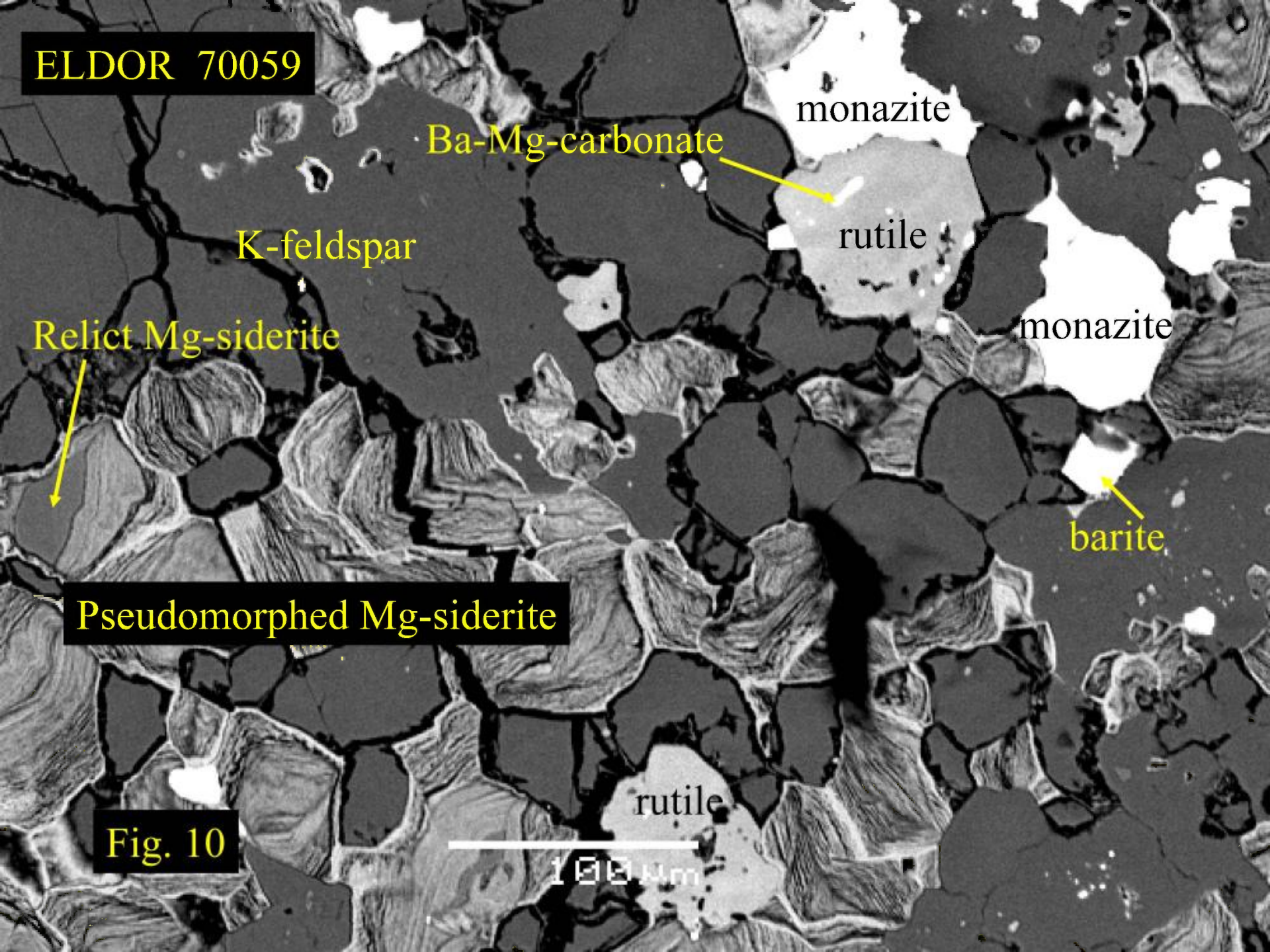
ELDOR 70059
monazite
Ba-Mg-carbonate
rutile
K-feldspar
monazite
Relict Mg-siderite
barite
Pseudomorphed Mg-siderite
rutile
100 µm

Fig. 10

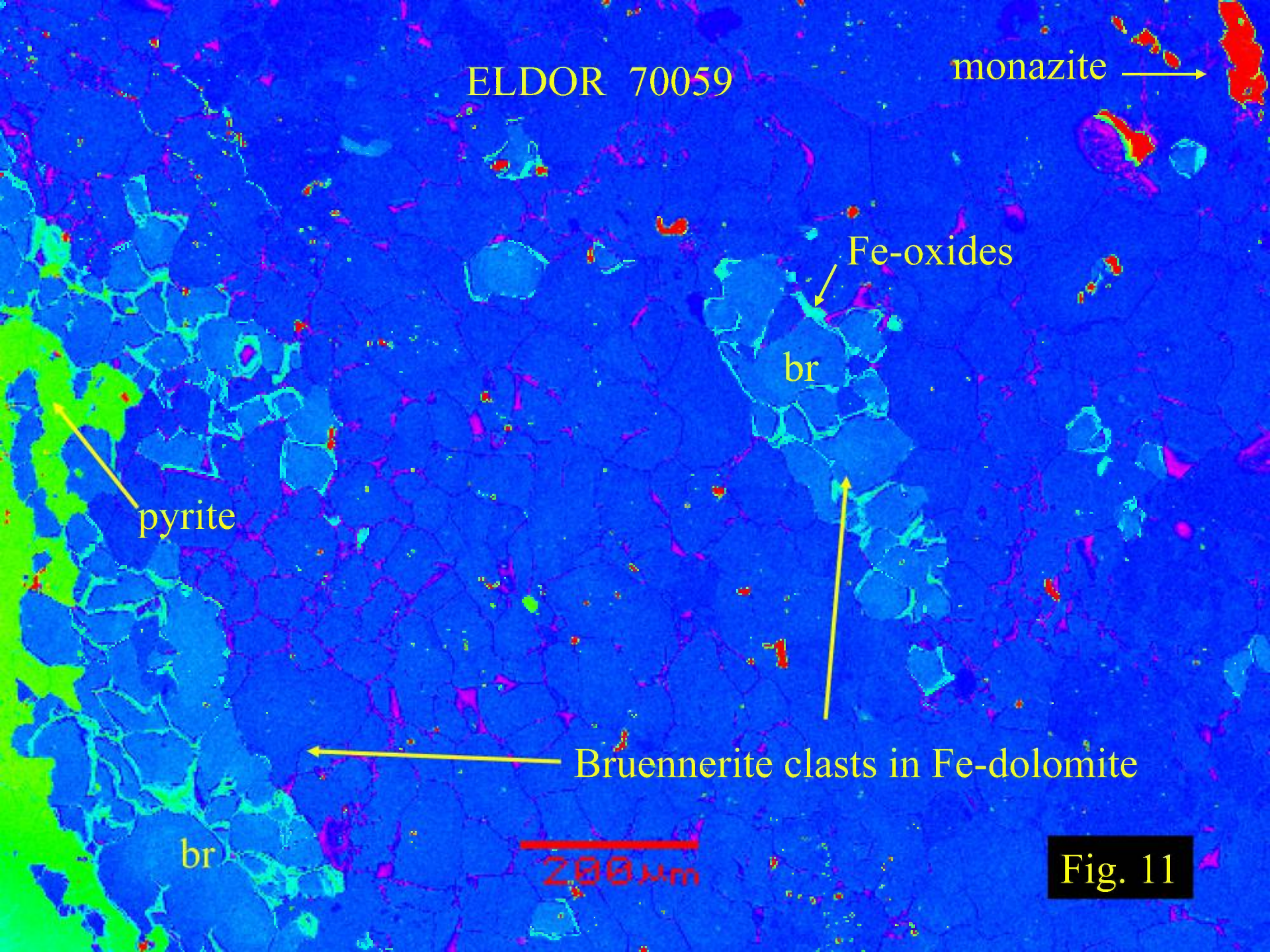
ELDOR 70059
monazite
Fe-oxides
br
pyrite
Bruennerite clasts in Fe-dolomite
br
200µm

Fig. 11

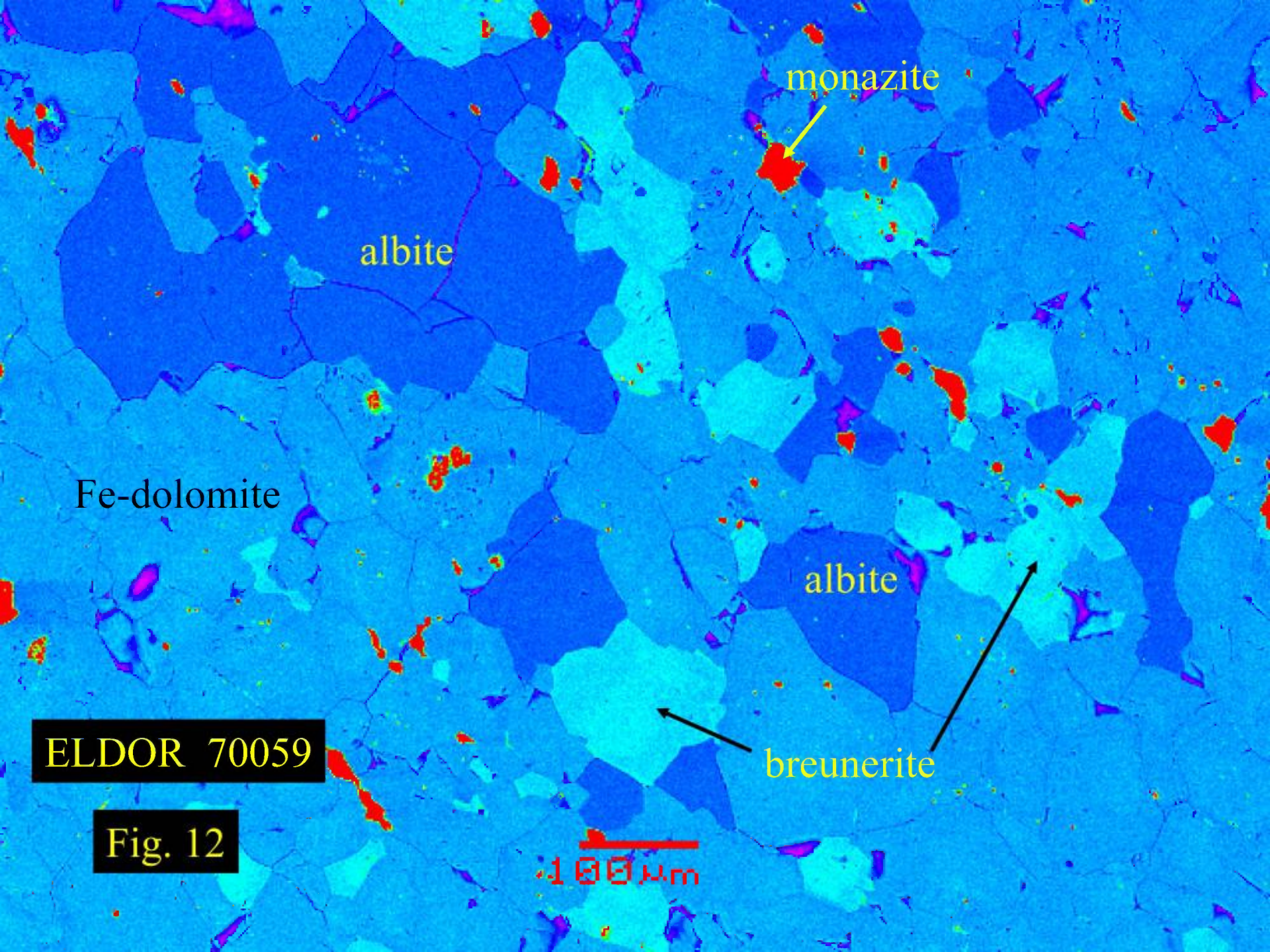

ELDOR 70059

Fig. 12

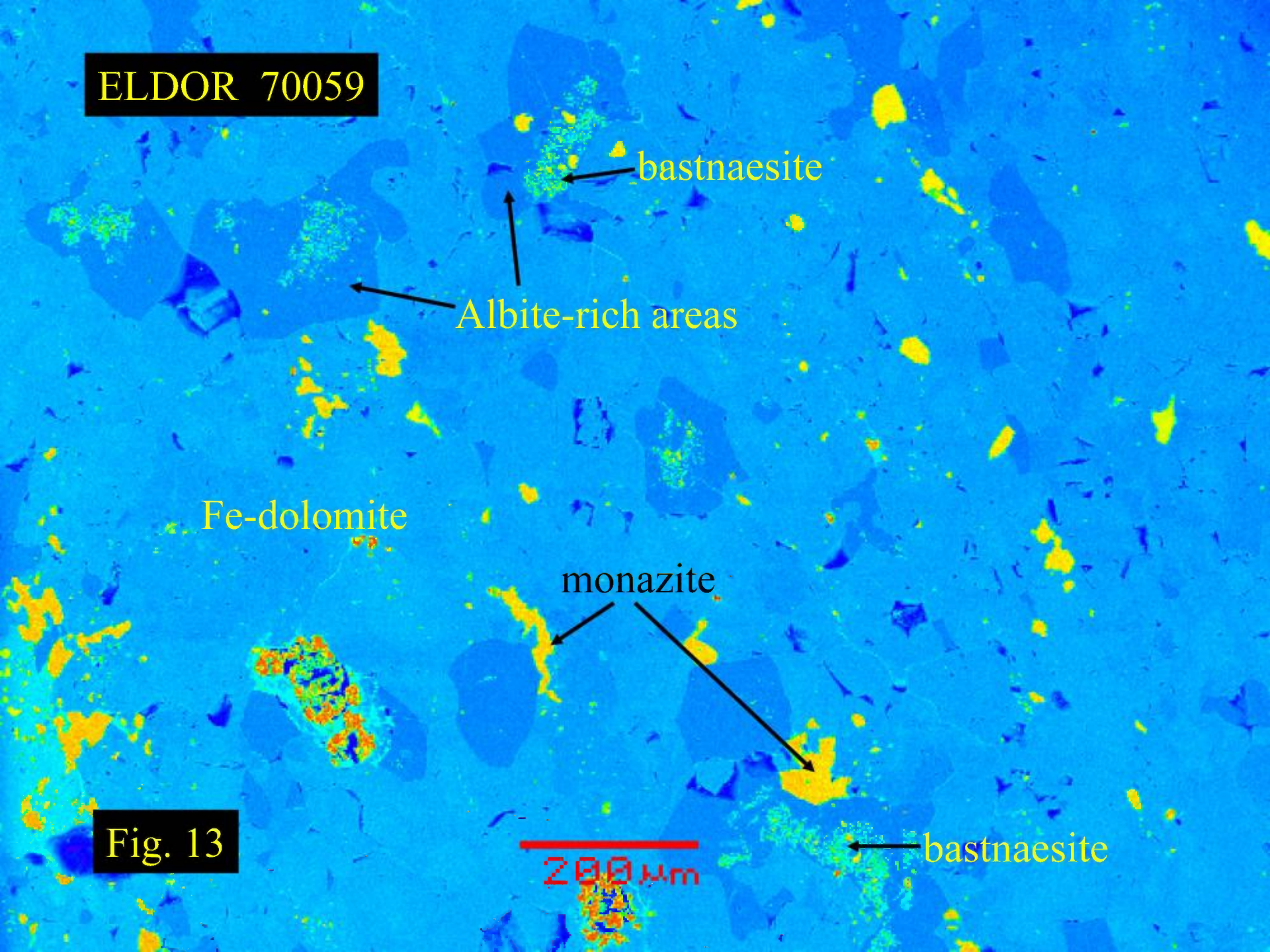
ELDOR 70059
bastnaesite
Albite-rich areas
Fe-dolomite
monazite
bastnaesite
200 µm

Fig. 13

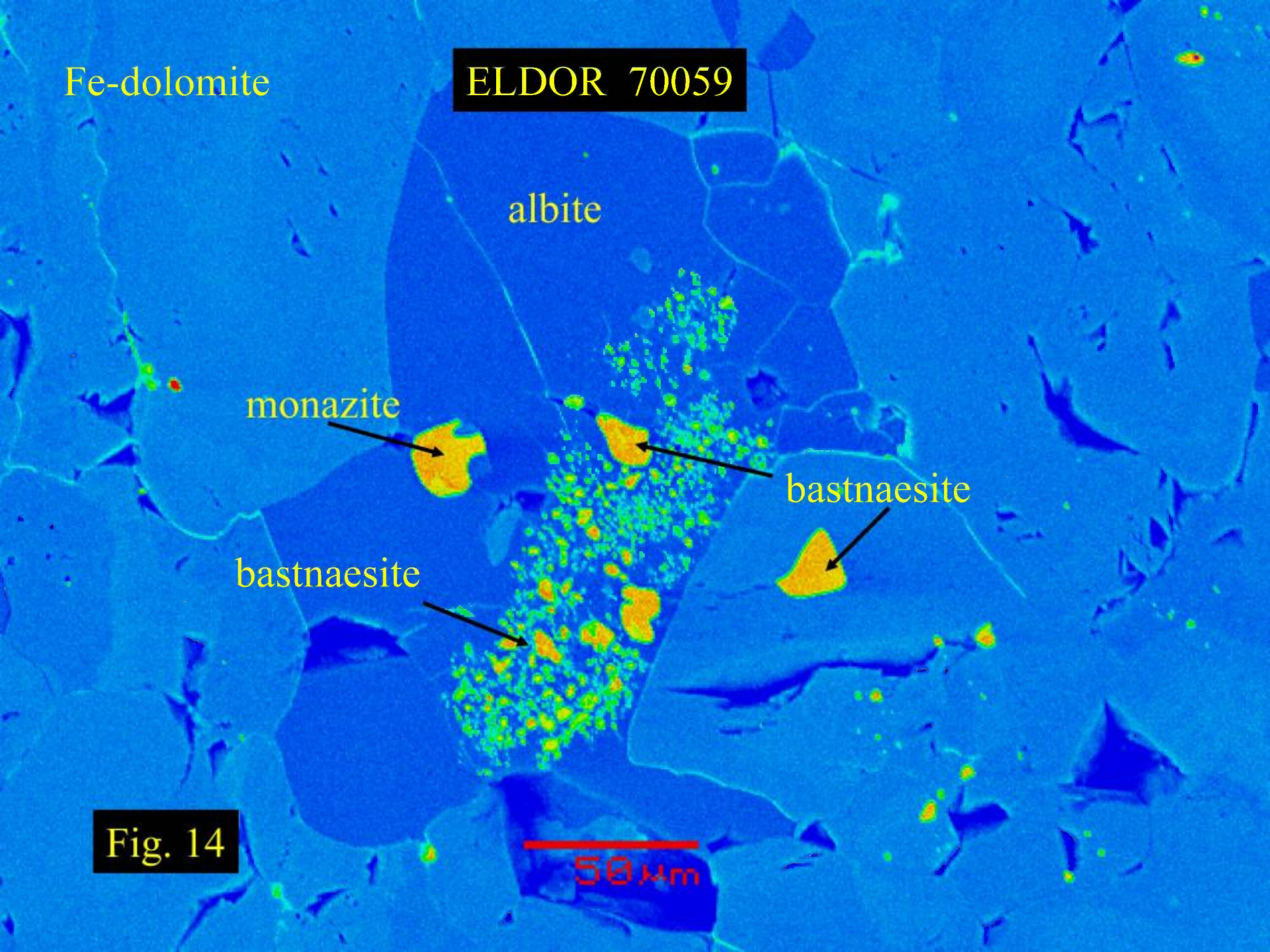
Fe-dolomite
ELDOR 70059
albite
monazite
bastnaesite
bastnaesite
50 µm

Fig. 14

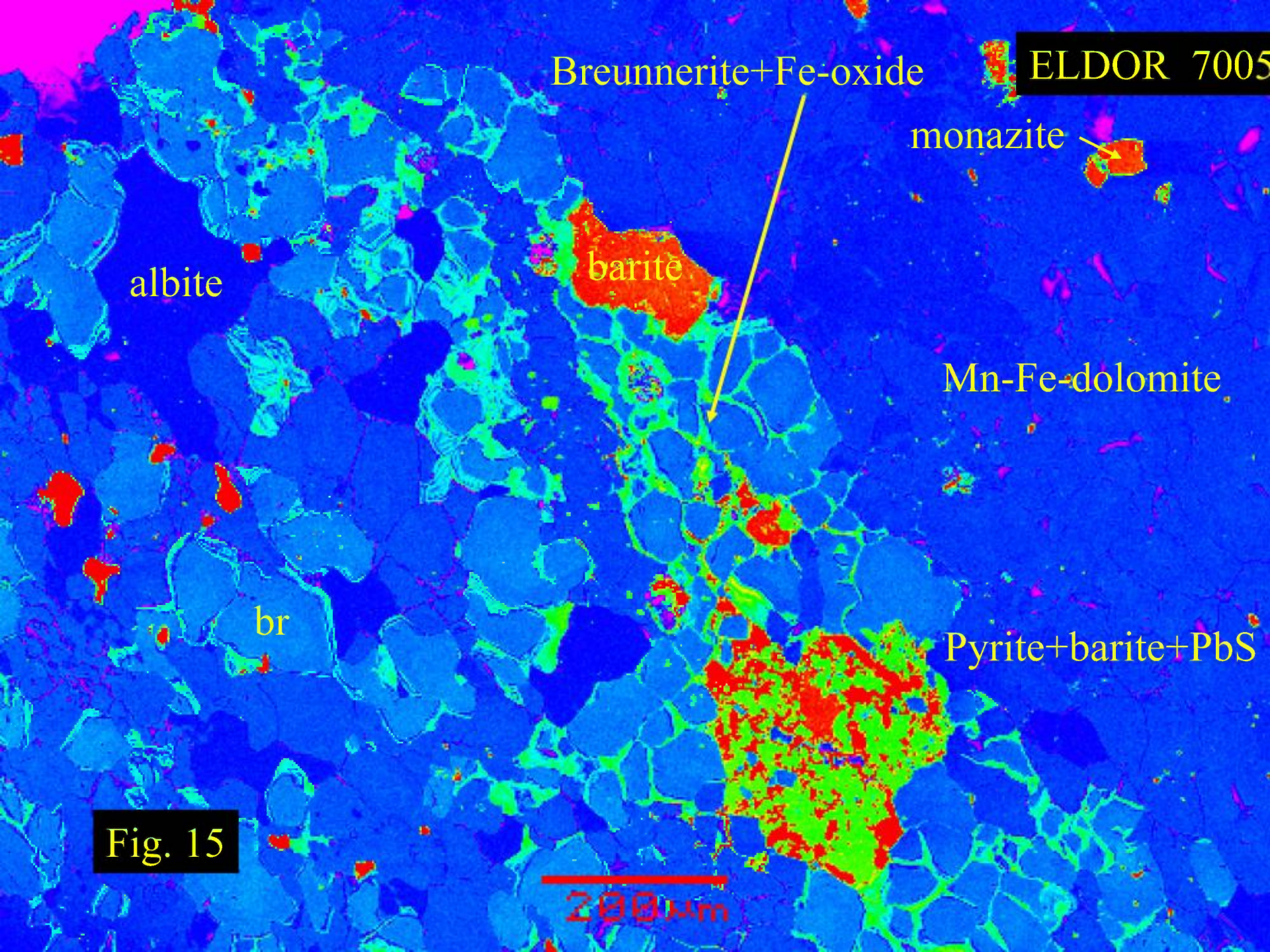
ELDOR 7005
Breunnerite+Fe-oxide
monazite
barite
albite
Mn-Fe-dolomite
br
Pyrite+barite+PbS
200µm

Fig. 15

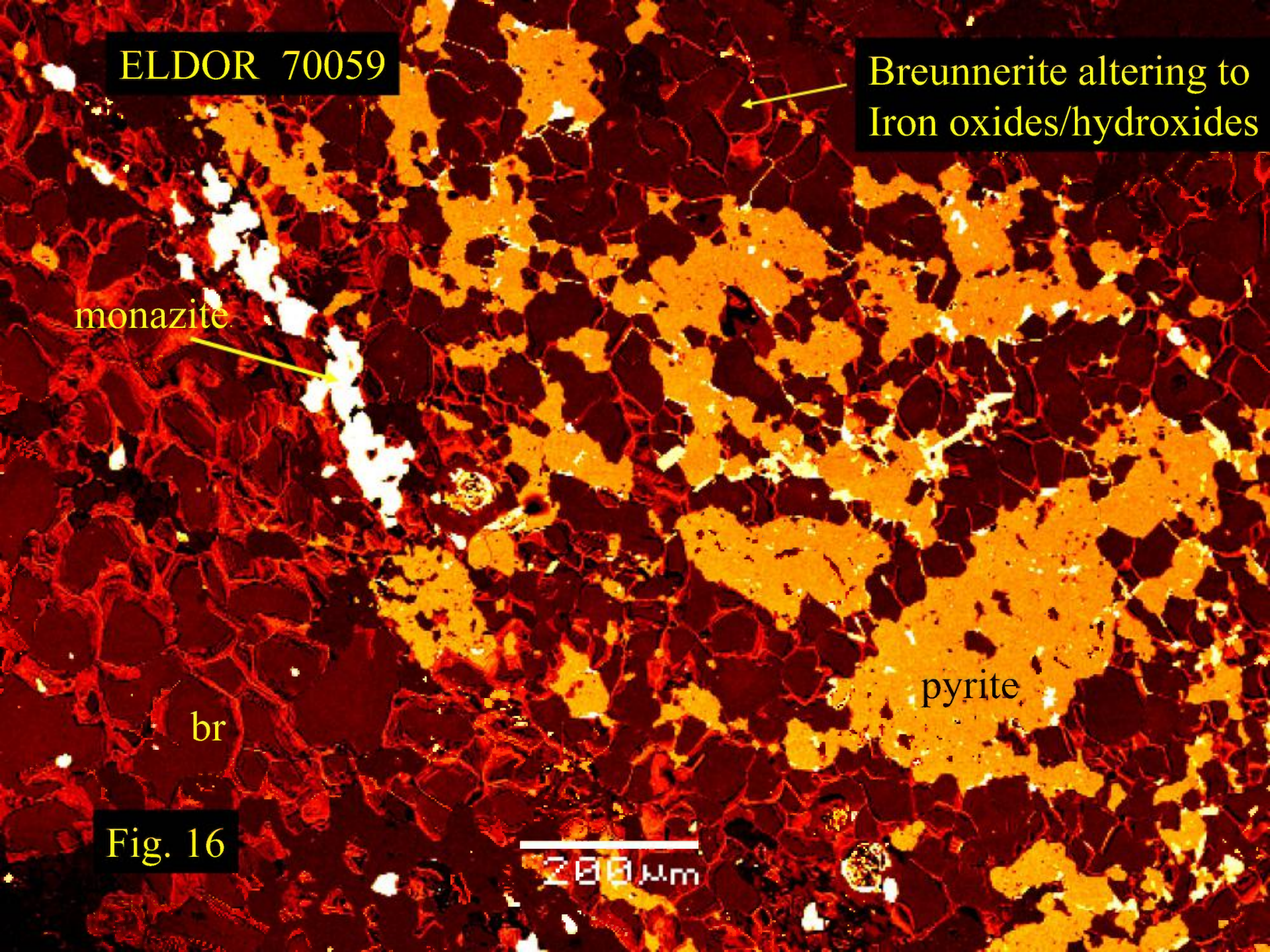
ELDOR 70059
Breunnerite altering to
Iron oxides/hydroxides
monazite
pyrite
br
200µm

Fig. 16

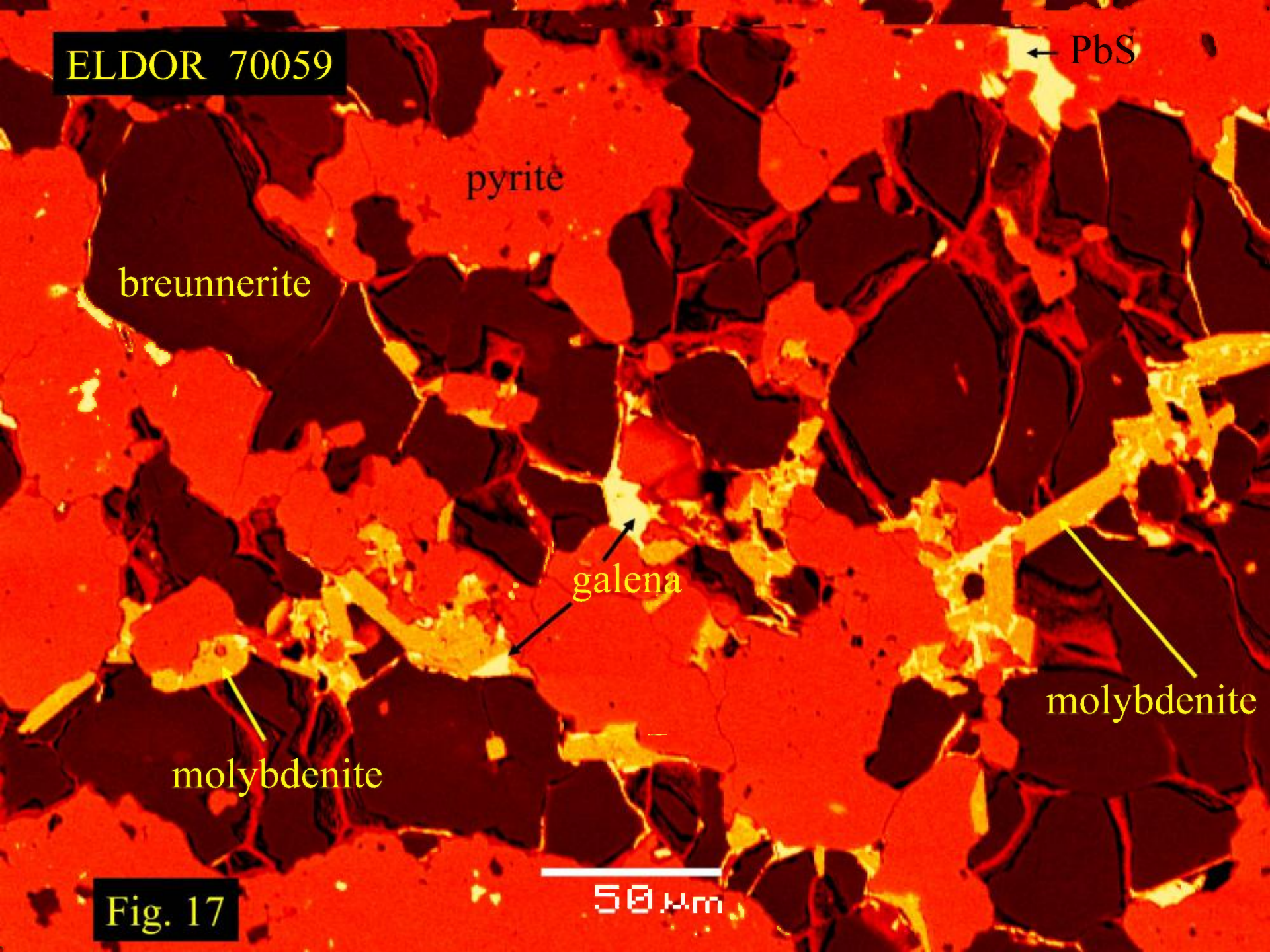
ELDOR 70059
PbS
pyrite
breunnerite
galena
molybdenite
molybdenite
50 µm

Fig. 17

DAHROUGE GEOLOGICAL-X08

teckcominco
Global Discovery Labs

Ref/I.D.: ELDOR CARBON/PRJ#20007
Report Date: 09 JUNE 2008
GDL Job No: V08-0412R

LAB NO	FIELD NUMBER	Nb(P) ppm	Ta(P) ppm	Nb(F) %	Ta(F) %
R0831449	28636	9	<3		
R0831450	28653	6	<3		
R0831451	28654	4	<3		
R0831452	28780	54	<3		
R0831453	29803			0.269	<0.001
R0831454	29811			1.023	0.054
R0831455	29819			0.540	0.054
R0831456	29822			1.542	0.036
R0831457	29905	12	<3		
R0831458	29976			1.757	0.126
R0831459	29982			1.200	<0.001
R0831460	29986			0.039	<0.001
R0831461	29988			0.093	<0.001
R0831462	29990			1.040	0.065
R0831462 rpt				1.023	0.063
R0831463	29992			0.067	<0.001
R0831464	39052			12.885	0.092
R0831465	39054			0.143	<0.001
R0831466	39061			0.451	<0.001
R0831467	39062			0.084	<0.001
R0831468	39375			0.071	<0.001
STD: Mica-Fe		267	30		
STD: OKA-1				0.373	
STD: TAN-1					0.236

I=insufficient sample
If requested analyses are not shown, results are to follow

ANALYTICAL METHODS
- Nb(P) X-Ray fluorescence / pressed pellet
- Ta(P) X-Ray fluorescence / pressed pellet
- Nb(F) X-Ray fluorescence/Fusion
- Ta(F) X-Ray fluorescence/Fusion

Fred Lo

Fred Lo, Chemist - Acme Laboratories

Teck Cominco Ltd.
Global Discovery Labs 1486 East Pender Street Vancouver, B.C. Canada V5L 1V8 Phone: (604) 685-3032 Fax: (604) 844-2686

Quality Analysis ... *Innovative Technologies*

Date Submitted: 15-May-09
Invoice No.: A09-2457
Invoice Date: 23-Jun-09
Your Reference:

Dahrouge Geological Consulting Ltd.
10509-81 Ave.
Suite 18
Edmonton AB T6E 1X7
Canada

ATTN: Darren Smith

CERTIFICATE OF ANALYSIS

20 Crushed Rock samples and 20 Pulp samples were submitted for analysis.

The following analytical packages were requested:

Code 4C (11+) Whole Rock Analysis-XRF
Code 4LITHO-Quant(11+) Major Elements Fusion ICP(WRA)/Trace Elements Fusion ICP/MS(WRA4B2)
Code 5A INAA(INAAGEO)

REPORT **A09-2457**

Notes:
Total includes all elements in % oxide to the left of total.

CERTIFIED BY :

Elitsa Hrischeva, Ph.D.
Quality Control

ACTIVATION LABORATORIES LTD.

1336 Sandhill Drive, Ancaster, Ontario Canada L9G 4V5 TELEPHONE +1.905.648.9611 or +1.888.228.5227 FAX +1.905.648.9613
E-MAIL ancaster@actlabsint.com ACTLABS GROUP WEBSITE http://www.actlabsint.com

Analyte Symbol	Nb	SiO2	Al2O3	Fe2O3(T)	MnO	MgO	CaO	Na2O	K2O	TiO2	P2O5	LOI	Total	Sc	Be	V	Cr	Co	Ni	Cu	Zn	Ga	Ge	As
Unit Symbol	%	%	%	%	%	%	%	%	%	%	%	%	%	ppm	ppm	ppm	ppm	ppm	ppm	ppm	ppm	ppm	ppm	ppm
Detection Limit	0.002	0.01	0.01	0.01	0.001	0.01	0.01	0.01	0.01	0.001	0.01		0.01	1	1	5	20	1	20	10	30	1	1	5
Analysis Method	FUS-XRF	FUS-ICP	FUS-ICP	FUS-ICP	FUS-ICP	FUS-ICP	FUS-ICP	FUS-ICP	FUS-ICP	FUS-ICP	FUS-ICP	FUS-ICP	FUS-ICP	FUS-ICP	FUS-ICP	FUS-ICP	FUS-MS	FUS-MS	FUS-MS	FUS-MS	FUS-MS	FUS-MS	FUS-MS	FUS-MS
67576	0.180	2.22	0.31	2.78	0.242	3.15	48.11	0.09	0.20	0.053	3.29	36.85	97.30	6	3	33	< 20	< 1	< 20	30	< 30	6	1	6
67577	0.104	0.76	0.11	0.78	0.135	1.23	53.78	0.08	0.06	0.104	2.71	39.27	99.02	4	1	9	120	< 1	30	10	< 30	6	1	< 5
67578	0.171	23.97	5.09	6.91	0.328	15.19	20.52	0.16	4.29	0.133	3.03	18.30	97.92	11	9	20	20	16	< 20	20	80	15	2	8
67579	0.211	22.17	7.84	6.78	0.275	15.53	16.96	0.08	5.33	0.974	5.12	16.82	97.87	11	28	93	20	16	40	20	120	22	2	7
67580	0.173	2.80	0.30	4.86	0.308	4.97	45.75	0.07	0.10	0.106	5.15	33.82	98.21	14	2	65	< 20	< 1	< 20	10	70	8	2	7
67581	0.860	32.99	8.99	7.29	0.211	21.60	7.43	0.24	7.62	0.569	1.12	10.79	98.87	5	12	94	30	19	< 20	30	130	18	1	< 5
67582	0.130	1.64	0.19	3.62	0.233	2.58	49.74	0.12	0.12	0.054	4.95	35.48	98.72	12	4	47	20	< 1	< 20	< 10	70	8	2	6
67583	0.027	1.14	0.13	2.99	0.218	2.55	49.91	0.11	0.04	0.021	5.41	36.16	98.68	9	4	32	< 20	< 1	< 20	10	70	9	2	9
67584	0.256	0.85	0.25	3.28	0.209	2.84	49.58	0.11	0.15	0.021	3.68	37.78	98.75	8	13	39	< 20	< 1	< 20	10	40	9	2	6
67585	0.634	8.22	0.40	29.21	0.854	12.45	20.08	0.05	< 0.01	0.592	7.54	15.86	95.26	68	3	364	< 20	10	< 20	10	620	15	3	14
67586	0.105	1.84	0.11	3.20	0.275	2.66	49.49	0.04	0.02	0.061	4.55	35.87	98.12	14	2	35	< 20	< 1	< 20	30	40	9	2	28
67587	0.665	3.84	1.12	6.92	0.421	11.22	30.14	0.16	0.68	0.117	7.10	30.78	92.50	11	21	95	20	8	< 20	20	90	15	3	12
67588	0.256	3.62	0.84	6.61	0.405	11.91	31.95	0.18	0.43	0.660	7.78	29.80	94.17	13	6	334	< 20	29	50	20	70	11	2	11
67589	0.220	2.89	0.90	10.87	0.545	10.40	30.31	0.41	0.14	1.491	7.59	26.29	91.81	24	7	672	< 20	28	40	20	100	11	2	18
67590	1.120	1.22	0.36	4.04	0.302	10.67	36.18	0.22	0.24	0.160	10.86	26.88	91.14	16	170	221	< 20	2	< 20	10	180	21	3	18
67591	0.240	0.67	0.19	4.26	0.302	7.40	48.35	0.08	0.15	0.048	5.11	21.27	87.83	12	96	101	< 20	< 1	< 20	20	120	9	1	9
67592	0.270	4.52	0.39	9.58	0.385	5.89	42.05	0.04	0.02	0.214	6.73	28.78	98.60	34	1	119	< 20	< 1	< 20	20	80	13	3	11
67593	0.191	4.79	0.31	20.63	0.513	7.11	34.59	0.04	0.02	0.376	8.46	21.97	98.82	46	1	190	< 20	19	< 20	10	290	14	3	13
67594	0.607	3.17	0.23	10.89	0.646	11.78	30.42	0.32	0.12	0.162	5.36	31.86	94.97	42	11	114	< 20	3	< 20	40	120	12	2	7
67595	0.290	4.16	0.76	10.88	0.257	9.16	33.74	0.45	0.60	0.163	18.18	20.99	99.34	26	10	84	< 20	17	< 20	10	90	18	2	9
67601	0.195	4.40	0.65	3.73	0.270	4.84	46.12	0.14	0.56	0.062	3.66	34.44	98.89	8	4	40	20	< 1	< 20	30	50	9	2	6
67602	0.082	0.53	0.08	0.85	0.146	1.20	55.06	0.10	0.06	0.001	2.28	40.20	100.5	4	1	8	< 20	< 1	< 20	10	< 30	7	1	< 5
67603	0.108	24.41	5.78	7.07	0.344	16.73	18.92	0.13	5.10	0.145	2.71	17.98	99.32	12	10	23	20	12	< 20	10	150	17	2	< 5
67604	0.149	21.84	7.98	6.95	0.290	16.98	17.14	0.08	5.42	0.911	4.34	18.37	100.3	11	19	93	20	15	50	20	160	24	2	6
67605	0.168	3.11	0.22	4.51	0.297	4.95	46.55	0.04	0.10	0.106	5.59	33.88	99.36	14	2	64	< 20	< 1	< 20	10	50	10	2	9
67606	0.454	34.76	9.77	7.37	0.180	23.19	5.74	0.23	8.32	0.497	0.79	9.37	100.2	4	11	96	30	19	< 20	20	140	18	2	< 5
67607	0.082	2.86	0.23	4.54	0.271	3.66	47.88	0.16	0.19	0.079	4.64	35.16	99.67	19	5	57	< 20	< 1	< 20	< 10	120	9	2	6
67608	0.021	1.16	0.12	2.95	0.256	3.10	49.86	0.13	0.06	0.030	4.83	37.14	99.63	12	5	33	< 20	< 1	< 20	10	70	10	2	8
67609	0.289	1.04	0.23	3.08	0.201	1.71	51.53	0.13	0.08	0.030	3.03	38.16	99.22	8	11	42	< 20	< 1	< 20	10	< 30	9	2	7
67610	0.601	9.31	0.49	23.53	0.943	14.44	20.41	0.06	0.04	0.589	7.62	17.27	94.69	78	3	295	< 20	5	< 20	20	230	16	3	22
67611	0.118	3.20	0.21	4.99	0.306	3.96	46.48	0.06	0.02	0.078	5.39	32.86	97.55	20	3	50	< 20	< 1	< 20	20	90	10	2	10
67612	0.728	3.42	1.03	7.53	0.473	12.02	31.91	0.20	0.61	0.081	7.77	31.87	96.91	14	26	89	< 20	10	< 20	10	80	17	3	12
67613	0.233	2.76	0.81	5.47	0.447	12.69	32.01	0.20	0.37	0.729	6.92	31.29	93.69	15	6	347	< 20	18	40	30	< 30	10	2	21
67614	0.213	3.56	1.16	10.54	0.546	10.19	29.28	0.54	0.23	1.856	7.91	27.84	93.65	25	10	705	< 20	24	40	30	90	11	2	27
67615	0.921	1.06	0.33	4.18	0.350	12.21	36.63	0.20	0.24	0.195	10.57	29.36	95.32	18	151	219	< 20	1	< 20	20	120	20	3	16
67616	0.280	0.84	0.18	4.65	0.317	7.70	48.24	0.08	0.10	0.074	5.74	21.63	89.56	13	113	109	< 20	< 1	< 20	20	40	10	2	16
67617	0.240	7.52	0.55	11.88	0.407	8.78	35.21	0.06	0.04	0.252	6.77	24.39	95.86	45	2	157	< 20	< 1	< 20	20	40	15	3	13
67618	0.188	10.34	0.55	17.58	0.518	12.07	29.40	0.06	< 0.01	0.324	7.87	20.49	99.19	74	2	166	< 20	3	< 20	10	250	16	3	13
67619	0.689	5.47	0.30	12.28	0.623	11.51	30.74	0.54	0.20	0.214	6.03	29.07	96.97	54	20	147	< 20	5	< 20	50	160	15	3	8
67620	0.281	8.11	1.42	13.88	0.279	9.56	27.40	0.84	1.08	0.257	12.57	22.35	97.74	35	23	141	20	24	50	30	< 30	24	2	32

Analyte Symbol	Rb	Sr	Y	Zr	Mo	Ag	In	Sn	Sb	Cs	Ba	La	Bi	Ce	Pr	Nd	Sm	Eu	Gd	Tb	Dy	Ho	Er	Tm
Unit Symbol	ppm	ppm	ppm	ppm	ppm	ppm	ppm	ppm	ppm	ppm	ppm	ppm	ppm	ppm	ppm	ppm	ppm	ppm	ppm	ppm	ppm	ppm	ppm	ppm
Detection Limit	2	2	2	4	2	0.5	0.2	1	0.5	0.5	3	0.1	0.4	0.1	0.05	0.1	0.1	0.05	0.1	0.1	0.1	0.1	0.1	0.05
Analysis Method	FUS-MS	FUS-ICP	FUS-ICP	FUS-ICP	FUS-MS	FUS-MS	FUS-MS	FUS-MS	FUS-MS	FUS-MS	FUS-ICP	FUS-MS	FUS-MS	FUS-MS	FUS-MS	FUS-MS	FUS-MS	FUS-MS	FUS-MS	FUS-MS	FUS-MS	FUS-MS	FUS-MS	FUS-MS
67576	8	4891	85	98	30	< 0.5	< 0.2	< 1	< 0.5	< 0.5	501	358	< 0.4	634	77.5	308	47.7	13.3	33.7	4.3	19.6	3.1	8.4	1.09
67577	< 2	5723	86	90	17	< 0.5	< 0.2	< 1	0.6	< 0.5	622	346	< 0.4	612	78.3	319	50.5	14.1	35.7	4.3	19.9	3.2	8.6	1.01
67578	133	1485	32	303	2	< 0.5	< 0.2	< 1	1.0	4.0	824	154	< 0.4	354	37.9	156	24.6	6.70	15.9	1.9	8.2	1.3	3.2	0.38
67579	153	1071	78	160	4	< 0.5	< 0.2	1	1.1	3.7	1238	414	< 0.4	855	107	422	63.6	17.8	43.2	4.8	20.3	3.0	7.7	0.87
67580	3	5161	120	257	22	< 0.5	< 0.2	< 1	0.8	< 0.5	318	377	< 0.4	711	92.6	383	62.4	17.9	45.5	5.7	26.6	4.3	11.6	1.39
67581	179	722	20	62	< 2	< 0.5	< 0.2	2	1.3	5.2	1421	84.1	< 0.4	236	22.8	88.6	14.1	4.03	8.6	1.1	4.5	0.7	1.8	0.22
67582	3	5271	85	174	< 2	< 0.5	< 0.2	< 1	1.1	< 0.5	461	395	< 0.4	721	92.9	391	61.2	16.4	43.0	4.8	21.2	3.3	8.5	0.96
67583	< 2	4842	141	62	4	< 0.5	< 0.2	< 1	1.4	< 0.5	526	477	< 0.4	801	104	427	69.7	19.8	54.3	7.2	32.8	5.2	13.2	1.50
67584	3	5454	85	153	< 2	< 0.5	< 0.2	< 1	0.6	< 0.5	677	420	< 0.4	802	97.5	392	61.3	16.7	41.9	4.8	20.9	3.3	8.7	0.99
67585	< 2	2768	55	672	5	< 0.5	0.6	12	1.5	< 0.5	2660	316	< 0.4	757	91.0	374	58.6	15.3	36.6	4.0	16.3	2.3	5.6	0.63
67586	< 2	5089	71	227	< 2	0.6	< 0.2	< 1	3.9	< 0.5	618	385	< 0.4	705	91.2	378	59.2	15.4	40.6	4.4	18.8	2.8	7.1	0.83
67587	18	1844	126	195	54	< 0.5	< 0.2	< 1	0.7	< 0.5	167	588	< 0.4	1270	154	619	93.6	25.7	64.3	7.3	31.8	4.9	13.1	1.55
67588	8	1358	137	591	5	< 0.5	< 0.2	< 1	1.0	< 0.5	140	408	< 0.4	805	103	420	69.4	19.4	51.2	6.7	31.3	5.2	14.3	1.85
67589	3	1729	58	89	< 2	< 0.5	0.3	1	0.9	< 0.5	152	368	< 0.4	719	95.5	389	57.9	14.6	37.6	3.8	15.9	2.3	6.1	0.73
67590	4	1752	149	369	3	< 0.5	< 0.2	< 1	0.7	< 0.5	142	808	< 0.4	1890	215	830	124	33.8	84.3	9.6	40.9	6.0	15.0	1.73
67591	< 2	1720	147	145	6	< 0.5	< 0.2	< 1	1.0	< 0.5	131	431	< 0.4	789	92.4	365	60.4	18.7	51.0	7.6	35.2	5.7	14.9	1.91
67592	< 2	4631	91	517	< 2	< 0.5	< 0.2	2	0.7	< 0.5	462	443	< 0.4	882	114	474	75.2	20.2	52.0	5.7	24.3	3.6	9.1	1.03
67593	< 2	3604	83	618	< 2	< 0.5	0.3	5	1.4	< 0.5	179	455	< 0.4	866	113	464	71.9	19.1	50.0	5.3	22.4	3.3	8.3	0.94
67594	4	2517	88	715	< 2	< 0.5	< 0.2	< 1	0.6	< 0.5	122	432	< 0.4	935	116	467	72.3	19.6	47.2	5.4	23.3	3.4	8.9	0.98
67595	3	2504	102	635	< 2	< 0.5	< 0.2	3	1.2	< 0.5	303	395	< 0.4	713	97.3	422	75.9	21.2	58.4	6.8	27.8	4.0	9.6	1.04
67601	21	4525	90	103	91	< 0.5	< 0.2	< 1	< 0.5	0.6	423	406	< 0.4	674	80.0	315	49.5	14.0	36.4	4.4	19.8	3.2	8.6	1.12
67602	< 2	5725	93	78	28	< 0.5	< 0.2	< 1	< 0.5	< 0.5	620	370	< 0.4	628	75.9	301	47.0	13.3	35.4	4.3	20.0	3.3	8.9	1.35
67603	154	1330	26	124	< 2	< 0.5	< 0.2	< 1	1.0	4.8	831	147	< 0.4	325	33.9	136	20.5	5.49	13.3	1.5	6.3	1.0	2.4	0.28
67604	155	1054	62	111	4	< 0.5	< 0.2	1	0.9	3.8	1180	516	< 0.4	865	104	408	58.7	15.3	38.5	3.9	16.2	2.4	6.3	0.74
67605	3	5273	108	244	11	< 0.5	< 0.2	< 1	0.8	< 0.5	320	408	< 0.4	752	97.0	400	64.0	18.0	46.1	5.6	24.9	4.0	10.5	1.16
67606	189	556	13	39	< 2	< 0.5	< 0.2	1	2.6	5.4	1327	59.1	< 0.4	162	15.5	59.8	9.4	2.71	5.8	0.7	2.9	0.5	1.1	0.15
67607	3	5415	78	121	< 2	< 0.5	< 0.2	2	1.9	< 0.5	464	392	< 0.4	685	87.5	359	55.6	14.8	37.9	4.2	18.5	2.9	7.4	0.91
67608	< 2	5177	136	59	5	< 0.5	< 0.2	< 1	0.9	< 0.5	535	529	< 0.4	861	107	425	66.7	18.8	52.3	6.6	30.5	4.9	12.6	1.39
67609	3	5892	80	152	< 2	< 0.5	< 0.2	< 1	< 0.5	< 0.5	625	400	< 0.4	779	92.5	373	56.5	15.5	38.9	4.4	19.2	3.0	7.8	0.95
67610	< 2	2700	53	630	< 2	< 0.5	0.6	11	1.6	< 0.5	2176	322	< 0.4	782	94.1	380	59.4	15.5	37.5	4.0	16.5	2.2	5.6	0.64
67611	< 2	4979	75	353	< 2	< 0.5	< 0.2	1	1.1	< 0.5	555	392	< 0.4	727	95.1	395	61.9	16.0	43.2	4.7	19.3	2.8	7.3	0.90
67612	14	2107	141	194	67	< 0.5	< 0.2	< 1	< 0.5	< 0.5	157	618	< 0.4	1350	163	645	99.6	27.6	69.6	8.0	34.8	5.4	14.2	1.74
67613	7	1378	135	621	< 2	< 0.5	< 0.2	< 1	< 0.5	< 0.5	120	391	< 0.4	779	98.9	405	66.7	18.7	50.7	6.5	30.0	5.1	14.5	1.91
67614	5	1806	59	87	< 2	< 0.5	0.3	2	1.2	< 0.5	140	391	< 0.4	760	99.4	404	59.1	14.9	38.8	3.9	16.2	2.4	6.1	0.76
67615	4	1875	146	333	3	< 0.5	< 0.2	< 1	< 0.5	< 0.5	127	814	< 0.4	1870	211	818	121	32.8	82.8	9.4	39.7	5.8	14.7	1.59
67616	2	1891	145	176	5	< 0.5	< 0.2	< 1	0.9	< 0.5	121	458	< 0.4	851	98.6	393	64.1	19.5	52.4	7.6	35.2	5.7	14.9	1.91
67617	< 2	3801	80	453	< 2	< 0.5	0.2	4	1.1	< 0.5	318	444	< 0.4	867	112	463	74.0	19.5	49.4	5.5	22.5	3.3	8.3	1.01
67618	< 2	3048	77	547	< 2	< 0.5	0.5	5	1.5	< 0.5	112	484	< 0.4	906	116	480	72.7	19.5	49.9	5.3	21.8	3.2	7.9	0.87
67619	4	2569	96	686	< 2	< 0.5	< 0.2	< 1	< 0.5	< 0.5	135	500	< 0.4	1100	135	541	82.8	22.1	53.8	6.0	25.5	3.8	9.8	1.20
67620	6	1960	85	669	< 2	< 0.5	< 0.2	3	1.0	< 0.5	326	358	< 0.4	613	80.2	339	60.5	16.5	47.1	5.5	22.8	3.4	8.2	0.93

Analyte Symbol	Yb	Lu	Hf	W	Tl	Pb	Th	U	Ta	Mass
Unit Symbol	ppm	ppm	ppm	ppm	ppm	ppm	ppm	ppm	ppm	g
Detection Limit	0.1	0.04	0.2	1	0.1	5	0.1	0.1	2	
Analysis Method	FUS-MS	FUS-MS	FUS-MS	FUS-MS	FUS-MS	FUS-MS	FUS-MS	FUS-MS	INAA	INAA
67576	5.8	0.76	1.5	< 1	< 0.1	< 5	43.2	39.0	66	1.564
67577	5.5	0.71	1.1	2	< 0.1	12	179	51.1	85	1.653
67578	2.0	0.25	3.3	< 1	0.3	8	22.6	49.7	65	1.535
67579	4.6	0.55	3.0	12	0.9	17	81.6	70.1	105	1.613
67580	7.2	0.91	2.6	< 1	0.3	47	472	187	306	1.152
67581	1.1	0.13	1.3	4	0.6	< 5	48.3	15.4	65	1.444
67582	5.1	0.63	1.9	< 1	< 0.1	61	411	180	250	1.258
67583	7.5	0.89	1.1	< 1	< 0.1	20	116	37.0	52	1.497
67584	5.4	0.67	1.0	< 1	< 0.1	37	258	31.3	84	1.733
67585	3.1	0.37	7.1	< 1	< 0.1	81	640	44.3	144	1.927
67586	4.3	0.51	2.8	< 1	0.3	47	438	124	187	1.773
67587	8.3	1.06	1.2	< 1	0.6	23	163	18.0	33	1.926
67588	10.1	1.33	6.1	16	0.3	150	215	185	160	1.929
67589	3.7	0.45	1.3	19	0.4	30	202	497	560	2.216
67590	8.5	0.96	2.2	2	0.5	17	158	54.7	72	1.969
67591	10.4	1.38	1.4	3	0.1	28	180	62.3	68	2.063
67592	5.2	0.63	4.8	< 1	< 0.1	51	887	333	453	1.681
67593	4.8	0.56	7.6	< 1	< 0.1	67	579	167	209	1.788
67594	5.5	0.66	3.3	< 1	0.1	110	1320	253	378	1.863
67595	4.8	0.52	9.7	3	< 0.1	15	42.2	877	719	1.965
67601	5.8	0.75	1.6	< 1	0.1	7	46.7	45.9	70	1.546
67602	5.8	0.73	0.9	< 1	< 0.1	15	179	50.3	73	1.672
67603	1.5	0.19	1.7	< 1	0.7	8	19.4	28.2	38	1.676
67604	3.7	0.44	2.0	5	1.0	14	54.1	40.6	59	1.685
67605	6.5	0.82	2.6	3	0.3	37	479	179	278	1.565
67606	0.7	0.09	0.8	2	0.7	5	30.0	9.6	40	1.612
67607	4.5	0.55	1.4	< 1	0.2	58	249	101	146	1.762
67608	7.0	0.85	1.0	< 1	< 0.1	14	94.1	24.4	35	1.719
67609	4.9	0.61	0.9	< 1	< 0.1	6	258	28.8	80	1.768
67610	3.1	0.34	6.0	2	< 0.1	18	641	36.7	126	1.663
67611	4.2	0.49	5.2	< 1	< 0.1	74	391	109	166	1.701
67612	9.0	1.13	1.7	< 1	0.5	8	177	12.6	19	1.877
67613	10.5	1.42	6.0	6	< 0.1	8	185	175	160	1.839
67614	3.8	0.47	1.3	20	0.4	34	194	445	535	1.973
67615	8.2	0.95	1.8	< 1	0.4	12	143	56.3	76	1.990
67616	10.3	1.35	1.6	3	< 0.1	13	185	73.4	83	1.861
67617	4.6	0.54	4.9	< 1	< 0.1	16	699	253	347	1.487
67618	4.4	0.52	5.3	< 1	< 0.1	88	613	143	181	1.345
67619	6.1	0.75	2.6	< 1	0.1	117	1410	262	410	1.985
67620	4.2	0.49	10.0	3	< 0.1	< 5	43.4	793	712	2.184

Quality Control

Analyte Symbol	Nb	SiO2	Al2O3	Fe2O3(T)	MnO	MgO	CaO	Na2O	K2O	TiO2	P2O5	LOI	Total	Sc	Be	V	Cr	Co	Ni	Cu	Zn	Ga	Ge	As
Unit Symbol	%	%	%	%	%	%	%	%	%	%	%	%	%	ppm	ppm	ppm	ppm	ppm	ppm	ppm	ppm	ppm	ppm	ppm
Detection Limit	0.002	0.01	0.01	0.01	0.001	0.01	0.01	0.01	0.01	0.001	0.01		0.01	1	1	5	20	1	20	10	30	1	1	5
Analysis Method	FUS-XRF	FUS-ICP	FUS-ICP	FUS-ICP	FUS-ICP	FUS-ICP	FUS-ICP	FUS-ICP	FUS-ICP	FUS-ICP	FUS-ICP	FUS-ICP	FUS-ICP	FUS-ICP	FUS-ICP	FUS-ICP	FUS-MS	FUS-MS	FUS-MS	FUS-MS	FUS-MS	FUS-MS	FUS-MS	FUS-MS
GXR-1 Meas																	< 20	5	40	1100	760	15		418
GXR-1 Cert																	12.0	8.20	41.0	1110	760	13.8		427
WMG-1 Meas																	800	207	2570	6540	120	10		49
WMG-1 Cert																	770	200	2700	5900	110	10.3		7.00
TAN-1 Meas																								
TAN-1 Cert																								
TAN-1 Meas																								
TAN-1 Cert																								
TAN-1 Meas																								
TAN-1 Cert																								
NIST 694 Meas		11.17	1.87	0.70	0.012	0.33	43.41	0.88	0.52	0.110	30.14					1679								
NIST 694 Cert		11.2	1.80	0.790	0.0116	0.330	43.6	0.860	0.510	0.110	30.2					1740								
DNC-1 Meas		46.76	18.43	10.04	0.146	10.12	11.28	1.93	0.18	0.487	0.08			31	< 1	156	280	57	250	140	80	13	1	< 5
DNC-1 Cert		47.0	18.3	9.93	0.149	10.1	11.3	1.87	0.234	0.480	0.0900			31.0	1.00	148	285	54.7	247	96.0	66.0	15.0	1.30	0.200
GBW 07113 Meas		72.49	12.76	3.16	0.144	0.15	0.59	2.46	5.52	0.283	0.06			5	4	< 5								
GBW 07113 Cert		72.8	13.0	3.21	0.140	0.160	0.590	2.57	5.43	0.300	0.0500			5.00	4.00	5.00								
MICA-FE Meas	0.028																							
MICA-FE Cert	0.0270																							
GXR-2 Meas																	30	7	< 20	100	430	37		115
GXR-2 Cert																	36.0	8.60	21.0	76.0	530	37.0		25.0
LKSD-3 Meas																	80	28	50	40	140			82
LKSD-3 Cert																	87.0	30.0	47.0	35.0	152			27.0
MAG-1 (Depleted) Meas																	90	20	40	40	130	22		21
MAG-1 (Depleted) Cert																	97.0	20.4	53.0	30.0	130	20.4		9.20
NIST 1633b Meas		49.23	28.70	11.49	0.019	0.78	2.16	0.27	2.37	1.308	0.60			41		308								
NIST 1633b Cert		49.2	28.4	11.1	0.0200	0.800	2.11	0.270	2.35	1.32	0.530			41.0		296								
OKA-1 Meas	0.380																							
OKA-1 Cert	0.370																							
W-2a Meas		52.17	15.27	10.96	0.164	6.33	10.95	2.20	0.61	1.076	0.14			35	1	280	90	42	60	140	80	17	2	< 5
W-2a Cert		52.4	15.4	10.7	0.163	6.37	10.9	2.14	0.626	1.06	0.130			36.0	1.30	262	92.0	43.0	70.0	110	80.0	17.0	1.00	1.20
NIST 696 Meas		4.49	54.21	8.18	0.006	0.02	0.02		0.06	2.612	0.05					409								
NIST 696 Cert		3.79	54.5	8.70	0.00400	0.0120	0.0180		0.00900	2.64	0.0500					403								
DTS-2b Meas		37.33	0.43			49.44	0.13							3		< 5								
DTS-2b Cert		39.4	0.450			49.4	0.120							3.00		22.0								
SY-4 Meas		49.09	20.13	6.07	0.105	0.51	7.92	7.00	1.60	0.284	0.14			< 1	3	< 5								
SY-4 Cert		49.9	20.69	6.21	0.108	0.54	8.05	7.10	1.66	0.287	0.131			1.1	2.6	8.0								
CTA-AC-1 Meas																		< 1		90	30			
CTA-AC-1 Cert																		2.72		54.0	38.0			
BIR-1a Meas		48.22	15.76	11.59	0.174	9.71	13.42	1.83	0.02	0.969	0.03			43	< 1	339	390	52	160	170	80	15	2	< 5
BIR-1a Cert		47.8	15.4	11.3	0.171	9.68	13.2	1.75	0.0300	0.960	0.0500			44.0	0.580	313	382	51.4	166	126	71.0	16.0	1.50	0.440
STM-2 Meas	0.027																							
STM-2 Cert	0																							
67590 Orig	1.118	1.18	0.36	3.97	0.305	10.78	36.55	0.23	0.25	0.161	10.94	26.88	91.60	16	171	223	< 20	2	< 20	20	150	21	3	16
67590 Dup	1.122	1.25	0.37	4.11	0.298	10.57	35.81	0.22	0.23	0.160	10.78	26.88	90.68	16	169	220	< 20	2	< 20	10	220	20	3	19
67610 Orig	0.601	9.31	0.49	23.53	0.943	14.44	20.41	0.06	0.04	0.589	7.62	17.27	94.69	78	3	295	< 20	5	< 20	20	230	16	3	22
67610 Split	0.610	9.30	0.46	22.65	0.913	14.29	20.93	0.06	0.02	0.597	7.24	16.97	93.42	74	3	330	< 20	3	< 20	10	170	16	3	15
67612 Orig		3.45	1.03	7.51	0.469	11.94	31.92	0.20	0.60	0.083	7.83	31.87	96.91	14	27	92	30	12	20	20	60	17	3	15
67612 Dup		3.39	1.03	7.54	0.476	12.11	31.89	0.19	0.61	0.080	7.70	31.87	96.90	14	24	86	< 20	9	< 20	10	110	16	3	10
67619 Orig	0.689	5.47	0.30	12.28	0.623	11.51	30.74	0.54	0.20	0.214	6.03	29.07	96.97	54	20	147	< 20	5	< 20	50	160	15	3	8
67619 Split	0.684	5.94	0.39	12.05	0.611	11.25	30.02	0.54	0.18	0.213	5.92	29.07	96.19	53	20	142	< 20	4	< 20	40	130	15	3	8
Method Blank Method Blank																								
Method Blank Method Blank	< 0.002																							

Quality Control

Analyte Symbol	Rb	Sr	Y	Zr	Mo	Ag	In	Sn	Sb	Cs	Ba	La	Bi	Ce	Pr	Nd	Sm	Eu	Gd	Tb	Dy	Ho	Er	Tm
Unit Symbol	ppm	ppm	ppm	ppm	ppm	ppm	ppm	ppm	ppm	ppm	ppm	ppm	ppm	ppm	ppm	ppm	ppm	ppm	ppm	ppm	ppm	ppm	ppm	ppm
Detection Limit	2	2	2	4	2	0.5	0.2	1	0.5	0.5	3	0.1	0.4	0.1	0.05	0.1	0.1	0.05	0.1	0.1	0.1	0.1	0.1	0.05
Analysis Method	FUS-MS	FUS-ICP	FUS-ICP	FUS-ICP	FUS-MS	FUS-MS	FUS-MS	FUS-MS	FUS-MS	FUS-MS	FUS-ICP	FUS-MS	FUS-MS	FUS-MS	FUS-MS	FUS-MS	FUS-MS	FUS-MS	FUS-MS	FUS-MS	FUS-MS	FUS-MS	FUS-MS	FUS-MS
GXR-1 Meas	3				18	34.0	0.8	18	122	2.7		8.7	1380	15.1		8.2	2.8	0.57	3.8	0.8	4.7			0.37
GXR-1 Cert	14.0				18.0	31.0	0.770	54.0	122	3.00		7.50	1380	17.0		18.0	2.70	0.690	4.20	0.830	4.30			0.430
WMG-1 Meas					< 2	2.7		< 1	20.5	< 0.5		8.6		16.4		9.0	2.3	0.74		0.4	2.5	0.5		0.20
WMG-1 Cert					1.40	2.70		2.20	1.80	0.480		8.20		16.0		9.00	2.30	0.820		0.300	2.80	0.500		0.200
TAN-1 Meas																								
TAN-1 Cert																								
TAN-1 Meas																								
TAN-1 Cert																								
TAN-1 Meas																								
TAN-1 Cert																								
NIST 694 Meas																								
NIST 694 Cert																								
DNC-1 Meas	4	143	16	39	< 2	< 0.5			5.1	< 0.5	107	4.1	< 0.4	8.1	1.07	4.8	1.4	0.60	1.9	0.4	2.8	0.6	2.0	0.51
DNC-1 Cert	4.50	145	18.0	41.0	0.700	0.0270			0.960	0.340	114	3.80	0.0200	10.6	1.30	4.90	1.38	0.590	2.00	0.410	2.70	0.620	2.00	0.380
GBW 07113 Meas		41	47	424							498													
GBW 07113 Cert		43.0	43.0	403							506													
MICA-FE Meas																								
MICA-FE Cert																								
GXR-2 Meas	83				< 2	11.6	< 0.2	< 1	33.7	5.5		29.3	< 0.4	53.7		20.4	3.8	0.69	3.2	0.6	3.2			0.29
GXR-2 Cert	78.0				2.10	17.0	0.252	1.70	49.0	5.20		25.6	0.690	51.4		19.0	3.50	0.810	3.30	0.480	3.30			0.300
LKSD-3 Meas	74				< 2	2.8		< 1	1.7	2.2		51.0		87.4		40.4	7.5	1.37		0.9	4.9			
LKSD-3 Cert	78.0				2.00	2.70		3.00	1.30	2.30		52.0		90.0		44.0	8.00	1.50		1.00	4.90			
MAG-1 (Depleted) Meas	150				< 2	< 0.5	< 0.2	4	2.5	8.6		45.7	< 0.4	85.4	9.74	35.6	7.0	1.43	5.7	1.0	5.2	1.0	2.9	0.40
MAG-1 (Depleted) Cert	149				1.60	0.0800	0.180	3.60	0.960	8.60		43.0	0.340	88.0	9.30	38.0	7.50	1.60	5.80	0.960	5.20	1.02	3.00	0.430
NIST 1633b Meas		1050									724													
NIST 1633b Cert		1040									709													
OKA-1 Meas																								
OKA-1 Cert																								
W-2a Meas	20	195	20	74	< 2	< 0.5			12.3	0.9	174	11.6	20.9	23.0		12.3	3.1	1.09		0.7	3.9	0.8	2.4	0.32
W-2a Cert	21.0	190	24.0	94.0	0.600	0.0460			0.790	0.990	182	10.0	0.0300	23.0		13.0	3.30	1.00		0.630	3.60	0.760	2.50	0.380
NIST 696 Meas				1050																				
NIST 696 Cert				1040																				
DTS-2b Meas											21													
DTS-2b Cert											16.0													
SY-4 Meas		1184	119	508							347													
SY-4 Cert		1191	119	517							340													
CTA-AC-1 Meas												> 2000		2960		1090	162	46.7	127	15.1				
CTA-AC-1 Cert												2176		3326		1087	162	46.7	124	13.9				
BIR-1a Meas	< 2	109	15	13	< 2	< 0.5		< 1	6.4	< 0.5	8	0.8	< 0.4	2.0	0.37	2.3	1.1	0.53	1.8	0.4	2.6	0.6	1.8	0.26
BIR-1a Cert	0.250	108	16.0	16.0	0.500	0.0360		0.650	0.580	0.00500	7.00	0.620	0.0200	1.95	0.380	2.50	1.10	0.540	1.85	0.360	2.50	0.570	1.70	0.260
STM-2 Meas																								
STM-2 Cert																								
67590 Orig	4	1769	151	362	3	< 0.5	< 0.2	1	0.6	< 0.5	142	801	< 0.4	1880	214	818	123	33.6	82.6	9.5	40.6	5.9	14.8	1.69
67590 Dup	4	1735	148	376	3	< 0.5	< 0.2	< 1	0.8	< 0.5	141	815	< 0.4	1900	216	841	125	34.1	85.9	9.7	41.3	6.1	15.3	1.77
67610 Orig	< 2	2700	53	630	< 2	< 0.5	0.6	11	1.6	< 0.5	2176	322	< 0.4	782	94.1	380	59.4	15.5	37.5	4.0	16.5	2.2	5.6	0.64
67610 Split	< 2	2629	52	622	< 2	< 0.5	0.5	8	1.9	< 0.5	2203	329	< 0.4	786	94.7	384	59.7	15.5	38.5	4.0	16.2	2.2	5.5	0.62
67612 Orig	15	2104	143	197	66	< 0.5	< 0.2	2	1.1	< 0.5	159	611	< 0.4	1330	161	637	99.3	27.6	69.8	8.1	35.2	5.5	14.5	1.78
67612 Dup	14	2110	138	191	68	< 0.5	< 0.2	< 1	< 0.5	< 0.5	155	625	< 0.4	1360	165	654	100	27.5	69.4	7.9	34.4	5.3	14.0	1.70
67619 Orig	4	2569	96	686	< 2	< 0.5	< 0.2	< 1	< 0.5	< 0.5	135	500	< 0.4	1100	135	541	82.8	22.1	53.8	6.0	25.5	3.8	9.8	1.20
67619 Split	5	2516	95	679	< 2	< 0.5	0.2	< 1	0.5	< 0.5	142	518	< 0.4	1120	137	552	85.0	22.3	54.7	6.0	26.0	3.8	10.0	1.28
Method Blank Method Blank																								
Method Blank Method Blank																								

Quality Control

Analyte Symbol	Yb	Lu	Hf	W	Tl	Pb	Th	U	Ta	Mass
Unit Symbol	ppm	ppm	ppm	ppm	ppm	ppm	ppm	ppm	ppm	g
Detection Limit	0.1	0.04	0.2	1	0.1	5	0.1	0.1	2	
Analysis Method	FUS-MS	FUS-MS	FUS-MS	FUS-MS	FUS-MS	FUS-MS	FUS-MS	FUS-MS	INAA	INAA
GXR-1 Meas	2.2	0.31	0.9	164	0.6	621	2.4	34.8		
GXR-1 Cert	1.90	0.280	0.960	164	0.390	730	2.44	34.9		
WMG-1 Meas	1.3	0.20	1.6	< 1		20	1.1	0.7		
WMG-1 Cert	1.30	0.210	1.30	1.30		15.0	1.10	0.650		
TAN-1 Meas									2360	
TAN-1 Cert									2360	
TAN-1 Meas									2360	
TAN-1 Cert									2360	
TAN-1 Meas									2350	
TAN-1 Cert									2360	
NIST 694 Meas										
NIST 694 Cert										
DNC-1 Meas	1.9	0.31	1.1	< 1	< 0.1	6	0.2	< 0.1		
DNC-1 Cert	2.01	0.320	1.01	0.200	0.0260	6.30	0.200	0.100		
GBW 07113 Meas										
GBW 07113 Cert										
MICA-FE Meas										
MICA-FE Cert										
GXR-2 Meas	1.9	0.30	7.7	2	1.0	213	8.9	3.3		
GXR-2 Cert	2.04	0.270	8.30	1.90	1.03	690	8.80	2.90		
LKSD-3 Meas	2.7	0.42	4.9	< 1		18	10.2	4.7		
LKSD-3 Cert	2.70	0.400	4.80	2.00		29.0	11.4	4.60		
MAG-1 (Depleted) Meas	2.6	0.39	3.8	1	0.3	15	11.6	3.1		
MAG-1 (Depleted) Cert	2.60	0.400	3.70	1.40	0.590	24.0	11.9	2.70		
NIST 1633b Meas										
NIST 1633b Cert										
OKA-1 Meas										
OKA-1 Cert										
W-2a Meas	2.1	0.31	2.6	< 1	0.1	15	2.1	0.5		
W-2a Cert	2.10	0.330	2.60	0.300	0.200	9.30	2.40	0.530		
NIST 696 Meas										
NIST 696 Cert										
DTS-2b Meas										
DTS-2b Cert										
SY-4 Meas										
SY-4 Cert										
CTA-AC-1 Meas	11.4	1.07	2.1				22.6	4.5		
CTA-AC-1 Cert	11.4	1.08	1.13				21.8	4.4		
BIR-1a Meas	1.7	0.26	0.6	< 1	< 0.1	< 5	< 0.1	< 0.1		
BIR-1a Cert	1.65	0.260	0.600	0.0700	0.0100	3.00	0.0300	0.0100		
STM-2 Meas										
STM-2 Cert										
67590 Orig	8.4	0.96	2.1	4	0.4	15	164	54.8		
67590 Dup	8.5	0.96	2.3	1	0.6	20	153	54.7		
67610 Orig	3.1	0.34	6.0	2	< 0.1	18	641	36.7	126	1.663
67610 Split	3.0	0.36	5.8	< 1	< 0.1	6	632	36.2	125	1.743
67612 Orig	9.2	1.15	2.3	12	0.4	8	195	13.2		
67612 Dup	8.9	1.12	1.1	< 1	0.5	8	159	12.0		
67619 Orig	6.1	0.75	2.6	< 1	0.1	117	1410	262	410	1.985
67619 Split	6.2	0.72	3.0	< 1	0.1	104	1410	262	434	2.077
Method Blank Method Blank									< 2	1.000
Method Blank Method Blank										

AGAT Laboratories

5623 McADAM ROAD
MISSISSAUGA, ONTARIO
CANADA L4Z 1N9
TEL (905)501-9998
FAX (905)501-0589
http://www.agatlabs.com

CLIENT NAME: DAHROUGE GEOLOGICAL CONSULTING LTD.
SUITE 18, 10509-81 AVE
EDMONTON, AB T6E1X7

ATTENTION TO: JUDY SMITH

PROJECT NO: REE Checks

AGAT WORK ORDER: 10T385783

ROCK ANALYSIS REVIEWED BY: Ron Cardinall, General Manager

DATE REPORTED: Mar 02, 2010

PAGES (INCLUDING COVER): 11

Should you require any information regarding this analysis please contact your client services representative at (905) 501 9998, or at 1-800-856-6261

*NOTES

All samples will be disposed of within 30 days following analysis. Please contact the lab if you require additional sample storage time.

AGAT Laboratories

5623 McADAM ROAD
MISSISSAUGA, ONTARIO
CANADA L4Z 1N9
TEL (905)501-9998
FAX (905)501-0589
http://www.agatlabs.com

Certificate of Analysis

AGAT WORK ORDER: 10T385783
PROJECT NO: REE Checks

CLIENT NAME: DAHROUGE GEOLOGICAL CONSULTING LTD.

ATTENTION TO: JUDY SMITH

Lithium Borate Fusion, ICP-MS finish

DATE SAMPLED: Feb 12, 2010 | DATE RECEIVED: Feb 12, 2010 | DATE REPORTED: Feb 26, 2010 | SAMPLE TYPE: Rock

Analyte:	Ag	Ba	Ce	Co	Cr	Cs	Cu	Dy	Er	Eu	Ga	Gd	Hf	Ho
Unit:	ug/g	ug/g	ug/g	ug/g	ug/g	ug/g	ug/g	ug/g	ug/g	ug/g	ug/g	ug/g	ug/g	ug/g
Sample Description RDL:	1	0.5	0.5	0.5	10	0.01	1	0.05	0.03	0.03	0.01	0.05	0.2	0.01
38703	<1	185	1160	49	<10	0.01	18	60.3	21.5	32.0	7.71	98.0	1.7	10.0
38721	<1	135	5600	9	11	0.03	<1	138.0	50.3	90.8	22.2	249	2.6	21.7
39052	1	1860	1410	19	150	4.55	<1	11.3	3.18	12.3	21.0	29.0	16.9	1.52
42857	2	980	482	24	85	3.73	<1	5.35	1.94	6.58	27.7	15.8	13.1	0.86
43003	<1	392	5230	6	<10	0.03	<1	185	55.6	115	20.0	362	1.2	26.4
43009	<1	454	>10000	6	18	0.08	<1	44.0	12.4	70.4	42.6	176	0.7	6.04
43013	<1	405	>10000	9	13	0.03	<1	94.7	23.8	111	42.2	285	0.4	12.6
43301	<1	730	3700	10	10	0.34	1	110	38.6	62.4	16.9	179	1.8	17.6
43859	<1	380	2760	3	<10	0.04	<1	41.3	12.3	36.2	11.7	103	0.9	5.98
45688	<1	478	5000	4	<10	0.04	<1	28.8	9.18	32.8	18.4	88.2	0.7	4.25
45808	<1	100	5120	10	<10	0.12	<1	71.7	25.6	57.5	19.6	160	0.9	11.2
47202	<1	75.8	727	26	<10	0.03	<1	30.7	10.1	20.1	7.82	60.2	2.6	4.75
47227	<1	298	470	10	30	0.30	<1	22.7	9.23	12.4	4.10	37.0	0.7	3.84
47229	<1	463	405	17	100	1.67	10	16.9	6.28	11.0	8.86	29.8	1.3	2.77
47239	<1	45.4	686	18	424	0.03	<1	33.3	13.5	18.2	3.64	54.4	1.2	5.70
54894	<1	185	924	23	10	0.03	<1	31.8	9.31	22.6	14.6	69.5	1.7	4.63
54867	<1	146	819	34	<10	0.01	<1	27.5	7.87	20.1	10.8	60.9	0.8	3.93
68405	<1	49.5	7550	5	13	0.03	<1	39.1	9.75	49.3	25.9	131	0.6	5.17
68428	<1	518	1990	9	12	0.08	<1	25.1	8.17	22.3	7.87	59.6	1.3	3.78
68437	<1	772	337	27	64	5.66	35	7.75	2.59	5.94	13.8	16.6	1.3	1.19
68514	<1	372	1280	16	21	0.07	62	25.1	9.03	19.5	6.27	53.5	2.8	3.93
68516	<1	360	617	3	<10	0.10	<1	9.9	3.92	7.07	2.76	18.7	<0.2	1.67
68523	<1	188	1200	15	<10	0.26	15	33.5	14.0	21.8	7.14	61.9	1.5	5.56
70010	<1	240	530	34	33	0.02	9	21.3	7.55	12.5	5.22	37.8	4.9	3.41
70048	2	2010	940	22	185	5.16	<1	9.40	2.44	9.24	21.8	21.1	24.1	1.24
70059	<1	2100	>10000	155	94	0.10	21	46.2	6.50	220	90.3	568	0.5	4.69

Certified By: Ron Cardinall

AGAT Laboratories
5623 McADAM ROAD
MISSISSAUGA, ONTARIO
CANADA L4Z 1N9
TEL (905)501-9998
FAX (905)501-0589
http://www.agatlabs.com

Certificate of Analysis

AGAT WORK ORDER: 10T385783

PROJECT NO: REE Checks

CLIENT NAME: DAHROUGE GEOLOGICAL CONSULTING LTD.

ATTENTION TO: JUDY SMITH

Lithium Borate Fusion, ICP-MS finish

DATE SAMPLED: Feb 12, 2010 | DATE RECEIVED: Feb 12, 2010 | DATE REPORTED: Feb 26, 2010 | SAMPLE TYPE: Rock

Analyte:	La	Lu	Mo	Nb	Nd	Ni	Pb	Pr	Rb	Sm	Sn	Sr	Ta	Tb
Unit:	ug/g	ug/g	ug/g	ug/g	ug/g	ug/g	ug/g	ug/g	ug/g	ug/g	ug/g	ug/g	ug/g	ug/g
Sample Description RDL:	0.5	0.01	2	0.2	0.1	1	1	0.03	0.2	0.03	1	0.1	0.1	0.01
38703	492	1.45	15	1330	642	31	18	164	4.6	107	6	1160	120	12.3
38721	2440	4.91	3	995	2800	24	342	763	0.6	379	32	2430	1.7	30.5
39052	600	0.29	3	>10000	498	50	248	155	199	53.6	36	1390	718	3.31
42857	161	0.18	<2	>10000	203	30	18	59.5	218	23.9	26	751	1020	1.51
43003	2340	4.77	4	382	2450	9	347	690	1.3	411	5	3510	2.3	43.0
43009	8925	1.01	6	295	3700	59	79	>1000	4.5	354	5	2780	0.4	16.1
43013	7070	1.49	20	600	4330	15	300	>1000	2.5	521	11	1790	0.6	28.4
43301	1770	2.90	15	660	1630	9	357	465	15.6	222	4	2890	10.7	23.1
43859	1230	0.90	9	310	1250	8	94	368	2.9	144	1	2930	29.7	11.0
45688	2830	0.72	47	908	1720	7	92	563	1.8	151	2	1890	2.6	8.71
45808	2580	2.17	2	1100	1860	9	53	583	2.1	224	6	2150	12.8	18.1
47202	277	0.83	<2	870	449	9	34	106	1.3	70.8	6	1600	210	7.07
47227	201	0.89	2	945	231	15	24	58.6	12.1	41.9	2	1790	52.0	4.62
47229	172	0.54	<2	1120	200	30	16	50.9	61.2	34.9	4	1050	39.5	3.69
47239	280	1.15	6	1490	356	31	37	96.2	1.3	64.2	2	1360	66.3	6.90
54894	356	0.62	<2	409	540	9	16	135	3.5	85.0	3	2310	103	7.78
54867	303	0.51	<2	120	482	10	22	118	0.2	76.3	2	1880	19.1	6.80
68405	4000	0.77	14	1540	2520	14	21	802	0.8	219	2	1280	20.1	12.6
68428	922	0.68	5	1560	750	74	43	221	4.7	89.9	2	4530	24.1	6.60
68437	132	0.22	5	730	151	46	12	38.6	213	22.9	10	1520	34.4	1.88
68514	456	0.86	3	1220	570	24	55	158	3.7	75.0	3	1990	52.2	6.17
68516	284	0.44	2	1500	194	11	4	60.6	5.0	25.3	1	6180	0.6	2.24
68523	455	1.96	27	3600	550	25	43	148	12.6	79.8	5	1170	27.0	7.42
70010	225	0.64	2	1590	250	41	603	63.9	1.3	43.4	5	1970	338.0	4.67
70048	328	0.15	2	>10000	291	62	326	98.6	226	37.2	37	1340	1180	2.48
70059	3620	0.39	127	156	>10000	320	737	>1000	13.4	>1000	<1	1710	1.9	3.44

Certified By: Ron Cardinall

AGAT Laboratories

5623 McADAM ROAD
MISSISSAUGA, ONTARIO
CANADA L4Z 1N9
TEL (905)501-9998
FAX (905)501-0589
http://www.agatlabs.com

Certificate of Analysis

AGAT WORK ORDER: 10T385783

PROJECT NO: REE Checks

CLIENT NAME: DAHROUGE GEOLOGICAL CONSULTING LTD.

ATTENTION TO: JUDY SMITH

Lithium Borate Fusion, ICP-MS finish

DATE SAMPLED: Feb 12, 2010 | DATE RECEIVED: Feb 12, 2010 | DATE REPORTED: Feb 26, 2010 | SAMPLE TYPE: Rock

Analyte:	Th	Tl	Tm	U	V	W	Y	Yb	Zn	Zr
Unit:	ug/g	ug/g	ug/g	ug/g	ug/g	ug/g	ug/g	ug/g	ug/g	ug/g
Sample Description RDL:	0.05	0.5	0.01	0.05	1	1	0.5	0.03	1	2
38703	153	<0.5	2.40	53.5	112	8	218	12.22	549	55
38721	420	<0.5	6.43	0.64	134	10	554	37.42	479	139
39052	>1000	<0.5	0.40	867	51	44	32.5	2.40	298	405
42857	467	0.8	0.23	720	98	10	35.6	1.49	348	625
43003	704	<0.5	6.93	0.93	80	5	682	39.01	1793	51
43009	185	<0.5	1.48	0.22	51	9	156	8.60	824	32
43013	378	<0.5	2.54	0.28	78	8	306	13.45	1572	13
43301	416	<0.5	4.60	25.4	61	5	441	24.37	608	124
43859	222	<0.5	1.38	43.5	26	2	150	7.68	49	64
45688	159	<0.5	1.07	1.67	59	7	107	5.93	397	64
45808	416	<0.5	3.13	5.89	119	9	273	18.07	908	60
47202	40.9	<0.5	1.20	762	137	4	107	6.68	174	269
47227	61.8	<0.5	1.22	44.0	37	4	96.8	7.32	58	22
47229	59.7	<0.5	0.77	21.9	98	5	60.4	4.36	77	47
47239	184	<0.5	1.76	54.4	234	5	140	9.60	104	40
54894	33.7	<0.5	1.01	990	102	7	101	5.45	83	211
54867	23.3	<0.5	0.84	628	134	5	87.7	4.41	140	152
68405	135	<0.5	1.06	10.7	48	7	137	6.24	76	39
68428	226	<0.5	0.97	29.1	58	2	89.5	5.62	67	159
68437	31.4	0.9	0.30	23.0	127	3	24.6	1.76	248	88
68514	454	<0.5	1.11	143	127	5	101	6.59	68	228
68516	4.31	<0.5	0.51	0.44	88	3	40.0	3.17	34	36
68523	210	3.9	2.09	46.6	106	6	149	14.10	210	180
70010	67.3	<0.5	0.90	442	91	6	88.1	5.03	795	304
70048	>1000	<0.5	0.27	>1000	31	30	26.1	1.44	463	617
70059	>1000	<0.5	0.54	2.19	18	4	97.0	4.29	447	20

Comments: RDL - Reported Detection Limit

Certified By: Ron Cardinall

AGAT Laboratories

5623 McADAM ROAD
MISSISSAUGA, ONTARIO
CANADA L4Z 1N9
TEL (905)501-9998
FAX (905)501-0589
http://www.agatlabs.com

Certificate of Analysis

AGAT WORK ORDER: 10T385783

PROJECT NO: REE Checks

CLIENT NAME: DAHROUGE GEOLOGICAL CONSULTING LTD.

ATTENTION TO: JUDY SMITH

Lithium Borate Fusion, ICP-OES finish (201076)

DATE SAMPLED: Feb 12, 2010 | DATE RECEIVED: Feb 12, 2010 | DATE REPORTED: Feb 20, 2010 | SAMPLE TYPE: Rock

Analyte:	Al2O3	BaO	CaO	Cr2O3	Fe2O3	K2O	MgO	MnO	Na2O	P2O5	SiO2	TiO2	SrO	LOI
Unit:	%	%	%	%	%	%	%	%	%	%	%	%	%	%
Sample Description RDL:	0.005	0.005	0.005	0.005	0.005	0.005	0.005	0.005	0.005	0.005	0.005	0.005	0.005	0.01
38703	0.543	0.025	32.07	<0.005	11.370	0.435	9.034	0.432	0.072	8.198	3.08	0.029	0.138	32.24
38721	0.150	0.016	31.46	<0.005	9.356	0.035	10.274	1.195	0.057	5.962	1.509	0.255	0.288	36.40
39052	7.345	0.223	6.098	<0.005	10.610	6.349	10.717	0.269	1.276	0.061	16.830	1.081	0.165	5.14
42857	6.069	0.128	9.821	<0.005	12.480	4.981	13.015	0.447	0.041	0.005	11.77	0.517	0.089	41.39
43003	0.045	0.049	30.387	<0.005	8.765	0.044	12.510	1.277	0.029	0.708	2.53	0.027	0.416	40.98
43009	0.114	0.058	29.670	<0.005	7.261	0.152	11.707	1.203	0.025	1.320	1.430	0.050	0.330	38.62
43013	0.065	0.049	27.820	<0.005	12.350	0.079	10.786	1.765	0.021	1.085	1.083	0.103	0.212	37.39
43301	0.661	0.090	34.090	<0.005	8.696	0.462	9.505	0.902	0.157	4.939	3.918	0.107	0.343	33.74
43859	0.202	0.048	43.850	<0.005	3.975	0.113	7.075	0.537	0.066	4.534	0.944	0.018	0.347	38.44
45688	0.065	0.062	34.350	<0.005	8.755	0.054	10.302	1.265	0.088	0.978	1.060	0.03	0.224	40.92
45808	0.300	0.013	29.520	<0.005	11.280	0.178	10.869	1.137	0.052	2.175	2.21	0.064	0.255	39.52
47202	0.141	0.011	30.818	<0.005	15.445	0.088	8.290	0.253	0.094	15.12	4.76	0.051	0.190	23.14
47227	1.157	0.038	32.640	0.005	6.153	0.458	12.842	0.335	0.344	3.539	4.301	0.061	0.212	38.01
47229	5.607	0.061	22.500	0.013	6.994	2.377	11.866	0.250	1.346	2.255	18.360	0.227	0.125	27.15
47239	0.165	0.007	31.240	0.050	12.410	0.105	10.412	0.436	0.066	4.745	0.659	0.010	0.162	36.95
54894	0.672	0.025	35.542	<0.005	8.825	0.506	7.880	0.206	0.523	18.82	5.13	0.074	0.274	19.37
54867	0.112	0.020	28.490	<0.005	19.770	0.034	8.121	0.207	0.892	17.410	7.922	0.132	0.223	15.86
68405	0.098	0.007	32.960	<0.005	6.141	0.030	11.430	0.774	0.028	0.862	2.406	0.048	0.152	41.94
68428	0.169	0.065	45.870	<0.005	4.794	0.147	4.596	0.379	0.133	4.186	1.618	0.085	0.537	36.06
68437	7.132	0.099	16.420	<0.005	10.325	5.720	13.765	0.300	0.098	2.635	27.846	0.639	0.181	14.62
68514	0.532	0.049	33.410	<0.005	8.882	0.134	10.883	0.392	0.231	5.640	2.047	0.094	0.236	34.66
68516	0.073	0.048	51.450	<0.005	2.702	0.102	2.310	0.259	0.089	2.434	2.140	0.031	0.733	38.55
68523	0.851	0.026	30.05	<0.005	42.48	0.541	5.623	0.121	0.102	6.631	3.197	0.083	0.139	7.64
70010	1.145	0.032	29.730	<0.005	9.092	0.188	10.440	0.369	0.555	5.594	7.405	0.147	0.234	33.49
70048	8.007	0.242	5.485	<0.005	9.984	6.738	12.399	0.197	1.377	0.009	19.850	1.128	0.159	4.91
70059	2.769	0.225	16.960	0.011	13.640	2.146	8.668	0.972	0.267	0.378	11.280	0.050	0.203	30.57

Certified By: Ron Cardinall

AGAT Laboratories

5623 McADAM ROAD
MISSISSAUGA, ONTARIO
CANADA L4Z 1N9
TEL (905)501-9998
FAX (905)501-0589
http://www.agatlabs.com

Certificate of Analysis

AGAT WORK ORDER: 10T385783
PROJECT NO: REE Checks

CLIENT NAME: DAHROUGE GEOLOGICAL CONSULTING LTD.

ATTENTION TO: JUDY SMITH

Lithium Borate Fusion, ICP-OES finish (201076)

DATE SAMPLED: Feb 12, 2010 | DATE RECEIVED: Feb 12, 2010 | DATE REPORTED: Feb 20, 2010 | SAMPLE TYPE: Rock

Analyte:	Total
Unit:	%
Sample Description RDL:	0.005
38703	97.66
38721	96.96
39052	66.16
42857	100.75
43003	97.76
43009	91.94
43013	92.81
43301	97.61
43859	100.14
45688	98.15
45808	97.57
47202	98.41
47227	100.09
47229	99.13
47239	97.42
54894	97.84
54867	99.19
68405	96.88
68428	98.64
68437	99.79
68514	97.19
68516	100.92
68523	97.48
70010	98.42
70048	70.48
70059	88.14

Comments: RDL - Reported Detection Limit

Certified By: Ron Cardinall

AGAT Laboratories
5623 McADAM ROAD
MISSISSAUGA, ONTARIO
CANADA L4Z 1N9
TEL (905)501-9998
FAX (905)501-0589
http://www.agatlabs.com

Certificate of Analysis

AGAT WORK ORDER: 10T385783

PROJECT NO: REE Checks

CLIENT NAME: DAHROUGE GEOLOGICAL CONSULTING LTD.

ATTENTION TO: JUDY SMITH

Sample Login Weight

DATE SAMPLED: Feb 12, 2010 | DATE RECEIVED: Feb 12, 2010 | DATE REPORTED: Feb 13, 2010 | SAMPLE TYPE: Rock

Analyte:	Sample Login Weight
Unit:	kg
Sample Description RDL:	0.01
38703	0.23
38721	0.21
39052	0.08
42857	0.24
43003	0.25
43009	0.20
43013	0.14
43301	0.31
43859	0.22
45688	0.25
45808	0.24
47202	0.23
47227	0.21
47229	0.25
47239	0.25
54894	0.30
54867	0.24
68405	0.23
68428	0.26
68437	0.28
68514	0.25
68516	0.27
68523	0.26
70010	0.29
70048	0.21
70059	0.31

Comments: RDL - Reported Detection Limit

Certified By: Ron Cardinall

AGAT Laboratories

5623 McADAM ROAD
MISSISSAUGA, ONTARIO
CANADA L4Z 1N9
TEL (905)501-9998
FAX (905)501-0589
http://www.agatlabs.com

Quality Assurance

CLIENT NAME: DAHROUGE GEOLOGICAL CONSULTING LTD.

AGAT WORK ORDER: 10T385783

PROJECT NO: REE Checks

ATTENTION TO: JUDY SMITH

Rock Analysis

RPT Date:		REPLICATE				Method Blank	REFERENCE MATERIAL				
PARAMETER	Batch	Sample Id	Original	Rep #1	RPD		Result Value	Expect Value	Recovery	Acceptable Limits	
										Lower	Upper
Lithium Borate Fusion, ICP-OES finish (201076)											
Al2O3	1	1661624	0.672	0.667	0.7%	< 0.005	19.56	20.69	94%	80%	120%
BaO	1	1661624	0.025	0.024	4.1%	< 0.005	0.04	0.04	100%	80%	120%
CaO	1	1661624	33.850	33.140	2.1%	< 0.005	8.11	8.05	100%	80%	120%
Cr2O3	1	1661624	< 0.005	<0.005		< 0.005				80%	120%
Fe2O3	1	1661624	8.405	8.418	0.2%	< 0.005	7.16	6.21	115%	80%	120%
K2O	1	1661624	0.506	0.525	3.7%	< 0.005	1.56	1.66	93%	80%	120%
MgO	1	1661624	7.505	7.408	1.3%	< 0.005	0.54	0.54	100%	80%	120%
MnO	1	1661624	0.206	0.205	0.5%	< 0.005	0.108	0.108	100%	80%	120%
Na2O	1	1661624	0.523	0.517	1.2%	< 0.005	6.74	7.10	94%	80%	120%
P2O5	1	1661624	17.920	17.740	1.0%	< 0.005	0.109	0.131	83%	80%	120%
SiO2	1	1661624	4.886	4.894	0.2%	< 0.005	46.8	49.9	93%	80%	120%
TiO2	1	1661624	0.074	0.078	5.3%	< 0.005	0.279	0.287	97%	80%	120%
SrO	1	1661624	0.274	0.278	1.4%	< 0.005	0.14	0.14	100%	80%	120%
LOI	1	1661624	19.37	19.28	0.5%	< 0.01	4.59	4.56	100%	80%	120%
Total	1	1661624	94.216	93.174	1.1%	< 0.005		100	96%	80%	120%
Lithium Borate Fusion, ICP-MS finish											
Ag	1	1661610	< 1	<1		< 1				70%	130%
Ba	1	1661610	150.7	152.4	1.1%	< 0.5	337	340	99%	70%	130%
Ce	1	1661610	5596.5	5662.8	1.2%	< 0.5	132	122	108%	70%	130%
Co	1	1661610	9.8	9.0	8.5%	< 0.5	2.5	2.8	89%	70%	130%
Cr	1	1661610	11	10	9.5%	< 10	13	12	108%	70%	130%
Cs	1	1661610	0.03	0.03	0.0%	< 0.01	1.5	1.5	100%	70%	130%
Cu	1	1661610	< 1	<1		< 1	5	7	71%	70%	130%
Dy	1	1661610	138.38	135.93	1.8%	< 0.05	19.0	18.2	104%	70%	130%
Er	1	1661610	50.32	49.16	2.3%	< 0.03	14.1	14.2	99%	70%	130%
Eu	1	1661610	90.86	92.37	1.6%	< 0.03	2.03	2.00	101%	70%	130%
Ga	1	1661610	22.27	23.61	5.8%	< 0.01	38	35	108%	70%	130%
Gd	1	1661610	249.75	246.72	1.2%	< 0.05	14.9	14.0	106%	70%	130%
Hf	1	1661610	2.6	2.5	3.9%	< 0.2	10.5	10.6	99%	70%	130%
Ho	1	1661610	21.70	21.46	1.1%	< 0.01	4.4	4.3	102%	70%	130%
La	1	1661610	2445.5	2478.4	1.3%	< 0.5	59	58	101%	70%	130%
Lu	1	1661610	4.91	4.90	0.2%	< 0.01	2.1	2.1	100%	70%	130%
Mo	1	1661610	3	3	0.0%	< 2				70%	130%
Nb	1	1661610	995.0	1010.3	1.5%	< 0.2	10	13	76%	70%	130%
Nd	1	1661610	2801.5	2790.1	0.4%	< 0.1	59	57	103%	70%	130%
Ni	1	1661610	24			< 1		9		70%	130%
Pb	1	1661610	342	348	1.7%	< 1	10	10	100%	70%	130%
Pr	1	1661610	763.45	755.46	1.1%	< 0.03	16	15.0	106%	70%	130%
Rb	1	1661610	0.6	0.6	0.0%	< 0.2	55	55	100%	70%	130%
Sm	1	1661610	379.61	386.00	1.7%	< 0.03	12.9	12.7	101%	70%	130%
Sn	1	1661610	32	34	6.1%	< 1				70%	130%
Sr	1	1661610	3021.8	3077.1	1.8%	< 0.1	1305	1191	109%	70%	130%
Ta	1	1661610	1.7	1.5	12.5%	< 0.1	0.9	0.9	100%	70%	130%
Tb	1	1661610	30.52	29.91	2.0%	< 0.01	2.7	2.6	103%	70%	130%

AGAT Laboratories

5623 McADAM ROAD
MISSISSAUGA, ONTARIO
CANADA L4Z 1N9
TEL (905)501-9998
FAX (905)501-0589
http://www.agatlabs.com

Quality Assurance

CLIENT NAME: DAHROUGE GEOLOGICAL CONSULTING LTD.

AGAT WORK ORDER: 10T385783

PROJECT NO: REE Checks

ATTENTION TO: JUDY SMITH

Rock Analysis (Continued)

RPT Date:		REPLICATE				Method Blank	REFERENCE MATERIAL				
PARAMETER	Batch	Sample Id	Original	Rep #1	RPD		Result Value	Expect Value	Recovery	Acceptable Limits	
										Lower	Upper
Th	1	1661610	420.65	417.94	0.6%	< 0.05	1.2	1.4	85%	70%	130%
Tl	1	1661610	< 0.5	<0.5		< 0.5				70%	130%
Tm	1	1661610	6.43	6.40	0.5%	< 0.01	2.3	2.3	100%	70%	130%
U	1	1661610	0.64	0.63	1.6%	< 0.05	0.75	0.8	93%	70%	130%
V	1	1661610	134	136	1.5%	< 1	6	8	75%	70%	130%
W	1	1661610	10	9	10.5%	< 1				70%	130%
Y	1	1661610	616.2	615.2	0.2%	< 0.5	122	119	102%	70%	130%
Yb	1	1661610	37.42	37.46	0.1%	< 0.03	15.1	14.8	102%	70%	130%
Zn	1	1661610	479	475	0.8%	< 1	101	93	108%	70%	130%
Zr	1	1661610	174	1558	159.8%	< 2	535	517	103%	70%	130%

Certified By: Ron Cardinall

AGAT Laboratories

5623 McADAM ROAD
MISSISSAUGA, ONTARIO
CANADA L4Z 1N9
TEL (905)501-9998
FAX (905)501-0589
http://www.agatlabs.com

Method Summary

CLIENT NAME: DAHROUGE GEOLOGICAL CONSULTING LTD.

AGAT WORK ORDER: 10T385783

PROJECT NO: REE Checks

ATTENTION TO: JUDY SMITH

PARAMETER	AGAT S.O.P	LITERATURE REFERENCE	ANALYTICAL TECHNIQUE
Rock Analysis			
Ag			ICP-MS
Ba		SY-4	ICP-MS
Ce		SY-4	ICP-MS
Co		SY-4	ICP-MS
Cr		SY-4	ICP-MS
Cs		SY-4	ICP-MS
Cu		SY-4	ICP-MS
Dy		SY-4	ICP-MS
Er		SY-4	ICP-MS
Eu		SY-4	ICP-MS
Ga		SY-4	ICP-MS
Gd		SY-4	ICP-MS
Hf		SY-4	ICP-MS
Ho		SY-4	ICP-MS
La		SY-4	ICP-MS
Lu		SY-4	ICP-MS
Mo			ICP-MS
Nb		SY-4	ICP-MS
Nd		SY-4	ICP-MS
Ni		SY-4	ICP-MS
Pb		SY-4	ICP-MS
Pr		SY-4	ICP-MS
Rb		SY-4	ICP-MS
Sm		SY-4	ICP-MS
Sn			ICP-MS
Sr		SY-4	ICP-MS
Ta		SY-4	ICP-MS
Tb		SY-4	ICP-MS
Th		SY-4	ICP-MS
Tl			ICP-MS
Tm		SY-4	ICP-MS
U		SY-4	ICP-MS
V		SY-4	ICP-MS
W			ICP-MS
Y		SY-4	ICP-MS
Yb		SY-4	ICP-MS
Zn		SY-4	ICP-MS
Zr		SY-4	ICP-MS
Al2O3	MIN-200-12015		ICP/OES
BaO	MIN-200-12015		ICP/OES
CaO	MIN-200-12015		ICP/OES
Cr2O3	MIN-200-12015		ICP/OES
Fe2O3	MIN-200-12015		ICP/OES
K2O	MIN-200-12015		ICP/OES
MgO	MIN-200-12015		ICP/OES
MnO	MIN-200-12015		ICP/OES
Na2O	MIN-200-12015		ICP/OES
P2O5	MIN-200-12015		ICP/OES
SiO2	MIN-200-12015		ICP/OES

AGAT Laboratories

5623 McADAM ROAD
MISSISSAUGA, ONTARIO
CANADA L4Z 1N9
TEL (905)501-9998
FAX (905)501-0589
http://www.agatlabs.com

Method Summary

CLIENT NAME: DAHROUGE GEOLOGICAL CONSULTING LTD.

AGAT WORK ORDER: 10T385783

PROJECT NO: REE Checks

ATTENTION TO: JUDY SMITH

PARAMETER	AGAT S.O.P	LITERATURE REFERENCE	ANALYTICAL TECHNIQUE
TiO2	MIN-200-12015		ICP/OES
SrO	MIN-200-12015		ICP/OES
LOI	MIN-200-12016		GRAVIMETRIC
Total	MIN-200-12015		CALCULATION
Sample Login Weight	MIN-200-12009		BALANCE

APPENDIX 22: NOMENCLATURE

Grain	
c.g.	coarse-grained
m.g.	medium-grained
f.g.	fine-grained
xst	crystal
anh	anhedral
subh	subhedral
euh	euhedral
irr	irregular

Minerals	
min	mineral
alb	albite
amph	amphibole
ap	apatite
bio	biotite
cc	calcite
clb	columbite
cpx	clinopyroxene
cpy	calcopyrite
dol	dolomite
dsp	diopside
epd	epidote
fl	fluorite
fsp	feldspar
grt	garnet
hem	hematite
ilm	ilmenite
mag	magnetite
mnz	monazite
phl	phlogopite
plag	plagioclase
po	pyrrhotite
py	pyrite
pych	pyrochlore
pyx	pyroxene
qtz	quartz
sid	siderite
sul	sulphides

Textures	
bnd	band
bndg	banding
brc	brecciated
diss	disseminated
frag	fragment
homo	homogeneous
mass	massive
pheno	phenocryst
sks	slicken slides
suc	sucrosic
textures	text
vnlet	veinlets
vns	veins
x-cut	cross cut
xstn	crystalline

Colour	
lt	light
med	medium
dk	dark
dkr	darker
b	blue
blk	black
br	brown
cr	cream
gr	green
gy	grey
og	orange
p	purple
pk	pink
r	red
w	white
y	yellow

Lithology	
litho	Lithology
Amt	Amphibolite
Carb	Carbonatite
Carb 1	Carb Stage 1
Carb 2	Carb Stage 2
Carb 3	Carb Stage 3
Carb 4	Carb Stage 4
Glim	Glimmerite
Gn	Gneiss
Phyl	Phyllite
Qtzite	Quartzite
S-Carb	Silico-Carb
Scht	Schist
Slct	Silicate
Syn	Synite

Other	
abnt	abundent
alt	altered
avg	average
CA	Core Axis
ctc	contact
few	few
mod	moderate
OC	outcrop
RA	radioactivity
rnd	rounded
STD	standard
str	strong
v	very
wk	weak
wthd	weathered
DUP	Duplicate

Names	
AH	Andy Hoffman
AK	Alex Knox
AL	Andrew Lafontaine
APR	Ashley Peter-Rennich
BP	Becky Partridge
BW	Bryce Wetthuhn
CR	Craig Ryan
DD	Deon Dicks
DS	Darren Smith
DT	Danny Trembly
EK	Elijah Koneak
LR	Laura Rapp
MG	Michael Guo
MH	Mike Hodge
MO	Craig Ryan
MP	Mireille Perreault
P	Patrick Lariviere ?
RD	Ramses D'Souza
RD	Ramses D'Souza
RL	Ryan Libke
TM	Trevor Martin